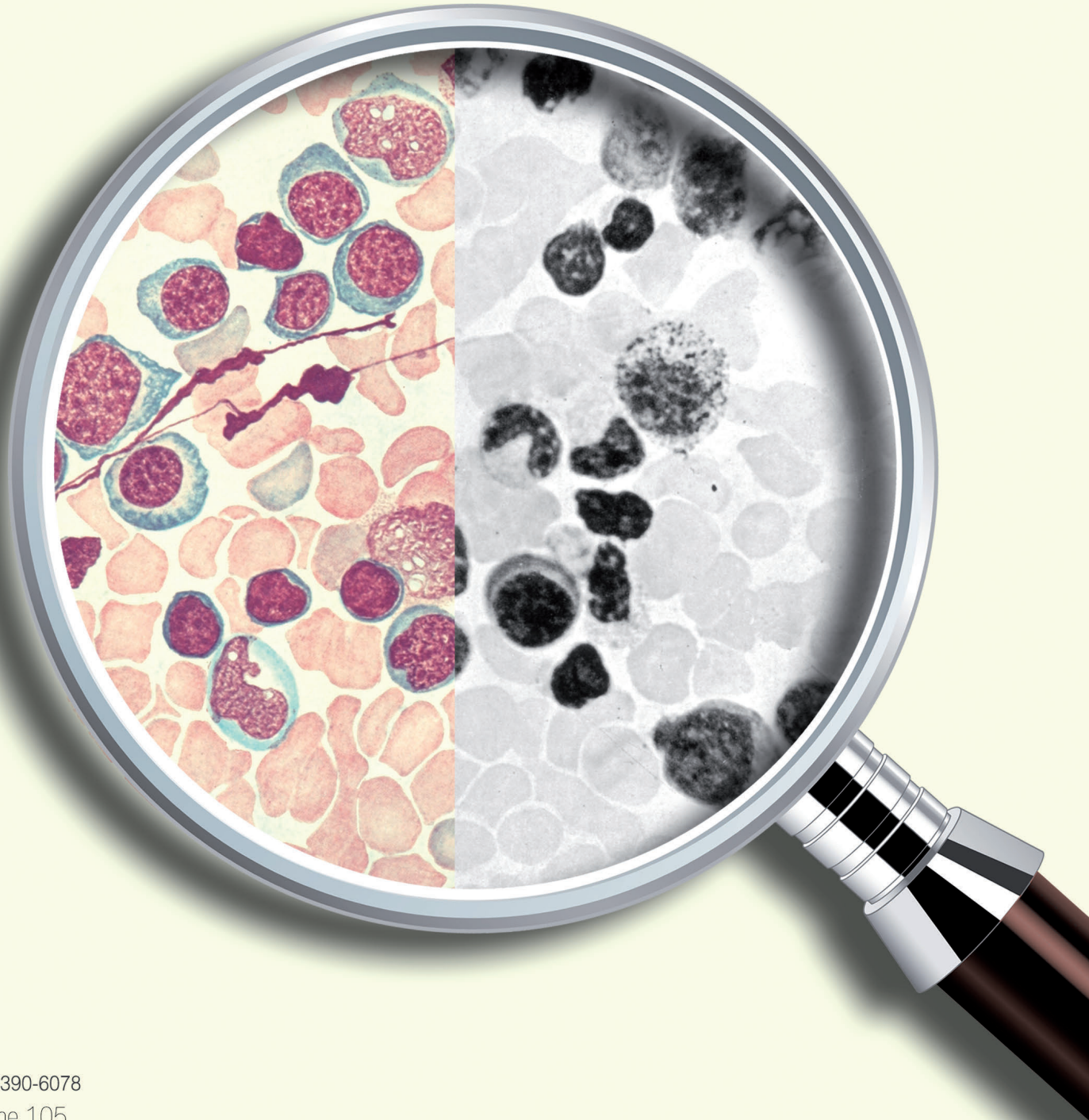


 **haematologica**

Journal of The Ferrata Storti Foundation



ISSN 0390-6078

Volume 105

AUGUST

2020 - 08

www.haematologica.org

haematologica

Looking for a definitive source
of information in hematology?

Haematologica is an Open Access
journal: all articles are completely
free of charge

Haematologica
is listed on *PubMed, PubMedCentral,*
DOAJ, Scopus and many other
online directories

5000 / amount of articles read daily

4300 / amount of PDFs downloaded daily

2.20 / gigabytes transferred daily

WWW.HAEMATOLOGICA.ORG

Editor-in-Chief

Luca Malcovati (Pavia)

Deputy Editor

Carlo Balduini (Pavia)

Managing Director

Antonio Majocchi (Pavia)

Associate Editors

Hélène Cavé (Paris), Monika Engelhardt (Freiburg), Steve Lane (Brisbane), PierMannuccio Mannucci (Milan), Simon Mendez-Ferrer (Cambridge), Pavan Reddy (Ann Arbor), Francesco Rodeghiero (Vicenza), Andreas Rosenwald (Wuerzburg), Davide Rossi (Bellinzona), Jacob Rowe (Haifa, Jerusalem), Wyndham Wilson (Bethesda), Swee Lay Thein (Bethesda)

Assistant Editors

Anne Freckleton (English Editor), Britta Dorst (English Editor), Cristiana Pascutto (Statistical Consultant), Rachel Stenner (English Editor),

Editorial Board

Jeremy Abramson (Boston); Paolo Arosio (Brescia); Raphael Bejar (San Diego); Erik Berntorp (Malmö); Dominique Bonnet (London); Jean-Pierre Bourquin (Zurich); Suzanne Cannegieter (Leiden); Francisco Cervantes (Barcelona); Nicholas Chiorazzi (Manhasset); Oliver Cornely (Köln); Michel Delforge (Leuven); Ruud Delwel (Rotterdam); Meletios A. Dimopoulos (Athens); Inderjeet Dokal (London); Hervé Dombret (Paris); Peter Dreger (Hamburg); Martin Dreyling (München); Kieron Dunleavy (Bethesda); Dimitar Efremov (Rome); Sabine Eichinger (Vienna); Jean Feuillard (Limoges); Carlo Gambacorti-Passerini (Monza); Guillermo Garcia Manero (Houston); Christian Geisler (Copenhagen); Piero Giordano (Leiden); Christian Gisselbrecht (Paris); Andreas Greinacher (Greifswald); Hildegard Greinix (Vienna); Paolo Gresele (Perugia); Thomas M. Habermann (Rochester); Claudia Haferlach (München); Oliver Hantschel (Lausanne); Christine Harrison (Southampton); Brian Huntly (Cambridge); Ulrich Jaeger (Vienna); Elaine Jaffe (Bethesda); Arnon Kater (Amsterdam); Gregory Kato (Pittsburg); Christoph Klein (Munich); Steven Knapper (Cardiff); Seiji Kojima (Nagoya); John Koreth (Boston); Robert Kralovics (Vienna); Ralf Küppers (Essen); Ola Landgren (New York); Peter Lenting (Le Kremlin-Bicetre); Per Ljungman (Stockholm); Francesco Lo Coco (Rome); Henk M. Lokhorst (Utrecht); John Mascarenhas (New York); Maria-Victoria Mateos (Salamanca); Giampaolo Merlini (Pavia); Anna Rita Migliaccio (New York); Mohamad Mohty (Nantes); Martina Muckenthaler (Heidelberg); Ann Mullally (Boston); Stephen Mulligan (Sydney); German Ott (Stuttgart); Jakob Passweg (Basel); Melanie Percy (Ireland); Rob Pieters (Utrecht); Stefano Pileri (Milan); Miguel Piris (Madrid); Andreas Reiter (Mannheim); Jose-Maria Ribera (Barcelona); Stefano Rivella (New York); Francesco Rodeghiero (Vicenza); Richard Rosenquist (Uppsala); Simon Rule (Plymouth); Claudia Scholl (Heidelberg); Martin Schrappe (Kiel); Radek C. Skoda (Basel); Gérard Socié (Paris); Kostas Stamatopoulos (Thessaloniki); David P. Steensma (Rochester); Martin H. Steinberg (Boston); Ali Taher (Beirut); Evangelos Terpos (Athens); Takanori Teshima (Sapporo); Pieter Van Vlierberghe (Gent); Alessandro M. Vannucchi (Firenze); George Vassiliou (Cambridge); Edo Vellenga (Groningen); Umberto Vitolo (Torino); Guenter Weiss (Innsbruck).

Editorial Office

Simona Giri (Production & Marketing Manager), Lorella Ripari (Peer Review Manager), Paola Cariati (Senior Graphic Designer), Igor Ebuli Poletti (Senior Graphic Designer), Marta Fossati (Peer Review), Diana Serena Ravera (Peer Review)

Affiliated Scientific Societies

SIE (Italian Society of Hematology, www.siematologia.it)

SIES (Italian Society of Experimental Hematology, www.siesonline.it)

Information for readers, authors and subscribers

Haematologica (print edition, pISSN 0390-6078, eISSN 1592-8721) publishes peer-reviewed papers on all areas of experimental and clinical hematology. The journal is owned by a non-profit organization, the Ferrata Storti Foundation, and serves the scientific community following the recommendations of the World Association of Medical Editors (www.wame.org) and the International Committee of Medical Journal Editors (www.icmje.org).

Haematologica publishes editorials, research articles, review articles, guideline articles and letters. Manuscripts should be prepared according to our guidelines (www.haematologica.org/information-for-authors), and the Uniform Requirements for Manuscripts Submitted to Biomedical Journals, prepared by the International Committee of Medical Journal Editors (www.icmje.org).

Manuscripts should be submitted online at <http://www.haematologica.org/>.

Conflict of interests. According to the International Committee of Medical Journal Editors (<http://www.icmje.org/#conflicts>), "Public trust in the peer review process and the credibility of published articles depend in part on how well conflict of interest is handled during writing, peer review, and editorial decision making". The ad hoc journal's policy is reported in detail online (www.haematologica.org/content/policies).

Transfer of Copyright and Permission to Reproduce Parts of Published Papers. Authors will grant copyright of their articles to the Ferrata Storti Foundation. No formal permission will be required to reproduce parts (tables or illustrations) of published papers, provided the source is quoted appropriately and reproduction has no commercial intent. Reproductions with commercial intent will require written permission and payment of royalties.

Detailed information about subscriptions is available online at www.haematologica.org. Haematologica is an open access journal. Access to the online journal is free. Use of the Haematologica App (available on the App Store and on Google Play) is free.

For subscriptions to the printed issue of the journal, please contact: Haematologica Office, via Giuseppe Belli 4, 27100 Pavia, Italy (phone +39.0382.27129, fax +39.0382.394705, E-mail: info@haematologica.org).

Rates of the International edition for the year 2019 are as following:

	<i>Institutional</i>	<i>Personal</i>
<i>Print edition</i>	<i>Euro 700</i>	<i>Euro 170</i>

Advertisements. Contact the Advertising Manager, Haematologica Office, via Giuseppe Belli 4, 27100 Pavia, Italy (phone +39.0382.27129, fax +39.0382.394705, e-mail: marketing@haematologica.org).

Disclaimer. Whilst every effort is made by the publishers and the editorial board to see that no inaccurate or misleading data, opinion or statement appears in this journal, they wish to make it clear that the data and opinions appearing in the articles or advertisements herein are the responsibility of the contributor or advisor concerned. Accordingly, the publisher, the editorial board and their respective employees, officers and agents accept no liability whatsoever for the consequences of any inaccurate or misleading data, opinion or statement. Whilst all due care is taken to ensure that drug doses and other quantities are presented accurately, readers are advised that new methods and techniques involving drug usage, and described within this journal, should only be followed in conjunction with the drug manufacturer's own published literature.

Direttore responsabile: Prof. Carlo Balduini; Autorizzazione del Tribunale di Pavia n. 63 del 5 marzo 1955.
Printing: Press Up, zona Via Cassia Km 36, 300 Zona Ind.le Settevene - 01036 Nepi (VT)



Table of Contents

Volume 105, Issue 8: August 2020

About the cover

- 1985** 100-YEAR-OLD HAEMATOLOGICA IMAGES: THE LONG ROAD FROM THE BEAUTY OF DRAWING TO THE OBJECTIVITY OF PHOTOGRAPHY
Carlo L. Balduini

Editorials

- 1986** Low-dose X-rays leave scars on human hematopoietic stem and progenitor cells: the role of reactive oxygen species
Masayuki Yamashita and Toshio Suda
- 1988** Busy signal: platelet-derived growth factor activation in myelofibrosis
Anna E. Marneth and Ann Mullally
- 1991** When the bond breaks – targeting adhesion of leukemia cells to the meninges
Lennart Lenk, Fotini Vogiatzi and Denis M. Schewe
- 1993** BCL2 dependency in diffuse large B-cell lymphoma: it's a family affair
Shannon M. Matulis and Lawrence H. Boise
- 1996** Insights into vitamin K-dependent carboxylation: home field advantage
Francis Ayombil and Rodney M. Camire

Perspective Article

- 1999** An agenda for future research projects in polycythemia vera and essential thrombocythemia
Tiziano Barbui et al.

Centenary Review Article

- 2004** Inherited thrombocytopenias: history, advances and perspectives
Alan T. Nurden and Paquita Nurden

Review Article

- 2020** Clonal hematopoietic mutations linked to platelet traits and the risk of thrombosis or bleeding
Alicia Veninga et al.
- 2032** Acquired von Willebrand syndrome: focused for hematologists
Massimo Franchini and Pier Mannuccio Mannucci

Guideline Article

- 2038** Kreuth V initiative: European consensus proposals for treatment of hemophilia using standard products, extended half-life coagulation factor concentrates and non-replacement therapies
Flora Peyvandi et al.

Articles

Hematopoiesis

- 2044** Human hematopoietic stem/progenitor cells display reactive oxygen species-dependent long-term hematopoietic defects after exposure to low doses of ionizing radiations
Elia Henry et al.

Macrophage Biology and Its Disorders

- 2056** Specialized pro-resolving lipid mediators are differentially altered in peripheral blood of patients with multiple sclerosis and attenuate monocyte and blood-brain barrier dysfunction
Gijs Kooij et al.

Iron Metabolism & its Disorders

- 2071** Transferrin receptor 1-mediated iron uptake plays an essential role in hematopoiesis
Shufen Wang et al.

Myeloproliferative Neoplasms

- 2083** Platelet-derived growth factor receptor β activation and regulation in murine myelofibrosis
Frederike Kramer et al.

Chronic Myeloid Leukemia

- 2095** A high-content cytokine screen identifies myostatin propeptide as a positive regulator of primitive chronic myeloid leukemia cells
Sofia von Palffy et al.

Acute Myeloid Leukemia

- 2105** Tuning mTORC1 activity dictates the response of acute myeloid leukemia to LSD1 inhibition
Amal Kamal Abdel-Aziz et al.

- 2118** EVI1 triggers metabolic reprogramming associated with leukemogenesis and increases sensitivity to L-asparaginase
Yusuke Saito et al.

Acute Lymphoblastic Leukemia

- 2130** Disrupting the leukemia niche in the central nervous system attenuates leukemia chemoresistance
Leslie M. Jonart et al.

Non-Hodgkin Lymphoma

- 2141** Quantification of minimal disseminated disease by quantitative polymerase chain reaction and digital polymerase chain reaction for *NPM-ALK* as a prognostic factor in children with anaplastic large cell lymphoma
Christine Damm-Welk et al.

- 2150** Specific interactions of BCL-2 family proteins mediate sensitivity to BH3-mimetics in diffuse large B-cell lymphoma
Victoria M. Smith et al.

Coagulation and its Disorders

- 2164** Vitamin K-dependent carboxylation of coagulation factors: insights from a cell-based functional study
Zhenyu Hao et al.

Blood Transfusion

- 2174** Red blood cell metabolism in Rhesus macaques and humans: comparative biology of blood storage
Davide Stefanoni et al.

Letters to the Editor

Letters are available online only at www.haematologica.org/content/105/8.toc

- e385** LJ000328, a novel ALK2/3 kinase inhibitor, represses hepcidin and significantly improves the phenotype of IRIDA
Audrey Belot et al.
<http://www.haematologica.org/content/105/8/e385>

- e389** Comparing the two leading erythroid lines BEL-A and HUDEP-2
Deborah E. Daniels et al.
<http://www.haematologica.org/content/105/8/e389>

- e395** Cloning and characterization of a novel druggable fusion kinase in acute myeloid leukemia
Christian Michel et al.
<http://www.haematologica.org/content/105/8/e395>
- e399** CD34⁺ acute myeloid leukemia cells with low levels of reactive oxygen species show increased expression of stemness genes and can be targeted by the BCL2 inhibitor venetoclax
Katharina Mattes et al.
<http://www.haematologica.org/content/105/8/e399>
- e404** Selinexor combined with cladribine, cytarabine, and filgrastim in relapsed or refractory acute myeloid leukemia
Ramzi Abboud et al.
<http://www.haematologica.org/content/105/8/e404>
- e408** Cryptic insertions of the immunoglobulin light chain enhancer region near *CCND1* in t(11;14)-negative mantle cell lymphoma
Carla Fuster et al.
<http://www.haematologica.org/content/105/8/e408>
- e412** Breast implant-associated Epstein-Barr virus-positive large B-cell lymphomas: a report of three cases
Socorro María Rodríguez-Pinilla et al.
<http://www.haematologica.org/content/105/8/e412>
- e415** Impact of relative dose intensity of standard regimens on survival in elderly patients aged 80 years and older with diffuse large B-cell lymphoma
Shin Lee et al.
<http://www.haematologica.org/content/105/8/e415>
- e419** ASK1 inhibition triggers platelet apoptosis via p38-MAPK-mediated mitochondrial dysfunction
Kurnegala Manikanta et al.
<http://www.haematologica.org/content/105/8/e419>
- e424** Activated protein C anticoagulant activity is enhanced by skeletal muscle myosin
Mary J. Heeb et al.
<http://www.haematologica.org/content/105/8/e424>

Case Reports

Case Reports are available online only at www.haematologica.org/content/105/8.toc

- e428** Clinical acceleration of *JAK2* p.V617F driven myeloproliferative disease due to a new uncommon homozygous *MPL* p.Y591D mutation
Jeremy Ong et al.
<http://www.haematologica.org/content/105/8/e428>
- e432** Evolutionary crossroads: morphological heterogeneity reflects divergent intra-clonal evolution in a case of high-grade B-cell lymphoma
Valentina Tabanelli et al.
<http://www.haematologica.org/content/105/8/e432>
- e437** Indolent EBV-positive T-cell lymphoproliferative disorder arising in a chronic pericardial hematoma: the T-cell counterpart of fibrin-associated diffuse large B-cell lymphoma?
Zhen Wang et al.
<http://www.haematologica.org/content/105/8/e437>

The origin of a name that reflects Europe's cultural roots.

Ancient Greek

αἷμα [haima] = blood
αἷματος [haimatos] = of blood
λόγος [logos] = reasoning

Scientific Latin

haematologicus (adjective) = related to blood

Scientific Latin

haematologica (adjective, plural and neuter,
used as a noun) = hematological subjects

Modern English

The oldest hematology journal,
publishing the newest research results.
2019 JCR impact factor = 7.116

100-YEAR-OLD HAEMATOLOGICA IMAGES: THE LONG ROAD FROM THE BEAUTY OF DRAWING TO THE OBJECTIVITY OF PHOTOGRAPHY

Carlo L. Balduini

Ferrata-Storti Foundation, Pavia, Italy

E-mail: CARLO L. BALDUINI - carlo.balduini@unipv.it

doi:10.3324/haematol.2020.261818

The first apparatuses for taking pictures under the microscope were developed in the late 19th century. The Ernst Leitz's company catalog from 1899 included an instrument for "projecting microscopic objects and taking photo-micrographs",¹ but the images obtained from these bulky devices were in gray scale and of very low quality. For a substantial improvement in the field of microphotography we had to wait until 1935, when the Kodak company launched the first multilayer photographic film that was capable of providing detailed color images. So, at the time of the birth of *Haematologica* in 1920, the only way to reproduce color images of cells and tissues seen under a microscope was to rely exclusively on the skill of specialized artists who could draw them. The images reproduced on the covers of the previous issues of *Haematologica* testify to the extraordinary ability of these artists. However, a drawing has a large margin of subjectivity and it is only the credibility of the author that testifies to its accuracy. To overcome this limit, starting in the 1930s, papers began to appear in *Haematologica* which reported gray scale, low resolution photographic images associated with a color drawing of the same microscopic field. With this approach, the authors intended to combine the objectivity of photography with

the ability of the designed plates to reproduce the smallest details. It was the end of an era, and a new one began.

The cover image of this issue of *Haematologica* was created by juxtaposing the photographic image of a cytological preparation alongside the image of the same microscopic field drawn by hand. The original images are shown in Figure 1. They were taken from an article published in *Haematologica* in 1936 by Edoardo Storti,² a pupil of Adolfo Ferrata and, decades later, one of the most active Editors of *Haematologica*. In the article, Storti reported on a patient with acute erythremic myelosis (now known as pure erythroid leukemia), thus providing further confirmation of the existence of this disease, described for the first time in *Haematologica* by Giovanni Di Guglielmo in 1928.^{3,4}

References

1. Leitz E, ed. Catalogue No 38: Microscopes and Accessory Apparatus. Wetzlar, Germany: Ernst Leitz; 1899.
2. Storti E. [Contributo allo studio della mielosi eritemica]. *Haematologica*. 1936;17:393-460.
3. Di Guglielmo G. [Le eritremie]. *Haematologica*. 1928;9:301-347.
4. Balduini CL. 100-Year Old *Haematologica* Images: Di Guglielmo Disease or Pure Erythroid Leukemia. *Haematologica*. 2020;105(3):525.

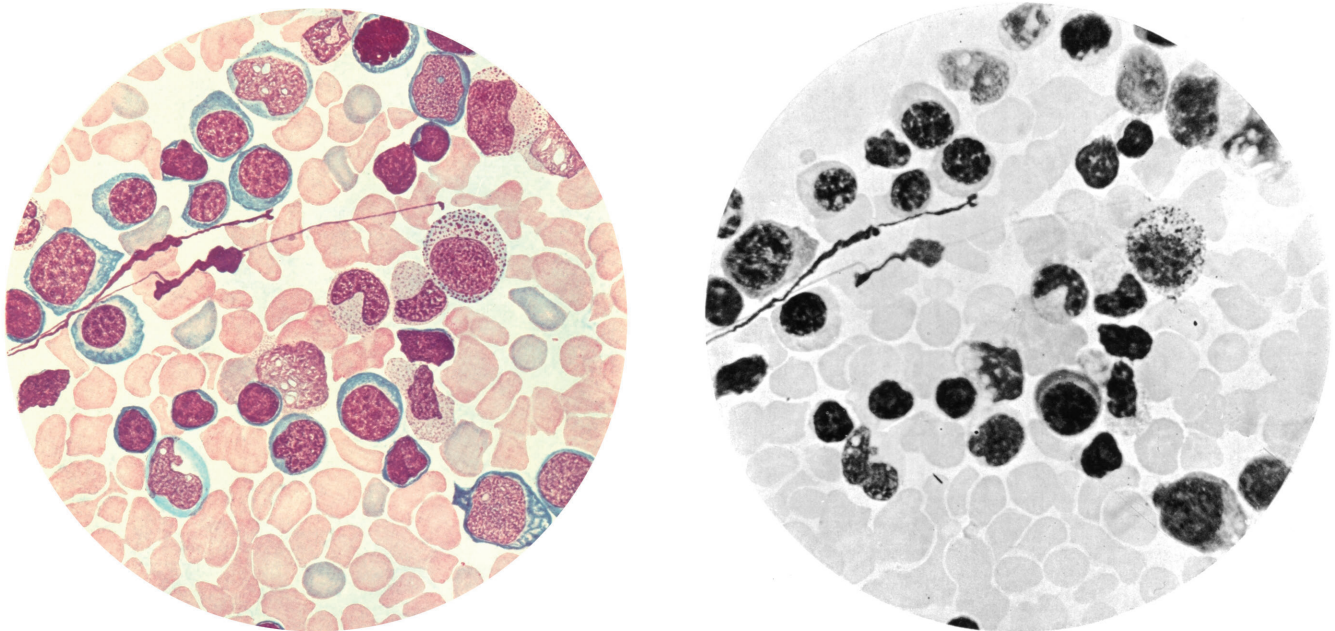


Figure 1. Peripheral blood (buffy coat smear) of a patient with acute erythremic myelosis. These images have been taken from an article published in *Haematologica* by Edoardo Storti in 1936² and the photo in gray scale was used to testify the genuineness of the color drawing.

Low-dose X-rays leave scars on human hematopoietic stem and progenitor cells: the role of reactive oxygen species

Masayuki Yamashita¹ and Toshio Suda^{2,3}

¹Division of Stem Cell and Molecular Medicine, Center for Stem Cell Biology and Regenerative Medicine, The Institute of Medical Science, The University of Tokyo, Tokyo, Japan; ²International Research Center for Medical Sciences, Kumamoto University, Kumamoto, Japan and ³Cancer Science Institute, National University of Singapore, Singapore

E-mail: TOSHIO SUDA - sudato@keio.jp

doi:10.3324/haematol.2020.254292

After Röntgen's discovery in 1895, an X-ray became a game changer in medicine.¹ It was discovered as an invisible ray of light that passes through many objects, including human bodies, and visualizes the internal organs and structures as silhouettes. As now seen in medical radiography, such as chest X-rays and computed tomography (CT) scans, X-rays have enabled investigation of deep tissues in humans that had been otherwise impossible without surgical intervention, contributing to the early detection and treatment of many diseases. However, as is often the case with new medicine, X-rays were shown to have a biohazard effect.² They are identified as a type of ionizing radiation (IR): a stream of high energy photons that are strong enough to ionize atoms and disrupt molecular bonds in biomolecules, including DNA. As DNA encodes an essential blueprint of a cell, the DNA-damaging property of X-rays can be toxic. This effect, although used for killing cancer cells in radiotherapy, has raised concerns about the effect of X-rays on normal tissues and whether the benefits exceed the risks.

Modern medicine relies heavily on radiography to assess human health. The annual doses of X-rays people receive are increasing. A recent study estimated that around 2% or 4,000,000 of the non-elderly adults in the US receive 20 milligray (mGy) or more per year due to medical requirements.³ Historically, risks associated with low-dose IR are considered to be almost negligible as it does not cause any acute toxicity, nor does it increase the risk of carcinogenesis, based on empirical linear fits of existing human data determined at high doses, such as those of Japanese atomic bomb survivors.⁴ Indeed, low-dose IR rarely induces DNA double strand breaks (DSB), which often cause mutations and are considered to be the most relevant lesion for the deleterious effects of IR.⁵ However, even though low-dose X-rays rarely cause DSB, they are reportedly less easy to repair than those induced by high-dose X-rays.⁶ Importantly, recent evidence suggests that cumulative doses of 50 mGy X-ray (doses equivalent to 5-10 brain CT scans when given in childhood) have long-term detrimental effects on human health, including a more than 3-fold increase in the risks of acute lymphoblastic leukemia and myelodysplastic syndrome.⁷ Furthermore, mouse studies demonstrate that low-dose X-rays affect function of long-lived tissue-specific stem cells, including hematopoietic stem cells (HSC).^{8,9} Thus, understanding the persistent effect of low-dose X-rays on human tissue-specific stem cells is of particular importance in precisely evaluating the risks posed by radiography on public health.

In this issue of *Haematologica*, Henry *et al.* compared the effects of low and high doses of X-rays on hematopoietic stem and progenitor cells (HSPC) obtained from human umbilical cord blood (CB) (Figure 1).¹⁰ HSPC sustain them-

selves *via* self-renewing ability, and give rise to all of the blood lineage cells, such as innate and acquired immune cells, erythrocytes and platelets, through multi-lineage differentiation. They found that a single dose of 20 mGy X-rays is sufficient to impair the self-renewing capacity of CB HSPC. Intriguingly, this effect is independent of canonical DNA damage response (DDR), as a 20 mGy dose fails to induce DSB markers γ -H2AX and 53BP1 foci, or DDR hallmarks phospho-ATM and -p53, all of which are induced by a 2.5 Gy dose. Instead, the authors demonstrate that it is mediated by reactive oxygen species (ROS), a highly reactive oxygen byproduct mainly generated *via* the cell respiratory process of oxidative phosphorylation (OXPHOS) in mitochondria, and p38/MAPK14, a key enzyme that, upon elevation of ROS, sends a signal to HSPC to inhibit their self-renewing potential.¹¹ Thus, the results of Henry *et al.* indicate that low-dose X-rays impair human CB HSPC function through ROS and p38/MAPK14, but not *via* canonical DDR *via* ATM or p53.

The high sensitivity of HSC to elevated levels of ROS is well established, first in ATM deficiency and later in the contexts of other stress conditions.¹¹⁻¹³ Similarly, p38/MAPK14 activation in response to ROS elevation is identified as a common downstream pathway responsible for impairment of self-renewal in HSC.^{11,12} In contrast, what is often unclear is the upstream mediator that causes ROS elevation. In the context of low-dose IR, mouse studies have uncovered the hypersensitivity of HSC and esophageal stem cells to low-dose IR that is mediated by ROS elevation, although the molecular link between low-dose IR and elevated ROS has not yet been investigated.^{8,9} It is estimated that approximately 90% of ROS can be generated during OXPHOS in mitochondria,¹⁴ mainly through functions of complexes I and III.¹⁵ Interestingly, the results shown by Henry *et al.* indicate that ROS elevation in human CB HSPC upon exposure to 20 mGy X-rays is closely associated with loss of mitochondrial membrane potential, which reflects a decrease in proton gradient across the cristae and often correlates with mitochondrial dysfunction.¹⁰ Apart from nucleus, mitochondria are the only organelle in mammalian cells that contain DNA, which can also be damaged by low-dose IR.¹⁶ Mitochondrial DNA (mtDNA) encodes proteins that consist of complexes I and ATP synthase, both of which are essential for proper electron transport and OXPHOS. Of note, these components are located in the so-called "common deletion" region of mtDNA that is commonly deleted upon exposure to low-dose IR. mtDNA is not protected by histones, and is thus potentially more susceptible to IR-induced damage compared to nuclear DNA. Moreover, mtDNA is located in matrix inside inner membranes where ROS is generated, and is thus more greatly affected by IR-induced oxidative stress

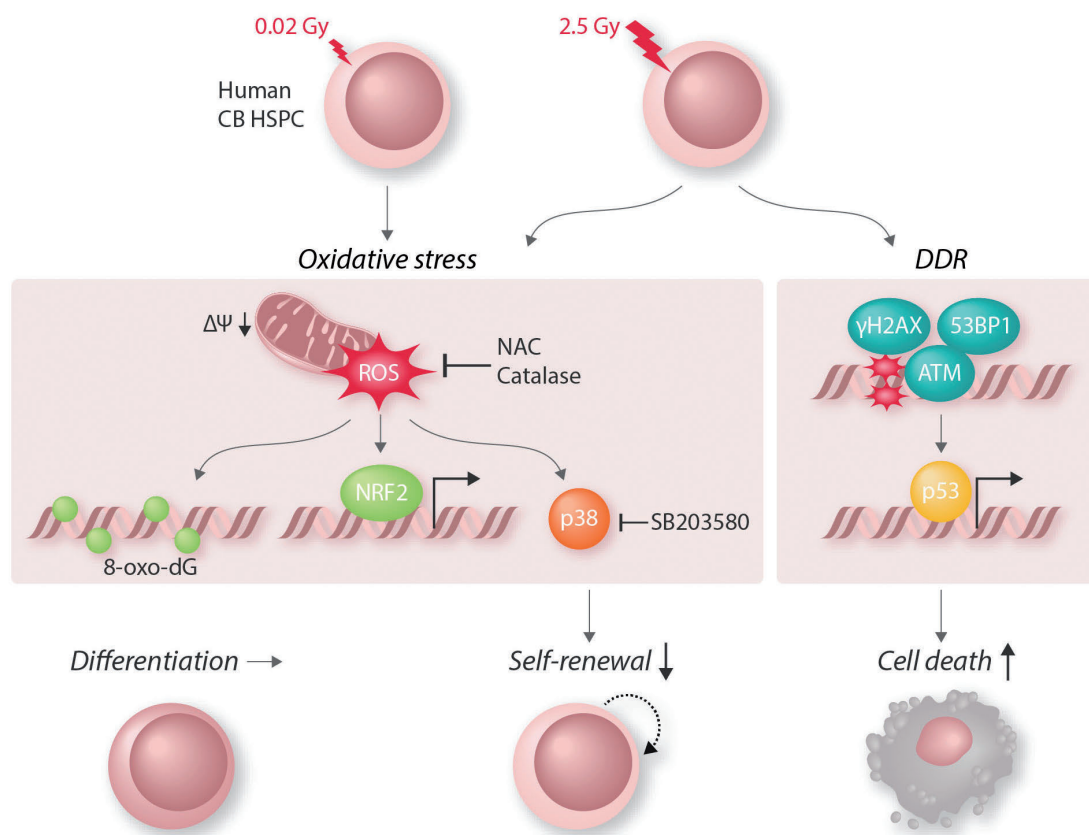


Figure 1. Response of human cord blood (CB) hematopoietic stem and progenitor cells (HSPC) to low- and high-dose X-ray irradiation demonstrated by Henri *et al.*¹⁰ A low dose of 0.02 Gy (20 mGy) X-rays induces reactive oxygen species (ROS) elevation coupled with decrease in mitochondrial membrane potential ($\Delta\Psi$), which leads to increase in oxidative stress represented by formation of 8-oxo-deoxyguanosine (8-oxo-dG) in DNA, nuclear expression of NRF2, and activation of p38/MAPK14. The p38/MAPK14 activation mediates a decline in self-renewing capacity of HSPC without affecting their differentiating potential. The low-dose X-rays do not induce γ -H2AX and 53BP1 foci that represents nuclear DNA double strand breaks (DSB), or canonical DNA damage response via phosphorylation of ATM and p53. In contrast, a high dose of 2.5 Gy X-ray irradiation causes both ROS elevation and nuclear DSB. As a result, ROS inhibition either by N-acetylcysteine (NAC) or catalase, or p38 inhibition by SB203580, can reverse the detrimental effect by low dose, but not high dose, of X-rays on self-renewal capacity of HSPC.

than nuclear DNA. Damage in mtDNA is not so simple as that in nuclear DNA, as a cell can contain more than 1,000 copies of mtDNA. Furthermore, numbers of mitochondria are dynamically changed by fusion and fission, which play critical roles in maintaining functional mitochondria *via* inter-mitochondrial complementation and quality control.¹⁷ In addition, damaged mitochondria can be removed by autophagy, which contributes to maintenance of self-renewal capacity of HSC.^{18,19} Henry *et al.* show that mitochondrial mass in HSPC does not seem to change after irradiation of 20 mGy X-rays.¹⁰ Although this observation should be validated by other methods,²⁰ it supports the idea that changes in mitochondrial mass are unlikely to be the cause of ROS elevation. Rather, it is tempting to speculate that damage in mtDNA induced by low-dose IR causes persistent changes in mitochondrial function that lead to initial elevation of ROS and long-term impairment of HSC function. This would be consistent with the results reported by Rodrigues-Moreira *et al.*, which demonstrate that low-dose X-rays cause biphasic elevations of ROS and the second wave of ROS elevation causes persistent reduction in self-renewing capacity of mouse bone marrow HSC.⁹ Mitochondrial dysfunction, but not constant elevation of ROS, is implicated in age-

associated decline in HSC function.¹⁸ Since involvement of mtDNA remains unknown, investigating whether aged HSC have mtDNA damage would be of particular interest. Collectively, identifying molecular ‘scars’ left by low-dose X-rays on HSC would help provide a precise evaluation of the long-term detrimental effects by medical radiographic examination and also find common mechanisms that underlie hematopoietic aging and disease.

References

1. Röntgen WC. On a New Kind of Rays. *Science*. 1896;3(59):227-231.
2. Daniel J. The X-Rays. *Science*. 1896;3(67):562-563.
3. Fazel R, Krumholz HM, Wang Y, et al. Exposure to low-dose ionizing radiation from medical imaging procedures. *N Engl J Med*. 2009;361(9):849-857.
4. Preston DL, Kusumi S, Tomonaga M, et al. Cancer incidence in atomic bomb survivors. Part III. Leukemia, lymphoma and multiple myeloma, 1950-1987. *Radiat Res*. 1994;137(2 Suppl):S68-97.
5. Hoeijmakers JH. Genome maintenance mechanisms for preventing cancer. *Nature*. 2001;411(6835):366-374.
6. Rothkamm K, Lobrich M. Evidence for a lack of DNA double-strand break repair in human cells exposed to very low x-ray doses. *Proc Natl Acad Sci U S A*. 2003;100(9):5057-5062.
7. Pearce MS, Salotti JA, Little MP, et al. Radiation exposure from CT scans in childhood and subsequent risk of leukaemia and brain

- tumours: a retrospective cohort study. *Lancet*. 2012;380(9840):499-505.
8. Fernandez-Antoran D, Piedrafita G, Murai K, et al. Outcompeting p53-Mutant Cells in the Normal Esophagus by Redox Manipulation. *Cell Stem Cell*. 2019;25(3):329-341.e6.
 9. Rodrigues-Moreira S, Moreno SG, Ghinatti G, et al. Low-Dose Irradiation Promotes Persistent Oxidative Stress and Decreases Self-Renewal in Hematopoietic Stem Cells. *Cell Rep*. 2017;20(13):3199-3211.
 10. Henry E, Souissi-Sahraoui I, Deynoux M, et al. Human hematopoietic stem/progenitor cells display ROS-dependent long-term hematopoietic defects after exposure to low dose of ionizing radiations. *Haematologica*. 2020;105(8):2044-2055.
 11. Ito K, Hirao A, Arai F, et al. Reactive oxygen species act through p38 MAPK to limit the lifespan of hematopoietic stem cells. *Nat Med*. 2006;12(4):446-451.
 12. Miyamoto K, Araki KY, Naka K, et al. Foxo3a is essential for maintenance of the hematopoietic stem cell pool. *Cell Stem Cell*. 2007;1(1):101-112.
 13. Tothova Z, Kollipara R, Huntly BJ, et al. FoxOs are critical mediators of hematopoietic stem cell resistance to physiologic oxidative stress. *Cell*. 2007;128(2):325-339.
 14. Balaban RS, Nemoto S, Finkel T. Mitochondria, oxidants, and aging. *Cell*. 2005;120(4):483-495.
 15. Nissanka N, Moraes CT. Mitochondrial DNA damage and reactive oxygen species in neurodegenerative disease. *FEBS Lett*. 2018;592(5):728-742.
 16. Kawamura K, Qi F, Kobayashi J. Potential relationship between the biological effects of low-dose irradiation and mitochondrial ROS production. *J Radiat Res*. 2018;59(suppl_2):ii91-ii97.
 17. Youle RJ, van der Bliek AM. Mitochondrial fission, fusion, and stress. *Science*. 2012;337(6098):1062-1065.
 18. Ho TT, Warr MR, Adelman ER, et al. Autophagy maintains the metabolism and function of young and old stem cells. *Nature*. 2017;543(7644):205-210.
 19. Ito K, Turcotte R, Cui J, et al. Self-renewal of a purified Tie2+ hematopoietic stem cell population relies on mitochondrial clearance. *Science*. 2016;354(6316):1156-1160.
 20. de Almeida MJ, Luchsinger LL, Corrigan DJ, Williams LJ, Snoeck HW. Dye-Independent Methods Reveal Elevated Mitochondrial Mass in Hematopoietic Stem Cells. *Cell Stem Cell*. 2017;21(6):725-729.e4.

Busy signal: platelet-derived growth factor activation in myelofibrosis

Anna E. Marneth¹ and Ann Mullally^{1,2,3}

¹Division of Hematology, Department of Medicine, Brigham and Women's Hospital, Harvard Medical School, Boston; ²Dana-Farber Cancer Institute, Harvard Medical School, Boston and ³Broad Institute, Cambridge, MA, USA.

E-mail: ANN MULLALLY - amullally@partners.org

doi:10.3324/haematol.2020.253708

The pathogenesis of myelofibrosis, a bone marrow (BM) disorder characterized by megakaryocytic hyperplasia and the deposition of extracellular matrix components such as reticulin, remains incompletely understood.

Using a mouse model of myelofibrosis (i.e. Gata-1^{low} mice), Kramer *et al.*¹ sought to identify key signaling molecules that play a role in early myelofibrosis development. GATA-1 is a transcription factor that is key to megakaryocyte development, and its downregulation results in expansion and abnormal maturation of megakaryocytes.² Importantly, low GATA-1 expression has been demonstrated in patients with myelofibrosis,³ and GATA-1 mutations are found in megakaryocytic leukemias.²

New key findings

Unlike several widely used myelofibrosis mouse models that rely on BM transplantation to engender fibrosis, primary Gata-1^{low} mice gradually develop myelofibrosis spontaneously.⁴ Due to its slow progression, this model allows for analysis at prefibrotic (5 months), early fibrotic (10 months), and overtly fibrotic (15 months) stages. A strength of the study by Kramer *et al.* is the application of an unbiased approach (i.e. RNA sequencing) to interrogate the changes that occur in receptor tyrosine kinase pathways during the development of myelofibrosis. Using bulk RNA sequencing on unfractionated BM (including stromal cells), the authors identified the platelet-derived growth factor (PDGF) pathway as significantly up-regulated in early fibrotic Gata-1^{low} mice compared to wild-type mice. Additionally, the authors analyzed protein expression of PDGF receptors and ligands

on BM sections at the three aforementioned time points; this allowed them to study the PDGF pathway in a spatio-temporal manner.

In addition to demonstrating increased transcript expression of PDGF receptor a (Pdgfra) and Pdgfrb, as well as the ligand Pdgfb, in fibrotic Gata-1^{low} mice, the authors employed a novel technique called *in situ* proximity ligation assay to determine protein localization. They found that the receptor PDGFR β and ligand PDGF-B are in close proximity in the setting of overtly fibrotic BM, suggesting binding of the ligand to the receptor and increased PDGF-B signaling. Furthermore, their data suggest that the most important cell types involved in PDGF signaling are megakaryocytes, which express PDGFR α and secrete the ligand PDGF-B, and spindle-shaped stromal cells which express PDGFR β (Figure 1).

Despite these findings, Kramer *et al.* did not detect increased PDGFR β tyrosine phosphorylation, a marker of receptor activation. They suggest that the phosphatase TC-PTP (PTPN2) may play a role in dephosphorylation of PDGFR β and show that TC-PTP is in close proximity to PDGFR β in fibrotic Gata-1^{low} mice. There are two main potential explanations for these findings. Either: (i) PDGF receptor activation is transient and rapidly down-regulated; or (ii) PDGF receptor activation is rapidly reset by phosphatases such as TC-PTP after ligand binding. Rapid downregulation would call into question the importance of the PDGF pathway in myelofibrosis, while a rapid reset may increase signaling in the presence of ligand and potentially contribute to the development of myelofibrosis. Further investigation of PDGF signaling in human myelofibrosis will be required to fully resolve this question.

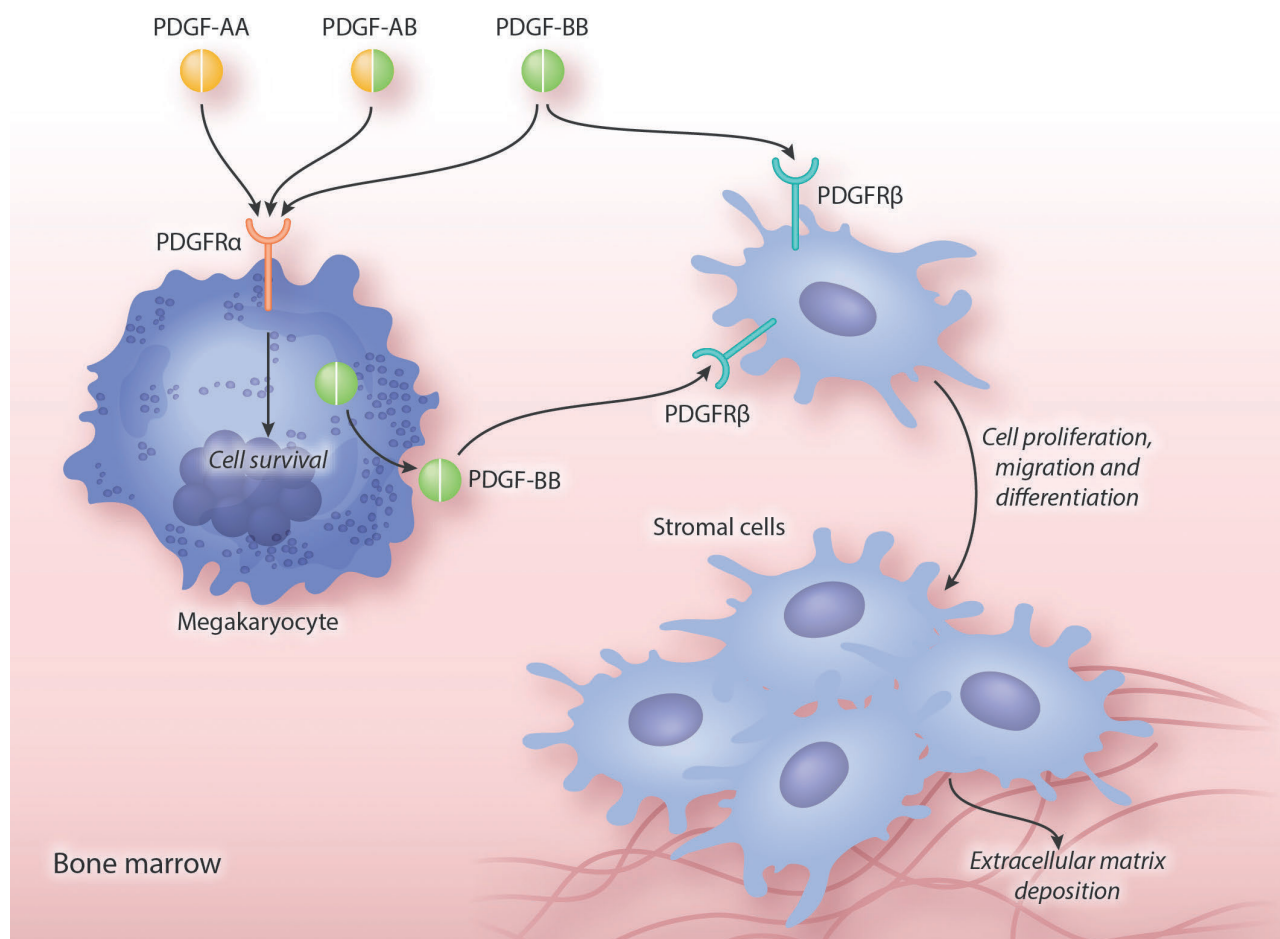


Figure 1. Platelet-derived growth factor (PDGF) signaling in myelofibrosis. Previous (human) data and the study by Kramer *et al.*¹ indicate that the ligands PDGF-A and PDGF-B and their receptors PDGFR α and PDGFR β play important roles in myelofibrosis development. PDGFR α is mainly expressed on megakaryocytes and can be activated by the dimeric ligands PDGF-AA, PDGF-AB, and PDGF-BB. PDGFR β is expressed on stromal cells and can be activated through the ligand PDGF-BB. PDGF-BB stimulates stromal cell proliferation, migration and differentiation, which in turn causes extracellular matrix deposition and myelofibrosis development.

Platelet-derived growth factor pathway as a potential biomarker for myelofibrosis development

Platelet-derived growth factors are growth factors for fibroblasts and stromal cells. Importantly, upregulation of the receptors PDGFR α in megakaryocytes and PDGFR β in stromal cells, as well as upregulation of their ligands PDGF-A and PDGF-B, has been shown in established human myelofibrosis.⁵⁻⁷ Moreover, the grade of myelofibrosis in myeloid malignancies correlates with the level of PDGFR β expression in activated fibroblasts.⁶ These data suggest that PDGF signaling contributes to myelofibrosis development.

Myelofibrosis occurs in the context of megakaryocyte disorders, encompassing both inherited bleeding and platelet disorders^{8,9} and myeloid malignancies, most commonly, myeloproliferative neoplasms (MPN). Although patients with MPN can present with *de novo* myelofibrosis (i.e. primary myelofibrosis, PMF), it can also occur as a complication of antecedent MPN (i.e. post-polycythemia myelofibrosis, PPV-MF or post-essential thrombocythemia myelofibrosis, PET-MF). In patients with PV and ET, it is currently difficult to predict who will progress to myelofibrosis. The study by Kramer *et al.* raises the ques-

tion of whether increased PDGF signaling could serve as an early biomarker for myelofibrosis development.

Bedekocivs *et al.*⁶ previously assessed PDGFR β expression in fibrotic and non-fibrotic BM from several myeloid malignancies and proposed that elevated PDGFR β expression could indicate a prefibrotic state. Kramer *et al.* found increased PDGFR α expression in the prefibrotic stage, but no increase in PDGFR β or the ligands PDGF-A and -B. In future studies, it would be informative to measure the dynamics of PDGF components in human myelofibrosis development, using a longitudinal study to determine their predictive and prognostic value.

Targeting the platelet-derived growth factor pathway

In conjunction with prior (human) studies, this study by Kramer *et al.* suggests that the PDGF pathway is a potential therapeutic target in myelofibrosis. PDGFR are one of the main targets of the tyrosine kinase inhibitor, imatinib.¹⁰ Treatment with imatinib has demonstrated clinical benefit in patients with hypereosinophilic syndromes and chronic myeloproliferative disorders who have chromosomal translocations involving PDGFR α and PDGFR β , respectively.^{11,12} Thrombopoietin (Thpo) is the major stimulant for

megakaryopoiesis and its overexpression engenders myelofibrosis in mouse models.¹³ Using a Thpo overexpression model, Decker *et al.*¹⁴ showed that stromal deletion of PDGFR α or treatment with imatinib suppressed stromal cell expansion and ameliorated myelofibrosis. In addition to imatinib, other methods of targeting the PDGF pathway are currently under investigation in different fibrosis models, such as PDGF/PDGFR-blocking antibodies and aptamers.¹⁵

Dual targeting of JAK and JAK/platelet-derived growth factor downstream pathways

Primary myelofibrosis is caused by MPN phenotypic driver mutations (i.e. in *JAK2*, *CALR* or *MPL*) that result in constitutive activation of JAK-STAT signaling.¹⁶ Although JAK2 inhibitors such as ruxolitinib reduce constitutional symptoms and splenomegaly, and may stabilize myelofibrosis, they do not have substantial disease-modifying activity in MPN. Inhibiting other tyrosine kinases including PDGF receptors is not sufficient either, since imatinib treatment in PMF was disappointing.¹⁷ A combinatorial approach involving JAK2 and PDGF inhibition in MPN could be considered, although hematologic toxicity is a real concern.¹⁸

An alternative treatment strategy involves simultaneously inhibiting JAK-STAT and MEK-ERK signaling. A recent MPN preclinical study showed that JAK2 inhibitors induce a strong reduction in STAT signaling but only marginally reduce MEK/ERK signaling.¹⁹ Multiplexed analyses of 34 secreted factors in *Jak2* V617F-mutant mice showed that transcript levels of the receptor *Pdgfra*, as well as the ligands *Pdgfa* and *Pdgfb*, were maintained in BM and spleen during ruxolitinib treatment.¹⁹ Additional experiments showed that PDGF signaling through MEK/ERK was not reduced upon ruxolitinib treatment. Combined treatment with JAK2 and MEK inhibitors was superior over inhibition with either compound alone in mouse models of *Jak2* V617F and MPLW515-induced myelofibrosis, and reduced *Pdgfra*, *Pdgfa*, and *Pdgfb* transcript expression. These data suggest that combined MEK/JAK2 inhibition may be efficacious in treating MPN.

Conclusions and future directions

In conclusion, Kramer *et al.* have methodically and elegantly analyzed the sequential changes that occur in the BM during the initiation and progression of myelofibrosis in *Gata1*^{low} mice and identified upregulation of the PDGF pathway as a hallmark of myelofibrosis. Their work suggests that increased PDGFR expression could be used as an early biomarker for myelofibrosis development. Given the paucity of reliable myelofibrosis biomarkers, this finding warrants further study in MPN patients. Additionally, now that next generation sequencing platforms are increasingly used to identify genetic predictors of progression to myelofibrosis in MPN, it would be interesting to study whether increased PDGF expression correlates with certain genetic subsets of MPN. Finally, given recent advancements enabling combined single-cell mutational and transcriptomic analyses,²⁰ it will be possible to determine precisely which cellular sub-populations in the BM (both hematopoietic and stromal) are involved in PDGF signaling early in the course of myelofibrosis. Since a multitude of profibrotic factors are up-regulated in myelofibrosis, the therapeutic

efficacy of inhibiting a single pathway, especially in advanced disease, may be limited. However, the identification and early targeting of pathways that are activated during the initial stages of myelofibrosis may prove more fruitful.

Acknowledgments

AM acknowledges support from the NIH (R01HL131835), the MPN Research Foundation and the Gabrielle's Angel Foundation for Cancer Research. Dr. Mullally is a Scholar of The Leukemia & Lymphoma Society.

References

- Kramer F, Demedde J, Mezheyskiet A, et al. Platelet-derived growth factor receptor β activation and regulation in murine myelofibrosis. *Haematologica* 2020;105(8):2083-2094.
- Shimizu R, Engel JD, Yamamoto M. GATA1-related leukaemias. *Nat Rev Cancer*. 2008; 8(4):279-287.
- Vannucchi AM, Pancrazzi A, Guglielmelli P, et al. Abnormalities of GATA-1 in megakaryocytes from patients with idiopathic myelofibrosis. *Am J Pathol*. 2005;167(3):849-858.
- Vannucchi AM, Bianchi L, Cellai C, et al. Development of myelofibrosis in mice genetically impaired for GATA-1 expression (GATA-1(low) mice). *Blood*. 2002;100(4):1123-1132.
- Bock O, Loch G, Büsche G, von Wasielewski R, Schlué J, Kreipe H. Aberrant expression of platelet-derived growth factor (PDGF) and PDGF receptor-alpha is associated with advanced bone marrow fibrosis in idiopathic myelofibrosis. *Haematologica*. 2005;90(1):133-134.
- Bedeckovics J, Kiss A, Beke L, Karolyi K, Méhes G. Platelet derived growth factor receptor-beta (PDGFRbeta) expression is limited to activated stromal cells in the bone marrow and shows a strong correlation with the grade of myelofibrosis. *Virchows Arch*. 2013;463(1):57-65.
- Gersuk GM, Carmel R, Pattengale PK. Platelet-derived growth factor concentrations in platelet-poor plasma and urine from patients with myeloproliferative disorders. *Blood*. 1989;74(7):2330-2334.
- Nurden AT, Nurden P. Inherited thrombocytopenias. *Haematologica*. 2007;92(9):1158-1164.
- Turro E, Greene D, Wijgaerts A, et al. A dominant gain-of-function mutation in universal tyrosine kinase SRC causes thrombocytopenia, myelofibrosis, bleeding, and bone pathologies. *Sci Transl Med*. 2016;8(328):328ra30.
- Pardanani A, Tefferi A. Imatinib targets other than bcr/abl and their clinical relevance in myeloid disorders. *Blood*. 2004;104(7):1931-1939.
- Cools J, DeAngelo DJ, Gotlib J, et al. A tyrosine kinase created by fusion of the PDGFRA and FIP1L1 genes as a therapeutic target of imatinib in idiopathic hypereosinophilic syndrome. *N Engl J Med*. 2003;348(13):1201-1214.
- Apperley JF, Gardembas M, Melo JV, et al. Response to imatinib mesylate in patients with chronic myeloproliferative diseases with rearrangements of the platelet-derived growth factor receptor beta. *N Engl J Med*. 2002;347(7):481-487.
- Villevall JL, Cohen-Solal K, Tulliez M, et al. High thrombopoietin production by hematopoietic cells induces a fatal myeloproliferative syndrome in mice. *Blood*. 1997;90(11):4369-4388.
- Decker M, Martinez-Morentin L, Wang G, et al. Leptin-receptor-expressing bone marrow stromal cells are myofibroblasts in primary myelofibrosis. *Nat Cell Biol*. 2017;19(6):677-688.
- Papadopoulos N, Lennartsson J. The PDGF/PDGFR pathway as a drug target. *Mol Aspects Med*. 2018;62:75-88.
- Marneth AE, Mullally A. The Molecular Genetics of Myeloproliferative Neoplasms. *Cold Spring Harb Perspect Med*. 2020;10(2):a034876.
- Mesa RA. Imatinib and tyrosine kinase inhibition, in the management of BCR-ABL negative myeloproliferative disorders. *Biologics*. 2007;1(2):129-138.
- Iurlo A, Gianelli U, Rapezzi D, et al. Imatinib and ruxolitinib association: first experience in two patients. *Haematologica*. 2014;99(6):e76-77.
- Stivala S, Codilupi T, Brkic S, et al. Targeting compensatory MEK/ERK activation increases JAK inhibitor efficacy in myeloproliferative neoplasms. *J Clin Invest*. 2019;129(4):1596-1611.
- Psaila B, Wang G, Rodriguez-Meira A, et al. Single-Cell Analyses Reveal Megakaryocyte-Biased Hematopoiesis in Myelofibrosis and Identify Mutant Clone-Specific Targets. *Mol Cell*. 2020;78(3):477-492.e8.

When the bond breaks – targeting adhesion of leukemia cells to the meninges

Lennart Lenk, Fotini Vogiatzi and Denis M. Schewe

Department of Pediatrics I, ALL-BFM Study Group, Christian-Albrechts University Kiel and University Medical Center Schleswig-Holstein, Kiel, Germany.

E-mail: DENIS M. SCHEWE - Denis.Schewe@uksh.de

doi:10.3324/haematol.2020.253609

A major clinical challenge in the treatment of acute lymphoblastic leukemia (ALL) is the involvement of the central nervous system (CNS), especially in children. CNS involvement can occur upon initial diagnosis and be a source of relapse.¹ Due to the high propensity of ALL cells to infiltrate the CNS and the lack of specific markers for their detection and eradication, patients receive high cumulative doses of intrathecal chemotherapy. This is associated with neurotoxicity, which may lead to acute complications and long-term developmental delay in children.² The CNS is regarded as a privileged “niche” in which ALL cells can persist due, for example, to the paucity of immune cells and the blood-brain barrier impairing accessibility of this sanctuary by chemotherapy.^{3,4} Thus, gaining a deeper understanding of how ALL

cells interact with the CNS microenvironment may open the field for novel targeted approaches to eradicate ALL cells in the CNS. In this issue of *Haematologica*, Jonart *et al.* describe how ALL cells seek shelter by adhering to meningeal cells, resulting in quiescence and chemoresistance. The authors propose interference with adhesion mechanisms as a novel therapeutic strategy in CNS leukemia⁵ (Figure 1).

Infiltration of the CNS can be observed in metastasis of solid cancers, as well as in hematologic malignancies including ALL, other leukemias and lymphomas. CNS metastasis of solid cancers mostly affects the brain parenchyma, but ALL cells predominantly reside in the leptomeninges, a conjunctive tissue surrounding the parenchyma and the ventricular choroid plexus.⁵⁻⁷ Hence, the mech-

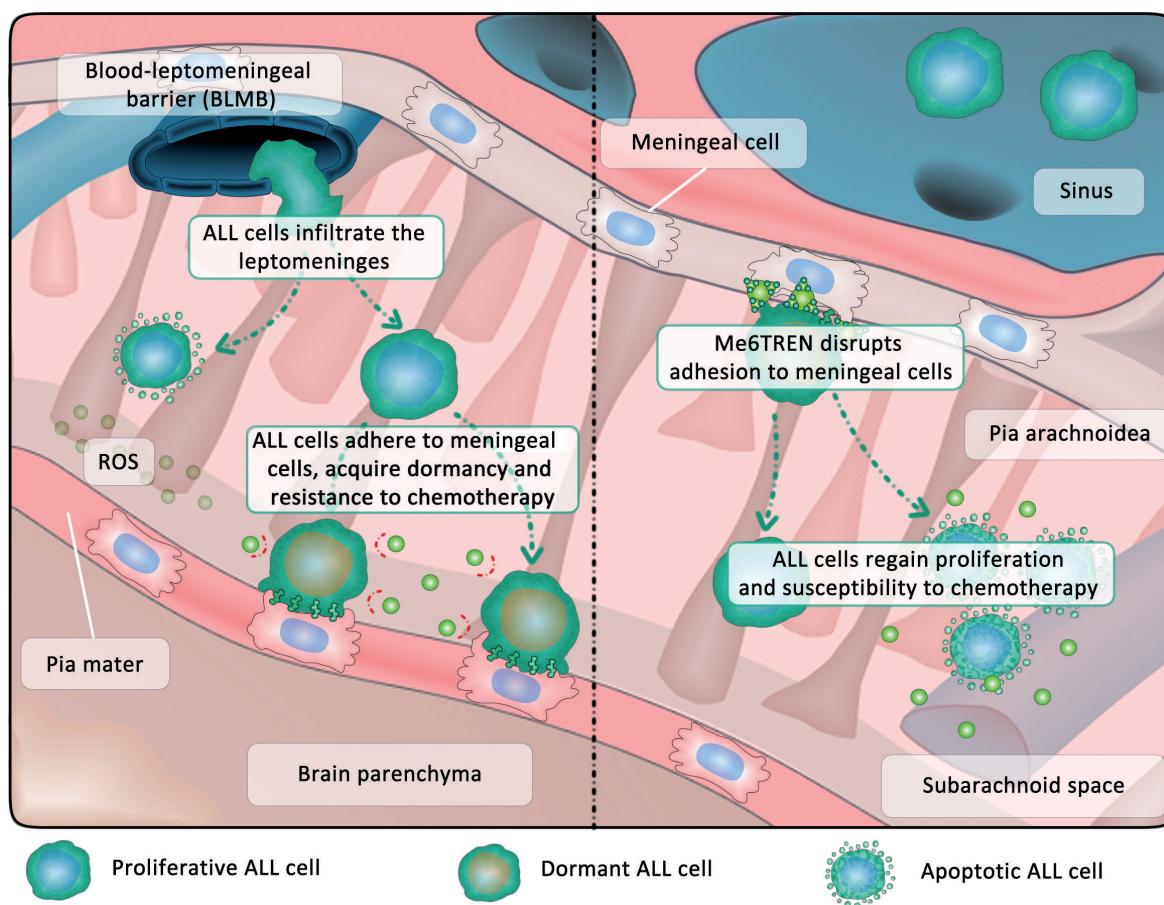


Figure 1. Leukemia cells seek shelter by adhering to meningeal cells. Acute lymphoblastic leukemia (ALL) cells breach the blood-leptomeningeal barrier and infiltrate the leptomeninges. They encounter a hostile microenvironment in which nutrients are scarce (cerebrospinal fluid) and levels of reactive oxygen species (ROS) are enhanced. By adhering to meningeal cells, ALL cells acquire a state of reversible quiescence (dormancy) rendering them less vulnerable to chemotherapy. Disrupting the adhesion of ALL cells to meningeal cells via Me6TREN mobilizes ALL cells from the niche, thereby restoring their susceptibility to chemotherapeutic agents.

anisms of CNS infiltration in solid tumors and hematologic malignancies likely differ fundamentally. To enter the CNS environment, ALL cells need to pass protective physiological barriers such as the blood-brain barrier, the blood-leptomeningeal barrier and the blood-cerebrospinal fluid barrier, which in physiological conditions ensure the controlled flux of molecules and passage of cells into the organ.³ The cerebrospinal fluid *per se* may also represent a hostile environment for ALL cells due to the limited quantity of proteins and the presence of reactive oxygen species.⁸ The CNS microenvironment may, therefore, critically affect the behavior of ALL cells in this niche.

To investigate the behavior of ALL cells in the CNS, Jonart *et al.* co-cultured B-cell precursor ALL and T-ALL cell lines as well as primary B-cell precursor ALL cells with primary human meningeal cells, modeling the leptomeningeal microenvironment.⁵ The authors found that ALL cells efficiently adhered to the primary human meningeal cells, rendering them less vulnerable to chemotherapy. Therapy sensitivity was markedly reduced when ALL cells were grown in direct contact with the meningeal cells and treated with methotrexate and cytarabine, two major compounds of CNS-directed chemotherapy in ALL. Direct contact with primary human meningeal cells also reduced proliferation of ALL cells, leading to the conclusion that chemoresistance was based on the acquisition of a dormant phenotype. Cellular dormancy is a state of transient G₀/G₁ arrest that may be induced by hostile microenvironments and that may be reversed when cells encounter favorable conditions again.⁹ Evidence that dormancy may represent a key mechanism of CNS disease and relapse in ALL is accumulating beyond this work.³ For example, patient-derived xenograft ALL cells recollected from murine meninges were shown to be less proliferative than cells recollected from the bone marrow.¹⁰ Furthermore, direct co-culture models of CNS leukemia showed G₀/G₁ arrest and resistance to methotrexate-mediated cytotoxicity *in vitro* in B-cell precursor ALL in dependence of the receptor tyrosine kinase MER.¹¹ Adhesion processes of leukemia cells to CNS microenvironmental structures have also recently been shown to play a crucial role in the invasion of leukemia cells into the CNS. Yao *et al.* showed that the interaction of leukemic cells expressing $\alpha 6$ -integrin with laminin on the abluminal surface of emissary blood vessels facilitates the cells' entry into the CNS.¹² Furthermore, the chemokine receptor CCR7 was found to promote adhesion and trafficking across the choroid plexus in T-ALL.¹³ With their recent report, Jonart *et al.* provide a further piece of the puzzle of CNS leukemia as they show that meningeal cells, presumably the cell entity that ALL cells mostly encounter in the CNS microenvironment after invading through the vasculature, promote ALL dormancy, survival and therapy resistance. This observation has important implications for understanding the mechanistic basis of CNS infiltration and relapse in ALL.

The study by Jonart *et al.* raises the questions of whether the acquisition of dormancy by adhesion to meningeal cells is a feature of every ALL cell in the CNS or whether this is only relevant in a fraction of cells undergoing selection by chemotherapy. Or, if all leukemic cells reaching the CNS adhere to meningeal cells and cease proliferation, how would they then go on to colonize the meninges and be clinically detectable? In their study, Jonart *et al.* detected a

small, slow cycling fraction of ALL cells recovered from the meninges of xenografted mice. Intriguingly, after treating leukemia-bearing mice with cytarabine, the authors found a 13-fold increase in the number of these quiescent cells whereas only a 5-fold relative increase was found in the bone marrow. This argues in favor of a small fraction of dormant cells that may survive treatment, as previously suggested,¹⁴ and in favor of the CNS microenvironment fostering the maintenance and enrichment of this fraction. Various molecules and pathways have recently been identified to be associated with CNS infiltration and relapse, some of which are also linked to cellular adhesion: the ZAP70 kinase regulates CXCR4 and CCR7,¹⁵ the receptor tyrosine kinase MER exposes structural similarity to neural adhesion molecules^{11,16} and phosphoinositide-3-kinase was shown to promote integrin-mediated adhesion.¹² It would be interesting to investigate whether cells enriching in the CNS after chemotherapy show a particularly high expression of these molecules.

If adhesion-mediated chemoresistance contributes to CNS relapse, how can this concept be exploited to establish novel targeted therapy approaches? One substantial advantage of compounds targeting general features such as adhesive interactions could be that they act on a variety of ALL cells irrespective of the genetic background. A previous report described promising results obtained from disrupting $\alpha 6$ integrin-laminin interactions via inhibition of phosphoinositide-3-kinase which delayed leukemic CNS engraftment in xenograft mouse models. However, the inhibitors used in this study, including idelalisib, which is already in clinical use, were shown to be unable to cross the blood-brain barrier.¹² Therefore, such approaches may be effective in preventing the entry of ALL cells into the CNS rather than targeting ALL cells already residing in the CNS.¹² CXCR4 is another key molecule associated with homing and adhesion processes in ALL in the CNS.¹⁵ The CXCR4 antagonist AMD3100 (plerixafor) reduced leukemia burden in peripheral organs of xenograft mice, but not in the CNS.⁶ Testing different compounds, Jonart *et al.* found a high efficacy of the small molecule inhibitor Tris[2-(dimethylamino)ethyl]amine (Me6TREN, Me6) in preventing the adhesion of ALL cells to meningeal cells *in vitro*, thereby restoring their sensitivity to cytarabine. When applied to mice bearing ALL cells, the addition of Me6TREN to cytarabine treatment resulted in diminished leukemic engraftment in the meninges as compared to that following treatment with cytarabine alone. Me6TREN was first described as a compound mobilizing hematopoietic progenitor cells from the bone marrow by upregulating matrix metalloproteinase-9 and disrupting the CCL12/CXCR4 axis, thereby outperforming AMD3100.¹⁷ Accordingly, compared to AMD3100, Me6TREN showed enhanced efficacy in disturbing the adhesion of ALL cells to meningeal cells in the work by Jonart *et al.*⁵ Me6TREN has proven to be well tolerated in mice.¹⁷ If Me6TREN is demonstrated to penetrate the CNS in pharmacokinetic and pharmacodynamics studies, this compound could indeed be considered as a drug for prevention and therapy of CNS disease.

Overall the study by Jonart *et al.* provokes some interesting questions for the future: Do the different cell types in the meninges, e.g., fibroblasts, endothelial cells and pericytes, have different impacts on CNS-infiltrating ALL cells?

Are meningeal cells also involved in specific homing of ALL cells into the CNS? Is adhesion-mediated chemoresistance of ALL cells in contact with meningeal cells simply a cause of decreased proliferation and therefore diminished vulnerability to chemotherapeutic agents or is an active process involved (e.g., regulation of drug transporters)? Furthermore, it would be interesting to determine whether adhesion capacity of ALL cells to the CNS microenvironment could be used to improve CNS diagnostics. A recent report suggests that surface expression of $\alpha 5$ -integrins on ALL cells is associated with the number of ALL cells in the cerebrospinal fluid detectable by diagnostic lumbar puncture.¹⁸ Finally, there is a need to consider that mobilizing dormant ALL cells by breaking adhesive bonds with meningeal cells may also confer potential risks. Re-awakening leukemic cells may cause a resumption of proliferation and therefore overt CNS disease, an aspect which will have to be clarified in the future.

The recent study by Jonart *et al.* shapes a sharper image of the complex mechanisms of both CNS infiltration and CNS relapse, and may ultimately contribute to improved strategies for targeted treatment of CNS leukemia in ALL.

References

- Pui CH, Howard SC. Current management and challenges of malignant disease in the CNS in paediatric leukaemia. *Lancet Oncol.* 2008;9(3):257-268.
- Cheung YT, Khan RB, Liu W, et al. Association of cerebrospinal fluid biomarkers of central nervous system injury with neurocognitive and brain imaging outcomes in children receiving chemotherapy for acute lymphoblastic leukemia. *JAMA Oncol.* 2018;4(7):e180089.
- Lenk L, Alsadeq A, Schewe DM. Involvement of the central nervous system in acute lymphoblastic leukemia. Opinions on molecular mechanisms and clinical implications based on recent data. *Cancer Metastasis Rev.* 2020;39(1):173-187.
- Frishman-Levy L, Shemesh A, Bar-Sinai A, et al. Central nervous system acute lymphoblastic leukemia: role of natural killer cells. *Blood.* 2015;125(22):3420-3431.
- Jonart LM, Ebadi M, Basile P, et al. Disrupting the leukemia niche in the central nervous system attenuates leukemia chemoresistance. *Haematologica.* 2020;105(8):2130-2140.
- Williams MTS, Yousafzai YM, Elder A, et al. The ability to cross the blood-cerebrospinal fluid barrier is a generic property of acute lymphoblastic leukemia blasts. *Blood.* 2016;127(16):1998-2006.
- Price RA. Histopathology of CNS leukemia and complications of therapy. *Am J Pediatr Hematol Oncol.* 1979;1(1):21-30.
- Basile P, Jonart LM, Ebadi M, Johnson K, Kerfeld M, Gordon PM. The meninges enhance leukaemia survival in cerebral spinal fluid. *Br J Haematol.* 2020;189(3):513-517.
- Aguirre-Ghiso JA. Models, mechanisms and clinical evidence for cancer dormancy. *Nat Rev Cancer.* 2007;7(11):834-846.
- Kato I, Nishinaka Y, Nakamura M, et al. Hypoxic adaptation of leukemic cells infiltrating the CNS affords a therapeutic strategy targeting VEGFA. *Blood.* 2017;129(23):3126-3129.
- Krause S, Pfeiffer C, Strube S, et al. Mer tyrosine kinase promotes the survival of t(1;19)-positive acute lymphoblastic leukemia (ALL) in the central nervous system (CNS). *Blood.* 2015;125(5):820-830.
- Yao H, Price TT, Canelli G, et al. Leukaemia hijacks a neural mechanism to invade the central nervous system. *Nature.* 2018;560(7716):55-60.
- Buonamici S, Trimarchi T, Ruocco MG, et al. CCR7 signalling as an essential regulator of CNS infiltration in T-cell leukaemia. *Nature.* 2009;459(7249):1000-1004.
- Ebinger S, Özdemir EZ, Ziegenhain C, et al. Characterization of rare, dormant, and therapy-resistant cells in acute lymphoblastic leukemia. *Cancer Cell.* 2016;30(6):849-862.
- Alsadeq A, Fedders H, Vokuhl C, et al. The role of ZAP70 kinase in acute lymphoblastic leukemia infiltration into the central nervous system. *Haematologica.* 2017;102(2):346-355.
- Chen J, Carey K, Godowski PJ. Identification of Gas6 as a ligand for Mer, a neural cell adhesion molecule related receptor tyrosine kinase implicated in cellular transformation. *Oncogene.* 1997;14(17):2033-2039.
- Zhang J, Ren X, Shi W, et al. Small molecule Me6TREN mobilizes hematopoietic stem/progenitor cells by activating MMP-9 expression and disrupting SDF-1/CXCR4 axis. *Blood.* 2014;123(3):428-441.
- Shah Scharff BFS, Modvig S, Thastrup M, et al. A comprehensive clinical study of integrins in acute lymphoblastic leukemia indicates a role of $\alpha 6$ /CD49f in persistent minimal residual disease and $\alpha 5$ in the colonization of cerebrospinal fluid. *Leuk Lymphoma.* 2020 Feb 28;1-5. [Epub ahead of print]

BCL2 dependency in diffuse large B-cell lymphoma: it's a family affair

Shannon M. Matulis and Lawrence H. Boise

Department of Hematology and Medical Oncology Emory School of Medicine and the Winship Cancer Institute, Emory University; Atlanta, GA, USA

E-mail: LAWRENCE H. BOISE - lboise@emory.edu

doi:10.3324/haematol.2020.253594

Diffuse large B-cell lymphoma (DLBCL) is the most common form of non-Hodgkin lymphoma, accounting for approximately 25% of all lymphomas.¹ DLBCL is highly heterogeneous, so responses to standard therapy, R-CHOP (rituximab plus cyclophosphamide, doxorubicin, vincristine, and prednisone) are mixed.² The response, as well as mechanisms of resistance to therapy, are associated with a cell's apoptotic threshold.³ Therefore, determining the molecular basis for a tumor's ability to survive can provide insights into drug resistance as well as opportunities for precision medicine. In this issue of *Haematologica*, Smith *et al.* demonstrate the

importance of the BCL2 family of anti-apoptotic proteins BCL2, BCLXL, and MCL1 in the survival of DLBCL, potentially revealing new treatment strategies.⁴

Inappropriate activation of oncogenes can result in cell death through the activation of pro-apoptotic proteins of the BCL2 family. Therefore, to survive the transformation process, tumor cells become more dependent on their anti-apoptotic BCL2 proteins (e.g., BCL2, BCLXL, and MCL1) than their normal counterparts.⁵⁻⁷ This dependency is the result of binding and neutralizing the pro-apoptotic family members (e.g., BIM, BAK, and BAX) and is often referred to as mitochondrial priming, as increased

priming results in a lower apoptotic threshold.⁵⁻⁷ Thus priming of anti-apoptotic BCL2 family proteins in cancer leads to increased sensitivity to therapy, as well as making BCL2 proteins excellent targets for therapy.⁵⁻⁷

Venetoclax (ABT-199) is a potent and selective inhibitor of BCL2.⁸ The importance of BCL2 in DLBCL is well established. The t(14;18) translocation, occurring in approximately 20% of DLBCL, juxtaposes BCL2 to the immunoglobulin heavy chain gene enhancers resulting in overexpression.⁹ While this translocation is most frequently found in the germinal center B-cell subtype of DLBCL, amplification and transcriptional upregulation of BCL2 are typically found in the activated B-cell molecular subtype.¹⁰ Despite this, the clinical success of venetoclax in DLBCL has been disappointing, with an overall response rate of only 18%, regardless of BCL2 expression level.¹¹

These findings led Smith *et al.* to propose a role for other anti-apoptotic proteins in DLBCL survival. To investigate this possibility, they employed venetoclax as well as A-1331852 and S63845, selective inhibitors for BCLXL and MCL1, respectively, as tools to determine the role of each anti-apoptotic protein in DLBCL survival. Using primary cells isolated from patients' samples, as well as a panel of cell lines representing the main subtypes of DLBCL, they demonstrated that all three

inhibitors displayed activity in both the patients' samples and the cell lines. About half of the cell lines were preferentially sensitive to only one inhibitor, suggesting sole dependence on that anti-apoptotic family member for survival.

However, four of the 18 cell lines and at least two of the seven patients' samples showed sensitivity to two inhibitors, suggesting co-dependence on more than one anti-apoptotic protein for survival, a characteristic reported in other hematologic malignancies.¹² Resistance to all three mimetics was seen in six of the 18 cell lines; however, the mechanism of resistance was not explored. To further support a role for MCL1 and BCLXL in DLBCL the authors showed that silencing the anti-apoptotic proteins with short interfering (si)RNA was sufficient to induce apoptosis in cell lines sensitive to S63845 and A-1331852, respectively.

Based on the sensitivity data, the authors determined the expression levels and ratios of the BCL2 proteins and found that expression was highly variable between cell lines. Concluding that expression alone could not account for sensitivity to the inhibitors they moved on to examine protein interactions. Previous studies in other hematologic malignancies had demonstrated that the binding pattern of pro-apoptotic proteins to anti-apoptotic proteins is also a predictor of sensitivity to these small molecule

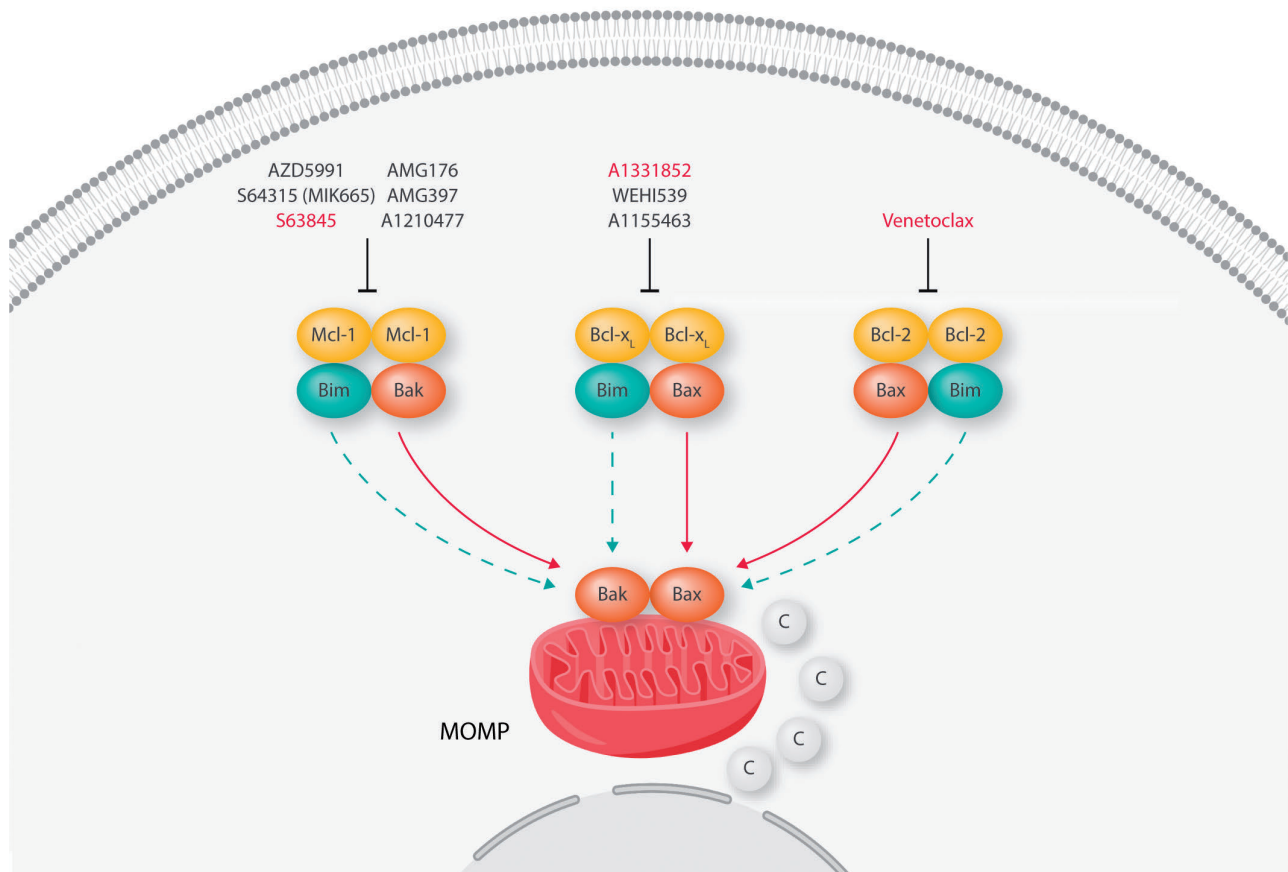


Figure 1. Schematic of the mechanism of action of selective BCL2 family inhibitors. Inhibitors disrupt interactions between anti-apoptotic BCL2 family members (green) and either the BH3-only activator protein BIM (orange) or the pro-apoptotic effectors BAX and BAK (red). This results in the release of activated effectors (solid arrows) or BIM, which can activate the effectors (dashed arrows) resulting in mitochondrial outer membrane permeabilization (MOMP) and cytochrome c release. The inhibitors in red were the ones used in the study by Smith *et al.*⁴

inhibitors, and this was found to be true in DLBCL as well.¹² Using co-immunoprecipitation, the authors showed BIM and BAX bound to BCL2 in BCL2-dependent/venetoclax-sensitive cell lines and BAX release upon drug treatment. In BCLXL-dependent/A-1331852-sensitive DLBCL lines, BIM, BAX, and BAK were bound to BCLXL and all three were released following treatment. The pro-apoptotic proteins BIM and BAK were bound to MCL1 and both displaced upon treatment with S63845 in MCL1-dependent cell lines.

BCL2 family expression data in the six resistant lines showed that five expressed some degree of all three anti-apoptotic proteins and one line expressed two. Furthermore, all six lines expressed BAK and/or BAX, with some variability in BIM expression. Co-immunoprecipitation assays performed in two of the resistant lines showed BIM binding to at least one anti-apoptotic protein but minimal binding of BAX or BAK. Displacement data following drug treatment in all six lines are necessary to gain a better understanding of the protein interactions driving this resistance. However, it remains unclear how a cell could be resistant to all three inhibitors. One possibility is that resistant cells utilize more than one BCL2 family member, requiring multiple inhibitors to be used in combination. Alternatively, the cells could be dependent on an anti-apoptotic BCL2 protein that was not tested. For example, BCL-w was recently reported to be overexpressed in DLBCL and investigating the role of this anti-apoptotic protein or that of BCL2A1 (A1/Bfl1) may reveal that it is implicated in cell survival in DLBCL.¹³ While there is not currently a selective inhibitor for BCL-w, testing cell lines that are resistant to venetoclax and A-1331852 with ABT-737, which was reported to inhibit BCL-w, may provide indirect evidence of dependency.¹⁴

The authors used both siRNA and CRISPR to discern the contribution of the displaced proteins to the initiation of apoptosis. BIM is necessary for S63845-induced apoptosis in the two cell lines tested, whereas its role in venetoclax- and A-1331852-induced apoptosis is cell-line dependent. BAK and BAX are involved to some degree in the apoptotic response to all three inhibitors, however the contribution of each in initiation *versus* amplification of the apoptotic signal is not entirely clear.

The authors suggest that activated BAX released from BCL2 directly activates BAK; however, previous studies indicate that BAX is a poor activator of BAK.¹⁵ An alternative explanation would be that displaced BIM is responsible for activating BAK. In the two BCLXL-dependent cell lines examined only one was protected from A-1331852-induced apoptosis when BAX was silenced and the apoptotic response was not altered in either in response to the silencing of BAK. Furthermore, CRISPR knockout of BAK appeared to have a minor, A-1331852 dose-independent, effect on apoptosis in the one cell line shown. Repeating these experiments on a larger panel of cell lines is necessary to understand the relative importance of these proteins in A-1331852-induced apoptosis. The BAX siRNA data support the authors' assertion that BAX is required for S63845-induced apoptosis; however, it remains unclear what protein(s) released from MCL1 are required to activate BAX. It should be noted that incomplete silencing of genes occurred in some experiments, which

could influence the interpretation of the results. Performing the mechanistic experiments with CRISPR knockouts of BIM and BAX, along with BAK, would provide further insight into the role of each of these proteins in BH3-mimetic-induced apoptosis in DLBCL. Regardless, the studies clearly point to the importance of several BCL2 family members in the survival of DLBCL cells and provide insights into a potential means of targeting these vulnerabilities.

The potential of *ex vivo* testing as a means to deliver precision medicine based on functional testing instead of genotype has been reported in multiple myeloma with venetoclax and also in acute myeloid leukemia.^{16,17} Given the data presented here, one could envisage a way this type of assay could be used in DLBCL. While venetoclax was not effective as a sole agent in DLBCL, it is being tested in combination with current therapeutics. Recently published data from the CAVALLI phase Ib trial demonstrate the benefit of combining venetoclax with R-CHOP or G-CHOP (obinutuzumab plus cyclophosphamide, doxorubicin, vincristine, and prednisone) in BCL2-positive, MYC-positive DLBCL, with seven of eight patients (87.5%) reaching complete remission.¹⁸ Additionally, a clinical trial evaluating the MCL1 inhibitor S64315 (MIK665) in MYC-positive DLBCL is currently recruiting (NCT02992483).¹⁹ *Ex vivo* testing of patients prior to therapy initiation or enrollment on a clinical trial could provide guidance on treatment and spare the patient from ineffective therapy.

References

1. Freedman AS, Jacobson CA, Ng A, Aster JC. Non-Hodgkin lymphoma. In: DeVita, Hellman, and Rosenberg's Cancer Principles & Practice of Oncology. 11th Edition, 2019. pp 1671-1707. Editors: DeRita VT Jr, Lawrence TS, Rosenberg SA. Published by Wolters Kluwer.
2. Liu Y, Barta SK. Diffuse large B-cell lymphoma: 2019 update on diagnosis, risk stratification, and treatment. *Am J Hematol*. 2019;94(5):604-616.
3. Ni Chonghaile T, Sarosiek KA, Vo TT, et al. Pretreatment mitochondrial priming correlates with clinical response to cytotoxic therapy. *Science*. 2011;334(6059):1129-1133.
4. Smith VM, Dietz A, Henz K, et al. Specific interactions of BCL-2 family proteins mediate sensitivity to BH3-mimetics in diffuse large B-cell lymphoma. *Haematologica*. 2020;105(8):2150-2163.
5. Certo M, Del Gaizo Moore V, Nishino M, et al. Mitochondria primed by death signals determine cellular addiction to antiapoptotic BCL2 family members. *Cancer Cell*. 2006;9(5):351-365.
6. Chipuk JE, Moldoveanu T, Llambi F, Parsons MJ, Green DR. The BCL2 family reunion. *Mol Cell*. 2010;37(3):299-310.
7. Davids MS, Letai A. Targeting the B-cell lymphoma/leukemia 2 family in cancer. *J Clin Oncol*. 2012;30(25):3127-3135.
8. Souers AJ, Levenson JD, Boghaert ER, et al. ABT-199, a potent and selective BCL2 inhibitor, achieves antitumor activity while sparing platelets. *Nat Med*. 2013;19(2):202-208.
9. Willis TG, Dyer MJ. The role of immunoglobulin translocations in the pathogenesis of B-cell malignancies. *Blood*. 2000;96(3):808-822.
10. Iqbal J, Neppalli VT, Wright G, et al. BCL2 expression is a prognostic marker for the activated B-cell-like type of diffuse large B-cell lymphoma. *J Clin Oncol*. 2006;24(6):961-968.
11. Davids MS, Roberts AW, Seymour JF, et al. Phase I first-in-human study of venetoclax in patients with relapsed or refractory non-Hodgkin lymphoma. *J Clin Oncol*. 2017;35(8):826-833.
12. Morales AA, Kurtoglu M, Matulis SM, et al. Distribution of Bim determines MCL1 dependence or codependence with BCLXL/BCL2 in MCL1-expressing myeloma cells. *Blood*. 2011;118(5):1329-1339.
13. Adams CM, Mitra R, Gong JZ, Eischen CM. Non-Hodgkin and Hodgkin lymphomas select for overexpression of BCLW. *Clin Cancer Res*. 2017;23(22):7119-7129.
14. Oltersdorf T, Elmore SW, Shoemaker AR, et al. An inhibitor of BCL2

- family proteins induces regression of solid tumours. *Nature*. 2005;435(7042):677-681.
15. Iyer S, Uren RT, Dengler MA, et al. Robust autoactivation for apoptosis by BAK but not BAX highlights BAK as an important therapeutic target. *Cell Death Dis*. 2020;11(4):268.
 16. Matulis SM, Gupta VA, Neri P, et al. Functional profiling of venetoclax sensitivity can predict clinical response in multiple myeloma. *Leukemia*. 2019;33(5):1291-1296.
 17. Swords RT, Azzam D, Al-Ali H, et al. Ex-vivo sensitivity profiling to guide clinical decision making in acute myeloid leukemia: a pilot study. *Leuk Res*. 2018;64:34-41.
 18. Zelenetz AD, Salles G, Mason KD, et al. Venetoclax plus R- or G-CHOP in non-Hodgkin lymphoma: results from the CAVALLI phase 1b trial. *Blood*. 2019;133(18):1964-1976.
 19. Adams CM, Clark-Garvey S, Porcu P, Eischen CM. Targeting the BCL2 family in B cell lymphoma. *Front Oncol*. 2019;8:636.

Insights into vitamin K-dependent carboxylation: home field advantage

Francis Ayombil¹ and Rodney M. Camire^{1,2}

¹Division of Hematology and the Raymond G. Perelman Center for Cellular and Molecular Therapeutics, The Children's Hospital of Philadelphia and ²Department of Pediatrics, Perelman School of Medicine, University of Pennsylvania, Philadelphia, PA, USA

E-mail: RODNEY M. CAMIRE - rcamire@penncmedicine.upenn.edu

doi:10.3324/haematol.2020.253690

Vitamin K-dependent (VKD) proteins play critical roles in blood coagulation, bone metabolism, and other physiologic processes. These proteins undergo a specific post-translational modification called gamma (γ)-carboxylation which is critical to their biologic function.¹ The reaction, which occurs in the endoplasmic reticulum (ER) and requires reduced vitamin K, carbon dioxide and oxygen as co-factors, is catalyzed by γ -glutamyl carboxylase (GGCX). GGCX converts several glutamic acid residues (Glu) on its protein substrate [e.g. prothrombin, FVII, FIX, FX, PC, PS, PZ, and bone Gla protein (BGP)] to γ -carboxy-glutamic acid, otherwise known as Gla.² How does this enzyme pick its protein substrate and modify specific glutamic acid residues? In work spanning over 30 years, researchers identified a critical sequence called the propeptide region that is N-terminal to the mature protein (Figure 1). GGCX binds the propeptide and directs carboxylation of 9-13 Glu residues on the so-called Gla domain in a processive fashion.² The signal sequence and propeptide region are removed by peptidases prior to secretion of the mature VKD protein (Figure 1). For the VKD coagulation factors, the enhanced net negative charge following carboxylation in the Gla domain allows for high affinity divalent metal ion binding.³ This changes the structural conformation of the Gla domain which facilitates binding to anionic phospholipids and localizes these proteins to the site of vascular injury.^{3,4} Defects of VKD protein carboxylation cause bleeding disorders, and inhibition of this pathway is the basis of warfarin anticoagulation.²

Acquiring mechanistic information about GGCX and deciphering how the propeptide influences carboxylation has been challenging. Since GGCX is an integral membrane ER protein (Figure 1), extracting it in a functional state is difficult and requires artificial conditions to study it. Early work used crude microsomal extracts or detergent-solubilized liver microsomes following warfarin treatment or vitamin K-deficient animals which contained the enzyme and small amounts of endogenous protein substrate (e.g. prothrombin).¹ Advancements to this system incorporated artificial peptide substrates for GGCX such as FLEEL (residues 5-9 of rat prothrombin).⁵ In the late 1980s, it was

recognized that the propeptide sequence is critical for VKD protein carboxylation.⁶ This insight led to the development of GGCX substrates that contained a propeptide sequence and portions of the Gla domain which are superior when compared to FLEEL alone.^{7,8} These and other substrates have been used to demonstrate the importance of propeptide affinity in substrate recognition using either crude preparations or purified forms of GGCX and increased our understanding about the enzyme.⁹ Further insights into the importance of the propeptide came from studies using mutant peptides and identification of naturally occurring mutations in the propeptide region of FIX.^{10,11} However, this knowledge about the function of GGCX was obtained outside of its natural environment under artificial conditions. To better understand VKD carboxylation in its native milieu, Tie and Stafford developed a cell-based reporter assay to study γ -carboxylation and the entire VKD cycle.¹² In this system, a chimeric reporter-protein, FIXgla-PC is used, in which the PC backbone was replaced at the N-terminus with the FIX Gla domain.^{12,13} This allowed for an ELISA-based quantification of carboxylated reporter protein using a capture antibody that recognizes only a fully carboxylated FIX Gla domain and an antibody against PC. The advantage of the system is that it allows for functional assessment of the VKD cycle enzymes, including GGCX, in an environment that requires the enzymes to interact with their physiologic substrates, a departure from systems previously employed.

In this issue of *Haematologica*, Hao *et al.* use this cell-based assay to study the role of the propeptide in directing carboxylation of VKD proteins.¹⁴ Previous studies indicate that the propeptide region of VKD coagulation factors show considerable variation in their affinities for GGCX with FX, FIX and PC showing high ($K_d \sim 1$ nM), intermediate ($K_d \sim 5$ nM), and low affinity ($K_d \sim 20$ nM), respectively (Figure 1).¹⁵ It is thought that these disparate affinities contribute to the heterogeneity in carboxylation in mammalian expression systems. Furthermore, it is thought that there is likely an optimal propeptide affinity that best directs carboxylation. To better understand how GGCX interacts with its protein substrates *via* propeptide binding in its natural environment, the authors created a series of chimeric

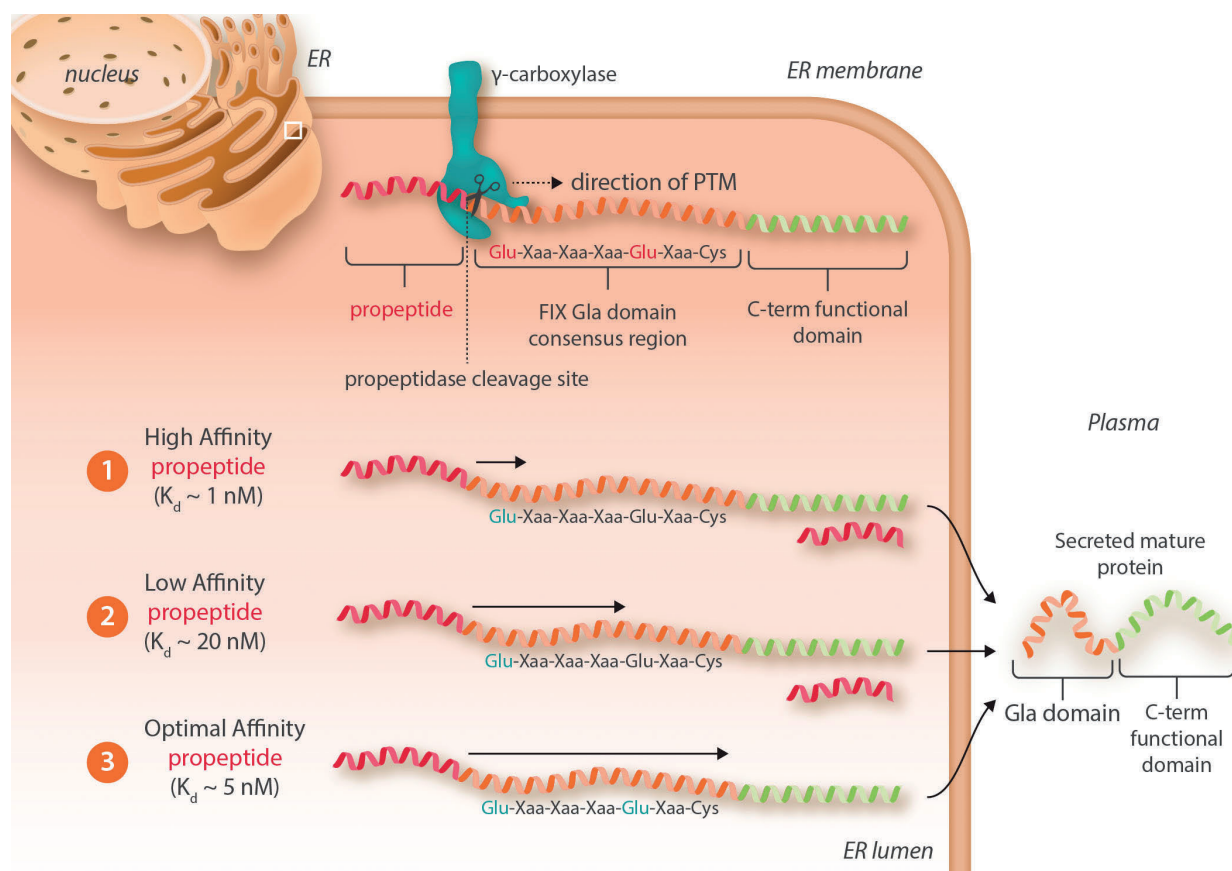


Figure 1. Carboxylation of vitamin K-dependent proteins by γ -carboxylase. The endoplasmic reticulum (ER) membrane-associated gamma-glutamyl carboxylase (GGCX) modifies glutamic acid (red) to gamma-carboxy-glutamic acid (Gla, blue) within the Gla domain. GGCX recognizes and binds the substrate via the propeptide region (red helix) in a processive fashion. The affinity of the GGCX-propeptide complex determines relative efficiency of carboxylation as follows: 1) high affinity propeptides ($K_d \sim 1$ nM) result in significant uncarboxylated protein; 2) low affinity propeptides ($K_d \sim 20$ nM) are associated with moderate to normal carboxylated protein; and 3) optimal affinity propeptides ($K_d \sim 5$ nM) produce efficiently carboxylated protein. Glu: glutamic acid residues; FIX: factor IX; PTM: post-translational modification; C-term: C-terminus.

proteins in their cell-based assay. Propeptide sequences having a broad range of affinities for GGCX derived from FX, FIX, PC, and BPG were attached individually to the FIXgla-PC chimeric reporter. Hao *et al.* found that the FIX propeptide was the most efficient at directing carboxylation while the high affinity propeptide from FX and the low affinity propeptides from PC and BPG had reduced efficiency.¹⁴ The data show that the FIX propeptide is optimal for both binding GGCX and releasing once the protein is carboxylated. These results differ when using synthetic propeptides, FLEEL and purified GGCX,⁹ highlighting the importance of the cell-based system. Interestingly, the BPG propeptide, known to have a low affinity for GGCX, did not direct carboxylation of the reporter protein harboring the FIX Gla domain, but did direct carboxylation if the BPG Gla domain was used. This suggests that other determinants within BPG are needed for carboxylation of this protein. Enhancing the affinity of BPG propeptide for GGCX by mutating the -6 and -10 position rescued carboxylation of the chimeric reporter. The picture with the FX propeptide appeared to be different. This propeptide binds very tightly to GGCX and attempts to weaken the binding by mutation at the -6 and -10 position were unsuccessful. However, further changes to the propeptide revealed that the entire N-terminal portion of the propeptide determines

carboxylation efficiency of VKD coagulation factors. Additional detailed investigation centered on known propeptide mutations. FIX mutations (-9 and -10 in the propeptide), for example, are known to cause warfarin hypersensitivity; a situation in which active FIX levels drop to <1% during anticoagulation therapy while the activity of other clotting factors is decreased to 30-40%.¹⁰ The authors show that, in the cell-based system, these FIX mutant proteins were indeed hypersensitive to warfarin. Again, these data highlight the power of using the cell-based system to gain information about clinically relevant mutations.

The cell-based functional study presented by Hao *et al.*¹⁴ provides further insights into GGCX function and the role of the propeptide during carboxylation in its natural environment. The findings are consistent with prior studies using purified GGCX and propeptide/FLEEL as a substrate. However, the work is nonetheless significant as it nicely shows that structure/function relationships about the propeptide and new insights about mutations in this region can be obtained. The finding that the FIX propeptide is optimal for efficient carboxylation should provide the framework to further understand the structural elements that mediate substrate recognition by GGCX and in the production of VKD coagulation factors. The work is also important as it highlights the power and utility of the cell-based

system to study GGCX and the entire vitamin K cycle. In fact, this group recently used this assay in a high-throughput capacity to screen small molecules that impact the vitamin K cycle, an exercise that would be not possible using prior approaches.¹⁶ In summary, this elegant report confirms the critical role that the propeptide region plays in carboxylation of VKD proteins and highlights the utility of a novel cell-based assay that enables researchers to study membrane-associated enzymes in their natural, home environment.

Acknowledgments

FA is supported by Grant T32 H107971 from NHLBI.

References

1. Tie J-K, Stafford D. Functional study of the vitamin K cycle enzymes in live cells. *Methods in Enzymol.* 2017;584:349-394.
2. Furie B, Furie BC. Molecular basis of vitamin K-dependent gamma-carboxylation. *Blood.* 1990;75(9):1753-1762.
3. Sunnerhagen M, Forsén S, Hoffrén A-M, Drakenberg T, Telemann O, Stenflo J. Structure of the Ca²⁺-free Gla domain sheds light on membrane binding of blood coagulation proteins. *Nat Struct Mol Biol.* 1995;2(6):504-509.
4. Huang M, Rigby AC, Morelli X, et al. Structural basis of membrane binding by Gla domains of vitamin K-dependent proteins. *Nat Struct Mol Biol.* 2003;10(9):751-756.
5. Suttie J, Hageman J. Vitamin K-dependent carboxylase. Development of a peptide substrate. *J Biol Chem.* 1976;251(18):5827-5830.
6. Jorgensen MJ, Cantor AB, Furie BC, Brown CL, Shoemaker CB, Furie B. Recognition site directing vitamin K-dependent gamma-carboxylation resides on the propeptide of factor IX. *Cell.* 1987;48(2):185-191.
7. Hubbard BR, Ulrich MM, Jacobs M, et al. Vitamin K-dependent carboxylase: affinity purification from bovine liver by using a synthetic propeptide containing the gamma-carboxylation recognition site. *Proc Natl Acad Sci U S A.* 1989;86(18):6893-6897.
8. Wu S, Soute B, Vermeer C, Stafford D. In vitro gamma-carboxylation of a 59-residue recombinant peptide including the propeptide and the gamma-carboxyglutamic acid domain of coagulation factor IX. Effect of mutations near the propeptide cleavage site. *J Biol Chem.* 1990;265(22):13124-13129.
9. Wu SM, Morris DP, Stafford DW. Identification and purification to near homogeneity of the vitamin K-dependent carboxylase. *Proc Natl Acad Sci U S A.* 1991;88(6):2236-2240.
10. Chu K, Wu S-M, Stanley T, Stafford DW, High KA. A mutation in the propeptide of factor IX leads to warfarin sensitivity by a novel mechanism. *J Clin Invest.* 1996;98(7):1619-1625.
11. Stanley TB, Wu S-M, Houben RJ, Mutucumarana VP, Stafford DW. Role of the propeptide and γ -glutamic acid domain of factor IX for in vitro carboxylation by the vitamin K-dependent carboxylase. *Biochemistry.* 1998;37(38):13262-13268.
12. Tie J-K, Jin D-Y, Straight DL, Stafford DW. Functional study of the vitamin K cycle in mammalian cells. *Blood.* 2011;117(10):2967-2974.
13. Yan SCB, Razzano P, Chao YB, et al. Characterization and novel purification of recombinant human protein C from three mammalian cell lines. *Nat Biotech.* 1990;8:655-661.
14. Hao Z, Jin DY, Stafford DW, Tie JK. Vitamin K-dependent carboxylation of coagulation factors: insights from a cell-based functional study. *Haematologica.* 2020;105(8):2164-2173.
15. Higgins-Gruber SL, Mutucumarana VP, Lin P-J, Jorgenson JW, Stafford DW, Straight DL. Effect of vitamin K-dependent protein precursor propeptide, vitamin K hydroquinone, and glutamate substrate binding on the structure and function of γ -glutamyl carboxylase. *J Biol Chem.* 2010;285(41):31502-31508.
16. Chen X, Li C, Jin D, et al. A cell-based high-throughput screen identifies drugs that cause bleeding disorders by off-targeting the vitamin K cycle. *Blood.* 2020 May 6. [Epub Ahead of print].

An agenda for future research projects in polycythemia vera and essential thrombocythemia

Tiziano Barbui,¹ Alessandro Maria Vannucchi,² Paola Guglielmelli,² Valerio De Stefano³ and Alessandro Rambaldi⁴

¹FROM Research Foundation, Papa Giovanni XXIII Hospital, Bergamo; ²Center of Research and Innovation of Myeloproliferative Neoplasms (CRIMM), Azienda Ospedaliera Universitaria Careggi and Department of Experimental and Clinical Medicine, University of Florence, Florence; ³Section of Hematology, Department of Radiological and Hematological Sciences, Catholic University and Fondazione Policlinico Universitario A. Gemelli IRCCS, Rome and ⁴Department of Oncology and Hematology, University of Milan, Milan and Azienda Socio Sanitaria Territoriale Papa Giovanni XXIII, Bergamo, Italy



Haematologica 2020
Volume 105(8):1999-2003

Introduction

The clinical course of essential thrombocythemia (ET) and polycythemia vera (PV) is characterized by an increased incidence of vascular complications and a tendency to progress to myelofibrosis (MF) or acute myeloid leukemia (AML). Over the past decade, new molecular and clinical knowledge in ET and PV has led to a significant improvement in the diagnostic, prognostic and therapeutic processes. Despite these advancements, many uncertainties remain concerning aspects of clinical decision-making. We identified some unmet needs in clinical practice and research that urgently require new scientific initiatives. For each of these, we reviewed the most significant existing evidence and made proposals for translational and clinical investigations. We acknowledge that several other clinically relevant unmet needs in the management of patients with PV and ET remain. These could not be addressed due to space constraints, and include, above all, prediction of evolution to secondary forms of myelofibrosis, identification of genetic predictors of survival and of specific subgroups of patients to include in intervention trials with novel drugs that are claimed to modify disease course.

Should we look for new diagnostic and prognostic criteria to distinguish pre-fibrotic myelofibrosis and essential thrombocythemia?

One of the major changes introduced by the 2016 World Health Organization (WHO) classification is the distinction between so called “true” ET and pre-fibrotic PMF. Insights from large series from reference institutions suggest that the proportion of ET patients who would be reclassified as pre-PMF according to these criteria may be as high as 15-30%.^{1,2}

Although some clinical and hematologic traits cluster preferentially with pre-PMF, with the exception of histopathology, no unique distinctive criterion contributes to diagnosis. The same holds true for the mutation landscape, since only a slight increase in *CALR* mutation frequency is observed in pre-PMF patients. On the other hand, there may be important differences in terms of disease course, clinical complications and overall prognosis. First, the rate of thrombosis seems to be quite similar in pre-PMF and ET (2% patient-years in both conditions).^{1,3,4} Risk variables associated with thrombosis appear to be similar in pre-PMF and ET, as supported by the results of a recent study where the International Prognostic Score of Thrombosis for Essential Thrombocythemia (IPSET-thrombosis) reliably predicted thrombosis in patient with pre-PMF.⁵ In contrast, bleeding episodes may be more frequent in pre-PMF as compared to ET.⁶ Of note, according to large retrospective series, the most distinctive feature between the two diseases is survival, uniformly worse in pre-PMF (ranging from 10.5 to 14.7 years) compared to ET (14.7-21.8 years) in which it was rather similar to the standardized European life expectancy.^{7,8} No specific risk model for survival has yet been developed for pre-PMF; whether that developed for the WHO 2008 definition of ET is proving satisfactory also for pre-PMF remains to be addressed.⁸ The same debate applies also to the recent molecular integrated scores MIPSS-70, that included fibrosis grade 1 *versus* grade 2/3 (the latter is one distinctive feature of overt-PMF *vs.* pre-PMF) as a significant variable for survival.⁹ Therefore, since expected survival is the key issue to discuss with a patient newly diagnosed with pre-PMF, acquiring such

Correspondence:

TIZIANO BARBUI
tbarbui@fondazionefrom.it

Received: March 4, 2020.

Accepted: April 14, 2020.

Pre-published: May 28, 2020.

doi:10.3324/haematol.2019.246207

Check the online version for the most updated information on this article, online supplements, and information on authorship & disclosures: www.haematologica.org/content/105/8/1999

©2020 Ferrata Storti Foundation

Material published in *Haematologica* is covered by copyright. All rights are reserved to the Ferrata Storti Foundation. Use of published material is allowed under the following terms and conditions:

<https://creativecommons.org/licenses/by-nc/4.0/legalcode>. Copies of published material are allowed for personal or internal use. Sharing published material for non-commercial purposes is subject to the following conditions: <https://creativecommons.org/licenses/by-nc/4.0/legalcode>, sect. 3. Reproducing and sharing published material for commercial purposes is not allowed without permission in writing from the publisher.



information definitely represents the most compelling unmet need in pre-PMF. A prospective registry collecting all new cases may be of significant help in finding an answer, but it may take several years. An alternative option may be a study enrolling not only all incident cases, but also retrospective ones, provided all the diagnoses are validated by a centralized panel of expert histopathologists and clinicians. Moreover, a comprehensive clinical and biologic database (with a tissue bank collecting samples at diagnosis and during follow up) should be made available. This approach may help to identify the causes of death in patients with pre-PMF, the rate of transformation to overt PMF and acute leukemia, and possibly allow predictive variables to be identified.

Should patients with essential thrombocythemia or polycythemia vera be stratified in genomic subgroups?

Recent publications have highlighted the prognostic contribution of genetic information in both ET and PV, which includes driver mutational status, karyotype abnormalities, and presence or absence of mutations in other myeloid genes. Next-generation sequencing (NGS) analysis identified the prognostic relevance of “adverse variants” in terms of inferior overall and shorter leukemia-free or fibrosis-free survival, including *ASXL1*, *SRSF2* and *IDH2* in PV and *SH2B3*, *SF3B1*, *U2AF1*, *TP53*, *IDH2*, and *EZH2* in ET.¹⁰ Although these studies have certainly contributed to advance our knowledge of the potential prognostic value of mutational genotyping in PV and ET, and provided informative tools to identify patients at higher risk of disease progression and leukemia transformation, this approach is still far from being considered relevant in clinical practice. In ET, *CALR* mutations have been shown to correlate with lower risk of thrombosis compared to *JAK2V617F* mutation and, indeed, the latter is included in the IPSET thrombosis score.^{11,12} In PV, there is some evidence that patients with higher *JAK2V617F* allele burden may be at increased risk of thrombosis;¹³ however, lack of prospective data weakens the value of this information. Future research should evaluate prospectively whether genetic data may add clinically relevant information on top of a conventional score for PV and the IPSET for ET; not an easy task, when considering that the rate of cardiovascular event is around 2% patient-years in ET and 2-3% in PV. Large, international registries may represent the most productive approach using series of patients carefully annotated according to the 2016 WHO classification.

Should cytoreduction be prescribed to all patients with polycythemia vera regardless of risk?

The first step in approaching a patient with PV is to identify the potential risk of developing major thrombotic or hemorrhagic complications. Patients are considered to be low-risk by age <60 years and absence of previous thrombosis,¹⁴ but this distinction is weakening. In fact, low-risk patients optimally treated with phlebotomy and low-dose aspirin still exhibit an annual rate of major thrombotic episodes of 2% patients/year; an estimate 2- and 3-fold higher than in the general population with, or without, multiple risk-factors, respectively.¹⁵ Thus, one may argue whether, in the presence of such residual risk of thrombosis, the conservative approach based on phlebotomy and aspirin is still appropriate. The greater added benefit of cytoreductive drugs over phlebotomy in

PV is based on the results of the Polycythemia Vera Study Group 01-PVSG study,¹⁶ a propensity score analysis of the European Collaboration on Low-dose Aspirin in Polycythemia Vera (ECLAP)¹⁷ prospective study and one recent retrospective cohort analysis.¹⁸ Nonetheless, experts discourage the use of cytoreductive drugs in clinical practice for young patients without previous thrombosis since the supposed leukemogenic risk associated with the currently available drugs, such as hydroxyurea, although largely uncertain, might outweigh the possible antithrombotic benefits.

However, although the prognostic and predictive role of leukocytosis is still debated, it may be worthwhile upgrading low-risk patients presenting with leukocyte counts greater than $11 \times 10^9/L$ to the high-risk category and, indeed, these have been included in randomized clinical trials testing hydroxyurea, and ruxolitinib (Mithridate trial; *clinicaltrials.gov identifier: NCT4116502*). Such a claim could be criticized since there has still been no formal demonstration of a clear advantage of cytoreductive therapy over a well-conducted phlebotomy policy. Therefore, we believe that young patients with no history of previous thrombosis could be exposed to cytoreductive treatment as long as they only receive drugs for which there is no evidence of promoting secondary leukemias or solid tumors. One such a drug is interferon, either in conventional or novel retard formulation, such as Ropeginterferon α -2ba which has recently been approved by the European Medicines Agency (EMA) for PV based on phase II and III studies.¹⁹ In these studies, an overall hematologic response in more than 80% of patients, good tolerability and evidence of molecular responses were found.²⁰ The ongoing randomized clinical trial (Low-PV), testing Ropeginterferon α -2ba in addition to conventional treatment, may hopefully provide a convincing answer to one of the clinical needs of patients with low-risk PV.

Can we improve the prevention and treatment of post-myeloproliferative neoplasms-acute myeloid leukemia?

Leukemia transformation of PV and ET is part of the natural history of these diseases.²¹ The risk of leukemic transformation is highest in PMF, but a sizeable proportion of PV and ET patients are involved, with an estimated risk of 3% and 1% at 10 years, respectively.²² It is likely that, in these patients, the unrestricted proliferation of bone marrow progenitors lasting for many years may itself favor the leukemic transformation, and, not surprisingly, older age, leukocytosis, and massive thrombocytosis represent significant risk factors in both PV and ET. Most importantly, biologic characteristics such as abnormal karyotype, presence of *SRSF2* or *IDH2* mutations are emerging risk factors in PV. In ET, anemia, older age, leukocytosis, and presence of *TP53* or *EZH2* mutations have been reported as risk factors.²² Therefore, NGS-based molecular profile performed at diagnosis and during the course of the disease may provide important information to identify patients at higher risk of disease progression and leukemia transformation.¹⁰

There is no evidence that hydroxyurea, interferon, anagrelide or ruxolitinib can slow down the intrinsic tendency of these diseases to transform into AML.²³ On the other hand, there are expectations that some new, targeted drugs may reduce the risk of leukemic transformation. Idasanutlin, an MDM2 inhibitor which modulates

MDM2/p53 interaction and restores p53 activity, produced clinical responses in PV both as monotherapy and in combination with interferon.²⁴ HDAC inhibitors like givinostat are equally non-genotoxic and active drugs in PV and ET.²⁵

As regards the therapeutic approach to post-myeloproliferative neoplasms-acute myeloid leukemia (MPN-AML), prognosis is largely dismal except for the few patients who undergo allogeneic hematopoietic stem cell transplantation (alloHSCT), preferably after debulking with induction chemotherapy. However, new drugs are particularly appealing in this setting, including enasidenib and ivosidenib for patients with *IDH2* or *IDH1* mutated AML, possibly in combination with azacitidine²⁶ or ruxolitinib (in case of enasidenib).²⁷ In addition, BCL2 inhibitors, like venetoclax or navitoclax, (alone or in combination with hypomethylating agents) and CPX-351, a dual-drug liposomal encapsulation of cytarabine and daunorubicin, are also under investigation. At the moment, however, results from rigorously designed clinical trials in this category of high-risk patients are still lacking and the little interest, if any, of pharma companies to promote studies in this setting represents a major problem. It is, therefore, a clear duty of the scientific community to promote academic trials for this unmet clinical need. Since alloHSCT remains the only potentially curative treatment option for these patients,²⁸ intensive treatment capable of achieving remission with a full or even incomplete hematologic reconstitution has to be made available. Apart from some new forthcoming protocols, registry collection of the outcomes of these patients is strongly recommended, particularly with the intent to identify biologic subgroups.

Are the current prevention methods for thrombosis adequate?

The current annual incidence of arterial and venous thrombosis in patients with PV and ET is 2.62% and 1.77%, respectively, a figure 1.5-fold and 3.2-fold higher than that in the general population.^{12,15-20} The antithrombotic role of cytoreductive drugs is uncertain. Hydroxyurea (HU) has demonstrated significant efficacy in preventing arterial thromboses, but doubts remain as to its ability to prevent recurrent venous thromboembolism (VTE),²⁹⁻³¹ particularly in patients with splanchnic venous thrombosis.^{32,33} The antithrombotic efficacy of interferon- α has not yet been convincingly demonstrated, and the performance of ruxolitinib in PV patients resistant/intolerant to HU is largely uncertain.³⁴ Although there is no direct evidence that thrombocytosis per se is a risk factor for thrombosis, the favorable effect of anagrelide *versus* HU in preventing the occurrence of venous thromboembolism in ET, as shown in the PT1 randomized clinical trial,³⁵ is of interest. However, the interpretation of that study is complicated by the heterogeneity of the patient population that was diagnosed according to WHO 2008 criteria. Of note, the ANAHYDRET study, that included patients with a diagnosis of ET that strictly followed WHO 2016 criteria, showed non-inferiority in terms of arterial and venous events.³⁶ As a whole, there is still no convincing evidence of a clear antithrombotic action of cytoreductive drugs in ET and PV, and new randomized clinical trials with thrombosis as the primary end point are warranted.

The indication of low-dose aspirin (LDA) is mainly based on a phase III trial in PV³⁷ and on retrospective studies in ET, but the quality of evidence is low.³⁸ However, new hypotheses are now being tested to improve the antithrombotic efficacy of aspirin in ET. These are based on the notion that accelerated release of new platelets in ET may accelerate the recovery of thromboxane (TX)A₂-dependent platelet function during the once-daily (od) LDA dosing interval. Accordingly, inhibition of the surrogate biomarker platelet TXA₂ by o.d. LDA is incomplete in $\geq 80\%$ of ET patients, but it was seen to be improved by a twice-daily regimen.^{39,40} In the phase II ARES randomized trial,⁴¹ most of the 245 ET patients treated with LDA displayed incomplete platelet inhibition, which was improved by shortening the dosing interval to 12 hours.⁴² The long-term superiority, compliance, and tolerability of an optimized LDA regimen is now being investigated in a clinical trial.

The prevention of recurrent venous thromboembolism by vitamin K-antagonists (VKA) was estimated in several retrospective studies showing an annual incidence of VTE recurrences as high as 5.6-6.5,^{31,43-46} that rose to as high as 12.8 after discontinuation.⁴⁵ In addition, the incidence of major bleeding on VKA of 1.7-1.8 per 100 patients/years^{44,45} is unsatisfactory when compared with non-MPN patients. As mentioned above, the addition of hydroxyurea to VKA has a weak effect³¹ and the combined treatment with LDA significantly increases the risk of bleeding with no substantial benefit on antithrombotic prevention.^{45,47} Thus, the prevention of recurrences after VTE is a crucial unmet clinical need in MPN, and innovative strategies are needed. Direct oral anticoagulants (DOAC) can represent a suitable alternative, but before embarking on a formal randomized comparative trial assessing DOAC *versus* warfarin, a retrospective analysis of treated cases may guide its design. In this regard, some preliminary evidence has been presented in the prospective multicenter observational REVEAL study.⁴⁷

Conclusion

We have highlighted some clinical topics about which the available evidence is limited. We believe these areas represent priorities for future research projects. Since both PV and ET are relatively rare diseases, and the outcomes of interest occur after long periods of observation, the methodology to conduct these studies cannot be reasonably based on conventional phase II/III design. Therefore, well organized observational and registry-based studies will play a key role in analyzing the clinical outcomes, hopefully with the help of a data mining approach and artificial intelligence techniques, as suggested by preliminary experiences in patients with PV treated with ruxolitinib.⁴⁸

Acknowledgments

This study was supported by Fondazione per la Ricerca Ospedale (FROM), Papa Giovanni XXIII Hospital, Bergamo, Italy; and by Associazione Italiana per la Ricerca sul Cancro, Grant 5 per Mille, Progetto MYNERVA (P.G. and A.M.V.) and Progetto ISM (AR)

References

- Guglielmelli P, Pacilli A, Rotunno G, et al. Presentation and outcome of patients with 2016 WHO diagnosis of prefibrotic and overt primary myelofibrosis. *Blood*. 2017;129(24):3227-3236.
- Rumi E, Boveri E, Bellini M, et al. Clinical course and outcome of essential thrombocythemia and prefibrotic myelofibrosis according to the revised WHO 2016 diagnostic criteria. *Oncotarget*. 2017;8(60):101735-101744.
- Carobbio A, Finazzi G, Guerini V, et al. Leukocytosis is a risk factor for thrombosis in essential thrombocythemia: Interaction with treatment, standard risk factors, and Jak2 mutation status. *Blood*. 2007;109(6):2310-2313.
- Carobbio A, Thiele J, Passamonti F, et al. Risk factors for arterial and venous thrombosis in WHO-defined essential thrombocythemia: An international study of 891 patients. *Blood*. 2011;117(22):5857-5859.
- Guglielmelli P, Carobbio A, Rumi E, et al. Validation of the IPSET score for thrombosis in patients with prefibrotic myelofibrosis. *Blood Cancer J*. 2020;10(2):21.
- Finazzi G, Vannucchi AM, Barbui T. Prefibrotic myelofibrosis: treatment algorithm 2018. *Blood Cancer J*. 2018;8(11):104.
- Barbui T, Thiele J, Passamonti F, et al. Survival and disease progression in essential thrombocythemia are significantly influenced by accurate morphologic diagnosis: A international study. *J Clin Oncol*. 2011;29(23):3179-3184.
- Tefferi A, Guglielmelli P, Larson DR, et al. Long-term survival and blast transformation in molecularly annotated essential thrombocythemia, polycythemia vera, and myelofibrosis. *Blood*. 2014;124(16):2507-2513.
- Guglielmelli P, Lasho TL, Rotunno G, et al. MIPSS70: Mutation-enhanced international prognostic score system for transplantation-age patients with primary myelofibrosis. *J Clin Oncol*. 2018;36(4):310-318.
- Tefferi A, Guglielmelli P, Lasho TL, et al. Mutation-enhanced international prognostic systems for essential thrombocythemia and polycythemia vera. *Br J Haematol*. 2020 Jan 16. [Epub ahead of print].
- Barbui T, Vannucchi AM, Buxhofer-Ausch V, et al. Practice-relevant revision of IPSET-thrombosis based on 1019 patients with WHO-defined essential thrombocythemia. *Blood Cancer J*. 2015;5:e369.
- Barbui T, Finazzi G, Carobbio A, et al. Development and validation of an International Prognostic Score of thrombosis in World Health Organization-essential thrombocythemia (IPSET-thrombosis). *Blood*. 2012;120(26):5128-5133.
- Vannucchi AM, Antonioli E, Guglielmelli P, et al. Clinical profile of homozygous JAK2 617V>F mutation in patients with polycythemia vera or essential thrombocythemia. *Blood*. 2007;110(3):840-846.
- Barbui T, Tefferi A, Vannucchi AM, et al. Philadelphia chromosome-negative classical myeloproliferative neoplasms: Revised management recommendations from European LeukemiaNet. *Leukemia*. 2018;32(5):1057-1069.
- Barbui T, Carobbio A, Rumi E, et al. To the editor: In contemporary patients with polycythemia vera, rates of thrombosis and risk factors delineate a new clinical epidemiology. *Blood*. 2014;124(19):3021-3023.
- Berk PD, Goldberg JD, Donovan PB, Fruchtman SM, Berlin NI, Wasserman LR. Therapeutic recommendations in polycythemia vera based on Polycythemia Vera Study Group protocols. *Semin Hematol*. 1986;23(2):132-143.
- Barbui T, Vannucchi AM, Finazzi G, et al. A reappraisal of the benefit-risk profile of hydroxyurea in polycythemia vera: A propensity-matched study. *Am J Hematol*. 2017;92(11):1131-1136.
- Enblom-Larsson A, Girodon F, Bak M, et al. A retrospective analysis of the impact of treatments and blood counts on survival and the risk of vascular events during the course of polycythemia vera. *Br J Haematol*. 2017;177(5):800-805.
- Gisslinger H, Zagrijtschuk O, Buxhofer-Ausch V, et al. Ropeginterferon alpha-2b, a novel IFN α -2b, induces high response rates with low toxicity in patients with polycythemia vera. *Blood*. 2015;126(15):1762-1769.
- Gisslinger H, Klade C, Georgiev P, et al. Ropeginterferon alpha-2b versus standard therapy for polycythemia vera (PROUD-PV and CONTINUATION-PV): a randomised, non-inferiority, phase 3 trial and its extension study. *Lancet Haematol*. 2020;7(3):196-e208.
- Tam CS, Nussenzweig RM, Popat U, et al. The natural history and treatment outcome of blast phase BCR-ABL - myeloproliferative neoplasms. *Blood*. 2008;112(5):1628-1637.
- Tefferi A, Mudireddy M, Mannelli F, et al. Blast phase myeloproliferative neoplasm: Mayo-AGIMM study of 410 patients from two separate cohorts. *Leukemia*. 2018;32(5):1200-1210.
- Björkholm M, Derolf ÅR, Hultcrantz M, et al. Treatment-related risk factors for transformation to acute myeloid leukemia and myelodysplastic syndromes in myeloproliferative neoplasms. *J Clin Oncol*. 2011;29(17):2410-2415.
- Mascarenhas J, Lu M, Kosiorek H, et al. Oral idasanutlin in patients with polycythemia vera. *Blood*. 2019;134(6):525-533.
- Rambaldi A, Iurlo A, Vannucchi AM, et al. Safety and efficacy of the maximum tolerated dose of givinostat in polycythemia vera: a two-part Phase Ib/II study. *Leukemia*. 2020 Feb 11. [Epub ahead of print].
- Odenike O. How I treat the blast phase of Philadelphia chromosome-negative myeloproliferative neoplasms. *Blood*. 2018;132(22):2339-2350.
- McKenney AS, Lau AN, Somasundara AVH, et al. JAK2/IDH-mutant-driven myeloproliferative neoplasm is sensitive to combined targeted inhibition. *J Clin Invest*. 2018;128(2):789-804.
- Lancet JE, Uy GL, Cortes JE, et al. Cpx-351 (cytarabine and daunorubicin) liposome for injection versus conventional cytarabine plus daunorubicin in older patients with newly diagnosed secondary acute myeloid leukemia. *J Clin Oncol*. 2018;36(26):2684-2692.
- Barbui T, De Stefano V, Ghirardi A, Masciulli A, Finazzi G, Vannucchi AM. Different effect of hydroxyurea and phlebotomy on prevention of arterial and venous thrombosis in Polycythemia Vera. *Blood Cancer J*. 2018;8(12):124.
- De Stefano V, Carobbio A, Di Lazzaro V, et al. Benefit-risk profile of cytoreductive drugs along with antiplatelet and antithrombotic therapy after transient ischemic attack or ischemic stroke in myeloproliferative neoplasms. *Blood Cancer J*. 2018;8(3):25.
- De Stefano V, Rossi E, Carobbio A, et al. Hydroxyurea prevents arterial and late venous thrombotic recurrences in patients with myeloproliferative neoplasms but fails in the splanchnic venous district. Pooled analysis of 1500 cases. *Blood Cancer J*. 2018;8(11):112.
- De Stefano V, Vannucchi AM, Ruggeri M, et al. Splanchnic vein thrombosis in myeloproliferative neoplasms: Risk factors for recurrences in a cohort of 181 patients. *Blood Cancer J*. 2016;6(11):e493.
- Sant'Antonio E, Guglielmelli P, Pieri L, et al. Splanchnic vein thromboses associated with myeloproliferative neoplasms: An international, retrospective study on 518 cases. *Am J Hematol*. 2020;95(2):156-166.
- Masciulli A, Ferrari A, Carobbio A, Ghirardi A, Barbui T. Ruxolitinib for the prevention of thrombosis in polycythemia vera: a systematic review and meta-analysis. *Blood Adv*. 2020;4(2):380-386.
- Harrison CN, Campbell PJ, Buck G, et al. Hydroxyurea compared with anagrelide in high-risk essential thrombocythemia. *N Engl J Med*. 2005;353(1):33-45.
- Gisslinger H, Gotic M, Holowiecki J, et al. Anagrelide compared with hydroxyurea in WHO-classified essential thrombocythemia: the ANAHYDRET Study, a randomized controlled trial. *Blood*. 2013;121(10):1720-1728.
- Landolfi R, Marchioli R, Kutti J, et al. Efficacy and Safety of Low-Dose Aspirin in Polycythemia Vera. *N Engl J Med*. 2004;350(2):114-124.
- Chu DK, Hillis CM, Leong DP, Anand SS, Siegal DM. Benefits and risks of antithrombotic therapy in essential thrombocythemia: A systematic review. *Ann Intern Med*. 2017;167(3):170-180.
- Pascale S, Petrucci G, Dragani A, et al. Aspirin-insensitive thromboxane biosynthesis in essential thrombocythemia is explained by accelerated renewal of the drug target. *Blood*. 2012;119(15):3595-3603.
- Dillinger JG, Sollier CBD, Sideris G, Ronez E, Henry P, Drouet L. Twice daily aspirin to improve biological aspirin efficacy in patients with essential thrombocythemia. *Thromb Res*. 2012;129(1):91-94.
- De Stefano V, Rocca B, Tosetto A, et al. The Aspirin Regimens in Essential Thrombocythemia (ARES) phase II randomized trial design: Implementation of the serum thromboxane B2 assay as an evaluation tool of different aspirin dosing regimens in the clinical setting. *Blood Cancer J*. 2018;8(6):49.
- Rocca B, Tosetto A, Betti S, et al. A randomized, double-blind trial of three aspirin regimens to optimize antiplatelet therapy in essential thrombocythemia. *Blood*. 2020 April 7. [Epub ahead of print].
- De Stefano V, Za T, Rossi E, et al. Recurrent thrombosis in patients with polycythemia vera and essential thrombocythemia: Incidence, risk factors, and effect of treatments. *Haematologica*. 2008;93(3):372-380.
- Hernández-Boluda J-C, Arellano-Rodrigo E, Cervantes F, et al. Oral anticoagulation to prevent thrombosis recurrence in poly-

- cythemia vera and essential thrombocythemia. *Ann Hematol.* 2015;94(6):911-918.
45. De Stefano V, Ruggeri M, Cervantes F, et al. High rate of recurrent venous thromboembolism in patients with myeloproliferative neoplasms and effect of prophylaxis with Vitamin K antagonists. *Leukemia.* 2016;30(10):2032-2038.
46. Wille K, Sadjadian P, Becker T, et al. High risk of recurrent venous thromboembolism in BCR-ABL-negative myeloproliferative neoplasms after termination of anticoagulation. *Ann Hematol.* 2019;98(1):93-100.
47. Zwicker JJ, Lessen DS, Colucci P, Paranagama D, Grunwald MR. Risk of hemorrhage in patients with polycythemia vera exposed to aspirin in combination with anticoagulants: results of a prospective, multicenter, observational cohort study (REVEAL). *Blood.* 2019;134 (Supplement 1):168.
48. Verstovsek S, De Stefano V, Heidel FH, et al. US Optum Database study in polycythemia vera patients: thromboembolic events (TEs) with hydroxyurea (HU) vs ruxolitinib switch therapy and machine-learning model to predict incidence of TEs and HU failure. *Blood.* 2019;134 (Supplement 1):1659.



Inherited thrombocytopenias: history, advances and perspectives

Alan T. Nurden and Paquita Nurden

Institut Hospitalo-Universitaire LIRYC, Pessac, France

Haematologica 2020
Volume 105(8):2004-2019

ABSTRACT

Over the last 100 years the role of platelets in hemostatic events and their production by megakaryocytes have gradually been defined. Progressively, thrombocytopenia was recognized as a cause of bleeding, first through an acquired immune disorder; then, since 1948, when Bernard-Soulier syndrome was first described, inherited thrombocytopenia became a fascinating example of Mendelian disease. The platelet count is often severely decreased and platelet size variable; associated platelet function defects frequently aggravate bleeding. Macrothrombocytopenia with variable proportions of enlarged platelets is common. The number of circulating platelets will depend on platelet production, consumption and lifespan. The bulk of macrothrombocytopenias arise from defects in megakaryopoiesis with causal variants in transcription factor genes giving rise to altered stem cell differentiation and changes in early megakaryocyte development and maturation. Genes encoding surface receptors, cytoskeletal and signaling proteins also feature prominently and Sanger sequencing associated with careful phenotyping has allowed their early classification. It quickly became apparent that many inherited thrombocytopenias are syndromic while others are linked to an increased risk of hematologic malignancies. In the last decade, the application of next-generation sequencing, including whole exome sequencing, and the use of gene platforms for rapid testing have greatly accelerated the discovery of causal genes and extended the list of variants in more common disorders. Genes linked to an increased platelet turnover and apoptosis have also been identified. The current challenges are now to use next-generation sequencing in first-step screening and to define bleeding risk and treatment better.

Correspondence:

ALAN NURDEN
nurdenat@gmail.com

Received: April 23, 2020.

Accepted: May 8, 2020.

Pre-published: June 11, 2020.

doi:10.3324/haematol.2019.233197

Check the online version for the most updated information on this article, online supplements, and information on authorship & disclosures: www.haematologica.org/content/105/8/2004

©2020 Ferrata Storti Foundation

Material published in *Haematologica* is covered by copyright. All rights are reserved to the Ferrata Storti Foundation. Use of published material is allowed under the following terms and conditions:

<https://creativecommons.org/licenses/by-nc/4.0/legalcode>.

Copies of published material are allowed for personal or internal use. Sharing published material for non-commercial purposes is subject to the following conditions:

<https://creativecommons.org/licenses/by-nc/4.0/legalcode>,

sect. 3. Reproducing and sharing published material for commercial purposes is not allowed without permission in writing from the publisher.



History

In the late 19th century improvements to the light microscope led to anucleate platelets being visualized in great numbers in human blood. Early pioneers in the field of platelet research included the Canadian William Osler, a Paris hematologist, George Hayem, who performed the first accurate platelet count, and the Italian Giulio Bizzozero.¹ In 1906, James Homer Wright confirmed that platelets were produced by bone marrow megakaryocytes.² When, in 1951, Harrington *et al.*³ observed purpura in a child of a mother with immune thrombocytopenic purpura, a maternal factor was said to be destroying the platelets. Anti-platelet antibodies were identified as the cause and platelet transfusions, immunosuppressive therapy and splenectomy became standard treatments. Acquired thrombocytopenia, often with defective platelet function, has many causes. For example, it may be an immune response linked to blood transfusions and drugs, a direct consequence of viral or bacterial infections, be the result of other hematologic disorders or be secondary to many major illnesses. However, some thrombocytopenias are inherited and Professors Jean Bernard and Jean-Pierre Soulier in Paris were pioneers in this domain, describing in 1948 what they called in French “*dystrophie thrombocytaire hémorragipare congénitale*”, later re-named the Bernard-Soulier syndrome (BSS).⁴ Strikingly, many platelets were enlarged and some were giant. A key to the molecular defect was the platelet deficit of sialic acid, a negatively charged monosaccharide terminating many of the oligosaccharides of platelet glycoproteins (GP) and

some glycolipids.⁵ The discovery that a major component of the platelet surface, first identified as “GPI”, was absent from platelets in BSS began the long road to defining the molecular landscape of inherited thrombocytopenias.⁶ This centenary review will take a concise look at this journey emphasizing major steps in the current understanding of these conditions and highlighting recent advances in what is an intriguing subset of Mendelian diseases.

Platelet production and lifespan

The platelet count is the result of a balance between the biogenesis, senescence and consumption of these cells. Briefly, CD34⁺ hematopoietic stem cells (HSC) first give rise to megakaryocyte-erythrocyte progenitors, a proportion of which will develop into colonies that mature by endomitosis to polylobulated megakaryocytes with a high DNA content (Figure 1). Megakaryocyte differentiation is regulated by transcription factors as well as by interactions with chemokines, cytokines and constituents of the extracellular matrix.⁷ Thrombopoietin, acting through its receptor Mpl, is a key factor.⁸ Mostly produced in the liver, thrombopoietin levels in blood are governed by the platelet number; feedback mechanisms stimulate HSC proliferation and megakaryopoiesis. The demarcation

membrane system of mature megakaryocytes is a membrane reservoir for platelet biogenesis. Migrating to the endothelial cell sinusoid barrier, mature megakaryocytes extend long, branched, protrusions, termed proplatelets, into the blood where under flow they release large numbers of platelets from their ends.^{9,10} This whole process is highly dependent on cytoskeletal proteins including myosin IIA, actin filaments and the tubulins that provide tracks for the transport of organelles with a Cdc42/RhoA regulatory circuit guiding transendothelial platelet biogenesis.¹¹ Type I collagen in the extracellular matrix is a negative regulator, preventing premature proplatelet formation. Early reports also insisted that megakaryocytes can migrate directly into the blood and accumulate in the lungs. Using two-photon microscopy, *in vivo* lineage tracing technologies and a series of lung transplants in mouse models, Lefrançais *et al.*¹² have confirmed that the lung is indeed a site for platelet biogenesis. In conditions of acute need, direct megakaryocyte rupture is an alternative pathway for platelet production.¹³

If unused in hemostatic events or pathological processes, human platelets circulate for 7-10 days (Figure 2). Platelet clearance due to senescence occurs in the liver. Loss of sialic acid through the action of neuraminidase during platelet aging exposes galactose or N-acetyl-galactosamine, residues that mediate platelet binding to the

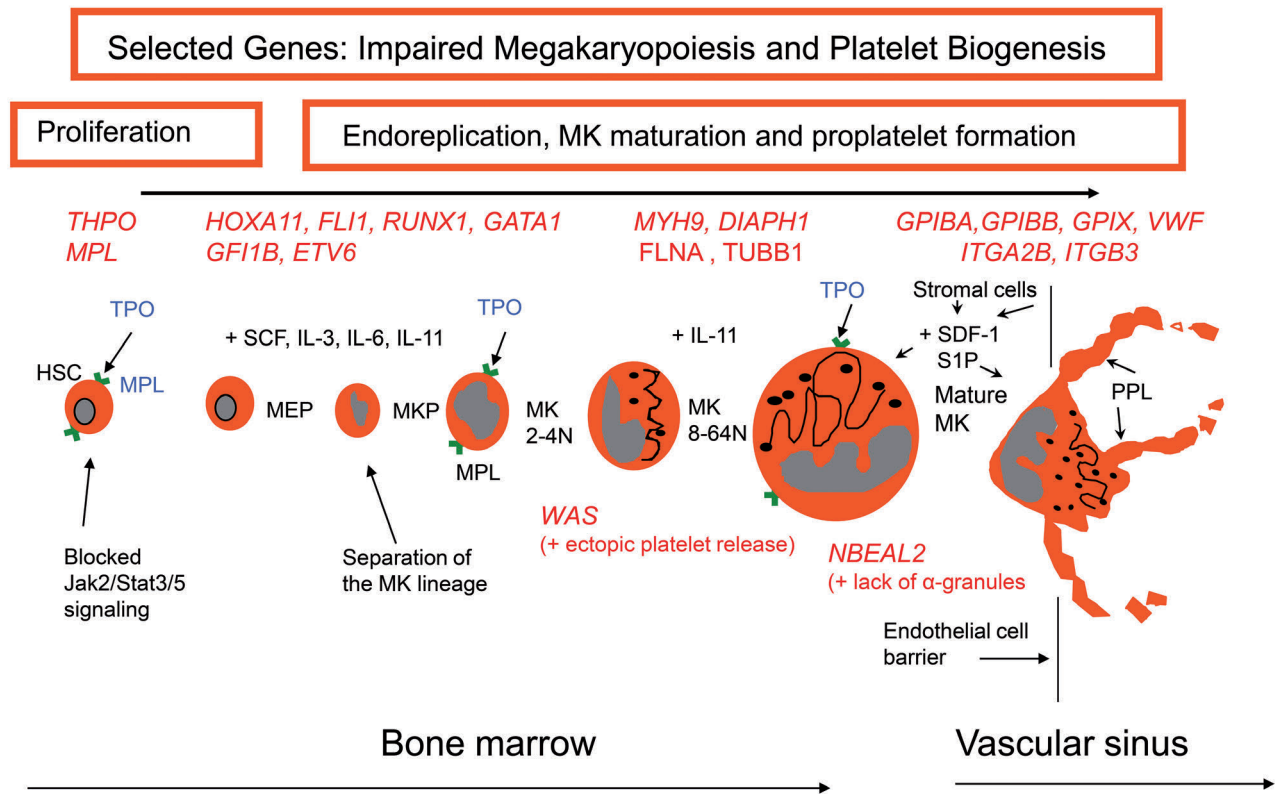


Figure 1. A schema of the major steps of megakaryopoiesis highlighting how inherited defects of selected genes cause thrombocytopenia. Megakaryocytes arise from hematopoietic stem cells that proliferate to first form megakaryocyte-erythrocyte progenitors, a proportion of which give rise to colony-forming megakaryocyte progenitors. These events require the interaction of thrombopoietin with its receptor and are under the influence of various growth factors (e.g. stem cell factor, cytokines and interleukins). The developing megakaryocytes undergo endomitosis to increase chromosome number; they then mature before migrating to the vascular sinus where they extend proplatelets or migrate themselves across the endothelial cell barrier into the vascular sinus. This latter step is under the influence of many factors including stromal derived growth factor-1 and sphingosine-1-phosphate. Selected genes with variants causing inherited thrombocytopenias are shown in red. HSC: hematopoietic stem cells; TPO: thrombopoietin; MPL: thrombopoietin receptor; MEP: megakaryocyte-erythrocyte progenitor; SCF: stem cell factor; IL: interleukin; MKP: megakaryocyte progenitor, MK: megakaryocyte; SDF-1: stromal derived growth factor-1; S1P: sphingosine-1-phosphate; PPL: proplatelet.

hepatocyte Ashwell-Morell receptor, an act that stimulates the synthesis of thrombopoietin.¹⁴ Subsequent studies using a mouse model additionally pointed to clearance by Kupffer cells in the liver sinusoids; here N-acetyl-galactosamine was recognized by the lectin, CLEC4A.¹⁵ State-of-the-art microscopy then pinpointed how Kupffer cells also recognized β -galactose on aged mouse or human platelets with a galactose-binding lectin mediating the phagocytosis.¹⁶ Most importantly, Kupffer cells were shown to continually scan circulating platelets with touch-and-go interactions as these latter pass through sinusoidal endothelial fenestrae.

In megakaryocytes, the role of apoptosis during pro-platelet formation and platelet biogenesis is controversial and largely unproven although it may intervene after platelet release or during stress situations such as infections and inflammation.¹⁷ In a classic paper, the pro-survival protein, Bcl-X_L, was proposed to constrain the pro-death Bak in platelets; the balance acting as a molecular clock for platelet survival.¹⁸ Others have shown how apoptotic pathways and necrosis engage pro-death proteins triggering mitochondrial membrane permeabilization, cytochrome C release and caspase activation leading to Ca²⁺-dependent exposure of phosphatidylserine, which is not only recognized by phagocytic cells but also leads to procoagulant activity.¹⁹

The following sections of this review will describe familial defects of platelet production and megakaryopoiesis; affected genes will be shown to interfere with HSC proliferation, megakaryocyte maturation and migration and the alteration of platelet lifespan. Many are

accompanied by an increased platelet size (Figure 2) while others have a normal platelet size or even small platelets (Figure 3). Platelet function is variably affected. While some thrombocytopenias are isolated, many are syndromic and/or associated with other conditions that may be of major clinical importance. Bleeding is mostly mucocutaneous, severe in some disorders, but infrequent or even absent in others, particularly when the decrease in platelet count is modest. A summary of the genes involved and the principle characteristics of each disorder are presented in *Online Supplementary Table S1*.

Classic inherited thrombocytopenias

We begin with a series of named inherited thrombocytopenias whose characterization has marked the history of inherited platelet disorders. In many of these syndromes, thrombocytopenia, defined as a platelet count $<150 \times 10^9/L$, is accompanied by platelet function defects that aggravate bleeding. In early studies genotyping mostly involved candidate gene sequencing and linkage studies.

Bernard-Soulier syndrome

The “GPI” lesion in BSS platelets was quickly shown to involve a complex of four distinct subunits each encoded by a distinct gene. The large, heavily glycosylated GPIb α is attached by a disulfide to the small GPIb β , while GPIX and GPV are non-covalently associated, all in a 2:2:2:1 stoichiometry. Bleeding in BSS patients is disproportionate to

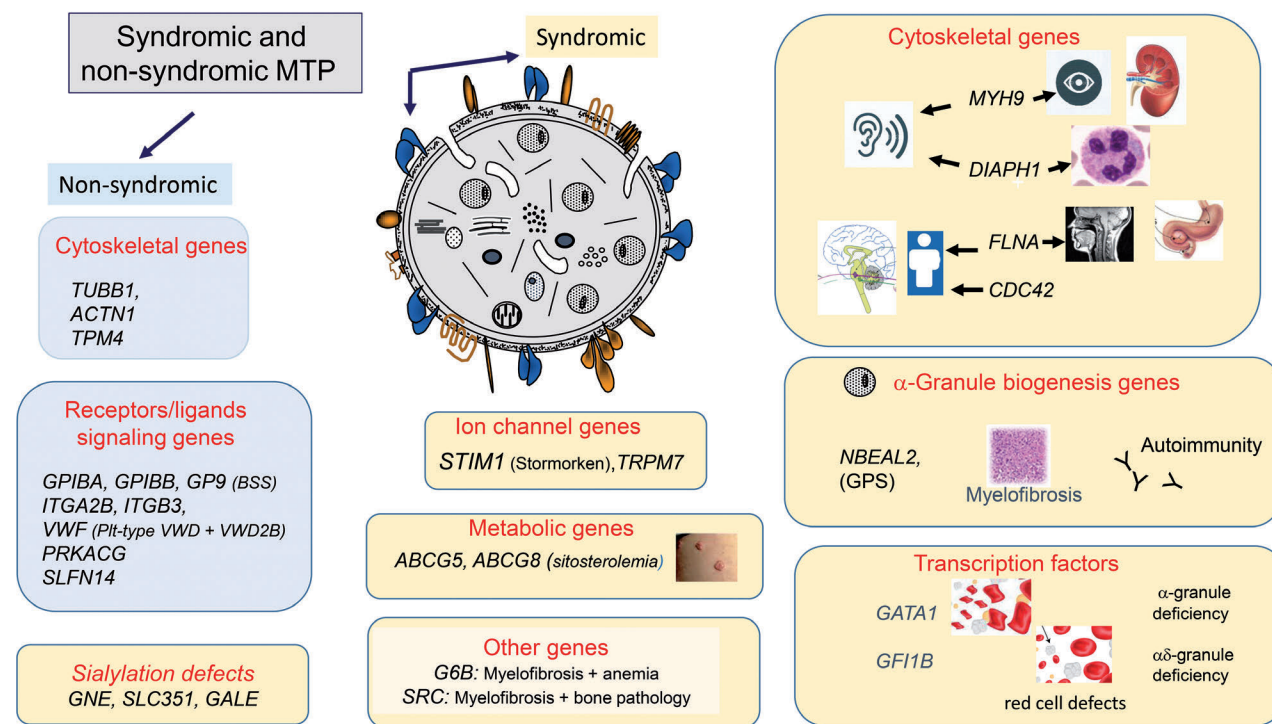


Figure 2. A cartoon showing genes causing non-syndromic and syndromic macrothrombocytopenias. The causative genes are grouped according to the nature of the encoded protein and/or the secondary condition(s) that may accompany the macrothrombocytopenia. MTP: macrothrombocytopenias; BSS: Bernard-Soulier syndrome; pit-type VWD: platelet-type von Willebrand syndrome; VWD2B: von Willebrand disease type 2B; GPS: gray platelet syndrome.

the degree of thrombocytopenia because the absence of GPIb α prevents the shear-dependent tethering of platelets to von Willebrand factor (VWF) in vascular lesions, an abnormality mimicked by the loss of ristocetin-induced platelet agglutination in a diagnostic test.^{20,21} The search for mutations first targeted *GP1BA*, the gene encoding GPIb α , but mutations in *GP1BB* and *GP9* were also quickly shown to cause BSS by preventing the surface expression of GPIb α .²² The generation and rescue of BSS in a mouse model confirmed the link between GPIb α loss and the appearance of giant platelets and, therefore, macrothrombocytopenia.²³ Typical findings in BSS and the mouse models are aberrant formation of the demarcation membrane system in megakaryocytes while fewer proplatelets protrude into the vascular sinus and these proplatelets are thicker with larger heads. While the loss of megakaryocyte interactions with extracellular proteins remains a plausible molecular basis of BSS, the absence of mechanical stabilizing interactions between GPIb, cytoskeletal proteins and internal membranes is another likely factor.

While classic BSS has autosomal recessive (AR) inheritance, mono-allelic forms with autosomal dominant (AD) transmission are a frequent cause of mild macrothrombocytopenia in Europe. The initial example was the Bolzano (p.A172V) mutation affecting GPIb α in Italian families, said to be responsible for Mediterranean macrothrombocytopenia, although other variants of *GP1BA* have since been described. More recently a series of single allele variants of *GP1BB* have been identified by whole exome sequencing (WES) in patients with mild macrothrombocytopenia.²⁴ The difference in phenotype given by AD single

allelic forms of BSS compared with heterozygosity for bi-allelic BSS has yet to be fully explained. A 1.5 to 3.0-Mb hemizygous mostly somatic deletion on chromosome 22q11.2 including *GP1BB* is seen in the Di-George and velocardiofacial syndromes in which multiple developmental defects are often accompanied by mild to moderate macrothrombocytopenia.²¹

Platelet-type von Willebrand disease and type 2B von Willebrand disease

GPIb α has seven leucine-rich repeats and flanking regions near its N-terminus; the mucin-like domain follows with the many negatively charged O-linked oligosaccharides that provide rigidity. In platelet-type von Willebrand disease, AD gain-of-function missense mutations within the leucine-rich repeats (and 1 deletion outside the repeats) promote spontaneous binding of large VWF multimers.²⁵ As a result, the higher molecular weight multimers are decreased or absent in plasma. Cross-linking of platelets by VWF favors platelet clumping and a high sensitivity to ristocetin-induced platelet agglutination. In culture, spontaneous binding of VWF multimers to maturing megakaryocytes inappropriately activates intracellular signaling pathways; as a result, there are fewer proplatelets and they have enlarged tips.²⁶ Furthermore, VWF-bound platelets are rapidly removed from the circulation in a process that is enhanced when aggregates are present. Bleeding is accentuated under conditions of stress, such as pregnancy when circulating large VWF multimers are elevated. Mention should also be made of type 2B von Willebrand disease, also with AD inheritance. In this condition single allele

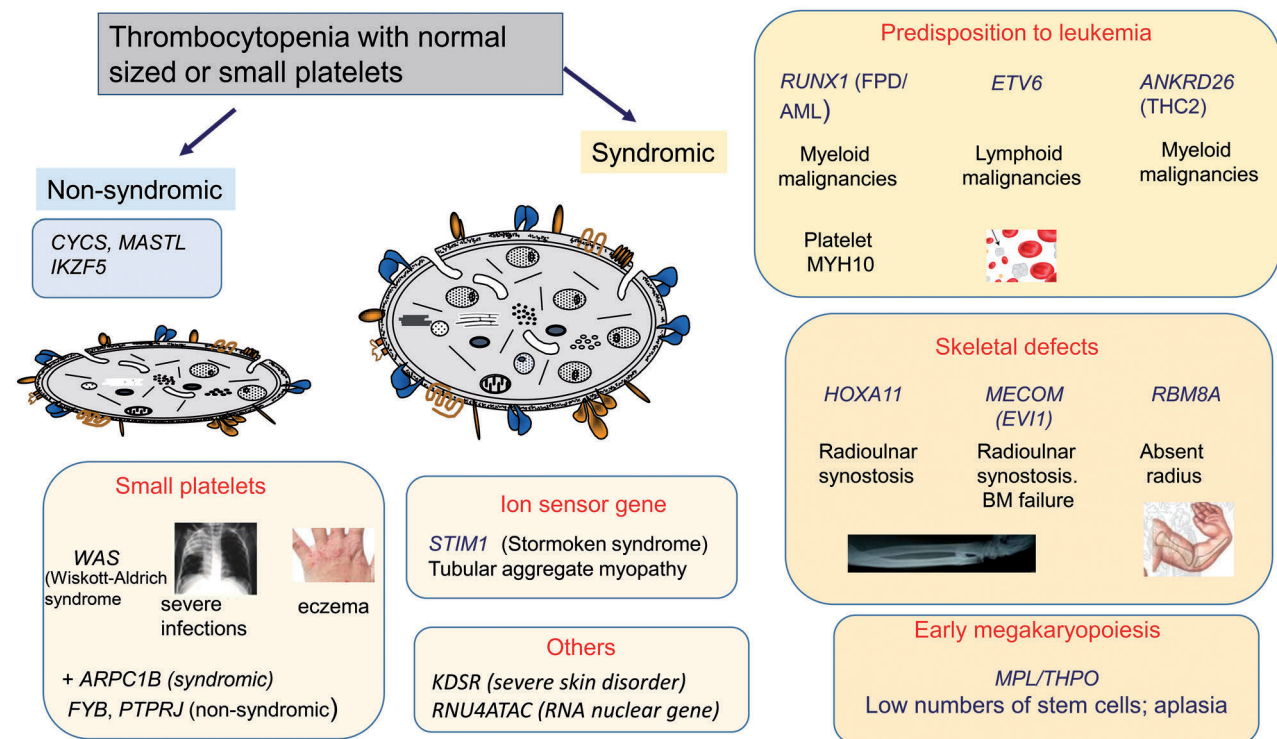


Figure 3. A cartoon showing genes causing non-syndromic and syndromic thrombocytopenias with normal sized or small platelets. The genes are grouped according to the nature of the encoded abnormal protein and to the accompanying secondary condition(s) that define the syndrome. BM: bone marrow.

gain-of-function mutations within exon 28 of VWF result in multimers that bind spontaneously to GPIb α .²⁷ Enlarged platelets and thrombocytopenia are features and the cross-linking of platelets by adsorbed VWF multimers leads to platelet clumping in many patients. Megakaryocytes in culture appear to bind VWF multimers leaking from their own cells; the mature megakaryocytes have larger platelet territories while proplatelet-like protrusions are fewer, shorter and the swellings larger.²⁸ Patients of French-Canadian descent with what was called the “Montreal platelet syndrome”, an inherited macrothrombocytopenia, in fact possessed the VWF p.V1316M mutation. Recent studies on both a mouse model and platelets from a patient with VWF V1316M have shown that platelet aggregation is also reduced due to the loss of essential signaling requirements for α IIb β 3 activation.²⁹ With regards to a possible loss of sialic acid from platelets of these patients, the same group showed that while endogenous neuraminidase translocated to the platelet surface, the desialylation threshold required for thrombocytopenia *in vivo* was not reached; intriguingly, N-glycans on α IIb and β 3 and not GPIb α , were most targeted.³⁰ But both platelet-type von Willebrand disease and type 2B von Willebrand disease are disorders in which increased platelet turnover contributes to the thrombocytopenia.

MYH9-related disease

Myosin, heavy chain 9 (MYH9), a subunit of myosin IIA, mediates intracellular contractile forces generated through ATP hydrolysis and the actin cytoskeleton. AD-inherited MYH9 variants are a common cause of moderate to severe macrothrombocytopenia and platelets can be very large.³¹ Cytochemical or immunofluorescence detection of inclusions (Döhle-like bodies) in leukocytes on blood smears facilitates the diagnosis.³² Myosin IIA is expressed in many tissues and MYH9-related disease will often become syndromic with age; symptoms include glomerulonephritis, potentially leading to renal failure (requiring dialysis or transplantation), sensorial hearing loss, early cataracts and elevated circulating liver enzymes indicating hepatic damage. Historically, combinations of macrothrombocytopenia with these conditions were known as May-Hegglin anomaly, and Epstein, Fechtner and Sebastian syndromes but all were later linked to mutations in MYH9.³³ Disease-causing variants are mostly missense but variants of all types have been described and affect both the N-terminal head or motor domain and C-terminal tail (responsible for dimerization and containing phosphorylation sites).^{33,34} Some residues are mutational hotspots, for example S96 and R702 in the head and R1165 and D1424 in the tail and genotype-phenotype correlations have been linked to disease evolution in MYH9-related disease. Notwithstanding the AD inheritance, some of the mutations are sporadic and somatic germinal mosaicism has been reported. Lacking contractile force, affected megakaryocytes show reduced migration to the vascular sinus and, together with altered proplatelet formation, this results in ectopic but reduced platelet release in the marrow.³⁵ Treatment includes slowing the extra-hematologic effects with cochlear or kidney transplantation and renin-angiotensin inhibitors in some cases.

Gray platelet syndrome and related disorders.

A qualitative disorder characterized by moderate macrothrombocytopenia with “gray-colored” platelets on a stained blood smear, gray platelet syndrome has mostly

AR inheritance. Patients have enlarged platelets lacking α -granules and their storage pool of proteins.³⁶ Thrombocytopenia is often progressive and bleeding highly variable. Enlarged spleens, myelofibrosis, high serum vitamin B12 levels and reduced platelet function help define the phenotype.³⁷ In 2011, three groups using different approaches including next-generation WES and RNA profiling showed that mutations in NBEAL2 caused gray platelet syndrome in large, but distinct cohorts of patients (data reviewed by Chen *et al.*³⁸). NBEAL2 is a scaffolding protein involved in α -granule ontogeny. Mouse *Nbeal2*^{-/-} models recapitulated the gray platelet syndrome phenotype and showed how the lack of the secretory pool of biologically active proteins affects wound healing, and has consequences for thrombosis and inflammation.³⁹ Cultured megakaryocytes from patients with NBEAL2 mutations interacted abnormally with extracellular matrix proteins, including type I collagen, with reduced proplatelet formation and branching.⁴⁰ Extensive emperipoiesis of neutrophils by the megakaryocytes is another feature of gray platelet syndrome. Although altered neutrophil structure and increased infections were reported in early studies on this syndrome, only recently was a role for NBEAL2 in immunity confirmed.⁴¹ New avenues for research on autoimmunity and inflammation in gray platelet syndrome have now opened.

The absence of platelet α -granules is also a characteristic of children with arthrogryposis, renal dysfunction and cholestasis (ARC) syndrome, a severe AR multisystem disorder especially affecting the kidneys and linked to mutations in VPS33B and VPS16B, genes encoding proteins involved in α -granule biogenesis; however, platelet count and size are often normal and this syndrome is not included in Online Supplementary Table S1.³⁸ A paucity of α -granules in platelets of patients with X-linked mutations in GATA1 is explained by its long-distance regulation of NBEAL2.⁴² The transcription factor, GATA1, in complex with its cofactor FOG1 acts as a gene repressor in hematopoietic cell lineages including megakaryocytes and red blood cells. It was first identified as a cause of macrothrombocytopenia with moderate to severe bleeding by Nichols *et al.*, who found a p.V205M mutation in siblings with severe thrombocytopenia and dyserythropoietic anemia.⁴³ Most GATA1 mutations result in dysmegakaryopoiesis with the marrow often containing an abundance of small megakaryocytes; the red blood cell abnormalities include features that can be observed in β -thalassemia and also congenital erythropoietic porphyria.²¹ Phenotypic variation is considerable and the condition often improves with age. A loss of collagen-induced platelet aggregation in some patients remains unexplained. Macrothrombocytopenia, an absence of platelet α -granules and red blood cell defects variably characterize patients with AD germline mutations in GFI1B, a transcriptional repressor and key regulator of hematopoiesis.^{44,45} The macrothrombocytopenia can be accompanied by platelet function defects and myelofibrosis; bleeding is mostly mild or even absent but may be severe after trauma. Abnormal megakaryocyte maturation and proplatelet formation contribute to the macrothrombocytopenia. The phenotype depends on the site and nature of the mutation and the GFI1B isoform affected.⁴⁶ Haploinsufficiency or non-functioning of GATA1 or GFI1B will change the activation of a number of genes coding for proteins maintaining platelet function.

Congenital amegakaryocytic thrombocytopenia

Born with severe thrombocytopenia but normal sized platelets, patients with congenital amegakaryocytic thrombocytopenia lack mature megakaryocytes in the bone marrow. Evolution to critical multi-lineage aplasia occurs before adulthood.^{47,48} In the majority of cases, AR mutations in the *MPL* gene make the cells incapable of binding thrombopoietin; as a result circulating thrombopoietin levels are very high.⁴⁷ Nonsense mutations with a complete loss of Mpl give rise to a severe form (type I) while missense mutations and the presence of residual Mpl may give a milder form of the disease (type II). The mutations lead to a loss of thrombopoietin binding or on rare occasions, altered receptor recycling. In culture, megakaryocytes from the patients with congenital amegakaryocytic thrombocytopenia fail to form colonies. The mutations can also affect stem cell maintenance. Disease severity depends on the extent of the interference with JAK2/STAT and MAPK signaling pathways, with there being residual signaling in type II disease. HSC transplantation has been the treatment of choice.⁴⁸ Progression to aplastic anemia or myelodysplastic syndrome is a risk. Rare homozygous mutations in the *THPO* gene with loss of thrombopoietin production or an inability to bind to Mpl can also lead to bone marrow aplasia. Note that because of the largely hepatic origin of thrombopoietin, these patients are unsuitable for bone marrow transplantation.⁴⁸ Conversely, both *MPL* and *THPO* gain-of-function mutations are a source of familial thrombocytosis.

Wiskott-Aldrich syndrome

Wiskott-Aldrich syndrome (WAS) is an X-linked disorder described by Alfred Wiskott in 1937 and Robert Aldrich in 1954. The syndrome is characterized by severe immunodeficiency, thrombocytopenia and small platelets. The clinical spectrum includes eczema, infections, autoimmune hemolytic anemia and cancer; bleeding is mostly mild but can be severe if the platelet count is very low and can prove fatal.⁴⁹ Hemizygous mutations in the *WAS* gene abrogate expression or alter function of WAS protein: the protein has multiple roles in the early stages of actin polymerization and in signal transduction with virtually all hematopoietic lineages affected.^{50,51} Megakaryocytes of WAS patients form proplatelets prematurely and shed platelets ectopically in the marrow.⁵² There is also a peripheral component to the thrombocytopenia with circulating autoantibodies and platelet destruction in the spleen making WAS a rare inherited thrombocytopenia in which splenectomy is still performed. Patients lacking WAS protein have a worse phenotype than those with residual amounts; milder forms are known as X-linked thrombocytopenia. Allogeneic HSC transplantation, first performed for WAS over 40 years ago, has a good prognosis for severe cases with a high risk of bleeding and also benefits immunodeficiency.⁵³ In the absence of matched donors gene therapy using a lentiviral vector encoding functional WAS protein is a promising alternative, even if full normalization of the platelet count is not achieved.⁵⁴

Familial platelet disorders with predisposition to myeloid or lymphoid malignancies

Defects of transcription factors are a major source of inherited thrombocytopenias (Figure 1). Those that inter-

fere with the early stages of megakaryocyte maturation are often accompanied by a risk of developing myeloid or lymphoid malignancies and this was first shown for AD thrombocytopenia caused by mutations of *RUNX1*.⁵⁵⁻⁵⁷ The thrombocytopenia is mild and platelet volume increases are modest, but platelet function is defective and a reduced dense granule secretion contributes to the mostly mild bleeding. Disease-causing variants occur across the gene with emphasis on the Runt homology domain that mediates DNA-binding and dimerization with the core binding factor (CBFA β), a complex essential for regulated proliferation and differentiation of HSC and normal megakaryopoiesis as well as suppression of erythroid gene expression. *RUNX1* mutations interfere with ploidy and prolong the expression of the cytoskeletal protein MYH10, whose natural loss triggers the switch from mitosis to endomitosis; the result is an abundance of immature megakaryocytes that fail to differentiate properly.²¹ Furthermore, *RUNX1* directly or indirectly regulates the synthesis of a number of platelet proteins thereby altering the function of those platelets that are affected. Decreased DNA repair, a pro-inflammatory environment and the prolonged life of HSC predispose patients to acute myeloid leukemia and related conditions. Most of the genetic variants act through haploinsufficiency but, significantly, those that act in a dominant negative manner have a higher probability of causing malignancy.⁵⁷

Myeloid malignancies and myelodysplastic syndromes are also a risk for patients with mutations in the 5' untranslated region of *ANKRD26*, which are associated with mostly moderate thrombocytopenia, mild bleeding and normal sized platelets (a condition also known as thrombocytopenia 2, *THC2*).⁵⁸⁻⁶⁰ Unexplained findings in some patients are a low density of $\alpha 2\beta 1$ integrin, decreased numbers of platelet α -granules and large, particulate structures formed of ubiquitinated proteins or proteasomes. As for mutations of *RUNX1*, patients with *ANKRD26* mutations have downregulated megakaryocyte maturation leading to an abundance of cells with hypolobulated nuclei. Mechanistically, mutations of the 5' untranslated region of *ANKRD26* prevent downregulation of this gene by *RUNX1* and *FLI1*, leading to increased *ANKRD26* protein with a lack of repression in the terminal stages of megakaryopoiesis.⁶⁰ Extramedullary hematopoiesis, a characteristic of inherited hemolytic anemia, and myeloproliferative and myelodysplastic syndromes, was reported in a case with *ANKRD26*-related thrombocytopenia.⁶¹ It should be noted that *THC2* also includes the Ser/Thr kinase *MASTL* without a tendency for malignancy, dealt with in a later section.

Mutations of *ETV6* lead to AD thrombocytopenia and a predisposition to acute lymphoblastic leukemia.⁶² *ETV6* is a tumor repressor gene with close links with *FLI1*. Red cell macrocytosis is said to accompany the thrombocytopenia in some families. An early study involving 130 families with suspected inherited thrombocytopenias identified *ETV6* gene variants in seven of them; four of the family members had developed B-cell acute lymphoblastic leukemia during childhood.⁶³ Thrombocytopenia was moderate as was the bleeding tendency; platelet size was normal but platelet spreading on fibrinogen was defective. Megakaryocytes in culture produced fewer proplatelets. Mutations within the consensus ETS DNA binding sites of *ETV6* resulted in reduced nuclear localization and transcriptional repression with cytoskeletal genes especially

affected. One mutation (p.R369W) involved a residue previously described as a somatic mutation in different forms of leukemia and cancer.⁶⁴

Linkage with skeletal disorders

Genetic defects responsible for inherited thrombocytopenias can be syndromic and involve a wide range of other organs and tissues as we have already seen for *MYH9*-related disease and WAS. Here we provide four examples in which the disease includes well-defined skeletal defects. The Paris-Trousseau syndrome combines macrothrombocytopenia and a panoply of developmental defects including dysmorphogenesis of the face and digits, possible pancytopenia, cardiac abnormalities and mental retardation, which are all characteristic of Jacobsen syndrome.²¹ The inheritance is largely AD with single allele expression of a small deletion in chromosome 11q23 that includes *FLI1*, an ETS transcription factor family member and a main regulator of megakaryopoiesis.⁶⁵ Genes targeted by *FLI1* include *MPL*, *GPIBA*, and *ITGA2* and a lack of transactivation early in megakaryocyte development due to a transient hemizygous loss of the affected allele is responsible for the pathology.⁶⁵ Dual populations of normal and immature megakaryocytes are generated, the latter with reduced polyploidization and persistence of the cytoskeletal protein, MYH10 (also see the section on *RUNX1*). Some of the α -granules in the enlarged platelets appear fused and giant.

In the thrombocytopenia with absent radius (TAR) syndrome, bilateral radius aplasia and various other developmental defects are accompanied at birth by severe thrombocytopenia but normal sized platelets. Initial studies identified a chromosome 1.21.1 heterozygous microdeletion in patients with TAR syndrome, but the genetics was only fully resolved when WES showed the necessity of a combination of the microdeletion including the *RBM8A* gene on one allele with one of two rare single nucleotide polymorphisms in regulatory regions of *RBM8A* on the second allele.⁶⁶ In fact, *RBM8A* codes for Y14, a nuclear and cytoplasmic protein that interacts with mRNA produced by splicing; how it relates to the TAR phenotype remains largely unknown. Hematopoietic progenitors have a reduced response to thrombopoietin and fail to differentiate into megakaryocytes in the marrow. Other hematologic defects include leukocytosis in some patients; enigmatically, the platelet count may correct with age.⁶⁷ TAR syndrome is to be distinguished from radio-ulnar synostosis with amegakaryocytic thrombocytopenia caused by a heterozygous truncating *HOXA11* mutation (RUSAT1) or, as determined by WES screening, by *de-novo* missense mutations in *MECOM* (RUSAT2) encoding oncoprotein EVI1 leading to altered activator protein-1 and transforming growth factor- β -mediated transcriptional responses.^{68,69} Both *HOXA11* and *MECOM* mutations cause defects in the early phase of megakaryopoiesis and the risk of trilineage marrow aplasia makes the patients candidates for HSC transplantation.

Defects of platelet biogenesis due to cytoskeletal protein defects

We have already highlighted how mutations affecting the myosin IIA heavy chain are a frequent cause of macrothrombocytopenia in *MYH9*-related disease. This

prompted research for mutations of genes encoding other cytoskeletal proteins in patients with congenital thrombocytopenia. X-linked mutations in *FLNA*, encoding filamin-A (FLNA), cause a syndromic disorder combined with periventricular nodular heterotopia/otopalatodigital syndromes and other developmental defects.²¹ It can also be associated with Ehlers-Danlos syndrome. We first showed that three patients in France also had macrothrombocytopenia and that bleeding could be severe.⁷⁰ Characterization of their genotype was aided by reports that mice with FlnA-null megakaryocytes prematurely release large and fragile platelets that are rapidly removed from the circulation.⁷¹ Curiously, platelets of some patients had giant α -granules. Cultured megakaryocytes from patients extended proplatelets with large swellings and released giant platelets.⁷¹ Filamin A promotes branching of actin filaments as well as anchoring membrane receptors and *FLNA* mutations associate with a loss of platelet adhesive function. Interestingly, a rare gain-of-function missense mutation caused isolated macrothrombocytopenia.⁷¹ Initially, *FLNA* mutations were speculated to cause macrothrombocytopenia through loss of the GPIb-FLNA interaction and involvement of RhoA (a GTPase); more recently an alternative mechanism has been proposed based on the loss of α IIb β 3-filamin A signaling.^{11,72}

Hearing loss and macrothrombocytopenia with moderate bleeding were reported in patients from two unrelated families with a heterozygous gain-of-function truncating mutation in *DIAPH1*; a variant identified by WES followed by crosschecking variants against a database of genes causing deafness.⁷³ *DIAPH1* is a member of the formin family of cytoskeletal proteins and is a regulator of actin filament formation. The above gain-of-function mutation resulted in cytoskeletal dysregulation and megakaryocytes with reduced but premature proplatelet formation similar to that seen in *MYH9*-related disease. The defect was linked to a loss of autoinhibition within the diaphanous autoregulatory domain and was distinguished from a frameshift modification that produced hearing loss in a group of families in South America but without hematologic problems.⁷³ Brief mention should also be made of moderate macrothrombocytopenia associated with a cluster of missense mutations detected by next-generation sequencing (NGS) in five out of 13 cases with AD missense mutations in *CDC42*.⁷⁴ *CDC42* is a small GTPase and a Rho family member and the mutations were said to affect the change between the active and inactive states of the molecule. The disease is syndromic and is associated with various developmental defects including intellectual disability, brain defects, muscle tone abnormalities, facial dysmorphism, and cardiac abnormalities although these were somewhat less apparent for patients with mutations causing macrothrombocytopenia. So far, few platelet function studies appear to have been performed but, on the basis of mouse models, both megakaryocyte maturation and platelet function are likely to be affected.¹¹ So far, bleeding has not been reported as a problem for the patients.

Mutations of *TUBB1* encoding β 1-tubulin cause macrothrombocytopenia through altered association with α -tubulin and defective microtubule assembly.^{75,76} The defect leads to altered megakaryocyte maturation with the production of fewer proplatelets with large tips but there is a high degree of phenotypic and genotypic variability and while the causal effect of some variants is clear,

other predicted pathological variants have little effect on platelet count or size. Interestingly, *TUBB1* dysfunction may lead to genome instability; co-segregation with myeloid malignancy has been reported, but this tendency needs confirmation as *TUBB1* mutations are relatively common. Thyroid dysgenesis has also been linked to *TUBB1* mutations in some patients. Variants identified by WES in exons 5 and 6 of *ACTB* encoding β -cytoplasmic actin cause syndromic thrombocytopenia by compromising microtubule organization during the final stages of megakaryocyte maturation, but bleeding has not been reported.⁷⁷ The defect has been located in five families and is accompanied by platelet size variability including large forms; associated and highly variable clinical features are given in *Online Supplementary Table S1*. The defect intervenes in the final stages of platelet biogenesis and preplatelet (a purported intermediate platelet precursor) fragmentation but no defects were seen in megakaryocyte proplatelet formation in culture.⁷⁷ Interestingly, variants in exons 2 to 4 give rise to a severe developmental disorder, Baraitser-Winter cerebrofrontofacial syndrome, but no thrombocytopenia.⁷⁷

Single allele missense mutations in *ACTN1* encoding α -actinin were first identified in Japanese patients with moderate thrombocytopenia and in a large French pedigree by WES and by genome-wide linkage analysis.^{78,79} Their presence was later revealed as quite common in a non-syndromic form of thrombocytopenia with mild or no bleeding although blood loss can be a problem after surgery. α -Actinin is a dimeric protein that cross-links actin filaments into bundles; mutations affecting functional domains act in a dominant-negative manner to disrupt actin filament organization and proplatelet structure in megakaryocytes. Platelet size changes are variable between patients. It is a quite common form of mild inherited thrombocytopenia.⁷⁸⁻⁸⁰

A final cytoskeletal gene identified by WES in two human pedigrees with macrothrombocytopenia is *TPM4* encoding tropomyosin 4, another actin-binding protein.⁸¹ A premature stop codon on a single allele segregated with platelet size increases and a low platelet count. Gene identification was helped by phenotype comparison with a mouse conditional knockout model and confirmed by short hairpin RNA knockdown of *TPM4* in normal human megakaryocytes. Platelet function was affected although bleeding was mild. Megakaryocytes in culture produced abundant proplatelets but with fewer branches and enlarged tips, the latter being a standard finding in patients with defects of genes encoding for cytoskeletal proteins, which results in a dynamic re-organization of the cytoskeleton.

Quite remarkably, all of the eight genes encoding cytoskeletal proteins and which give rise to macrothrombocytopenia do so with AD inheritance (*Online Supplementary Table S1*).

Abnormal integrin interactions with extracellular matrix proteins

The final steps of megakaryocyte maturation and the migration of these cells towards the vascular sinus depend not only on cytoskeletal proteins, but also on interactions between surface receptors and extracellular matrix con-

stituents. Glanzmann thrombasthenia is the classic disorder of platelet function; with AR inheritance; bleeding occurs because thrombus formation and platelet aggregation fail in the absence or non-functioning of integrin α IIb β 3. Caused by AR mutations in *ITGA2B* and *ITGB3*, the platelet count is normal in the absence of major bleeding.⁸² However, rare gain-of-function mutations affecting the structure of α IIb or β 3 can give rise to macrothrombocytopenia. Our group made the initial report in 1998, describing a single allele p.R995Q mutation in the α IIb cytoplasmic domain; this was later shown to be associated with a null allele.⁸³ Platelet aggregation was much decreased with surface α IIb β 3 at 18%, the macrothrombocytopenia was modest and bleeding infrequent. The affected residue forms an intracellular salt bridge with D723 of β 3, itself mutated in a variant of Glanzmann thrombasthenia with macrothrombocytopenia (detailed in Nurden *et al.*⁸²). Breaking this bond leads to conformational changes that are transmitted to the extracellular domains with a “partial” activation of α IIb β 3. Since these reports, macrothrombocytopenia with AD inheritance has been shown for other intracytoplasmic or membrane proximal gain-of-function variants affecting α IIb β 3.^{84,85} One hypothesis is that the partially activated integrin on megakaryocytes modifies megakaryocyte contact with extracellular matrix proteins in the marrow. This may promote cytoskeletal re-organization with proplatelets having fewer branches and enlarged tips. Interestingly, a gain-of-function mutation affecting α IIb β 3 had a dominant phenotypic effect with respect to a loss-of-function variant.⁸⁶

Next-generation sequencing is expanding the landscape of inherited thrombocytopenias

Careful phenotyping and the use of NGS have led to the identification of a number of new genes responsible for inherited thrombocytopenia with or without large platelets or accompanying platelet function defects. Some have been discussed in preceding sections, others, confined to a limited number of families or of unusual phenotype and with links to signaling pathways, are presented below. All of the upwards of 40 genes now recognized as causative of inherited thrombocytopenia are included in *Online Supplementary Table S1*.

Microthrombocytopenia

The classic disorder with a low platelet count and small platelets is WAS, but microthrombocytopenia and a similar phenotype including eczema, leukocytoclastic vasculitis, eosinophilia and elevated IgA and IgE levels was recently linked in two unrelated patients by WES to AR mutations in *ARPC1B*, a gene that encodes a subunit of the human actin-related protein 2/3 complex (Arp2/3).⁸⁷ In fact, Arp2/3 acts with WAS protein in regulating the branching of actin filaments and plays a central role in cell migration, vesicular trafficking and cytokinesis. Platelets from the patients showed defective spreading. Loss of Arp2/3 function is syndromic in that it predisposed to inflammatory disease although many of the immunodeficiencies characteristic of WAS have so far not been observed. Microthrombocytopenia was also linked by NGS in two consanguineous families to a loss-of-function homozygous AR mutation in *FYB*, encoding the cytosolic

adaptor protein ADAP (SLAP-130) for the Fyn tyrosine kinase.⁸⁸ The bleeding syndrome in these families was mild. As discussed by the authors, studies using mouse *Adap^{-/-}* models showed that the small platelets had a short survival (also a feature of WAS) and defective α IIb β 3 activation, findings confirmed in the patients. Subsequent whole sternum three-dimensional confocal microscopy and intravital two-photon microscopy detected reduced megakaryocyte maturation in *Adap^{-/-}* mice with signs of ectopic release of platelet-like particles within the bone marrow.⁸⁹ Biallelic mutations in *PTPRJ*, encoding CD148, a master regulator of Src family kinases and the most abundant membrane-bound tyrosine phosphatase in platelets and megakaryocytes, were next shown to result in non-syndromic microthrombocytopenia in two siblings with mild bleeding.⁹⁰ Loss of CD148 was accompanied by platelet aggregation defects, particularly in relation to GPVI signaling. The thrombocytopenia was again linked to ectopic platelet release within the bone marrow, a characteristic of WAS.

Src, a universal tyrosine kinase

A gain-of-function, heterozygous E727K mutation was identified in *SRC* by WES in nine members of a large family; it was linked to thrombocytopenia, a low content of α -granules and reduced platelet function.⁹¹ The thrombocytopenia was syndromic with myelofibrosis, the disease being accompanied by bone defects including mild facial dysmorphism. The marrow showed trilineage dysplasia with immature megakaryocytes poorly able to form proplatelets. Platelets were variable in size and morphologically abnormal; they responded poorly to collagen with reduced GPVI signaling. The gain-of-function mutation was suggested to lift autoinhibition with spontaneous Src activation and upgraded protein tyrosine phosphorylation. The abnormalities were reproduced in a zebrafish model. The mutation may have a feedback on Mpl function.

Mutations affecting ion gradients

Stormorken syndrome was described many years ago as a “multifaceted bleeding syndrome” in which an unusual form of macrothrombocytopenia was associated with reduced platelet survival and upgraded prothrombin consumption.⁹² It was linked to a spontaneous expression of phosphatidylserine on platelets. Platelet function and thrombus formation under flow were affected. Much later it resurfaced as a syndromic macrothrombocytopenia with a range of clinical features including mild anemia, asplenia, myopathy with tubular aggregates, miosis, immune dysfunction, ichthyosis and dyslexia.^{93,94} Bleeding is life-long but is mostly mild. Heterozygous gain-of-function AD variants in *STIM1* identified by WES are the cause of the disease. *STIM1* is a Ca^{2+} -sensor within the endoplasmic reticulum; on Ca^{2+} -depletion conformational changes induce its coiled-coil 1 domain to elongate and interact with ORAI1, a surface membrane channel that mediates store-operated calcium entry into cells. ORAI1 can be affected in rare cases with miosis and non-progressive myopathy but without significant platelet abnormalities. The mutations make *STIM1* (and secondarily ORAI1) constitutively active, favoring Ca^{2+} entry into platelets and presumably megakaryocytes. The York platelet syndrome, with large and morphologically abnormal platelets with giant opaque organelles also had gain-of-function mutations in *STIM1* thereby expanding the spectrum of

Stormorken syndrome.⁹⁴ WES and comparison with mouse models led us to identify variants in the *TRPM7* gene in two French index cases with macrothrombocytopenia and with a possible link to atrial fibrillation in one family.⁹⁵ *TRPM7* is both a kinase and an ion channel primarily linked to Mg^{2+} homeostasis; its absence in mice or disease-causing variants in man were both accompanied by cytoskeletal changes in megakaryocytes.

Other miscellaneous defects

Patients in three families with an often strong bleeding history, moderate thrombocytopenia and enlarged platelets were linked by WES to heterozygous mutations within *SLFN14* (Schlafen family member 14).⁹⁶ *SLFN14* locates to the nucleus, where it acts as an endoribonuclease and is possibly involved in RNA surveillance. The variants in patients with macrothrombocytopenia localize to the ATPase-AAA-4 domain. The protein is known to associate with ribosomes where it regulates RNA degradation; *SLFN14* expression was reduced in the patients and a dominant-negative effect was suggested.⁹⁷ Platelet dense granule content was low and platelet aggregation particularly reduced with collagen, modestly reduced and reversible with ADP but normal with arachidonic acid. In a separate study, severe macrothrombocytopenia but with AR inheritance was linked through WES to a homozygous missense mutation in the *PRKACG* gene encoding the gamma-catalytic subunit of the cyclic adenosine monophosphate (cAMP)-dependent protein kinase A.⁹⁸ Protein kinase A phosphorylates multiple substrates in platelets and in its absence platelet activation and cytoskeletal organization (with extensive degradation of filamin A) were impaired. However the very low platelet count ($<10 \times 10^9/\text{L}$) precluded platelet aggregation testing. Significantly, megakaryocytes from this patient had a defect in proplatelet formation. Next in this section are AR mutations in *G6B* (*MPIG6B*) encoding the megakaryocyte and platelet inhibitory receptor, G6b-B, a critical regulator of hematopoietic lineage differentiation and megakaryocyte function and platelet production.⁹⁹ The mutations were detected by WES screening of four families with macrothrombocytopenia. One feature was the presence of focal myelofibrosis atypically even in children. Bleeding was moderate and accompanied by anemia and leukocytosis. In a mouse model megakaryocytes were abnormal with reduced proplatelet formation. G6b-B regulates the activity of the tyrosine phosphatases Shp1 and Shp2. Nonetheless, platelet aggregation to ADP was only minimally affected.

Severe thrombocytopenia observed in four Spanish families was associated with a disorder of ceramide biosynthesis with WES linking the disease to AR mutations in *KDSR* encoding 3-ketodihydrosphingosine reductase, a lipid enzyme that localizes to the endoplasmic reticulum.¹⁰⁰ Interestingly, in at least two of these cases the platelet count was normal at birth but fell rapidly to around $30 \times 10^9/\text{L}$ or lower. Impaired platelet biogenesis was speculated to be due to decreased synthesis of sphingosine-1 phosphate but formal proof of this is lacking. Another disorder in which the platelet count falls after birth is Roifman syndrome in which moderate thrombocytopenia accompanies a variable syndromic disorder characterized by growth retardation, spondylo-epiphyseal dysplasia, cognitive delay and hypogammaglobulinemia.¹⁰¹ Interestingly, the disease is driven by AR variants in the small RNA nuclear gene *RNU4ATAC* that intervenes in intron splicing. The platelets

were unusually round and had altered tubulin and actin levels with *DIAPH1* being one of the affected genes.

Finally, mention must be made of *IKZF5* encoding a transcription factor known as Pegasus that was highlighted by whole genome sequencing of over 13,000 individuals enrolled in the National Institute for Health Research Bioresource and including 233 cases of isolated thrombocytopenia.¹⁰² Various causal missense variants were detected in patients with isolated thrombocytopenia but mild or no bleeding; the mutations (sometimes *de novo*) were proposed to interfere with DNA binding and to selectively alter the expression of a series of proteins expressed in megakaryocytes and platelets. The thrombocytopenia was mild and platelet size was normal. The platelet α -granule content was low but the platelet aggregation response was reported as inconsistent. The megakaryocytes produced fewer proplatelets.

Thrombocytopenia, apoptosis and deficient glycosylation

Early apoptosis with phagocytosis of platelets by macrophages in the spleen or glycosylation changes followed by platelet clearance in the liver are potential causes of inherited thrombocytopenia. Although evidence for such mechanisms remains incomplete, the identification of some mutations, largely by NGS, has revived interest, particularly in deficient glycosylation.

Apoptosis

Non-syndromic mild AD thrombocytopenia but with little or no bleeding and platelets of normal size is associated with mutations in the *CYCS* gene encoding mitochondrial cytochrome c, a disease first reported in New Zealand.^{103,104} Although normal-looking megakaryocytes were present in the bone marrow, the number of naked nuclei was increased. Their presence as well as platelets in the marrow space was indicative of ectopic release. Electron microscopy revealed platelets lacking glycogen stores and the microtubule coil. Culture of megakaryocytes from the patients showed that abnormal and normal platelets were both released. Whether or not *CYCS* mutations, so far limited to three families, lead to loss of mitochondrial inner membrane potential and platelet phosphatidylserine expression remains speculative. Mention must also be made of a missense p.E167D mutation in *MASTL*, coding for a microtubule-associated Ser/Thr kinase, in a large family first reported many years previously. The mutation was linked to moderate thrombocytopenia (with normal sized platelets), incomplete differentiation of high ploidy megakaryocytes and a propensity to mild bleeding.^{58,105} Recent studies on a mouse knock-in model suggest that this is a gain-of-function mutation leading to platelet survival changes and to platelets that extend unusually long pseudopods and contain hyper-stabilized microtubules.¹⁰⁶ In mice, *Mastl* inhibits protein phosphatase 2, an important negative regulator of several major platelet activation pathways. The result is an increased propensity of platelets to form aggregates, reduced platelet survival and increased signs of apoptosis.

Desialylation and other glycosylation changes

An early study showed macrothrombocytopenia and

neutropenia in a patient with a specific defect in α -2,3-sialylation and rapid platelet clearance by the Ashwell-Morell receptor in the liver but the gene defect was not identified.¹⁰⁷ More recent studies using WES have linked macrothrombocytopenia with AR mutations of *GNE* encoding UDP-N-acetylglucosamine 2-epimerase/N-acetylmannosamine kinase, a bi-functional enzyme essential for N-acetylneuraminic acid synthesis (the principle sialic acid of human platelets).¹⁰⁸⁻¹¹⁰ Interestingly *GNE* mutations are also a cause of myopathy and in the above studies macrothrombocytopenia was either syndromic or isolated depending on the report. Severe menorrhagia and bleeding into the corpus luteum in affected women were noteworthy. Platelets were large and the numbers of reticulated (young) platelets often increased, features suggesting accelerated platelet clearance. Precise quantification of the platelet sialic acid deficiency and a direct measure of platelet survival have not, however, been made.

A necessary step in the synthesis of oligosaccharides is the transport of cytidine monophosphate-bound sialic acid to the Golgi apparatus. This requires a transporter protein *SLC35A1*, whose molecular deficiency was recently reported in two siblings with moderate thrombocytopenia, giant platelets, and mild bleeding.¹¹¹ The macrothrombocytopenia is syndromic, featuring delayed psychomotor development, epilepsy, ataxia, microcephaly and choreiform movements. Exome sequencing highlighted a homozygous missense mutation in *SLC35A1* in both siblings; their consanguineous parents were heterozygous. Lectin binding confirmed abnormally high β -galactose exposure on platelets from the patients and increased numbers of reticulated platelets. Bone marrow biopsies showed a high percentage of immature megakaryocytes, yet in culture megakaryocytes from the patients showed normal maturation and proplatelet formation. However quantification of platelet survival using a non-obese diabetic/severe combined immunodeficiency mouse model confirmed that the patients' platelets had a very short lifespan. In a separate study, severe thrombocytopenia with enlarged platelets and dysplastic megakaryocytes was the characteristic of six members of a consanguineous family in whom WES and homozygosity mapping revealed a homozygous mutation in *GALE*, encoding UDP-galactose-4-epimerase, an enzyme responsible for UDP-galactose inter-conversion with UDP-glucose and UDP-N-acetylglucosamine inter-conversion with UDP-N-acetylglucosamine.¹¹² Some individuals also showed mild anemia and febrile neutropenia while galactosemia is a feature of mutations of this gene. With predicted protein instability, the enzyme retained 40% of its normal activity. Knockdown of *GALE* in hematopoietic cells slowed the proliferation of these cells in liquid culture; larger colonies possibly reflected an increased presence of immature cells.

Macrothrombocytopenia and sitosterolemia

An unusual inherited macrothrombocytopenia with epigenetic or environmental implications is sitosterolemia. In this condition, giant platelets associate with AR mutations in *ABCG5* and *ABCG8*, genes which code for proteins that act as cellular transporters of plant sterols, the latter accumulating at high levels in blood and tissues.¹¹³ Xanthomas, premature atherosclerosis and hemolytic anemia are other

features; not all patients develop hematologic abnormalities while macrothrombocytopenia can also be isolated. Studies in mice show knock-on effects with sterol intercalation within the demarcation membrane system of megakaryocytes leading to release of hyper-reactive enlarged platelets with deregulation of multiple signaling pathways including GPIIb α shedding.¹¹⁴

Diagnosis

The continuing difficulties in diagnosis of inherited thrombocytopenias should not be underestimated. While classic disorders such as BSS, *MYH9*-related disease and WAS are now relatively straightforward to identify, the majority are not and in the absence of a well-defined family history of bleeding, new cases can still be confused with immune thrombocytopenic purpura. Diagnostic algorithms with steps based on clinical data and laboratory testing aid the work-up and management of patients.¹¹⁵⁻¹¹⁸ The widespread use of whole blood electronic counters to evaluate platelet count and size has helped, while assessing platelet function, distinguishing between syndromic or non-syndromic forms, identifying associated hematologic or marrow defects are important parts of any strategy. A successful diagnosis avoids unnecessary splenectomy and/or the use of drugs given for immune thrombocytopenic purpura. It helps to predict disease evolution, and is indispensable for selecting patients for HSC transplantation or gene therapy. Noteworthy advances have been the application of Human Phenotype Ontology terms and the identification of phenotype clusters of associated pathologies as an aid to establishing phenotype/genotype relationships.¹¹⁹ Nonetheless preparing an extensive Human Phenotype Ontology listing is not always compatible with day-to-day hospital practice. Classic tests for evaluating platelet function, such as aggregometry (Born platelet aggregometer, impedance aggregometry or other methods), secretion assays, flow cytometry, western blotting and electron microscopy, are time consuming, expensive to perform and require trained personnel. Critically, many such tests are difficult or impossible to perform when the platelet count is low. Cytochemical or immunofluorescence staining of blood smears is a recognized first step for detecting enlarged platelets, and is particularly useful in third-world countries.^{32,117} The evaluation of platelet spreading on single protein substrates provides more information.¹²⁰ The use of computer-based high-throughput testing of platelet function and thrombus formation under flow on extracellular matrix proteins on microchips is full of promise but has been little tested for thrombocytopenias.¹²¹

As highlighted throughout our review, applying NGS to inherited thrombocytopenias is greatly expanding the list of causative genes as well as increasing the number of variants implicated in the classic diseases. The initial success of WES in genotyping gray platelet syndrome and the TAR syndromes led to the BRIDGE-Bleeding and Platelet Disorders (BRIDGE-BPD) project, orchestrated by Professor W. Ouwehand, which combines the unique sequencing and bioinformatics resources of the Sanger Institute in Cambridge (UK).¹²² The Genotyping and Platelet Phenotyping (GAPP) consortium led by Professor S. Watson in Birmingham, UK has been another major player.¹²³ As the number of causal genes for all forms of

inherited platelet disorders increased, BRIDGE-BPD and GAPP both put together platforms to test patients for potentially pathogenic variants against previously identified target genes concentrating on exomes, untranslated regions and selected intronic regions.¹²⁴⁻¹²⁷ Indeed, GAPP designed a gene panel specific for inherited thrombocytopenias.¹²⁷ In contrast, the ThromboGenomics Consortium (Department of Haematology, University of Cambridge, UK) included a limited number of genes causal for other blood and thrombotic disorders; the panel was regularly updated and a large cohort of 2,396 patients screened.^{125,126} The use of NGS and high-throughput procedures for diagnosing platelet disorders including thrombocytopenias has quickly expanded worldwide as is illustrated by reports from Italy, Japan, Spain, France, Holland and Scandinavia as well as North America.^{46,60,77,78,80,87,108,113,128, 129}

The question now is not whether to apply NGS procedures in the mainstream of diagnosis but when and how.¹²⁸ Certainly, a strong argument can now be made to use them upfront: early identification of a causal mutation in a known gene will avoid much unnecessary biological characterization, as we have stated recently in this journal.¹³⁰ It is certainly necessary if prenatal diagnosis or HSC transplantation is on the agenda. Nonetheless, upwards of 200 potential gene variants can be located for each patient, so prioritizing and filtering the variants is key.¹³¹ Variant selection includes the exclusion of synonymous variants and those with a minor allele frequency >0.01 in the normal population. Therefore, in the absence of a previously validated mutation in a known causal gene for inherited thrombocytopenia much care must be taken. Only for a limited number of cases can linkage in large families be performed. Data evaluation in terms of quality control, depth of coverage of each gene, the conservation of affected nucleotides or amino acids, the choice of *in silico* pathogenicity prediction software, and the classification of variants according to appropriate genetic guidelines have been nicely reviewed elsewhere.^{125,131}

In taking account of these advances, the fundamentals for a systematic approach to the diagnosis and management of inherited thrombocytopenia remain largely those expertly outlined in a recent European Hematology Association consensus report on mild and moderate bleeding disorders, to which the reader is directed.¹³² In the context of immune thrombocytopenia, a systematic approach includes careful primary tier assessment of the basic clinic-pathological information for each new patient prior to next stage investigations and, if needed, referral to a specialist center. The recommendations in this European Hematology Association report are very useful in emergency situations and for prevention or control of spontaneous bleeding, such as epistaxis or gum bleeding and at-risk situations, including dental and surgical procedures or traumatic events when immediate practical decisions must be made.

Treatment

As with all inherited platelet disorders, spontaneous bleeding includes epistaxis, gum bleeding, easy bruising and petechiae while gastrointestinal hemorrhage occurs in some severe cases; bleeding may be prolonged after cuts, trauma, or surgery, while for women, menorrhagia and childbirth are added risks.^{133,134} For example, in a European

study of pregnancy, the risk of bleeding was greater when mothers had a severe bleeding history and a platelet count below $50 \times 10^9/L$. Platelet count appeared more important as a parameter than the genetic cause of the inherited thrombocytopenia.¹³⁵ Clearly, studies support the classic theory that a primary role of platelets is to maintain vascular integrity.¹³⁵ Nevertheless, many subjects with new forms of inherited thrombocytopenias have modest reductions in platelet count and will bleed rarely or not at all in normal life. Bleeding in such patients depends not only on the extent of the fall in platelet count but also on the nature of accompanying functional defects. Furthermore, much evidence has accumulated on the non-hemostatic roles of platelets.¹³⁶ Using mouse models, Goerge *et al.* observed that thrombocytopenia rapidly leads to bleeding in inflamed skin and brain due to the loss of vascular integrity.¹³⁷ Much needs to be learned on how the genetic defects described in our review influence the non-hemostatic roles of platelets.

Managing bleeding in inherited thrombocytopenia is much the same as in all inherited platelet disorders, with platelet and red blood cell transfusions being the first options. The use of recombinant activated factor VII is especially recommended in BSS in which the absence of a major surface constituent (GPIb-IX-V) makes isoantibody formation likely and platelet transfusion ineffective.¹³⁸ Tranexamic acid or local measures are the most frequent options for mild bleeding and tranexamic acid is counseled prior to surgery or childbirth if the thrombocytopenia is severe, with platelet concentrates on standby. A quantitated bleeding score, such as the International Society of Thrombosis and Haemostasis Bleeding Assessment Tool, is useful for assessing disease severity but will not predict bleeding risk.¹³⁹⁻¹⁴¹ Curing the disease is still at its debut for inherited thrombocytopenia. Human stem cell and allogeneic bone marrow transplants have been used very successfully in children with WAS in whom the immunodeficiency is accompanied by a major bleeding risk.⁵³ It has also been used in congenital amegakaryocytic thrombocytopenia and more recently in gray platelet syndrome, in which a positive effect was noted on myelofibrosis, but each procedure has its complications in terms of donor matching and the choice of conditioning regime.^{21,48,142} Lentivirus-based gene therapy is already a proven therapy in WAS when donor-matching for HSC transplantation is a problem, although restoration of the platelet count remains incomplete.⁵⁴ Clearly the gain *versus* risk profile for the patient must be evaluated case-by-case and current gene therapy procedures can only be considered when a patient's long-term survival is in question or perhaps when CRISPR-Cas gene editing becomes available. One highly promising, non-invasive approach to raising the platelet count is the use of the thrombopoietin-mimetics, eltrombopag or romiplostim.¹⁴³ Although bleeding is generally mild in *MYH9*-related disease, eltrombopag was first used successfully prior to surgery in a case with aggravated thrombocytopenia over 10 years ago.¹⁴⁴ Thrombopoietin-mimetics have more recently been used for a patient with a *DIAPH1* mutation prior to hip arthroplasty and as a "bridge" for a child with WAS and severe thrombocytopenia awaiting HSC transplantation.^{145,146} The goal in such situations is to transiently increase the platelet count to $>50 \times 10^9$ platelets/L. Romiplostim has been successful in correcting the platelet count resulting from mutations in

THPO in congenital amegakaryocytic thrombocytopenia in which the patient's own thrombopoietin is absent or non-functional.¹⁴⁷ Overall, a careful and complete diagnosis is essential for the optimal management of patients, not only for those in need of special care but also to avoid over-reacting for patients with little risk of bleeding.

Perspectives

It is clear that we have entered a new era in the diagnosis of inherited thrombocytopenias with the arrival of WES, whole genome sequencing and selected high-throughput sequencing platforms. A feature of the reports so far is the large genetic heterogeneity. Crucial for the future will be a better understanding of regulatory DNA elements and untranslated regions, a new science that will include epigenomic profiling.¹⁴⁸ The challenges of whole genome sequencing are great but the potential to identify possible pathological traits hidden up to now, including difficult copy number variations and sequence variations deep within introns, is vast. The study of RNA sorting during platelet biogenesis and of the modulating influence of miRNA is also important.¹⁴⁹ Despite current technological advances, a high proportion of new cases of inherited thrombocytopenia remain without diagnosis; this proportion is often estimated to be around 50% but can be as high as 70% or more depending on the extent to which patients with easily identified disorders have been prescreened.^{127,128,150,151} Assigning a significance to the variants is key, because in the absence of confirmation with follow-up biological studies, including the use of mouse, zebrafish or *Drosophila* models or site-directed mutagenesis in megakaryocyte-related cells, the alternative is to use sophisticated bioinformatics; new variants are being variously graded as highly significant and likely pathogenic to those of unknown significance.^{126,131} An early meta-analysis of genome-wide association studies identified 68 common single-nucleotide variants that influenced platelet count or platelet volume; genes already linked to inherited thrombocytopenia, such as *THPO*, *GPIBA*, *TUBB1* and the pro-survival gene, *BAK*, were included, but the majority involved genes with no known link to megakaryopoiesis.¹⁵² Evaluating the sum of the effects of large combinations of single nucleotide variants and of novel gene variants of unknown significance has barely started yet and they may be disease-modulating, particularly if including heterozygous variants of known causal genes.¹⁵³ Their identification will require large study groups and high-powered bioinformatics beyond the scope of most individual laboratories.

A major challenge posed by inherited thrombocytopenia is identifying how patients, sometimes within the same family, with an identical genotype can vary so much clinically. In a GAPP study, there were descriptions of patients with excessive bleeding, mild thrombocytopenia and platelet dense granule secretion but with an enrichment of heterozygous *FLI1* and *RUNX1* hypomorphic mutations that were proposed to modulate phenotype.¹⁵⁴ On the basis of data from the ThromboGenomics project, we identified a disease-modifying *TUBB1* mutation in a patient with classic type I Glanzmann thrombasthenia who, confusingly, also had giant platelets and macrothrombocytopenia.¹⁵⁵ Such studies must be just the tip of the iceberg but the benefit of screening against large

gene panels is that some patients thought to have a monogenic condition may in fact be seen to have digenic or oligogenic pathologies. The extent of bleeding or predisposition to leukemia may crucially depend on gene variants that are different from those causing the primary disease. An early example is the *ARID5B* risk allele for leukemia in patients with *ETV6*-linked thrombocytopenias.¹⁵⁶ A future step for modern technologies is to identify variants and gene modulators able to influence phenotype and bleeding - either by protecting against or by exaggerating the primary disease. This will be key to improving prognosis and prevention.

The use of cost-effective NGS procedures, with the continued updating of gene panels, will require national networks with links to high-performance bioinformatics centers able to best analyze the data, perform variant filtering as well as the quality control of the sequencing procedures. As we have proposed elsewhere, this will be best done for Europe with a consensus¹³² in which the European

Hematology Association can be a leader providing guidelines, as is already the case with its comprehensive roadmap for hematology research.¹⁵⁷ Early recognition of a germline mutation facilitates appropriate treatment, better monitoring for disease progression, proper donor selection for HSC transplantation (family members must also be tested to ensure that they do not carry the mutation), as well as optimal genetic counseling of the affected patients and their family. Quite clearly for many patients the associated pathologies are clinically more serious than the bleeding risk and for some there is an obvious age-dependence. Improving the quality of life of patients and, at the same time, avoiding their stigmatization requires comprehensive ethical considerations.¹⁵⁸ It is crucial to decide how to provide delicate genetic information concerning a potential risk for leukemia or cancer, especially when potentially causal variants are found in young children, or how to deal with the coincidental identification of gene defects likely to predict other major illnesses.

References

- Balduini CL, Melazzini F. Research at the heart of hematology: thrombocytopenias and platelet function disorders. *Haematologica*. 2017;102(2):203-205.
- Lee RE, Young RH, Castleman B. James Homer Wright: a biography of the enigmatic creator of the Wright stain on the occasion of its centennial. *Am J Surg Pathol*. 2002;26(1):88-96.
- Harrington WJ, Minnich V, Hollingsworth JW, Moore CV. Demonstration of a thrombocytopenic factor in the blood of patients with thrombocytopenic purpura. *J Lab Clin Med*. 1951;38(1):1-10.
- Bernard J, Soulier JP. Sur une nouvelle variété de dystrophie thrombocytaire hémorragique congénitale. *Sem Hop*. 1948;24 (Spec. No.):3217-3223.
- Gröttum KA, Solum NO. Congenital thrombocytopenia with giant platelets: a defect in the platelet membrane. *Br J Haematol*. 1969;16(3):277-290.
- Nurden AT, Caen JP. Specific roles for platelet surface glycoproteins in platelet function. *Nature*. 1975;255(5511):720-722.
- Chang Y, Bluteau D, Debili N, Vainchenker W. From haematopoietic stem cells to platelets. *J Thromb Haemost*. 2007;5(Suppl 1):318-327.
- Kaushansky K, Lok S, Holly RD, et al. Promotion of megakaryocyte progenitor expansion and differentiation by the c-Mpl ligand thrombopoietin. *Nature*. 1994;369 (6481):568-571.
- Machlus KR, Italiano JE. The incredible journey: from megakaryocyte development to platelet formation. *J Cell Biol*. 2013;201(6):785-796.
- Junt T, Schulze H, Chen Z, et al. Dynamic visualization of thrombopoiesis within bone marrow. *Science*. 2007;317(5845):1767-1770.
- Dütting S, Gaits-Iacovoni F, Stegner D, et al. A Cdc42/RhoA regulatory circuit downstream of glycoprotein Ib guides transendothelial platelet biogenesis. *Nat Commun*. 2017;8:15838.
- Lefrançais E, Ortiz-Munoz G, Cadrillier A, et al. The lung is a site of platelet biogenesis and a reservoir for haematopoietic progenitors. *Nat New Biol*. 2017;544(7648):105-109.
- Nishimura S, Nagasaki M, Kunishima S, et al. IL-1 α induces thrombopoiesis through megakaryocyte rupture in response to acute platelet needs. *J Cell Biol*. 2015;209(3):453-466.
- Grozovsky R, Begonja AJ, Liu K, et al. The Ashwell-Morell receptor regulates hepatic thrombopoietin production via JAK2-STAT3 signaling. *Nat Med*. 2015;21(1):47-54.
- Li Y, Fu Y, Ling T, et al. Sialylation on O-glycans protects platelets from clearance by liver Kupffer cells. *Proc Natl Acad Sci U S A*. 2017;114(31):8360-8365.
- Deppermann C, Kratofil RM, Peiseler M, et al. Macrophage galactose lectin is critical for Kupffer cells to clear aged platelets. *J Exp Med*. 2020;217(4):e20190723.
- McArthur K, Chappaz S, Kile BT. Apoptosis in megakaryocytes and platelets: the life and death of a lineage. *Blood*. 2018;131(6):605-610.
- Mason KD, Carpinelli MR, Fletcher JJ, et al. Programmed mutations in Bernard-Soulier platelet life span. *Cell*. 2007;128(6):1173-1186.
- Jackson SP, Schoenwaelder S. Procoagulant platelets: are they necrotic? *Blood*. 2010;116(12):2011-2018.
- Berndt MA, Andrews RK. Bernard-Soulier syndrome. *Haematologica*. 2011;96(3):355-359.
- Favier R, Raslova H. Progress in understanding the diagnosis and molecular genetics of macrothrombocytopenias. *Br J Haematol*. 2015;170(5):626-639.
- Savoia A, Kunishima S, De Rocco D, et al. Spectrum of mutations in Bernard-Soulier syndrome. *Hum Mutat*. 2014;35(9):1033-1045.
- Poujol C, Ware J, Nieswandt B, Nurden AT, Nurden P. Absence of GPIIb α is responsible for aberrant membrane development during megakaryocyte maturation: ultrastructural study using a transgenic model. *Exp Hematol*. 2002;30(4):352-360.
- Sivapalaratnam S, Westbury SK, Stephens JC, et al. Rare variants in GPIIb α are responsible for autosomal dominant macrothrombocytopenia. *Blood*. 2017;129(4):520-524.
- Othman M. Platelet-type von Willebrand disease: three decades in the life of a rare bleeding disorder. *Blood Rev*. 2011;25(4):147-153.
- Bury L, Malara A, Momi S, Petitto E, Balduini A, Gesele P. Mechanisms of thrombocytopenia in platelet-type von Willebrand disease. *Haematologica*. 2019;104(7):1473-1481.
- Federici A, Mannucci PM, Castaman G, et al. Clinical and molecular predictors of thrombocytopenia and risk of bleeding in patients with von Willebrand disease type 2B: a cohort study of 67 patients. *Blood*. 2009;113(3):526-534.
- Nurden P, Gobbi G, Nurden A, et al. Abnormal VWF modifies megakaryocytopoiesis: studies of platelets and megakaryocyte cultures from patients with von Willebrand disease type 2B. *Blood*. 2010;115(13):2649-2656.
- Casari C, Berrou E, Lebreton M, et al. Von Willebrand factor mutation promotes thrombocytopenia by inhibiting integrin α IIb β 3. *J Clin Invest*. 2013;123(12):5071-5081.
- Dupont A, Soukaseum C, Cheptou M, et al. Relevance of platelet desialylation and thrombocytopenia in type 2B von Willebrand disease: preclinical and clinical evidence. *Haematologica*. 2019;104(12):2493-2500.
- Pecci A, Ma X, Savoia A, Adelstein RS. MYH9: structure, functions and role of non-muscle myosin IIA in human disease. *Gene*. 2018;664:152-167.
- Greinacher A, Pecci A, Kunishima S, et al. Diagnosis of inherited platelet disorders on a blood smear: a tool to facilitate worldwide diagnosis of platelet disorders. *J Thromb Haemost*. 2017;15(7):1511-1521.
- Heath KE, Campos-Barros A, Toren A, et al. Non-muscle myosin heavy chain IIA mutations define a spectrum of autosomal dominant macrothrombocytopenias: May-

- Hegglin anomaly and Fechtner, Sebastien, Epstein and Alport-like syndromes. *Am J Hum Genet.* 2001;69(5):1033-1045.
34. Saposnik B, Binard S, Fenneteau O, et al. French MYH9 network. Mutation spectrum and genotype-phenotype correlations in a large French cohort of MYH9-related disorders. *Mol Genet Genomic Med.* 2014;2(4):297-312.
 35. Aguilar A, Pertuy F, Eckly A, et al. Importance of environmental stiffness for megakaryocyte differentiation and proplatelet formation. *Blood.* 2016;128(16):2022-2032.
 36. Breton-Gorius J, Vainchenker W, Nurden A, Levy-Toledano S, Caen J. Defective alpha-granule production in megakaryocytes from gray platelet syndrome: ultrastructural studies of bone marrow cells and megakaryocytes growing in culture from blood cell precursors. *Am J Pathol.* 1981;102(1):10-19.
 37. Gunay-Aygun M, Zivony-Elboun Y, Gumruk F, et al. Gray platelet syndrome: natural history of a large patient cohort and locus assignment to chromosome 3p. *Blood.* 2010;116(23):4990-5001.
 38. Chen CH, Lo RW, Urban D, Pluthero FG, Kahr WH. α -granule biogenesis: from disease to discovery. *Platelets.* 2017;28(2):147-154.
 39. Deppermann C, Cherpokova D, Nurden P, et al. Gray platelet syndrome and defective thrombo-inflammation in Nbeal2-deficient mice. *J Clin Invest.* 2013;123(8):3331-3342.
 40. Di Buduo CA, Alberelli AC, Glembotsky AC, et al. Abnormal proplatelet formation and emperipolesis in cultured human megakaryocytes from gray platelet syndrome patients. *Sci Rep.* 2016;6:23213.
 41. Sowerby JM, Thomas DC, Clare S, et al. NBEAL2 is required for neutrophil and NK cell function and pathogen defense. *J Clin Invest.* 2017;127(9):3521-3526.
 42. Wijgaerts A, Wittevrongel C, Thys C, et al. The transcription factor GATA1 regulates NBEAL2 expression through a long-distance enhancer. *Haematologica.* 2017;102(4):695-706.
 43. Nichols KE, Crispino JD, Poncz M, et al. Familial dyserythropoietic anaemia and thrombocytopenia due to an inherited mutation in GATA1. *Nat Genet.* 2000;24(3):266-270.
 44. Stevenson WS, Morel-Kopp MC, Chen Q, et al. GFI1B mutation causes a bleeding disorder with abnormal platelet function. *J Thromb Haemost.* 2013;11(11):2039-2047.
 45. Monteferrario D, Bolar NA, Mameth AE, et al. A dominant negative GFI1B mutation in the gray platelet syndrome. *New Engl J Med.* 2014;370(3):245-253.
 46. Van Oorschot R, Mameth AE, Bergevoet SM, et al. Inherited missense variants that affect GFI1B function do not necessarily cause bleeding diatheses. *Haematologica.* 2019;104(6):e260-e264.
 47. Ballmaier M, Germeshausen M, Schulze H, et al. c-Mpl mutations are the cause of congenital amegakaryocytic thrombocytopenia. *Blood.* 2001;97(1):139-146.
 48. Plo I, Bellané-Chantelot, Mosca M, Mazzi S, Marty C, Vainchenker W. Genetic alterations of the thrombopoietin/MPL/JAK2 axis impacting megakaryopoiesis. *Front Endocrinol (Lausanne).* 2017;8:234.
 49. Imai K, Morio T, Zhu Y, et al. Clinical course of patients with WASP gene mutations. *Blood.* 2004;103(2):456-464.
 50. Thrasher AJ, Burns SO. WASP: a key immunological multitasker. *Nat Rev Immunol.* 2010;10(3):182-192.
 51. Mahlaoui N, Pellier I, Mignot C, et al. Characteristics and outcome of early-onset, severe forms of Wiskott-Aldrich syndrome. *Blood.* 2013;121(9):1510-1516.
 52. Sabri S, Foudi A, Boukour S, et al. Deficiency in the Wiskott-Aldrich protein induces premature proplatelet formation and platelet production in the bone marrow compartment. *Blood.* 2006;108(1):134-140.
 53. Aiuti A, Biasco L, Scarauzza S, et al. Lentiviral hematopoietic stem cell gene therapy in patients with Wiskott-Aldrich syndrome. *Science.* 2013;341(6148):1233-1235.
 54. Ferrua F, Cicalese MP, Galimberti S, et al. Lentiviral haemopoietic stem/progenitor cell gene therapy for treatment of Wiskott-Aldrich syndrome: interim results of a non-randomized, open-label, phase 1/2 clinical study. *Lancet Haematol.* 2019;6(5):e239-e253.
 55. Song WJ, Sullivan MG, Legare RD, et al. Haploinsufficiency of CBFA2 causes familial thrombocytopenia with propensity to develop acute myelogenous leukemia. *Nat Genet.* 1999;23(2):166-175.
 56. Lordier L, Bluteau D, Jalil A, et al. RUNX1-induced silencing of non-muscle myosin heavy chain IIB contributes to megakaryocyte polyploidization. *Nat Commun.* 2012;3:717.
 57. Morgan NV, Daly M. Gene of the issue: RUNX1 mutations and inherited bleeding. *Platelets.* 2017;28(2):208-210.
 58. Drachman JG, Jarvik GP, Mehaffey MG. Autosomal dominant thrombocytopenia: incomplete megakaryocyte differentiation and linkage to chromosome 10. *Blood.* 2000;96(1):118-125.
 59. Noris P, Perrotta S, Seri M, et al. Mutations in ANKRD26 are responsible for a frequent form of inherited thrombocytopenia: analysis of 78 patients from 21 families. *Blood.* 2011;117(24):6673-6680.
 60. Bluteau D, Balduini A, Balayn A, et al. Thrombocytopenia-associated mutations in the ANKRD26 regulatory region induce MAPK hyperactivation. *J Clin Invest.* 2014;124(2):580-591.
 61. Zaninetti C, Melazzini F, Croci GA, Boveri E, Balduini CL. Extramedullary hematopoiesis: a new feature of inherited thrombocytopenias. *J Thromb Haemost.* 2017;15(11):2226-2229.
 62. Di Paola J, Porter CC. ETV6-related thrombocytopenia and leukemia predisposition. *Blood.* 2019;134(8):663-667.
 63. Noetzi L, Lo RW, Lee-Sherick AB, et al. Germline mutations in ETV6 are associated with thrombocytopenia, red cell macrocytosis and predisposition to lymphoblastic leukemia. *Nat Genet.* 2015;47(5):535-538.
 64. Melazzini F, Palombo F, Balduini A, et al. Clinical and pathogenic features of ETV6-related thrombocytopenia with predisposition to acute lymphoblastic leukemia. *Haematologica.* 2016;101(11):1333-1342.
 65. Raslova H, Komura E, Le Couedic JP, et al. Fli1 monoallelic expression combined with its hemizygous loss underlies Paris-Trousseau/Jacobsen thrombopenia. *J Clin Invest.* 2004;114(1):77-84.
 66. Albers CA, Paul DS, Schulze H, et al. Compound inheritance of a low-frequency regulatory SNP and a rare null mutation in exon-junction complex subunit RBM8A causes TAR syndrome. *Nat Genet.* 2012;44(4):435-439.
 67. Manukjan G, Bösing H, Schmutz M, Straub G, Schulze H. Impact of genetic variants on haematopoiesis in patients with thrombocytopenia absent radii (TAR) syndrome. *Br J Haematol.* 2017;179(4):606-617.
 68. Thompson AA, Nguyen LT. Amegakaryocytopenia and radio-ulnar synostosis are associated with HOXA11 mutation. *Nat Genet.* 2000;26(4):397-398.
 69. Nijhori T, Ouchi-Uchiyama M, Sasahara Y, et al. Mutations in MECOM, encoding oncoprotein EVI1, cause radioulnar synostosis with amegakaryocytic thrombocytopenia. *Am J Hum Genet.* 2015;97(6):848-854.
 70. Nurden P, Debili N, Coupry I, et al. Thrombocytopenia resulting from mutations in filamin A can be expressed as an isolated syndrome. *Blood.* 2011;118(22):5928-5937.
 71. Begonja AJ, Hoffmeister KM, Hartwig JH, Falet H. FlnA-null megakaryocytes prematurely release large and fragile platelets that circulate poorly. *Blood.* 2011;118(8):2285-2295.
 72. Donada A, Balayn N, Silva D, et al. Disrupted filamin A/ α IIb β 3 interaction induces macrothrombocytopenia by increasing RhoA activity. *Blood.* 2019;133(16):1778-1788.
 73. Stritt S, Nurden P, Turro E, et al. A gain-of-function variant in DIAPH1 causes dominant macrothrombocytopenia and hearing loss. *Blood.* 2016;127(23):2903-2914.
 74. Martinelli S, Krumbach OHF, Pantaleoni F, et al. Functional dysregulation of CDC42 causes diverse developmental phenotypes. *Am J Hum Genet.* 2018;102(2):309-320.
 75. Kunishima S, Kobayashi R, Itoh TJ, Hamaguchi M, Saito H. Mutation of the beta1-tubulin gene associated with congenital macrothrombocytopenia affecting microtubule assembly. *Blood.* 2009;113(2):458-461.
 76. Burley K, Westbury SK, Mumford AD. TUBB1 variants and human platelet traits. *Platelets.* 2018;29(2):209-211.
 77. Latham SL, Ehmke M, Reinke PYA, et al. Variants in exons 5 and 6 of ACTB cause syndromic thrombocytopenia. *Nat Commun.* 2018;9(1):4250.
 78. Kunishima S, Okuno Y, Yoshida K, et al. ACTN1 mutations cause congenital macrothrombocytopenia. *Am J Hum Genet.* 2013;92(3):431-438.
 79. Guéguen P, Roualt K, Chen JM, et al. A missense mutation in the alpha-actinin 1 gene (ACTN1) is the cause of autosomal dominant macrothrombocytopenia in a large French family. *PLoS One.* 2013;8(9):e74728.
 80. Bottega R, Marconi C, Faleschini M, et al. ACTN1-related thrombocytopenia: identification of novel families for phenotypic characterization. *Blood.* 2015;125(5):869-872.
 81. Pleines I, Woods J, Chappaz S, et al. Mutations in tropomyosin 4 underlie a rare form of human macrothrombocytopenia. *J Clin Invest.* 2017;127(3):814-829.
 82. Nurden AT, Fiore M, Nurden P, Pillois X. Glanzmann thrombasthenia: a review of ITGA2B and ITGB3 defects with emphasis on variants, phenotypic variability, and mouse models. *Blood.* 2011;118(23):5996-6005.
 83. Nurden AT, Pillois X, Fiore M, et al. Expanding the mutation spectrum of the α IIb β 3 integrin in Glanzmann thrombasthenia: screening of the ITGA2B and ITGB3 genes in a large international cohort. *Hum Mutat.* 2015;36(5):548-561.

84. Nurden P, Bordet JC, Pillois X, Nurden AT. An intracytoplasmic $\beta 3$ Leu718 deletion in a patient with a novel platelet phenotype. *Blood Adv*. 2017;1(8):494-499.
85. Bury L, Falcinelli E, Chiasserini D, Springer TA, Italiano JE Jr, Gresele P. Cytoskeletal perturbation leads to platelet dysfunction and thrombocytopenia in variant forms of Glanzmann thrombasthenia. *Haematologica*. 2016;101(1):46-56.
86. Bury L, Zetterburg E, Leino EB, et al. A novel variant Glanzmann thrombasthenia due to co-inheritance of a loss and a gain-of-function mutation of ITGB3: evidence of a dominant effect of gain-of-function mutations. *Haematologica*. 2018;103(6):e259-e263.
87. Kahr WH, Pluthero FG, Elkadri A, et al. Loss of the Arp2/3 complex component ARPC1B causes platelet abnormalities and predisposes to inflammatory disease. *Nat Commun*. 2017;8:14816.
88. Hamamy H, Makrythanasis P, Al-Allawi N, Muhsin AA, Antonarakis SE. Recessive thrombocytopenia likely due to a homozygous pathogenic variant in the FYB gene: case report. *BMC Med Genet*. 2014;15:135.
89. Spindler M, van Eeuwijk JMM, Schurr Y, et al. ADAP deficiency impairs megakaryocyte polarization with ectopic proplatelet release and causes microthrombocytopenia. *Blood*. 2018;132(6):635-646.
90. Marconi C, Di Buduo CA, LeVine K, et al. Loss-of-function mutations in PTPRJ cause a new form of inherited thrombocytopenia. *Blood*. 2019;133(12):1346-1357.
91. Turro E, Greene D, Wijgaerts A, et al. A dominant gain-of-function in universal tyrosine kinase SRC causes thrombocytopenia, myelofibrosis, bleeding and bone pathologies. *Sci Transl Med*. 2016;8(328):328ra330.
92. Stormorken H, Holmsen H, Sund R, et al. Studies on the haemostatic defect in a complicated syndrome. An inverse Scott syndrome platelet membrane abnormality. *Thromb Haemost*. 1995;74(5):1244-1251.
93. Nesin V, Wiley G, Kousi M, Ong EC, et al. Activating mutations in STIM1 and ORAI1 cause overlapping syndromes of tubular myopathy and congenital myosis. *Proc Natl Acad Sci U S A*. 2014;111(11):4197-4202.
94. Markello T, Chen D, Kwan JW, et al. York platelet syndrome is a CRAC channelopathy due to gain-of-function mutations in STIM1. *Mol Genet Metab*. 2015;114(3):474-482.
95. Stritt S, Nurden P, Favier R, et al. TRPM7 channel function deregulates thrombopoiesis through altered cellular homeostasis and cytoskeletal architecture. *Nat Commun*. 2016;7:11097.
96. Fletcher SJ, Johnson B, Lowe GC, et al. SLFN14 mutations underlie thrombocytopenia with excessive bleeding and platelet secretion defects. *J Clin Invest*. 2015;125(9):3600-3605.
97. Fletcher SJ, Pisareva VP, Khan AO, Tcherepanov A, Morgan NV, Pisarev AV. Role of the novel endoribonuclease SLN14 and its disease-causing mutations in ribosomal degradation. *RNA*. 2018;24(7):939-949.
98. Manchev VT, Hilpert M, Berrou E, et al. A new form of macrothrombocytopenia induced by a germline mutation in the PRKACG gene. *Blood*. 2014;124(16):2554-2563.
99. Hofmann I, Geer MJ, Vögtle T, et al. Congenital macrothrombocytopenia with focal myelofibrosis due to mutations in human G6b-B is rescued in humanized mice. *Blood*. 2018;132(13):1399-1412.
100. Takeichi T, Torrello A, Lee JYW, et al. Biallelic mutations in KDSR disrupt ceramide synthesis and result in a spectrum of keratinization disorders associated with thrombocytopenia. *J Invest Dermatol*. 2017;137(11):2344-2353.
101. Heremans J, Garcia-Perez JE, Turro E, et al. Abnormal differentiation of B cells and megakaryocytes in patients with Roifman syndrome. *J Allergy Clin Immunol*. 2018;142(2):630-646.
102. Lentaigne C, Greene D, Sivapalaratnam S, et al. Germline mutations in the transcription factor IKZF5 cause thrombocytopenia. *Blood*. 2019;134(23):2070-2081.
103. Morison IM, Cramer-Bordé EM, Cheesman EJ, et al. A mutation of human cytochrome C enhances the intrinsic apoptotic pathway but causes only thrombocytopenia. *Nat Genet*. 2008;40(4):387-389.
104. Ledgerwood EC, Dunstan-Harrison C, Ong L, Morison IM. CYCS gene variants associated with thrombocytopenia. *Platelets*. 2019;30(5):672-674.
105. Gandhi MJ, Cummings CL, Drachman JG. FLJ14813 missense mutation: a candidate for autosomal dominant thrombocytopenia on chromosome 10. *Hum Hered*. 2003;55(1):66-70.
106. Hurtado B, Trakala M, Ximenez-Embun P, et al. Thrombocytopenia-associated mutations in Ser/Thr kinase MASTL deregulate actin cytoskeletal dynamics in platelets. *J Clin Invest*. 2018;128(12):5351-5367.
107. Jones C, Denecke J, Strater R, et al. A novel type of macrothrombocytopenia associated with a defect in alpha2,3 sialylation. *Am J Pathol*. 2011;179(4):1969-1977.
108. Izumi R, Niihori T, Suzuki N, et al. GNE myopathy associated with congenital thrombocytopenia: a report of two sibs. *Neuromuscul Disord*. 2014;24(12):1068-1072.
109. Revel-Vilk S, Shai E, Turro E, et al. GNE variants causing autosomal recessive macrothrombocytopenia without associated muscle wasting. *Blood*. 2018;132(17):1851-1854.
110. Futterer J, Dalby A, Lowe GC, et al. UK GAPP Study group. Mutation in GNE is associated with severe congenital thrombocytopenia. *Blood*. 2018;132(17):1855-1858.
111. Kauskot A, Pascreau T, Adam F, et al. A mutation in the gene coding for the sialic acid transporter SLC35A1 is required for platelet survival but not proplatelet formation. *Haematologica*. 2018;103(12):e613-e617.
112. Seo A, Gulsuner S, Pierce S, et al. Inherited thrombocytopenia associated with mutation of UDP-galactose-4-epimerase (GALE). *Hum Molec Genet*. 2019;28(1):133-142.
113. Bastida JM, Benito R, Janusz K, et al. Two novel variants of the ABCG5 gene cause xanthelasmas and macrothrombocytopenia: a brief review of hematologic abnormalities of sitosterolemia. *J Thromb Haemost*. 2017;15(9):1859-1866.
114. Kanaji T, Kanaji S, Montgomery RR, Patel SB, Newman PJ. Platelet hyperreactivity explains the bleeding abnormality and macrothrombocytopenia in a murine model of sitosterolemia. *Blood*. 2013;122(15):2732-2742.
115. Balduini CL, Cattaneo M, Fabris F, et al. Inherited thrombocytopenias: a proposed diagnostic algorithm from the Italian Gruppo di Studio delle Plastrine. *Haematologica*. 2003;88(5):582-592.
116. Bolton-Maggs PFB, Chalmers EA, Collins PW, et al. A review of inherited platelet disorders with guidelines for their management on behalf of the UKHCDO. *Br J Haematol*. 2006;135(5):603-633.
117. Noris P, Biino G, Pecci A, et al. Platelet diameters in inherited thrombocytopenias: analysis of 376 patients with all known disorders. *Blood*. 2014;124(6):e4-e10.
118. Gresele P. Diagnosis of inherited platelet function disorders: guidance from the SSC of the ISTH. *J Thromb Haemost*. 2015;13(2):314-322.
119. Westbury SK, Turro E, Greene D, et al. Human Phenotype Ontology annotation and cluster analysis to unravel genetic defects in 707 cases with unexplained bleeding and platelet disorders. *Genome Med*. 2015;7(1):36.
120. Khan AO, Maclachlan A, Lowe JC, et al. High-throughput platelet spreading analysis: a tool for the diagnosis of platelet-based bleeding disorders. *Haematologica*. 2020;105(3):e124-e128.
121. Van Geffen JP, Brouns SLN, Batista J, et al. High-throughput elucidation of thrombus formation reveals sources of platelet function variability. *Haematologica*. 2019;104(6):1256-1267.
122. Lentaigne C, Freson K, Laffan MA, Turro E, Ouwehand WH. On behalf of the BRIDGE-BPD Consortium and the ThromboGenomics Consortium. Inherited platelet disorders: towards DNA-based diagnosis. *Blood*. 2016;127(33):2814-2823.
123. Johnson B, Lowe GC, Futterer J, et al. Whole exome sequencing identifies genetic variants in inherited thrombocytopenia with secondary qualitative function defects. *Haematologica*. 2016;101(10):1170-1179.
124. Simeoni I, Stephens JC, Hu F, et al. A high-throughput sequencing test for diagnosing inherited bleeding, thrombotic and platelet disorders. *Blood*. 2016;127(23):2791-2803.
125. Downes K, Megy K, Duarte D, et al. Diagnostic high-throughput sequencing of 2,396 patients with bleeding, thrombotic and platelet disorders. *Blood*. 2019;134(23):2082-2091.
126. Megy K, Downes K, Simeoni I, et al. Curated disease-causing genes for bleeding, thrombotic, and platelet disorders: communication from the SSC of the ISTH. *J Thromb Haemost*. 2019;17(8):1253-1260.
127. Johnson B, Doak R, Allsup D, et al. A comprehensive targeted next-generation sequencing panel for genetic diagnosis of patients with suspected inherited thrombocytopenia. *Res Pract Thromb Haemost*. 2018;2(4):640-652.
128. Bastida JM, Lozano ML, Benito R, et al. Introducing high-throughput sequencing into mainstream genetic diagnosis practice in inherited platelet disorders. *Haematologica*. 2018;103(1):148-162.
129. Leino E, Gabrielate M, Ostrup O, et al. Outcome of an enhanced diagnostic pipeline for patients suspected of inherited thrombocytopenia. *Br J Haematol*. 2019;186(2):373-376.
130. Nurden AT, Nurden P. High-throughput sequencing for rapid diagnosis of inherited platelet disorders: a case for a European consensus. *Haematologica*. 2018;103(1):6-8.
131. Freson K, Turro E. High-throughput sequencing approaches for diagnosing hereditary bleeding and platelet disorders. *J Thromb Haemost*. 2017;15(7):1262-1272.
132. Rodeghiero F, Pabinger I, Ragni M, et al. Fundamentals for a systematic approach to

- mild and moderate inherited bleeding disorders: an EHA consensus report. *HemaSphere*. 2019;3(5):e286.
133. Noris P, Schlegel N, Kierys C, et al. Analysis of 339 pregnancies in 181 women with 13 different forms of inherited thrombocytopenia. *Haematologica*. 2014;99(8):1387-1394.
 134. Orsini S, Noris P, Bury L, et al. Bleeding risk of surgery and its prevention in patients with inherited platelet disorders. *Haematologica*. 2017;102(7):1192-1203.
 135. Gimbrone MA Jr, Aster RH, Cotran RS, Corkery J, Jandl JH, Folkman J. Preservation of vascular integrity in organs perfused in vitro with a platelet-rich medium. *Nature*. 1969;222(5188):33-36.
 136. Nurden AT. The biology of the platelet with special reference to inflammation, wound healing and immunity. *Front Biosci (Landmark Ed)*. 2018;23:726-751.
 137. Goerge T, Ho-Tin-Noe B, Carbo C, et al. Inflammation induces hemorrhage in thrombocytopenia. *Blood*. 2008;111(10):4958-4964.
 138. Poon MC, D'Oiron R. Alloimmunization in congenital deficiencies of platelet surface glycoproteins: focus on Glanzmann's thrombasthenia and Bernard-Soulier's syndrome. *Semin Thromb Haemost*. 2018;44(6):604-614.
 139. Rodeghiero F, Tosetto A, Abshire T, et al. ISTH/SSC joint VWF and Perinatal/Pediatric Hemostasis Subcommittees Working Group. ISTH/SSC bleeding assessment tool: a standardized questionnaire and a proposal for a new bleeding score for inherited bleeding disorders. *J Thromb Haemost*. 2010;8(9):2063-2065.
 140. Gesele P, Orsini S, Noris P, et al. Validation of the ISTH/SSC bleeding assessment tool for inherited platelet disorders: a communication from the Platelet Physiology SSC. *J Thromb Haemost*. 2020;18(3):732-739.
 141. Fasulo MR, Biquzzi E, Abbattista M, et al. The ISTH bleeding assessment tool and the risk of future bleeding. *J Thromb Haemost*. 2018;16(1):125-130.
 142. Favier R, Roussel X, Audia S, et al. Correction of severe myelofibrosis, impaired platelet function abnormalities in a patient with gray platelet syndrome successfully treated by stem cell transplantation. *Platelets*. 2019 Sep 10:1-5 [Epub ahead of print].
 143. Ghanima W, Cooper N, Rodeghiero F, Godeau B, Bussel JB. Thrombopoietin receptor agonists: ten years later. *Haematologica*. 2019;104(6):1112-1123.
 144. Pecci A, Gesele P, Kierys C, et al. Eltrombopag for the treatment of the inherited thrombocytopenia deriving from MYH9 mutations. *Blood*. 2010;116(26):5832-5837.
 145. Westbury SK, Downes K, Burney C, et al. Phenotypic description and response to thrombopoietin receptor agonist in DIAPH1-related disorder. *Blood Adv*. 2018;2(18):2341-2346.
 146. Gabelli M, Marzollo A, Notarangelo LD, Basso G, Putti MC. Eltrombopag use in a patient with Wiskott-Aldrich syndrome. *Pediatr Blood Cancer*. 2017;64(12).
 147. Pecci A, Ragab I, Bozzi V, et al. Thrombopoietin mutation in congenital amegakaryocytic thrombocytopenia treatable with romiplostim. *EMBO Mol Med*. 2018;10(1):63-75.
 148. Barbosa M, Joshi RS, Garg P, et al. Identification of rare de novo epigenetic variations in congenital disorders. *Nat Commun*. 2018;9(1):2064.
 149. Fisher MS, Di Paola J. Genomics and transcriptomics of megakaryocytes and platelets: implications for health and disease. *Res Pract Thromb Haemost*. 2018;2(4):630-639.
 150. Almazni I, Stapley R, Morgan NV. Inherited thrombocytopenia: update on genes and genetic variants which may be associated with bleeding. *Front Cardiovasc Med*. 2019;6:80.
 151. Savoia A. Molecular basis of inherited thrombocytopenias: an update. *Curr Opin Hematol*. 2016;23(5):486-492.
 152. Gieger C, Radakrishnan A, Cvejic A, et al. New gene functions in megakaryopoiesis and platelet formation. *Nature*. 2011;489(7376):201-208.
 153. Astle WJ, Elding H, Jiang T, et al. The allelic landscape of human blood cell trait variation and links to common complex disease. *Cell*. 2016;167(5):1415-1429.
 154. Stockley J, Morgan NV, Bem D, et al. Enrichment of FLI1 and RUNX1 mutations in families with excessive bleeding and platelet dense granule secretion defects. *Blood*. 2013;122(25):4090-4093.
 155. Guillet B, Bayart S, Pillois X, Nurden P, Caen JP, Nurden AT. A Glanzmann thrombasthenia family associated with a TUBB1-related macrothrombasthenia. *J Thromb Haemost*. 2019;17(12):2211-2215.
 156. Karastaneva A, Nebral K, Schlagenhauf A, et al. Novel phenotypes observed in patients with ETV6-linked leukemia/familial thrombocytopenia syndrome and a biallelic ARID5B risk allele as leukaemogenic cofactor. *J Med Genet*. 2019;jmedgenet-2019-106339. [Epub ahead of print]
 157. Engert A, Balduini C, Brand A, et al. The European Haematology Association roadmap for haematology research: a consensus document. *Haematologica*. 2016; 101(2):115-208.
 158. Greinacher A, Eekels JJM. Simplifying the diagnosis of inherited platelet disorders? The new tools do not make it easier. *Blood*. 2019;133(23):2478-2483.



Clonal hematopoietic mutations linked to platelet traits and the risk of thrombosis or bleeding

Alicia Veninga,^{1,*} Ilaria De Simone,^{1,*} Johan W.M. Heemskerk,¹
Hugo ten Cate,^{1,2,3} and Paola E.J. van der Meijden^{1,2}

¹Department of Biochemistry, Cardiovascular Research Institute Maastricht (CARIM), Maastricht University, Maastricht; ²Thrombosis Expertise Center, Heart and Vascular Center, Maastricht University Medical Center, Maastricht and ³Department of Internal Medicine, Maastricht University Medical Center, Maastricht, the Netherlands

*AV and IDS contributed equally as co-first authors.

ABSTRACT

Platelets are key elements in thrombosis, particularly in atherosclerosis-associated arterial thrombosis (atherothrombosis), and hemostasis. Megakaryocytes in the bone marrow, differentiated from hematopoietic stem cells are generally considered as a uniform source of platelets. However, recent insights into the causes of malignancies, including essential thrombocytosis, indicate that not only inherited but also somatic mutations in hematopoietic cells are linked to quantitative or qualitative platelet abnormalities. In particular cases, these form the basis of thrombo-hemorrhagic complications regularly observed in patient groups. This has led to the concept of clonal hematopoiesis of indeterminate potential (CHIP), defined as somatic mutations caused by clonal expansion of mutant hematopoietic cells without evident disease. This concept also provides clues regarding the importance of platelet function in relation to cardiovascular disease. In this summative review, we present an overview of genes associated with clonal hematopoiesis and altered platelet production and/or functionality, like mutations in *JAK2*. We consider how reported CHIP genes can influence the risk of cardiovascular disease, by exploring the consequences for platelet function related to (athero)thrombosis, or the risk of bleeding. More insight into the functional consequences of the CHIP mutations may favor personalized risk assessment, not only with regard to malignancies but also in relation to thrombotic vascular disease.

Correspondence:

P.E.J. VAN DER MEIJDEN
p.vandermeijden@maastrichtuniversity.nl

Received: January 31, 2020.

Accepted: May 4, 2020.

Pre-published: June 18, 2020.

doi:10.3324/haematol.2019.235994

Check the online version for the most updated information on this article, online supplements, and information on authorship & disclosures: www.haematologica.org/content/105/8/2020

©2020 Ferrata Storti Foundation

Material published in *Haematologica* is covered by copyright. All rights are reserved to the Ferrata Storti Foundation. Use of published material is allowed under the following terms and conditions:

<https://creativecommons.org/licenses/by-nc/4.0/legalcode>.

Copies of published material are allowed for personal or internal use. Sharing published material for non-commercial purposes is subject to the following conditions:

<https://creativecommons.org/licenses/by-nc/4.0/legalcode>, sect. 3. Reproducing and sharing published material for commercial purposes is not allowed without permission in writing from the publisher.



Introduction

Atherosclerotic cardiovascular disease is a chronic inflammatory condition that frequently occurs in the aging population.¹ Current understanding is that upon rupture or erosion of an atherosclerotic plaque, a thrombus is formed of aggregated platelets and fibrin which can become vaso-occlusive.² Furthermore, platelets contribute to ensuing thrombo-inflammatory reactions through their multiple interactions with vascular cells, leukocytes and the coagulation system, thereby promoting disease progression.³

Platelets are formed from megakaryocytes in the bone marrow (BM) through a differentiation and maturation process known as megakaryopoiesis. Several transcription factors have been identified over the years that regulate megakaryopoiesis and platelet production, and understanding of key transcriptional regulators is still expanding. Mutations in genes encoding for these transcription factors, along with epigenetic regulators, are accompanied with quantitative and/or qualitative platelet abnormalities, causing thrombo-hemorrhagic complications.⁴ Multiple growth factors control megakaryopoiesis and platelet production, of which thrombopoietin and its binding to the thrombopoietin receptor plays a primary role.⁵ Megakaryocytes undergo endomitosis to become polyploid and during maturation

extensive reorganization of cytoskeletal proteins is required for proplatelet formation and the budding of platelets.⁶

A number of recent studies stipulate that the incidence of cardiovascular disease (CVD), such as coronary artery disease, heart failure and ischemic stroke, is higher in patients with so-called somatic driver mutations in hematopoietic stem or progenitor cells, resulting in a clonal expansion of a subpopulation of blood cells.¹ This process, referred to as clonal hematopoiesis of indeterminate potential (CHIP), was proposed to define individuals with somatic clonal mutations in genes related to hematologic malignancies with variant allele fractions of >2%, but without a known hematologic malignancy or other clonal disorder.⁷ This premalignant state is considered to be relatively frequent in the elderly population, where somatic mutations accumulate in a variety of genes controlling hematopoietic stem cell maintenance, expansion and survival. Although CHIP increases the risk of developing hematologic cancer, mostly myeloid neoplasms, the absolute risk is still small. Several excellent recent reviews describe in detail the etiology of clonal hematopoiesis and its relation with CVD.^{1,8,9} So far, attention has mainly been focused on proposed mechanisms of accelerated inflammation-driven atherosclerosis and increased thrombosis risk through altered function of innate immune cells.

In the present paper, we took a different approach. We confined our search to the current evidence on CHIP mutations that are directly or indirectly linked to qualitative or quantitative platelet traits. Starting from the Online Mendelian Inheritance in Man (OMIM) database complemented with recent literature, we selected and discussed genes that were linked to clonal hematopoiesis as well as to the platelet traits count and function. Since CHIP mutations appeared not to be only associated with increased platelet count and/or function, but also with decreases in these platelet traits, its potential relation to both (athero)thrombotic and hemostatic disorders is presented in this review.

Section 1: Clonal mutations in genes associated with increased platelet count and/or function

For several genes encoding for transcription regulators (*ASXL1*), epigenetic regulators (*DNMT3A*, *IDH2*) and cell signaling proteins (*ABL1*, *BCR*, *BRAF*, *JAK2*, *SH2B3*), clonal mutations are known that enhance platelet production, which can be accompanied by enhanced platelet functionality. Related effects are described for several genes with divergent roles (*ABCB6*, *SF3B1*) (Table 1 and Figure 1).

ABCB6

Multiple so-called ABC transporters play a role in lipid trafficking, and thus may contribute to atherosclerosis. However, the *ABCB6* gene product (*ATP binding cassette subfamily B member 6*) facilitates the ATP-dependent import of porphyrins and heme into mitochondria.¹⁰ Markedly, germline mutations of *ABCB6* are associated with several disease phenotypes, including dyschromatosis, microphthalmia and pseudo-hyperkalemia.

The gene *ABCB6* is highly expressed in BM megakaryocyte progenitor cells and megakaryocytes, but only moderately in platelets. Evidence regarding CVD mainly comes from animal studies. In mice, deficiency in *Abcb6*

increased megakaryopoiesis and thrombopoiesis, resulting in an increased platelet count and larger platelet volume, effects that were explained by higher oxidative stress in the presence of accumulating porphyrins.¹¹ The platelets produced in these mice were hyper-reactive and furthermore, against a high-lipid background, attracted leukocytes, thus enhancing atherosclerosis.^{10,11}

In patients with acute promyelocytic or myeloid leukemia, RNA expression levels of *ABCB6* are reduced, suggesting the occurrence of also acquired clonal mutations in this gene.¹² However, so far no strong association with CHIP has been found.⁸

ASXL1

The transcriptional regulator *Additional sex combs like 1* (*ASXL1*) is a chromatin-binding protein, which acts as tumor suppressor and is implicated in the maintenance of normal hematopoiesis. Somatic mutations of this gene are found in patients with a variety of myeloid malignancies, including acute myeloid leukemia (AML), chronic myelomonocytic leukemia (CMML), myelodysplastic syndrome (MDS), and myeloproliferative neoplasm (MPN).¹⁵ In particular, mutations in *ASXL1* are detected in 10% of MDS patients and 40% of CMML patients.¹⁴ Hence, this gene is considered as a driver of leukemia and myelodysplasia. The majority of (somatic) mutations provoke a truncation of the C-terminus of the protein, resulting in a loss of transcription regulation. In addition, the truncated form can interact with other proteins to modulate cell proliferation.¹⁵ In mouse models, transgenic expression of a C-terminal truncated *Asxl1* mutant resulted in age-dependent anemia, thrombocytosis, and morphological dysplasia.¹³ A similar type of thrombocytosis is seen in MDS-refractory anemia patients, carrying *ASXL1* mutations.¹⁵ The prevalence of acquired hematopoietic mutations in *ASXL1* in a healthy population of 60-69 years of age was estimated at 1.5%, and was associated with twice the risk of developing CVD.¹⁶

BCR and ABL1

The somatic gene effects of *Breakpoint cluster region protein* (*BCR*) and *Abelson murine leukemia viral oncogene homolog 1* (*ABL1*) are highly related, if only because the two proteins share signaling pathways. The proto-oncogene *ABL1* contains an auto-inhibitory SH3 domain which, when deleted, turns it into an oncogene. During a somatic reciprocal translocation of chromosomes 22 and 9, both genes can fuse together. The encoded BCR-ABL1 fusion protein is frequently detected in patients with chronic myeloid leukemia (CML) (90%) or acute lymphoblastic leukemia (ALL) (30%).¹⁷ While CML patients mostly carry the 210 amino-acid variant of BCR-ABL, in ALL patients also a shorter 185 amino-acid variant is present. Both fusion forms display constitutive protein tyrosine kinase activity.¹⁷

The current understanding is that aberrant roles of BCR and ABL1 in hematopoiesis are a consequence of fusion formation, although the main evidence comes from case studies. A fusion variant has been described, which is associated with an increased platelet count, although the mechanism is still unclear.¹⁸ In the few healthy adults carrying a BCR-ABL1 fusion mutation hematopoietic malignancies were not detected. On the other hand, BCR-ABL1 fusions can be considered as indicators for a premalignant state, while the absolute risk of developing CVD is smaller than for the *JAK2* V617F mutation.¹⁹

Table 1. Relevant genes in clonal hematopoiesis with effects on platelet traits and disease.

Gene name	Gene (OMIM)	Protein function	Overall role in hematopoiesis	Germline/ somatic	Inherited disease classification (OMIM, PMID)	Somatic phenotype (OMIM, PMID)	Mutation effect on protein	Mutation effect on platelet traits	Thrombosis risk	Bleeding risk	Predisposition to malignancy	Ref. platelet traits
ABCB6	605452	Mitochondrial transporter	Mitochondrial stability	G, S	Dyschromatosis universalis hereditaria 3 (615402); Microphthalmia (614497); Pseudohyperkalemia familial 2 (609153); Blood group Langereis system (111600)	Undefined	Loss-of-function	Count ↑, size ↑, function ↑ (m)	Yes	No	Undefined	11
ABL1	189980	Signaling regulator	Proliferation and survival of HSC	G, S	Congenital heart defect skeletal malformations syndrome (617602)	Leukemia Philadelphia chromosome-positive resistant to imatinib (608232)	Gain-of-function	Count ↑	n.d.	No	ALL, CML	18
ASXL1	612990	Transcription regulator	Tumor suppression; maintenance of normal hematopoiesis	G, S	Bohring-Opitz syndrome (605039)	Myelodysplastic syndrome somatic (614286)	Loss-of-function	Count ↑ (h, m)	Yes	No	Aplastic anemia, AML, CMML, MDS, MPN	13
BCR	151410	Signaling regulator	Development and survival of HSC	S	Undefined	Acute lymphocytic leukemia Philadelphia chromosome positive somatic (613065); Chronic myeloid leukemia Philadelphia chromosome positive somatic (608232)	Gain-of-function	Count ↑	n.d.	No	ALL, CML	18
BRAF	164757	Signaling protein kinase	Controlling development and proliferation of HSC	G, S	Cardiofaciocutaneous syndrome (115150); LEOPARD syndrome 3 (613707); Noonan syndrome 7 (613706)	Adenocarcinoma of lung somatic (211980); Colorectal and other cancers somatic	Gain-of-function	Count ↑/=	n.d.	n.d.	HCL, solid cancers	20
DNMT3A	602769	Epigenetic regulator	Tumor suppression	G, S	Tatton-Brown-Rahman syndrome (615879)	Acute myeloid leukemia somatic (601626)	Loss-of-function	Count ↑	Yes	No	AML, CMML, MDS, MPN (including ET, PV)	26,28
ETV6	600618	Transcription repressor	Development and survival of HSC; when fused either proto-oncogene or tumor suppressor	G, S	Thrombocytopenia 5 (616216)	Acute myeloid leukemia somatic (601262)	Loss-of-function	Count ↓, size =, function ↓	No	Yes	ALL (pre-B), AML, MDS	49
FANCA	607139	DNA repair protein	Chromosomal stability regulating differentiation of HSC	G, S	Fanconi anemia complementation group A (227650)	Undefined	Loss-of-function	Count ↓ (h, m)	No	Yes	AML, MDS, solid cancers	50
FANCC	613899	DNA repair protein	Protection against cytotoxicity	G, S	Fanconi anemia complementation group C (227645)	Undefined	Loss-of-function	Count ↓	No	Yes	AML, MDS, solid cancers	50

continued on the next page

continued from the previous page

Gene name	Gene (OMIM)	Protein function	Overall role in hematopoiesis	Germline/somatic	Inherited disease classification (OMIM, PMID)	Somatic phenotype (OMIM, PMID)	Mutation effect on protein	Mutation effect on platelet traits	Thrombosis risk	Bleeding risk	Predisposition to malignancy	Ref. platelet traits
FLII	193067	Transcription regulator	Development and maintenance of HSC	G, S	Bleeding disorder platelet-type 21 (617443)	Ewing sarcoma (29977059)	Loss-of-function	Count ↓, size ↑,	No	Yes	Solid cancers	82,85
							Gain-of-function	function ↓ Count ↑, function ↑	n.d.	No	Lymphoblastic leukemia, lymphoma	87
GATA1	305371	Transcription regulator	Development and differentiation of HSC and megakaryocytes	G, S	Anemia X-linked with/without platelet abnormalities (300835); Thrombocytopenia (314050, 300367)	Leukemia megakaryoblastic with/without Down syndrome somatic (190685)	Loss-of-function	Count ↓, size ↑, function ↓ (m)	Yes	Yes	AMKL (in Down syndrome)	88,91
							Gain-of-function	Count ↑	Yes	No	MPN (including ET, PV), AMKL (in non-Down syndrome)	93
GATA2	137295	Transcription regulator	Development and survival of HSC	G, S	Emberger syndrome (614038); Immunodeficiency 21 (614172)	Acute myeloid leukemia (601626); Myelodysplastic syndrome (614286); Predisposition to infection and chronic myelomonocytic leukemia (25359990)	Loss-of-function	Count ↓	n.d.	n.d.	AML, CMML, MDS	55
							Gain-of-function	n.d.	n.d.	n.d.	CML	56
GFI1B	604383	Transcription regulator	Development and mobilization of HSC and megakaryocytes	G, S	Bleeding disorder platelet-type 17, Gray platelet syndrome (187900)	Acute myeloid leukemia (26851695)	Loss-of-function	Count ↓, size ↑, function ↓	no	Yes	Various leukemias	63,65
IDH2	147650	Epigenetic regulator (indirect)	Development and differentiation of HSC	G, S	D-20 hydroxyglutaric aciduria 2 (613657)	Myeloproliferative neoplasm (20428194); Acute myeloid leukemia (20884716)	Gain-of-function	Count ↑/=	n.d.	Yes	AML, solid cancers	31
JAK2	147796	Signaling regulator	Proliferation and survival of HSC	G, S	Thrombocythemia 3 (614521)	Erythrocytosis somatic (133100); Acute myeloid leukemia somatic (601626); Myelofibrosis somatic (254450), Polycythemia vera somatic (263300); Thrombocythemia 3 (614521); Budd-Chiari syndrome somatic; (600880)	Gain-of-function	Count ↑, size ↑/=, function ↑ (h, m)	Yes	No	MPN (including ET, PV)	36,38
SF3B1	605590	Splicing factor	Development of HSC	S	Undefined	Myelodysplastic syndrome somatic (614286)	Unclear	Count ↑ (h, m)	Yes	No	ET, MDS, MPD	40
SH2B3	605093	Signaling regulator	Development of megakaryocytes and platelet production	G, S	B-precursor acute lymphoblastic Leukemia (23908464)	Erythrocytosis somatic (133100); Myelofibrosis somatic (254450); Thrombocythemia somatic (187950)	Loss-of-function	Count ↑, function ↑ (m)	Yes	No	MPN	44,45
SMAD4	600993	Transcription regulator	Tumor suppression	G, S	Hemorrhagic telangiectasia syndrome (175050); Myhre syndrome (139210); Polyposis juvenile intestinal (174900)	Pancreatic cancer somatic (260350)	Loss-of-function	Count ↓, size =, function ↓ (m)	No	Yes	AML, solid cancers	67

continued on the next page

continued from the previous page

Gene name	Gene (OMIM)	Protein function	Overall role in hematopoiesis	Germline/ somatic	Inherited disease classification (OMIM, PMID)	Somatic phenotype (OMIM, PMID)	Mutation effect on protein	Mutation effect on platelet traits	Thrombosis risk	Bleeding risk	Predisposition to malignancy	Ref. platelet traits
TET2	612839	Epigenetic regulator	Tumor suppression	S	Undefined	Myelodysplastic syndrome somatic (614286)	Loss-of-function	Count = (m)	Yes	No	MDS	95
TP53	191170	Transcription regulator	Quiescing of HSC; tumor suppression	G, S	Bone marrow failure syndrome 5 (618165); Li-Fraumeni syndrome (151623); Adrenocortical carcinoma pediatric (202300); Basal cell carcinoma 7 (614740); Choroid plexus papilloma (260500); Colorectal cancer (114500); Glioma susceptibility 1 (137800)	Breast cancer somatic (114480); Hepatocellular carcinoma somatic (114550); Nasopharyngeal carcinoma somatic (607107); Pancreatic cancer somatic (260350); Colorectal cancer (114500); Glioma susceptibility 1 (137800); Osteosarcoma (259500)	Loss-of-function	Count ↓ (h) = (m), size ↑, function ↓ (m)	n.d.	n.d.	Solid cancers, various leukemias	71,72
WAS	300392	Signaling regulator	Morphogenic development of HSC	G, S	Neutropenia severe congenital X-linked (300299); Thrombocytopenia X-linked (313900); Wiskott-Aldrich syndrome (301000)	Juvenile myelomonocytic leukemia (29316027); Somatic mosaicism in Wiskott-Aldrich syndrome (19129986)	Loss-of-function	Count ↓, size ↓, function unclear (h, m)	No	Yes	lymphoma, lymphoblastic leukemia, MDS, MPD	77,79
							Gain-of-function	Count ↓/=, size =	n.d.	n.d.	AML, MDS, JMML	75

ALL: acute lymphoblastic leukemia; AMKL: acute megakaryoblastic leukemia; AML: acute myeloid leukemia; CML: chronic myeloid leukemia; CMML: chronic myelomonocytic leukemia; ET: essential thrombocythemia; HSC: hematopoietic stem cell; JMML: juvenile myelomonocytic leukemia; MDS: myelodysplastic syndrome; MPN: myeloproliferative neoplasms; OMIM: Online Mendelian Inheritance in Man; PMID: PubMed reference number; PV: polycythemia vera. (h) is mutation effect on platelet trait found in human, (m) is in mice

BRAF

The serine-threonine protein kinase BRAF is an essential partner in the mitogenic RAS/RAF/MEK/ERK signaling pathway. The *BRAF* proto-oncogene is expressed in all tissues, where it controls cell proliferation, apoptosis, and differentiation. In addition, BRAF is necessary for embryonic development, as *Braf*-deficient embryos die because of disturbed blood vessel formation.²⁰

Evidence on the role of BRAF in normal megakaryopoiesis comes from work mainly with immortalized human megakaryoblastic cell lines. Upon stimulation with thrombopoietin, differentiation and proliferation of the cells appeared to rely on BRAF-mediated signaling to ERK.²¹ Downregulation of BRAF thus lowered the number of megakaryocytic lineage cells, a phenomenon that was confirmed *in vivo* in chimeric mice.²⁰

In the Noonan, LEOPARD and cardiofaciocutaneous syndromes, patients carry germline mutations in *BRAF* in regions distinct from those of somatic cancerous mutations. However, only limited changes in BRAF signaling are reported.²² On the other hand, somatic gain-of-function mutations in the *BRAF* gene accumulate in patients with AML, malignant lymphomas or solid cancers.²³ Next to more common point mutations, rare chromosomal translocations are described for this gene.²⁴

A frequently observed gain-of-function mutation

(V600E) is the driver mutation present in different cancers, including melanomas, solid cancers and hairy cell leukemia (HCL). Patients who suffer from HCL have low blood cell counts, likely due to BM aberrations and splenomegaly.²⁵ Whether megakaryopoiesis is altered due to a constitutively increased MEK/ERK signaling *via* BRAF still needs to be confirmed.

DNMT3A

Clonal mutations of three genes (*DNMT3A*, *IDH2*, *TET2*) have been reported which, directly or indirectly, affect histone methylation and hence these can be considered as epigenetic regulators.

The gene *DNA methyltransferase 3α* (*DNMT3A*) encodes for a DNA methylation enzyme that regulates gene imprinting, chromosome inactivation and tumor suppression. Genetic mutations in the *DNMT3A* gene occur in the rare Tatton-Brown-Rahman syndrome which, as far as is known, is not accompanied by hematopoietic aberrations.

In several acquired blood cancers, but especially in adults with AML, somatic mutations in *DNMT3A* have been reported.²⁶ About a quarter of all AML patients with *de novo* disease carry variant forms of this protein, most commonly with R882H mutation. The loss-of protein-function in those patients resulted in chromosomal islands of hypomethylation.²⁷ The same mutation, albeit less fre-

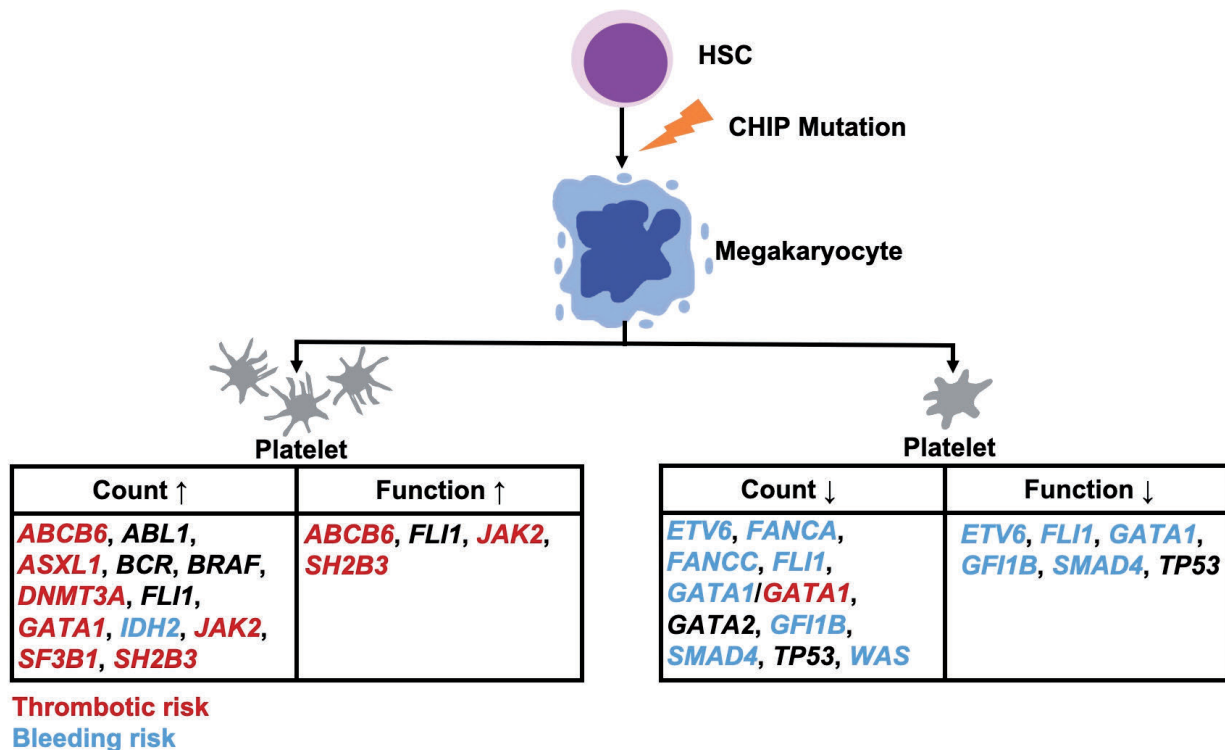


Figure 1. Clonal hematopoiesis of indeterminate potential (CHIP)-related genes affecting platelet traits and the risk of thrombosis or bleeding. Mutations in genes associated with a thrombotic or bleeding risk are indicated in red and blue, respectively. For genes indicated in black, no such associations are known yet.

quent, can occur in patients with CMML, MDS or MPN.²⁶ It is considered that *DNMT3A* mutations in hematopoietic stem cells lead to a pre-leukemic state, waiting for additional mutations to induce leukemia. The time interval from first appearance of the mutation to disease is, however, unclear.²⁶

In agreement with its relevance for clonal hematopoiesis, a recent report points to an increased incidence of acquired *DNMT3A* mutations in the elderly, with a prevalence of about 15% at 60-69 years of age.¹ Combined with a *JAK2* V617F mutation (see below), the mutated *DNMT3A* gene associates with essential thrombocythemia (ET) and polycythemia vera (PV).²⁶ Current understanding is that first acquisition of a *DNMT3A* mutation followed by *JAK2* will result in an ET phenotype. On the other hand, first appearance of the *JAK2* mutation may result in a PV phenotype.²⁶ Overall, *DNMT3A* mutations in AML patients are associated with higher platelet counts than patients with WT-*DNMT3A*; however, the absolute count is still low (<150x10⁹/L).²⁸

Regarding atherosclerosis development and atherothrombosis, studies report increased inflammation, linked to mutated *DNMT3A*, possibly due to a higher production of cytokines.²⁹ Indeed, in patients carrying an acquired mutation of *DNMT3A*, the risk of CVD appears to be doubled.¹ The higher platelet count observed in AML patients with *DNMT3A* mutations likely occurs secondary to the pro-inflammatory phenotype. So far, no mechanism has been found to link *DNMT3A* mutations directly to platelet traits.

IDH2

The enzyme *isocitrate dehydrogenase NADP⁺ 2* (IDH2)

localized in mitochondria generates NADPH from NADP⁺, whilst catalyzing the oxidative decarboxylation of isocitrate, ultimately producing D-2-hydroxy-glutarate. By producing NADPH, IDH2 regulates the mitochondrial redox balance, hence mitigating cellular oxidative damage.³⁰ As expected, genetic mutations in *IDH2* are described to be associated with metabolic diseases. On the other hand, somatic mutations of *IDH2* are found in several cancers, including hematologic malignancies, sarcomas and colon cancer. This is compatible with a role of IDH2 as epigenetic regulator, although the direct evidence for epigenetic effects is still indirect.

The most frequent clonal mutations in *IDH2*, identified in patients with *de novo* AML, concern the protein arginine residues R140Q and R172K. These variants cause a gain-of-function resulting in an abnormal, damaging production of D-2-hydroxyglutaric acid, leading to a hypermethylated state of DNA and histones.³⁰ In comparison to non-carriers, AML patients carrying the somatic *IDH2* mutations showed a higher platelet count, although the absolute platelet count was still low (<150x10⁹/L).³¹ The same trend for platelet count has also been found in MDS patients.³² Next to this, in primary myelofibrosis, *IDH* mutations can form a risk factor for leukemic transformation.³³ No association with thrombotic events is known for these patient groups, but bleeding was more common in mutant-carrying patients. In the elderly, the percentage of individuals with clonal hemostasis driver mutations in *IDH2* appeared to be rather low at around 1%.¹⁶ Together, this suggests only mild effects of somatic changes in this gene on clonal hematopoiesis, associated with a slight increase in platelet count by a so far unknown mechanism and an increased bleeding tendency.

JAK2

The non-receptor tyrosine kinase *Janus kinase 2* (JAK2) is one of the general regulators of cell survival and proliferation, by controlling, for example, cytokine receptor signaling pathways. Also in hematopoiesis, JAK2 controls precursor cell maintenance and function.³⁴ Inherited mutations of *JAK2* are detected in patients with hereditary thrombocytosis,³⁵ while somatic mutations of the gene link to various phenotypes including erythrocytosis.

A well-known acquired *JAK2* variant is the mutation V617F, which is carried by the majority of patients with MPN, i.e. in nearly all PV patients and half of patients with ET or primary myelofibrosis. In general, the V617F mutation affects the proliferation of myeloid cells and leads to increased inflammatory responses.³⁴ However, this somatic mutation as such is not considered to enhance the risk of thrombotic events in patients with ET or PV.³⁶ Nevertheless, platelets from *JAK2* V617F-positive patients demonstrated an enhanced activation status and procoagulant potential. In addition, the fraction of immature platelets, which can be more active than mature platelets, was higher in carriers of the *JAK2* V617F mutation versus non-carriers.³⁷

Transgenic mice have been generated carrying the human *JAK2* V617F mutation in the megakaryocyte lineage.³⁸ The *JAK2* V617F megakaryocytes responded better to thrombopoietin, and displayed a greater migratory ability, proplatelet formation and increased ploidy. The produced platelets responded stronger to multiple agonists.

In aging healthy individuals, the prevalence of the *JAK2* V617F variant is only 1%, but carriers have a 10-fold increased risk of CVD.¹⁶ Depending on the degree of mutation expansion, subjects may develop MPN instead of CHIP.⁸ How or under which conditions the thrombocytosis is linked to somatic *JAK2* mutations aggravating CVD is still a matter of debate and requires further investigation.

SF3B1

The gene *splicing factor 3B subunit 1* (*SF3B1*) encodes for a core component of the RNA spliceosome machinery.³⁹ Somatic mutations in this gene, along with other genes of the spliceosome, have been identified in over half of MDS patients.³⁹ Common mutations in the *SF3B1* gene are those of K700E, K666N and R625C.⁴⁰ To study the impact of the frequent K300E mutation, a conditional knock-in mouse model was developed, which revealed a RNA splicing defect similar as suggested in MDS patients harboring this mutation.³⁹ Regarding the thrombotic risk, studies revealed that patients carrying a mutated *SF3B1* gene had higher platelet counts and were more prone to develop CVD than patients without mutation,⁴⁰ although the altered molecular players are unclear. Furthermore, a sequencing study identified *SF3B1* mutations in 5% of ET patients.⁴¹ In the aging healthy population, clonal hematopoietic mutations of *SF3B1* appear to be infrequent, ranging from 2 to 5%.⁴²

SH2B3

The signaling adaptor protein *Src homology 2 B3* (SH2B3, also named LNK) acts as an interactor of JAK2, and negatively regulates thrombopoietin-induced megakaryopoiesis. An associated inherited disease is B-precursor acute lymphoblastic leukemia. Somatic mutations in the *SH2B3* gene are found in >5% of MPN patients. These

concern frameshift and missense mutations throughout the whole gene, often co-existing with mutations in driver genes, including *JAK2*, *CALR* and *MPL*.⁴³ The loss-of-function of SH2B3 can lead to a higher expansion of hematopoietic stem cells, acting by increased thrombopoietin signaling and megakaryopoiesis.⁴⁴ The higher platelet and leukocyte counts may worsen atherosclerosis and the thrombotic risk.⁴³ In *Sh2b3* knockout mice, it was found that hyperlipidemia aggravated both atherosclerosis and thrombosis, likely due to positive platelet priming.⁴⁵ Whether this priming event due to *SH2B3* mutations also occurs in humans, is not known.

Section 2: Clonal mutations in genes associated with decreased platelet count and/or function

Several mutations in genes encoding for transcription regulators (*ETV6*, *GATA2*, *GFI1B*, *SMAD4*), cell signaling proteins (*TP53*, *WAS*), and other proteins (*FANCA*, *FANCC*) are linked to impaired hematopoiesis, causing thrombocytopenia of varying severity with evidence for concomitant platelet function defects (Table 1 and Figure 1).

ETV6

The transcriptional repressor *E26 transformation-specific variant 6* (*ETV6*) serves to maintain the development of hematopoietic stem cells in the BM as a continuous survival signal. It acts by inhibiting other transcription factors, such as FLI1. However, it appears not to be required for embryonic stem cell expansion.⁴⁶

ETV6 is known as a proto-oncogene, since it can be a fusion partner with over 30 other genes, but in case of truncating mutations it acts as a tumor suppressor gene. Depending on the fusion site, the fused protein can alter the transcription levels of *ETV6* target genes, which may support the development of leukemia.^{46,47} On the other hand, germline heterozygous *ETV6* mutations have been identified in some patients with dominantly inherited thrombocytopenia.⁴⁸ Such patients seem to have a predisposition to hematologic malignancies, most commonly ALL, AML or MDS. Given that the complete loss of *ETV6* is lethal, truncating or protein-inactivating mutations are mainly found as somatic events, and rarely as germline variants.⁴⁶

As a transcriptional repressor, *ETV6* has an established role in megakaryocyte and platelet (patho)physiology. Patients with germline *ETV6* variants show a large expansion of immature megakaryocyte colony-forming units, accompanied by a reduced formation of proplatelets, thus explaining the thrombocytopenia. The mutant platelets are of normal size, although characterized by aberrant cytoskeleton organization, lower levels of small GTPases, and defective clot retraction.⁴⁹ Evidence is lacking to link clonal variants of *ETV6* to thrombotic phenotypes; however, a related bleeding tendency has been described.

FANCA, FANCC

The proteins *Fanconi anemia complementation group A and C* (*FANCA/C*) are repair factors after DNA damage or apoptosis. Inherited mutations in either gene are seen in the disorder Fanconi anemia, where patients in 60-70% of the cases show a mutation in *FANCA* and in 15% a muta-

tion in *FANCC*. Such patients suffer from progressive bone marrow failure, pancytopenia and predisposition to cancer.⁵⁰ Knockout mouse studies revealed that *FANCA* is needed for normal megakaryopoiesis and platelet production. Megakaryocytes in the deficient mice were found to be in a senescent state.⁵⁰

In humans, heterozygous mutations of *FANCA* are observed in a proportion of patients with AML.⁵¹ However, carriers of such mutations do not seem to have a significant risk of developing cancer.⁵² On the other hand, *FANCA* deletion mutations, especially in combination with other germline mutations, might contribute to breast cancer susceptibility.⁵³ The phenotype coupled to somatic mutations in *FANCA* and/or *FANCC* is probably linked to genomic instability caused by defective FANC proteins.⁵¹ How these somatic mutations contribute to CHIP-related CVD needs to be established.

GATA2

In immature hematopoietic stem cells, the transcription factor *GATA-binding factor 2* (*GATA2*) is expressed earlier than *GATA1*, and becomes down-regulated upon differentiation.⁵⁴ This has also been observed in *Gata2*-knockout mice, revealing that *GATA2* is required for hematopoietic stem cell and progenitor cell development.⁵⁵ In humans, congenital *GATA2* deficiency is accompanied by a hypocellular and dysplastic bone marrow, resulting in low platelet counts.⁵⁵ Furthermore, germline deletion mutations in the *GATA2* gene are associated with an increased predisposition to infection, AML, CMML or MDS.

On the other hand, a somatic mutation (L359V) in *GATA2* has been identified in approximately 10% of patients in the progression phase of CML.⁵⁶ This concerns a gain-of-function resulting in increased transcription factor activity, in contrast to gene deletion. Reports indicate that in approximately 50% of patients with any *GATA2* mutation, the megakaryocyte development is abnormal.⁵⁷ Unlike *GATA1*, *GATA2* regulates platelet GPIIb rather than GPIb expression.⁵⁴ Variants of *GATA2* have also been associated with increased susceptibility for coronary artery disease,⁵⁸ linking this gene to CHIP.

GFI1B

Another transcription regulator crucial for erythroid and megakaryocytic differentiation is *growth factor independent 1B transcription repressor* (*GFI1B*). As a DNA-binding protein, it regulates the dormancy and mobilization of hematopoietic stem cells.⁵⁹ Next to the full-size protein of 330 amino acids implicated in megakaryopoiesis, a shorter form is expressed that may rather regulate erythroid development.⁶⁰ The longer protein modulates the expression of several proto-oncogenes and tumor suppressor genes.⁵⁹ Accordingly, a functional disturbance of *GFI1B* can contribute to leukemia development. In mice, genetic deletion of *Gfi1b* resulted in early lethality, where the embryos showed failed megakaryocyte development.⁶¹

For human *GFI1B*, both germline and somatic mutations have been identified. These generally result in a truncated or a dysfunctional form of the protein, thereby reducing DNA binding and transcription repressor activity.⁶² In the inherited disorder gray platelet syndrome, patients with a *GFI1B* mutation display (macro)thrombocytopenia with platelets that are reduced in α -granules.⁶³ The patient's platelets were also found to be reduced in GPIb and GPIIb/IIIa expression, whereas that of the

hematopoietic precursor marker CD34 was markedly increased. The suggestion that, in these and other patients with a truncating mutation of *GFI1B*, megakaryocyte development is impaired was recently supported by platelet proteome analysis.⁶⁴ In mice, a megakaryocyte-specific deletion of *Gfi1b* enhanced the expansion of megakaryocytes, but resulted in severe thrombocytopenia.⁶⁵ Here, the (tubulin) cytoskeleton appeared to be underdeveloped in the mutant megakaryocytes, explaining an inadequate proplatelet formation.

Whole-exome sequencing efforts have revealed the presence of alternative *GFI1B* splice variants, which is accompanied by impaired megakaryocyte differentiation and thrombopoiesis.⁶⁰ However, in heterozygous carriers, platelet counts and function were in normal ranges. Little is known about clonal hematopoiesis. A somatic mutation of *GFI1B* has been identified in patients with AML.⁵⁹

SMAD4

The 'vascular' transcription factor *SMAD family member 4* (*SMAD4*) acts as a tumor suppressor, triggered by signaling pathways evoked by transforming growth factor- β or bone morphogenetic protein.⁶⁶ Within the cellular nucleus, *SMAD4* forms a complex with other *SMAD* isoforms to control gene expression. In mice, *SMAD4* was found to play a role especially in vascular development.⁶⁶ On the other hand, a megakaryocyte-specific deficiency of *SMAD4* is described, causing mild thrombocytopenia with partially dysfunctioning platelets, likely as a consequence of altered promoter activities.⁶⁷

In humans, both somatic and inherited mutations of *SMAD4* are known. Inherited mutations of the gene present with distinct phenotypes, ranging from a vascular bleeding disorder (hereditary hemorrhagic telangiectasia) to gastro-intestinal and bone marrow abnormalities.⁶⁸ Somatic mutations of the 358-515 amino-acid region are linked to pancreatic carcinoma.⁶⁹ During the screening for somatic driver mutations linked to clonal hematopoiesis, a similar mutation of *SMAD4* was found.¹⁶ Mutations in *SMAD4* are related to a bleeding rather than thrombotic phenotype.

TP53

The tumor suppressor *tumor protein p53* (*TP53* or *p53*) is a critical player in cell cycle progression and apoptosis. Herein, *TP53* maintains the quiescent state of hematopoietic stem cells, and controls DNA damage responses upon cellular stress.⁷⁰ In megakaryocytic cells derived from *Tp53* knockout mice, cell size and polyploidization were increased due to higher DNA synthesis and decreased apoptosis. In human cell cultures, *TP53* knockdown affected the expression of platelet integrins, granule components and cytoskeletal proteins, which was accompanied by functional platelet defects.⁷¹

Regarding human disease, the *TP53* deletion occurring in multiple myeloma is accompanied by a lowering in platelet count.⁷² In this context, mutant *TP53* forms are considered to drive clonal hematopoiesis *via* the epigenetic regulator *EZH2*, leading to overmethylation of histone H3. This can down-regulate several genes associated with self-renewal and differentiation of hematopoietic stem cells.⁷⁰ A common consequence is expansion of the affected hematopoietic cell clones. Markedly, the *TP53* gene is top ranking in mutated genes found in CHIP.⁷³ How mutated *TP53* in hematopoietic cells contributes to

CHIP-associated CVD still remains to be determined. Few studies have shown that there is higher expression of pro-inflammatory cytokines in *p53*-deficient murine leukocytes, which may accelerate the development of CVD.⁹ However, there is no evidence directly linking platelet traits to CVD development.

WAS

The *Wiskott-Aldrich syndrome* (WAS) protein is selectively expressed in hematopoietic cells, where it regulates actin cytoskeleton rearrangements. In the classical X-linked Wiskott-Aldrich syndrome, patients suffer from thrombocytopenia with smaller sized platelets and recurrent infections, due to an impaired functionality or availability of WAS.⁷⁴ A milder phenotype is that of X-linked thrombocytopenia, in which patients only suffer from bleeding because of low platelet count.⁷⁴ Rare inherited mutations that instead cause constitutive WAS activation are seen in patients with X-linked neutropenia, experiencing recurrent bacterial infections while having normal platelet count and size.⁷⁵ In addition, these patients show an increased predisposition for AML or MDS.⁷⁶

In classical Wiskott-Aldrich syndrome patients, the prevalence of malignancy is 13-22%, mostly due to development of lymphoma, but also to lymphoblastic leukemia, MDS or MPD.⁷⁶ The thrombocytopenia is likely caused by increased platelet removal. In *Was*-deficient mice, platelet turnover was shortened, with proteomic evidence for alterations in proteins of metabolic and proteasomal pathways.⁷⁷ Furthermore, in both the mutant mice and patients, there is evidence for a hyperactivation status of the platelets, thus explaining the higher elimination rate. Several groups reported on alterations in integrin activation in the patient's platelets.^{78,79} However, one patient study concluded platelet activation properties were normal.⁸⁰

There is limited evidence for the presence of somatic mutations in the WAS gene. This mainly concerns gain-of-function mutations, associated with poor outcome in patients with juvenile myelomonocytic leukemia.⁸¹ This suggested a clonal role of the gene in the pre-malignant state.

Section 3: Clonal mutations in other genes

For the genes *FLI1* and *GATA1* encoding for transcription regulators, whether the mutation is gain-of-function or loss-of-function likely determines its respective effect on platelet count and/or function. Mutations in *TET2* have been associated with increased inflammation-induced atherosclerosis and thrombotic disease, although possible effects on platelets remain to be established (Table 1 and Figure 1).

FLI1

The protein *Friend leukemia virus integration 1* (FLI1) is a member of the ETS transcription factor family, which is highly expressed in the hematopoietic lineage and endothelial cells. Due to a faulty vasculature, *Fli1* knockout mice die during embryonic development, but heterozygous mice are viable without apparent phenotype.⁸² Detailed studies indicate that FLI1 plays an important role in both erythropoiesis and megakaryopoiesis by regulating the expression of multiple genes.⁸³ It acts together with the transcription factor

GABPA, especially in later phases of megakaryopoiesis. This is exemplified by the fact that, in *Fli1* knockout mice, megakaryocytes are specifically reduced in the expression of late-stage genes, e.g. genes encoding for glycoprotein (GP)Ib α , GPIIX and platelet factor 4.⁸²

In humans, heterozygous mutations in *FLI1* are commonly grouped together as 'Bleeding disorder platelet-type 21' (Phenotype MIM 617443). Examples are the Jacobsen syndrome and Paris-Trousseau syndrome, which are characterized by a heterozygous partial deletion of chromosome 11, encompassing the *FLI1* gene. Such patients characteristically suffer from abnormal growth and mental retardation, accompanied by thrombocytopenia, most likely due to impaired megakaryopoiesis.⁸⁴ In the Paris-Trousseau syndrome, platelets are enlarged and contain large fused α -granules.⁸⁴ In patients with a mutated *FLI1* gene, presenting with congenital macrothrombocytopenia, also an impaired agonist-induced platelet aggregation has been reported.⁸⁵

In the case of somatic mutations, *FLI1* can become fusion partner with the transcriptional repressing gene *EWSR1*, a condition known as Ewing sarcoma.⁸⁶ The effect on platelets is unclear. On the other hand, *in vitro* studies have indicated that the overexpression of *FLI1* in stem cells enhances megakaryopoiesis, thrombopoiesis, and platelet functionality.⁸⁷ Furthermore, deregulated high levels of FLI1 are found in various types of cancer. In agreement with this, a predisposition to pre-T-cell lymphoblastic leukemia and lymphoma is described for transgenic mice over-expressing *Fli1* in the hematopoietic progenitor cells.⁸³ It remains to be established whether *FLI1* is a main contributing gene in CHIP-related CVD.

GATA1

The transcription factor *GATA-binding protein 1* (GATA1) controls the development and production of megakaryocytes, platelets and erythrocytes. In mouse studies, the loss of *Gata1* in the megakaryocyte lineage resulted in smaller size megakaryocytes and a defect in proplatelet formation. The *Gata1*-deficient platelets were larger in size, showed an excess in rough endoplasmic reticulum, and contained fewer α -granules.⁸⁸ Furthermore, the deficient mice were impaired in red blood cell development, and often died because of anemia.⁸⁹ Consistent with this, *GATA1* is highly expressed in human megakaryocytes and erythroid cells. Mutations in *GATA1* can appear as germline or somatic. Inherited mutations associate with hematopoietic disorders, characterized by low blood cell counts. On the other hand, somatic mutations often result in the production of shorter GATA1 variants, for example, in cases of AMKL (acute megakaryoblastic leukemia) or Down syndrome.⁵⁴ Here, platelets tend to be low in counts and display an atypical morphology.

A common consequence of germline *GATA1* mutations in hematopoietic disorders is the altered interaction of GATA1 with its co-factor FOG1, i.e. a zinc finger protein co-operating with GATA1 to regulate cell differentiation. This has been reported for patients with X-linked thrombocytopenia, or other forms of macrothrombocytopenia, who experience bleeding diatheses.⁹⁰ The patient's megakaryocytes are abnormal in structure and the platelets show decreased numbers of α -granules.⁹⁰ Patients with primary myelofibrosis, having upstream driver mutations resulting in low GATA1 levels in megakaryocytes, show an increased risk of both thrombosis and

bleeding. Mice with *Gata1*^{low} mutation resemble this phenotype, demonstrating similar megakaryocyte abnormalities, such as abnormal P-selectin localization, and thrombo-hemorrhagic events. The prothrombotic state was ascribed to increased platelet-leukocyte interactions through P-selectin.⁹¹

In cultured megakaryocytes, GATA1 has been shown to regulate the expression of GPIIb (fibrinogen receptor) and GPIb (von Willebrand factor receptor). Markedly, in *GATA1*-deficient megakaryocytes, expression levels of GPIIb can be maintained by GATA2 substitution, whereas those of GPIb are decreased.⁵⁴ As expected, inherited mutations of *GATA1* are accompanied by a bleeding phenotype rather than by an increased risk of thrombosis. On the other hand, high levels of *GATA1* transcripts are found in patients with ET or PV.⁹² Overexpression of *GATA1* in mice results in a similar phenotype.⁹³ Regarding CHIP, somatic gain-of-function may increase the cardiovascular risk including atherothrombosis, whereas loss-of-function may be more associated with bleeding.

TET2

The protein *Tet oncogene family member 2* (TET2) has a key role in DNA methylation, explaining how it functions as a tumor suppressor, maintaining normal hematopoiesis. The *TET* gene product in particular represses the transcription of inflammatory molecules, such as interleukin-6 and -8, which are known as pro-atherogenic mediators.^{1,94} This explains why somatic loss-of-function mutations in *TET2* are associated with an increased inflammation tendency. Similarly, as described for *DNMT3A*, the mutations may increase the burden of atherosclerosis and arterial CVD.

Murine *Tet2*-null models are used to confirm that CHIP-like mutations lead to inflammation-driven cardiovascular pathologies,^{7,95} markedly without changes in blood cell counts. In the aging population, clonal hematopoietic mutations of *TET2* have a prevalence of 2.5%.¹⁶ On the other hand, such mutations are found in approximately 25% of patients with myeloid neoplasms, and are then associated with an increased cardiovascular risk.⁷ It is still not clear to what extent the mutations affect megakaryopoiesis or platelet function, either directly or indirectly *via* enhanced inflammation.

Conclusions and perspectives

As outlined above, somatic mutations in multiple genes affecting hematopoiesis contribute as a risk factor to the development of CVD. So far, studies have focused on the effects of somatic and CHIP-linked mutations on blood cells, linking to increased inflammation, atherosclerotic disease and thrombosis risk. In this review, we provide evidence that many of the common CHIP genes are involved in quantitative (count) and/or qualitative (function) platelet traits, and therefore in this way can influence CVD, in particular triggered by thrombo-inflammatory mechanisms. On the other hand, insight is gained in a link between mutations in CHIP genes and impairment of hematopoiesis and hemostatic function.

Reactive (secondary) thrombocytosis, which is not due

to a primary hematologic disorder but driven by inflammatory stimuli, trauma or acute bleeding, does not seem to increase the risk of thrombotic or hemorrhagic complications.⁹⁶ In line with this, the degree of elevation in the platelet count does not correlate with the thrombosis risk in myeloproliferative disease, where clonal (primary) thrombocytosis has been demonstrated.⁹⁷ This indicates that the platelet count as such is not the only determinant of the increased thrombosis risk in myeloproliferative disorders.^{98,99} Also, several CHIP mutations (e.g. *DNMT3A* mutations) can indirectly cause a rise in platelet count by inducing increased expression of inflammatory molecules that subsequently upregulate the thrombopoietin production by the liver. However, the combination of alterations in count and function may play an essential role in CHIP mutations related to thrombosis. So far, we have found evidence of seven CHIP-related genes (*ABCB6*, *ASXL1*, *DNMT3A*, *GATA1*, *JAK2*, *SF3B1*, *SH2B3*) with elevated platelet counts and an associated thrombotic risk (Figure 1). For the other genes, there is not enough evidence to make estimates of this kind; only for *ABCB6*, *JAK2* and *SH2B3* mutations is it known that the elevated platelet count is accompanied by a hyper-reactive platelet phenotype. Apparently, information regarding the functional status of platelets in the context of CHIP mutations is still scarce and further studies are needed to elucidate the contribution of platelets to the risk of thrombosis.

One of the most thoroughly investigated conditions, demonstrating the consequences of altered platelet traits due to somatic driver mutations, is essential thrombocytopenia. Markedly, in these patients, there appears to be no direct correlation between platelet count and thrombosis. On the other hand, the *JAK2* V617F mutation is known to increase the thrombosis risk in ET patients, when compared to patients without the mutation.¹⁰⁰ The reported enhanced activation status of platelets in *JAK2* V617F-positive patients provides a strong indication that platelet function changes induced by a CHIP mutation contribute to the risk of thrombosis, thus explaining part of the risk associations of CHIP mutations with CVD. Platelet reactivity also involves interactions with leukocytes, secretion of pro-inflammatory mediators and release of extracellular vesicles that may all contribute to CVD, like atherosclerosis and atherothrombosis. Given the increasing prevalence of CHIP mutations in the elderly who are prone to develop CVD (along with malignancies), more thorough investigation of platelet function linked to CHIP mutations would be worthwhile. Greater insight into the functional consequences of such acquired mutations may also favor personalized risk assessment, not only with regard to malignancies, but also in relation to thrombotic vascular disease.

Acknowledgments

AV is supported by the Dutch Landsteiner Foundation for Blood Transfusion Research (1711). *IDS* is supported by a joint PhD scholarship of Maastricht and Reading Universities, and by the European Union's Horizon 2020 research and innovation program under the Marie Skłodowska-Curie grant agreement n. 766118.

References

- Jaiswal S, Libby P. Clonal haematopoiesis: connecting ageing and inflammation in cardiovascular disease. *Nat Rev Cardiol.* 2020;17(3):137-144.
- Libby P, Pasterkamp G. Requiem for the 'vulnerable plaque'. *Eur Heart J.* 2015;36(43):2984-2987.
- Van der Meijden PE, Heemskerck JW. Platelet biology and functions: new concepts and future clinical perspectives *Nat Rev Cardiol.* 2019;16(3):166-179.
- Daly ME. Transcription factor defects causing platelet disorders. *Blood Rev.* 2017;31(1):1-10.
- Bianchi E, Norfo R, Pennucci V, et al. Genomic landscape of megakaryopoiesis and platelet function defects. *Blood.* 2016;127(10):1249-1259.
- Machlus KR, Italiano JE Jr. The incredible journey: From megakaryocyte development to platelet formation. *J Cell Biol.* 2013;201(6):785-796.
- Steenma DP. Clinical consequences of clonal hematopoiesis of indeterminate potential. *Blood Adv.* 2018;2(22):3404-3410.
- Haybar H, Shahrabi S, Ghanavat M, Khodadi E. Clonal hematopoiesis: genes and underlying mechanisms in cardiovascular disease development. *J Cell Physiol.* 2019;234(6):8396-8401.
- Sano S, Wang Y, Walsh K. Clonal Hematopoiesis and Its Impact on Cardiovascular Disease. *Circ J.* 2018;83(1):2-11.
- Boswell-Casteel RC, Fukuda Y, Schuetz JD. ABCB6, an ABC transporter impacting drug response and disease. *AAPS J.* 2017;20(1):8.
- Murphy AJ, Sarazy V, Wang N, et al. Deficiency of ATP-binding cassette transporter B6 in megakaryocyte progenitors accelerates atherosclerosis in mice. *Arterioscler Thromb Vasc Biol.* 2014;34(4):751-758.
- Abraham A, Karathedath S, Varatharajan S, et al. ABCB6 RNA expression in leukemias: expression is low in acute promyelocytic leukemia and FLT3-ITD-positive acute myeloid leukemia. *Ann Hematol.* 2014;93(3):509-512.
- Nagase R, Inoue D, Pastore A, et al. Expression of mutant *Asxl1* perturbs hematopoiesis and promotes susceptibility to leukemic transformation. *J Exp Med.* 2013;215(6):1729-1747.
- Carbuccia N, Murati A, Trouplin V, et al. Mutations of *ASXL1* gene in myeloproliferative neoplasms. *Leukemia.* 2009;23(11):2183-2186.
- Yang H, Kurtenbach S, Guo Y, et al. Gain of function of *ASXL1* truncating protein in the pathogenesis of myeloid malignancies. *Blood.* 2018;131(3):328-341.
- Acuna-Hidalgo R, Sengul H, Steehouwer M, et al. Ultra-sensitive sequencing identifies high prevalence of clonal hematopoiesis-associated mutations throughout adult life. *Am J Hum Genet.* 2017;101(1):50-64.
- Guo JQ, Wang JY, Arlinghaus RB. Detection of BCR-ABL proteins in blood cells of benign phase chronic myelogenous leukemia patients. *Cancer Res.* 1991;51(11):3048-3051.
- Yamagata T, Mitani K, Kanda Y, et al. Elevated platelet count features the variant type of BCR/ABL junction in chronic myelogenous leukaemia. *Br J Haematol.* 1996;94(2):370-372.
- Valent P, Kern W, Hoermann G, et al. Clonal hematopoiesis with oncogenic potential (CHOP): separation from CHIP and roads to AML. *Int J Mol Sci.* 2019;20(3):789.
- Kamata T, Kang J, Lee TH, et al. A critical function for B-Raf at multiple stages of myelopoiesis. *Blood.* 2005;106(3):833-840.
- Garcia J, de Gunzburg J, Eychene A, et al. Thrombopoietin-mediated sustained activation of extracellular signal-regulated kinase in UT7-Mpl cells requires both Ras-Raf-1 and Rap1-B-Raf-dependent pathways. *Mol Cell Biol.* 2001;21(8):2659-2670.
- Sarkozy A, Carta C, Moretti S, et al. Germline BRAF mutations in Noonan, LEOPARD, and cardiofaciocutaneous syndromes: molecular diversity and associated phenotypic spectrum. *Hum Mutat.* 2009;30(4):695-702.
- Xu Y, Wertheim G, Morrisette JJD, Bagg A. BRAF kinase domain mutations in de novo acute myeloid leukemia with monocytic differentiation. *Leuk Lymphoma.* 2017;58(3):743-745.
- Palanisamy N, Ateeq B, Kalyana-Sundaram S, et al. Rearrangements of the RAF kinase pathway in prostate cancer, gastric cancer and melanoma. *Nat Med.* 2010;16(7):793-798.
- Falini B, Martelli MP, Tiacci E. BRAF V600E mutation in hairy cell leukemia: from bench to bedside. *Blood.* 2016;128(15):1918-1927.
- Yang L, Rau R, Goodell MA. DNMT3A in haematological malignancies. *Nat Rev Cancer.* 2015;15(3):152-165.
- Yang L, Rodriguez B, Mayle A, et al. DNMT3A loss drives enhancer hypomethylation in FLT3-ITD-associated leukemias. *Cancer Cell.* 2016;29(6):922-934.
- Hou HA, Kuo YY, Liu CY, et al. DNMT3A mutations in acute myeloid leukemia: stability during disease evolution and clinical implications. *Blood.* 2012;119(2):559-568.
- Leoni C, Montagner S, Rinaldi A, et al. Dnmt3a restrains mast cell inflammatory responses. *Proc Natl Acad Sci U S A.* 2017;114(8):E1490-E1499.
- Tefferi A. Novel mutations and their functional and clinical relevance in myeloproliferative neoplasms: JAK2, MPL, TET2, ASXL1, CBL, IDH and IKZF1. *Leukemia.* 2010;24(6):1128-1138.
- DiNardo CD, Ravandi F, Agresta S, et al. Characteristics, clinical outcome, and prognostic significance of IDH mutations in AML. *Am J Hematol.* 2015;90(8):732-736.
- DiNardo CD, Jabbour E, Ravandi F, et al. IDH1 and IDH2 mutations in myelodysplastic syndromes and role in disease progression. *Leukemia.* 2016;30(4):980-984.
- Yonal-Hindilerden I, Daglar-Aday A, Hindilerden F, et al. The clinical significance of IDH mutations in essential thrombocythemia and primary myelofibrosis. *J Clin Med Res.* 2016;8(1):29-39.
- Perner F, Perner C, Ernst T, Heidel FH. Roles of JAK2 in Aging, Inflammation, Hematopoiesis and Malignant Transformation. *Cells.* 2019;8(8):854.
- Mead AJ, Rugless MJ, Jacobsen SE, Schuh A. Germline JAK2 mutation in a family with hereditary thrombocytosis. *N Engl J Med.* 2012;366(10):967-969.
- Fleischman AG, Tyner JW. Causal role for JAK2 V617F in thrombosis. *Blood.* 2013;122(23):3705-3706.
- Barbui T, Finazzi G, Falanga A. Myeloproliferative neoplasms and thrombosis. *Blood.* 2013;122(13):2176-2184.
- Hobbs CM, Manning H, Bennett C, et al. JAK2V617F leads to intrinsic changes in platelet formation and reactivity in a knock-in mouse model of essential thrombocythemia. *Blood.* 2013;122(23):3787-3797.
- Mupo A, Seiler M, Sathiseelan V, et al. Hemopoietic-specific SF3b1-K700E knock-in mice display the splicing defect seen in human MDS but develop anemia without ring sideroblasts. *Leukemia.* 2017;31(3):720-727.
- Lin CC, Hou HA, Chou WC, et al. SF3B1 mutations in patients with myelodysplastic syndromes: the mutation is stable during disease evolution. *Am J Hematol.* 2014;89(8):E109-115.
- Tefferi A, Vannucchi AM, Barbui T. Essential thrombocythemia treatment algorithm 2018. *Blood Cancer J.* 2018;8(1):2.
- McKerrell T, Park N, Moreno T, et al. Leukemia-associated somatic mutations drive distinct patterns of age-related clonal hemopoiesis. *Cell Rep.* 2015;10(8):1239-1245.
- Maslah N, Cassinat B, Verger E, et al. The role of LNK/SH2B3 genetic alterations in myeloproliferative neoplasms and other hematological disorders. *Leukemia.* 2017;31(8):1661-1670.
- Takizawa H, Eto K, Yoshikawa A, et al. Growth and maturation of megakaryocytes is regulated by Lnk/Sh2b3 adaptor protein through crosstalk between cytokine- and integrin-mediated signals. *Exp Hematol.* 2008;36(7):897-906.
- Wang W, Tang Y, Wang Y, et al. LNK/SH2B3 loss of function promotes atherosclerosis and thrombosis. *Circ Res.* 2016;119(6):e91-e103.
- Hock H, Shimamura A. ETV6 in hematopoiesis and leukemia predisposition. *Semin Hematol.* 2017;54(2):98-104.
- Kim CA, Phillips ML, Kim W, et al. Polymerization of the SAM domain of TEL in leukemogenesis and transcriptional repression. *EMBO J.* 2001;20(15):4173-4182.
- Di Paola J, Porter CC. ETV6-related thrombocytopenia and leukemia predisposition. *Blood.* 2019;134(8):663-667.
- Poggi M, Canault M, Favier M, et al. Germline variants in ETV6 underlie reduced platelet formation, platelet dysfunction and increased levels of circulating CD34+ progenitors. *Haematologica.* 2017;102(2):282-294.
- Pawlikowska P, Fouchet P, Vainchenker W, et al. Defective endomitosis during megakaryopoiesis leads to thrombocytopenia in *Fanca*^{-/-} mice. *Blood.* 2014;124(24):3613-3623.
- Tischkowitz MD, Morgan NV, Grimwade D, et al. Deletion and reduced expression of the *Fanconi anemia FANCA* gene in sporadic acute myeloid leukemia. *Leukemia.* 2004;18(3):420-425.
- Garcia MJ, Benitez J. The *Fanconi anaemia/BRCa* pathway and cancer susceptibility. Searching for new therapeutic targets. *Clin Transl Oncol.* 2008;10(2):78-84.
- Solyom S, Winqvist R, Nikkila J, et al. Screening for large genomic rearrangements in the *FANCA* gene reveals extensive deletion in a Finnish breast cancer family. *Cancer Lett.* 2011;302(2):113-118.
- Crispino JD. GATA1 in normal and malignant hematopoiesis. *Semin Cell Dev Biol.* 2005;16(1):137-147.
- Ganapathi KA, Townsley DM, Hsu AP, et al. GATA2 deficiency-associated bone marrow disorder differs from idiopathic aplastic anemia. *Blood.* 2015;125(1):56-70.
- Zhang SJ, Shi JY, Li JY. GATA-2 L359 V mutation is exclusively associated with

- CML progression but not other hematological malignancies and GATA-2 P250A is a novel single nucleotide polymorphism. *Leukoc Res.* 2009;33(8):1141-1143.
57. Dickinson RE, Milne P, Jardine L, et al. The evolution of cellular deficiency in GATA2 mutation. *Blood.* 2014;123(6):863-874.
 58. Connelly JJ, Wang T, Cox JE, et al. GATA2 is associated with familial early-onset coronary artery disease. *Plos Genet.* 2006; 2(8):e139.
 59. Anguita E, Candel FJ, Chaparro A, Roldan-Etcheverry JJ. Transcription Factor GFI1B in Health and Disease. *Front Oncol.* 2017;7:54.
 60. Polfus LM, Khajuria RK, Schick UM, et al. Whole-exome sequencing identifies loci associated with blood cell traits and reveals a role for alternative GFI1B splice variants in human hematopoiesis. *Am J Hum Genet.* 2016;99(2):481-488.
 61. Saleque S, Cameron S, Orkin SH. The zinc-finger proto-oncogene GFI1b is essential for development of the erythroid and megakaryocytic lineages. *Genes Dev.* 2002; 16(3):301-306.
 62. Moroy T, Vassen L, Wilkes B, Khandanpour C. From cytopenia to leukemia: the role of Gfi1 and Gfi1b in blood formation. *Blood.* 2015;126(24):2561-2569.
 63. Monteferrario D, Bolar NA, Marneth AE, et al. A dominant-negative GFI1B mutation in the gray platelet syndrome. *N Engl J Med.* 2013;370(3):245-253.
 64. Van Oorschot R, Hansen M, Koornneef JM, et al. Molecular mechanisms of bleeding disorder associated GFI1B (Q287*) mutation and its affected pathways in megakaryocytes and platelets. *Haematologica.* 2019;104(7):1460-1472.
 65. Beauchemin H, Shooshtarizadeh P, Vadnais C, et al. GFI1b controls integrin signaling-dependent cytoskeleton dynamics and organization in megakaryocytes. *Haematologica.* 2017;102(3):484-497.
 66. Mao X, Debenedittis P, Sun Y, et al. Vascular smooth muscle cell Smad4 gene is important for mouse vascular development. *Arterioscler Thromb Vasc Biol.* 2012;32(9): 2171-2177.
 67. Wang Y, Jiang L, Mo X, et al. Megakaryocytic Smad4 regulates platelet function through Syk and ROCK2 expression. *Mol Pharmacol.* 2017;92(3):285-296.
 68. Gallione CJ, Repetto GM, Legius E, et al. A combined syndrome of juvenile polyposis and hereditary haemorrhagic telangiectasia associated with mutations in MADH4 (SMAD4). *Lancet.* 2004;363(9412):852-859.
 69. Schutte M, Hruban RH, Hedrick L, et al. DPC4 gene in various tumor types. *Cancer Res.* 1996;56(11):2527-2530.
 70. Chen S, Wang Q, Yu H, et al. Mutant p53 drives clonal hematopoiesis through modulating epigenetic pathway. *Nat Commun.* 2019;10(1):5649.
 71. Apostolidis PA, Woulfe DS, Chavez M, et al. Role of tumor suppressor p53 in megakaryopoiesis and platelet function. *Exp Hematol.* 2012;40(2):131-142.
 72. Shah V, Johnson DC, Sherborne AL, et al. Subclonal TP53 copy number is associated with prognosis in multiple myeloma. *Blood.* 2018;132(23):2465-2469.
 73. Xie M, Lu C, Wang J, et al. Age-related mutations associated with clonal hematopoietic expansion and malignancies. *Nat Med.* 2014;20(12):1472-1478.
 74. Zhu Q, Zhang M, Blaese RM, et al. The Wiskott-Aldrich syndrome and X-linked congenital thrombocytopenia are caused by mutations of the same gene. *Blood.* 1995;86(10):3797-3804.
 75. Devriendt K, Kim AS, Mathijs G, et al. Constitutively activating mutation in WASP causes X-linked severe congenital neutropenia. *Nat Genet.* 2001;27(3):313-317.
 76. Keszei M, Kritikou JS, Sandfort D, et al. Wiskott-Aldrich syndrome gene mutations modulate cancer susceptibility in the p53 +/- murine model. *Oncoimmunology.* 2018;7(9):e1468954.
 77. Sereni L, Castiello MC, Villa A. Platelets in Wiskott-Aldrich syndrome: Victims or executioners? *J Leukoc Biol.* 2018;103(3):577-590.
 78. Shcherbina A, Cooley J, Lutskiy MI, et al. WASP plays a novel role in regulating platelet responses dependent on alphaIIb beta3 integrin outside-in signalling. *Br J Haematol.* 2010;148(3):416-427.
 79. Kim H, Falet H, Hoffmeister KM, Hartwig JH. Wiskott-Aldrich syndrome protein (WASP) controls the delivery of platelet transforming growth factor-beta1. *J Biol Chem.* 2013;288(48):34352-34363.
 80. Gerrits AJ, Leven EA, Frelinger AL, et al. Effects of eltrombopag on platelet count and platelet activation in Wiskott-Aldrich syndrome/X-linked thrombocytopenia. *Blood.* 2015;126(11):1367-1378.
 81. Coppe A, Nogara L, Pizzuto MS, et al. Somatic mutations activating Wiskott-Aldrich syndrome protein concomitant with RAS pathway mutations in juvenile myelomonocytic leukemia patients. *Hum Mutat.* 2018;39(4):579-587.
 82. Pang L, Xue HH, Szalai G, et al. Maturation stage-specific regulation of megakaryopoiesis by pointed-domain Ets proteins. *Blood.* 2006;108(7):2198-2206.
 83. Li Y, Luo H, Liu T, et al. The ets transcription factor Fli-1 in development, cancer and disease. *Oncogene.* 2015;34(16):2022-2031.
 84. Favier R, Jondeau K, Boutard P, et al. Paris-Trousseau syndrome : clinical, hematological, molecular data of ten new cases. *Thromb Haemost.* 2003;90(5):893-897.
 85. Saultier P, Vidal L, Canault M, et al. Macrothrombocytopenia and dense granule deficiency associated with FLI1 variants: ultrastructural and pathogenic features. *Haematologica.* 2017;102(6):1006-1016.
 86. Delattre O, Zucman J, Plougastel B, et al. Gene fusion with an ETS DNA-binding domain caused by chromosome translocation in human tumours. *Nature.* 1992;359(6391):162-165.
 87. Vo KK, Jarocho DJ, Lyde RB, et al. FLI1 level during megakaryopoiesis affects thrombopoiesis and platelet biology. *Blood.* 2017;129(26):3486-3494.
 88. Vyas P, Ault K, Jackson CW, et al. Consequences of GATA1 deficiency in megakaryocytes and platelets. *Blood.* 1999;93(9):2867-2875.
 89. Fujiwara Y, Browne CP, Cunniff K, et al. Arrested development of embryonic red cell precursors in mouse embryos lacking transcription factor GATA-1. *Proc Natl Acad Sci USA.* 1996;93(22):12355-12358.
 90. Freson K, Devriendt K, Mathijs G, et al. Platelet characteristics in patients with X-linked macrothrombocytopenia because of a novel GATA1 mutation. *Blood.* 2001;98(1):85-92.
 91. Zetterberg E, Verrucci M, Martelli F, et al. Abnormal P-selectin localization during megakaryocyte development determines thrombosis in the gata1low model of myelofibrosis. *Platelets.* 2014;25(7):539-547.
 92. Lally J, Boasman K, Brown L, et al. GATA-1: A potential novel biomarker for the differentiation of essential thrombocythemia and myelofibrosis. *J Thromb Haemost.* 2019; 17(6):896-900.
 93. Yamaguchi Y, Zon LI, Ackerman SJ, et al. Forced GATA-1 expression in the murine myeloid cell line M1: induction of c-Mpl expression and megakaryocytic/erythroid differentiation. *Blood.* 1998;91(2):450-457.
 94. Kaasinen E, Kuismin O, Rajamaki K, et al. Impact of constitutional TET2 haploinsufficiency on molecular and clinical phenotype in humans. *Nat Commun.* 2019;10(1):1252.
 95. Fuster JJ, MacLauchlan S, Zuriaga MA, et al. Clonal hematopoiesis associated with TET2 deficiency accelerates atherosclerosis development in mice. *Science.* 2017;355(6327):842-847.
 96. Vannucchi AM, Barbui T. Thrombocytosis and thrombosis. *Hematology Am Soc Hematol Educ Program.* 2007:363-370.
 97. Schafer AI. Thrombocytosis. *N Engl J Med.* 2004;350(12):1211-1219.
 98. Hengeveld PJ, Hazenberg MD, Biezeveld MH, Raphael MF [Risk of thrombosis in reactive thrombocytosis]. *Ned Tijdschr Geneesk.* 2018;162:D2697.
 99. Scharf RE. Molecular complexity of the megakaryocyte-platelet system in health and disease. *Hamostaseologie.* 2016;36(3): 159-160.
 100. Falanga A, Marchetti M. Thrombosis in myeloproliferative neoplasms. *Semin Thromb Hemost.* 2014;40(3):348-358.



Acquired von Willebrand syndrome: focused for hematologists

Massimo Franchini¹ and Pier Mannuccio Mannucci²

¹Department of Transfusion Medicine and Hematology, Carlo Poma Hospital, Mantua and

²Fondazione IRCCS Ca' Granda Ospedale Maggiore Policlinico, Angelo Bianchi Bonomi Hemophilia and Thrombosis Center, Milan, Italy

Haematologica 2020
Volume 105(8):2032-2037

ABSTRACT

The acquired von Willebrand syndrome (AvWS) is a rare bleeding disorder with laboratory findings similar to those of inherited von Willebrand disease. However, unlike the inherited disease, AvWS occurs in persons with no personal and family history of bleeding and is often associated with a variety of underlying diseases, most frequently lymphoproliferative, myeloproliferative and cardiovascular disorders. After the presentation of a typical case, in this narrative review we discuss the more recent data on the pathophysiology, clinical, laboratory and therapeutic aspects of this acquired bleeding syndrome. We chose to focus particularly on those aspects of greater interest for the hematologist.

Introduction

Acquired von Willebrand syndrome (AvWS) is a rare but probably underestimated bleeding disorder characterized by laboratory findings and clinical presentations similar to those of inherited von Willebrand disease (vWD).¹⁻⁸ Differing from vWD, a bleeding disorder due to quantitative or qualitative genetic defects of von Willebrand factor (vWF),^{9,10} AvWS usually occurs more frequently in adults with no personal or family history for a bleeding diathesis. Although it was first recognized more than 50 years ago (it was described in 1968 in a patient with systemic lupus erythematosus), AvWS has gained renewed interest in the last few years due to its association with relatively frequent cardiovascular disorders, including congenital heart defects, aortic stenosis, and the use of left ventricular assist devices.¹¹⁻¹⁵ In addition to these, many other underlying diseases are associated with AvWS, ranging from solid and hematologic cancers to autoimmune diseases.¹⁶⁻¹⁸ Various mechanisms are implied in the pathophysiology of AvWS, the majority of them leading to the increased degradation or clearance of circulating vWF. This article reviews current knowledge on the mechanisms, diagnostic, clinical and therapeutic aspects of AvWS, focusing particularly on those cases associated with hematologic disorders. AvWS associated with cardiovascular diseases is not discussed here because it requires particular diagnostic and treatments strategies which were extensively and recently analyzed.^{11-15,19,20} A brief description of an individual case provides an example which allows us to introduce the main characteristics and management of the syndrome.

Clinical case

A 70-year old man presented to the emergency room of the main Mantua city hospital in north east Italy with spontaneous gingival bleeding. Apart from mild fatigue and headache, the patient felt well, with no bruising or other hemorrhagic symptoms. His medical history was positive for hypertension under satisfactory drug control but negative for a bleeding diathesis, and he had undergone an inguinal herniotomy 20 years earlier with no hemorrhagic complications. On physical examination, there was mild cutaneous and conjunctival pallor, blood oozing from the gums, and lymphadenomegaly at superficial stations (maximum diameter, 2 cm). Blood tests revealed normocytic anemia (hemoglobin 9 g/dL), with normal white cell and platelet counts. With a normal prothrombin time, the activated partial thromboplastin time (APTT) was mildly prolonged (ratio, 1.29; normal range, 0.82-1.18), but its full correction with a normal plasma mixing test excluded

Correspondence:

PIER MANNUCCIO MANNUCCI
piermannuccio.mannucci@policlinico.mi.it

Received: April 14, 2020.

Accepted: May 27, 2020.

Pre-published: June 18, 2020.

doi:10.3324/haematol.2020.255117

Check the online version for the most updated information on this article, online supplements, and information on authorship & disclosures: www.haematologica.org/content/105/8/2032

©2020 Ferrata Storti Foundation

Material published in *Haematologica* is covered by copyright. All rights are reserved to the Ferrata Storti Foundation. Use of published material is allowed under the following terms and conditions:

<https://creativecommons.org/licenses/by-nc/4.0/legalcode>.

Copies of published material are allowed for personal or internal use. Sharing published material for non-commercial purposes is subject to the following conditions:

<https://creativecommons.org/licenses/by-nc/4.0/legalcode>,

sect. 3. Reproducing and sharing published material for commercial purposes is not allowed without permission in writing from the publisher.



a coagulation inhibitor. Screening for lupus anticoagulant was also negative. Factor VIII coagulant activity (FVIII:C) was 40% (normal range, 50-150%), von Willebrand factor antigen (vWF:Ag) was 18% (normal range, 50-120%), ristocetin co-factor activity (vWF:RCo) was 29% (normal range, 50-150%), and the collagen binding activity (vWF:CB) was 37% (normal range, 50-150%). Following the observation of slightly elevated serum proteins (8.8 g/dL; normal range, 6.5-8.0 g/dL), electrophoresis showed increased concentrations in the beta (β) (2.58 g/dL; normal range, 0.6-0.9 g/dL) and gamma (γ) (2.36; normal range, 0.8-1.4 g/dL) regions, with a double spike at a concentration of 1.67 g/dL (Figure 1). Immunofixation confirmed a double monoclonal component, IgM kappa (κ). Immunoglobulin assays showed serum IgG levels of 5.39 g/L (normal range, 7-16 g/L), IgA 0.11 g/L (normal range, 0.7-4 g/L), but very high IgM at 63.7 g/L (normal range, 0.4-2.3 g/L). Bone marrow biopsy detected increased cellularity (90%) that accounted for at least 40% of interstitial cellular aggregates of lymphoid, lymphoplasmacytoid and plasma cells, that at immunohistochemical analysis were positive for CD20, IgM and κ light chains but negative for CD5, CD23, D1 cyclin and lambda (λ) light chains. Megakaryocytic and myelo-erythroid lineages were represented but depressed. An abdominal ultrasound showed no hepatosplenomegaly nor lymphadenopathy. On the basis of these findings a diagnosis of AvWS associated with Waldenstrom macroglobulinemia was made. The patient underwent a test with desmopressin (DDAVP) given subcutaneously at a dose of 0.3 μ g/kg in an attempt to increase vWF and FVIII plasma levels, but no increase was observed at 1, 2 and 4 hours post injection. Due to the very high serum levels of the IgM monoclonal component, the patient underwent four plasma apheretic procedures (each with the removal of 1.5 plasma volume), resulting in a significant reduction in the monoclonal component, and normalization of vWF/FVIII parameters (vWF:Ag 86%, vWF:RCo 77%, vWF:CB 69%, and FVIII:C 84%). The patient was treated with six monthly cycles of bendamustine-rituximab, with a good partial response (IgM 6 g/L, normal hemoglobin and

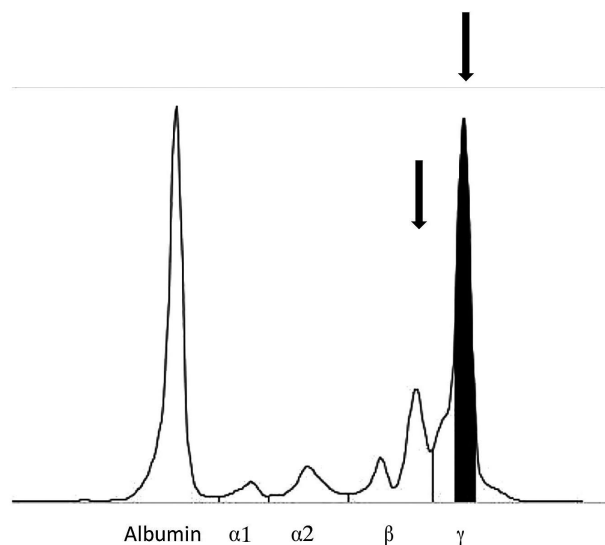


Figure 1. Example clinical case of acquired von Willebrand syndrome. Patient's serum protein electrophoresis. The arrows indicate a double spike within the beta (β) and gamma (γ) regions, respectively.

hemostasis test values, complete disappearance of the enlarged lymph nodes). This positive response was maintained at a 3-year follow up, and a recent bone marrow biopsy showed a normal trilineage hematopoiesis with less than 10% lymphoplasmacytoid cells.

Pathophysiology, clinical presentation, diagnosis

Pathophysiology

In the past, AvWS was considered a very rare hemorrhagic disease. The more recent discovery of its association with relatively frequent cardiovascular disorders suggests that its prevalence is higher than previously thought.^{19,20} Unlike acquired hemophilia (another rare acquired bleeding disorder caused by autoantibodies that neutralize FVIII coagulant activity),^{21,25} the complex pathophysiology of AvWS involves various and different mechanisms.¹⁶⁻¹⁸ Most cases are due to an increased plasma clearance of vWF caused by such mechanisms as antibodies, cell adsorption, shear stress or increased proteolysis. At variance with acquired hemophilia, AvWS almost always occurs in association with an underlying disorder;¹⁶⁻¹⁸ besides cardiovascular disorders, those more frequently associated are lymphoproliferative disorders [multiple myeloma, chronic lymphocytic leukemia, monoclonal gammopathy of undetermined significance (MGUS), Waldenstrom macroglobulinemia], and, less frequently, other hematologic malignancies (myeloproliferative neoplasms including essential thrombocythemia, polycythemia vera, primary myelofibrosis, and chronic myeloid leukemia), solid malignancies, and autoimmune disorders (Table 1).^{16-18,24,25} In a registry of the International Society of Thrombosis and Haemostasis (ISTH) that collected data from 211 AvWS cases, lymphoproliferative disorders were the most frequent underlying disorder in 48% of cases, whereas myeloproliferative neoplasms and solid tumors accounted for 15% and 5% of cases.¹⁶⁻¹⁸ Mohri *et al.*, in a prospective study evaluating 206 patients with a range of hematologic disorders, estimated that AvWS was present in approximately 10% of these patients.²⁵ The different underlying disorders lead to AvWS through different mechanisms. In patients with hypothyroidism, the syndrome is caused by the decreased synthesis of an otherwise qualitatively normal vWF, and this can be reversed by l-thyroxine therapy.^{26,27} In most other cases, the synthesis of vWF in megakaryocytes and endothelial cells and its release in circulation are normal, so that AvWS recognizes other mechanistic pathways. In cardiac valvulopathies and left ventricular assist devices, sheering of high-molecular-weight (HMW) vWF multimers by mechanical stress or proteolysis induced by ADAMTS 13 (a disintegrin and metalloproteinase with a thrombospondin type 1 motif, member 13) are involved.²⁸⁻³³ In cases associated with plasma cell dyscrasias (MGUS and multiple myeloma), as well as in autoimmune diseases such as systemic lupus erythematosus, circulating autoantibodies directed against functional or non-functional vWF domains have been reported.³¹⁻³³ Antibody binding to vWF leads to the formation of immune complexes that are cleared from the circulation by the reticulo-endothelial system. Antibodies that neutralize platelet-related vWF activities (inhibitors) have seldom been reported. Finally, a mechanism involving the selective adsorption of HMW multimers on tumor cells leading to their enhanced plasma clearance has been

described in lymphoproliferative diseases (multiple myeloma, Waldenström's macroglobulinemia, non-Hodgkin lymphoma, hairy cell leukemia) and solid cancers.³⁵ In MGUS, the aberrant expression on abnormal plasma cells of the glycoprotein Ib (the principal platelet receptor of vWF) was associated with its selective binding to these cells.³⁴ vWF adsorption onto the cell membranes and subsequent plasma clearance has also been involved in AvWS associated with myeloproliferative neoplasms.³⁵ For example, adsorption on platelets is the mechanism in essential thrombocythemia, with an inverse relationship between platelet count and the plasma defect of HMW multimers.³⁵ In addition, essential thrombocythemia and other myeloproliferative neoplasms may cause the syndrome through increased plasma vWF proteolysis.

Clinical features

The bleeding diathesis usually occurs rather late in life in persons with no past and family history of bleeding. The main symptoms are mild to moderately severe mucocutaneous bleeding (ecchymosis, epistaxis, menorrhagia, gastrointestinal tract bleeding), similar to inherited vWD, or excessive bleeding following trauma or surgical procedures, particularly when FVIII:C is low. Gastrointestinal bleeding is usually associated with the detection of angiodysplasia. The mechanism of this vascular abnormality, which has also been described in inherited type 2 and type 3 vWD, involves the defect of HMW vWF multimers, that characterizes all AvWS cases¹⁰ with the only exception of those associated with hypothyroidism. According to the ISTH registry,¹⁶⁻¹⁸ patients with AvWS associated with lymphoproliferative disorders have more severe bleeding symptoms than those with other underlying conditions, even though bleeding-related deaths have seldom been reported. As mentioned above, lymphoproliferative disorders account for a significant proportion of AvWS cases, ranging from 30% to 48%. A few studies have investigated the association of myeloproliferative neoplasms with AvWS.³⁵⁻³⁸ Mital *et al.*, in two studies involving 312 consecutive patients with essential thrombocythemia (n=170) or polycythemia vera (n=142), found prevalences of 20% and 12%, respectively, and they recommend that persons with these disorders and a bleeding tendency should be screened for the presence of an underlying AvWS.^{35,36} A high prevalence was also found by Rottenstreich *et al.*³⁷ in 173 patients with thrombocythemia (n=116) or polycythemia (n=57),³⁷ meaning that 55% of those with thrombocythemia and 49% of those with polycythemia had an AvWS. Younger age, higher platelet count and hemoglobin levels, as well as the presence of the *JAK2*^{V617F} somatic mutation, independently pre-

dicted the syndrome in patients with thrombocythemia but not in polycythemia, the only predictor being a higher platelet count.³⁷ Furthermore, Mital *et al.*,³⁸ in an investigation of 21 patients with systemic mastocytosis, found a high rate of AvWS accompanied by mild to moderate symptoms of mucocutaneous bleeding (ecchymosis, menorrhagia, epistaxis).

Diagnosis

In the absence of a family history of bleeding, the diagnosis of AvWS is usually based on the laboratory tests used to diagnose inherited vWD.^{39,40} A defect in primary hemostasis is demonstrated by a prolonged skin bleeding time or prolonged closure time with PFA-100.⁴⁰ Plasma samples usually show normal or mildly decreased vWF:Ag contrasting with a more marked decrease in vWF:RCo and vWF:CB.⁴⁰ The latter qualitative platelet-related activity assays of vWF are frequently lower than the quantitative vWF:Ag assay, resulting in vWF:RCo/vWF:Ag ratios that are often below 0.7, similar to type 2A vWD.⁴⁰ When FVIII:C is low, a prolonged APTT is also observed. vWF multimer electrophoresis is warranted to demonstrate the defect of HMW multimers that helps to distinguish AvWS from type 1 vWD.^{9,10} Measurement of the plasma vWF propeptide, which reflects the degree of vWF biosynthesis, is not currently recommended to distinguish inherited vWD from AvWS^{41,42} because the latter is often characterized by an accelerated clearance of vWF from the circulation but normal synthesis, so that propeptide levels are normal. At variance with acquired hemophilia, autoantibodies that inhibit platelet-related vWF activity play a mechanistic role in a minority of AvWS cases.^{43,44} Nevertheless, because the presence of neutralizing antibodies seems to be associated with a more severe bleeding tendency, antibody screening should be performed in all AvWS cases. The most common method used to look for an inhibitory activity against vWF is based upon mixing studies (patient plasma mixed with normal plasma and incubated at 37°C), followed by the measurement of both residual vWF:RCo and vWF:CB.⁴⁰⁻⁴⁴ However, an inhibitor is seldom demonstrated and the antibodies that bind vWF and accelerate its plasma clearance without neutralizing vWF activity cannot be detected with this method. Enzyme-linked immunosorbent assays (ELISA) are an option that has, however, not yet been adequately standardized.⁴⁵ Overall, diagnosis of AvWS is difficult, and a correct workup should consider all information from both clinical and case history evaluation as well as laboratory results. In particular, the differential diagnosis with milder forms of inherited vWD is important given the difference in therapeutic approach (see below).

Table 1. Conditions associated with the acquired von Willebrand syndrome.

Conditions	
Cancers	Hematologic: MGUS, multiple myeloma, Waldenström macroglobulinemia, chronic lymphocytic leukemia, hairy cell leukemia, lymphomas, essential thrombocythemia, polycythemia vera, chronic myeloid leukemia. Solid: Wilm's tumor, lung and bladder adenocarcinoma.
Autoimmune diseases	Systemic lupus erythematosus, autoimmune thyroid disorders, connective tissue diseases, GvHD.
Drug-induced	Antibiotics (griseofulvin, ciprofloxacin), anticonvulsants (valproic acid), plasma volume expander (HES).
Other	Cardiovascular disorders (aortic stenosis, congenital cardiac defects, mitral valve prolapse, left ventricular assist devices), infections (viral, parasitical), uremia, gastrointestinal angiodysplasia, diabetes.

MGUS: monoclonal gammopathy of unknown significance; GvHD: graft-versus-host disease; HES: hydroxyethyl starch.

Treatment

There are three main treatment goals for patients with AvWS: the control of acute bleeding, its prevention in high-risk situations, and the achievement of a stable remission or cure of the syndrome.^{46,47} Removal of the underlying disorder (i.e. by means of surgery, chemotherapy, radiotherapy and/or immunosuppressants), which is not within the scope of this review, is the only potentially curative approach. However, treatment of the associated condition may not be feasible, and a partial remission does not always ameliorate the bleeding symptoms.

As far as the hemostatic therapies are concerned, a range of different medications have been used: desmopressin (DDAVP), vWF/FVIII concentrates, antifibrinolytic agents, high-dose intravenous immunoglobulins (HDIVIg), plasmapheresis and recombinant activated factor VII (rFVIIa).^{46,47}

The synthetic analog of DDAVP, given intravenously or subcutaneously at the dose of 0.3 µg/kg, was used to control or prevent bleeding in the AvWS.^{48,49} The ISTH registry reported an overall success rate with DDAVP of approximately 30%, although this varied according to the underlying disorder: lower in cardiovascular disorders (10%) and myeloproliferative neoplasms (21%), and higher in autoimmune (33%) and lymphoproliferative (44%) disorders.¹⁶⁻¹⁸ In a prospective trial performed in ten patients with MGUS, plasma vWF levels increased in all patients after DDAVP, but the increase was short-lasting.⁴⁴ A short plasma half-life of vWF following DDAVP administration has also been observed in the context of other lymphoproliferative disorders and is thought to be related to the presence of anti-vWF antibodies. A transient effect of DDAVP was also observed in patients with myeloproliferative neoplasms, mainly due to adsorption or proteolytic cleavage of the released vWF. It is advisable to closely monitor FVIII:C and vWF:RCo/vWF:CB plasma levels after DDAVP in order to maintain these at levels that are sufficient to prevent or treat bleeds.

As far as replacement therapy is concerned, several plasma-derived concentrates containing vWF have been used in AvWS.¹⁶⁻¹⁸ In the ISTH registry, vWF/FVIII concentrates showed a favorable response in approximately 40% of cases,¹³ with dosages ranging between 30-100 vWF:RCo units/kg. The half-life of infused vWF is shorter than in inherited vWD, thus requiring higher doses of vWF/FVIII concentrate to ensure adequate hemostatic plasma levels.¹⁶⁻¹⁸ Plasma FVIII:C and vWF:RCo must be monitored when administering DDAVP, particularly in patients undergoing invasive or surgical procedures.

The antifibrinolytic agents most commonly used in

AvWS are the lysine analogs ε-aminocaproic acid, administered at a dose of 50-60 mg/kg every 4-6 hours, and tranexamic acid, at a dose of 20-25 mg/kg every 8-12 hours.⁵⁰ These drugs can be given orally, intravenously or topically, and act by inhibiting plasminogen activation. Antifibrinolytics are primarily used as adjuvants together with DDAVP or vWF/FVIII concentrates for surgery and bleeding, particularly at sites with high fibrinolytic activity (i.e. gastrointestinal and oral tracts); however, these drugs may be used alone for minor bleeding episodes.

The ISTH registry reported a 33% success rate in clinical cases receiving HDIVIg in AvWS, especially for lymphoproliferative disorders (37%), solid tumors (100%), and immunological diseases (50%).¹⁶⁻¹⁸ HDIVIg is especially useful in cases associated with MGUS.⁴⁴ In a prospective trial which enrolled ten patients with AvWS and MGUS, HDIVIg was more effective than DDAVP and vWF/FVIII concentrates because there was a more sustained increase in FVIII/vWF activities and shortening of bleeding time for at least 15-20 days in all IgG-MGUS cases.⁴⁴ In contrast, no response was observed in patients with IgM class MGUS (IgM-MGUS).⁴⁴ In addition, prophylactic infusions of HDIVIg every 21 days stopped recurrent gastrointestinal bleeding in patients with IgG-MGUS. The mechanisms of action of HDIVIg may involve an anti-idiotypic effect, blockage of reticulo-endothelial Fc-receptors, or capture of the circulating immune complexes by the immunoglobulins.⁵⁵ The recommended doses of HDIVIg are 1 g/kg for two days or 0.4 g/kg for five days.⁵¹⁻⁵⁴ The increase in vWF and FVIII:C levels usually occurs within 24-48 hours and may last up to 3-4 weeks; thus, additional courses of HDIVIg every 21 days are necessary to maintain a clinical response. On the whole, HDIVIg represent an important therapeutic tool for the management of AvWS, especially for cases associated with IgG monoclonal gammopathies, lymphoproliferative disorders, and multiple myeloma associated IgG paraproteins.⁴⁴ Due to the delay in the post-infusion increase in vWF and FVIII:C levels, HDIVIg is not effective in the management of acute bleeding; in these cases, the medication must be administered together with shorter-acting agents such as DDAVP and vWF/FVIII concentrates.⁵¹⁻⁵⁴ The main goal of plasmapheresis is to temporarily eliminate autoantibodies and paraproteins from the circulation. This procedure is particularly effective in IgM-MGUS, which generally responds poorly to other treatments. Finally, rFVIIa, usually administered at a dose of 90 µg/kg for a median of three doses, has been successfully used when bleeding associated with AvWS is unresponsive to DDAVP and vWF/FVIII concentrates.⁵⁵⁻⁵⁹

Table 2 summarizes the multiple therapeutic strategies available for the treatment or prevention of bleeding in

Table 2. Hemostatic therapies in acquired von Willebrand syndrome associated with different underlying diseases.

Underlying diseases	Therapy
Cardiovascular	vWF/FVIII concentrates, antifibrinolytics
Lymphoproliferative	HDIVIg
- IgG MGUS	Plasmapheresis, DDAVP, vWF/FVIII concentrates, antifibrinolytics, rFVIIa
- IgM MGUS	DDAVP, vWF/FVIII concentrates, antifibrinolytics, rFVIIa, HDIVIg
- Lymphoma, myeloma	
Myeloproliferative	DDAVP, vWF/FVIII concentrates, antifibrinolytics
Autoimmune	HDIVIg, DDAVP, vWF/FVIII concentrates

MGUS: monoclonal gammopathy of unknown significance; vWF: von Willebrand factor; FVIII: factor VIII; HDIVIg: high-dose intravenous immunoglobulin; DDAVP: desmopressin; rFVIIa: recombinant activated factor VII.

AvWS. DDAVP and vWF/FVIII concentrates typically give a prompt but short-lived improvement in vWF and FVIII levels. High doses of vWF/FVIII concentrates usually result in higher response rates, particularly in cases associated with lymphoproliferative disorders, which represent the most challenging condition to treat, and in the context of myeloproliferative neoplasms. In these cases, the short plasma residence time of vWF must be taken into account when dosages and intervals of administration of DDAVP and vWF/FVIII concentrates are planned. Patients with IgG autoantibodies or paraproteins usually respond to HDIVIg with longer-lasting effects. In addition, antifibrinolytics may be helpful as adjuvant therapy, particularly for the management of mucocutaneous bleeds.

Conclusions

Acquired von Willebrand syndrome is a highly heterogeneous bleeding disorder, usually characterized by mild to moderate hemorrhagic symptoms that may sometimes be severe, especially when the disease becomes manifest following surgery. Although AvWS is rare, our perception

is that its true incidence is underestimated due to the diagnostic complexity. When laboratory findings suggest vWD in a patient with a negative personal and family history of a bleeding diathesis, possible AvWS-associated conditions should be explored. We advise screening for AvWS in those patients with conditions potentially associated with this syndrome, particularly onco-hematologic disorders, at the time of the onset of abnormal and otherwise unexplained bleeding and before undergoing invasive or surgical procedures.

The diagnostic workup of patients with suspected AvWS is challenging. This is mainly due to the overlap in clinical and laboratory features with those of inherited vWD. Diagnosis requires the close integration of hematologists with laboratory experts. Similarly, a close interaction between clinicians from different specialties (i.e. hematology, oncology, rheumatology, cardiology) is needed to appropriately manage patients with AvWS. Besides the control or prevention of bleeding, which often requires the combination of multiple hemostatic medications, the mainstay of treatment is the removal of the underlying conditions. When feasible, this is the only way to cure AvWS.

References

- Michiels JJ, Michiels JJ, Budde U, et al. Acquired von Willebrand syndromes: clinical features, aetiology, pathophysiology, classification and management. *Best Pract Res Clin Haematol.* 2001;14(2):401-436.
- Kumar S, Pruthi RK, Nichols WL. Acquired von Willebrand's syndrome: a single institution experience. *Am J Hematol.* 2003;72(4):243-247.
- Franchini M, Lippi G. Recent acquisitions in acquired and congenital von Willebrand disorders. *Clin Chim Acta.* 2007;377(1-2):62-69.
- Franchini M, Lippi G. Acquired von Willebrand syndrome: an update. *Am J Hematol.* 2007;82(5):368-375.
- Franchini M, Lippi G, Favaloro EJ. Advances in hematology. Etiology and diagnosis of acquired von Willebrand syndrome. *Clin Adv Hematol Oncol.* 2010;8(1):20-24.
- Mital A. Acquired von Willebrand syndrome. *Adv Clin Exp Med.* 2016;25(6):1337-1344.
- Charlebois J, Rivard GE, St-Louis J. Management of acquired von Willebrand syndrome. *Transfus Apher Sci.* 2018;57(6):721-723.
- Menegatti M, Biguzzi E, Peyvandi F. Management of rare acquired bleeding disorders. *Hematology Am Soc Hematol Educ Program.* 2019;2019(1):80-86.
- Leebeek FW, Eikenboom JC. Von Willebrand's disease. *N Engl J Med.* 2016;375(21):2067-2080.
- Mannucci PM. New therapies for von Willebrand disease. *Blood Adv.* 2019;3(21):3481-3487.
- Vincentelli A, Susen S, Le Toumeau T, et al. Acquired von Willebrand syndrome in aortic stenosis. *N Engl J Med.* 2003;349(4):343-349.
- Loscalzo J. From clinical observation to mechanism--Heyde's syndrome. *N Engl J Med.* 2012;367(20):1954-1956.
- Otto CM, Prendergast B. Aortic-valve stenosis--from patients at risk to severe valve obstruction. *N Engl J Med.* 2014;371(8):744-756.
- Mehta R, Athar M, Girgis S, Hassan A, Becker RC. Acquired Von Willebrand Syndrome (AVWS) in cardiovascular disease: a state of the art review for clinicians. *J Thromb Thrombolysis.* 2019;48(1):14-26.
- Horiuchi H, Doman T, Kokame K, Saiki Y, Matsumoto M. Acquired von Willebrand syndrome associated with cardiovascular diseases. *J Atheroscler Thromb.* 2019;26(4):303-314.
- Federici AB, Rand JH, Bucciarelli P, et al. Acquired von Willebrand syndrome: data from an International registry. *Thromb Haemost.* 2000;84(2):345-349.
- Federici AB, Budde U, Rand JH. Acquired von Willebrand syndrome 2004: international registry. *Hämostaseologie.* 2004;24(1):50-55.
- Federici AB, Budde U, Castaman G, Rand JH, Tiede A. Current diagnostic and therapeutic approaches to patients with acquired von Willebrand syndrome: a 2013 update. *Semin Thromb Hemost.* 2013;39(2):191-201.
- Muslem R, Caliskan K, Leebeek FWG. Acquired coagulopathy in patients With left ventricular assist devices. *J Thromb Haemost.* 2018;16(3):429-440.
- Thomas J, Kostousov V, Teruya J. Bleeding and thrombotic complications in the use of extracorporeal membrane oxygenation. *Semin Thromb Hemost.* 2018;44(1):20-29.
- Coppola A, Favaloro EJ, Tufano A, Di Minno MND, Cerbone AM, Franchini M. Acquired inhibitors of coagulation factors: Part I-acquired hemophilia A. *Semin Thromb Hemost.* 2012;38(5):433-446.
- Franchini M, Mannucci PM. Acquired haemophilia: a 2013 update. *Thromb Haemost.* 2013;110(6):1114-1120.
- Tiede A, Abdul Karim F, Jiménez-Yuste V, et al. Factor VIII activity and bleeding risk during prophylaxis for severe hemophilia A: a population pharmacokinetic model. *Haematologica.* 2020 Apr 23. doi: 10.3324/haematol.2019.241554. [Epub ahead of print]
- Veyradier A, Jenkins CS, Fressinaud E, Meyer D. Acquired von Willebrand syndrome: from pathophysiology to management. *Thromb Haemost.* 2000;84(2):175-182.
- Mohri H, Tanabe J, Ohtsuka M, et al. Acquired von Willebrand disease associated with multiple myeloma: characterization of an inhibitor to von Willebrand factor. *Blood Coagul Fibrinolysis.* 1995;6(6):561-566.
- Bruggers CS, McElligott K, Rallison ML. Acquired von Willebrand disease in twins with autoimmune hypothyroidism: Response to desmopressin and L-thyroxine therapy. *J Pediatr.* 1994;125(6 Pt 1):911-913.
- Franchini M, de Gironcoli M, Lippi G, et al. Efficacy of desmopressin as surgical prophylaxis in patients with acquired von Willebrand disease undergoing thyroid surgery. *Haemophilia.* 2002;8(2):142-144.
- Tsai HM, Sussman II, Nagel RL. Shear stress enhances the proteolysis of von Willebrand factor in normal plasma. *Blood.* 1994;83(8):2171-2179.
- Yoshida K, Tobe S, Kawata M, Yamaguchi M. Acquired and reversible von Willebrand disease with high shear stress aortic valve stenosis. *Ann Thorac Surg.* 2006;81(2):490-494.
- Pareti FI, Lattuada A, Bressi C, et al. Proteolysis of von Willebrand factor and shear stress-induced platelet aggregation in patients with aortic valve stenosis. *Circulation.* 2000;102(11):1290-1295.
- Mohri H, Motomura S, Kanamori H, et al. Clinical significance of inhibitors in acquired von Willebrand syndrome. *Blood.* 1998;91(10):3623-3629.
- Gan TE, Sawers RJ, Koutris J. Pathogenesis of antibody-induced acquired von Willebrand syndrome. *Am J Hematol.* 1980;9(4):363-371.
- Richard C, Cuadrado MA, Prieto M, et al.

- Acquired von Willebrand disease in multiple myeloma secondary to adsorption of von Willebrand factor by plasma cells. *Am J Hematol.* 1990;35(2):114-117.
34. Scrobobhaci ML, Daniel MT, Levy Y, Marolleau JP, Brouet JC. Expression of Gplb on plasma cells in a patient with monoclonal IgG and acquired von Willebrand disease. *Br J Haematol.* 1993;84(3):471-475.
 35. Mital A, Prejzner W, Bieniaszewska M, Hellmann A. Prevalence of acquired von Willebrand syndrome during essential thrombocythemia: a retrospective analysis of 170 consecutive patients. *Pol Arch Med Wewn.* 2015;125(12):914-920.
 36. Mital A, Prejzner W, Świętkowska-Stodulska R, Hellmann A. Factors predisposing to acquired von Willebrand syndrome during the course of polycythemia vera - retrospective analysis of 142 consecutive cases. *Thromb Res.* 2015;136(4):754-757.
 37. Rottenstreich A, Kleinstern G, Krichevsky S, Varon D, Lavie D, Kalish Y. Factors related to the development of acquired von Willebrand syndrome in patients with essential thrombocythemia and polycythemia vera. *Eur J Intern Med.* 2017;41:49-54.
 38. Mital A, Prejzner W, Hellmann A. Acquired von Willebrand syndrome during systemic mastocytosis: an analysis of 21 cases. *Pol Arch Intern Med.* 2018;128(7):491-493.
 39. Federici AB. Acquired von Willebrand syndrome: is it an extremely rare disorder or do we see only the tip of the iceberg? *J Thromb Haemost.* 2008;6(4):565-568.
 40. Favaloro EJ, Facey D, Grispo L. Laboratory assessment of von Willebrand factor. Use of different assays can influence the diagnosis of von Willebrand's disease, dependent on differing sensitivity of sample preparation and differential recognition of high molecular weight VWF forms. *Am J Clin Pathol.* 1995;104(3):264-271.
 41. van Genderen PJ, Boertjes RC, van Mourik JA. Quantitative analysis of von Willebrand factor and its propeptide in plasma in acquired von Willebrand syndrome. *Thromb Haemost.* 1998;80(3):495-498.
 42. Eikenboom J, Federici AB, Dirven RJ, et al; MCMDM-1VWD Study Group. VWF propeptide and ratios between VWF, VWF propeptide, and FVIII in the characterization of type 1 von Willebrand disease. *Blood.* 2013;121(12):2336-2339.
 43. Fricke WA, Brinkhous KM, Garris JB, Roberts HR. Comparison of inhibitory and binding characteristics of an antibody causing acquired von Willebrand syndrome: an assay for von Willebrand factor binding by antibody. *Blood.* 1985;66(3):562-569.
 44. Mannucci PM, Lombardi R, Bader R, et al. Studies of the pathophysiology of acquired von Willebrand's disease in seven patients with lymphoproliferative disorders or benign monoclonal gammopathies. *Blood.* 1984;64(3):614-621.
 45. Siaka C, Rugeri L, Caron C, Goudemand J. A new ELISA assay for diagnosis of acquired von Willebrand syndrome. *Haemophilia.* 2003;9(3):303-308.
 46. Federici AB. Therapeutic approaches to acquired von Willebrand syndrome. *Expert Opin Investig Drugs.* 2000;9(2):347-354.
 47. Tiede A, Rand JH, Budde U, Ganser A, Federici AB. How I treat the acquired von Willebrand syndrome. *Blood.* 2011;117(25):6777-6785.
 48. Franchini M. The use of desmopressin as a hemostatic agent: a concise review. *Am J Hematol.* 2007;82(8):731-735.
 49. Biguzzi E, Siboni SM, Peyvandi F. Acquired von Willebrand syndrome and response to desmopressin. *Haemophilia.* 2018;24(1):e25-e28.
 50. Franchini M, Mannucci PM. The never ending success story of tranexamic acid in acquired bleeding. *Haematologica.* 2020;105(5):1201-1205.
 51. Federici AB. Use of intravenous immunoglobulin in patients with acquired von Willebrand syndrome. *Hum Immunol.* 2005;66(4):422-430.
 52. Federici AB, Rossi V, Sacchi E, Franchini M. Are intravenous immunoglobulins really inappropriate in acquired von Willebrand syndrome? *Blood Transfus.* 2012;10(3):402-403.
 53. Stone ME, Mazzeffi M, Derham J, Korshin A. Current management of von Willebrand disease and von Willebrand syndrome. *Curr Opin Anaesthesiol.* 2014;27(3):353-358.
 54. Michiels JJ, van Vliet HH. Acquired von Willebrand disease in monoclonal gammopathies: Effectiveness of high-dose intravenous gamma globulin. *Clin Appl Thromb Hemost.* 1999;5(3):152-157.
 55. Colella MP, Duarte GC, Marques JF Jr, De Paula EV. Haemostatic management of extreme challenges to haemostasis in acquired von Willebrand syndrome. *Haemophilia.* 2012;18(3):e188-191.
 56. Friederich PW, Wever PC, Briët E, Doorenbos CJ, Levi M. Successful treatment with recombinant factor VIIa of therapy-resistant severe bleeding in a patient with acquired von Willebrand disease. *Am J Hematol.* 2001;66(4):292-294.
 57. Franchini M, Veneri D, Lippi G. The use of recombinant activated factor VII in congenital and acquired von Willebrand disease. *Blood Coagul Fibrinolysis.* 2006;17(8):615-619.
 58. Smaradottir A, Bona R. A case of acquired von Willebrand syndrome successfully treated with recombinant factor VIIa during thyroidectomy. *Thromb Haemost.* 2004;92(3):666-667.
 59. Karger R, Weippert-Kretschmer M, Budde U, Kretschmer V. Diagnosis and therapeutic management in a patient with type 2B-like acquired von Willebrand syndrome. *Blood Coagul Fibrinolysis.* 2011;22(2):144-147.



Kreuth V initiative: European consensus proposals for treatment of hemophilia using standard products, extended half-life coagulation factor concentrates and non-replacement therapies

Flora Peyvandi,^{1,2} Karin Berger,^{3,4} Rainer Seitz,⁵ Anneliese Hilger,⁵ Marie-Laure Hecquet,⁶ Michael Wierer,⁶ Karl-Heinz Buchheit,⁶ Brian O'Mahony,^{7,8} Amanda Bok,⁸ Mike Makris,⁹ Ulrich Mansmann,⁴ Wolfgang Schramm¹⁰ and Pier Mannuccio Mannucci⁴

¹Fondazione IRCCS Ca' Granda Ospedale Maggiore Policlinico, Angelo Bianchi Bonomi Hemophilia and Thrombosis Center and Fondazione Luigi Villa, Milan, Italy; ²Università degli Studi di Milano, Department of Pathophysiology and Transplantation, Milan, Italy; ³University Hospital, Ludwig-Maximilian University, Department of Medicine III, Munich, Germany; ⁴Institute for Medical Information Processing, Biometry and Epidemiology (IBE), Ludwig-Maximilian-University, Munich, Germany; ⁵Paul-Ehrlich-Institut, Langen, Germany; ⁶European Directorate for the Quality of Medicines and Healthcare, Strasbourg, France; ⁷Trinity College, Dublin, Ireland; ⁸European Haemophilia Consortium, Brussels, Belgium; ⁹Sheffield Haemophilia and Thrombosis Centre, Sheffield, UK and ¹⁰Department of Transfusion Medicine and Haemostasis, Ludwig-Maximilians-University, Munich, Germany

ABSTRACT

This report contains the updated consensus recommendations for optimal hemophilia care produced in 2019 by three Working Groups (WG) on behalf of the European Directorate for Quality of Medicines and Healthcare in the frame of the Kreuth V Initiative. WG1 recommended access to prophylaxis for all patients, the achievement of plasma factor trough levels of at least 3-5% when extended half-life factor VIII (FVIII) and FIX products are used, a personalized treatment regimen, and a choice of chromogenic assays for treatment monitoring. It was also emphasized that innovative therapies should be supervised by hemophilia comprehensive care centers. WG2 recommended mandatory collection of postmarketing data to assure the long-term safety and efficacy of new hemophilia therapies, the establishment of national patient registries including the core data recommended by the European Medicines Agency and the International Society on Thrombosis and Haemostasis, with adequate support under public control, and greater collaboration to facilitate a comprehensive data evaluation throughout Europe. WG3 discussed methodological aspects of hemophilia care in the context of access decisions, particularly for innovative therapies, and recommended that clinical studies should be designed to provide the quality of evidence needed by regulatory authorities, HTA bodies and healthcare providers. The dialogue between all stakeholders in hemophilia care and patient organizations should be fostered to implement these recommendations.

Correspondence:

FLORA PEYVANDI,
flora.peyvandi@unimi.it

Received: November 18, 2019.

Accepted: May 20, 2020.

Pre-published: May 28, 2020.

doi:10.3324/haematol.2019.242735

Check the online version for the most updated information on this article, online supplements, and information on authorship & disclosures: www.haematologica.org/content/105/8/2038

©2020 Ferrata Storti Foundation

Material published in *Haematologica* is covered by copyright. All rights are reserved to the Ferrata Storti Foundation. Use of published material is allowed under the following terms and conditions:

<https://creativecommons.org/licenses/by-nc/4.0/legalcode>.

Copies of published material are allowed for personal or internal use. Sharing published material for non-commercial purposes is subject to the following conditions:

<https://creativecommons.org/licenses/by-nc/4.0/legalcode>,

sect. 3. Reproducing and sharing published material for commercial purposes is not allowed without permission in writing from the publisher.



Introduction

The Wildbad Kreuth Initiative started in 1999 with a seminar including experts from 15 European Community member states. This was followed over the next few years by a series of four meetings. Treatment of hemophilia has always been the focus of the initiative, given the increasing number of diagnosed patients and the importance of providing them with optimal therapies. The objectives of the Initiative were to evaluate the state of hemophilia therapy, identify areas in need of further studies, and provide updated recommendations for optimal use of blood

products for treatment. The first Kreuth meeting also dealt with the optimal use of the available products in hemophilia therapy, emphasizing that the main priority was the safety of blood and blood products. Attention was also given to the need to guarantee an effective treatment, ensuring that all subjects with coagulation disorders can benefit from these lifesaving therapies.¹

The following Kreuth meetings were periodically convened under the joint auspices of the Ludwig-Maximilian University of Munich (LMU), the Paul Ehrlich Institute (PEI), and the Council of Europe through its European Directorate for the Quality of Medicines and Healthcare (EDQM), under the aegis of the European Committee on Blood Transfusion (CD-P-TS). The latter institution provides resolutions that are non-binding but that are still strong indications for member states. The second Kreuth meeting in 2009 was attended by 110 transfusion medicine experts, hemophilia clinicians and regulatory authority representatives from 38 countries. New recommendations were provided regarding the best clinical practice on hemophilia, home treatment, genetic counselling and equal treatment across European member states.²

The following two meetings in 2013 and 2016 focused on the optimal use of coagulation factors and provided the opportunity to review trends in the use of factor concentrates.^{3,4} A total of 12 recommendations were made in 2016, dealing with national protocols or guidelines for the management of aging patients with hemophilia, the minimum utilization of FVIII and FIX concentrates in each country, treatment for hepatitis C with direct-acting antiviral agents, genotype analysis for all patients with severe hemophilia, access to bypassing agents and immune tolerance for those with inhibitors, individualization of treatment regimens with extended half-life products and the attainment of the highest possible rate of bleeding prevention by increasing the trough plasma factor levels. The recommendations emerging from the 2013 and 2016 Kreuth meetings were subsequently incorporated by the EDQM into proposals for resolutions adopted by the Committee of Ministers of the Council of Europe, with the objective of increasing their visibility and providing official support. The 2017 Resolution [Resolution CM/Res(2017)43 on principles concerning hemophilia therapies]⁵ listed 17 principles.

The 2019 meeting was the most recent opportunity for the official delegates nominated by 26 Council of Europe members and observer states, along with members from the academia, the European Hemophilia Consortium (EHC) and the European Medicines Agency (EMA), to review trends in the use of standard half-life coagulation factor concentrates, but also of the new extended half-life products and non-replacement therapies.

Methodology

The “Wildbad Kreuth Initiative V – Optimal Treatment of hemophilia symposium” that took place in June 2019 involved clinicians, regulators and patient organizations from 26 European countries.

The participants were experts invited by the Scientific Programme Committee, as well as delegates appointed by the Council of Europe (CoE) Member States on the invitation of the EDQM, plus delegates from the patient organizations, the European Hemophilia Consortium (EHC)

and World Federation of Hemophilia (WFH), and the European Medicines Agency (EMA). Several of the participating experts are active members of the European Association for Hemophilia and Allied Disorders (EAHAD) or other scientific societies. Industry representatives had the opportunity to participate in the open sessions, but were excluded from the discussion and formulation of the recommendations.

The topics of the symposium were defined by the Scientific Committee on the basis of the results and recommendations of the previous symposia and the latest developments in the field of therapies for hemophilia. During the subsequent open plenary sessions, the invited experts presented an overview of the current state-of-the-art on hemophilia therapy in Europe and treatment progress on the topics predefined by the Scientific Committee. Their solid scientific background and in-depth knowledge of the particular situation of hemophilia treatment in their own countries enabled the chosen delegates taking part to elaborate the recommendations to be presented to the Health Authorities of the CoE Member States.

The experts met in three different working groups to discuss and develop the new recommendations. Each working group was responsible for one of the following areas of discussion:

- clinical evaluation of hemophilia therapy;
- collection of data on hemophilia therapy;
- methodological aspects of hemophilia therapy.

Each working group prepared an interim report which was then discussed with the general assembly. If the report received full and unanimous consensus, it would then go forward for final approval. Based on the final report, this manuscript was prepared and circulated among all participants of all three working groups. Literature research was based on articles published in peer reviewed journals. Medline and PubMed were also searched for all articles published in English in the last ten years. Furthermore, data were extracted from the abstracts of the more recent international congresses.

Recommendation 1

Prophylactic treatment should be available to all hemophilia patients, with or without inhibitors, and access to physiotherapy should be provided.

Prophylaxis in hemophilia is considered the standard of care to prevent joint bleeding and related arthropathy, with the objective of preserving a normal musculoskeletal function. Manco-Johnson established the superiority of prophylactic *versus* on-demand therapy in a randomized clinical trial in 2007.⁶ Primary prophylaxis in hemophilia should start at a very young age (≤ 2 years of age) before joint disease develops, and usually requires coagulation factor infusions 2-3 times per week, whereas secondary prophylaxis begins after the onset of joint disease.⁷ There are many prophylactic schedules, although the optimum dosing regimen is still to be defined. Prophylaxis with standard half-life coagulation factor products is usually given at a dose of 25-40 IU/kg 2-3 times per week,^{7,8} whereas with the extended half-life products, prophylaxis regimens with intervals of 3-5 days in hemophilia A and once every 7-14 days in hemophilia B can be effectively implemented.⁹⁻¹¹

Currently, the availability of a non-replacement therapy administered subcutaneously such as emicizumab makes

prophylaxis accessible to all patients with hemophilia A, including those with FVIII inhibitors, and this may help to reduce bleeding events and improve quality of life.^{12,13}

For optimal care of hemophilia, the multidisciplinary team of specialists should include physiotherapists who should be involved from diagnosis and deal with the functional recovery after each musculoskeletal bleeding. They should also provide a rehabilitation program tailored to tackle all the problems related to this chronic condition.¹⁴

Recommendation 2

With increased treatment options, appropriate instruments should be developed to personalize treatment regimens for all patients with hemophilia A and B.

The aim of prophylaxis is to minimize or abolish bleeding events, and thus improve quality of life in patients. Prophylaxis regimens with standard and extended half-life products have been shown to be effective at preserving joint function and preventing bleeding episodes, although significant variability was seen among individuals exposed to the same treatment regimen.¹⁵ Inter- and intra-individual variability in coagulation factor pharmacokinetics is thought to be the main determinant of uncertainty in the standardization of prophylaxis regimens. Appropriate tools must be developed to personalize treatment regimens, taking into account each patient's individual lifestyle and pharmacokinetic profile.¹⁶ The individualization of prophylaxis is the best strategy to improve patients' quality of life with the ambitious goal of zero bleeding in the near future.

Recommendation 3

With extended half-life therapies, a minimum trough level of 3-5% should be achieved to preserve joint status.

Patients with severe hemophilia suffer from repeated and prolonged spontaneous bleeding episodes, mainly in muscles and joints, that result in disabling musculoskeletal damage and chronic arthropathy. The aim of prophylaxis in hemophilia is to reduce the risk of bleeding in order to preserve normal musculoskeletal function. Prophylaxis dosing regimens using standard half-life FVIII and FIX products can achieve trough plasma levels of 1-2%,¹⁷ but the introduction of extended half-life products significantly improves efficacy by achieving higher trough levels. A further improvement due to the forthcoming second-generation extended half-life products and gene therapies might lead to a further increase in the achievement of almost normal trough factor levels. For the time being, with the opportunities provided by the availability of extended half-life products, the aim should be to achieve a minimum trough level of 3-5% in order to preserve joint function.

Recommendation 4

For the post infusion measurement of extended half-life products chromogenic assays should be used.

Hemophilia patients must be monitored by laboratory testing in order to assess the optimal plasma factor levels after concentrate infusion. One-stage clotting or chromogenic substrate assays have been used for monitoring post-infusion levels. However, with the introduction of extended half-life products, discrepancies between one-stage and chromogenic assays have been observed. The choice of APTT reagents in the one-stage assays, and particularly the source of the contact activator, can influence

assay sensitivity to the extended half-life products. This may lead to factor levels in patients being under- or over-estimated according to the assay used for monitoring, with a potential negative effect on management. Therefore, experts recommended the adoption of a practical approach of switching from one-stage clotting assays to chromogenic assays.^{18,19}

Recommendation 5

When using non-replacement therapies, for example for patients on emicizumab, some laboratory issues should be considered to correctly measure the procoagulant activity, FVIII levels after infusion of FVIII concentrate and in the estimation of FVIII inhibitors.

Novel non-replacement therapies that reduce the effect of natural anticoagulants rather than replace the deficient factor have been developed. One approach is based upon the use of a monoclonal antibody (concizumab) against tissue factor pathway inhibitor (TFPI); another emerging class is based on small interference RNA (siRNA) that reduces antithrombin expression. A different approach is represented by a bispecific antibody (emicizumab) that mimics the co-factor function of FVIII by bridging FIXa and FX. Special consideration should be given to laboratory monitoring in patients on the aforementioned novel approaches, especially for emicizumab, since this is the first non-replacement drug approved by both European and US medicine regulatory agencies (the EMA and the US Food and Drug Administration) for prophylaxis in adult and pediatric patients with hemophilia A, with and without inhibitors, and is currently used in clinical practice.

Emicizumab does not affect the prothrombin and thrombin time, but tests based on intrinsic coagulation are affected by this drug.^{19,20} Conventional one-stage clotting assay over-estimates the procoagulant activity of emicizumab, so that a modified FVIII one-stage clotting assay should be used to monitor this activity. The chromogenic FVIII assay is sensitive to emicizumab and provides an indirect measure of the procoagulant activity and drug concentration when reagents of human origin are used. However, there is no evidence that the procoagulant activity or emicizumab concentrations are correlated with its hemostatic efficacy when assessed by the chromogenic assay employing human reagents. The measurement of plasma FVIII levels after *in vitro* addition of FVIII concentrate and the measurement of anti-FVIII inhibitor titer by the conventional Bethesda method employing human reagents are affected by the drug in treated patients. Therefore, in order to measure post-infusion FVIII levels, and accurately detect the inhibitor titer, a chromogenic assay can be used, but only with reagents of bovine origin that are insensitive to the presence of the drug.^{19,23}

Recommendation 6

The management of patients with hemophilia, particularly those using non-replacement therapies and gene therapies, should be supervised by Comprehensive Care Centres, such as the certified European Haemophilia Comprehensive Care Centres (EHCCC).

Hemophilia patients with and without inhibitors in Europe will be using more and more novel subcutaneous and innovative non-replacement therapies such as emicizumab. Hemophilia specialists must manage these patients in comprehensive care centers, particularly in the event of major intercurrent bleeds or surgery, because the physicians involved must have sufficient knowledge of

the novel drugs to be able to handle any side effect. The need for additional hemostatic drugs, such as bypassing agents, at the time of breakthrough bleeding and surgery may increase the risk of thrombosis, and this must be carefully evaluated. In general, patients should be managed by EHCCC. The future objective of these expert centers should be the preparation and standardization of specific healthcare packages integrating comprehensive procedures for the management of hemophilia patients (with and without inhibitors) using emicizumab and other novel drugs during prophylaxis, with or without the addition of other hemostatic drugs during intercurrent bleeds or at the time of a surgery. The European Association for Hemophilia and Allied Disorders (EAHAD) and the European Hemophilia Consortium (EHC) need to update their joint European certification system, moving from the current self-documentation provided by each center to the implementation of audit visits that are going to be the basis on which the decision whether or not to issue a certificate will be taken.

Recommendation 7

Postmarketing data collection for the long-term safety and efficacy of all products should be mandatory. Every country should establish a national patient registry for hemophilia and other inherited bleeding disorders, covering all treatment modalities and patient-relevant outcomes.

From the beginning, the Kreuth Initiative for optimal use of blood products has been producing recommendations for hemophilia treatment,⁴ but so far the issue of data collection has not been addressed. Clinical registries are important tools, particularly in the context of rare diseases such as hemophilia characterized by a limited number of patients available for clinical trials. Registries may also help to collect long-term real-life data on the usage of products and patient-relevant treatment outcomes, thus providing valuable safety information. Registries should be set up in each European country on a national basis, and ideally should include all patients with inherited bleeding disorders.

Although recent EMA guidelines set standards for clinical studies,²⁴ the design and conduct of the currently available studies are characterized by several differences which prevent comparative data analysis. Registries may provide relevant complementary real-life data across a variety of products.²⁵ Alongside the reporting obligations laid down by the pharmacovigilance legislation, registries should also collect comprehensive postmarketing safety information on all treatment modalities.

Recommendation 8

Dedicated data governance, evaluation and reporting should be implemented with adequate sustainable financial support under public control. Core data elements as recommended by the European Medicines Agency (EMA)^{24,26} and minimal dataset for post-registration surveillance should be implemented according to the communication from the International Society on Thrombosis and Haemostasis (ISTH) Scientific and Standardization Subcommittee (SSC) on Factor VIII, Factor IX and Rare Coagulation Disorders.²⁷

Although there are a number of ongoing registries in Europe, their organization and status, as well as the amount and quality of collected data, is quite variable.²⁸ There are various models of registries, and promoters may be patient organizations, scientific societies, networks of

treatment centers or government institutions. Important questions need to be answered and solutions found for the problems related to each registry. How is the collection of data organized (preferably as user-friendly online portals)? How are data integrity and quality assured? Who owns the data? Who performs which analysis? How and by whom are results reported and eventually published? Additional challenges may also be presented by some degree of reluctance from hemophilia caregivers to share their patients' data and to make the effort needed to enter the data into a registry. To tackle these challenges, the German Transfusion Act was updated to include mandatory adherence to the German Hemophilia Register Participation agreement. The organization of registries is a complex affair, and requires thorough planning, and substantial and sustainable support. Given the importance and relevance of the data for the scientific evaluation of hemophilia treatment by regulatory agencies, and the particular sensitivity of patient data, registries and their funding need to be under public control. In order to enable meaningful evaluation and comparative analysis, a minimum set of common data elements should be included, as recently recommended by the EMA.²⁶ Detailed guidance concerning the data set required for post-registration surveillance was also previously communicated by the ISTH Scientific and Standardization Committee on Factor VIII, Factor IX and Rare Coagulation Disorders.²⁷

Recommendation 9

Collaboration at the European level should be encouraged, by strengthening and harmonizing existing registries in order to facilitate pooling and comprehensive evaluation of data.

Greater collaboration is essential in order to have more data available for evaluation, and to enable data pooling and a comprehensive evaluation of data across all treatment modalities at a European level. Although the performance, co-operation and outputs of the registries currently operative in Europe are not satisfactory,²⁸ the way forward is not to advocate a single new, pan-European super-registry, but to strengthen and harmonize those already existing, as well as to encourage the establishment of common tools and strategies for their optimal use. This is an important and ambitious task which requires the support of all stakeholders, including patients, those responsible for their treatment, and academia, regulatory authorities and policymakers involved in health care.

Recommendation 10

Data collection should include direct reporting from patients using appropriate electronic industry-independent tools. Its use should be supported by education, user-friendly applications, and positive feedback to the patients.

The ultimate success of any kind of hemophilia registry depends on the participation and commitment of the caregivers and the willingness of patients to provide their data. In particular, the accuracy and completeness of the collected data are closely related to the tools made available for reporting them to the registry. Data collection by direct reporting from patients through electronic tools is an attractive approach, provided any bias resulting from industry-developed applications is excluded, and treating physicians supervise its management and exercise quality control. Appropriate information and education about the background, instruments and goals of each registry, and provision of user-friendly applications are particularly

important. It is also important to provide patients with a positive feedback to underline the value of their contributions.

Recommendation 11

Clinical studies should be performed to provide the best possible evidence needed for regulatory authorities, health technology assessment (HTA) bodies, academia and healthcare providers.

Clinical trials conducted during the drug licensing process provide the most important information for predicting the efficacy and value of new medicines. While clinical trial data are the gold-standard of the evidence-based efficacy needed by regulatory authorities and health care providers, their usefulness often has limitations with respect to HTA and determining their value within the framework of cost-effectiveness studies, primarily carried out in the interest of the decision-making processes of payers. The purpose of most clinical trials is to test hypotheses about the efficacy and side effects of medications compared against placebo or a selected comparator therapy. HTA aims to answer questions about how these findings can be translated into clinical practice and change the standard of care, but also on how to estimate cost-effectiveness, with the goal of informing decisions intended to ensure value for money. Most clinical trials often do not focus on end points such as the relevant patient outcomes requested by HTA bodies and/or payers. These limitations have acquired greater importance since regulatory authorities introduced new initiatives such as adaptive licensing in order to accelerate access to innovative treatments, particularly in the context of orphan or rare diseases. Smaller and shorter trials may be able to provide evidence faster, but they will fail to generate enough information for patient assessment of relevant outcomes and for cost-effectiveness. To minimize these gaps of knowledge, and to provide sufficient evidence to promote effective HTA and cost effectiveness analysis, clinical trial designs for innovative therapies should be optimized to reduce uncertainty, eliminate bias, decrease costs, and accelerate patient access.

Recommendation 12

A process to reach better agreement on relevant indicators and methods should be started in order to meet the needs of regulatory authorities, HTA bodies, academia and healthcare providers, that have different foci, responsibilities and requirements.

There is a strong need for a multidisciplinary consensus on measurable, patient-relevant outcome indicators which reflect the benefits of new and innovative hemophilia therapies. Consensus on the choice of outcome assessment instruments should also be reached in order to allow for a more effective combination of data from different sources. These goals will be necessary to obtain harmonized and transparent decision-making processes. Another subject for discussion should be whether outcomes should be collected in clinical trials or if data from

other sources such as observational studies including registries should be complementary sources to assess benefit within hemophilia care. Furthermore, a minimum set of methods for outcome determination would help the different decision makers to make their assessment. Because hemophilia is a chronic rare disease, and concrete patient-relevant outcomes such as avoidance of joint damage cannot be evaluated at the time of market entry of innovative therapies, it is important to identify appropriate surrogate indicators and agree on statistical methods for prognostic calculations in order to provide estimates also on medium- to long-term consequences.

Recommendation 13

A dialogue with agencies and academia should be started in order to reach understanding of relevant outcomes and to ensure comprehensive and consistent reporting.

Health Technology Assessment bodies and/or payers request information on patient-relevant clinical end points in order to provide the evidence of therapeutic benefit of new or innovative therapies compared to the standard of care. These hard end points are mainly morbidity, mortality and quality of life, but these only partially reflect the benefits associated with innovative hemophilia therapies.²⁹ Although mortality in hemophilia was very high before the introduction of replacement therapy, nowadays it is almost comparable to that of the general population, so it cannot be seen as an appropriate outcome to be measured at the time of drug evaluation and market entry.³⁰ Repeated joint bleeds cause morphological changes and in the long run lead to arthropathy; but many years of follow up would be required to assess hemophilic arthropathy and its consequences. Multifactorial influences lead to individual variations in a small patient population such as hemophilia pertaining to the bleeding phenotype, development of arthropathy, and inhibitory antibodies. Thus, the measurement of health-related quality of life (HRQoL) might be a reasonable indicator of the long-term outcome and effectiveness of the therapeutic intervention chosen. It can also be converted into utility values to enable the assessment of the quality-adjusted life years gained, and to calculate cost-effectiveness. Both hemophilia disease-specific instruments and generic instruments are available and should be implemented as a standard procedure.

Acknowledgments

Co-sponsoring by Paul Ehrlich Institut, the Ludwig-Maximilian University of Munich and the European Directorate for the Quality of Medicines and Healthcare. Thanks to Isabella Garagiola, Ph.D. from Angelo Bianchi Bonomi Hemophilia and Thrombosis Center for helping us in the preparation of the manuscript and to all participants and delegates who actively participated in the discussion with the three working groups, providing their own input and helping to produce this Kreuth V European consensus for treatment of hemophilia.

References

- Schramm W, von Auer F, Delaney F, Seitz R. Blood Safety in the European Community: An Initiative for Optimal Use. Wildbad Kreuth, 20-22 May, 1999. Conference Proceedings. ISBN 3-00-005705-6.
- Berger K, Klein HG, Seitz R, Schramm W, Spieser JM. The Wildbad Kreuth initiative: European current practices and recommendations for optimal use of blood components. *Biologicals*. 2011;39(3):189-193.
- Giangrande P, Seitz R, Behr-Gross ME, et al. Kreuth III: European consensus proposals for treatment of haemophilia with coagulation factor concentrates. *Haemophilia*. 2014;20(3):322-325.
- Giangrande PLF, Peyvandi F, O'Mahony B, et al. Kreuth IV: European consensus proposals for treatment of haemophilia with coagula-



Ferrata Storti Foundation

Human hematopoietic stem/progenitor cells display reactive oxygen species-dependent long-term hematopoietic defects after exposure to low doses of ionizing radiations

Elia Henry,^{*1,2,3,4} Inès Souissi-Sahraoui,^{*1,2,3,4} Margaux Deynoux,^{1,2,3,4} Andréas Lefèvre,^{1,2,3,4} Vilma Barroca,^{1,2,3,4} Anna Campalans,^{3,4,5} Véronique Ménard,^{3,4,6} Julien Calvo,^{1,2,3,4} Françoise Pflumio,^{#1,2,3,4} and Marie-Laure Arcangeli^{#1,2,3,4}

Haematologica 2020
Volume 105(8):2044-2055

¹INSERM, U1274, Laboratory "Niche, Cancer and Hematopoiesis"; ²CEA, DRF-JACOB-IRCM-SCSR-LSHL, UMR "Genetic stability, Stem Cells and Radiation"; ³UMR "Genetic stability, Stem Cells and Radiation" Université de Paris; ⁴UMR "Genetic stability, Stem Cells and Radiation", Université Paris-Saclay; ⁵CEA, DRF-JACOB-IRCM-SIGRR-LRIG, UMR "Genetic stability, Stem Cells and Radiation" and ⁶UMR "Genetic stability, Stem Cells and Radiation", F-92265 Fontenay-aux-Roses, France

*EH and IS-S contributed equally as co-first authors.

#FP and M-LA contributed equally as co-senior authors.

ABSTRACT

Hematopoietic stem cells are responsible for life-long blood cell production and are highly sensitive to exogenous stresses. The effects of low doses of ionizing radiations on radiosensitive tissues such as the hematopoietic tissue are still unknown despite their increasing use in medical imaging. Here, we study the consequences of low doses of ionizing radiations on differentiation and self-renewal capacities of human primary hematopoietic stem/progenitor cells (HSPC). We found that a single 20 mGy dose impairs the hematopoietic reconstitution potential of human HSPC but not their differentiation properties. In contrast to high irradiation doses, low doses of irradiation do not induce DNA double strand breaks in HSPC but, similar to high doses, induce a rapid and transient increase of reactive oxygen species (ROS) that promotes activation of the p38MAPK pathway. HSPC treatment with ROS scavengers or p38MAPK inhibitor prior exposure to 20 mGy irradiation abolishes the 20 mGy-induced defects indicating that ROS and p38MAPK pathways are transducers of low doses of radiation effects. Taken together, these results show that a 20 mGy dose of ionizing radiation reduces the reconstitution potential of HSPC suggesting an effect on the self-renewal potential of human hematopoietic stem cells and pinpointing ROS or the p38MAPK as therapeutic targets. Inhibition of ROS or the p38MAPK pathway protects human primary HSPC from low-dose irradiation toxicity.

Correspondence:

MARIE-LAURE ARCANGELI
marie-laure.arcangeli@inserm.fr

Received: May 14, 2019.

Accepted: November 27, 2019.

Pre-published: November 28, 2019.

doi:10.3324/haematol.2019.226936

Check the online version for the most updated information on this article, online supplements, and information on authorship & disclosures: www.haematologica.org/content/105/8/2044

©2020 Ferrata Storti Foundation

Material published in *Haematologica* is covered by copyright. All rights are reserved to the Ferrata Storti Foundation. Use of published material is allowed under the following terms and conditions:

<https://creativecommons.org/licenses/by-nc/4.0/legalcode>.

Copies of published material are allowed for personal or internal use. Sharing published material for non-commercial purposes is subject to the following conditions:

<https://creativecommons.org/licenses/by-nc/4.0/legalcode>, sect. 3. Reproducing and sharing published material for commercial purposes is not allowed without permission in writing from the publisher.



Introduction

Hematopoietic stem cells (HSC) give rise to all blood cell types over the entire life of an organism. In adult mammals, they are located in very specific microenvironments of the bone marrow (BM), allowing maintenance of HSC functions.¹ In humans, HSC are enriched in the CD34⁺ CD38^{low} CD90⁺ CD45RA⁻ cell population that also contains immature progenitors, hereafter called HSPC.^{2,3} Hematopoietic stem/progenitor cells (HSPC) are multipotent and mainly slow cycling cells. They possess a self-renewal potential that allows them to sustain the continuous generation of blood cells. Quiescence and self-renewal are regulated by several extrinsic factors, such as cytokines, extracellular matrix proteins and adhesion molecules,^{4,5} as well as intrinsic factors, such as transcription factors (TAL1,⁶⁻⁸ GATA-2, etc.⁹), proteins implicated in DNA damage repair pathways,¹⁰⁻¹² and cell cycle regulators.¹³⁻¹⁵ Mutations in genes involved in DNA repair induce BM failure with exhaustion of the

HSC pool, demonstrating that preserving genome integrity is crucial for HSC long-term maintenance (reviewed by Biechonski and Milyavsky).¹⁶ For instance, *ku80*, *lig4* and *atm*-deficient mice exhibit defects in HSC maintenance and self-renewal.¹⁰⁻¹² *Atm*-deficient HSC harbor increased levels of reactive oxygen species (ROS) responsible for their loss of hematopoietic reconstitution capacity¹⁰ that can be rescued by treatment with the antioxidant N-acetylcystein (NAC). Indeed, increased ROS in HSC induce their differentiation and their exhaustion^{17,18} and quiescent HSC with the lowest level of ROS have the highest hematopoietic reconstitution potential compared to 'activated' HSC harboring higher ROS levels.¹⁷ Interestingly, in mouse and human, ROS and DNA damage accumulate in HSC upon serial transplantation resulting in decreased self-renewal capacities. NAC-treated HSC are protected against the accumulation of oxidative DNA damage.^{18,19}

Ionizing radiations (IR) represent the main source of DNA damage and ROS. Importantly, the human population is increasingly exposed to low doses of IR (LDIR, <100 mGy) due to the recurrent use of medical imaging.²⁰ Studies have shown that combinations of several computed tomography (CT) scans (thoracic or cranial) can increase the risk of developing cancer.²¹ Indeed, having more than five CT scans (corresponding to a cumulative dose of 30 mGy) can lead to a 3-fold increase in the risk of developing pediatric leukemia. Moreover, a recent study showed that 20 mGy LDIR affects the fundamental properties of HSC in mouse.²² In this context, it is crucial to study the consequences of LDIR exposure in human cells, in particular in human HSC. Here we show through combining *in vitro* and *in vivo* studies that a single acute 20 mGy LDIR decreases human HSPC serial clonogenic and reconstitution potentials, and that these effects are mediated through a ROS/p38MAPK-dependent signaling pathway.

Methods

Primary cells

Cord blood (CB) samples were collected from healthy infants with the informed written consent of the mothers according to the Declaration of Helsinki. Samples were obtained in collaboration with the Clinique des Noriets, Vitry-sur-Seine, and with the Cell Therapy Department of Hôpital Saint-Louis, Paris, France. Samplings and experiments were approved by the Institutional Review Board of INSERM (Opinion n. 13-105-1, IRB00003888). CD34⁺ cells were purified by immuno-magnetic selection using a CD34 MicroBeads kit (Miltenyi Biotec, Paris, France). For each experiment, we used a pool of CD34⁺ cells from different healthy infants to diminish individual variability.

Low dose of ionizing radiations

20 mGy LDIR was delivered with a dose rate of 20 mGy/minute (min) using a Cobalt 60 Irradiator (Alcyon). 2.5 Gy was delivered with a dose rate of 1 Gy/min.

Flow cytometry and cell sorting

CD34⁺CD38^{low} cells and CD34⁺CD38^{low}CD45RA⁺CD90⁺ HSPC were isolated after labeling with human specific monoclonal antibodies (MoAbs, see *Online Supplementary Table S1* for details). Cell sorting was performed using either a Becton Dickinson (BD)-FACS-ARIA3 SORP or a BD-FACS-Influx (laser 488, 405, 355, 561 and 633, BD Bioscience). Flow cytometry experiments are described in the *Online Supplementary Methods*.

Transplantation assays

NOD.Cg-Prkdc(scid) Il2rg(tm1Wjl)/SzJ (NSG) mice (Jackson Laboratory, Bar Harbor, ME, USA) were housed in the pathogen-free animal facility of IRCM, CEA, Fontenay-aux-Roses, France. Adult 8-12-week old NSG mice received a 3 Gy sublethal irradiation using a GSRD1 γ -irradiator (source Cesium137, GSM) and were anesthetized with isoflurane before intravenous retro-orbital injection (i.v.) of human cells as described in the *Online Supplementary Methods*. All experimental procedures were carried out in compliance with French Ministry of Agriculture regulations (animal facility registration n.: A9203202, Supervisor: Michel Bedoucha, APAFIS #9458-2017033110277117v2) for animal experimentation and in accordance with a local ethical committee (#44).

Immunofluorescence

Immunofluorescence was performed on cell-sorted HSPC irradiated and incubated 30 min, 1 hour (h), or 3 h at 37°C in MyeloCult medium, as previously described.²²⁻²⁴ Details of the methods used are available in the *Online Supplementary Methods*.

Drug treatments

CD34⁺ cells or CD34⁺ CD38^{low}CD45RA⁺CD90⁺ HSPC were treated with several drugs as described in the *Online Supplementary Methods*.

Colony forming unit-cell assay

Colony forming unit-cell assay (CFU-C) and serial platings were performed as previously described;⁶ see *Online Supplementary Methods* for details. Depending on CB pool samples, 60-80 colonies were generated from 500 HSPC non-irradiated or irradiated at 20 mGy.

Primary and extended long-term culture initiating cell assays

Long-term culture initiating cell assay was performed as previously described⁶ and is described in detail in the *Online Supplementary Methods*.

Intracellular flow cytometry

Ki67, cleaved caspase 3, phospho-p38MAPK (P-p38, phosphorylation on Thr180/Tyr182), phospho-ATM, p53 and phospho-p53 staining were performed as previously described⁴ (Ki67) and according to the manufacturer's instructions, respectively. More details can be found in the *Online Supplementary Methods*.

Carboxyfluorescein diacetate succinimidyl ester staining

3x10⁵ CD34⁺ cells were labeled with carboxyfluorescein diacetate succinimidyl ester (CFSE) (2.5 μ M, Sigma, France) and cultured in StemSpan medium supplemented with cytokines (Stem Cell Technologies), as described in the *Online Supplementary Methods*.

Reactive oxygen species quantification and mitochondria activity assay

Reactive oxygen species quantification was performed with fresh CD34⁺ cells using CellRox Orange reagent following the manufacturer's instructions (ref. C10443, Molecular Probes, ThermoFisher Scientific). Mitochondrial activity assay was performed using mitotracker green (MTG) and TMRE products, according to the manufacturer's instructions (Molecular Probes, ThermoFisher Scientific).

Statistical analysis

Mann and Whitney (M&W) and Kruskal and Wallis (K&W)

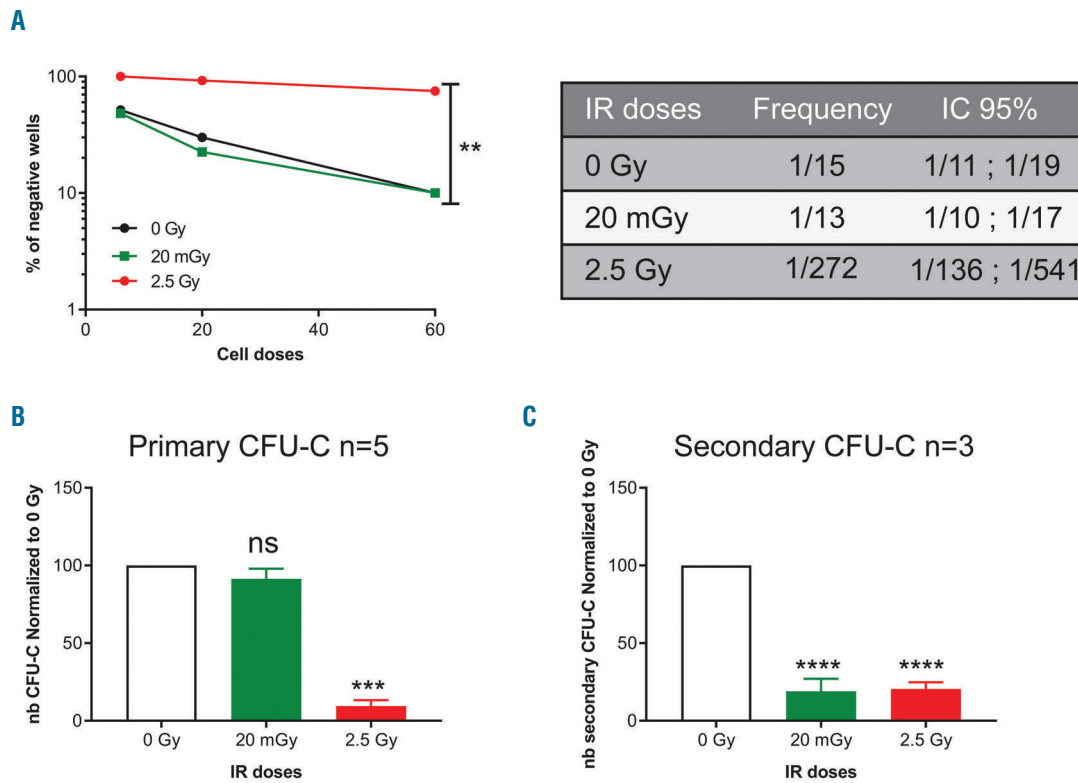


Figure 1. Low doses (LD) of ionizing radiations (IR) exposure of human hematopoietic stem progenitor cells (HSPC) leads to deficient serial colony forming unit-cell assay (CFU-C) and primary and extended long-term culture initiating cell (LTC-IC) potentials. CD34⁺ CD38^{low} CD45RA⁻ CD90⁺ HSPC were sorted from pools of independent cord blood (CB) samples by cell sorting and exposed to the indicated IR doses prior to *in vitro* cultures. (A) LTC-IC assay in limiting dilution (pool of 2 experiments, 120 wells/IR dose). Irradiated CD34⁺ CD38^{low} CD45RA⁻ CD90⁺ HSPC were seeded on MS5 stromal cells in limiting dilution for five weeks then plated in methylcellulose for 12 days. LTC-IC frequency was calculated using LCalc software. (B) Primary CFU-C assay (cumulative results from 4 independent experiments with HSPC isolated from 4 independent pools of CB samples). HSPC (500 cells/plate) were plated in CFU-C condition for 12-14 days and the number (nb) of CFU-C was quantified. Results are normalized to the non-irradiated conditions. (C) Primary CFU-C were pooled and replated in methylcellulose for 12-14 days. Shown are the nb of secondary CFU-C. Results are normalized to the sham-irradiated conditions (cumulative results from 3 independent experiments). Results are shown as mean ± standard error of mean. ***P*<0.01, ****P*<0.001, *****P*<0.0001 (Mann-Whitney statistics).

non-parametric statistical analyses were used. **P*<0.05, ***P*<0.01, ****P*<0.001, *****P*<0.0001.

Results

A 20 mGy dose of irradiation decreases serial replating capacity of human hematopoietic stem/progenitor cells

To understand the impact of HSPC exposure to LDIR, we first performed serial long-term culture initiating cell (LTC-IC) and CFU tests as surrogate assays to study human HSPC properties, i.e. self-renewal and differentiation capacities.²⁵⁻²⁷ Human CD34⁺CD38^{low}CD45RA⁻CD90⁺ HSPC were purified, irradiated and cultured with the MS5 stromal cell line in LTC medium for five weeks or plated directly in semi-solid methylcellulose cultures. In LTC-IC limiting dilution analyses, every single well was harvested independently at the end of the culture and plated in CFU-C assay. The LTC-IC frequency obtained after a 20 mGy irradiation of HSPC was similar to the LTC-IC frequency of sham-irradiated HSPC (1/15) suggesting that LDIR do not affect LTC-IC frequency. In contrast, a high (2.5 Gy) irradiation dose induced a drastic drop in LTC-IC frequency (1/272) (Figure 1A). In addition, 2.5 Gy-irradiated HSPC directly seeded in CFU-C conditions after IR produced

very few colonies compared to control cells whereas 20 mGy-irradiated HSPC generated a similar number of CFU-C to sham-irradiated HSPC (Figure 1B and *Online Supplementary Figure S1A*). No difference in the quality of CFU-C was observed between sham and 20 mGy conditions (*Online Supplementary Figure S1B*). These primary LTC-IC and primary CFU-C assays show that 20 mGy LDIR do not alter HSPC frequency and clonogenicity *in vitro* and do not induce any myelo/erythroid differentiation bias in primary cultures (*Online Supplementary Figure S1B*). To characterize whether LDIR have deleterious effects on human HSPC self-renewal potential *in vitro*, serial replatings were performed for both CFU-C and LTC-IC assays.²⁵⁻²⁷ We observed that 20 mGy and 2.5 Gy-irradiated CD34⁺CD38^{low}CD45RA⁻CD90⁺ HSPC produced lower numbers of secondary colonies in contrast to sham-irradiated HSPC, showing that 20 mGy alters their serial clonogenic potential (Figure 1C and *Online Supplementary Figure S1C*). This result was also obtained after picking up and replating individual primary CFU-GM colonies (*Online Supplementary Figure S1D*). In the case of LTC-IC, secondary/extended cultures were initiated using cells expressing high CD34 surface expression (CD34^{hi}), purified after the initial five weeks of LTC-IC culture (*Online Supplementary Figure S1E*) and seeded for five additional weeks in LTC-IC conditions at limiting dilution. Of note, we were not

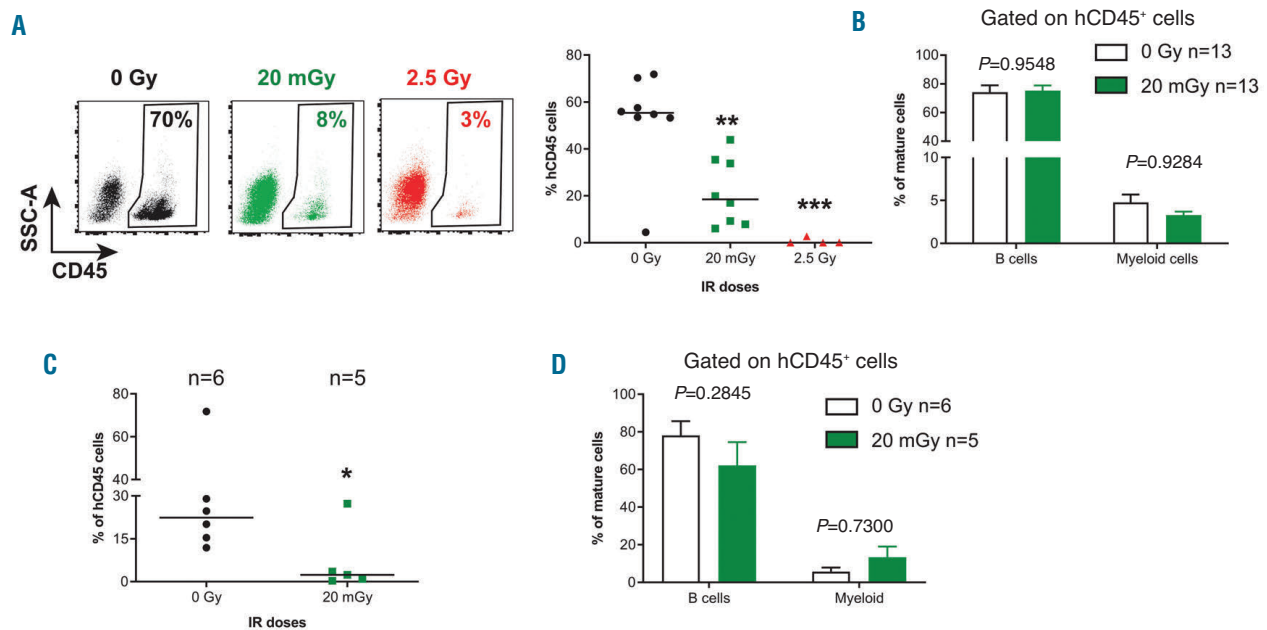


Figure 2. Hematopoietic reconstitution capacities of human hematopoietic stem cells (HSC) after *in vivo* exposure to low doses (LD) of ionizing radiations (IR). NSG mice were transplanted with 5.10^4 CD34⁺ CB cells and 13 to 16 weeks post graft mice were irradiated or not with the indicated doses then immediately sacrificed. Bone marrow (BM) cells were recovered and characterized by flow cytometry (*Online Supplementary Figure S2A and B*). An equivalent of 5.10^4 CD34⁺ CD19⁺ BM cells were injected in secondary recipient mice. (A) Dot plots of representative engraftment levels (left: human hCD45⁺ cells) in secondary recipient mice and human engraftment levels obtained in the BM of 9 secondary NSG mice (right: 2 independent experiments are pooled). Results of a third experiment is shown in *Online Supplementary Figure S2D* since engraftment levels of control mice were lower. (B) Proportion of engrafted human B cells and myeloid cells based respectively on CD19 and CD14/CD15 expression gated in human CD45⁺ cells, in secondary recipient mice. (C) Human hematopoietic reconstitution of CD34⁺ CD38^{low} Lin^{neg} BM cells purified by cell sorting from primary mice and transplanted in secondary recipient mice. Shown are human cell reconstitution in the BM of secondary recipient mice 13 weeks later. (D) Proportion of engrafted human B cells and myeloid cells gated within human CD45⁺ cell compartment in secondary mice after human CD34⁺ CD38^{low} Lin^{neg} BM cell transplants. Results are shown as mean \pm standard error of mean. * $P < 0.05$; ** $P < 0.01$, *** $P < 0.001$ (Mann-Whitney statistics).

able to perform such extended LTC-IC with the 2.5 Gy condition due to very low cell quantities in the cultures. Interestingly, there was a 2-fold decrease in the extended LTC-IC frequency of 20 mGy-irradiated HSPC compared to sham-irradiated HSPC (1/275 vs. 1/128) (*Online Supplementary Figure S1F*) showing a defect in long-term HSPC maintenance. This decrease in secondary LTC-IC frequency induced by 20 mGy LDIR was also found in bulk culture conditions with 20 mGy-irradiated HSPC generating fewer CFU-C than sham-irradiated cells after secondary LTC-IC cultures (*Online Supplementary Figure S1G*). Taken together, these results suggest that a single exposure to 20 mGy LDIR impairs the *in vitro* self-renewal potential of human CD34⁺CD38^{low}CD45RA⁻CD90⁺ HSPC.

A 20 mGy dose of irradiation decreases human hematopoietic stem/progenitor cell hematopoietic reconstitution potential

We then studied the effect of 20 mGy LDIR on *in vivo* HSC functions. To do so, NSG mice were first engrafted with human CD34⁺ cells. Sixteen weeks later, once human hematopoiesis was stabilized, engrafted mice were exposed to 0, 20 mGy and 2.5 Gy IR doses and sacrificed immediately after irradiation. Bone marrow (BM) cells were harvested and phenotype analysis was performed. The levels of human CD45⁺ cells and the percentage of Lin^{neg}CD34⁺ cells recovered from NSG BM were similar in the irradiated and non-irradiated groups (*Online Supplementary Figure S2A and B*). Furthermore, no increase of apoptosis of human cells engrafted in NSG mouse BM

was observed in mice irradiated at 20 mGy compared to non-irradiated mice (*Online Supplementary Figure S2C*). To study the consequences of irradiation on human HSC functions (i.e. reconstitution and differentiation potential), BM cells containing 5.10^4 human CD45⁺CD34⁺CD19⁺ cells were transplanted in secondary NSG mice. Human hematopoietic development in the secondary recipient mice was analyzed 13-16 weeks later. Human engraftment levels in mice receiving 20 mGy and 2.5 Gy-irradiated BM cells were decreased compared to sham-irradiated BM cells (Figure 2A and *Online Supplementary Figure S2D*) showing that 20 mGy-irradiated BM cells are less efficient than non-irradiated BM cells to reconstitute human hematopoiesis in secondary recipient mice. However, in the 20 mGy condition, some human cells were still detected in the BM of secondary recipient mice. Among them, human B CD19⁺ lymphocytes and CD14⁺/CD15⁺ myeloid cells were produced at the same proportion than in non-irradiated conditions, indicating that the few HSC that survived LDIR had maintained their differentiation capacities (Figure 2B). To exclude a non-cell autonomous effect of LDIR on HSPC mediated by irradiated hematopoietic or non-hematopoietic BM cells during the transplantation, we purified human CD34⁺CD38^{low} cells from the BM of control and 20 mGy-irradiated mice before transplantation in secondary NSG mice. As in the previous experiment, human cell engraftment in secondary recipients showed a reduced hematopoietic reconstitution capacity when 20 mGy-irradiated CD34⁺CD38^{low} cells were used (Figure 2C) and again no difference in the differentiation

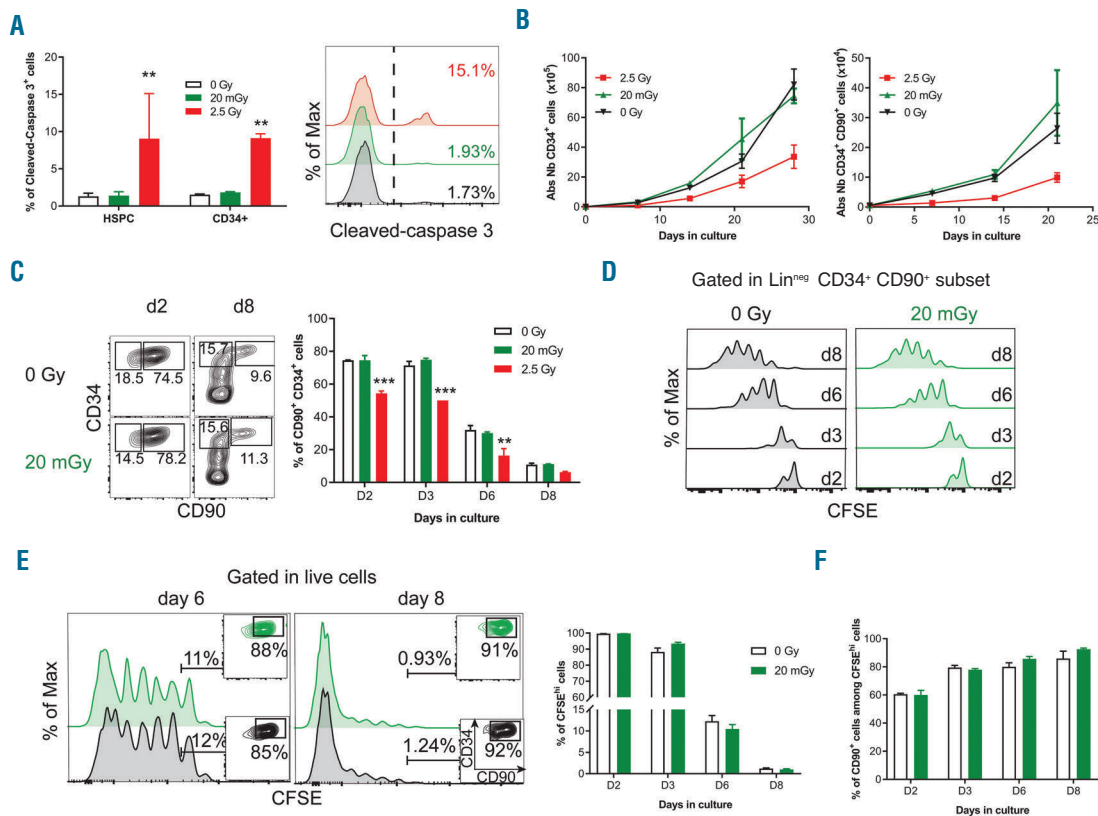


Figure 3. Low doses (LD) of ionizing radiations (IR) do not induce apoptosis and do not modify the cell cycle in human hematopoietic stem progenitor cells (HSPC). (A) CD34⁺ cells were irradiated and cultured for 6 hours (h) at 37 °C, then stained for cell surface markers and fixed. Cleaved-caspase 3 protein expression was analyzed by FACS. Percentage of cleaved-caspase 3⁺ cells on CD34⁺ CD38^{low} CD45RA⁺ CD90⁺ HSPC and on total CD34⁺ (left panel) and overlay histograms of cleaved-caspase 3 expression on HSPC (right panel) are represented in function of IR doses. One representative experiment out of two is shown. (B) Sorted CD34⁺ CD38^{low} CD45RA⁺ CD90⁺ HSPC were irradiated or not and co-cultured with MS5 stroma cell line for several days. At several time points, cells were enumerated and stained for cell surface markers. The numbers of CD34⁺ cells (left) and Lin^{neg}CD34⁺CD90⁺ cells (right) were monitored over time. One representative experiment out of two is shown. (C-F) Sorted CD34⁺ CD38^{low} CD45RA⁺ CD90⁺ HSPC were first stained with carboxyfluorescein hydroxysuccinimidyl ester (CFSE), irradiated and cultured for several days. One representative experiment out of two is shown. (C) Differentiation of CD34⁺ CD38^{low} CD45RA⁺ CD90⁺ HSPC in culture was followed by using expression levels of CD90 and CD34 surface markers. Dot plots (left panel) represent CD90 and CD34 expression after 2 and 8 days of culture for control and 20 mGy-irradiated HSPC. Histogram bars (right panel) represent the percentage of Lin^{neg}CD34⁺CD90⁺ cells at different days of culture after IR. (D) Levels of carboxyfluorescein succinimidyl ester (CFSE) fluorescence in the Lin^{neg}CD34⁺CD90⁺ subset at different days of culture in control and 20 mGy conditions. No differences in cell division can be detected between both conditions. (E) Histogram representing CFSE staining in the HSPC-derived bulk cells at days 6 and 8 of culture in control and 20 mGy conditions (left panels). Histogram bars show CFSE labeling loss over culture time in the bulk population (right panel). (F) Percentage of Lin^{neg}CD34⁺CD90⁺ cells in CFSE^{hi} cells in control and in 20 mGy conditions. Results are shown as mean±standard error of mean. ***P*<0.01, ****P*<0.001 (Mann and Whitney statistics). Abs Nb: absolute numbers.

of the engrafted HSC was shown (Figure 2D) showing a cell-autonomous effect of LDIR in HSPC. Taken together these results indicate that 20 mGy LDIR affects the hematopoietic reconstitution capacity of human HSPC.

Low doses of ionizing radiations do not induce apoptosis nor alter cell cycle of hematopoietic stem/progenitor cells

To characterize the mechanisms activated by 20 mGy LDIR in human primary HSPC, we first investigated if LDIR trigger apoptosis. Analysis of caspase 3 cleavage showed that 2.5 Gy irradiation increases CD34⁺CD38^{low}CD45RA⁺CD90⁺ HSPC apoptosis (Figure 3A, red histograms), whereas 20 mGy LDIR had no significant effect on the percentage of cleaved caspase 3-expressing HSPC compared to sham-irradiated HSPC (Figure 3A, green histograms). As increased HSPC cell cycle can lead to self-renewal defects and HSC exhaustion,²⁸ we also determined if 20 mGy LDIR could alter HSPC proliferation. 20 mGy and sham-irradiated CD34⁺CD38^{low}CD45RA⁺CD90⁺

HSPC generated the same number of CD34⁺ and CD34⁺CD90⁺ cells *in vitro* (Figure 3B, left and right panel, respectively) whereas 2.5 Gy-irradiated HSPC did not proliferate efficiently. Moreover, the proportion of CD34⁺CD90⁺ cells evolved similarly during culture period after no irradiation or 20 mGy LDIR, strengthening the lack of effect of a 20 mGy irradiation on HSPC differentiation (Figure 3C). We studied the cell division rate of irradiated HSPC after staining with CFSE and during culture in serum free medium with cytokines. The number of cell divisions was the same for sham- or 20 mGy-irradiated HSPC (Figure 3D). After 6 and 8 days of culture, no difference in CFSE^{hi} cell (the most immature cells)²⁸ proportion was observed between 20 mGy and control HSPC (Figure 3E) and 90% of these CFSE^{hi} cells expressed the immature markers CD34 and CD90²⁹ regardless of the culture time and irradiation conditions considered (Figure 3F). These results show that 20 mGy LDIR does not impair either proliferation or differentiation of the most immature HSPC in cytokine-stimulating conditions.

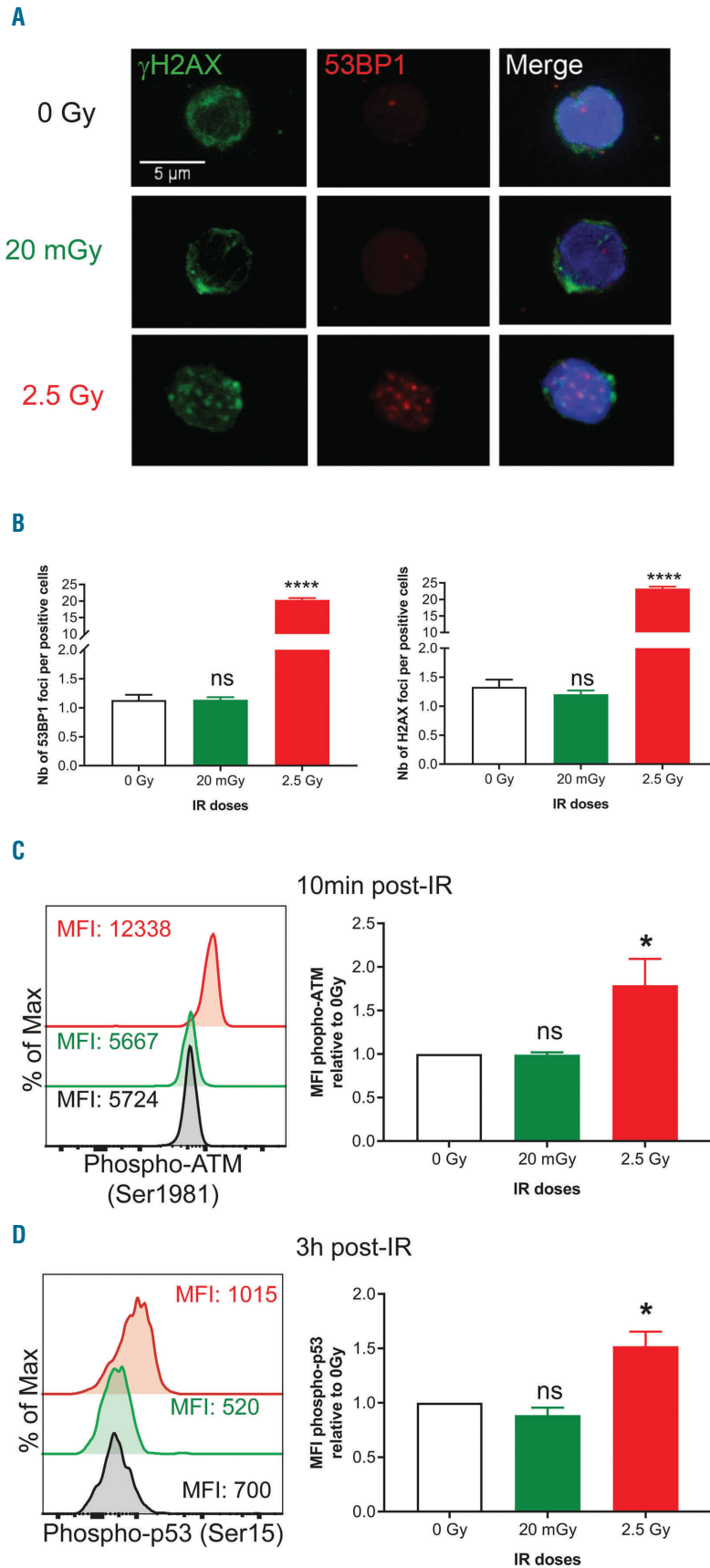


Figure 4. Low doses (LD) of ionizing radiations (IR) do not induce DNA double strand breaks nor activate ATM-dependent/p53-dependent DNA repair pathway in human hematopoietic stem progenitor cells (HSPC). CD34⁺ CD38^{low} CD45RA⁻ CD90⁺ HSPC were purified by cell sorting and exposed to different doses of IR as indicated. (A) γ H2AX and 53BP1 foci were examined by confocal microscopy 30 minutes (min) post IR (at least 100 cells by condition were analyzed). (B) Number (Nb) of 53BP1 (left panel) and γ H2AX (right panel) foci by positive HSPC. (C and D) CD34⁺ cells were irradiated, cultured 10 min (C) or 3 hours (h) (D) at 37 °C, stained for cell surface markers then fixed. (C) Analysis of ATM-phosphorylation on Ser1981 by FACS in CD34⁺ CD38^{low} CD45RA⁻ CD90⁺ HSPC (one representative experiment out of 4). (D) Analysis of p53-phosphorylation on Ser15 (left) and p53 protein expression (right) in CD34⁺ CD38^{low} CD45RA⁻ CD90⁺ HSPC by FACS 3 h post IR (one representative experiment out of 5). Results are shown as mean \pm standard error of mean. * P <0.05, **** P <0.0001 (Mann and Whitney statistics).

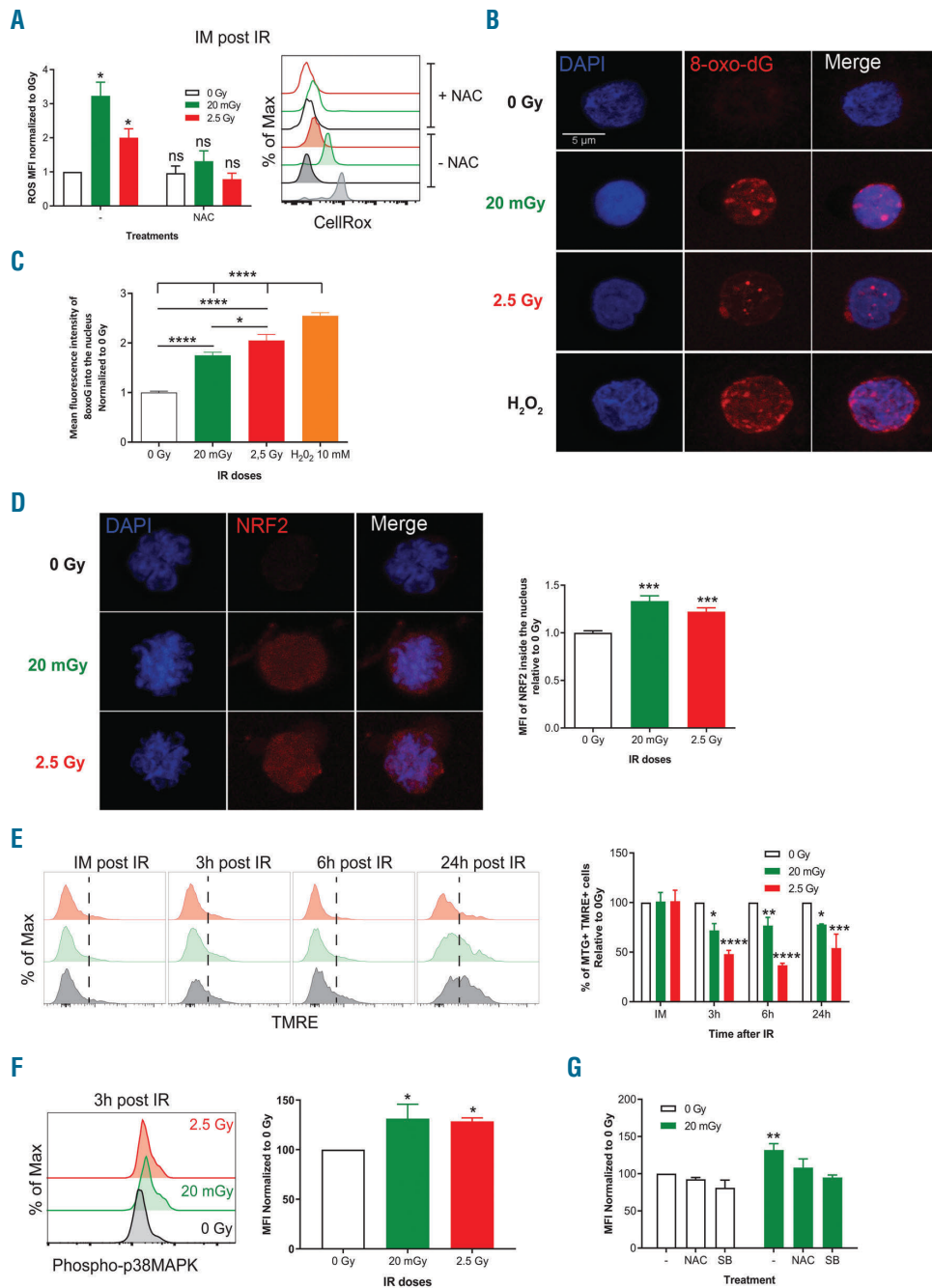


Figure 5. Low doses (LD) of ionizing radiations (IR) induce transitory reactive oxygen species (ROS) increase, 8-Oxo-dG DNA lesions and p38MAPK activation with altered mitochondrial activity in hematopoietic stem progenitor cells (HSPC). (A) ROS levels were quantified in CD34⁺ CD38^{low} CD45RA⁻ CD90⁻ HSPC using CellRox Orange probe immediately after IR. (Left) Pool of CellRox Orange mean of fluorescence relative to 0 Gy condition, right overlay histograms showing CellRox Orange fluorescence. One representative experiment out of four is shown (see also *Online Supplementary Figure S4*). Results are shown as mean±standard error of mean. (B and C) CD34⁺ CD38^{low} CD45RA⁻ CD90⁻ HSPC were purified by cell sorting and exposed to different doses of IR or H₂O₂ as indicated. Shown are 8-oxo-dG lesions quantified by confocal microscopy 30 minutes post IR (at least 50 cells were screened by condition in 3 independent experiments. Blue: Dapi, Red: 8-oxo-dG). Histograms represent the intensity of fluorescence of 8-oxo-dG staining within HSPC nucleus. To avoid heterogeneity, mean fluorescence intensity (MFI) has been normalized to the sham-irradiated condition. (D) CD34⁺ CD38^{low} CD45RA⁻ CD90⁻ HSPC were purified by cell sorting and exposed to different doses of IR as indicated. Shown are NRF2 staining quantified by confocal microscopy 2 hours (h) post IR (at least 50 cells were screened by condition in 2 independent experiments. Blue: Dapi, Red: NRF2). Histograms represent the intensity of fluorescence of NRF2 staining within HSPC nucleus. To avoid heterogeneity, MFI has been normalized to the sham-irradiated condition. (E) Mitochondrial activity was monitored over time by using TMRE (membrane potential, left panel) and MTG (mitochondrial mass) probes in HSPC. Shown is the frequency of TMRE⁺ cells over time in culture for one representative experiment out of three independent experiments and the mitochondria activation (% of MTG⁺ TMRE⁺ cells, right panel) over time in culture (pool of the 3 independent experiments). (F) CD34⁺ cells were irradiated and cultured 2 h at 37 °C followed by cell surface marker staining and then fixed. Phosphorylation of p38MAPK on Thr180/Tyr182 was analyzed by flow cytometry. Overlay histograms of p38MAPK phosphorylation on CD34⁺ CD38^{low} CD45RA⁻ CD90⁻ HSPC (left panel) are represented for the three irradiation conditions. Overlay histograms are from one representative experiment out of three. Histogram bars (right panel) show the MFI of phospho-p38MAPK in CD34⁺ CD38^{low} CD45RA⁻ CD90⁻ HSPC (n=3 independent experiments). (G) CD34⁺ cells were treated with NAC, SB203580 (SB) or untreated for 1 h at 37 °C then irradiated and cultured 2 h at 37 °C. Staining for cell surface markers was performed and then cells were fixed. Phosphorylation of p38MAPK on Thr180/Tyr182 was analyzed by flow cytometry. Histogram bars show mean of fluorescence of phospho-p38MAPK in CD34⁺ CD38^{low} CD45RA⁻ CD90⁻ HSPC (n=3 independent experiments). Results are shown as mean±standard error of mean. *P<0.05, **P<0.01, ***P<0.001, ****P<0.0001 (Mann-Whitney statistics).

Low doses of ionizing radiations do not induce DNA double strand breaks nor activate ATM or p53 signaling pathway

Since irradiation usually induces DNA double strand breaks (DSB), we quantified the number of H2AX and 53BP1 foci 30 min post irradiation (Figure 4A). In contrast to a 2.5 Gy irradiation, a 20 mGy irradiation did not increase the number of H2AX and 53BP1 foci compared to sham-irradiated CD34⁺CD38^{low}CD45RA⁻CD90⁺ HSPC indicating that 20 mGy LDIR does not induce DNA DSB (Figure 4B). We then studied the DNA damage response (DDR) path-

way after exposure to LDIR by quantification of ATM and p53 phosphorylation 10 min and 3 h after irradiation. As expected, 2.5 Gy-irradiated HSPC exhibited an increased ATM and p53 phosphorylation compared to control HSPC (Figure 4C and D). In contrast, no increase in ATM or p53 phosphorylation was detected after exposure to 20 mGy (Figure 4C and D). Importantly, the expression of p53 protein was not modified by IR (*Online Supplementary Figure S3*). Altogether these results indicate that 20 mGy LDIR does not induce DNA DSB nor activate p53 and ATM-dependent DNA damage repair pathway in human HSPC.

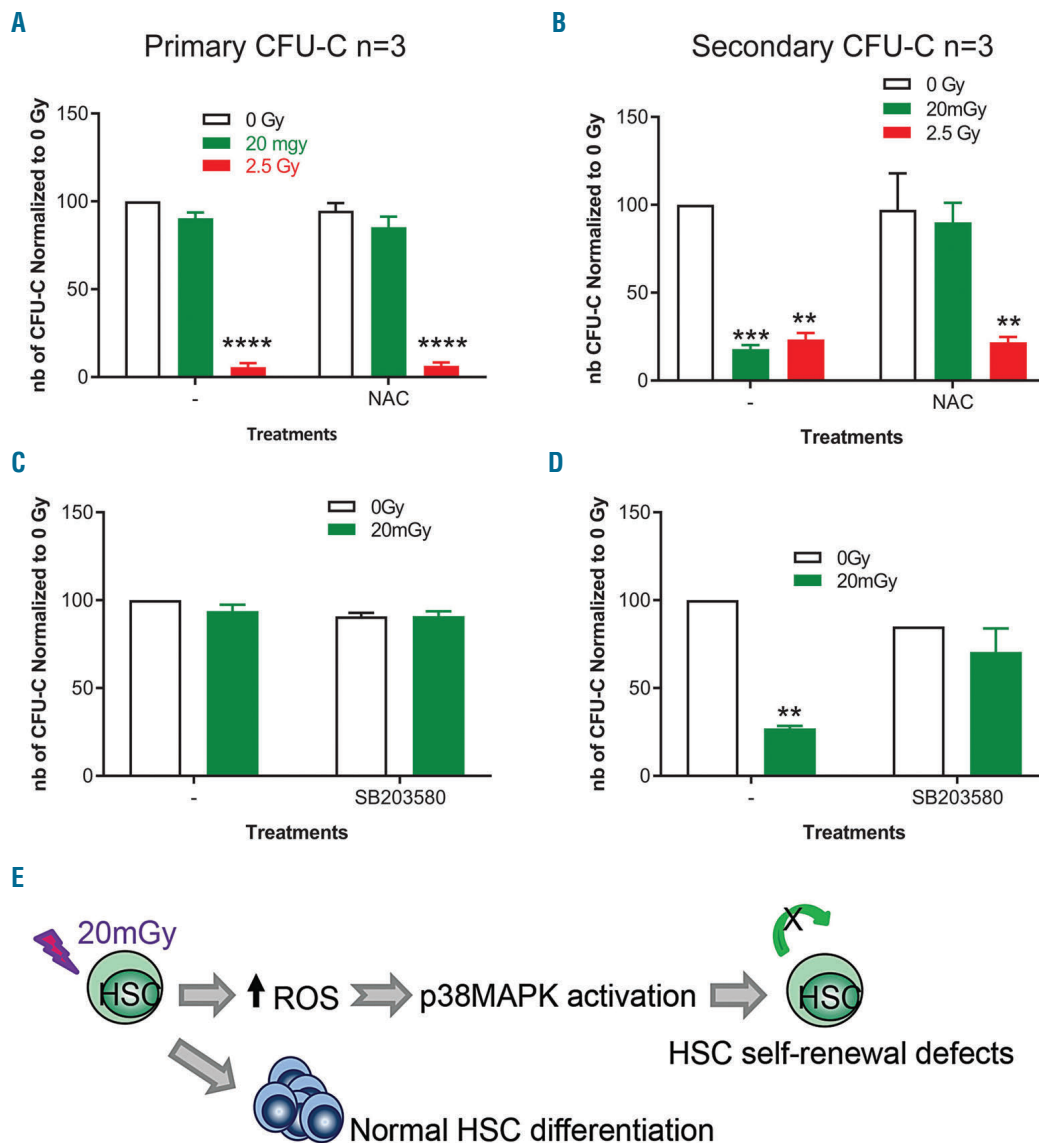


Figure 6. Low doses (LD) of ionizing radiations (IR) induce a transitory increase of ROS in CD34⁺ CD38^{low} CD45RA⁻CD90⁺ hematopoietic stem progenitor cells (HSPC) that alters their serial clonogenic potential. (A) Colony forming unit-cell (CFU-C) assay. Cumulative results from 3 independent experiments with CD34⁺ CD38^{low} CD45RA⁻CD90⁺ HSPC from 3 independent pools of cord blood (CB) samples. Sorted CD34⁺ CD38^{low} CD45RA⁻CD90⁺ HSPC were pre-treated or not with N-acetylcysteine (NAC) prior to IR and plated (500 cells/plate) in CFU-C conditions for 12-14 days. Shown are the number (nb) of CFU-C (primary CFU-C). Results are normalized to the sham-irradiated conditions. (B) Primary CFU-C were pooled and replated in CFU-C conditions for 12-14 days. Shown are the nb of secondary CFU-C, normalized to the sham-irradiated conditions (cumulative results from 3 independent experiments). (C) Sorted CD34⁺ CD38^{low} CD45RA⁻CD90⁺ HSPC were pre-treated or not with SB203580 prior to IR and plated (500 cells/plate) in CFU-C conditions for 12-14 days. Shown are the nb of CFU-C (primary CFU-C). Results are normalized to the sham-irradiated conditions. (D) Primary CFU-C were pooled and replated in CFU-C conditions for 12-14 days. Shown are the nb of secondary CFU-C, normalized to the sham-irradiated conditions (cumulative results from 2 experiments with CD34⁺ CD38^{low} CD45RA⁻CD90⁺ HSPC from two independent pools of CB samples). (E) Model explaining how LDIR can impair HSC self-renewal through ROS-p38MAPK dependent pathway. Results are shown as mean+standard error of mean. **P<0.01, ***P<0.001, ****P<0.0001 (Mann-Whitney statistics).

Low doses of ionizing radiations increase reactive oxygen species levels, 8-oxo-dG lesions, induce NRF2 translocation into the nucleus, activate p38MAPK pathway and delay mitochondrial activation

Since irradiation is known to promote ROS production,^{10,18,30} we next quantified ROS levels after LDIR exposure. ROS levels in CD34⁺CD38^{low}CD45RA⁻CD90⁺ HSPC after exposure to LDIR were measured immediately or 3 h after irradiation of CD34⁺ cells. Menadione and NAC treatments were used to respectively induce and inhibit ROS production. Increased ROS levels in HSPC were observed immediately after exposure to 20 mGy LDIR and to a lesser extent after exposure to 2.5 Gy, as compared to no irradiation (Figure 5A and *Online Supplementary Figure S4A and B*). These ROS increased levels were transient as no further difference in ROS levels could be detected 3 h after irradiation (*Online Supplementary Figure S4C*). NAC pretreatment of HSPC significantly decreased this early burst of ROS after 20 mGy and 2.5 Gy exposure. As increased ROS levels can lead to 8-oxo-dG lesions, as well as NRF2 translocation into the nucleus, we looked for 8-oxo-dG lesions in DNA of irradiated *versus* sham-irradiated HSPC^{30,31} and NRF2 location into HSPC.^{22,24} As expected sham-irradiated and H₂O₂-treated (control) cells exhibited respectively no and highly detectable anti-8-oxo-dG nuclear labeling. After exposure to 20 mGy, 8-oxo-dG staining was detected in the HSPC nucleus showing that 20 mGy LDIR can induce 8-oxo-dG lesions in DNA (Figure 5B and C). Similarly, the NRF2 protein was found in the nucleus of 20 mGy- and 2.5 Gy-irradiated HSPC compared to sham-irradiated cells (Figure 5D). As an increase in ROS is also associated with a delay in mitochondrial activation,³² we used mitotracker green (MTG) and TMRE probes to study respectively mitochondrial mass and membrane potential. Of note, CB CD34⁺ cells and CB HSPC are mainly quiescent, therefore there is very little mitochondrial activation (TMRE^{neg}) (Figure 5E, first left panel, and *data not shown*). HSPC exposure to LDIR did not alter the mitochondrial mass (MTG) of CD34⁺ cells in short-term culture (*Online Supplementary Figure S5A*). However, a delay in mitochondrial activation occurred (MTG⁺ TMRE⁺ HSPC) as soon as 3 h post IR (Figure 5E and *Online Supplementary Figure S5B*), suggesting that LDIR affect mitochondrial activity. In line with mitochondria activation, autophagy activation was monitored after IR (*Online Supplementary Figure S6*). The CytoID probe was used to follow autophagy in HSPC.^{33,34} As expected, after treatment with chloroquine and rapamycin, autophagy was detected in CD34⁺ cells (*Online Supplementary Figure S6A*). Besides, LDIR did not induce autophagy in HSPC after a different culture time (*Online Supplementary Figure S6B and C*). Finally, we investigated whether the observed increase of ROS can lead to p38MAPK activation as previously documented.¹⁹ Thr180/Tyr18 phosphorylation was used as a marker of p38MAPK activation. As a positive control of p38MAPK activation, increased p38MAPK phosphorylation (P-p38MAPK) can be detected in PMA-treated HSPC (*Online Supplementary Figure S5C*). In irradiated HSPC, we observed an increase of P-p38MAPK after exposure to 20 mGy and 2.5 Gy IR compared to sham-irradiated controls, suggesting that LDIR can activate p38MAPK pathway in HSPC similarly to high irradiation doses (2.5 Gy)³⁵ (Figure 5F). To further confirm that p38MAPK acti-

vation was due to the early transient increase in ROS levels, HSPC were treated with NAC or SB203580, a p38MAPK inhibitor, prior to 20 mGy irradiation. As expected, SB203580 prevented increased p38MAPK phosphorylation in 20 mGy-irradiated HSPC (Figure 5G). NAC treatment resulted in the same decrease in p38MAPK phosphorylation in 20 mGy-irradiated HSPC (Figure 5G). Altogether, these results show that LDIR increase ROS levels leading to DNA 8-oxo-dG lesions, NRF2 translocation into the nucleus and p38MAPK activation in 20 mGy-irradiated HSPC.

20 mGy-dependent reactive oxygen species increase and p38MAPK activation lead to defects in the serial clonogenic potential of hematopoietic stem/progenitor cells

As increased ROS levels can lead to HSC loss of potentials,¹⁸ we then asked if ROS-dependent pathways could explain the HSPC functional defects after LDIR exposure. To this end, serial CFU-C assays were performed using sorted CD34⁺CD38^{low}CD45RA⁻CD90⁺ HSPC pre-treated or not with NAC before exposure to LDIR and cultures. 20 mGy-irradiated HSPC generated the same number of primary CFU-C compared to sham-irradiated HSPC with or without NAC treatment (Figure 6A and *Online Supplementary Figure S7A*). However, 20 mGy-irradiated HSPC treated with NAC before IR, but not 2.5 Gy-irradiated cells, were capable of generating equivalent numbers of secondary CFU-C compared to sham-irradiated HSPC, showing that NAC treatment prior to exposure to 20 mGy protected HSPC from the loss of *in vitro* serial clonogenic potential (Figure 6B and *Online Supplementary Figure S7B*). This result was obtained when the serial plating assays were performed with the whole cell population harvested from primary CFU cultures (Figure 6B), and also after picking up and replating individual primary CFU-GM colonies (*Online Supplementary Figure S7C*). Rescue of secondary replating properties of HSPC after 20 mGy LDIR was also obtained using HSPC pretreatment with Catalase, another antioxidant enzyme (*Online Supplementary Figure S7D*). These results show that preventing ROS production with antioxidants before LDIR exposure rescues the *in vitro* serial clonogenic potentials of HSPC.

Finally, we wondered whether ROS-mediated p38MAPK activation was involved in LDIR-induced HSC self-renewal defects. HSPC were pre-treated with SB203580, a specific inhibitor of p38MAPK, prior to 20 mGy irradiation and serial CFU-C assays. No difference in the number of primary CFU-C was detected with SB203580 pretreated HSPC regardless of the irradiation dose used (Figure 6C and *Online Supplementary Figure S7E*). However, whereas SB203580-untreated 20 mGy-irradiated HSPC generated very few secondary CFU-C, SB203580 treatment of HSPC protected their capacity to generate secondary CFU-C as efficiently as sham-irradiated HSPC (Figure 6D and *Online Supplementary Figure S7F*), suggesting that p38MAPK pathway activation participates in LDIR-mediated HSPC defects. Based on all these results, we propose a model in which 20 mGy LDIR rapidly increases ROS amounts in HSPC that induce p38MAPK activation altogether leading to a defect in the long-term maintenance of the clonogenic potential of CD34⁺CD38^{low}CD45RA⁻CD90⁺ HSPC (Figure 6E).

Discussion

Here we show that exposure to a single 20 mGy LDIR alters the functional properties of human HSPC. No defect in HSPC differentiation potential tested in primary cultures was detected after exposure to LDIR. However, HSPC irradiated at 20 mGy *in vivo* in the NSG mouse BM harbored a defect in human hematopoietic reconstitution potential. This defect was cell-intrinsic since 20 mGy-irradiated CD34⁺CD38^{low} cells isolated after *in vivo* irradiation failed to serially reconstitute NSG mice as efficiently as non-irradiated cells; the same was observed with *in vivo* 20 mGy-irradiated bulk BM cells. This *in vivo* phenotype was also observed *in vitro* when using LDIR-exposed CD34⁺CD38^{low}CD45RA⁺CD90⁺ HSPC in serial CFU-C and LTC-IC assays, supporting the fact that these effects are cell-autonomous and not limited to transplantation conditions. Likewise, *in vitro*, HSPC exposure to 20 mGy induced a loss of secondary CFU-C potential as well as a decrease in secondary LTC-IC frequency. Altogether, based on the use of *in vivo* assays and *in vitro* surrogate assays to evaluate the self-renewal potential,²⁵⁻²⁷ these functional results strongly argue for an effect of 20 mGy LDIR on the long-term HSC functional properties, most likely through a loss of self-renewal potential. Of note, 20 mGy LDIR has been shown to decrease self-renewal capacity in murine HSC as well.²²

High-dose ionizing radiations (HDIR) (2.5 Gy) are known to induce DNA DSB in human HSPC, rejoining is delayed, and H2AX foci persist leading to a loss of HSC functions partly related to apoptosis and activation of p53 pathway.²⁵ Despite the publication of several studies over the past few years,³⁶⁻³⁸ little is known about which pathway is used to repair DNA DSB in human HSPC.¹⁶ In the present work, we tested if a single 20 mGy LDIR can alter cell cycle and induce apoptosis, and cause DNA DSB in HSPC. Surprisingly, and in contrast to HDIR, 20 mGy irradiation did not induce obvious cell cycle defects nor promote apoptosis in HSPC, since no increased cleaved caspase 3 protein was detected after exposure to 20 mGy LDIR. Moreover, no significant increase in H2AX and 53BP1 foci numbers was revealed, suggesting that 20 mGy LDIR does not produce DNA DSB. Finally, neither p53 nor ATM pathway was activated after 20 mGy exposure. However, and similarly to HDIR, 20 mGy irradiation led to 8-oxo-dG lesions in HSPC DNA. No such lesion was observed in sham-irradiated cells. Altogether, 20 mGy LDIR does not induce classic DNA damage and repair pathways usually activated by γ -irradiation but rather triggers 8-oxo-dG-dependent DNA damage that can be linked to uncontrolled increase in ROS levels. Moreover, NRF2 protein was found in the nucleus of 20 mGy-irradiated HSPC. Indeed, increased ROS levels were detected immediately after HSPC exposure to 20 mGy and, in line with this, we could observe that 20 mGy-irradiated HSPC had a delay in mitochondrial activation compared to control cells. Our results and those from Romeo's lab²² suggest that the transient increase in ROS levels is likely to be responsible for HSPC defects after LDIR exposure. We tested this hypothesis using antioxidant treatment of HSPC prior to exposure to LDIR. Importantly, pre-treatment of HSPC with NAC or Catalase prior to LDIR exposure did rescue the loss of *in vitro* serial clonogenic potential of HSPC. In mouse, irradiation can induce p38MAPK activation through increased levels of ROS.^{19,35} Prevention

of p38MAPK activation leads to decreased IR toxicity in HSC.³⁵ It is also known that dormant HSC have little or no p38MAPK activation, and that p38MAPK activation in HSC is associated with differentiation and loss of HSC self-renewal.^{17,39} In humans, the function of the p38MAPK pathway is still not fully understood but preventing p38MAPK activation allows HSC maintenance/expansion *in vitro*.^{40,41} Interestingly, in our model, we observed a ROS-dependent p38MAPK activation in human HSPC after exposure to both 2.5 Gy and 20 mGy IR. The involvement of the p38MAPK pathway in the LDIR-mediated HSC self-renewal defects was then confirmed in serial replating CFU-C assays. Indeed, pre-treatment of HSPC with a specific inhibitor of p38MAPK prior to LDIR rescued their serial replating capacities. This is in agreement with the fact that HSC treatments either with NAC or p38MAPK inhibitor increase LTC-IC frequency and promote higher hematopoietic reconstitution upon serial transplantation.^{18,19} It is important to highlight that two other studies on the effect of LDIR have also shown that LDIR did not induce classic DNA damage and repair pathways, but rather an oxidative stress (increase in ROS level and NRF2 nuclear localization).^{22,42} Therefore, oxidative stress induction seems to be a feature of exposure to LDIR, leading either to a differentiation defect in the case of cycling stem cells⁴² or a self-renewal defect in the case of quiescent stem cells, as we observed for human HSPC; this is also the case for mouse HSC.²²

Increased ROS levels as well as p38MAPK activation in HSC are associated with aging and stress during serial transplantation.^{17,18,43} The aging phenomenon is clearly a strong driver of differentiation and expansion of myeloid-biased HSPC.⁴⁴ Here we were not able to detect any bias toward myelopoiesis when analyzing the progeny of the surviving LDIR-treated human HSC after serial transplantation, maybe due to the NSG mouse model, as the NSG BM microenvironment is more supportive of B-cell rather than myeloid-cell differentiation.⁴⁵ Moreover, all experiments were performed with HSPC from CB, i.e. young HSPC. Thus, although it is tempting to speculate that exposure to LDIR may induce early/accelerated aging of the human HSC, we have no formal proof of that. Since radiation sensitivity and transplantation efficiency are highly dependent on the ontogenic origin of HSPC,⁴⁶⁻⁴⁸ aged HSPC may be more sensitive to LDIR. Another feature of HSC aging is higher risk of leukemic transformation, especially in the presence of an oncogenic-initiating event such as a mutation of the epigenetic modifiers *DNMT3a* or *TET2*, as observed in blood from elderly people.⁴⁹ A very interesting and important question for the future would be to determine if aged HSC exposed to LDIR are more prone to (pre)leukemic transformation, especially when HSC contain primary oncogenic mutations.

To sum up, in contrast to HDIR, 20 mGy does not induce DNA DSB, nor apoptosis and a defect in the cell cycle. However, both 20 mGy and 2.5 Gy IR induce 8-oxo-dG lesions in DNA, increase ROS levels, and activate the p38MAPK pathway leading to HSC self-renewal defects. Nevertheless, only 20 mGy-LDIR effects were counteracted by use of antioxidants prior to irradiation exposure, indicating there are major differences between these two IR doses. These results show for the first time that a dose as low as 20 mGy can have a huge impact on human HSC through both similar and also different molecular mechanisms to those of high IR doses.

Acknowledgments

We acknowledge the midwives from Clinique des Noriets in Vitry-sur-Seine and the Cell therapy department of Hôpital Saint Louis in Paris, France, especially Prof. J. Larghero, for providing cord blood samples free of charge and the families who agreed to donate the samples for research purposes. This work was made possible thanks to multiple platforms (Flow cytometry, Microscopy, Irradiation and animal facilities) of IRCM, Fontenay-aux-Roses, France. We are thus grateful to J Tilliet and N Dechamps for their great technical help during this project. A special thanks to J Bernardino and JB Lahaye for their devoted work at the irradiation platform from IRCM but also to C. Villagrasa, Y. Ristic and M. Razanajotovo-Derichebourg for their

precious help at the irradiation platform, laboratory of dosimetry of ionizing radiation, IRSN, Fontenay-aux-Roses, France. Finally, we acknowledge Paul-Henri Roméo, Franck Yates, Christophe Carles, Benjamin Uzan and Rima Haddad for helpful discussions and manuscript reviewing.

Funding

This study was supported by grants from INSERM, CEA (Segment Radiobiologie), Ligue Nationale contre le Cancer (équipe labellisée from 2014 to 2017), Région Ile de France/Cancéropole, Electricité de France and the European network RISK-IR. I-SS was supported by the European network RISK-IR and EH is a PhD fellow from the Ligue Nationale Contre le Cancer.

References

- Mendelson A, Frenette PS. Hematopoietic stem cell niche maintenance during homeostasis and regeneration. *Nat Med.* 2014; 20(8):833-846.
- Doulatov S, Notta F, Laurenti E, Dick JE. Hematopoiesis: a human perspective. *Cell Stem Cell.* 2012;10(2):120-136.
- Majeti R, Park CY, Weissman IL. Identification of a hierarchy of multipotent hematopoietic progenitors in human cord blood. *Cell Stem Cell.* 2007;1(6):635-645.
- Arcangeli ML, Frontera V, Bardin F, et al. JAM-B regulates maintenance of hematopoietic stem cells in the bone marrow. *Blood.* 2011;118(17):4609-4619.
- Yu VW, Scadden DT. Hematopoietic Stem Cell and Its Bone Marrow Niche. *Curr Top Dev Biol.* 2016;118:21-44.
- Benyoucef A, Calvo J, Renou L, et al. The SCL/TAL1 Transcription Factor Represses the Stress Protein DDIT4/REDD1 in Human Hematopoietic Stem/Progenitor Cells. *Stem Cells.* 2015;33(7):2268-2279.
- Brunet de la Grange P, Armstrong F, Duval V, et al. Low SCL/TAL1 expression reveals its major role in adult hematopoietic myeloid progenitors and stem cells. *Blood.* 2006; 108(9):2998-3004.
- Correia NC, Arcangeli ML, Pflumio F, Barata JT. Stem Cell Leukemia: how a TALented actor can go awry on the hematopoietic stage. *Leukemia.* 2016; 30(10):1968-1978.
- Orkin SH. Diversification of haematopoietic stem cells to specific lineages. *Nat Rev Genet.* 2000;1(1):57-64.
- Ito K, Hirao A, Arai F, et al. Regulation of oxidative stress by ATM is required for self-renewal of haematopoietic stem cells. *Nature.* 2004;431(7011):997-1002.
- Nijnik A, Woodbine L, Marchetti C, et al. DNA repair is limiting for haematopoietic stem cells during ageing. *Nature.* 2007; 447(7145):686-690.
- Rossi DJ, Bryder D, Seita J, Nussenzweig A, Hoeijmakers J, Weissman IL. Deficiencies in DNA damage repair limit the function of haematopoietic stem cells with age. *Nature.* 2007;447(7145):725-729.
- Cheng T, Rodrigues N, Dombkowski D, Stier S, Scadden DT. Stem cell repopulation efficiency but not pool size is governed by p27(kip1). *Nat Med.* 2000;6(11):1235-1240.
- Matsumoto A, Takeishi S, Kanie T, et al. p57 is required for quiescence and maintenance of adult hematopoietic stem cells. *Cell Stem Cell.* 2011;9(3):262-271.
- Zou P, Yoshihara H, Hosokawa K, et al. p57(Kip2) and p27(Kip1) cooperate to maintain hematopoietic stem cell quiescence through interactions with Hsc70. *Cell Stem Cell.* 2011;9(3):247-261.
- Biechonski S, Milyavsky M. Differences between human and rodent DNA-damage response in hematopoietic stem cells: at the crossroads of self-renewal, aging and leukemogenesis. *Transl Cancer Res.* 2013; 2(5):372-383.
- Jang YY, Sharkis SJ. A low level of reactive oxygen species selects for primitive hematopoietic stem cells that may reside in the low-oxygenic niche. *Blood.* 2007;110(8):3056-3063.
- Yahata T, Takanashi T, Muguruma Y, et al. Accumulation of oxidative DNA damage restricts the self-renewal capacity of human hematopoietic stem cells. *Blood.* 2011; 118(11):2941-2950.
- Ito K, Hirao A, Arai F, et al. Reactive oxygen species act through p38 MAPK to limit the lifespan of hematopoietic stem cells. *Nat Med.* 2006;12(4):446-451.
- Pearce MS. Patterns in paediatric CT use: an international and epidemiological perspective. *J Med Imaging Radiat Oncol.* 2011;55(2):107-109.
- Pearce MS, Salotti JA, Little MP, et al. Radiation exposure from CT scans in childhood and subsequent risk of leukaemia and brain tumours: a retrospective cohort study. *Lancet.* 2012;380(9840):499-505.
- Rodrigues-Moreira S, Moreno SG, Ghinatti G, et al. Low-dose irradiation promotes persistent oxidative stress and decreases self-renewal in hematopoietic stem cells. *Cell Rep.* 2017;20(13):3199-3211.
- Milyavsky M, Gan OI, Trotter M, et al. A distinctive DNA damage response in human hematopoietic stem cells reveals an apoptosis-independent role for p53 in self-renewal. *Cell Stem Cell.* 2010;7(2):186-197.
- Picou F, Debeissat C, Bourgeois J, et al. n-3 Polyunsaturated fatty acids induce acute myeloid leukemia cell death associated with mitochondrial glycolytic switch and Nrf2 pathway activation. *Pharmacol Res.* 2018;136:45-55.
- Hao QL, Thiemann FT, Petersen D, Smogorzewska EM, Crooks GM. Extended long-term culture reveals a highly quiescent and primitive human hematopoietic progenitor population. *Blood.* 1996;88(9):3306-3313.
- Petzer AL, Hogge DE, Landsdorp PM, Reid DS, Eaves CJ. Self-renewal of primitive human hematopoietic cells (long-term-culture-initiating cells) in vitro and their expansion in defined medium. *Proc Natl Acad Sci U S A.* 1996;93(4):1470-1474.
- Rizo A, Dontje B, Vellenga E, de Haan G, Schuringa JJ. Long-term maintenance of human hematopoietic stem/progenitor cells by expression of BMI1. *Blood.* 2008;111(5):2621-2630.
- Nakamura-Ishizu A, Takizawa H, Suda T. The analysis, roles and regulation of quiescence in hematopoietic stem cells. *Development.* 2014;141(24):4656-4666.
- Notta F, Doulatov S, Laurenti E, Poepl A, Jurisica I, Dick JE. Isolation of single human hematopoietic stem cells capable of long-term multilineage engraftment. *Science.* 2011;333(6039):218-221.
- Walter D, Lier A, Geiselhart A, et al. Exit from dormancy provokes DNA-damage-induced attrition in haematopoietic stem cells. *Nature.* 2015;520(7548):549-552.
- Haghdoost S, Czene S, Naslund I, Skog S, Harms-Ringdahl M. Extracellular 8-oxo-dG as a sensitive parameter for oxidative stress in vivo and in vitro. *Free Radic Res.* 2005;39(2):153-162.
- Cabon L, Bertaux A, Brunelle-Navas MN, et al. AIF loss deregulates hematopoiesis and reveals different adaptive metabolic responses in bone marrow cells and thymocytes. *Cell Death Differ.* 2018;25(5):983-1001.
- Chabi S, Uzan B, Naguibneva I, et al. Hypoxia regulates lymphoid development of human hematopoietic progenitors. *Cell Rep.* 2019;29(8):2307-2320.e6.
- Gomez-Puerto MC, Folkerts H, Wierenga AT, et al. Autophagy Proteins ATG5 and ATG7 Are Essential for the Maintenance of Human CD34(+) Hematopoietic Stem-Progenitor Cells. *Stem Cells.* 2016; 34(6):1651-1663.
- Wang Y, Liu L, Zhou D. Inhibition of p38 MAPK attenuates ionizing radiation-induced hematopoietic cell senescence and residual bone marrow injury. *Radiat Res.* 2011;176(6):743-752.
- de Laval B, Pawlikowska P, Petit-Cocault L, et al. Thrombopoietin-increased DNA-PK-dependent DNA repair limits hematopoietic stem and progenitor cell mutagenesis in response to DNA damage. *Cell Stem Cell.* 2013;12(1):37-48.
- Kraft D, Rall M, Volcic M, et al. NF-kappaB-dependent DNA damage-signaling differ-

- entially regulates DNA double-strand break repair mechanisms in immature and mature human hematopoietic cells. *Leukemia*. 2015;29(7):1543-1554.
38. Shao L, Feng W, Lee KJ, Chen BP, Zhou D. A sensitive and quantitative polymerase chain reaction-based cell free in vitro non-homologous end joining assay for hematopoietic stem cells. *PLoS One*. 2012;7(3):e33499.
 39. Tesio M, Tang Y, Mudder K, et al. Hematopoietic stem cell quiescence and function are controlled by the CYLD-TRAF2-p38MAPK pathway. *J Exp Med*. 2015;212(4):525-538.
 40. Baudet A, Karlsson C, Safaee Talkhonchek M, Galeev R, Magnusson M, Larsson J. RNAi screen identifies MAPK14 as a druggable suppressor of human hematopoietic stem cell expansion. *Blood*. 2012; 119(26):6255-6258.
 41. Zou J, Zou P, Wang J, et al. Inhibition of p38 MAPK activity promotes ex vivo expansion of human cord blood hematopoietic stem cells. *Ann Hematol*. 2012;91(6):813-823.
 42. Fernandez-Antoran D, Piedrafita G, Murai K, et al. Outcompeting p53-Mutant Cells in the Normal Esophagus by Redox Manipulation. *Cell Stem Cell*. 2019;25(3):329-341.e6.
 43. Rube CE, Fricke A, Widmann TA, et al. Accumulation of DNA damage in hematopoietic stem and progenitor cells during human aging. *PLoS One*. 2011;6(3):e17487.
 44. Akunuru S, Geiger H. Aging, Clonality, and Rejuvenation of Hematopoietic Stem Cells. *Trends Mol Med*. 2016;22(8):701-712.
 45. Ito R, Takahashi T, Katano I, Ito M. Current advances in humanized mouse models. *Cell Mol Immunol*. 2012;9(3):208-214.
 46. Hernandez L, Terradas M, Camps J, Martin M, Tusell L, Genesca A. Aging and radiation: bad companions. *Aging Cell*. 2015;14(2):153-161.
 47. Holyoake TL, Nicolini FE, Eaves CJ. Functional differences between transplantable human hematopoietic stem cells from fetal liver, cord blood, and adult marrow. *Exp Hematol*. 1999;27(9):1418-1427.
 48. Kollman C, Howe CW, Anasetti C, et al. Donor characteristics as risk factors in recipients after transplantation of bone marrow from unrelated donors: the effect of donor age. *Blood*. 2001;98(7):2043-2051.
 49. Xie M, Lu C, Wang J, et al. Age-related mutations associated with clonal hematopoietic expansion and malignancies. *Nat Med*. 2014;20(12):1472-1478.



Ferrata Storti Foundation

Haematologica 2020
Volume 105(8):2056-2070

Specialized pro-resolving lipid mediators are differentially altered in peripheral blood of patients with multiple sclerosis and attenuate monocyte and blood-brain barrier dysfunction

Gijs Kooij,^{1,2*} Claudio Derada Troletti,^{1*} Alessandro Leuti,^{3,4} Paul C. Norris,² Ian Riley,² Maria Albanese,⁵ Serena Ruggieri,⁶ Stephania Liberos,² Susanne M.A. van der Pol,¹ Bert van het Hof,¹ Yoëlle Schell,¹ Gisella Guerrero,⁴ Fabio Buttari,⁷ Nicola Biagio Mercuri,^{4,5} Diego Centonze,^{5,7} Claudio Gasperini,⁶ Luca Battistini,⁴ Helga E. de Vries,¹ Charles N. Serhan,^{2#} Valerio Chiurchiù^{3,4#}

¹Amsterdam UMC, Vrije Universiteit Amsterdam, Department of Molecular Cell Biology and Immunology, MS Center Amsterdam, Amsterdam Neuroscience, Amsterdam, the Netherlands; ²Center for Experimental Therapeutics and Reperfusion Injury, Department of Anesthesiology, Perioperative and Pain Medicine, Brigham and Women's Hospital and Harvard Medical School, Boston, MA, USA; ³Department of Medicine, Campus Bio-Medico University of Rome, Rome, Italy; ⁴European Center for Brain Research, IRCCS Santa Lucia Foundation, Rome, Italy; ⁵Neurology Unit, Department of Neurosciences, University of Rome Tor Vergata, Rome, Italy; ⁶Neurology Unit, San Camillo Forlanini Hospital, Rome, Italy and ⁷Unit of Neurology and Unit of Neurorehabilitation, IRCCS Istituto Neurologico Mediterraneo (INM) Neuromed, Pozzilli, IS, Italy

*GK and CDT contributed equally as first authors.

#ECNS and VC contributed equally as co-senior authors.

ABSTRACT

Chronic inflammation is a key pathological hallmark of multiple sclerosis (MS) and suggests that resolution of inflammation, orchestrated by specialized pro-resolving lipid mediators (LM), is impaired. Here, through targeted-metabololipidomics in peripheral blood of patients with MS, we revealed that each disease form was associated with distinct LM profiles that significantly correlated with disease severity. In particular, relapsing and progressive MS patients were associated with high eicosanoids levels, whereas the majority of pro-resolving LM were significantly reduced or below limits of detection and correlated with disease progression. Furthermore, we found impaired expression of several pro-resolving LM biosynthetic enzymes and receptors in blood-derived leukocytes of MS patients. Mechanistically, differentially expressed mediators like LXA₄, LXB₄, RvD1 and PD1 reduced MS-derived monocyte activation and cytokine production, and inhibited inflammation-induced blood-brain barrier dysfunction and monocyte transendothelial migration. Altogether, these findings reveal peripheral defects in the resolution pathway in MS, suggesting pro-resolving LM as novel diagnostic biomarkers and potentially safe therapeutics.

Correspondence:

VALERIO CHIURCHIÙ
v.chiurchiu@hsantalucia.it

CHARLES N. SERHAN
cserhan@bwh.harvard.edu

Received: February 13, 2019.

Accepted: November 21, 2019.

Pre-published: November 28, 2019.

doi:10.3324/haematol.2019.219519

Check the online version for the most updated information on this article, online supplements, and information on authorship & disclosures: www.haematologica.org/content/105/8/2056

©2020 Ferrata Storti Foundation

Material published in *Haematologica* is covered by copyright. All rights are reserved to the Ferrata Storti Foundation. Use of published material is allowed under the following terms and conditions:

<https://creativecommons.org/licenses/by-nc/4.0/legalcode>.

Copies of published material are allowed for personal or internal use. Sharing published material for non-commercial purposes is subject to the following conditions:

<https://creativecommons.org/licenses/by-nc/4.0/legalcode>,

sect. 3. Reproducing and sharing published material for commercial purposes is not allowed without permission in writing from the publisher.



Introduction

Multiple sclerosis (MS) is the most common chronic inflammatory demyelinating disease of the central nervous system (CNS) associated to uncontrolled/excessive neuro-inflammation and autoimmunity.^{1,2} The underlying immunopathogenesis of the disease has been extensively studied and is currently thought to involve an initial alteration of peripheral and brain immune responses, as well as a disruption of the blood-brain barrier (BBB). Subsequently, this leads to a substantial infiltration of autoreactive lymphocytes and innate immune cells causing demyelination, axonal loss, and ultimately neurodegeneration.³⁻⁶ Nevertheless, there is still an unmet need for new diagnostic and therapeutic options, especially for the progressive forms of MS for which almost no drugs are available (with the exception of the off-label rituximab and the recently approved ocrelizumab for the management of pri-

mary progressive MS). Recent studies suggest that chronic inflammation and autoimmunity could be a consequence of failure to resolve inflammation, and this resolution of inflammation is mediated by newly discovered metabolites termed specialized pro-resolving lipid mediators (SPM),⁷ temporally and spatially synthesized from ω -3 polyunsaturated fatty acids [eicosapentaenoic acid (EPA) and docosahexaenoic acid (DHA)].^{7,8} During the process of resolution of inflammation, the very same cells recruited to the inflammatory milieu and that produce inflammatory mediators (mainly innate immune cells) undergo a temporal lipid mediator (LM) class switch, whereby they stop producing classical eicosanoids (prostaglandins, leukotrienes, thromboxanes) from ω -6 arachidonic acid and start to biosynthesize SPM mainly from ω -3 EPA and DHA,^{7,8} through the stereoselective and concerted action of the same enzymes engaged in classical eicosanoids production, namely cyclo-oxygenase (COX) COX-2, lipoxygenases (LOX) LOX-5, LOX-12 and LOX-15, as well as cytochrome P450 and several pathway specific epoxide hydrolases.⁷ These LM are potent and extinguish the eicosanoid-induced inflammation by activating local resolution programs,⁷⁻⁹ also by directly modulating oxidative stress¹⁰ and T-cell responses,¹¹ via five separate G protein-coupled receptors (e.g. ALX/FPR2, GPR32/DRV1, ChemR23/ERV, BLT1 and GPR18/DRV2),⁹ without evoking unwanted side effects as opposed to the immunosuppressive agents that are currently most used as disease-modifying treatments. Despite the increase in data suggesting that SPM metabolism and functions are differentially altered in several chronic peripheral and brain inflammatory diseases,^{7,10,12,15} research on these LM in MS and how they contribute to disease is of high interest. Given this, we aimed to determine whether MS patients at different phases of disease, compared to healthy subjects, displayed different levels and abilities to endogenously synthesize and respond to ω -6- and ω -3-derived pro-inflammatory (eicosanoids) and pro-resolving LM (lipoxins, resolvins, protectins and maresins) by means of targeted lipid metabololipidomics in human plasma and by evaluating the expression of their enzymes and key target receptors in peripheral blood mononuclear cells (PBMC). Finally, we investigated whether specific SPM could modulate the inflammatory response of MS patient-derived monocytes and whether they could attenuate inflammation-induced BBB dysfunction as well as monocyte-transendothelial migration, which all represent key pathological hallmarks of MS pathogenesis.¹⁴

Methods

Multiple sclerosis patients

Peripheral blood was collected from two different cohorts. The first cohort was admitted to the neurological clinic of the University Hospital Tor Vergata, Rome, (14 females and 6 males, mean age 34.51 ± 3.35 years) and the second cohort to the San Camillo Hospital of Rome (13 females and 5 males, mean age 38.24 ± 2.76 years). Both cohorts were diagnosed as suffering from relapsing-remitting MS (RR-MS, $n=26$) or primary progressive (P-MS, $n=12$). Fifteen age-matched healthy subjects (HS, $n=15$) were used as controls. See Table 1 and *Online Supplementary Methods* for diagnostic details. All subjects gave their written informed consent to the study which was approved by the ethics committees of Tor Vergata Hospital and of San Camillo Hospital, Rome.

Liquid chromatography-tandem mass spectrometry-based metabololipidomics and analysis

Total lipids were extracted from plasma samples with solid phase C18 cartridges. Liquid chromatography-tandem mass spectrometry (LC-MS-MS) was used to perform absolute quantifications of all LM.^{15,16} Lipidomics data were analyzed by principal component analysis using SIMCA 13.0.3 software (MKS Data Analytics Solution Umea, Sweden) and by volcano plots using MetaboAnalyst (<http://www.metaboanalyst.ca>).

Human leukocyte and brain endothelial cell treatments

Freshly isolated PBMC from HS or MS patients were left untreated or pretreated with SPM and then stimulated with Imiquimod and ssRNA40 for five hours in presence of brefeldin A.¹⁷⁻¹⁹ Human brain endothelial cell line hCMEC/D3 cells were grown and treated with TNF- α in the presence or absence of SPM.²⁰

Flow cytometry

Peripheral blood mononuclear cells were assayed for surface immunophenotype (CD14, CD16, CD69) and intracellular cytokine production (TNF- α , IL-1 β , IL-6 and IL-12) by multiple fluorochrome-conjugated antibody staining. hCMEC/D3 were assayed for anti-ICAM-1 (REK-1) and SPM receptors (GPR32, ALX/FPR2 and GPR18) through primary specific antibodies followed by fluorochrome-conjugated secondary antibodies.^{11,17}

Real-time quantitative polymerase chain reaction

Total RNA was extracted from PBMC and hCMEC/D3, and retro-transcribed to cDNA. Specific probes for SPM receptors and SPM biosynthetic enzymes were used to assess relative mRNA

Table 1. Demographic data of patients with multiple sclerosis (MS) and control subjects.

	Healthy	Relapsing MS	Remitting MS	Progressive MS
N. of subjects	n=14	n=14	n=12	n=12
Mean age	36.12 ± 1.77	36.82 ± 2.91	37.67 ± 2.23	38.82 ± 2.54
Female/male	9/6	10/4	9/3	8/4
Disease duration* (years)	–	3.6	4.2	6.1
Mean EDSS	–	<3 (1.5–3)	<3 (1–1.5)	>3 (4–6)
Corticosteroids* (yes/no)	0	0/0	0/0	0/0
DMT* (yes/no)	0	0/0	0/0	0/0
N. of Gd+ T2 brain MRI lesions (%)	0	10-20 (65%)	10-20 (45%)	>20 (50%)

*Disease duration was defined as the time from disease onset to the time of sampling (in years). #At time of sampling. EDSS: Expanded Disability Status Scale scores; DMT: disease modifying treatments; Gd: gadolinium; MRI: magnetic resonance imaging.

Table 2. Human plasma lipid mediator (LM) (pg/mL).

			HS	MS	P
AA bioactive metabolome	Q1	Q3			
AA	303	259	13940 ± 1942	12480 ± 811.1	0.4127
LTB4	335	195	32.79 ± 11.55	63.16 ± 16.25	0.2958
20-OH-LTB4	351	195	–	–	–
20-COOH-LTB4	365	195	–	–	–
5S,12S-diHETE	335	195	21.04 ± 11.04	64.11 ± 40.07	0.2406
5S,15S-diHETE	335	115	10.78 ± 5.02	47.30 ± 14.48	0.1336
PGD2	351	233	1.69 ± 0.44	8.42 ± 1.63	0.0211
PGE2	351	189	3.84 ± 1.22	16.37 ± 2.68	0.0098
PGF2a	353	193	8.55 ± 3.14	14.74 ± 1.69	0.0768
TBX2	369	169	63.14 ± 20.03	209.60 ± 40.96	0.0289
5-HETE	319	115	199.6 ± 39.91	345.20 ± 97.29	0.1588
12-HETE	319	179	657.10 ± 145.50	1472.00 ± 180.20	0.0095
15-HETE	319	219	56.98 ± 14.84	102.70 ± 11.85	0.0348
LXA4	351	115	0.65 ± 0.56	1.85 ± 0.88	0.4077
LXB4	351	221	1.64 ± 0.44	4.71 ± 1.66	0.2705
AT-LXA4	351	115	3.56 ± 1.69	6.57 ± 1.59	0.2797
AT-LXB4	351	221	–	–	–
DHA bioactive metabolome					
DHA	327	283	25330.00 ± 3090.00	22690.00 ± 3133.00	0.6247
RvD1	375	121	0.19 ± 0.09	0.68 ± 0.32	0.2735
RvD2	375	215	–	–	–
RvD3	375	147	–	–	–
RvD4	375	101	–	–	–
RvD5	359	199	0.38 ± 0.15	1.37 ± 0.43	0.1794
RvD6	359	101	–	–	–
AT-RvD1	375	121	–	–	–
AT-RvD3	375	147	–	–	–
PD1	359	153	0.02 ± 0.01	0.14 ± 0.03	0.0325
AT-PD1	359	153	–	–	–
PDX			0.43 ± 0.15	2.08 ± 0.65	0.1182
Maresin 1	359	221	–	–	–
17-HDHA	343	245	71.47 ± 17.66	114.70 ± 12.40	0.0588
14-HDHA	343	205	310.20 ± 91.26	784.90 ± 130.90	0.0333
4-HDHA	359	101	30.19 ± 6.94	69.51 ± 18.37	0.1810
7-HDHA	359	250	5.68 ± 1.29	7.23 ± 1.06	0.4185
EPA bioactive metabolome					
EPA	301	259	6605.00 ± 1296.00	4606.00 ± 341.80	0.0472
RvE1	349	195	–	–	–
RvE2	333	253	–	–	–
RvE3	333	201	–	–	–
18-HEPE	317	259	75.50 ± 28.23	49.89 ± 8.10	0.2445
15-HEPE	317	219	18.54 ± 5.76	17.85 ± 2.32	0.6215
12-HEPE	317	179	244.70 ± 66.11	393.70 ± 49.88	0.0895
5-HEPE	317	115	27.07 ± 7.79	30.16 ± 6.90	0.7989

HS: healthy subjects; MS: multiple sclerosis.

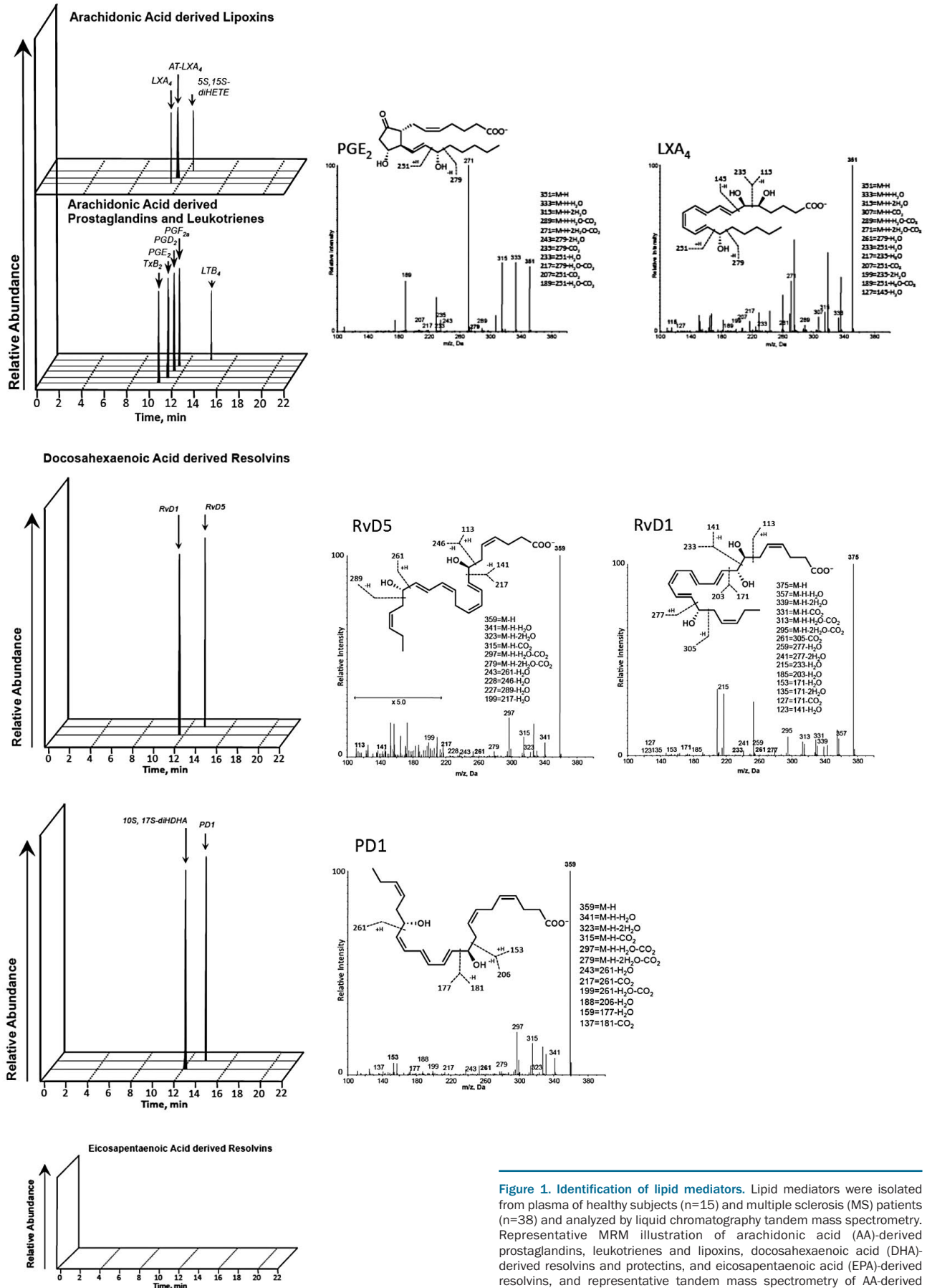


Figure 1. Identification of lipid mediators. Lipid mediators were isolated from plasma of healthy subjects (n=15) and multiple sclerosis (MS) patients (n=38) and analyzed by liquid chromatography tandem mass spectrometry. Representative MRM illustration of arachidonic acid (AA)-derived prostaglandins, leukotrienes and lipoxins, docosahexaenoic acid (DHA)-derived resolvins and protectins, and eicosapentaenoic acid (EPA)-derived resolvins, and representative tandem mass spectrometry of AA-derived PGE₂ and LXA₄, DHA-derived RvD1, RvD5 and PD1.

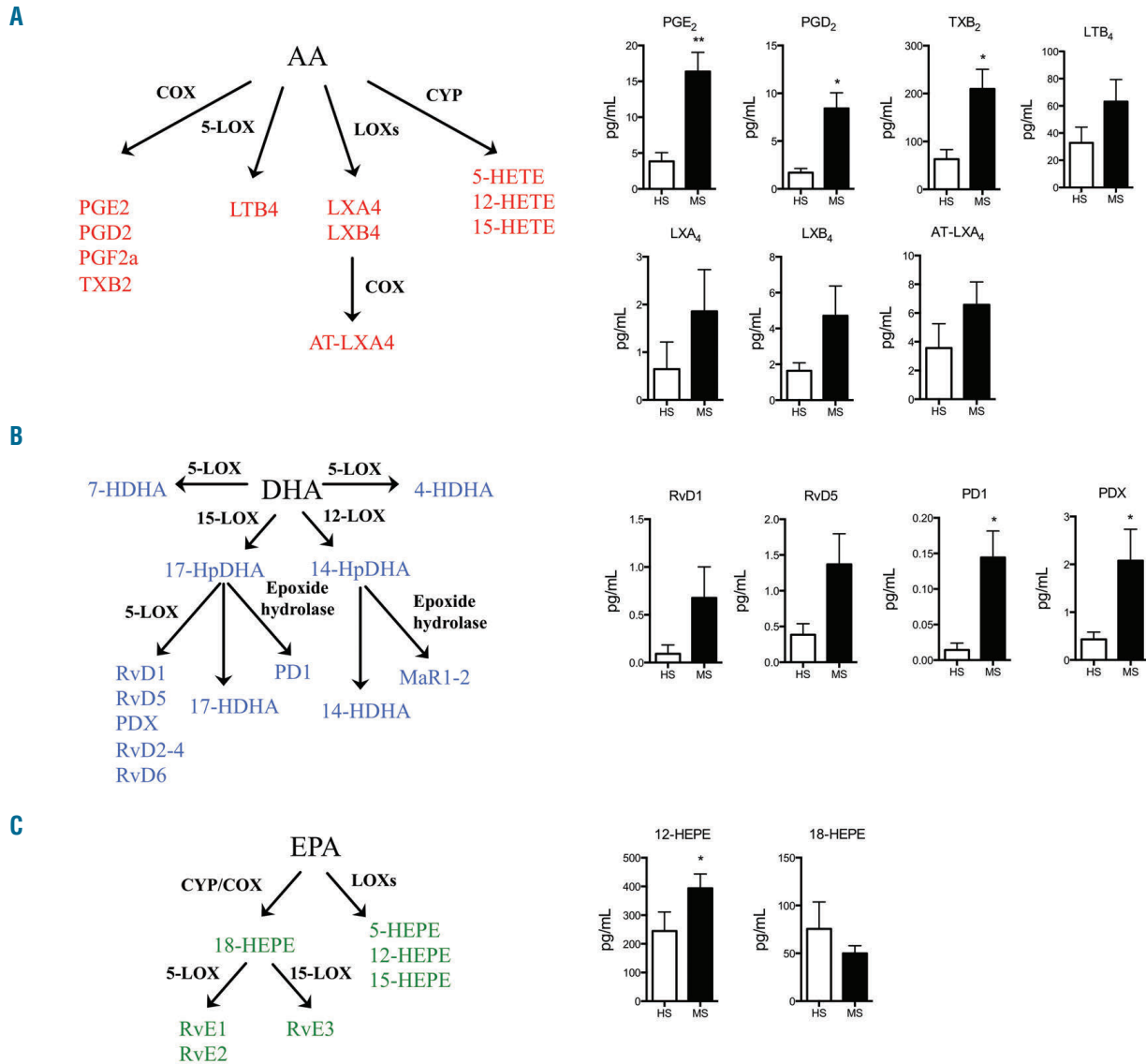


Figure 2. Multiple sclerosis (MS) patients show altered lipid mediators profiles in blood. Lipid mediators (LM) were isolated from plasma of healthy subjects (HS, n=15) and MS patients (n=38) and analyzed by liquid chromatography tandem mass spectrometry. (A) Schematic representation of the arachidonic acid (AA)-derived respective LM biosynthetic pathways and their selected values between HS and MS. (B) Schematic representation of the docosahexaenoic acid (DHA)-derived respective LM biosynthetic pathways and their selected values between HS and MS. (C) Schematic representation of the eicosapentaenoic acid (EPA)-derived respective LM biosynthetic pathways and their selected values between HS and MS. Data are presented as means pg/mL±standard error of mean. **P*<0.05 or ***P*<0.01 compared to HS, determined by Student t-test.

abundance for each gene in respect with beta actin or GAPDH expression.

Electric cell-substrate impedance sensing

hCMEC/D3 cells were seeded on collagen-coated 96W10idf electric cell-substrate impedance sensing (ECIS) arrays (Ibidi). Trans-endothelial electrical resistance (TEER) of hCMEC/D3 cells was measured at multiple frequencies,²¹ and TNF-α was added as maximum barrier resistance was reached, in the presence or absence of different SPM. Subsequently, TEER was measured over time and finally analyzed.²²

ELISA

hCMEC/D3 culture supernatants harvested 24 hours after TNF-α treatment in the presence or absence of SPM were meas-

ured for the levels of CCL2/MCP-1 by its commercial ELISA Kit (Invitrogen, the Netherlands) according to the manufacturer's instructions.

Transwell migration of monocytes

In vitro monocyte transendothelial cell migration assay was performed using a collagen 1-coated Transwell system. Briefly, hCMEC/D3 cells were cultured alone or with TNF-α upon which resting or SPM-treated purified human monocytes were added to the transwell filters.^{23,24} Transmigrated cells were determined through flow cytometry.

Statistical analysis

All data were expressed as means±standard error of mean (SEM). Differences between groups were compared using Student

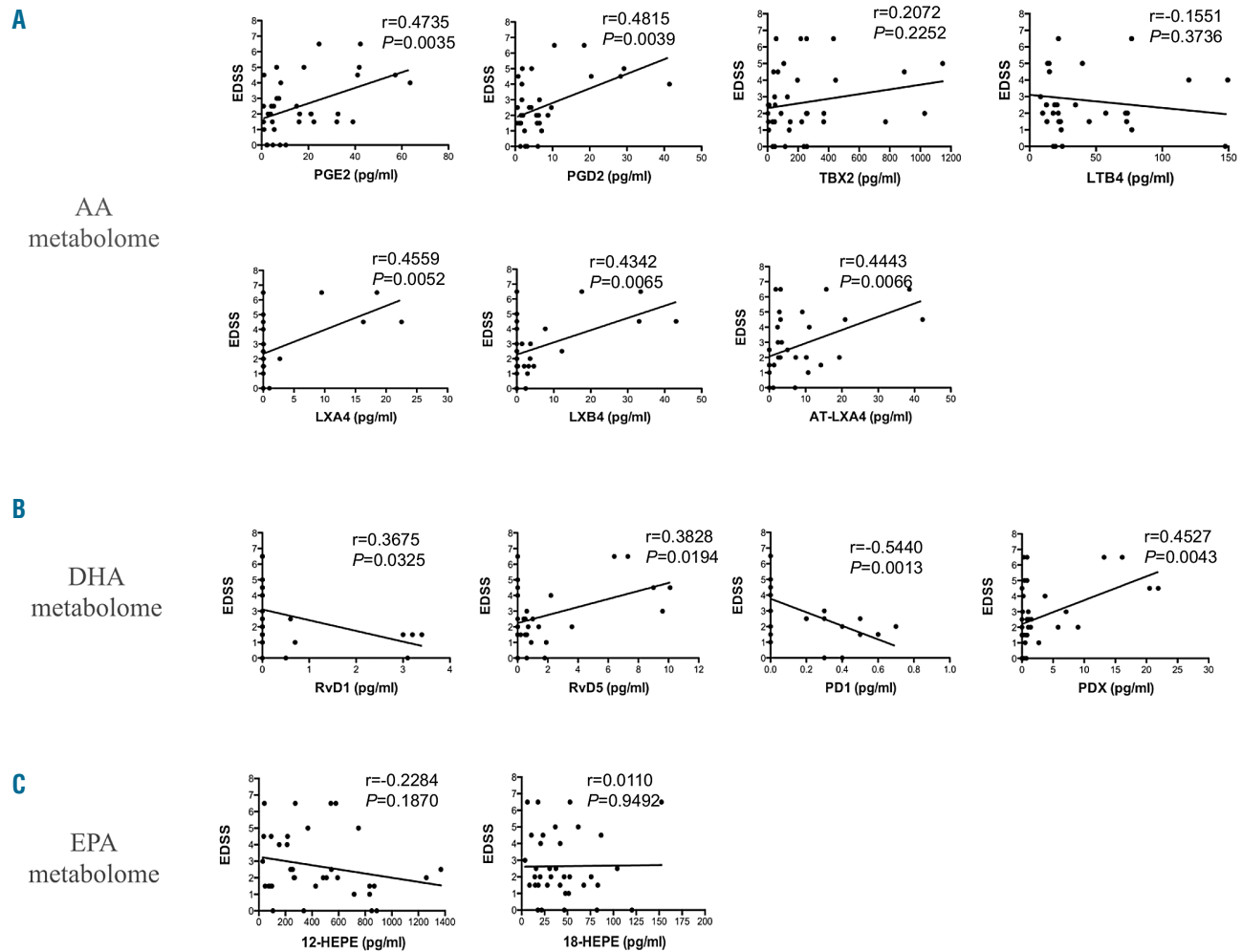


Figure 3. Correlations between Expanded Disability Status Scale (EDSS) scores of patients and lipid mediators. Correlation plots between EDSS values and levels (pg/mL) of specific lipid mediators of the AA metabolome (A), DHA metabolome (B) and EPA metabolome (C) in the entire cohort of patients with multiple sclerosis. Data were compared by Spearman's rank correlation coefficient ($P < 0.05$).

t-test (two groups) or one-way ANOVA (multiple groups) followed by a *post hoc* Bonferroni test. $P < 0.05$ was considered statistically significant.

Results

Multiple sclerosis patients show altered lipid mediators profiles in the blood

To address potential differences in LM profiles between MS patients and healthy donors, involving both pro-inflammatory and specialized pro-resolving lipid mediators (SPM), we performed targeted LM metabololipidomics on human plasma samples using liquid chromatography tandem mass spectrometry (LC-MS/MS) in two different cohorts of MS patients, analyzing 42 distinct LM from the endogenous substrates AA, DHA and EPA based on published criteria for each LM (i.e. matching chromatographic retention times (RT), fragmentation patterns, and six characteristic and diagnostic ions).^{15,16} This analysis revealed a pronounced biosynthesis of 27 of these LM in the blood of healthy donors and MS

patients (Table 2), and the identification of key LM, including leukotriene B₄ (LTB₄), resolvin (Rv) D1, RvD5 and protectin D1 (Figure 1). Quantitation of LM was performed using signature ion pairs *via* multiple reaction monitoring (MRM) and revealed marked differences in several LM of each metabolome between MS patients and healthy subjects (Figure 2). In particular, total MS patients showed significantly higher blood levels of many AA-derived pro-inflammatory LM, such as prostaglandins (PG) PGE₂, PGD₂ (Figure 2A) and hydroxyeicosatetraenoic acids (HETE) 12-HETE and 15-HETE (*Online Supplementary Figure S1A*), as well as increases, although not significant, in leukotriene B₄ and in AA-derived pro-resolving mediators lipoxins (LX)A₄ and LXB₄ (Figure 2A). Furthermore, as for LM derived from the DHA metabolome, we observed that MS patients displayed significantly higher levels of pathway markers 17-HDHA and 14-HDHA (*Online Supplementary Figure S1B*); however, among the ten possible DHA-derived SPM (D-series resolvins, protectins and maresins), only four were detected, e.g. RvD1, RvD5, PD1 and PDX, and these were all generally increased in MS patients, with PD1 and PDX

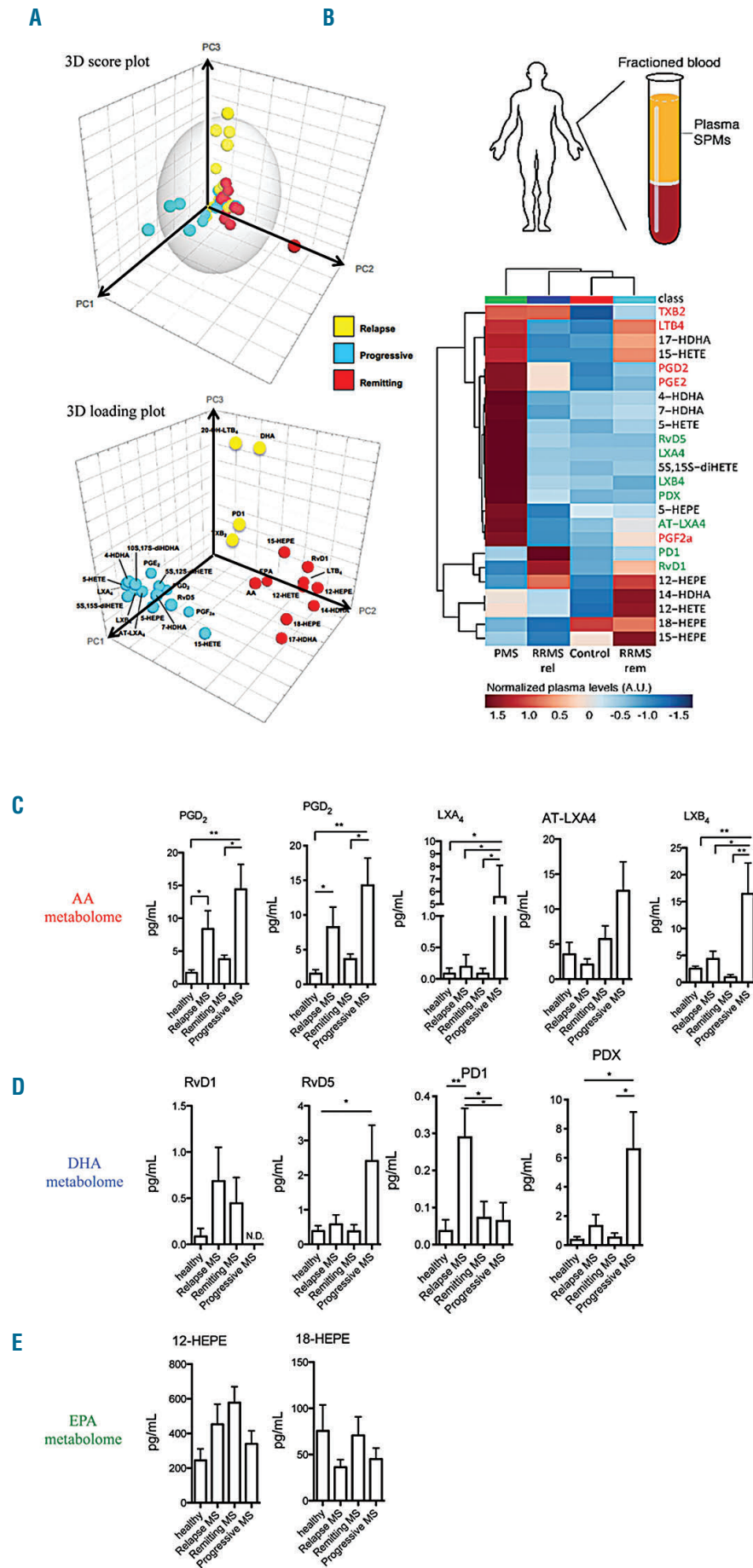


Figure 4. Lipid mediators (LM) are differentially altered in multiple sclerosis (MS) patients according to clinical disease phase. LM were isolated from plasma of healthy subjects (n=15), relapsing MS (n=14), remitting MS (n=12), and progressive MS (n=12) patients and analyzed by liquid chromatography tandem mass spectrometry. (A) Principal component analysis (PCA) of the LM profile. (Top) 3D score plot. (Bottom) 3D loading plot. (B) Heat map of LM fingerprint. Pro-inflammatory LM are shown in red, anti-inflammatory/pro-resolving LM are shown in green and pathway intermediates in black (C-E) Selected values of LM of AA metabolome (C), DHA metabolome (D), and EPA metabolome (E) from healthy subjects, relapsing, remitting and progressive MS patients. Data are presented as means pg/mL±standard error of mean. *P<0.05, **P<0.01, ***P<0.001 determined by one-way ANOVA followed by Bonferroni's multiple comparison test.

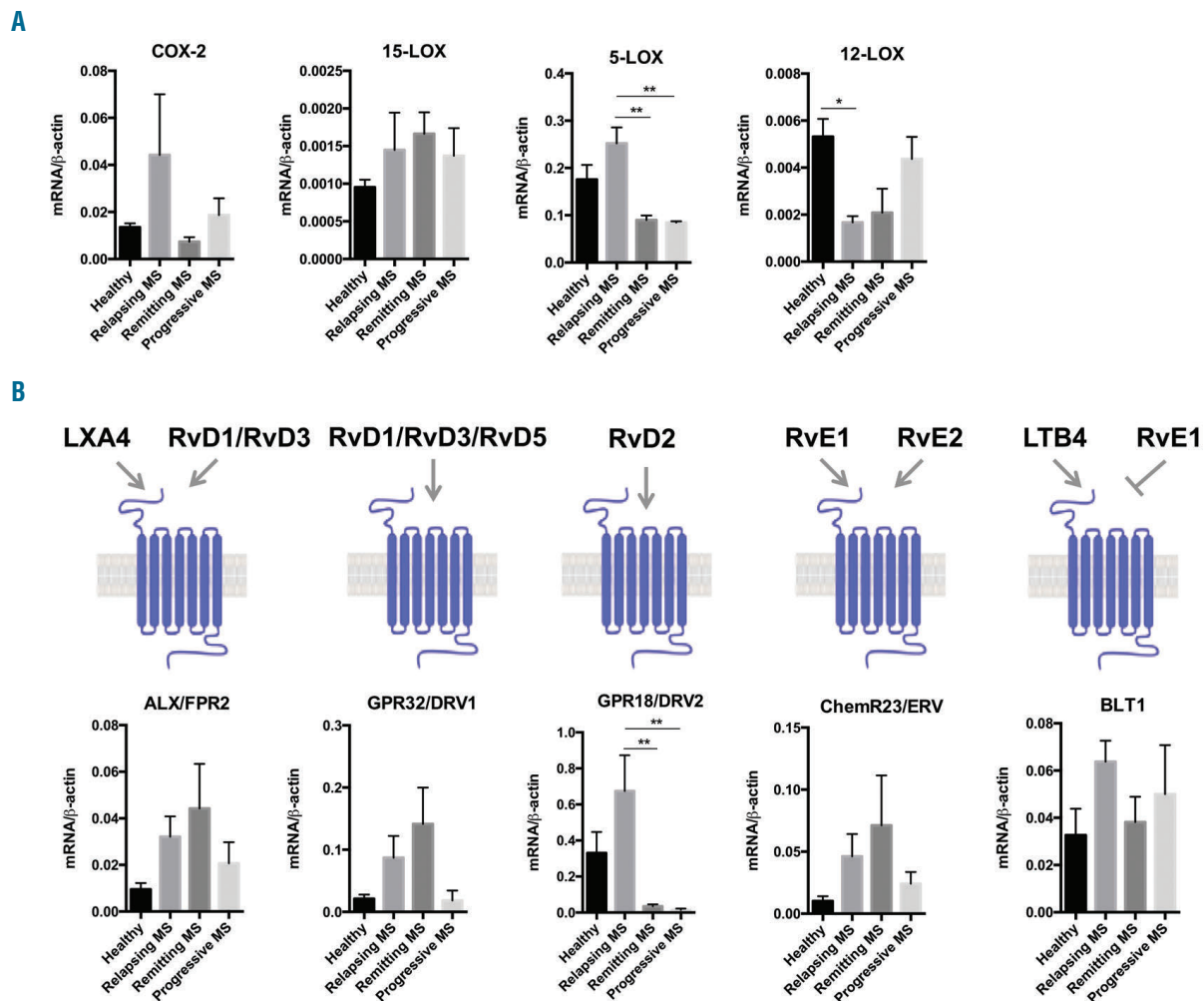


Figure 5. Specialized pro-resolving mediators biosynthetic enzymes and receptors are differentially expressed in multiple sclerosis (MS) patients according to the clinical disease phase. Peripheral blood mononuclear cells (PBMC, 2×10^6 cells) from healthy subjects ($n=5$), relapsing MS ($n=7$), remitting MS ($n=5$), and progressive MS ($n=5$) patients were quantified for their mRNA content by quantitative real-time polymerase chain reaction (qRT-PCR) of lipid mediator biosynthesizing enzymes COX-2, 5-LOX, 12-LOX and 15-LOX (A) and of SPMs receptors ALX/FPR2, GPR32/DRV1, GPR18/DRV2, ChemR23/ERV and BLT1 (B). Data are means \pm standard error of mean of 5-7 independent experiments. * $P < 0.05$, ** $P < 0.01$ determined by one-way ANOVA followed by Bonferroni's multiple comparison test.

being significant (Figure 2B). Of note, other DHA-derived SPM, such as RvD2, RvD3, RvD4 RvD6, AT-RvD1, AT-RvD3 and maresin (MaR) 1 were undetectable (Table 2). Among the EPA-derived lipid mediators, only 12-HEPE was significantly higher and 18-HEPE was slightly lower in MS patients; levels of E-series resolvins (RvE 1-3) were not identified in these patient samples (Table 2 and Figure 2C). Of interest, the total levels of AA and DHA were almost unchanged between MS patients and healthy subjects, while those of EPA were significantly reduced (*Online Supplementary Figure S1*). We next observed that all the LM that were increased in MS significantly correlated with disease severity, evaluated as Expanded Disability Status Scale (EDSS) scores, except for LTB₄ and EPA-derived 12-HEPE and 5-HEPE (Figure 3). In contrast, RvD1 and PD1 showed a negative correlation, inasmuch as their levels progressively decreased with clinical score (Figure 3B). Interestingly, we did not observe any correlation with the age and gender of patients, whereby levels of SPM were fairly constant in both males and females (*data not shown*).

Specialized pro-resolving lipid mediators, their biosynthetic enzymes and receptors are differentially expressed in multiple sclerosis patients according to disease phase

Since MS is characterized by different and independent forms of the disease,¹⁻³ we next stratified the metabololipidomics analysis according to disease clinical subtype. Using unbiased PCA (Figure 4A), we observed that each form of disease and healthy subjects were associated with distinct LM profiles. Indeed, relapse patients were associated with a cluster characterized by few LM, including PD1 and TXB₂ and remitting patients with a cluster that included several HEPE and HETE, as well as LTB₄ and RvD1, while progressive patients gave a cluster that included the most abundant and diversified LM, from pro-inflammatory PGE₂ and PGD₂ to anti-inflammatory LXA₄ and LXB₄. In particular, ANOVA analysis showed that many AA-derived pro-inflammatory and pro-resolving mediators, including PGD₂, PGE₂, LXA₄, LXB₄ (Figure 4B) as well as TXB₂ (*Online Supplementary Figure S2A*) fol-

lowed a similar trend, being generally increased in both relapsing MS and progressive MS patients compared to healthy subjects (with PGD₂ and PGE₂ being also significant for relapsing MS and LXA₄ and LXB₄ for progressive MS), while showing reduced levels in remitting MS patients compared to clinically active forms. For all of these LM, progressive patients consistently displayed higher levels compared to relapsing patients (Figure 4B and C). Of note, levels of their precursor AA moved in the opposite direction (*Online Supplementary Figure S2A*), suggesting an active metabolic conversion into such LM associated to disease phase. Other key metabolites of AA, including HETE, PGF_{2a} and LTB₄, appeared with specific trends of expression, with 5-HETE being mostly found in progressive MS and 12-HETE in remitting MS, while 15-HETE and PGF_{2a} steadily increased along disease forms (*Online Supplementary Figure S2A*). Levels of aspirin-triggered (AT) lipoxins were detected only for AT-LXA₄, which was particularly present in progressive patients (Table 2 and Figure 4B). As for the DHA metabolome, pro-resolving LM RvD5 and PDX were slightly increased in relapsing MS and significantly increased in progressive MS, with remitting MS showing similar levels compared to healthy subjects (Figure 4C). Furthermore, RvD1 and PD1 were increased in relapsing MS, with the latter being also significant and showing a reduction in both remitting and progressive patients, while the former being reduced in remitting MS and undetectable in progressive MS (Figure 4C). Of interest, the levels of their precursor DHA, although showing an initial, yet not significant, increase in relapsing MS, were progressively reduced along disease forms (*Online Supplementary Figure S2B*). Other pathway makers and metabolites of DHA were significantly increased, especially in remitting (14-HDHA and 17-HDHA) or progressive (17-HDHA and 4-HDHA) patients (*Online Supplementary Figure S2B*). As for EPA metabolome, levels of 15-HEPE and 18-HEPE were reduced in relapsing and progressive MS, returning back to control levels in remitting MS, showing a similar trend as their precursor EPA (Figure 4D and *Online Supplementary Figure S2C*). However, 12-HEPE was particularly high in both relapsing and remitting MS (Figure 4E). Specific LM fingerprints are also shown by volcano plots when comparing every two groups against each other, with SPM like RvD1 and PD1 being reduced along disease progression and others like LXB₄ and pro-inflammatory prostaglandins being produced during the active phases of disease, especially in progressive patients (*Online Supplementary Figure S3*).

Of note, both cohorts of healthy donors and MS patients displayed an almost identical LM profile (*Online Supplementary Figure S4*), with pro-inflammatory AA-derived prostanoids being induced in relapsing and progressive patients and reduced during remission, whereas lipoxins being slightly induced during the relapsing phase and even more during the progressive phase. As for the DHA- and EPA-derived SPM, both cohorts showed an induction of RvD1 and PD1 during the relapsing phase, which were both reduced or even undetected along disease progression, and showed a significant induction of RvD5 in progressive patients. The only SPM that was discordant was PDX, being significantly induced during the relapsing phase in the first cohort of MS patients, whereas in the second cohort, PDX was markedly induced in progressive patients (*Online Supplementary Figure S4*).

Having observed that each clinical form of MS is char-

acterized by differential profiles in the levels of SPM, we next sought to evaluate whether this was associated to contradistinctive capacities to produce them and/or to respond to them. Thus, we further characterized the different forms of MS by investigating the mRNA expression of the main SPM biosynthetic enzymes and their known receptors in peripheral blood leukocytes. While COX-2 and 5-LOX were particularly induced in relapsing MS to be then strongly reduced in both remitting and progressive patients, 15-LOX was consistently found in all MS forms (Figure 5A). On the contrary, 12-LOX expression was antithetical, inasmuch as its levels were substantially reduced in relapsing and remitting MS and started to recover in progressive MS patients (Figure 5A). As for SPM receptor expression, ALX/FPR2, DRV1 and ERV all displayed a similar pattern, with their expression levels being induced in relapsing MS, reaching their highest expression in remitting MS, and then exhibiting a reduction in progressive MS (Figure 5B). In addition, while BLT1 receptor expression was induced only in the active phases of the disease, DRV2 was strongly induced in relapsing MS and markedly reduced in both remitting and progressive patients, to expression levels much lower than healthy subjects (Figure 5B).

Specific specialized pro-resolving mediators attenuate monocyte inflammatory responses in multiple sclerosis patients

The observed differences of MS patients in producing distinct SPM profiles prompted us to examine whether peripheral blood leukocytes of MS patients were responsive to the immunomodulatory activity of disease-affected SPM. Accordingly, we tested the ability of SPM that showed an initial induction in relapsing MS patients and are subsequently diminished along disease progression (RvD1 and PD1), and SPM that showed a higher expression in relapsing MS patients and no induction in remitting MS (LXA₄, LXB₄), to evaluate their potential to affect the activation and cytokine production of activated monocytes obtained from RRMS patients, i.e. in the disease phase where such mediators were initially increased and then decreased. To do so, we analyzed the expression of activation markers and inflammatory cytokines in SPM-treated monocytes that were then challenged with two different viral Toll-like receptors (TLR) agonists: TLR7 and TLR8 (see *Online Supplementary Figure S5A* for gating strategy). As expected, the simultaneous stimulation of monocytes of relapsing MS patients with selective agonists of viral Toll-like receptors (TLR) 7 and TLR8 induced a strong upregulation of the activation marker CD69 on their cell surface compared to resting monocytes (Figure 6A). Treatment of activated monocytes with LXA₄, LXB₄, RvD1 or PD1 caused a significant reduction in CD69 surface expression (Figure 6A), indicating an overall ability of these SPM to attenuate the general activation of myeloid cells. More specifically, all these tested SPM were equally able to significantly reduce the intracellular production of several pro-inflammatory cytokines. Indeed, the high levels of TNF- α , IL-1 β , IL-6 and IL-12 production from activated monocytes of relapsing MS patients were equivalently and significantly reduced by LXA₄, LXB₄, RvD1 and PD1, although RvD1 and PD1 showed a higher vigor in reducing IL-6 production (Figure 6B and *Online Supplementary Figure S5B*). The immunomodulatory activity of these SPM was even

more evident in activated monocytes of healthy donors (*Online Supplementary Figure S6A and B*) inasmuch as all tested SPM induced an even stronger reduction of CD69 and of all pro-inflammatory cytokines, suggesting that although their pro-resolving actions are equally functional in health and disease, cells of MS patients are probably less responsive to SPM. Of note, besides reducing pro-inflammatory cytokines production, LXA₄, LXB₄, RvD1 and PD1 all equally enhanced the production of the typical anti-inflammatory cytokine IL-10 produced from

TLR7/8-activated monocytes (Figure 6C). Interestingly, the SPM-induced effect on cytokine reduction was not observed with monocytes treated with the pro-inflammatory LM LTB₄ (*Online Supplementary Figure S6C*).

Specific specialized pro-resolving mediators counteract blood-brain barrier dysfunction and attenuate monocyte transendothelial migration

A key pathological feature of MS is BBB dysfunction that ultimately leads to monocyte transmigration into the

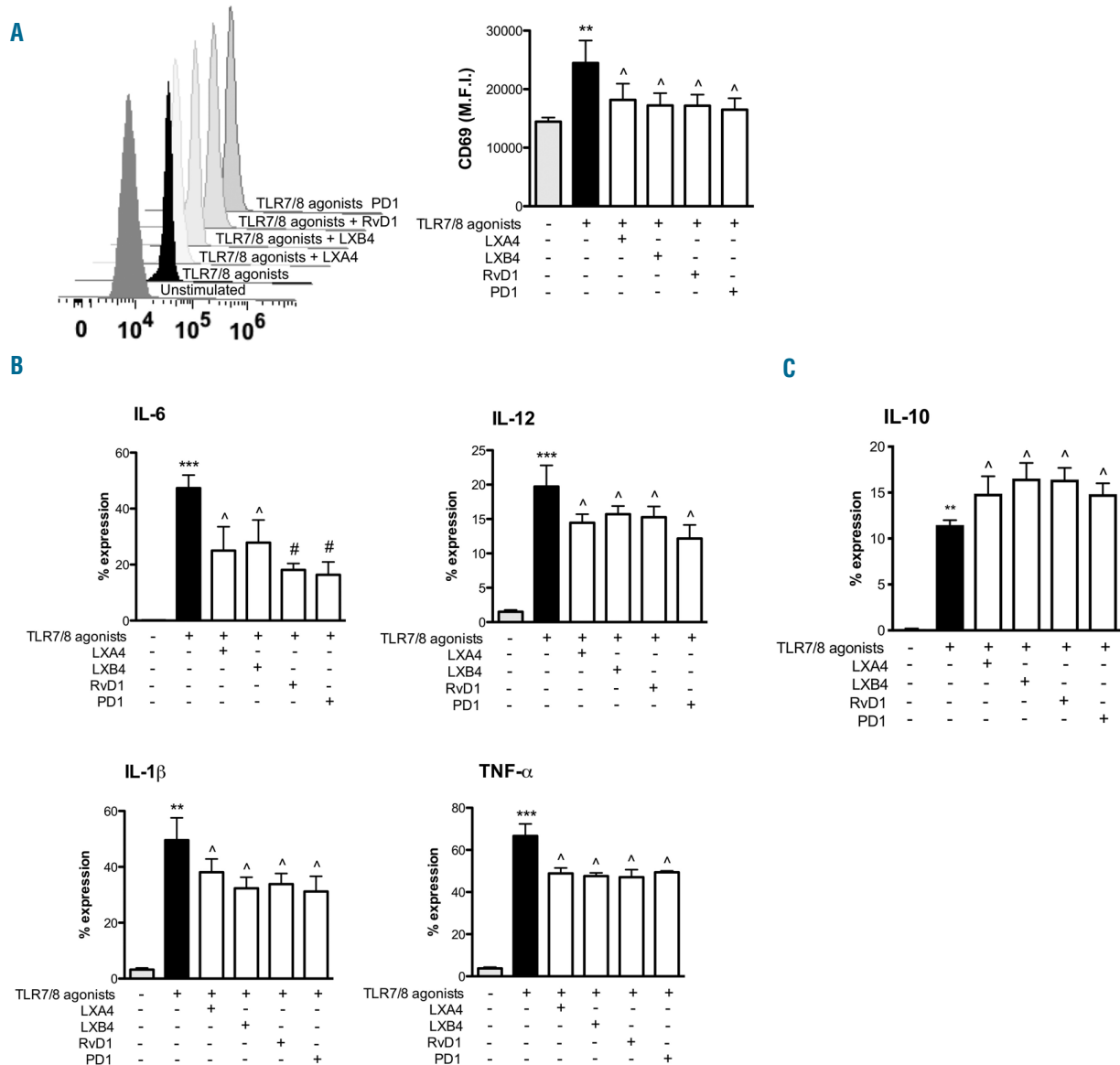


Figure 6. Specialized pro-resolving mediators reduce monocyte activation and cytokine production in multiple sclerosis (MS) patients. Peripheral blood mononuclear cells (PBMC, 2×10^6 cells) from relapsing MS patients ($n=5$) were left untreated or pre-treated with LXA, LXB₄, RvD1 or PD1 for 30 minutes. Cells were then stimulated with Imiquimod (Toll-like receptor 7 agonist) and ssRNA40 (Toll-like receptor 8 agonist) for five hours in absence or presence of Brefeldin A, stained at the cell surface and intracellularly, and analyzed by flow cytometry by gating on CD14⁺ monocytes. (A) Surface expression of CD69 positive monocytes. Data are shown as representative flow cytometry histograms and as means of fluorescence intensity (MFI)±standard error of mean of five independent experiments. ** $P<0.01$ compared to control cells and ^ $P<0.05$ compared to TLR7/TLR8 agonists, determined by one-way ANOVA followed by Bonferroni's multiple comparison test. (B) Cytofluorimetric plots and percentages of intracellular pro-inflammatory cytokine production (IL-6, IL-12, IL-1β and TNF-α) from CD14⁺ monocytes. Data are presented as means± standard error of mean (SEM) of five independent experiments. ** $P<0.01$ and *** $P<0.001$ compared to control cells, ^ $P<0.05$ and # $P<0.001$ compared to TLR7/TLR8 agonists, determined by one-way ANOVA followed by Bonferroni's multiple comparison test. (C) Cytofluorimetric plots and percentages of intracellular IL-10 production from CD14⁺ monocytes. Data are presented as means±SEM of four independent experiments. ** $P<0.01$, ^ $P<0.05$ and # $P<0.001$ compared to TLR7/TLR8 agonists, determined by one-way ANOVA followed by Bonferroni's multiple comparison test.

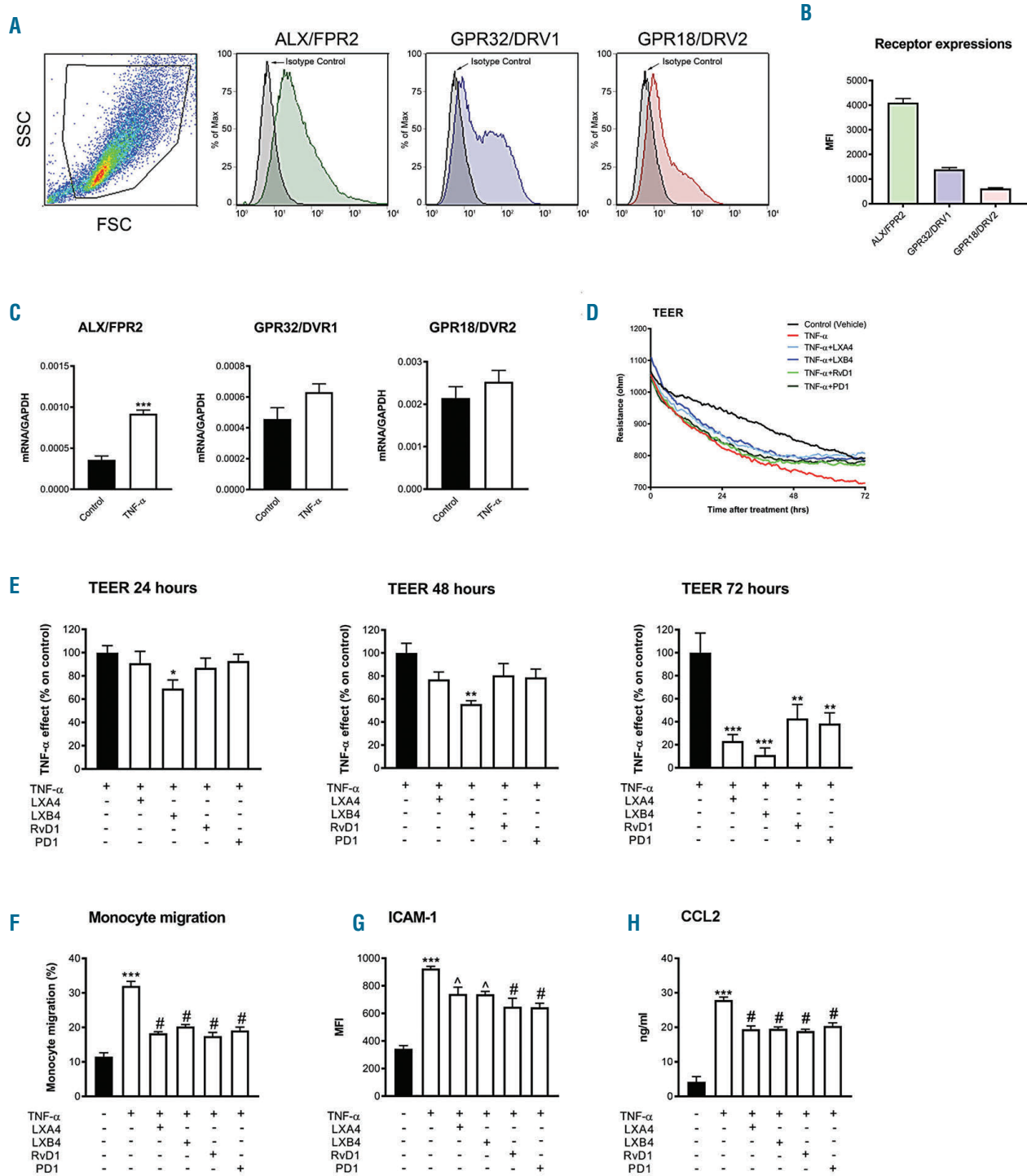


Figure 7. Specialized pro-resolving mediators (SPM) improve blood brain barrier (BBB) function and reduce monocyte transmigration and activation. (A) Representative scatter plots of forward scatter versus side scatter from human brain endothelial cells (BEC) and representative overlays histogram plot gated on live cells for GPR18/DRV2, GPR32/DRV1 and ALX/FPR2 surface expression. (B) Quantification of surface expression. Data are means±standard error of mean (SEM) of four independent experiments. (C) SPM receptors mRNA content in resting or TNF- α -activated BEC. Data are means±SEM of three independent experiments. Statistical analysis was carried out using Student *t*-test. ****P*<0.001. (D and E) The functional effect of TNF- α (5 ng/mL) in the presence or absence of LXA₄, LXB₄, RvD1 or PD1 on BBB function was assessed by measuring the trans-endothelial electrical resistance (TEER) of BEC. Confluent BEC monolayer was treated as described and TEER was measured over time. Data are shown as representative TEER curves of three independent experiments. Graphs showing the TNF- α effect at selected time-points, plotted as % TNF- α effect of control BEC±SEM of three independent experiments. Statistical analysis was carried out using Student *t*-test. **P*<0.05, ***P*<0.01, ****P*<0.001. (F-H) Confluent BEC were stimulated for 24 hours with TNF- α in the presence or absence of LXA₄, LXB₄, RvD1 or PD1. Human monocytes (1x10⁵ cells/well) were left untreated or treated with LXA₄, LXB₄, RvD1 or PD1 prior plated on BEC. Cells were incubated for eight hours before harvesting the transmigrated cells. (F) Percentage of monocyte transmigration evaluated by flow cytometry. Data are shown as means±SEM of three independent experiments. ****P*<0.001 compared to control cells and #*P*<0.001 compared to TNF- α stimulated cells, determined by one-way ANOVA followed by Bonferroni's multiple comparison test. ICAM-1 expression by flow cytometry (G) and CCL2 secretion was measured by ELISA (H). Data are means±SEM of three independent experiments. ****P*<0.001 compared to control cells, ^*P*<0.05 and #*P*<0.001 compared to TNF- α stimulated cells, determined by one-way ANOVA followed by Bonferroni's multiple comparison test.

CNS by crossing the inflamed and disrupted BBB. Therefore, we addressed the question as to whether the differentially expressed SPM were able to counteract inflammation-induced BBB dysfunction, by using human brain endothelial cells (BEC) as a BBB model. We first assessed if these cells responded to SPM by looking at the expression pattern of specific SPM receptors. We found that BEC mainly express ALX/FPR2 and to a lesser extent GPR18/DVR2 and GPR32/DVR1 (Figure 7A and B). Interestingly, such marked ALX/FPR2 expression was even more evident when BEC were stimulated with TNF- α , inasmuch as inflamed cells underwent a significant upregulation of ALX/FPR2 mRNA, while they only showed a slight increase in GPR18/DVR2 and GPR32/DVR1 expression (Figure 7C). Next, we assessed whether LXA₄, LXB₄, RvD1 and PD1 were capable of counteracting inflammation-induced BBB dysfunction by measuring TEER in real-time. We found that these SPM were able to rescue the TNF- α -mediated decrease in TEER in a time-dependent manner, at both a 10 nM (Figure 7D and E) and 100 nM concentration (*Online Supplementary Figure S7*), with LXB₄ starting to have a significant effect as early as at 24 hours (h) (at 10 nM but not at 100 nM) and with all SPM significantly rescuing TEER after 72 h (at both concentrations). Of note, no dose-dependency in SPM potency in rescuing TEER was observed, except for 100 nM LXA₄ that showed a significant impact at 48 h. In view of these results, we next sought to investigate the SPM effect on monocyte transendothelial migration by using this human BBB model. Treatment with LXA₄, LXB₄, RvD1 or PD1 significantly inhibited the migration of monocytes across BEC (Figure 7F) and this action was associated with a significant reduction in the expression of endothelial adhesion molecule ICAM-1 and chemokine CCL2 (Figure 7G and H), thereby accounting for a potent anti-inflammatory action of the pro-resolving LM in preventing inflammation-induced BBB dysfunction.

Discussion

This study provides an unprecedented comprehensive overview of the LM signature in plasma from MS patients with different clinical forms of the disease compared to healthy controls. Targeted LM metabololipidomics using LC-MS-MS with subsequent analyses revealed that relapsing MS patients display most of the AA-derived prostaglandins (i.e. PGD₂ and PGE₂) as well as of DHA-derived SPM like PD1 and RvD1 (and partly PDX), which were all reduced in remitting MS patients. In addition, progressive MS patients not only were characterized by the co-presence of all pro-inflammatory mediators (all of them even in higher levels than relapsing patients) but also on the appearance of some AA-derived or DHA-derived SPM, such as LXA₄ and LXB₄, RvD5 and PDX. Of note, the levels of PD1 and RvD1 were significantly reduced or even undetected along disease progression.

In line with the general concepts that bioactive LM undergo temporal and spatial production during inflammation, that SPM appear at the peak of acute inflammation in order to later reduce inflammation by activating endogenous resolution programs,^{7,10} and that chronic inflammation may result from failed resolution mechanisms,^{12,13} our results display that during the acute phase of

the disease (relapsing form) there is an imbalance between pro-inflammatory and pro-resolving LM, in favor of the former, and an insufficient or lack of expression of many key SPM (including E-resolvins, maresins and the rest of D-resolvins), which may in turn affect the outcome of remission and thereby, in theory, even lead to disease progression, although further studies are needed to fully clarify this. Indeed, over 80% of individuals with MS initially develop a clinical pattern with periodic relapses that reflect acute inflammation in the CNS and myelin disruption as well as induced activation of innate immune cells and pro-inflammatory mediators in peripheral blood, followed by continuous remissions during which self-remyelination occurs and symptoms decrease or temporarily disappear.^{6,25} Repeated relapses and remissions lead to less and less effective remyelination, appearance of scar-like plaques (scleroses) and thus after 10-20 years, patients might evolve into a progressive form of the disease, characterized by an irreversible disruption of peripheral and central immune tolerance, neurodegeneration, and permanent cortical and subcortical gray matter atrophy.²⁶ More than a dozen disease-modifying (and mostly anti-inflammatory) agents are available to reduce the frequency of transient episodes of neurological disability and limit the accumulation of CNS lesions, but these systemically applied agents not only are exclusive for RR-MS patients and not for progressive patients, but also result in severe side-effects, and none of these prevents or reverses the neurological deterioration.²⁷ Therefore, we set out to investigate whether impairments of endogenous processes to resolve inflammation correlate with MS progression to ultimately provide tools to either slow down inflammatory activation and simultaneously promote neuroprotection or prevent disease progression. The primary objective of our study was to identify pro-inflammatory and pro-resolving LM and validate their structures in peripheral blood of MS patients and healthy controls, and secondly, to correlate levels with clinical outcomes. To this aim, targeted metabololipidomics allowed us to reveal the full spectrum of LM in plasma samples of healthy donors and of MS patients with different clinical disease forms. We found that acute MS patients are able to produce only very few SPM (i.e. lipoxins, RvD1 and PD1). This is suggestive of a defective resolution program during MS that could not only result in a partial recovery, but could also eventually increase the probability of evolving into the progressive form, as substantiated by an inverse correlation of such SPM with clinical severity. Our observed presence of high levels of few SPM (LXA₄, LXB₄, RvD5 and PDX) in progressive MS, which instead positively correlate with clinical severity, is indicative of a last, but ineffective, attempt of the body to respond to an even higher inflammatory status, where all pro-inflammatory LM are consistently produced in high amounts and are also associated to disease severity. This is particularly relevant for LXA₄ and LXB₄ that are metabolically derived from arachidonic acid, and that are the actual initiators of the metabolic switch from the omega-6 pro-inflammatory eicosanoids to the omega-3 SPM. Indeed, MS patients attempt to induce a compensatory boost of these two lipoxins in order to promote the subsequent production of all SPM, which is reflected only in an increased production of RvD5 and PDX (whose potency is much lower than its stereoisomer PD1) and not by an induction of all other SPM. Of note, typical SPM that are usually produced later

in the inflammatory process, and that appear also during chronic stages, namely RvD3 and RvD4, are undetected in all MS phases, further suggesting that, although progressive patients endeavor in a last attempt to boost a lipoxin-mediated metabolic switch towards SPM, this is not followed by actual SPM production.

Our findings are in line with the only other study that analyzed a few of such LM in MS, whereby RvD1 and PD1 were induced in highly active MS patients.²⁸ However, this study, which was performed on cerebrospinal fluid samples, not only analyzed a smaller cohort of patients and did not take into consideration healthy subjects, but was able to detect only one-third of the LM that have been measured here. Furthermore, and most importantly, our metabololipidomics analysis was performed on three clinically distinct MS forms, which included not only MS with active relapse phases, but also patients with clear signs of remission or progression, allowing us to have a complete overview of a vast array of LM and observe how they vary along disease phases and during progression.

The recent evidence that several chronic inflammatory diseases are associated with altered SPM metabolism also supports our findings. Indeed, decreased production of lipoxins and resolvins (especially RvD1) have been linked to the pathogenesis of chronic obstructive pulmonary disease,²⁹ type-2 diabetes and obesity,^{30,31} inflammatory bowel disease,^{32,33} and rheumatoid arthritis.³⁴ In addition, an imbalance between pro-inflammatory leukotrienes and pro-resolving SPM was observed in atherosclerosis.³⁵ Of note, the notion that also neuroinflammatory and neurodegenerative diseases might be linked to a dysfunctional resolution of inflammation has very recently been put forward, and an impaired pro-resolution pathway, involving both specific SPM (i.e. LXA₄ and RvD1) and their receptors was found in post-mortem brain tissues of patients with Alzheimer disease,^{36,37} where clinical trials with DHA show a reduced peripheral inflammation associated with increases in specific SPM.³⁸ Accordingly, our observed significant and progressive reduction of DHA during MS, reaching very low levels in progressive patients, once again support a defect in producing its SPM derivatives. In line with this, Holmann *et al.* described deficiencies in polyunsaturated fatty acid (PUFA) and subsequent replacement by non-essential fatty acids in MS.³⁹ Along these lines, untargeted metabolomics analysis of plasma samples derived from mice with experimental autoimmune encephalomyelitis (EAE), the most commonly used animal model for MS, revealed similar profound alterations in the omega-3 and omega-6 PUFA pathways, with several metabolites of PUFA being significantly lower in EAE mice including RvD1.⁴⁰ Importantly, RvD1 supplementation ameliorated clinical signs of EAE, illustrating *in vivo* efficacy of SP during neuro-inflammation.⁴⁰ Epidemiological studies suggest that in particular omega-3 PUFA supplementation is linked with improved clinical outcomes in patients with MS.^{27,41,42} However, although the levels of AA and DHA could be restored by supplementation in MS patients, the efficacy of PUFA supplementation remains to be established.

Next, we further investigated the profile of peripheral blood leukocytes, and our analysis revealed distinctive expressions patterns of SPM biosynthetic enzymes and receptors in each clinical form of MS. Relapsing MS patients showed increased expression of COX-2 and 5-

LOX as well as of all five identified receptors (ALX/FPR2, GPR2/DRV1, GPR18/DRV2, ChemR23/ERV and BLT1). Interestingly, 12-LOX, which is responsible for maresins production, was consistently lower in all MS phases compared to healthy donors. Furthermore, the expression of SPM enzymes and receptors decreased along disease progression, with the exception of 15-LOX (that remained constant in all MS phases) and of ALX/FPR2, GPR32/DRV1, and ChemR23/ERV that further increased only during remission, thus suggesting their possible involvement in promoting pro-resolution programs and neuroprotection, but subsequently dropped in progressive MS patients.

It is worth mentioning that the levels of SPM observed in the different disease phases might also be a consequence of a differential utilization and/or degradation, as well as a different expression, of their target receptors. Indeed, progressive patients bear the lowest amount of all SPM target receptors, yet they continue to express high levels of the proinflammatory BLT1 receptor, whose action is only blocked by E-series resolvins that are never to be found in all MS phases.

Although many types of leukocytes are involved in disease progression, activated monocytes are believed to be one of the first to arrive to the brain and initiate inflammation.⁴³ In MS, the majority of monocytes display a classical inflammatory phenotype and are hyperactive.⁴⁴ Here we found that monocytes isolated from RR-MS patients not only displayed a more activated and pro-inflammatory status (since their expression of CD69 and cytokines were, indeed, much higher than monocytes of healthy subjects), but also that specific SPM significantly inhibited such inflammatory responses in both healthy monocytes and those of RR-MS patients. However, the ability of SPM to modulate the inflammatory response of these peripheral cells was more evident in cells of healthy subjects, suggesting that, despite expressing comparable levels of pro-resolving receptors, MS patient-derived monocytes are less susceptible to SPM. These findings confirm and extend earlier reports in which such SPM were shown to reduce the inflammatory profile of human monocytes upon a pro-inflammatory stimulus.⁴⁵⁻⁴⁷ Of note, such SPM-induced effect is of crucial importance in preventing priming and activation of autoreactive T cells (especially Th1 and Th17 cells) and natural killer cells, whose pathogenicity are strictly dependent on monocyte-derived cytokines.

Of note, the onset of MS starts when activated and autoreactive peripheral immune cells cross the BBB and start to damage myelin. In this process, BBB endothelial cells are key regulators of the neuroinflammatory response, inasmuch as when inflamed they lead to BBB disruption, upregulation of several adhesion molecules and production of chemokines, ultimately favoring leukocyte transmigration and subsequent MS lesion development.⁴⁸ However, BBB endothelial cells also play an important role during the resolution phase of inflammation *via* the secretion of pro- and anti-inflammatory mediators that co-ordinate both leukocyte traffic and barrier function.⁴⁹ In this context, despite the fact that a great number of studies have shown the anti-inflammatory and pro-resolving effect of SPM on various cell types of the immune system, their potential impact on inflamed BBB has never been reported. Our results show for the first time, not only that BBB endothelial cells express several pro-resolving receptors, which are increased upon inflam-

mation, but also that specific SPM (LXA₄, LXB₄, RvD1 and PD1) can prevent inflammation-induced BBB dysfunction, and reduce monocyte transmigration, as well as expression of ICAM-1 adhesion molecule and production of CCL2 chemokine. Our results confirm and extend previous findings in which SPM have been shown to positively regulate endothelial barrier functions through different mechanisms of action. Indeed, it has been shown that LXA₄ and RvD1 were able to protect LPS-induced barrier integrity and function *via* suppression of reactive oxygen species (ROS) production,⁵⁰ inhibition of the NF- κ B pathway⁵¹ or induction of the antioxidant protein Nrf2.⁵² Furthermore, SPM like (AT)-LXA₄, RvD1, RvD2, and MaR1 were reported to reduce monocyte/macrophage infiltration and chemotaxis both *in vitro* and *in vivo*,^{53,54} with RvD1 also being able to induce a switch to the anti-inflammatory M2 phenotype on monocyte-derived brain macrophages in the murine model of MS.⁴⁰ Although several studies report the anti-inflammatory role of different SPM (LXA₄ in particular) on vascular endothelial cells or monocytes/macrophages, in terms of reduction of ICAM-1 expression^{55,56} and CCL2 production,⁵⁷ we are the first to reveal potent SPM effects on the BBB, therefore providing novel tools to counteract inflammation-induced BBB dysfunction.

In conclusion, we provide here a comprehensive profiling of the LM signature in plasma from MS patients with different clinical forms of the disease compared to healthy controls. Importantly, our data indicate that key SPM are

lacking at different disease stages, which not only indicates a failed resolution response in these individuals, but may also provide an explanation as to why the disease progresses. It may also hint at novel therapeutic strategies aimed at boosting their endogenous production or at activating their target receptors. At a functional level, we here show that LXA₄, LXB₄, RvD1 and PD1 significantly reduce the inflammatory profile of MS-patient-derived monocytes and potentially inhibit inflammation-induced BBB dysfunction and monocyte-BBB traversal, which are key pathological hallmarks of MS lesion development. Although further investigations are needed to verify whether SPM impairment is also associated to demyelination and behavior/motor functions in MS patients, this study highlights the potential to use SPM as novel blood biomarkers for MS diagnosis and provides novel tools to ultimately limit MS pathogenesis at several clinical disease stages.

Funding

This study was supported by the Italian Foundation of Multiple Sclerosis (FISM grant 2017/R/O8 to VC) and Ministry of Health, Progetto Giovani Ricercatori (GR-2016-02362380 to VC), Nauta Fonds and VUmc MS Center Amsterdam (to GK), Dutch MS Research Foundation (14-878MS to GK), by the European Union's Seventh Framework Program FP7 under Grant agreement 607962 (nEUROinflammation) (to CDT) and studies in the CNS laboratories were supported by NIH/NIGMS (Grant P01GM095467). GK was supported by an IBRO Research Fellowship.

References

- Noseworthy JH, Lucchinetti C, Rodriguez M, Weinshenker BG. Multiple sclerosis. *N Engl J Med*. 2000;343:938-952.
- Dendrou CA, Fugger L, Friese MA. Immunopathology of multiple sclerosis. *Nat Rev Immunol* 2015;15:545-558.
- Compston A, Coles A. Multiple sclerosis. *Lancet*. 2008;372(9648):1502-1517.
- Dutta R, Trapp BD. Mechanisms of neuronal dysfunction and degeneration in multiple sclerosis. *Prog Neurobiol*. 2011; 93(1):1-12.
- Calabrese M, Magliozzi R, Ciccarelli O, Geurts JJ, Reynolds R, Martin R. Exploring the origins of grey matter damage in multiple sclerosis. *Nat Rev Neurosci*. 2015; 16(3):147-58.
- Mahad DH, Trapp BD, Lassmann H. Pathological mechanisms in progressive multiple sclerosis. *Lancet Neurol*. 2015; 14(2):183-193.
- Serhan CN. Pro-resolving lipid mediators are leads for resolution physiology. *Nature*. 2014;510(7503):92-101.
- Chiang N, Serhan CN. Structural elucidation and physiologic functions of specialized pro-resolving mediators and their receptors. *Mol Aspects Med*. 2017;58:114-129.
- Chiurchiù V, Leuti A, Maccarrone M. Bioactive lipids and chronic inflammation: managing the fire within. *Front Immunol*. 2018;9:38.
- Leuti A, Maccarrone M, Chiurchiù V. Proresolving Lipid Mediators: Endogenous Modulators of Oxidative Stress. *Oxid Med Cell Longev*. 2019;2019:8107265.
- Chiurchiù V, Leuti A, Dalli J et al. Proresolving lipid mediators resolvin D1, resolvin D2, and maresin 1 are critical in modulating T cell responses. *Sci Transl Med*. 2016;8(353):353ra111.
- Nathan C, Ding A. Nonresolving inflammation. *Cell* (2010);140:871-882.
- Krashia P, Cordella A, Nobili A, La Barbera L, Federici M, Leuti A, Campanelli F, Natale G, Marino G, Calabrese V, Vedele F, Ghiglieri V, Picconi B, Di Lazzaro G, Schirinzi T, Sancesario G, Casadei N, Riess O, Bernardini S, Pisani A, Calabresi P, Viscomi MT, Serhan CN, Chiurchiù V, D'Amelio M, Mercuri NB. Blunting neuroinflammation with resolvin D1 prevents early pathology in a rat model of Parkinson's disease. *Nat Commun*. 2019; 10(1):3945.
- Lopes Pinheiro MA, Kooij G, Mizee MR et al. Immune cell trafficking across the barriers of the central nervous system in multiple sclerosis and stroke. *Biochim Biophys Acta*. 2016;1862(3):461-471.
- English JT, Norris PC, Hodges RR, Dartt DA, Serhan CN. Identification and profiling of specialized pro-resolving Mediators in human tears by lipid mediator metabolomics. *Prostaglandins Leukot Essent Fatty Acids*. 2017;117:17-27.
- Werz O, Gerstmeier J, Libreros S et al. Human macrophages differentially produce specific resolvin or leukotriene signals that depend on bacterial pathogenicity. *Nat Commun*. 2018;9(1):59.
- Chiurchiù V, Leuti A, Cencioni MT et al. Modulation of monocytes by bioactive lipid anandamide in multiple sclerosis involves distinct Toll-like receptors. *Pharmacol Res*. 2016;113(Pt A):313-319.
- Hong S, Tian H, Lu Y et al. Neuroprotectin/protectin D1: endogenous biosynthesis and actions on diabetic macrophages in promoting wound healing and innervation impaired by diabetes. *Am J Physiol Cell Physiol*. 2014;307(11):C1058-C1067.
- Bonnans C, Vachier I, Chavis C, Godard P, Bousquet J, Chanez P. Lipoxins are potential endogenous antiinflammatory mediators in asthma. *Am J Respir Crit Care Med*. 2002;165(11):1531-1535.
- Weksler B, Romero IA, Couraud PO. The hCMEC/D3 cell line as a model of the human blood brain barrier. *Fluids Barriers CNS*. 2013;10(1):16.
- Mizee MR et al. Astrocyte-derived retinoic acid: a novel regulator of blood-brain barrier function in multiple sclerosis. *Acta Neuropathol*. 2014;128(5):691-703.
- Lopez-Ramirez MA, Reijerkerk A, de Vries HE, Romero IA. Regulation of brain endothelial barrier function by microRNAs in health and neuroinflammation. *FASEB J*. 2016;30(8):2662-2672.
- Vogel DY et al. GM-CSF promotes migration of human monocytes across the blood brain barrier. *Eur J Immunol*. 2015; 45(6):1808-1819.
- Kooij G, Mizee MR, van Horsen J et al. Adenosine triphosphate-binding cassette transporters mediate chemokine (C-C motif) ligand 2 secretion from reactive astrocytes: relevance to multiple sclerosis pathogenesis. *Brain*. 2011;134(Pt 2):555-570.
- Lublin FD, Reingold FC, Cohen JA et al. Defining the clinical course of multiple sclerosis. 2014;37(1):1-103.

- rosis: the 2013 revisions. *Neurology*. 2014;83(3):278-286.
26. Reich DS, Lucchinetti CF, Calabresi PA. Multiple Sclerosis. *N Engl J Med*. 2018; 378(2):169-180.
 27. Chiurciu V. Novel targets in multiple sclerosis: to oxidative stress and beyond. *Curr Top Med Chem*. 2014;14(22):2590-2599.
 28. Prüss H, Rosche B, Sullivan AB *et al*. Proresolution lipid mediators in multiple sclerosis - differential, disease severity dependent synthesis - a clinical pilot trial. *PLoS One*. 2013;8(2):e55859.
 29. Hsiao H-M, Thatcher TH, Colas RA, Serhan CN, Phipps RP, Sime PJ. Resolvin D1 reduces emphysema and chronic inflammation. *Am J Pathol*. 2015;185:3189-31201.
 30. Hellmann J, Tang Y, Kosuri M, Bhatnagar A, Spite M. Resolvin D1 decreases adipose tissue macrophage accumulation and improves insulin sensitivity in obese-diabetic mice. *FASEB J* 2011;25:2399-23407.
 31. Clària J, Dallì J, Yacoubian S, Gao F, Serhan CN. Resolvin D1 and resolvin D2 govern local inflammatory tone in obese fat. *J Immunol*. 2012;189:2597-25605.
 32. Bento AF, Claudino RF, Dutra RC, Marcon R, Calixto JB. Omega-3 fatty acid-derived mediators 17(R)-hydroxy docosahexaenoic acid, aspirin-triggered resolvin D1 and resolvin D2 prevent experimental colitis in mice. *J Immunol*. 2011;187:1957-1969.
 33. Schwanke RC, Marcon R, Bento AF, Calixto JB. EPA- and DHA-derived resolvins' actions in inflammatory bowel disease. *Eur J Pharmacol*. 2016;785:156-164.
 34. Perretti M, Norling LV. Actions of SPM in regulating host responses in arthritis. *Mol Aspects Med*. 2017;58:57-64.
 35. Fredman G, Hellmann J, Proto JD, Kuriakose G, Colas RA, Dorweiler B, *et al*. An imbalance between specialized pro-resolving lipid mediators and pro-inflammatory leukotrienes promotes instability of atherosclerotic plaques. *Nat Commun*. 2016;7:12859.
 36. Wang X, Zhu M, Hjorth E, Cortés-Toro V, Eyjolfsson H, Graff C, *et al*. Resolution of inflammation is altered in Alzheimer's disease. *Alzheimers Dement*. 2015;11:40.e-50.e.
 37. Zhu M, Wang X, Hjorth E, Colas RA, Schroeder L, Granholm A-C, *et al*. Pro-resolving lipid mediators improve neuronal survival and increase A β phagocytosis. *Mol Neurobiol*. 2016;53:2733-2749.
 38. Fiala M, Halder RC, Sagong B, Ross O, Sayre J, Porter V, *et al*. -3 supplementation increases amyloid- β phagocytosis and resolvin D1 in patients with minor cognitive impairment. *FASEB J*. 2015;29:2681-2689.
 39. Holman RT, Johnson SB, Kokmen E. Deficiencies of polyunsaturated fatty acids and replacement by nonessential fatty acids in plasma lipids in multiple sclerosis. *Proc Natl Acad Sci U S A*. 1989;86(12):4720-4724.
 40. Poisson LM, Suhail H, Singh J *et al*. Untargeted plasma metabolomics identifies endogenous Metabolite with Drug-like properties in chronic animal model of multiple sclerosis. *J Biol Chem*. 2015; 290(52):30697-30712.
 41. Jelinek GA, Hadgkiss EJ, Weiland TJ, Pereira NG, Marck CH, van der Meer DM. Association of fish consumption and Ω 3 supplementation with quality of life, disability and disease activity in an international cohort of people with multiple sclerosis. *Int J Neurosci*. 2013;123(11):792-800.
 42. Weinstock-Guttman B, Baier M, Park Y *et al*. Low fat dietary intervention with omega-3 fatty acid supplementation in multiple sclerosis patients. *Prostaglandins Leukot Essent Fatty Acids*. 2005;73(5):397-404.
 43. Reder AT, Genc K, Byskosh PV, Porrini AM. Monocyte activation in multiple sclerosis. *Mult Scler* 1998; 4: 162-168.
 44. Chuluundorj D, Harding SA, Abernethy D, La Flamme AC. Expansion and preferential activation of the CD14(+)/CD16(+) monocyte subset during multiple sclerosis. *Immunol Cell Biol*. 2014;92(6):509-517.
 45. Singh A *et al*. Lipoxin A4, a 5-lipoxygenase pathway metabolite, modulates immune response during acute respiratory tularemia. *J Leukoc Biol*. 2017;101(2):531-542.
 46. Gu Z, Lamont GJ, Lamont RJ, Uriarte SM, Wang H, Scott DA. Resolvin D1, resolvin D2 and maresin 1 activate the GSK3 anti-inflammatory axis in TLR4-engaged human monocytes. *Innate Immun*. 2016;22(3):186-195.
 47. Koltsida O, Karamnov S, Pырillou K *et al*. Toll-like receptor 7 stimulates production of specialized pro-resolving lipid mediators and promotes resolution of airway inflammation. *EMBO Mol Med*. 2013;5(5):762-775.
 48. Ortiz GG, Pacheco-Moisés FP, Macías-Islas M \acute{A} *et al*. Role of the blood-brain barrier in multiple sclerosis. *Arch Med Res*. 2014; 45(8):687-697.
 49. Kadl A, Leitinger N. The role of endothelial cells in the resolution of acute inflammation. *Antioxid Redox Signal*. 2005;7(11-12):1744-1754.
 50. Chattopadhyay R, Raghavan S, Rao GN. Resolvin D1 via prevention of ROS-mediated SHP2 inactivation protects endothelial adherens junction integrity and barrier function. *Redox Biol*. 2017;12:438-455.
 51. Zhang X, Wang Y, Gui P, *et al*. Resolvin D1 reverts lipopolysaccharide-induced TJ proteins disruption and the increase of cellular permeability by regulating IB signaling in human vascular endothelial cells. *Oxid Med Cell Longev*. 2013;2013:185715.
 52. Pang H, Huang YP, Liu ZJ, *et al*. Effect of lipoxin A4 on lipopolysaccharide-induced endothelial hyperpermeability. *Scientific World Journal*. 2011;11:1056-1067.
 53. Jones CN, Dallì J, Dimisko L, Wong E, Serhan CN, Irimia D. Microfluidic chambers for monitoring leukocyte trafficking and humanized nano-proresolving medicines interactions. *Proc Natl Acad Sci U S A*. 2012;109(50):20560-20565.
 54. Akagi D, Chen M, Toy R, Chatterjee A, Conte MS. Systemic delivery of proresolving lipid mediators resolvin D2 and maresin 1 attenuates intimal hyperplasia in mice. *FASEB J*. 2015;29(6):2504-2513.
 55. Baker N, O'Meara SJ, Scannell M, Madema P, Godson C. Lipoxin A4: anti-inflammatory and anti-angiogenic impact on endothelial cells. *J Immunol*. 2009;182(6):3819-26.
 56. Chinthamani S, Odusanwo O, Mondal N, Nelson J, Neelamegham S, Baker OJ. Lipoxin A4 inhibits immune cell binding to salivary epithelium and vascular endothelium. *Am J Physiol Cell Physiol*. 2012; 302(7):C968-C978.
 57. Merched AJ, Ko K, Gotlinger KH, Serhan CN, Chan L. Atherosclerosis: evidence for impairment of resolution of vascular inflammation governed by specific lipid mediators. *FASEB J*. 2008;22(10):3595-606.

Transferrin receptor 1-mediated iron uptake plays an essential role in hematopoiesis

Shufen Wang,^{1,2*} Xuyan He,^{1*} Qian Wu,¹ Li Jiang,¹ Liyun Chen,¹ Yingying Yu,¹ Pan Zhang,¹ Xin Huang,³ Jia Wang,³ Zhenyu Ju,⁴ Junxia Min¹ and Fudi Wang^{1,2,3}

¹The First Affiliated Hospital, School of Public Health, Institute of Translational Medicine, Zhenjiang Provincial Key Laboratory of Pancreatic Disease, Zhejiang University School of Medicine, Hangzhou; ²Beijing Advanced Innovation Center for Food Nutrition and Human Health, China Agricultural University, Beijing; ³Department of Nutrition, Precision Nutrition Innovation Center, School of Public Health, Zhengzhou University, Zhengzhou and ⁴Key Laboratory of Regenerative Medicine of Ministry of Education, Institute of Aging and Regenerative Medicine, Jinan University, Guangzhou, China

*SW and XH contributed equally as co-first authors.



Haematologica 2020
Volume 105(8):2071-2082

ABSTRACT

Transferrin receptor 1 (Tfr1) mediates the endocytosis of diferric transferrin in order to transport iron, and Tfr1 has been suggested to play an important role in hematopoiesis. To study the role of Tfr1 in hematopoiesis, we generated hematopoietic stem cell (HSC) specific Tfr1 knockout mice. We found that *Tfr1* conditional knockout mice reached full term but died within one week of birth. Further analyses revealed that *Tfr1*-deficient HSC had impaired development of all hematopoietic progenitors except thrombocytes and B lymphocytes. In addition, *Tfr1*-deficient cells had cellular iron deficiency, which blocked the proliferation and differentiation of hematopoietic precursor cells, attenuated the commitment of hematopoietic lineages, and reduced the regeneration potential of HSC. Notably, hemin rescued the colony-forming capacity of *Tfr1*-deficient HSC, whereas expressing a mutant Tfr1 that lacks the protein's iron-transporting capacity failed to rescue hematopoiesis. These findings provide direct evidence that Tfr1 is essential for hematopoiesis through binding diferric transferrin to supply iron to cells.

Introduction

Hematopoietic stem cells (HSC) are essential for the continuous replenishment of the hematopoietic system throughout the lifespan of an organism.¹⁻⁴ HSC regulate development^{5,6} and undergo important changes during aging.⁷ However, precisely how HSC orchestrate the delicate balance between proliferation, differentiation, and self-renewal remains one of the major topics of study in the field of stem cell biology.

Iron is essential for a variety of fundamental metabolic processes and is incorporated into many proteins in the form of cofactors such as heme and iron-sulfur clusters. In adults, a substantial proportion of iron is present in the liver and the hematopoietic system. Excess iron in the liver is clinically relevant, as individuals with systemic iron overload often develop liver cirrhosis and hepatocellular carcinoma.⁸ On the other hand, hematopoiesis is sensitive to iron deficiency, and insufficient iron leads to iron deficiency anemia.⁹ Although iron serves as an essential cofactor for enzymes involved in cell proliferation and differentiation, the precise mechanism that regulates iron homeostasis in HSC is unknown.

Transferrin receptor 1 (Tfr1) facilitates the uptake of iron at the cell surface by internalizing diferric transferrin.¹⁰ Tfr1 is ubiquitously expressed in mammalian tissues and has been called the “cellular iron gate”.¹¹ Tfr1 is essential for erythropoiesis, a process that consumes the majority of circulating iron.¹² Accordingly, mice that globally lack Tfr1 (*i.e.* homozygous *Tfr1* knockout mice) are embryonic lethal; moreover, although heterozygous *Tfr1* knockout mice survive to adulthood they have microcytic hypochromic erythrocytes, consistent with Tfr1's essential role in erythropoiesis.¹³ In addition, Tfr1 plays an important role in the develop-

Correspondence:

FUDI WANG
fwang@zju.edu.cn

JUNXIA MIN
junxiamin@zju.edu.cn

Received: April 17, 2019.

Accepted: October 4, 2019.

Pre-published: October 10, 2019.

doi:10.3324/haematol.2019.224899

Check the online version for the most updated information on this article, online supplements, and information on authorship & disclosures: www.haematologica.org/content/105/8/2071

©2020 Ferrata Storti Foundation

Material published in *Haematologica* is covered by copyright. All rights are reserved to the Ferrata Storti Foundation. Use of published material is allowed under the following terms and conditions:

<https://creativecommons.org/licenses/by-nc/4.0/legalcode>. Copies of published material are allowed for personal or internal use. Sharing published material for non-commercial purposes is subject to the following conditions: <https://creativecommons.org/licenses/by-nc/4.0/legalcode>, sect. 3. Reproducing and sharing published material for commercial purposes is not allowed without permission in writing from the publisher.



ment and proliferation of lymphocytes.¹⁴ A recent study found that patients who carry a homozygous mutation in the *TFR1* gene have reduced T-cell and B-cell proliferation, as well as reduced antibody production.¹⁵

Several key questions remain, however, regarding the function of Tfr1 in hematopoiesis. First, because previous studies focused on mature hematopoietic lineages, whether Tfr1 plays a role in upstream of hematopoiesis (for example, in stem cells, progenitors, and precursor cells) is unknown. Second, Tfr1 plays a role in signal transduction pathways other than iron uptake and is required for maintaining intestinal epithelial homeostasis,¹⁶ thus raising the question of whether the function of Tfr1 in hematopoiesis is independent of its iron-uptake function. Finally, because *Tfr1* knockout embryos die at embryonic stage E10.5-E12.5, the embryo's iron demands at later stages of development have not been investigated.

To address these key questions, we generated mice that lack *Tfr1* expression selectively in HSC and used this model to study the role of Tfr1 in hematopoiesis. We found that loss of Tfr1 in HSC does not affect the production of hematopoietic stem/progenitor cells (HSPC) in the fetal liver (FL) but markedly impairs the expansion of functional HSC in the bone marrow (BM). Mechanistically, iron uptake rather than signal transduction appears to be the key function of Tfr1 in hematopoiesis, and iron uptake mediated by Tfr1 is required for the differentiation of HSPC, particularly in mid-gestation.

Methods

All animal experiments were approved by the Institutional Animal Care and Use Committee of Zhejiang University. *Tfr1^{fl/fl}* mice on the C57BL/6J background were obtained from Dr. Ying Shen.¹⁷ To generate HSC-specific Tfr1 knockout mice (*Tfr1^{fl/fl};Vav-Cre*, referred to hereafter as cKO mice), we crossed female *Tfr1^{fl/fl}* mice with male *Tfr1^{fl/wt};Vav-Cre* transgenic mice; the *Vav-Cre* line we used was B6.Cg-*Commd10^{Tg(Vav1-cre)A2Kio}*, the *Vav-Cre* transgene is expressed mainly in hematopoietic cells.¹⁸ Hematological parameters, blood smears, embryo dissection and single-cell isolation, flow cytometric analysis, evaluation of intracellular iron status, iron parameters, colony formation assays, and transplantation assays are described in the *Online Supplementary Materials and Methods*. Except where indicated otherwise, all summary data are presented as the mean \pm standard deviation. The Student's *t*-test was used to compare two groups, multiple groups were subjected to analysis of variance (ANOVA) with Bonferroni *post hoc* test comparison, and the log-rank (Mantel-Cox) test for survival curve analysis (GraphPad version 7). *P*-values <0.05 were considered statistically significant.

Results

Tfr1 is expressed at higher levels in hematopoietic progenitor cells than in HSC and mature cell lineages

First, we measured Tfr1 expression in mouse FL HSPC and the different stages of erythroid differentiation using multiparametric flow cytometry and the gating strategies shown in Figure 1A-B. As shown in Figure 1C-D, Tfr1 expression was extremely low in Lin⁺Sca1⁺cKit⁺ subsets, virtually undetectable on the surface of long-term HSC, short-term HSC, multipotent progenitors, and common

myeloid progenitors. In contrast, Tfr1 expression was relatively high in granulocyte/monocyte progenitors and common lymphoid progenitors, and was highest in megakaryocyte/erythrocyte progenitors. In erythroid lineage, Tfr1 expression was high in pro-erythroblast, and gradually decreased with the differentiation of erythroblast. These findings at the protein level were generally consistent with RNA sequencing data (*Online Supplementary Figure S1*) that we extracted from previous studies.^{19,20} In addition, *Tfr1* expression was higher in progenitors/precursors (early T-cell progenitors, progenitor B cells, and granulocyte monocyte progenitors) compared to their mature counterparts (T cells, B cells, NK cells, granulocytes, and monocytes) (*Online Supplementary Figure S1*), suggesting that Tfr1 may play a more important role in the progenitor/precursor stages than in stem cells.

HSC-specific loss of Tfr1 causes early postnatal lethality

To examine further the role of Tfr1 in hematopoiesis, we generated HSC-specific *Tfr1* cKO mice. The cKO offspring were born at the expected Mendelian ratio but smaller and paler than control (*Tfr1^{fl/fl}*) littermates (Figure 2A). Importantly, although cKO pups were born at the expected Mendelian ratio, homozygous cKO pups failed to thrive and died by postnatal day 7 (P7), whereas both heterozygous and control littermates grew normally (Figure 2B-C). We confirmed the knockout efficiency in both mRNA and protein level. *Tfr1* mRNA was virtually non-detectable in the BM of cKO mice (Figure 2D) and Tfr1 (CD71) expression in cKO HSPC significantly decreased compared to control littermates by flow cytometry analysis (Figure 2E-F).

Tfr1-deficient HSC have multiple lineage defects in hematopoiesis

A possible explanation for the early postnatal mortality and paleness of the cKO mice is that the *Tfr1*-deficient HSC may perturb erythropoiesis. To test this possibility, we examined various hematopoietic organs. In peripheral blood, cKO mice had significantly fewer red blood cells, fragmented and irregularly shaped (*Online Supplementary Figure S2*), as well as reduced erythrocyte mean corpuscular volume (MCV), mean corpuscular hemoglobin (MCH), mean corpuscular hemoglobin concentration (MCHC), and hemoglobin concentration (*Online Supplementary Table S1*) compared to control, indicating that cKO mice had microcytic hypochromic anemia. In addition, cKO pups had reduced numbers of white blood cells and reticulocytes, and increased numbers of platelets (*Online Supplementary Table S1*).

To examine the role of Tfr1 in the development of proerythroblasts into mature red blood cells, we performed flow cytometry using the markers Ter119 and CD44.^{21,22} The number of early basophilic erythroblasts (R2), polychromatophilic erythroblasts (R3), and orthochromatophilic erythroblasts (R4) decreased significantly in cKO mice compared to controls (Figure 3A). In addition, orthochromatophilic erythroblasts (R4) and mature erythrocytes (R5) decreased significantly in the spleen of cKO mice (*Online Supplementary Figure S3A*). These data indicate that erythrocyte development is severely blocked in the early stages in the absence of Tfr1. Moreover, cKO mice had fewer Mac1⁺Gr1⁺ (mature macrophage/granulocyte) cells in the spleen and liver

compared to control littermates (Figure 3B); in contrast, the number of B220⁺ cells in the liver and spleen was similar between cKO and control mice (Figure 3C). We also found significantly fewer cells in the thymus of cKO mice (Figure 3D), particularly CD4⁺CD8⁺ T cells (Figure 3E). Taken together, these results indicate that Tfr1 is required for the generation of T cells, macrophages, granulocytes, and erythrocytes, but is not required for the production of B cells or platelets.

Loss of *Tfr1* impairs hematopoiesis in the BM

During late embryogenesis, HSC populate the BM, providing stem cells and progenitor cells for all blood cell lin-

eages; thus, during postnatal development the BM becomes the primary site of hematopoiesis.²³ Hematoxylin and eosin staining revealed significantly fewer cells in cKO BM compared to control littermates (Figure 3F-G). Specifically, hematopoietic stem cells (LSK, Lin⁻Sca1⁺cKit⁺) and hematopoietic progenitor cells (HPC, Lin⁻Sca1⁻cKit⁺) were extremely rare in the BM of cKO pups (Figure 3H and *Online Supplementary Figure S3B*). The reduced number of LSK cells in the BM of cKO mice was accompanied by a significant increase of apoptotic cells (Figure 3I). Thus, Tfr1 plays a critical role in hematopoiesis in the BM and is required for the survival of HSC in the BM of postnatal mice.

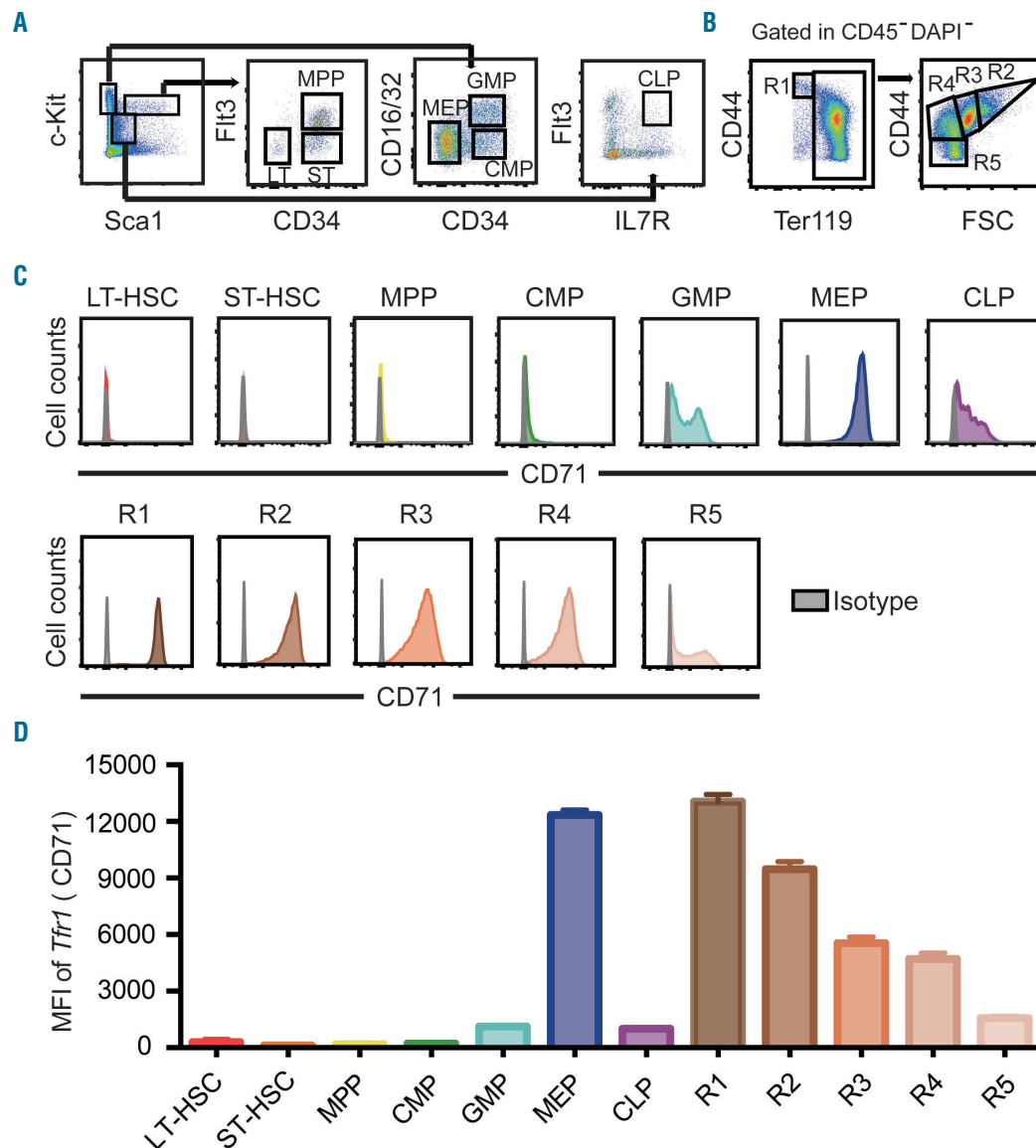


Figure 1. Tfr1 expression in hematopoietic stem/progenitor cells. (A) Representative gating strategy for analyzing long-term hematopoietic stem cells (HSC) (LT-HSC, Lin⁻cKit⁺Sca1⁺CD34⁻Flt3⁻), short-term HSC (ST-HSC, Lin⁻cKit⁺Sca1⁺CD34⁺Flt3⁻), multipotent progenitor (MPP, Lin⁻cKit⁺Sca1⁺CD34⁺Flt3⁺) cells, common myeloid progenitor (CMP, Lin⁻cKit⁺Sca1⁻CD34⁺CD16/32^{int}) cells, granulocyte-macrophage progenitor (GMP, Lin⁻cKit⁺Sca1⁻CD34⁺CD16/32^{int}) cells, megakaryocyte-erythroid progenitor (MEP, Lin⁻cKit⁺Sca1⁻CD34⁻CD16/32^{int}) cells, and common lymphoid progenitor (CLP, Lin⁻cKit^{int}Sca1^{int}IL-7R⁺Flt3⁺) cells. (B) Erythrocytes gating strategy was used based on the expression levels of Ter119 and CD44: R1, proerythroblasts (Ter119⁺CD44^{int}); R2, early basophilic erythroblasts (CD44^{int}FSC^{int}); R3, polychromatophilic erythroblasts (CD44^{int}FSC^{med}); R4, orthochromatophilic erythroblasts (CD44^{med}FSC^{med}); and R5, mature erythrocytes (CD44⁺FSC⁺). (C) Flow cytometric analysis of Tfr1 expression in HSPC and erythroblasts in fetal liver of E16.5 mouse embryos. Grey histogram: isotype control (Rat IgG2a, κ-PE). (D) Quantification of the flow cytometry data in C, showing the mean fluorescence intensity (MFI) of Tfr1 in the indicated hematopoietic stem/progenitor cells (HSPC) and erythroblasts.

Loss of *Tfr1* in HSC causes impaired development of various cell lineages in the FL

Our finding that cKO pup were anemic at birth (Figure 4A) suggests that hematopoiesis is impaired in prenatal development. Moreover, definitive hematopoiesis involves the colonization of the FL, thymus, spleen, and ultimately the BM.^{5,6} Therefore, we harvested FL cells from cKO and control embryos at E14.5, E16.5, and E18.5 and performed hematopoietic phenotyping using multi-color flow cytometry. Our analysis revealed no difference between cKO and control embryos at E14.5. However, during later stages of development, the cKO embryos became progressively smaller and paler than control siblings (Figure 4B). The most prominent difference was a significant decrease in lineage-positive (Lin⁺) cells beginning at E16.5 and becoming much more pronounced by E18.5 (Figure 4C-D), indicating that some cell lineages were severely impaired.

To examine this effect in further detail, we measured the development of erythroid, myeloid, and lymphoid cells in FL. With respect to erythropoiesis, we found no effect at E14.5. In contrast, R1 and R3 increased at both E16.5 and

E18.5, and R4 and R5 significantly reduced at E18.5 (Figure 4E); thus, progressive erythropenia in cKO embryos occurs after E14.5. With respect to myelopoiesis and lymphogenesis, we found reduced numbers of both Mac1⁺Gr1⁺ granulocytes and CD3⁺ T cells in the cKO embryos beginning at E14.5, whereas the number of CD19⁺ B cells was similar between cKO and control embryos (Figure 4F). These results indicate that the loss of *Tfr1* in HSC causes impaired development of myeloid cells, erythrocytes, and T cells but spares B-cell development in the FL, consistent with our results obtained in neonatal mice.

Given the inability of cKO mice to produce several mature cell lineages, we examined HSPC in the FL of cKO and control embryos at E16.5, the gestational stage in which Lin⁺ cells dramatically decreased. Interestingly, we found no difference between cKO and control embryos, with the exception of a slight albeit significant increase in granulocyte/macrophage progenitors (Figure 4G). These data suggest that in the FL, *Tfr1* preferentially functions at the progenitor/precursor stage rather than the HSC stage, consistent with our findings shown in Figure 1 and *Online Supplementary Figure S1*.

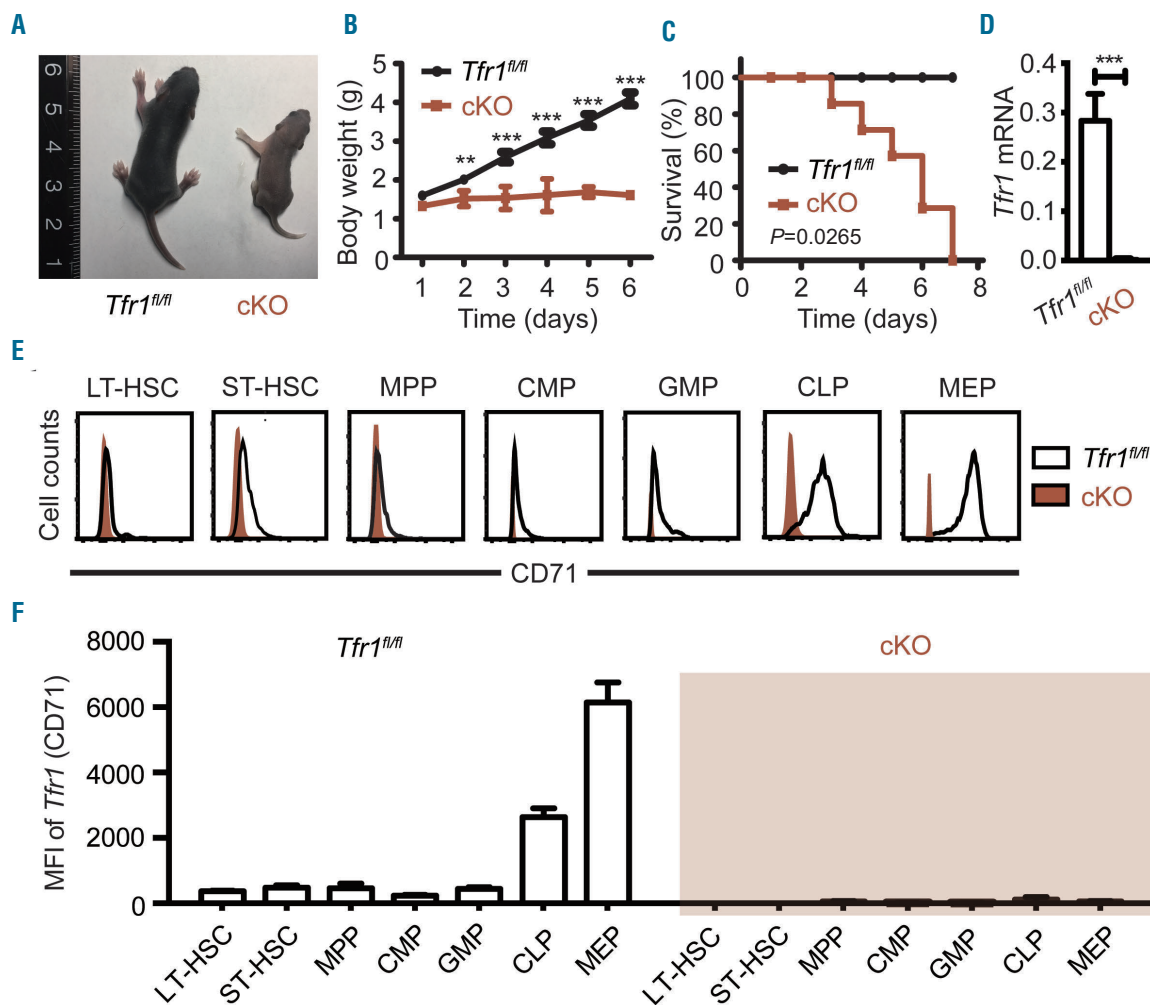


Figure 2. Loss of *Tfr1* in hematopoietic stem cells results in early postnatal lethality. (A) Representative images of a control (*Tfr1^{fl/fl}*) and a *Tfr1* conditional knockout (cKO) mouse at P6. (B) Body weight of control and cKO mice at the indicated days after birth (n=4 for each group). (C) Kaplan–Meier survival curve for control and cKO mice (n=7 for each group). (D) *Tfr1* mRNA was measured in bone marrow cells obtained from control and cKO mice (n=3 for each group). (E) Flow cytometric analysis of *Tfr1* expression in hematopoietic stem/progenitor cells (HSPC) in fetal liver of E14.5 mouse embryos. Open histogram: *Tfr1^{fl/fl}* control; red histogram: cKO. (F) Quantification of the flow cytometry data in (D). The mean fluorescence intensity (MFI) of *Tfr1* in the indicated HSPC. ***P*<0.01; ****P*<0.001.

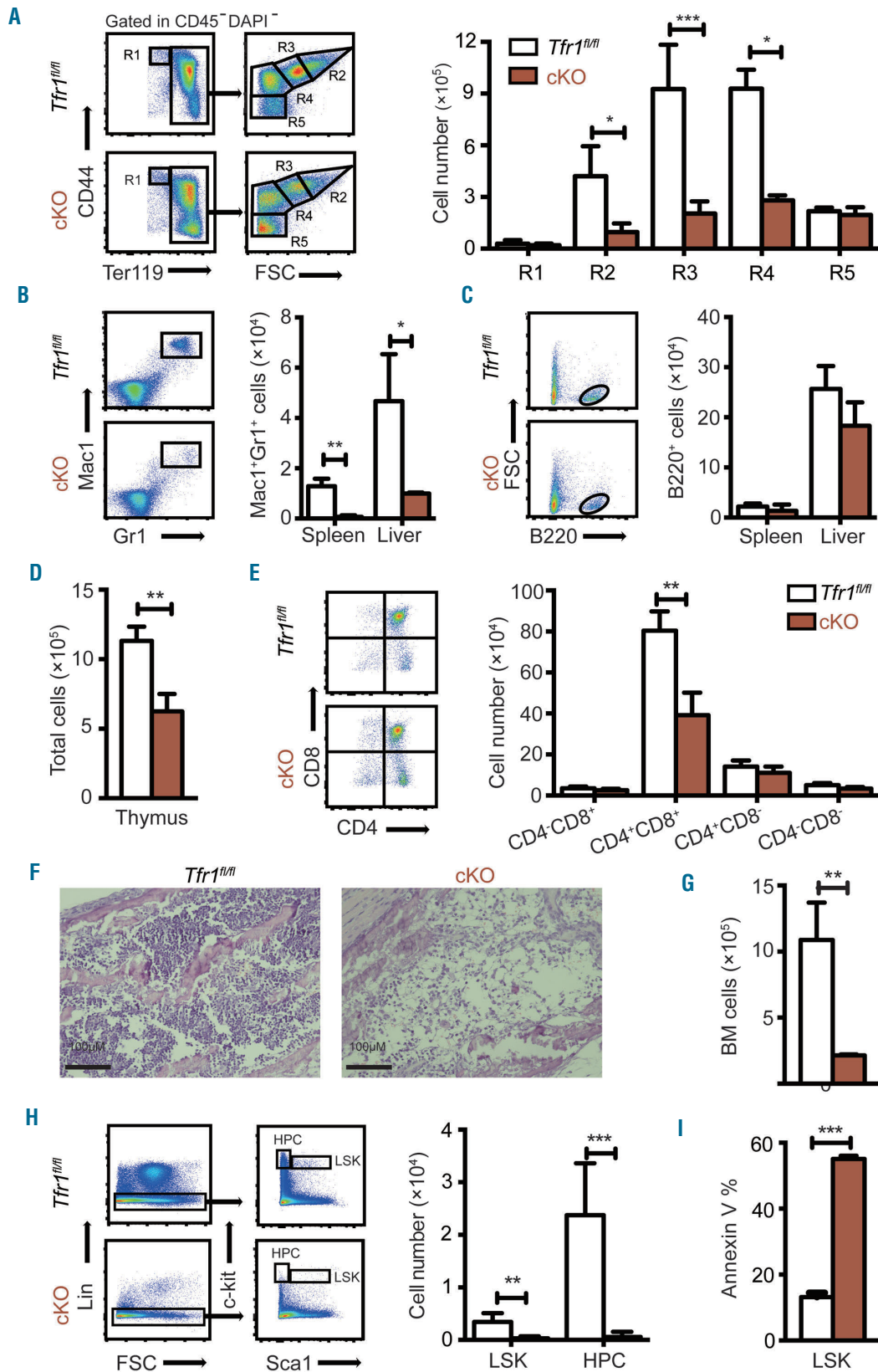


Figure 3. Neonatal *Tfr1* conditional knockout mice have defects in multiple cell lineages. (A) Gating strategy (left panel) and the absolute number of erythrocytes (right panel) at the indicated differentiation stages measured in the bone marrow of control and *Tfr1* knockout (cKO) mice at P3 (n=4 per group). (B, C) Gating strategy (left panel) and absolute numbers (right panel) of Mac1⁺Gr1⁺ myeloid cells (B) and B220⁺ B cells (C) in the spleen and liver of control and cKO mice (n=4 for each group). (D) Total number of cells in the thymus. (E) Cells were gated according to CD4 and CD8 expression (left panel), and the absolute cell numbers are shown at the right. (F) H&E-stained bone marrow sections obtained from a control and cKO mouse at P3. (G) Total number of cells in the bone marrow of control and cKO mice at P3 (n=4 for each group). (H) Absolute numbers of LSK (Lin-cKit⁺Sca1⁺) and hematopoietic progenitor cells (HPC) (Lin-cKit⁺Sca1⁻) cells in the bone marrow of control and cKO mice at P3 (n = 4 for each group). (I) Percentage of Annexin V-positive LSK cells in control and cKO mice (n=4 for each group). **P*<0.05; ***P*<0.01; ****P*<0.001.

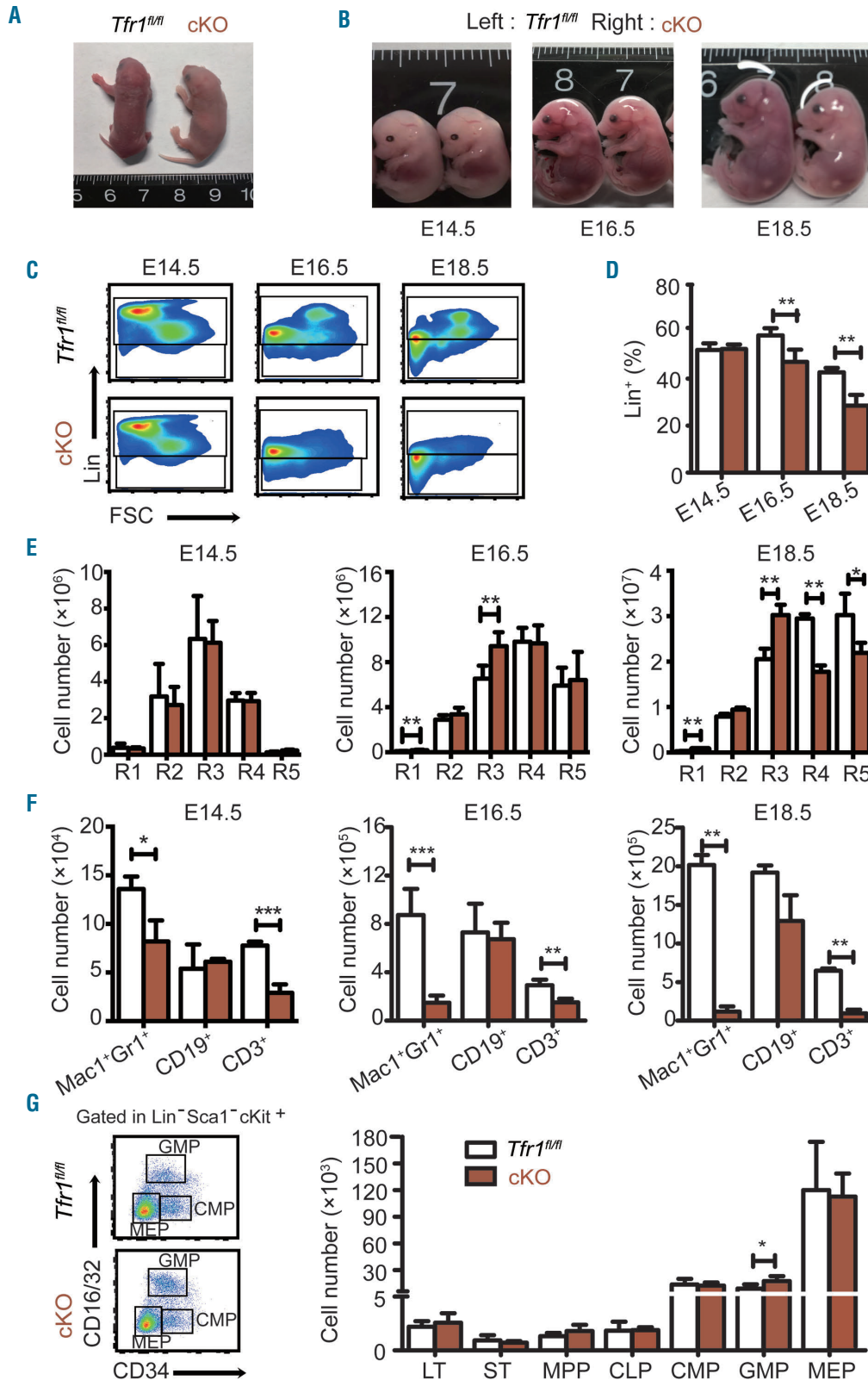


Figure 4. Loss of *Tfr1* in hematopoietic stem cells causes progressively impaired cellular maturation in fetal liver. (A) Representative images of a control and *Tfr1* knockout (cKO) embryo at P1. (B) Representative images of control and cKO embryos at E14.5, E16.5, and E18.5. (C) Representative flow cytometric profiles of Lin⁺ and Lin⁻ cell populations in the liver of control and cKO embryos at E14.5, E16.5, and E18.5. (D) Percentage of Lin⁺ cells in the liver of control and cKO embryos at E14.5, E16.5, and E18.5 (n=5 per group). (E) Absolute numbers of the indicated erythrocyte development stages in the liver of control and cKO embryos at E14.5, E16.5, and E18.5 (n=5 per group). (F) Absolute number of myeloid cells (Mac1⁺Gr1⁺), B cells (CD19⁺), and T cells (CD3⁺) in the liver of control and cKO embryos at E14.5, E16.5, and E18.5 (n=5 per group). (G) Hematopoietic progenitor cells (HPC) were gated for fetal liver cells in control and cKO embryos using flow cytometry (left panel). The bar graph (right panel) shows the absolute numbers of LT, ST, MPP, CLP, CMP, GMP, and MEP cells in control and cKO fetal liver cells at E16.5 (n = 5 for each group); note the break in the y-axis. LT: long-term HSC; ST: short-term HSC; MPP: multipotent progenitor cells; CLP: common lymphoid progenitor cells; CMP: common myeloid progenitor cells; GMP: granulocyte/monocyte progenitor cells; MEP: megakaryocyte/erythrocyte progenitor cells. *P<0.05; **P<0.01; ***P<0.001.

Loss of *Tfr1* in HSC causes intracellular iron decrease in hematopoietic cells in postnatal mice

Given that the principal function of Tfr1 is iron uptake through the cell membrane, we reasoned that the loss of Tfr1 might cause cellular iron deficiency, thereby affecting systemic iron levels. Therefore we evaluated intracellular iron concentration in hematopoietic cells by loading BM derived HSPC with the iron-sensitive fluorophore calcein-AM, which is quenched upon binding ferrous iron (Fe^{2+}).²⁴ Intracellular iron was significantly lower in cKO erythrocytes compared to control cells at all five stages (Figure 5A-B). In addition, intracellular iron was lower in cKO Lin⁺ mature cells (Figure 5C), as well as LSK and HPC cells (Figure 5D), compared to their respective controls.

Next, we measured systematic iron levels and found that cKO pups have higher levels of serum iron (Figure 5E), transferrin saturation (Figure 5F), and serum hepcidin (Figure 5G). Considering smaller sizes of the livers and spleens in cKO pups compared to the controls (*Online Supplementary Figure S4A-B*), we found that liver non-heme iron was significantly higher than control measured either in $\mu\text{g/g}$ wet weight or absolute amount of iron (Figure 5H-I). In contrast, splenic non-heme iron levels of cKO in $\mu\text{g/g}$ wet weight didn't change (Figure 5J), whereas the absolute amount of iron decreased (Figure 5K). In the muscle of cKO pups, non-heme iron ($\mu\text{g/g}$ wet weight) increased (Figure 5L). In addition, whole body non-heme iron levels ($\mu\text{g/g}$ wet weight) in cKO pups were significantly increased (Figure 5M), whereas the absolute amount of body iron (μg) remained unchanged (Figure 5N). Taken together, these data suggest that hematopoietic *Tfr1* deficiency significantly impaired iron uptake of hematopoietic cells, in turn led to iron redistribution to other organs (*e.g.* serum, liver and muscle).

Loss of *Tfr1* in HSC affects iron homeostasis in mature cells but not HSPC in the FL

Next, we investigated whether Tfr1 affects iron homeostasis differently between prenatal and postnatal stages of development. Intracellular iron levels were lower in cKO Lin⁺ cells at E16.5 (Figure 5O), which is consistent with decreased numbers of mature cells. Interestingly, intracellular iron levels and ferritin protein levels (*Online Supplementary Figure S5A*) in both LSK and HPC cells were similar between cKO and control embryos at E16.5 (Figure 5P), indicating that loss of Tfr1 does not affect intracellular iron in HSPC during prenatal development. Meanwhile, we found no difference between cKO and control HPC cells with respect to the mRNA levels of various membrane iron transporters and *Alas2*, catalyzing the rate-limiting step of heme biosynthesis in erythroid cells (*Online Supplementary Figure S5B*). Therefore, we hypothesized that hematopoietic Tfr1 is required for differentiation into lineages in which iron plays an essential role. In addition, we quantified expression levels of critical transcription factors required for cell fate determination of HSC.¹ We found significant decreases of a subset of transcription factors involved in the development and differentiation of HPC, including *Gli1*, *C/EBP α* , *Fli*, *PU.1*, *Gata2*, *Notch1*, and *Gata3* (*Online Supplementary Figure S5C*).

Loss of *Tfr1* in HSC impairs the regeneration capacity of HSPC

The maintenance and survival of HSPC requires an interplay between these cells and their niche within the

BM.²⁵ Therefore, we speculated whether loss of Tfr1 in cKO HSPC disrupts this niche, leading to a feedback loop that impairs hematopoiesis. To test this possibility, we performed a transplantation assay to measure the regenerative capacity of HSPC in recipient BM. We used FL cells obtained from E14.5 embryos, as cells at this stage were only mildly affected in the cKO mice.

To determine their short-term regenerative capacity, FL cells were isolated from cKO and control mice expressing the alloantigen CD45.2 and injected into the tail vein in lethally irradiated CD45.1 recipient mice. We found that recipient mice that received control cells had 100% survival, whereas mice that received cKO cells all died within 12 days of transplantation (Figure 6A). Next, we performed competitive BM transplants in order to assess the long-term regenerative capacity and found that recipient mice that received 50% cKO cells and 50% CD45.1 competitor cells had virtually no donor-derived cKO cells in their peripheral blood by four weeks post-transplantation (Figure 6B). In addition, virtually no contribution of cKO HSPC or committed cell lineages in the recipient mice was measured 16 weeks after transplantation (Figure 6C-E). Finally, we found virtually no contribution of cKO HSPC to myeloid cells, B cells in the spleen, or T cells in the thymus of the recipient mice (Figure 6F). These results indicate that Tfr1 is required for both the short-term and long-term regeneration of FL cells.

Upon transplantation, HSPC migrate to the recipient's BM, where they home to their proper niche. When we analyzed BM cells in lethally irradiated CD45.1 recipient mice 40 hours after transplanted with CD45.2 cKO or control FL cells, no difference was found (Figure 6G), indicating that the homing process is not impaired in cKO FL cells. Taken together, these results suggest that the reduced regenerative capacity in Tfr1-deficient HSPC is due to a cell-autonomous mechanism.

Hemin treatment rescues the proliferation and differentiation defects in Tfr1-deficient HSPC

The results described above indicate that the composition of cKO HSPC is normal in the early stages of embryonic development. Thus, other modes of iron delivery might be presented in order to support the demand of FL HSPC for iron. To examine whether an alternative modes of iron deliver is able to bypass the loss of Tfr1 in cKO HSPC, we performed various *in vitro* rescue experiments using a methylcellulose colony formation assay with FL cells obtained from E14.5 embryos. cKit⁺ cells were sorted and then cultured in a methylcellulose medium containing IL-6, IL-3, stem cell factor, and erythropoietin. We found that colony-forming units (CFU) were formed by control cells, whereas cKO cells failed to develop any of these CFU (Figure 7A). These results are consistent with

in vivo data and suggest that the differentiation of both myeloid and erythrocyte cell lineages are blocked in cKO mice. Next, we treated the cells with 5 μM holo-transferrin (holo-Tf), 10 μM ferric ammonium citrate (FAC), 10 μM hemin, or 0.25 μM Fe (III)/8-hydroxyquinoline (Fe/8-HQ), a highly membrane-permeable complex that delivers iron directly into the cells,²⁶ thereby bypassing Tfr1. Interestingly, at these concentrations of both hemin and Fe/8-HQ partially rescued the colony-forming capacity of cKO cells, whereas holo-Tf and FAC had no effect (Figure

7A). The effect of hemin on the colony-forming capacity was concentration-dependent, and 50 μM hemin was sufficient to rescue the colony-forming capacity of cKO cells to control levels (Figure 7B). In contrast, 0.25 μM Fe/8-HQ failed to rescue CFU-GEMM forming capacity of cKO

cells, while Fe/8-HQ at a higher dose of 0.5 μM was toxic (data not shown). These results suggest that heme may serve as an alternative iron source other than Tf-iron in order to meet the cellular iron demand in FL HSPC in the absence of Tfr1.

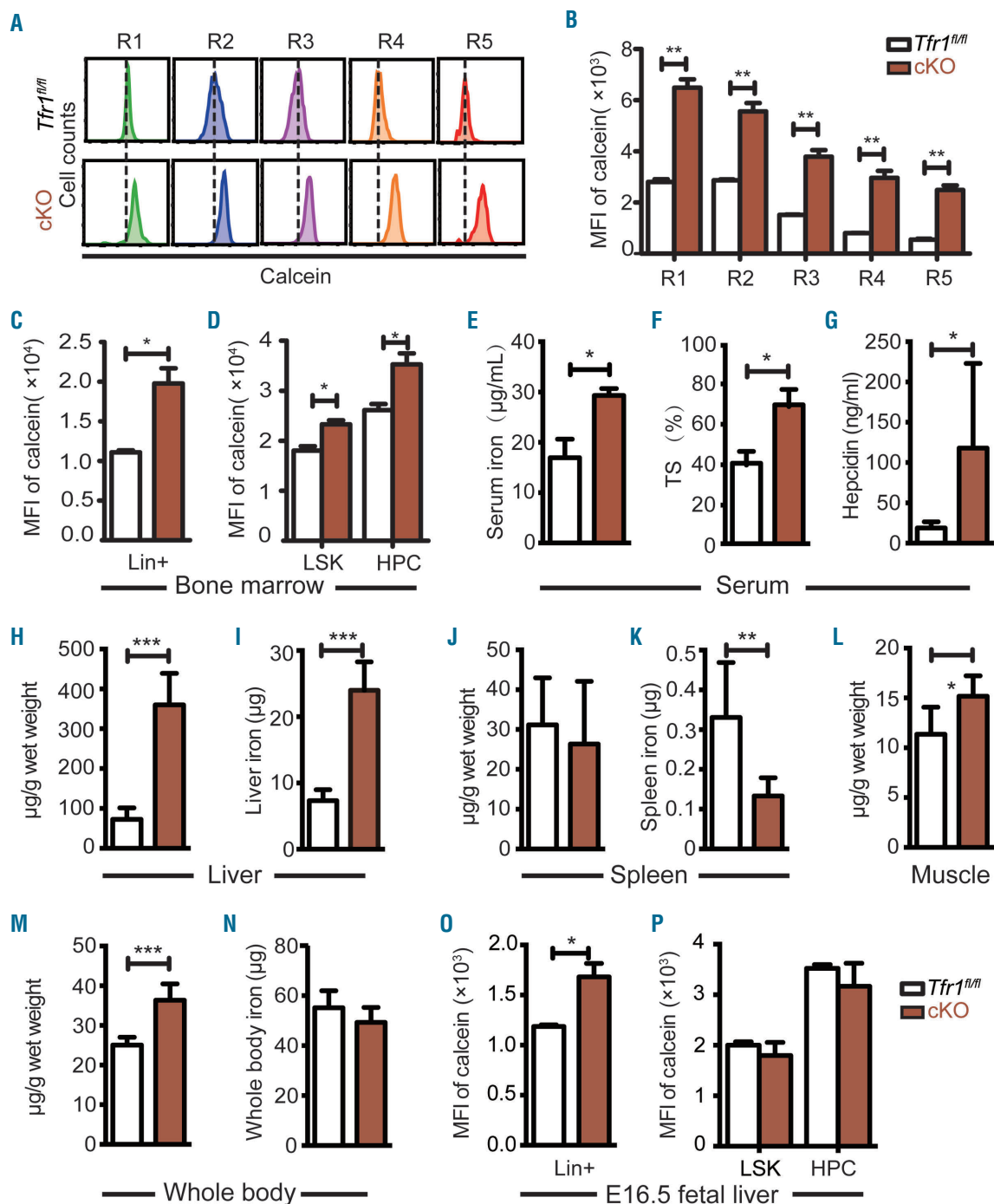


Figure 5. Postnatal *Tfr1* conditional knockout mice have dysregulated cellular iron homeostasis. (A) Flow cytometric analysis of calcein fluorescence was measured in the indicated stages of erythroid differentiation. (B) Relative mean fluorescence intensity (MFI) of calcein in figure 5A (n=4 per group). (C-D) Relative mean fluorescence intensity (MFI) of calcein measured in mature hematopoietic (Lin⁺) cells (C) and LSK and hematopoietic progenitor cells (HPC) cells (D) obtained from control and *Tfr1* knockout (cKO) bone marrow (n=4 per group). (E) Serum iron concentration, (F) transferrin saturation, and (G) serum hepcidin. (H-I) Liver non-heme iron, (J-K) spleen non-heme iron, (L) muscle non-heme iron, and (M-N) whole body non-heme iron were measured in control and cKO pups at P3 (n=5 per group). (O-P) Relative mean fluorescence intensity (MFI) of calcein measured in Lin⁺ cells (O), LSK (Lin⁺cKit⁺Sca1^{hi}) and HPC (Lin⁺cKit⁺Sca1^{lo}) cells (P) obtained from control and cKO livers at E16.5 (n = 4 for each group). *P<0.05; **P<0.01; ***P<0.001.

Overexpressing wild-type *Tfr1* but not the R654A mutant rescues *Tfr1*-deficient HSPC

Noncanonical functions of Tfr1 have been reported, including maintaining intestinal epithelial function independent of iron uptake,¹⁶ cell survival,²⁷ and regulating mitochondrial morphology.²⁸ Additionally, the missense mutation R654A in *Tfr1* prevents Tf binding without affecting the receptor's ability to bind Hfe protein.²⁹ We therefore expressed either wild-type *Tfr1* or mutant *Tfr1* in cKO FL cells using lentivirus infection. Expressing wild-

type *Tfr1* in cKO cells rescued the colony-forming capacity; interestingly, expressing the *Tfr1*^{L622A} mutant (which lacks the ability to bind Hfe) partially rescued, whereas expressing the *Tfr1*^{R654A} mutant was completely unable to rescue the impaired colony-forming capacity of cKO cells (Figure 7C). These results suggest that its function in iron uptake rather than signal transduction is the sole mechanism by which Tfr1 controls differentiation and survival in the hematopoietic system.

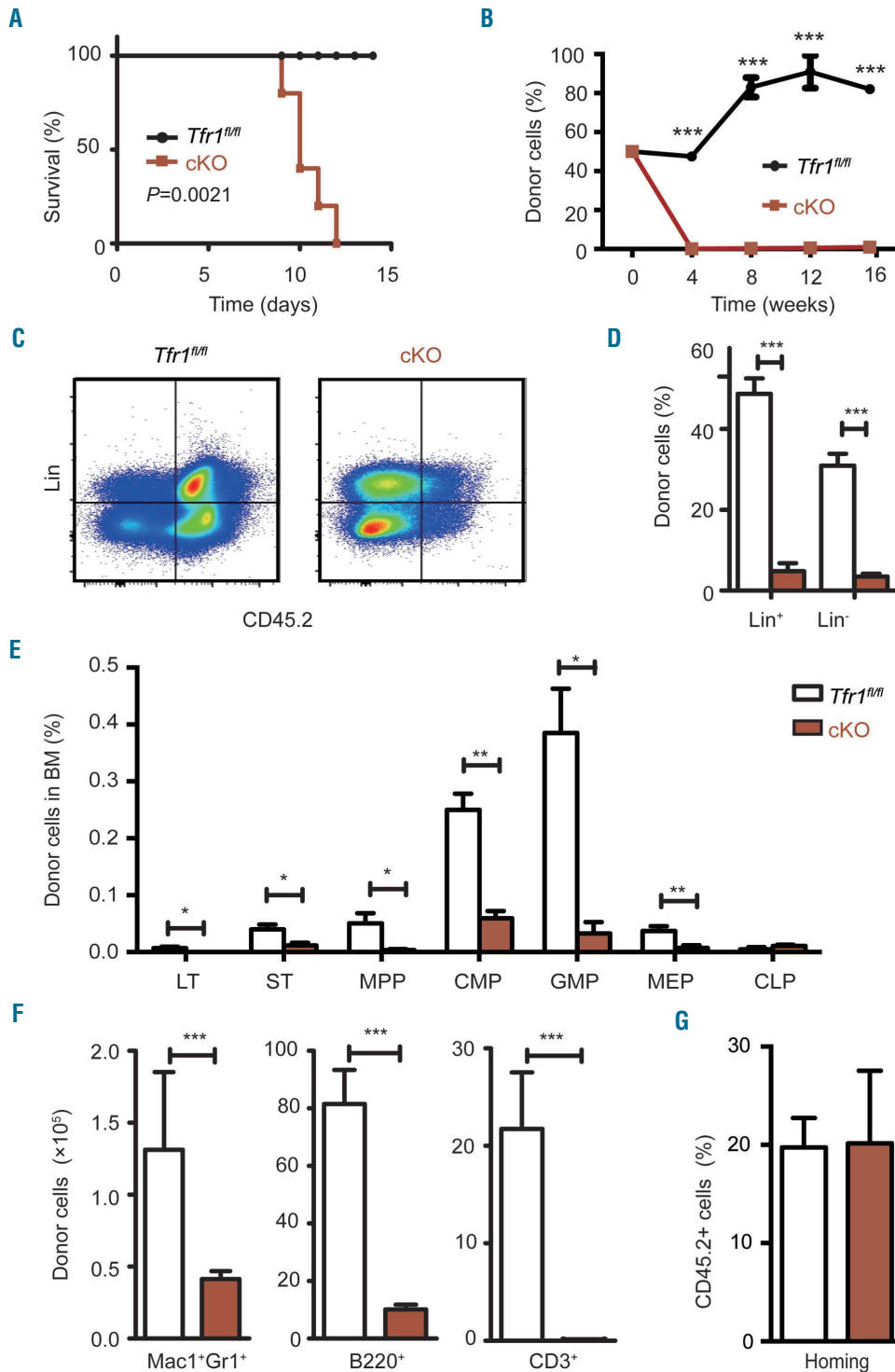


Figure 6. *Tfr1* knockout hematopoietic stem cells have impaired capacity for restoring hematopoiesis following transplantation. (A) Kaplan–Meier survival curve of CD45.1 mice that were lethally irradiated and then transplanted with fetal liver cells obtained from CD45.2 control or *Tfr1* knockout (cKO) embryos (n=5 recipients per group). (B) Recipient mice received a 50/50 combination of the indicated donor-derived fetal liver (CD45.2) cells and competitor (CD45.1) cells were measured at the indicated time points following transplantation (n=3 recipients per group). (C) Donor-derived (CD45.2) lineage-negative cells (Lin⁻) and mature hematopoietic cells (Lin⁺) were gated by flow cytometry. (D) The percentage of donor-derived Lin⁻ and Lin⁺ cells in the recipient bone marrow cells after transplantation for 16 weeks. (E) The absolute number of donor-derived LT (long-term HSC), ST (short-term HSC), MPP (multipotent progenitor cells), CMP (common myeloid progenitor cells), GMP (granulocyte/monocyte progenitor cells), MEP (megakaryocyte/erythrocyte progenitor cells), and CLP (common lymphoid progenitor cells) were measured 16 weeks after co-transplantation with control and cKO donor cells (n=3 for each group). (F) The absolute number of donor-derived myeloid cells (Mac1⁺Gr1⁺) and B cells (B220⁺) in the spleen, and T cells (CD3⁺) in the thymus of recipient mice 16 weeks after co-transplantation with control and cKO cells (n=3 for each group). (G) Homing efficiency of fetal liver cells obtained from either control or cKO mice 40 hours after transplantation into lethally irradiated recipient mice (n=3 per group). *P<0.05; **P<0.01; ***P<0.001.

Discussion

Tfr1 has long been used as a marker of red blood cells and is believed to play an essential role in erythropoiesis; however, its role in HSPC is poorly understood. Here, we generated and characterized a mouse model in which Tfr1 expression was deleted specifically in HSC and observed profoundly impaired BM function and defects in multiple cell lineages. These defects, which cause cKO offspring to die within one week of age, indicate that Tfr1 plays an essential role in hematopoiesis.

Specifically, our HSC-specific Tfr1-deficient mouse model allowed us to systematically dissect the role of *Tfr1* in the development of erythrocytes, granulocytes, thrombocytes, and lymphocytes. Our findings of microcytic hypochromic anemia in neonatal cKO pups and progressive erythropenia in FL of cKO embryos reveal that Tfr1 is required for erythropoiesis at an early stage, as loss of *Tfr1* primarily blocked the differentiation of erythroblast precursors (*e.g.* proerythroblasts, polychromatophilic erythroblasts), leading to decreased mature erythrocytes. In addition, although T-cell development was severely impaired in cKO mice, B-cell development was largely unaffected. These findings are supported by previous experiments showing that developing T cells derived from *Tfr1*^{-/-} ES cells arrested in an early stage, whereas B-cell development was affected less severely.¹⁴ Moreover, a recent study by Wang *et al.* found that *Tfr1*^{fl/fl}; *Cd4-Cre* mice develop normally, but have reduced production of pro-inflammatory cytokines.³⁰

Although the production of B cells was generally unaffected in our cKO mice, antibody production was likely affected given that patients with a mutation in the *TFR1* gene have severe hypogammaglobulinemia.¹⁵ Importantly, we found that monocyte development is severely blocked in embryonic development in cKO mice, providing the first direct evidence that Tfr1 plays an important role in monocyte development, which is consistent with studies demonstrating the role of Tfr1 in monocytes.³¹⁻³³

A wide range of peripheral blood cell types were decreased in cKO mouse, while the number of platelets was increased. On one hand, iron deficiency anemia has been shown to cause reactive thrombocytosis in both patients³⁴ and animal models,³⁵ and iron deficiency itself can promote megakaryopoiesis.³⁶ On the other hand, megakaryocytes are reported to arise directly from stem-like megakaryocyte-committed progenitor cells, a population that shares many features with multipotent HSC and serves as a megakaryocyte lineage-restricted emergency pool,³⁷ these progenitor cells might escape the impaired proliferation that affects other cell types.

Although, *Tfr1*^{fl/fl}; *Vav-Cre* mice have concomitant deletion of *Tfr1* in hematopoietic and endothelial cells, it remains elusive with respect to the effect of endothelial Tfr1 on systemic iron regulation. Most recently, Canali *et al.* and Koch *et al.* independently reported that liver sinusoidal endothelial cells (LSEC) are the major source of bone morphogenetic proteins (BMP), which are essential to the hepcidin expression.^{38,39} Specifically, it is suggested

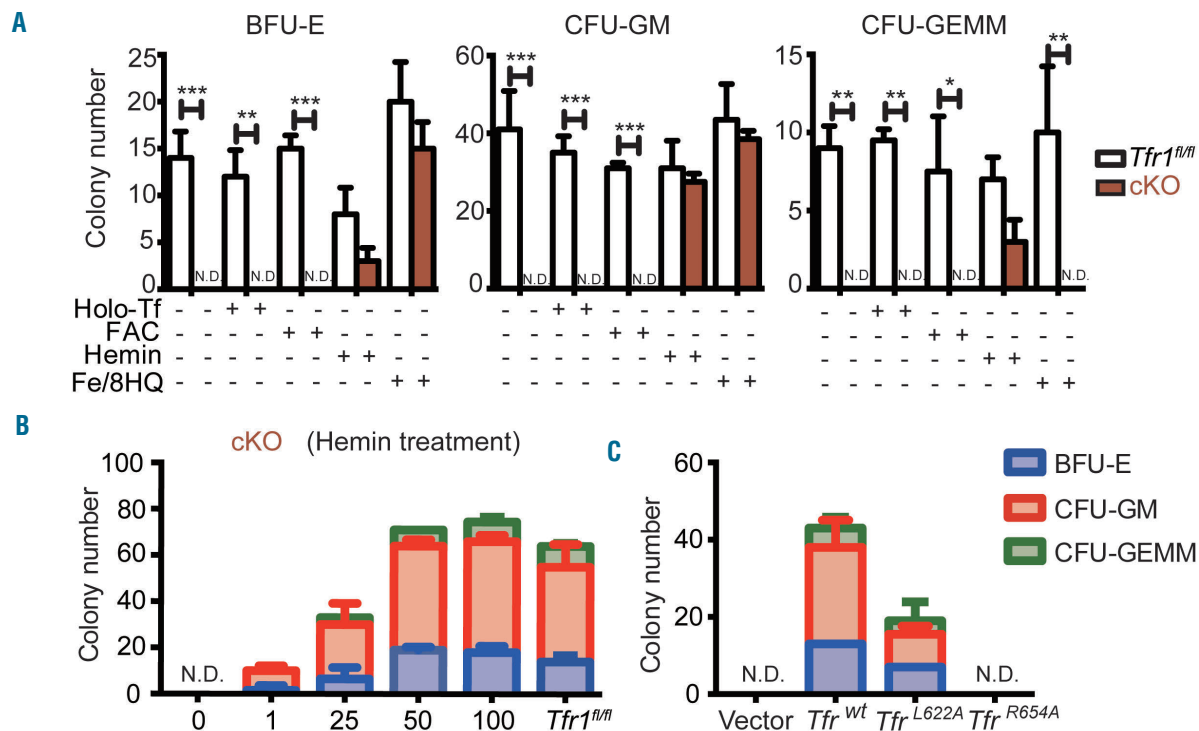


Figure 7. Treating *Tfr1* knockout hematopoietic stem/progenitor cells with hemin restores their differentiation capacity. (A) *In vivo* colony assays were performed using hematopoietic stem/progenitor cells (HSPC) obtained from control and *Tfr1* knockout (cKO) embryos at E14.5 ($n=3$ for each group) and treated with or without 5 μ M holo-transferrin (holo-Tf), 10 μ M ferric ammonium citrate (FAC), 10 μ M hemin, or 0.25 μ M Fe (III)/8-hydroxyquinoline (Fe/8-HQ). Colonies were measured on day 12, and the number of erythrocyte burst-forming units (BFU-E), granulocyte/macrophage colony-forming units (CFU-GM), and granulocytes, erythrocytes, macrophages, and megakaryocyte colony-forming units (CFU-GEMM) is shown. (B) Number of CFU formed by HSPC of cKO fetal liver treated with the indicated concentrations of hemin, and control cells. (C) Number of CFU formed by HSPC infected with the indicated *Tfr1*-expressing lentivirus. N.D.: not detectable. * $P<0.05$; ** $P<0.01$; *** $P<0.001$.

that downregulation of liver hepcidin expression could be attributed to iron overload resulted from depletion of *Bmp2* or *Bmp6* in LSEC. On the contrary, our *Tfr1^{fl/fl};Vav-Cre* mice had increased levels of liver and serum hepcidin. Interestingly, *Stat5a/b^{fl/fl;TC}* (Tie2-Cre driven *Stat5a/b* gene deletion in HSC and endothelial cells) mutant mice displayed a 50% reduction of *Tfr1* mRNA and protein expression, higher liver and serum iron levels, and elevated transferrin saturation,⁴⁰ which phenotypes are similar to those observed in our *Tfr1^{fl/fl};Vav-Cre* mice. Therefore, it is possible that serum iron and organ iron could be attributed to concomitant deletion of *Tfr1* in both hematopoietic and endothelial cells.

Interestingly, we found that iron storage is similar between cKO embryos and control embryos, indicating that the maternal transfer of iron is unaffected by the loss of *Tfr1* in the embryo's HSC. Previous studies showed that neonatal iron status is significantly correlated with three placental heme iron transporters⁴¹ and that newborn absorb a significantly higher fraction of heme iron compared to non-heme iron.⁴² In this respect, it is interesting to note that our *in vitro* colony-forming assay revealed that heme may serve as an alternative source of iron during early embryonic development.

Given that intracellular iron homeostasis is controlled by a complex molecular network, it is possible that transporters of non-transferrin bound iron⁴³⁻⁴⁶ may also play a role in hematopoiesis. Several studies revealed compelling evidence of other iron transporters in hematopoiesis. For example, the putative heme transporter FLVCR (group C feline leukemia virus receptor) did not appear to be essential for HSC function.⁴⁷ *Slc39a14^{-/-}* mice had no effect on hematological parameters,⁴⁸ either. In addition, *Slc11a2^{-/-}* mice only showed impaired erythropoiesis.⁴⁹ While, *Tfr2*-deficient mice had an increased red blood cell count and terminal erythropoiesis in the BM.⁵⁰ In general, none

of the aforementioned knockout mouse models present with hematopoietic impairments as severe as our HSC-specific *Tfr1*-deficient mice. Thus, although other currently unknown transporters and/or other modes of iron delivery may play a role in iron uptake in HSPC, *Tfr1* is clearly the predominant pathways for iron uptake, particularly in the downstream differentiation of progenitor cells.

In addition to its central role in facilitating cellular iron uptake, *Tfr1* also appears to play a role in signal transduction in intestinal homeostasis.¹⁶ We found that overexpressing of wild-type *Tfr1* but not the R654A mutant rescued both differentiation and proliferation. Interestingly, the L622A mutant only partially rescued the defects in cKO cells, possibly because *Tfr1*-Hfe may also regulate hematopoiesis. These results indicate that iron uptake but not signal transduction is the main mechanism by which *Tfr1* promotes the differentiation and survival of hematopoietic cells.

In conclusion, we provide direct *in vivo* evidence that *Tfr1* plays an essential role in hematopoiesis. In particular, we show that *Tfr1* is required for the differentiation of HSPC into a range of mature cell types. Importantly, our results indicate that iron uptake appears to be the principal mechanism by which *Tfr1* mediates the differentiation and survival of hematopoietic cells, thereby underscoring the important role that intracellular iron homeostasis plays in hematopoiesis.

Acknowledgments

The authors would like to thank the grants from the National Natural Science Foundation of China (31930057 and 31530034 to FW, 31570791 and 91542205 to JM, and 31701034 to QW) and the National Key R&D Program of China (2018YFA0507802 to FW and 2018YFA0507801 to JM). The authors thank the members of the Wang and Min laboratory for helpful discussions.

References

- Orkin SH, Zon LI. Hematopoiesis: an evolving paradigm for stem cell biology. *Cell*. 2008;132(4):631-644.
- Doulatov S, Notta F, Laurenti E, Dick JE. Hematopoiesis: a human perspective. *Cell Stem Cell*. 2012;10(2):120-136.
- Copley MR, Beer PA, Eaves CJ. Hematopoietic stem cell heterogeneity takes center stage. *Cell Stem Cell*. 2012;10(6):690-697.
- Wilson A, Laurenti E, Oser G, et al. Hematopoietic stem cells reversibly switch from dormancy to self-renewal during homeostasis and repair. *Cell*. 2008;135(6):1118-1129.
- Dzierzak E, Speck NA. Of lineage and legacy: the development of mammalian hematopoietic stem cells. *Nat Immunol*. 2008;9(2):129-136.
- Medvinsky A, Rybtsov S, Taoudi S. Embryonic origin of the adult hematopoietic system: advances and questions. *Development*. 2011;138(6):1017-1031.
- Rossi DJ, Jamieson CH, Weissman IL. Stem cells and the pathways to aging and cancer. *Cell*. 2008;132(4):681-696.
- Bacon BR, Adams PC, Kowdley KV, et al. Diagnosis and management of hemochromatosis: practice guideline by the American Association for the Study of Liver Diseases. *Hepatology*. 2011;54(1):328-343.
- Camaschella C. Iron-deficiency anemia. *N Engl J Med*. 2015;372(5):485-486.
- Hentze MW, Muckenthaler MU, Andrews NC. Balancing acts: Molecular control of mammalian iron metabolism. *Cell*. 2004;117(3):285-297.
- Gammella E, Buratti P, Cairo G, Recalcati S. The transferrin receptor: the cellular iron gate. *Metallomics*. 2017;9(10):1367-1375.
- Papanikolaou G, Pantopoulos K. Systemic iron homeostasis and erythropoiesis. *IUBMB Life*. 2017;69(6):399-413.
- Levy JE, Jin O, Fujiwara Y, Kuo F, Andrews NC. Transferrin receptor is necessary for development of erythrocytes and the nervous system. *Nat Genet*. 1999;21(4):396-399.
- Ned RM, Swat W, Andrews NC. Transferrin receptor 1 is differentially required in lymphocyte development. *Blood*. 2003;102(10):3711-3718.
- Jabara HH, Boyden SE, Chou J, et al. A missense mutation in TFRC, encoding transferrin receptor 1, causes combined immunodeficiency. *Nat Genet*. 2016;48(1):74-78.
- Chen AC, Donovan A, Ned-Sykes R, Andrews NC. Noncanonical role of transferrin receptor 1 is essential for intestinal homeostasis. *Proc Natl Acad Sci U S A*. 2015;112(37):11714-11719.
- Zhou JH, Wang XT, Zhou L, et al. Ablation of TFR1 in Purkinje cells inhibits mGlu1 trafficking and impairs motor coordination, but not autistic-like behaviors. *J Neurosci*. 2017;37(47):11335-11352.
- Chen MJ, Yokomizo T, Zeigler BM, Dzierzak E, Speck NA. Runx1 is required for the endothelial to haematopoietic cell transition but not thereafter. *Nature*. 2009;457(7231):887-891.
- Bagger FO, Sasivarevic D, Sohi SH, et al. BloodSpot: a database of gene expression profiles and transcriptional programs for healthy and malignant haematopoiesis. *Nucleic Acids Res*. 2016;44(D1):D917-D924.
- Lara-Astiaso D, Weiner A, Lorenzo-Vivas E, et al. Immunogenetics. Chromatin state dynamics during blood formation. *Science*. 2014;345(6199):943-949.
- Chen K, Liu J, Heck S, et al. Resolving the distinct stages in erythroid differentiation based on dynamic changes in membrane protein expression during erythropoiesis. *Proc Natl Acad Sci U S A*. 2009;

- 106(41):17413-17418.
22. Liu J, Zhang J, Ginzburg Y, et al. Quantitative analysis of murine terminal erythroid differentiation in vivo: novel method to study normal and disordered erythropoiesis. *Blood*. 2013;121(8):e43-e49.
 23. Cumano A, Godin I. Ontogeny of the hematopoietic system. *Annu Rev Immunol*. 2007;25:745-785
 24. Kakhlon O, Cabantchik ZI. The labile iron pool: characterization, measurement, and participation in cellular processes. *Free Radic Biol Med*. 2002;33(8):1037-1046.
 25. Kiel MJ, Morrison SJ. Uncertainty in the niches that maintain haematopoietic stem cells. *Nat Rev Immunol*. 2008;8(4):290-301.
 26. Petrat F, Rauen U, de Groot H. Determination of the chelatable iron pool of isolated rat hepatocytes by digital fluorescence microscopy using the fluorescent probe, phen green SK. *Hepatology*. 1999; 29(4):1171-1179.
 27. Jian J, Yang Q, Huang X. Src regulates Tyr (20) phosphorylation of transferrin receptor-1 and potentiates breast cancer cell survival. *J Biol Chem*. 2011;286(41):35708-35715.
 28. Senyilmaz D, Virtue S, Xu X, et al. Regulation of mitochondrial morphology and function by stearoylation of TFR1. *Nature*. 2015;525(7567):124-128.
 29. Schmidt PJ, Toran PT, Giannetti AM, Bjorkman PJ, Andrews NC. The transferrin receptor modulates Hfe-dependent regulation of hepcidin expression. *Cell Metab*. 2008;7(3):205-214.
 30. Wang Z, Yin W, Zhu L, et al. Iron drives T helper cell pathogenicity by promoting RNA-binding protein PCBP1-mediated proinflammatory cytokine production. *Immunity*. 2018;49(1):80-92.
 31. Ludwiczek S, Aigner E, Theurl I, Weiss G. Cytokine-mediated regulation of iron transport in human monocytic cells. *Blood*. 2003; 101(10):4148-4154.
 32. Kim S, Ponka P. Effects of interferon-gamma and lipopolysaccharide on macrophage iron metabolism are mediated by nitric oxide-induced degradation of iron regulatory protein 2. *J Biol Chem*. 2000;275(9):6220-6226.
 33. Testa U, Kühn L, Petrini M, Quaranta MT, Pelosi E, Peschle C. Differential regulation of iron regulatory element-binding protein(s) in cell extracts of activated lymphocytes versus monocytes-macrophages. *J Biol Chem*. 1991;266(21):13925-13930.
 34. Voudoukis E, Karmiris K, Oustamanolakis P, et al. Association between thrombocytosis and iron deficiency anemia in inflammatory bowel disease. *Eur J Gastroenterol Hepatol*. 2013;25(10):1212-1216.
 35. Choi SI, Simone JV, Jackson CW. Megakaryocytopoiesis in experimental iron deficiency anemia. *Blood*. 1974;43(1):111-120.
 36. Evstatiev R, Bukaty A, Jimenez K, et al. Iron deficiency alters megakaryopoiesis and platelet phenotype independent of thrombopoietin. *Am J Hematol*. 2014;89(5):524-529.
 37. Haas S, Hansson J, Klimmeck D, et al. Inflammation-induced emergency megakaryopoiesis driven by hematopoietic stem cell-like megakaryocyte progenitors. *Cell Stem Cell*. 2015; 17(4):422-434.
 38. Canali S, Zumbrennen-Bullough KB, Core AB, et al. Endothelial cells produce bone morphogenetic protein 6 required for iron homeostasis in mice. *Blood*. 2017; 129(4):405-414.
 39. Koch P-S, Olsavszky V, Ulbrich F, et al. Angiocrine Bmp2 signaling in murine liver controls normal iron homeostasis. *Blood*. 2017;129(4):415-419.
 40. Zhu BM, McLaughlin SK, Na R, et al. Hematopoietic-specific Stat5-null mice display microcytic hypochromic anemia associated with reduced transferrin receptor gene expression. *Blood*. 2008;112 (5):2071-2080.
 41. Best CM, Pressman EK, Cao C, et al. Maternal iron status during pregnancy compared with neonatal iron status better predicts placental iron transporter expression in humans. *FASEB J*. 2016;30(10):3541-3550.
 42. Young MF, Griffin I, Pressman E, et al. Maternal hepcidin is associated with placental transfer of iron derived from dietary heme and nonheme sources. *J Nutr*. 2012; 142(1):33-39.
 43. Goetz DH, Holmes MA, Borregaard N, et al. The neutrophil lipocalin NGAL is a bacteriostatic agent that interferes with siderophore-mediated iron acquisition. *Mol Cell*. 2002; 10(5):1033-1043.
 44. Yang J, Goetz D, Li JY, et al. An iron delivery pathway mediated by a lipocalin. *Mol Cell*. 2002;10(5):1045-1056.
 45. Kaplan J. Mechanisms of cellular iron acquisition: another iron in the fire. *Cell*. 2002;111(5):603-606.
 46. Oudit GY, Sun H, Trivieri MG, et al. L-type Ca(2+) channels provide a major pathway for iron entry into cardiomyocytes in iron-overload cardiomyopathy. *Nat Med*. 2003; 9(9):1187-1194.
 47. Byon JC, Chen J, Doty RT, Abkowitz JL. FLVCR is necessary for erythroid maturation, may contribute to platelet maturation, but is dispensable for normal hematopoietic stem cell function. *Blood*. 2013;122(16): 2903-2910.
 48. Jenkitkasemwong S, Wang CY, Coffey R, et al. SLC39A14 is required for the development of hepatocellular iron overload in murine models of hereditary hemochromatosis. *Cell Metabolism*. 2015;22(1):138-150.
 49. Gunshin H, Fujiwara Y, Custodio AO, et al. Slc11a2 is required for intestinal iron absorption and erythropoiesis but dispensable in placenta and liver. *J Clin Invest*. 2005; 115(5):1258-1266.
 50. Nai A, Lidonnici MR, Rausa M, et al. The second transferrin receptor regulates red blood cell production in mice. *Blood*. 2015; 125(7):1170-1179.

Platelet-derived growth factor receptor β activation and regulation in murine myelofibrosis

Frederike Kramer,^{1,2} Jens Dornedde,¹ Artur Mezheyski,³ Rudolf Tauber,¹ Patrick Micke³ and Kai Kappert^{1,2,4}

¹Charité - Universitätsmedizin Berlin, corporate member of Freie Universität Berlin, Humboldt-Universität zu Berlin, and Berlin Institute of Health, Institute of Laboratory Medicine, Clinical Chemistry and Pathobiochemistry, Berlin, Germany; ²Charité - Universitätsmedizin Berlin, corporate member of Freie Universität Berlin, Humboldt-Universität zu Berlin, and Berlin Institute of Health, Center for Cardiovascular Research (CCR), Berlin, Germany; ³Department of Immunology, Genetics and Pathology, Uppsala University, Uppsala, Sweden and ⁴DZHK (German Centre for Cardiovascular Research), partner site Berlin, Berlin, Germany



Haematologica 2020
Volume 105(8):2083-2094

ABSTRACT

There is prevailing evidence to suggest a decisive role for platelet-derived growth factors (PDGF) and their receptors in primary myelofibrosis. While PDGF receptor β (PDGFR β) expression is increased in bone marrow stromal cells of patients correlating with the grade of myelofibrosis, knowledge on the precise role of PDGFR β signaling in myelofibrosis is sparse. Using the Gata-1^{low} mouse model for myelofibrosis, we applied RNA sequencing, protein expression analyses, multispectral imaging and, as a novel approach in bone marrow tissue, an *in situ* proximity ligation assay to provide a detailed characterization of PDGFR β signaling and regulation during development of myelofibrosis. We observed an increase in PDGFR β and PDGF-B protein expression in overt fibrotic bone marrow, along with an increase in PDGFR β -PDGF-B interaction, analyzed by proximity ligation assay. However, PDGFR β tyrosine phosphorylation levels were not increased. We therefore focused on regulation of PDGFR β by protein tyrosine phosphatases as endogenous PDGFR β antagonists. Gene expression analyses showed distinct expression dynamics among PDGFR β -targeting phosphatases. In particular, we observed enhanced T-cell protein tyrosine phosphatase protein expression and PDGFR β -T-cell protein tyrosine phosphatase interaction in early and overt fibrotic bone marrow of Gata-1^{low} mice. *In vitro*, T-cell protein tyrosine phosphatase (*Ptpn2*) knockdown increased PDGFR β phosphorylation at Y⁷⁵¹ and Y¹⁰²¹, leading to enhanced downstream signaling in fibroblasts. Furthermore, *Ptpn2* knockdown cells showed increased growth rates when exposed to low-serum growth medium. Taken together, PDGF signaling is differentially regulated during myelofibrosis. Protein tyrosine phosphatases, which have so far not been examined during disease progression, are novel and hitherto unrecognized components in myelofibrosis.

Introduction

Primary myelofibrosis (PMF) is a malignant hematologic disorder characterized by the clonal proliferation of hematopoietic stem cells (HSC) in the bone marrow. Patients display symptoms of ineffective hematopoiesis such as anemia, thrombocytopenia and related extramedullary hematopoiesis resulting in splenomegaly. The bone marrow of PMF patients shows dysplastic megakaryocytes, neoangiogenesis and, as a central pathological feature, progressive fibrosis.¹ The development of myelofibrosis is mainly ascribed to the overproduction of pro-fibrotic cytokines and growth factors by malignant immature cells of the megakaryocytic lineage. As a consequence, fibroblasts proliferate and produce extensive amounts of extracellular matrix (ECM) components, leading to impaired hematopoietic function of the bone marrow.²

Correspondence:

KAI KAPPERT
kai.kappert@charite.de

Received: May 14, 2019.

Accepted: October 29, 2019.

Pre-published: October 31, 2019.

doi:10.3324/haematol.2019.226332

Check the online version for the most updated information on this article, online supplements, and information on authorship & disclosures: www.haematologica.org/content/105/8/2083

©2020 Ferrata Storti Foundation

Material published in *Haematologica* is covered by copyright. All rights are reserved to the Ferrata Storti Foundation. Use of published material is allowed under the following terms and conditions:

<https://creativecommons.org/licenses/by-nc/4.0/legalcode>. Copies of published material are allowed for personal or internal use. Sharing published material for non-commercial purposes is subject to the following conditions: <https://creativecommons.org/licenses/by-nc/4.0/legalcode>, sect. 3. Reproducing and sharing published material for commercial purposes is not allowed without permission in writing from the publisher.



Abberantly activated janus kinase-signal transducer and activator of transcription (JAK-STAT) signaling has been identified as a driver of clonal cells in PMF patients.³ Somatic mutations in *JAK2*,⁴ the thrombopoietin receptor *MPL*⁵ and *CALR*⁶ are the most prevalent genetic aberrations. These, however, are also frequently found in other myeloproliferative neoplasms (MPN), making a definite diagnosis of early PMF problematic. Thus, efforts are directed towards novel and valid diagnostic markers.

Platelet-derived growth factors (PDGF) have been implicated in the progression of bone marrow fibrosis.^{7,8} PDGF-A and -B, as well as PDGF receptor α (PDGFR α) and PDGF receptor β (PDGFR β) expression is increased in the bone marrow of PMF patients, regardless of driver mutations.^{9,10} The PDGF system comprises five dimeric ligands: PDGF-AA, -AB, -BB, -CC and -DD.¹¹ The two cognate transmembrane receptors, PDGFR α and PDGFR β , dimerize upon ligand binding and cross-phosphorylate intracellular tyrosine residues. These phosphorylated residues serve as binding sites for downstream signaling components and activate, among others, phospholipase C γ (PLC γ), phosphatidylinositol 3-kinase (PI3K), and JAK-STAT signaling.¹² A large proportion of PDGF derive from megakaryocytes, from where the ligands act on their receptors in a paracrine and autocrine manner.¹⁵ Whereas PDGFR α binds PDGF-A, -B and -C, PDGFR β can only be activated by PDGF-B and -D. Therefore, depending on the ligand dimers, PDGFR α and PDGFR β can form homo- and, if co-expressed, heterodimers.¹⁴ Distinct functions of PDGFR α and PDGFR β have been ascribed to the discrete, cell-type specific expression of the receptors. The receptors are predominantly expressed by cells of mesenchymal origin; within the bone marrow, PDGFR α expression is highest in megakaryocytes, whereas PDGFR β is almost exclusively expressed in fibroblasts.^{9,10} Therefore, PDGFR β has been attributed a major role in the proliferation of bone marrow stromal cells in myelofibrosis. Different mechanisms are involved in the regulation of PDGF signaling, e.g. injury and pro-inflammatory cytokines affect expression of the ligands and receptors.¹⁵ Furthermore, protein tyrosine phosphatases (PTP) dephosphorylate intracellular tyrosine residues of PDGF receptors and negatively regulate PDGF signaling.

PDGFR β expression in activated fibroblasts correlates with the grade of myelofibrosis in the bone marrow of PMF patients.¹⁰ However, the mechanisms of transformation from malign clonal proliferation of HSC to myelofibrosis and the involvement of the PDGF system are not fully understood. In particular, the expression dynamics of PDGFR β , the interaction with the ligand PDGF-B, and a possible regulation by PTP during the development of bone marrow fibrosis have not been thoroughly addressed. Using the Gata-1^{low} mouse model for PMF, this study concentrates on PDGFR β and its relevance in stromal cell proliferation. These mice show reduced Gata-1 expression in megakaryocytes, which have a high proliferation rate while remaining immature and releasing reduced platelet numbers. Therefore, Gata-1^{low} mice develop fibrosis in the bone marrow that resembles the development of myelofibrosis in PMF patients.¹⁶ For a detailed characterization, we performed whole transcriptome analyses, protein expression and localization analyses in pre-fibrotic, early fibrotic and overt fibrotic bone marrow. Furthermore, we applied a proximity ligation

assay (PLA) as a novel, sensitive technique for the quantification of protein expression, interaction of PDGFR β with its ligand PDGF-B, as well as PDGFR β tyrosine phosphorylation and the interaction of PDGFR β with T-cell protein tyrosine phosphatase (TC-PTP) for a detailed evaluation of PDGFR β activation status in bone marrow fibrosis *in situ*. Finally, we provide evidence for the regulation of PDGFR β by TC-PTP in fibroblasts *in vitro*.

Methods

Mouse model

Gata-1^{low} mice were purchased from Jackson Laboratory (Bar Harbour, ME, USA) and bred according to standards of the animal facility at the Center for Cardiovascular Research of Charité – Universitätsmedizin Berlin (Berlin, Germany). All littermates were genotyped using polymerase chain reaction (PCR) according to the standard protocol provided by Jackson. Hemizygous males and age-matched wild-type (WT) littermates were euthanized at 5, 10 and 15 months of age.

Further material and methods used in this study are described in the *Online Supplementary Appendix*.

Statistical analysis

Results presented as boxplots show the median, with whiskers representing minima and maxima; bar graphs show mean and standard deviation. Statistical differences between a Gata-1^{low} and the age-matched WT control group were determined using unpaired Student *t*-test. For comparison of multiple groups, analysis of variance with *post hoc* Tukey correction was used. Statistical analyses were performed using GraphPad Prism 6.01 (GraphPad Software Inc., San Diego, CA, USA). *P* < 0.05 was considered statistically significant.

Results

Development of myelofibrosis in the bone marrow of Gata-1^{low} mice

We determined different stages of bone marrow fibrosis in a cohort of Gata-1^{low} mice, which served as time points for all subsequent analyses: 5 months, 10 months and 15 months of age. Mice of all ages were normal in body weight (Figure 1A). As early as 5 months of age, Gata-1^{low} mice showed a pronounced splenomegaly (Figure 1B), whereas liver weight remained normal at all ages (Figure 1C). Mice displayed time-dependent, progressive anemia (Figure 1D) and a slight increase in leukocytes starting at month 10 (Figure 1E). Platelets were markedly reduced at all ages (Figure 1F). To determine fibrotic stages in Gata-1^{low} mice, we stained murine femoral bone marrow for reticulum fibers (Figure 1I). We did not observe an apparent accumulation of reticulum fibers in the bone marrow of Gata-1^{low} mice at month 5, whereas there was a time-dependent increased deposition of fibers at month 10 and 15. Hence, month 5 was defined as a pre-fibrotic, month 10 as an early fibrotic, and month 15 as an overt fibrotic stage in Gata-1^{low} mice. To monitor the induction of collagen production in the bone marrow of Gata-1^{low} mice, we analyzed type I collagen *Col1a1* and type III collagen *Col3a1* gene expression by qPCR (Figure 1G and H). We observed a significant decrease in *Col1a1* gene expression in the pre-fibrotic stage. However, a marked increase in gene expression of the two collagens was detected in early

fibrotic bone marrow and remained increased in overt fibrotic bone marrow of 15-month-old *Gata-1*^{low} mice.

Differential expression of receptor tyrosine kinases and their ligands in myelofibrosis

Since receptor tyrosine kinases (RTK) and RTK-activating ligands have been attributed an important role in myelofibrosis, we investigated transcriptomic changes by RNA sequencing (RNAseq) analyses with a focus on RTK

(Figure 2A) and their cognate ligands (Figure 2B). Interestingly, a high number of RTK showed a significant increase in gene expression; among which *Ptk7*, *Tie1*, *Flt1*, *Fgfr1* and the PDGF receptors *Pdgfra* and *Pdgfrb*. Although many ligands were not significantly regulated in early fibrotic bone marrow of *Gata-1*^{low} mice, we observed an induction of *Ptn*, *Efnb1*, *Pgf*, *Angpt2*, *Angpt4*, *Igf2* and *Efna2*. To classify transcriptionally up-regulated genes to their biological function, we further performed gene ontology

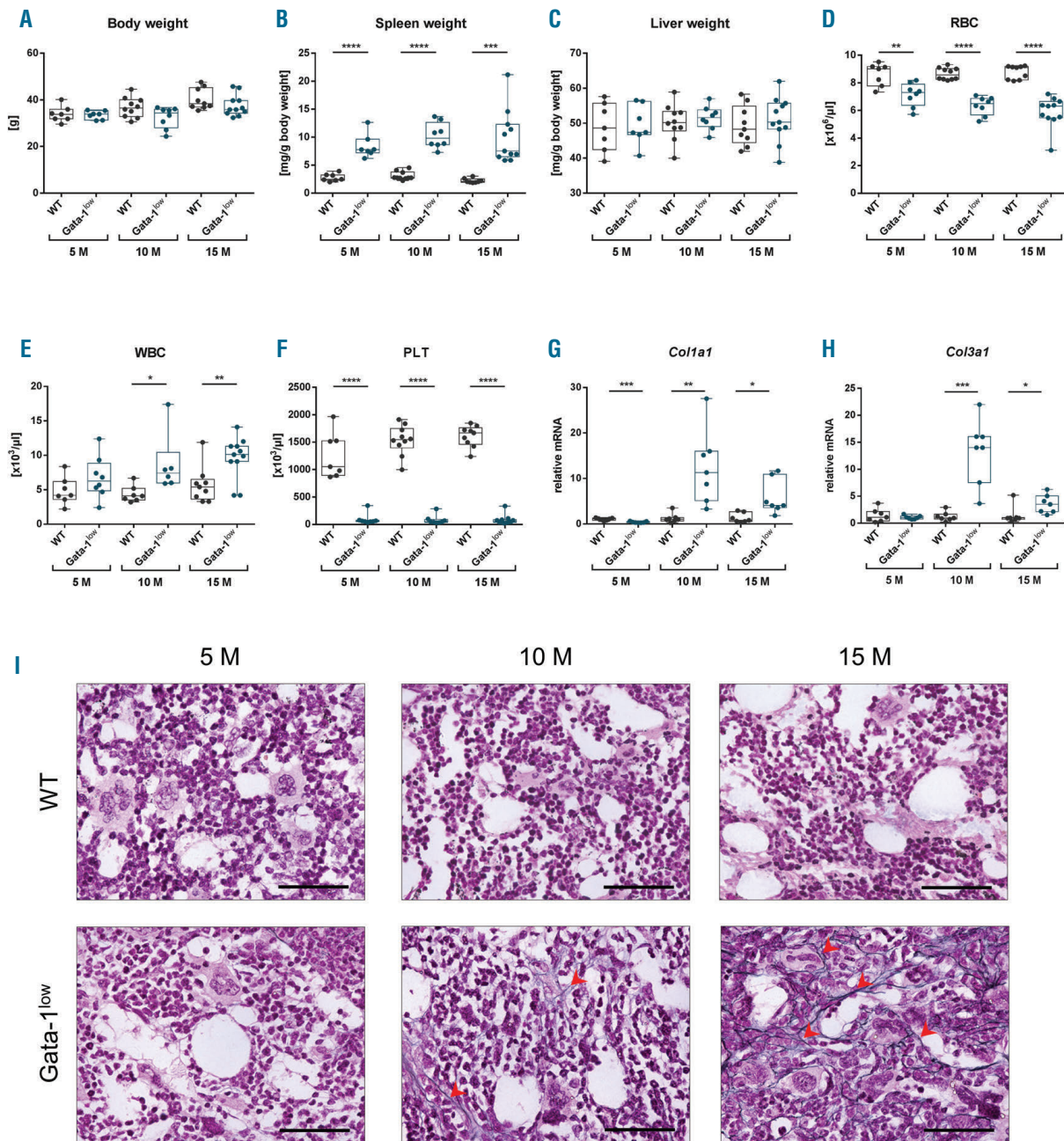


Figure 1. Characteristics of the *Gata-1*^{low} mouse model for primary myelofibrosis at 5 months (5 M), 10 months (10 M), and 15 months (15 M) of age. (A) Body weight of *Gata-1*^{low} mice and age-matched wild-type (WT) controls. (B) Spleen weight per g body weight. (C) Liver weight per g body weight. (D) Red blood cell (RBC) counts. (E) White blood cell (WBC) counts. (F) Platelet (PLT) counts. (G) Quantitative polymerase chain reaction analyses of type I collagen *Col1a1* and (H) type III collagen *Col3a1*. (I) Representative images of reticulum-stained femoral bone marrow showing increasing amount of reticulum fibers in the bone marrow of *Gata-1*^{low} mice, indicated by red arrowheads. Scale bar=50 μm. n=7-11 mice per group. **P*≤0.05, ***P*≤0.01, ****P*≤0.001, *****P*≤0.0001 versus the control group by Student *t*-test.

enrichment analyses (Figure 2C). Interestingly, genes implicated in PDGF binding (*Pdgfa*, *Pdgfb*, *Pdap1*, *Pdgfra*, *Pdgfrb*, *Col1a1*, *Col1a2*, *Col2a1*, *Col3a1*, *Col4a1*, *Col5a1* and *Col6a1*) were most over-represented within the up-regulated genes, followed by ECM structural constituents and genes referring to collagen binding.

Expression dynamics of platelet-derived growth factor signaling components during the development of myelofibrosis

Platelet-derived growth factors and their receptors are linked to bone marrow fibrosis, as was inferred from their increased expression in PMF patients.^{9,10} However, data addressing the expression dynamics during the develop-

ment of myelofibrosis are sparse. In order to characterize the expression pattern of PDGF signaling components at different stages of bone marrow fibrosis, we analyzed gene expression of the ligand and receptor genes in the bone marrow of *Gata-1^{low}* mice by quantitative PCR (qPCR). Here, we observed that gene expression of both receptor genes *Pdgfra* and *Pdgfrb* was highly induced in early fibrotic bone marrow from 10-month-old *Gata-1^{low}* mice and remained increased in overt fibrotic bone marrow of 15-month-old *Gata-1^{low}* mice (Figure 3A and B). Interestingly, *Pdgfrb* gene expression was significantly decreased in pre-fibrotic bone marrow of 5-month-old *Gata-1^{low}* mice, as also detected for *Col1a1* gene expression. qPCR analyses of the ligand genes *Pdgfa* and *Pdgfb*

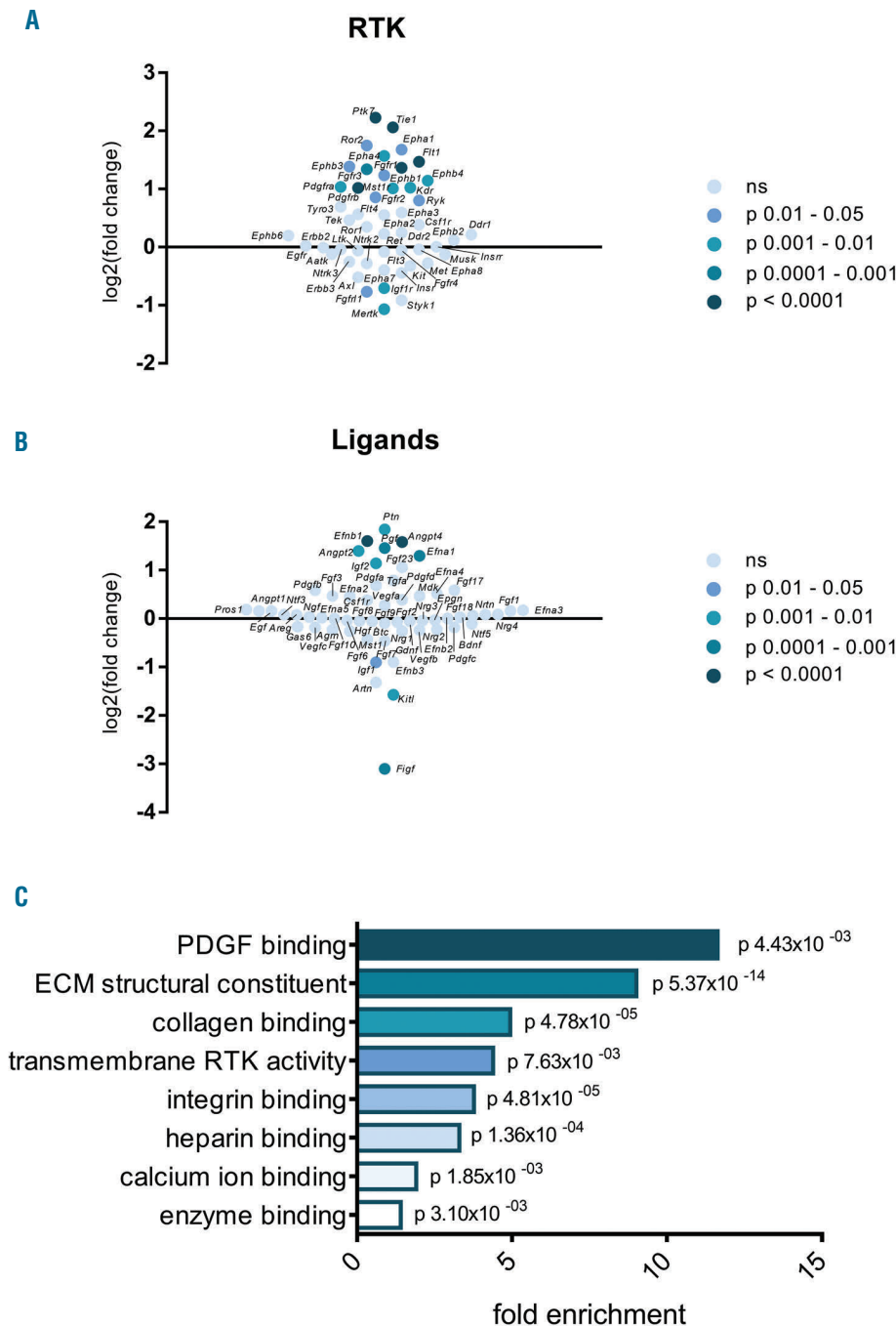


Figure 2. RNA sequencing analyses showing gene expression of receptor tyrosine kinases (RTK), their ligands and gene ontology enrichment analysis. Total RNA from femoral bone marrow of 10-month-old mice (n=3 *Gata-1^{low}* vs. n=3 wild-type mice) was analyzed. (A) Gene expression of RTK. (B) Gene expression of their cognate ligands. (C) Gene ontology enrichment analysis of over-expressed genes.

revealed a major increase in ligand gene expression at the early fibrotic stage (Figure 3C and D). We again observed a decrease in *Pdgfa* gene expression in pre-fibrotic bone marrow, whereas *Pdgfa* gene expression was increased in early and overt fibrotic bone marrow. *Pdgfb* expression was significantly up-regulated only in early fibrotic bone marrow and remained at nearly baseline level in pre-fibrotic and overt fibrotic bone marrow of *Gata-1^{low}* mice.

To validate the gene expression data, we further analyzed protein expression using an *in situ* proximity ligation assay (PLA) in a single recognition approach (Figure 3E). By this method, two oligonucleotide-coupled secondary antibodies (PLA probes) detect a single primary antibody. Through ligation, oligonucleotides are joined to a circle when in close proximity and serve as template for polymerization. A polymerase replicates the DNA circles and a concatemeric product is generated. Fluorescently-labeled nucleotides enable the detection of a rolling circle product (RCP), which can be visualized and quantified as a distinct fluorescent dot.^{17,18} Corresponding negative controls, positive controls, and results from the quantitative

analyses by proximity ligation assay (PLA) in comparison to quantified protein expression data acquired from multiplex staining are shown in *Online Supplementary Figures S1-S3*. Although we observed a heterogenic protein expression in *Gata-1^{low}* mice, there was a steady increase in PDGF receptor protein expression during the development of myelofibrosis (Figure 3F and G; original PLA images are shown in *Online Supplementary Figures S4*). When analyzing PDGF-A and PDGF-B protein expression by single recognition PLA, we again observed high heterogeneity among age-matched *Gata-1^{low}* mice. We did not detect a significant increase in PDGF-A expression, while PDGF-B protein expression was significantly increased in overt fibrotic bone marrow of 15-month-old *Gata-1^{low}* mice (Figure 3H and I, original PLA images are shown in *Online Supplementary Figures S4*).

To visualize the cell type-specific expression of the PDGF signaling components, we performed multiplexed staining of PDGF signaling components in the bone marrow (Figure 4). We observed PDGFR α expression predominantly in megakaryocytes, whereas PDGFR β

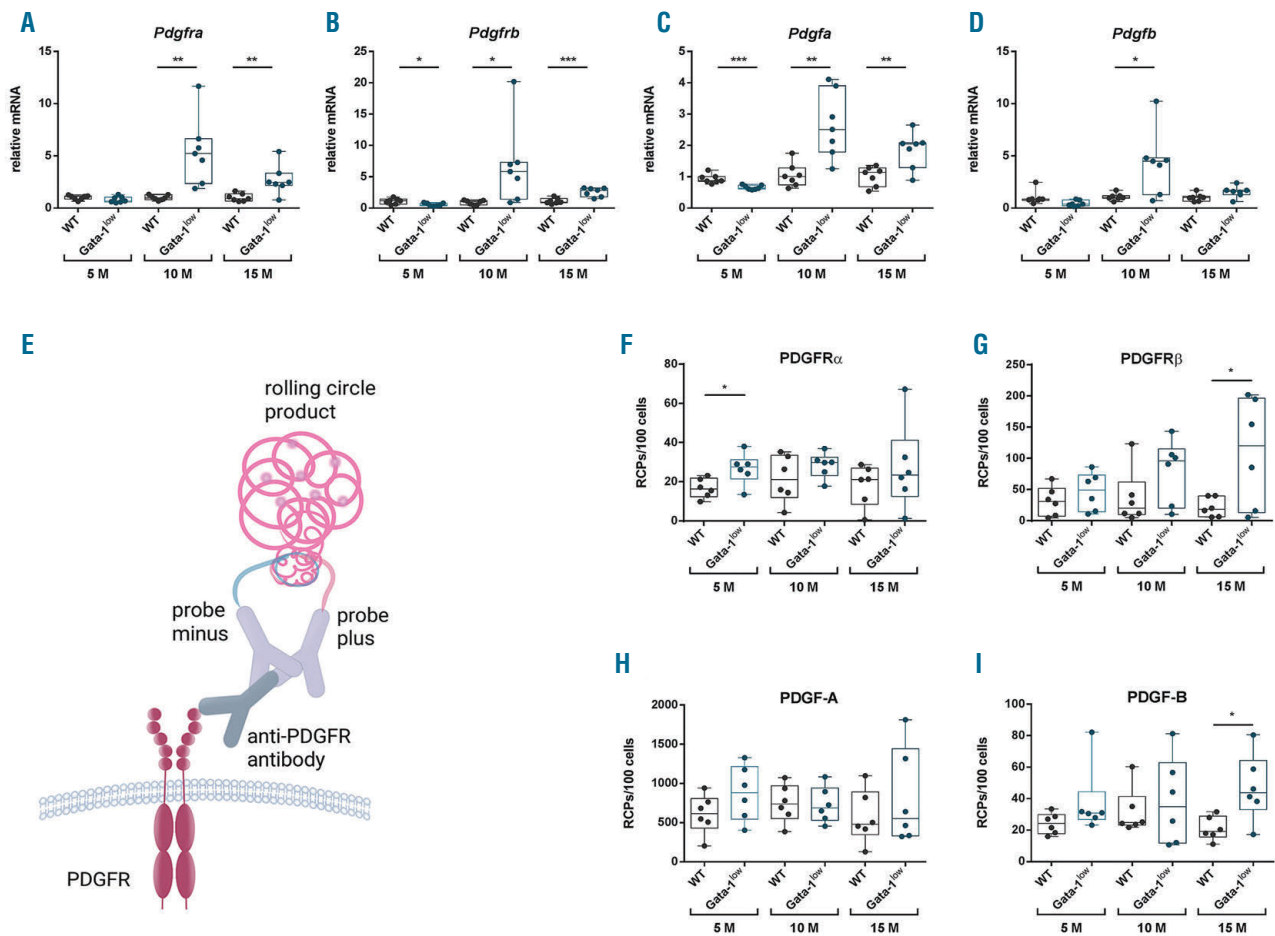


Figure 3. Expression of platelet-derived growth factors (PDGF) and their receptors in the bone marrow of *Gata-1^{low}* mice at 5 months (5 M), 10 months (10 M) and 15 months (15 M) of age. (A) Quantitative polymerase chain reaction (qPCR) analyses of *Pdgfra*, (B) *Pdgfrb*, (C) *Pdgfa*, and (D) *Pdgfb* in the bone marrow of *Gata-1^{low}* mice and age-matched wild-type (WT) controls. n=7 mice per group. (E) Illustration of a single recognition proximity ligation assay (PLA) as a sensitive means to quantify protein expression *in situ*. (F) Quantitative analyses of PDGFR α , (G) PDGFR β , (H) PDGF-A, and (I) PDGF-B protein expression by single recognition PLA in the bone marrow of *Gata-1^{low}* mice and age-matched WT controls. n=6 mice per group. 3170-7935 nucleated cells per mouse were analyzed for the presence of rolling circle products (RCP). * $P \leq 0.05$, ** $P \leq 0.01$, *** $P \leq 0.001$ versus the control group by Student t-test.

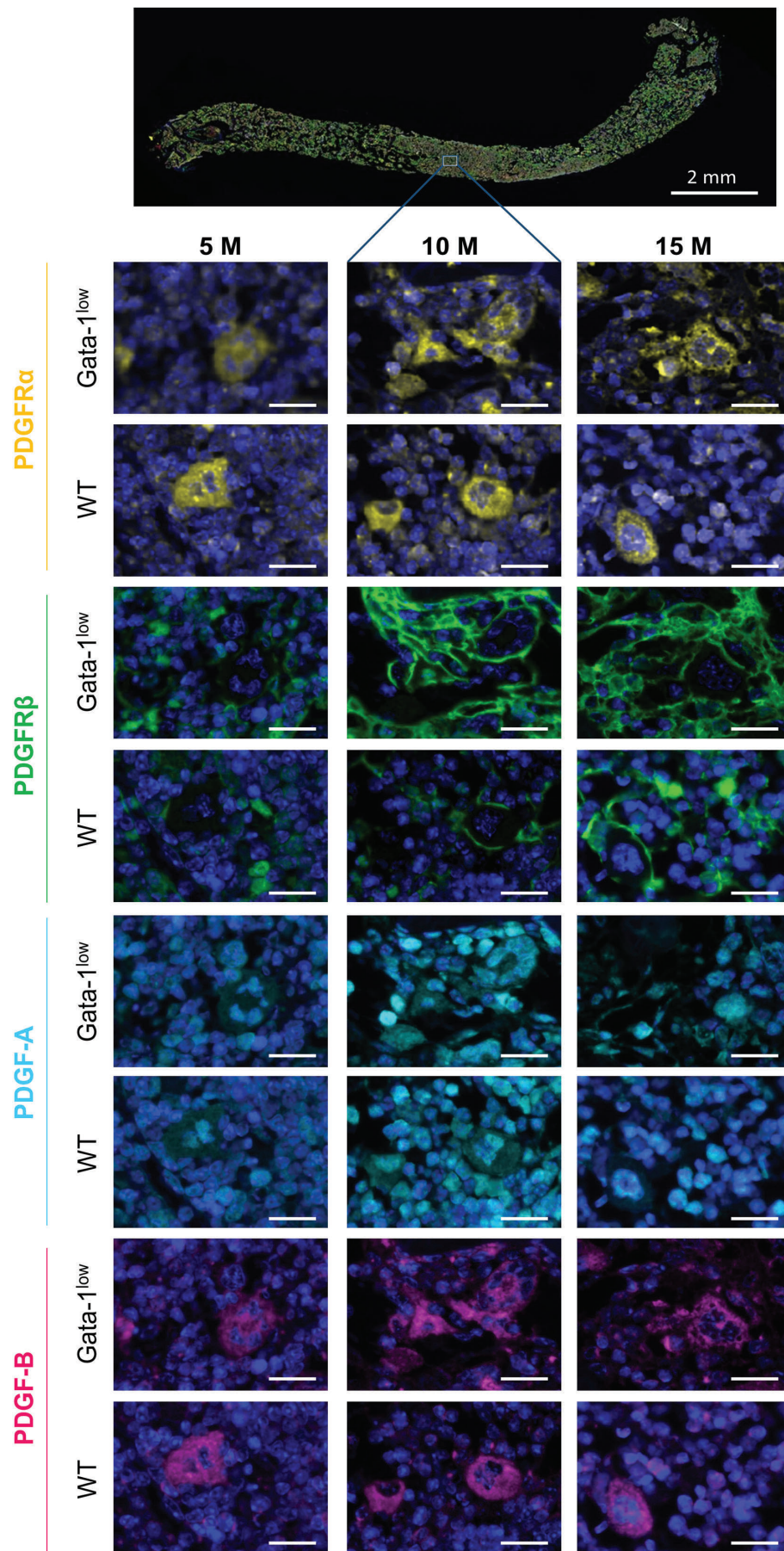


Figure 4. Multiplex staining of platelet-derived growth factors (PDGF) and their receptors in the bone marrow of Gata-1^{low} mice at 5 months (5 M), 10 months (10 M) and 15 months (15 M) of age. Representative images showing femoral bone marrow of Gata-1^{low} mice and wild-type (WT) control mice stained for PDGF receptor α (PDGFR α , yellow), PDGF receptor β (PDGFR β , green), PDGF-A (cyan) and PDGF-B (magenta). 10 images at 40x magnification were acquired within the femoral bone marrow for each group. Nuclei were counterstained with DAPI (blue), scale bars in lower panels=20 μ m.

marked spindle-shaped stromal cells in early and overt fibrotic bone marrow of Gata-1^{low} mice. Staining of the ligand PDGF-A showed expression in a wide variety of different hematopoietic cells, whereas PDGF-B mainly derived from megakaryocytes, suggesting a paracrine effect of PDGF-B on PDGFR β in bone marrow fibrosis.

Whereas megakaryocyte dysplasia and proliferation is a defining feature of PMF, fibroblast proliferation leading to a progressive fibrosis is the key pathological aspect of PMF. Given the distinct expression of PDGFR β in stromal cells of early fibrotic and fibrotic bone marrow, we further concentrated on the dynamics of PDGFR β and its ligand PDGF-B.

Ligand-activation and regulation of PDGFR β during the development of myelofibrosis

The increased protein expression of PDGFR β and its ligand PDGF-B in overt myelofibrosis prompted us to investigate the interaction of both signaling components *in situ*. To analyze PDGFR β -PDGF-B binding, we performed a PLA using combined primary antibodies detecting PDGFR β and PDGF-B (Figure 5A). The assay allows for the detection and quantification of signals and showed an increased interaction of receptor and ligand in overt fibrotic bone marrow of 15-month-old Gata-1^{low} mice (Figure 5B, original PLA images are shown in *Online Supplementary Figures S5*). This is in accordance with enhanced protein

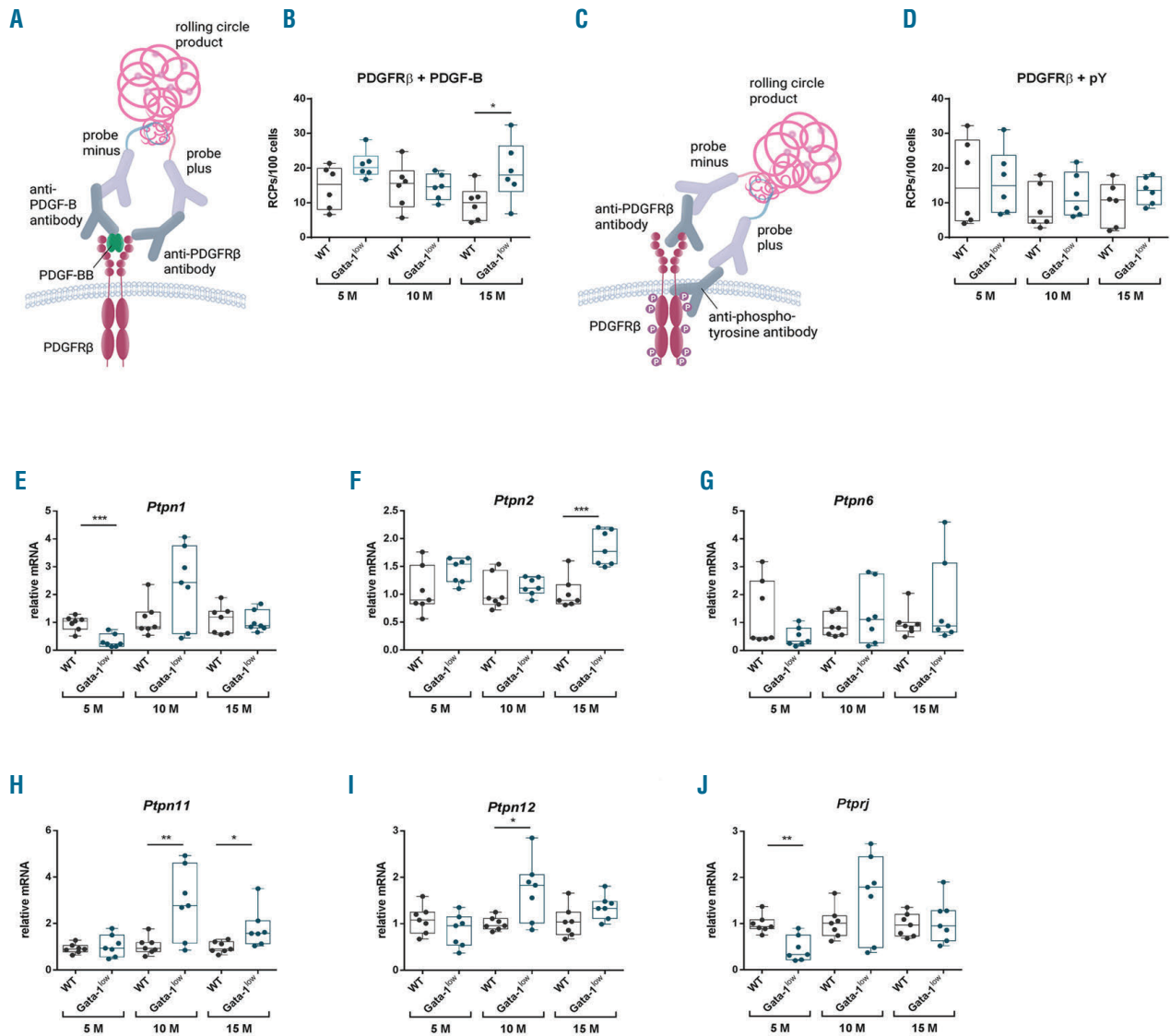


Figure 5. Interaction analysis of platelet-derived growth factor receptor β (PDGFR β) with PDGF-B and PDGFR β tyrosine phosphorylation in the bone marrow of Gata-1^{low} mice at 5 months (5 M), 10 months (10 M) and 15 months (15 M) of age. (A) Illustration of a proximity ligation assay (PLA) for the analysis of PDGFR β -PDGF-B interaction. (B) Quantitative analysis of PDGFR β -PDGF-B interaction by PLA in the bone marrow of Gata-1^{low} mice and age-matched wild-type (WT) controls. (C) Illustration of a PLA for the analysis of PDGFR β tyrosine phosphorylation. (D) Quantitative analysis of PDGFR β tyrosine phosphorylation by PLA in the bone marrow of Gata-1^{low} mice and age-matched WT controls, n=6 mice per group, 2670-9001 nucleated cells per mouse were analyzed for the presence of rolling circle products (RCP). (E) qPCR analyses of *Ptpn1*, (F) *Ptpn2*, (G) *Ptpn6*, (H) *Ptpn11*, (I) *Ptpn12* and (J) *Ptpnj*, n=7 mice per group, *P \leq 0.05, **P \leq 0.01, ***P \leq 0.001 versus the control group by Student t-test.

expression of both PDGFR β and PDGF-B in the bone marrow of 15-month-old Gata-1^{low} mice and suggests an increased activation of intracellular signaling in the overt fibrotic stage. To further analyze the activation status of the receptor, we applied a PLA combining PDGFR β and phosphotyrosine-targeting primary antibodies to analyze PDGFR β phosphorylation *in situ* (Figure 5C). Surprisingly, we did not observe increased PDGFR β tyrosine phosphorylation at any stage of myelofibrosis in Gata-1^{low} mice (Figure 5D, original PLA images are shown in *Online Supplementary Figure 5*). To verify these results, we per-

formed both an enzyme-linked immunosorbent assay (ELISA) with isolated protein from fresh frozen material and *in situ* staining for PDGFR β phosphorylation at Y⁷⁵¹. In line with the PLA data, no differences in tyrosine phosphorylation were detectable between the WT animals and Gata-1^{low} mice at all ages (*data not shown*). These results suggest the presence of further counter-regulatory mechanisms, such as PTP. Therefore, to investigate the contribution of the different PTP regarding the PDGFR β phosphorylation status, we screened RNAseq data from 10-month-old Gata-1^{low} mice and WT controls for differ-

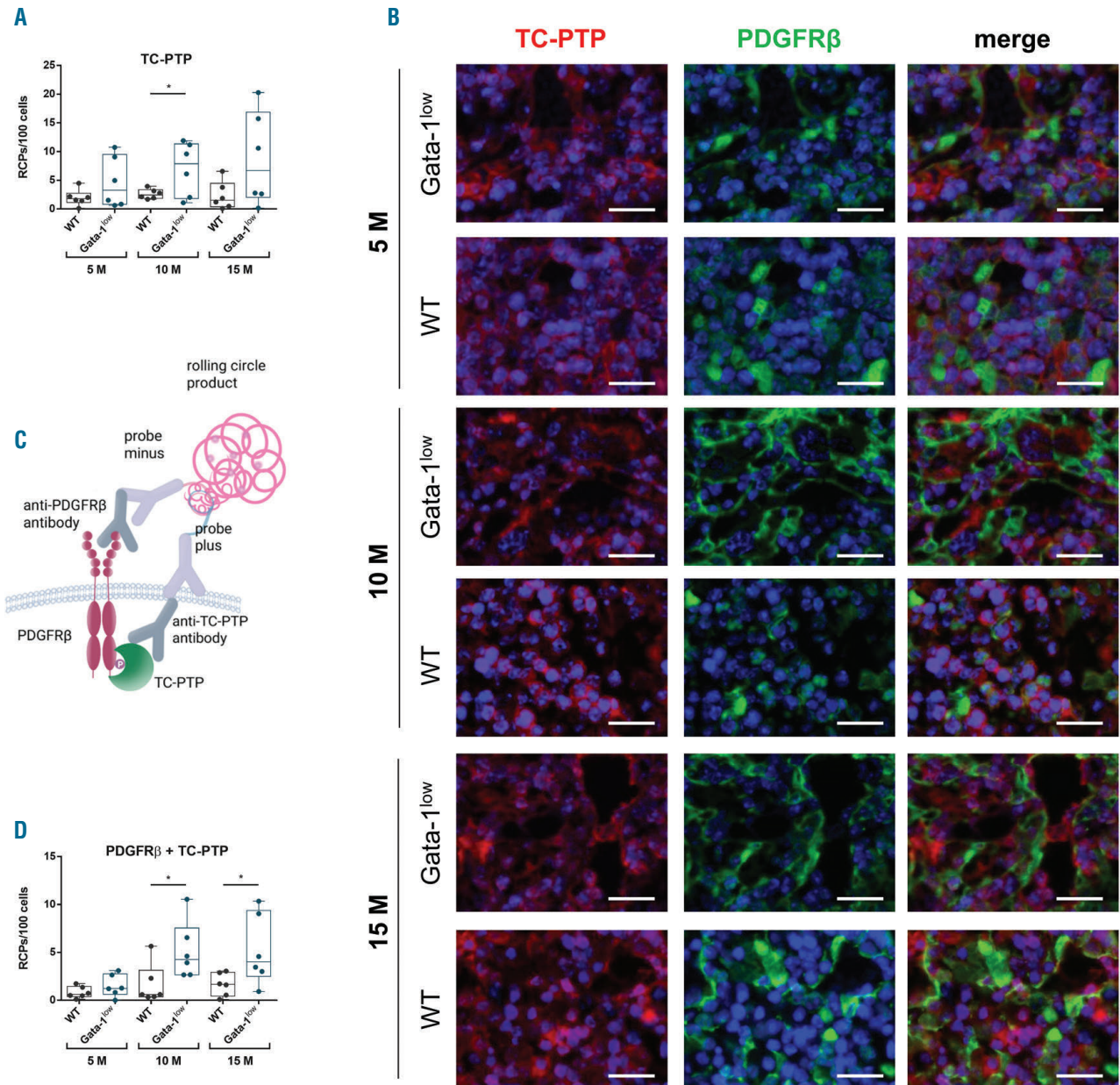


Figure 6. Expression and interaction dynamics of the phosphatase T-cell protein tyrosine phosphatase (TC-PTP) and platelet-derived growth factor receptor β (PDGFR β) in the bone marrow of Gata-1^{low} mice at 5 months (5 M), 10 months (10 M) and 15 months (15 M) of age. (A) Quantitative analyses of TC-PTP protein expression by single recognition proximity ligation assay (PLA) in the bone marrow of Gata-1^{low} mice and age-matched wild-type (WT) controls. (B) Representative images showing femoral bone marrow of Gata-1^{low} mice stained for PDGF receptor β (PDGFR β , green) and TC-PTP (red). Nuclei were counterstained with DAPI (blue), scale bars=20 μ m. (C) Illustration of a PLA for the analysis of PDGFR β -TC-PTP interaction. (D) Quantitative analysis of PDGFR β -TC-PTP interaction by PLA in the bone marrow of Gata-1^{low} mice and age-matched WT controls, n=6 mice per group. 4051-9101 nucleated cells per mouse were analyzed for the presence of rolling circle products (RCP). * $P \leq 0.05$ versus the control group by Student t-test.

ential expression of all classical PTP and the dual-specific phosphatase *Pten*. These analyses included the six PTP which are known to target PDGFR β .¹⁹⁻²² However, *Ptpn1* (encoding PTP1B), *Ptpn2* (encoding TC-PTP), *Ptpn6* (encoding SHP-1), *Ptpn11* (encoding SHP-2), *Ptpn12* (encoding PTP-PEST), and *Ptprj* (encoding DEP-1) were not differentially expressed in the bone marrow of early fibrotic, 10-month-old mice (*data not shown*). To complement these data with gene expression analyses for Gata-1^{low} mice of all ages, and to overcome the small sample size (n=3 mice per group) in the RNAseq analyses, we

performed qPCR analyses for *Ptpn1*, *Ptpn2*, *Ptpn6*, *Ptpn11*, *Ptpn12*, and *Ptprj*. Indeed, in the gene expression analyses we observed distinct expression dynamics among gene expression of these PTP (Figure 5E-J). Overall, the data generated by qPCR from early fibrotic bone marrow of 10-month-old Gata-1^{low} mice displayed pronounced biological variances, possibly contributing to the lack of significance within the RNAseq data. Interestingly, *Ptpn1* and *Ptprj* gene expression, analyzed by qPCR, showed decreased expression in pre-fibrotic bone marrow. There was an increased expression of *Ptpn11* and *Ptpn12* in early

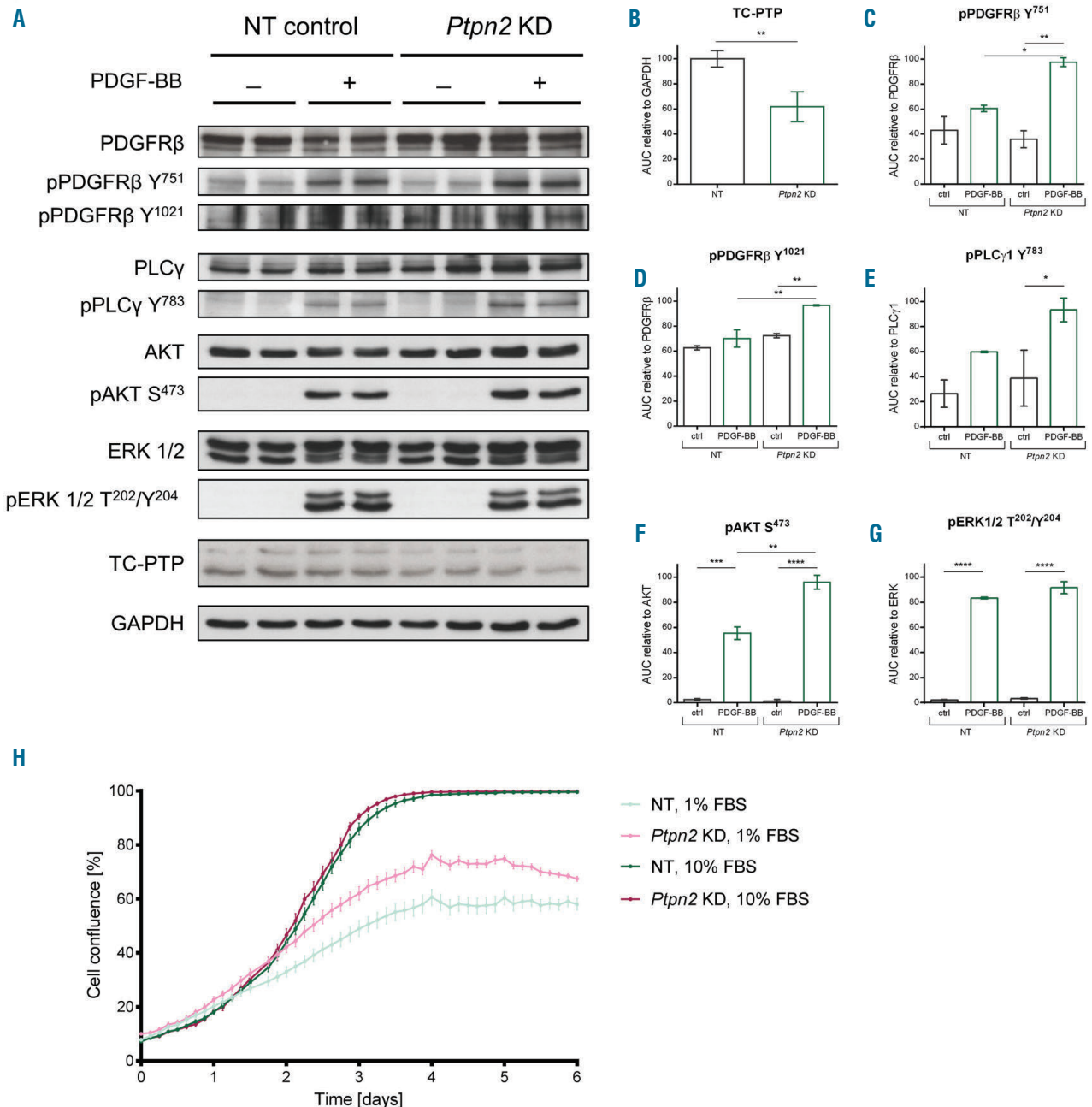


Figure 7. Regulation of platelet-derived growth factor receptor β (PDGFR β) signaling and proliferation of NIH-3T3 fibroblasts by T-cell protein tyrosine phosphatase (TC-PTP). (A) Immunoblot of *Ptpn2* knock down (KD) and non-targeting (NT) control cells, untreated (-) and stimulated with 50 ng/mL PDGF-BB (+) for 5 minutes. (B) Densitometric analyses of TC-PTP, (C) pPDGFR β Y⁷⁵¹, (D) pPDGFR β Y¹⁰²¹, (E) pPLC γ 1 Y⁷⁸³, (F) pAKT S⁴⁷³, (G) pERK1/2 T²⁰²/Y²⁰⁴. (H) Proliferation curves of *Ptpn2* KD and NT control cells cultured in 1% and 10% fetal bovine serum (FBS). * $P \leq 0.05$, ** $P \leq 0.01$, *** $P \leq 0.001$, **** $P \leq 0.0001$ by analysis of variance with *post hoc* Tukey correction.

fibrotic bone marrow. In overt fibrotic bone marrow, *Ptpn2* and *Ptpn11* gene expression was enhanced. Since TC-PTP (*Ptpn2*) has previously been ascribed an essential role in normal hematopoietic function,^{23,24} we further focused on PDGFR β regulation by TC-PTP. Given the conclusive increase in *Ptpn2* gene expression in overt fibrotic bone marrow, we next analyzed TC-PTP protein expression in the different fibrotic stages in Gata-1^{low} mice. Quantitative analysis of TC-PTP protein expression by PLA confirmed an increased expression in early and overt myelofibrosis (Figure 6A, original PLA images are shown in *Online Supplementary Figure S5*). In addition, *in situ* imaging showed ubiquitous expression of TC-PTP in the bone marrow of Gata-1^{low} mice (Figure 6B). TC-PTP staining was positive in a wide variety of hematopoietic cells, megakaryocytes and in spindle-shaped cell structures, raising the question if TC-PTP directly regulates PDGFR β in bone marrow stromal cells. To determine the interaction of PDGFR β and TC-PTP, we again applied the sensitive proximity ligation technique (Figure 6C) and detected increased interaction of PDGFR β and TC-PTP in early and overt fibrotic bone marrow of Gata-1^{low} mice (Figure 6D, original PLA images are shown in *Online Supplementary Figure S5*).

TC-PTP in PDGFR β signaling and proliferation in fibroblasts *in vitro*

Our findings of increased PDGFR β and TC-PTP expression and interaction led us to further analyze the regulation of PDGFR β by TC-PTP in fibroblasts *in vitro*. We knocked down *Ptpn2* in NIH-3T3 fibroblasts and stimulated cells with PDGF-BB (Figure 7A). Transfection with *Ptpn2*-targeting siRNA resulted in a moderate but significant knockdown (KD) compared to cells transfected with non-targeting (NT) siRNA (Figure 7B). We observed a consecutive increase in PDGFR β phosphorylation at Y⁷⁵¹ and downstream AKT signaling in *Ptpn2* KD cells (Figure 7C and F). However, there was no substantial effect on downstream ERK signaling (Figure 7G). PDGFR β phosphorylation at Y¹⁰²¹, as well as downstream PLC γ activation, was increased in *Ptpn2* KD cells (Figure 7D and E). We further monitored proliferation of *Ptpn2* KD cells (Figure 7H) and did not find any evident differences in proliferation in cells cultured in complete growth medium containing 10% fetal bovine serum (FBS). However, when cells were exposed to serum-reduced medium (1% FBS), *Ptpn2* KD cells showed increased growth rates compared to NT control cells.

Discussion

In this study, we provide detailed analyses of the expression patterns of PDGFR β signaling in the bone marrow of Gata-1^{low} mice at different fibrotic disease stages using RNAseq, qPCR, *in situ* protein expression analyses, multiplex staining and PLA. Early and overt fibrotic bone marrow was characterized by increased expression of PDGF signaling components and overt fibrosis by an increase in PDGFR β -PDGF-B interaction. Since PDGFR β tyrosine phosphorylation levels were not increased, the regulation of PDGFR β by PTP was investigated. *Ptpn2* gene as well as TC-PTP protein expression was increased in fibrotic bone marrow of Gata-1^{low} mice. Furthermore, enhanced PDGFR β -TC-PTP interaction was observed in

early and overt myelofibrosis, potentially counteracting PDGFR β phosphorylation. Likewise, *Ptpn2* KD increased PDGFR β tyrosine phosphorylation at Y⁷⁵¹ and Y¹⁰²¹ and resulted in enhanced downstream AKT and PLC γ 1 signaling in fibroblasts. Furthermore, *Ptpn2* KD cells showed a growth condition-dependent increase in expansion rate. Thus, while PDGF signaling is differentially regulated during PMF, PTP seem novel and so far unrecognized components in disease development. Previously not applied in bone marrow, PLA might add to diagnostics as a novel technique.

Intense efforts have been made to understand the mechanisms leading to PMF, focusing on genetic analysis. However, the PMF-associated driver mutations leading to aberrant activation of JAK-STAT signaling are not unique to PMF but also occur in other MPN, namely essential thrombocythemia and polycythemia vera. Although one of the driver mutations is sufficient to induce PMF in patients, they are often accompanied by other mutations and epigenetic changes.^{25,26} However, there is still no distinct molecular marker available for the respective MPN, emphasizing that the underlying mechanisms directing the different MPN are not yet understood. The discovery of JAK-STAT-associated mutations led to the development of JAK inhibitors and since its US Food and Drug Administration approval in 2011, the JAK1/2 inhibitor ruxolitinib has become part of combined standard therapy for PMF patients. Long-term treatment with ruxolitinib reduces spleen size and prolongs the overall survival of PMF patients.²⁷ However, there is no improvement or reversal of bone marrow fibrosis. Furthermore, efficacy of ruxolitinib is limited by drug resistance,²⁸ and JAK inhibition does not abrogate clonal proliferation.²⁹ Recently, PDGFR α signaling was shown to remain active despite JAK2 inhibition *in vivo* and is a cell-intrinsic bypass for maintaining downstream ERK signaling upon ruxolitinib treatment.³⁰ To date, allogeneic stem cell transplantation is the only curative treatment for PMF; however, transplantation is only suitable for a subset of high-risk patients and limited by comorbidities and donor availability.^{31,32}

Gata-1^{low} mice were characterized by a marked thrombocytopenia, splenomegaly and progressive anemia starting before 5 months of age. Enrichment analyses of RNAseq data from early fibrotic bone marrow of Gata-1^{low} mice revealed that genes implicated in PDGF binding are most over-represented within the up-regulated genes. We further observed enhanced PDGFR β and PDGF-B protein expression at 15 months of age, along with an increase in PDGFR β -PDGF-B interaction, analyzed by PLA.

However, we did not detect an increase in PDGFR β tyrosine phosphorylation in the bone marrow of Gata-1^{low} mice. This observation raised the question as to whether other mechanisms are involved in the regulation of the receptor in fibrotic bone marrow. Since a number of PTP have been identified, which site-selectively dephosphorylate PDGFR β , namely PTP1B, TC-PTP, SHP-1, SHP-2, PTP-PEST and DEP-1,¹⁹⁻²² an increased expression of these PTP might be responsible for the absence of an increased PDGFR β phosphorylation. Indeed, our data showed distinct dynamics in gene expression of these PTP.

We observed decreased *Ptpn1* and *Ptpn12* gene expression in pre-fibrotic bone marrow in Gata-1^{low} mice. The relevance of these PTP as potential diagnostic markers could be validated in a translational clinical approach. In contrast, *Ptpn2*, *Ptpn11* and *Ptpn12* showed an increased gene

expression during the development of myelofibrosis in Gata-1^{low} mice. *Ptpn11*, encoding the phosphatase SHP-2, has been described as positive regulator by mediating binding of Grb2 and thus promotes ERK signaling.^{33,34} Therefore, interpretation of enhanced *Ptpn11* expression is complex and context dependent. *Ptpn12*, coding for PTP-PEST, has previously been implicated in dendritic cell migration and macrophage fusion.^{35,36} However, data on *Ptpn12* involvement in bone marrow malignancies are scarce. *Ptpn2* and its gene product TC-PTP, however, play a pivotal role in normal hematopoietic and stromal cell function, as emphasized by studies using TC-PTP deficient mice. Homozygous mice die 3-5 weeks after birth with severe defects in hematopoiesis.²⁴ Transplantation experiments further suggest that TC-PTP knockout leads to changes in the bone marrow microenvironment, which impede normal HSC function.²⁴ This supports the findings in our study, which indicate that TC-PTP expression in bone marrow stromal cells and the interaction with PDGFR β might be important mediators of changes in the bone marrow microenvironment during the development of myelofibrosis. *Ptpn2* gene expression was increased in overt fibrotic bone marrow of Gata-1^{low} mice, implicating the importance of TC-PTP also with regard to PDGFR β regulation. TC-PTP is ubiquitously expressed but shows strong expression in cells of the different hematopoietic lineages. We observed TC-PTP expression in hematopoietic cells, megakaryocytes as well as in stromal cells within the bone marrow. In addition to PDGFR β , TC-PTP dephosphorylates EGFR and JAK-STAT signaling components.^{37,38} Importantly, there are several lines of evidence showing TC-PTP is involved in a number of bone marrow alterations.^{23,24,39} Ultimately, a pharmacological approach with a highly efficient modulator of TC-PTP activity *in vivo* will be needed to provide evidence for TC-PTP contribution to the pathogenesis of myelofibrosis, which is a limitation of our study. A direct pharmacological intervention of TC-PTP *in vivo*, however, is not currently available. Consistent with other studies,²¹ we were able to show a counter-regulation of PDGFR β by TC-PTP in fibroblasts *in vitro*. *Ptpn2* KD resulted in enhanced PDGFR β tyrosine phosphorylation at Y⁷⁵¹, which serves as a binding site for PI3K.⁴⁰ Conclusively, we detected an increase in downstream AKT activation as a central mediator of cell proliferation. PDGFR β phosphorylation also activates Ras and downstream ERK signaling,⁴¹ however, we did not observe increased ERK signaling in *Ptpn2* KD cells. *Ptpn2* KD further led to increased PDGFR β tyrosine phosphorylation at Y¹⁰²¹, resulting in enhanced downstream PLC γ 1 activation, suggesting a possible role of downstream protein kinase C and Ca²⁺ signaling.

We observed that *Ptpn2* KD fibroblasts cultured in com-

plete growth medium containing 10% FBS did not have an apparent superiority in proliferation. However, we detected increased growth rates in *Ptpn2* KD cells exposed to reduced-serum media containing 1% FBS. This suggests that under conditions of high abundance of growth factor differences in proliferation in *Ptpn2* KD cells are abolished, while these are apparent during serum-deprivation. Other studies using murine skin cancer models showed that TC-PTP controls proliferation and survival *via* AKT and STAT3 activation.^{42,43} Furthermore, emphasizing the role of TC-PTP in hematopoietic cells, TC-PTP controls T-cell proliferation.⁴⁴ Our data, based on a moderate KD, indicate that more discrete changes in TC-PTP expression controls cell growth mainly when the availability of growth components is limited.

In this study, we applied a PLA as a novel technique to analyze *in situ* alterations in bone marrow disease progression. The data acquired by PLA are generally in good agreement with our data acquired by multiplex staining, as another antibody-based method. While some discrepancies remained, further optimization regarding this tissue-specific approach are desired. This refers in particular to fluorescent signals, which are distinct from the clearly recognizable RCP. Those are most likely not ascribed to primary antibody binding but are caused by binding of oligonucleotides conjugated to secondary antibodies (PLA probes). Indeed, such signals have also been observed using DNA probes in *in situ* hybridization (FISH) approaches on bone marrow tissue and are associated with eosinophils.⁴⁵ Future studies in patient material are warranted to evaluate the applicability of the PLA as a diagnostic tool in early disease stages, to monitor disease progression and response to JAK inhibition. These analytical methods should carefully consider pre-analytic processing such as specific decalcification protocols and archiving conditions for long-term storage of specimens.

In summary, PDGF signaling components display major alterations in bone marrow fibrosis. While PDGF and their cognate receptors are dynamically regulated, PTP represent previously unrecognized contributors that control PDGF signaling in myelofibrosis. As this study focused on PDGFR β -TC-PTP interaction within the bone marrow *in situ* microenvironment, future examination of PDGFR β regulation by TC-PTP in primary stromal cells from mouse models and from PMF patients will help to elucidate the precise role of TC-PTP in the development of bone marrow disease.

Funding

The authors would like to thank the Stiftung für Pathobiochemie und Molekulare Diagnostik for funding to KK and the Sonnenfeld Stiftung (Berlin) for a doctoral scholarship to FK.

References

- O'Sullivan JM, Harrison CN. Myelofibrosis: clinicopathologic features, prognosis, and management. *Clin Adv Hematol Oncol*. 2018;16(2):121-131.
- Tefferi A. Pathogenesis of myelofibrosis with myeloid metaplasia. *J Clin Oncol*. 2005;23(33):8520-8530.
- Kleppe M, Kwak M, Koppikar P, et al. JAK-STAT pathway activation in malignant and nonmalignant cells contributes to MPN pathogenesis and therapeutic response. *Cancer Discov*. 2015;5(3):316-331.
- Baxter EJ, Scott LM, Campbell PJ, et al. Acquired mutation of the tyrosine kinase JAK2 in human myeloproliferative disorders. *Lancet*. 2005;365(9464):1054-1061.
- Pikman Y, Lee BH, Mercher T, et al. MPLW515L is a novel somatic activating mutation in myelofibrosis with myeloid metaplasia. *PLoS Med*. 2006;3(7):e270.
- Klampfl T, Gisslinger H, Harutyunyan AS, et al. Somatic mutations of calreticulin in myeloproliferative neoplasms. *N Engl J Med*. 2013;369(25):2379-2390.
- Caenazzo A, Pietrogrande F, Polato G, et al. Changes in the mitogenic activity of platelet-derived growth factor(s) in patients with myeloproliferative disease. *Acta Haematol*. 1989;81(3):131-135.
- Reilly JT. Pathogenesis of idiopathic

- myelofibrosis: role of growth factors. *J Clin Pathol.* 1992;45(6):461-464.
9. Bock O, Loch G, Busche G, von Wasielewski R, Schlue J, Kreipe H. Aberrant expression of platelet-derived growth factor (PDGF) and PDGF receptor-alpha is associated with advanced bone marrow fibrosis in idiopathic myelofibrosis. *Haematologica.* 2005;90(1):133-134.
 10. Bedekovics J, Kiss A, Beke L, Karolyi K, Mehes G. Platelet derived growth factor receptor-beta (PDGFRbeta) expression is limited to activated stromal cells in the bone marrow and shows a strong correlation with the grade of myelofibrosis. *Virchows Arch.* 2013;463(1):57-65.
 11. Fredriksson L, Li H, Eriksson U. The PDGF family: four gene products form five dimeric isoforms. *Cytokine Growth Factor Rev.* 2004;15(4):197-204.
 12. Heldin CH, Ostman A, Ronnstrand L. Signal transduction via platelet-derived growth factor receptors. *Biochim Biophys Acta.* 1998;1378(1):F79-113.
 13. Wickenhauser C, Hillienhof A, Jungheim K, et al. Detection and quantification of transforming growth factor beta (TGF-beta) and platelet-derived growth factor (PDGF) release by normal human megakaryocytes. *Leukemia.* 1995;9(2):310-315.
 14. Heldin CH, Westermark B. Mechanism of action and in vivo role of platelet-derived growth factor. *Physiol Rev.* 1999;79(4):1283-1316.
 15. Bonner JC. Regulation of PDGF and its receptors in fibrotic diseases. *Cytokine Growth Factor Rev.* 2004;15(4):255-273.
 16. Vannucchi AM, Bianchi L, Cellai C, et al. Development of myelofibrosis in mice genetically impaired for GATA-1 expression (GATA-1^{low} mice). *Blood.* 2002;100(4):1123-1132.
 17. Soderberg O, Leuchowius KJ, Gullberg M, et al. Characterizing proteins and their interactions in cells and tissues using the in situ proximity ligation assay. *Methods.* 2008;45(3):227-232.
 18. Fredriksson S, Gullberg M, Jarvius J, et al. Protein detection using proximity-dependent DNA ligation assays. *Nat Biotechnol.* 2002;20(5):473-477.
 19. Klinghoffer RA, Kazlauskas A. Identification of a putative Syp substrate, the PDGF beta receptor. *J Biol Chem.* 1995;270(38):22208-22217.
 20. Markova B, Herrlich P, Ronnstrand L, Bohmer FD. Identification of protein tyrosine phosphatases associating with the PDGF receptor. *Biochemistry.* 2003;42(9):2691-2699.
 21. Persson C, Savenhed C, Bourdeau A, et al. Site-selective regulation of platelet-derived growth factor beta receptor tyrosine phosphorylation by T-cell protein tyrosine phosphatase. *Mol Cell Biol.* 2004;24(5):2190-2201.
 22. Kappert K, Paulsson J, Sparwel J, et al. Dynamic changes in the expression of DEP-1 and other PDGF receptor-antagonizing PTPs during onset and termination of neointima formation. *FASEB J.* 2007;21(2):523-534.
 23. Wiede F, Chew SH, van Vliet C, et al. Strain-dependent differences in bone development, myeloid hyperplasia, morbidity and mortality in ptpn2-deficient mice. *PLoS One.* 2012;7(5):e36703.
 24. You-Ten KE, MuiSE ES, Itie A, et al. Impaired bone marrow microenvironment and immune function in T cell protein tyrosine phosphatase-deficient mice. *J Exp Med.* 1997;186(5):683-693.
 25. Vannucchi AM, Lasho TL, Guglielmelli P, et al. Mutations and prognosis in primary myelofibrosis. *Leukemia.* 2013;27(9):1861-1869.
 26. Martinez-Calle N, Pascual M, Ordonez R, et al. Epigenomic profiling of myelofibrosis reveals widespread DNA methylation changes in enhancer elements and ZFP36L1 as a potential tumor suppressor gene epigenetically regulated. *Haematologica.* 2019;104(8):1572-1579.
 27. Verstovsek S, Mesa RA, Gotlib J, et al. Long-term treatment with ruxolitinib for patients with myelofibrosis: 5-year update from the randomized, double-blind, placebo-controlled, phase 3 COMFORT-I trial. *J Hematol Oncol.* 2017;10(1):55.
 28. Harrison CN, Vannucchi AM, Kiladjian JJ, et al. Long-term findings from COMFORT-II, a phase 3 study of ruxolitinib vs best available therapy for myelofibrosis. *Leukemia.* 2016;30(8):1701-1707.
 29. Deininger M, Radich J, Bum TC, Huber R, Paranagama D, Verstovsek S. The effect of long-term ruxolitinib treatment on JAK2p.V617F allele burden in patients with myelofibrosis. *Blood.* 2015;126(13):1551-1554.
 30. Stivala S, Codilupi T, Brkic S, et al. Targeting compensatory MEK/ERK activation increases JAK inhibitor efficacy in myeloproliferative neoplasms. *J Clin Invest.* 2019;130:1596-1611.
 31. Kroger NM, Deeg JH, Olavarria E, et al. Indication and management of allogeneic stem cell transplantation in primary myelofibrosis: a consensus process by an EBMT/ELN international working group. *Leukemia.* 2015;29(11):2126-2133.
 32. McLoman DP, Yakoub-Agha I, Robin M, Chalandon Y, Harrison CN, Kroger N. State-of-the-art review: allogeneic stem cell transplantation for myelofibrosis in 2019. *Haematologica.* 2019;104(4):659-668.
 33. Ronnstrand L, Arvidsson AK, Kallin A, et al. SHP-2 binds to Tyr763 and Tyr1009 in the PDGF beta-receptor and mediates PDGF-induced activation of the Ras/MAP kinase pathway and chemotaxis. *Oncogene.* 1999;18(25):3696-3702.
 34. Dance M, Montagner A, Salles JP, Yart A, Raynal P. The molecular functions of Shp2 in the Ras/Mitogen-activated protein kinase (ERK1/2) pathway. *Cell Signal.* 2008;20(3):453-459.
 35. Rhee I, Davidson D, Souza CM, Vacher J, Veillette A. Macrophage fusion is controlled by the cytoplasmic protein tyrosine phosphatase PTP-PEST/PTPN12. *Mol Cell Biol.* 2013;33(12):2458-2469.
 36. Rhee I, Zhong MC, Reizis B, Cheong C, Veillette A. Control of dendritic cell migration, T cell-dependent immunity, and autoimmunity by protein tyrosine phosphatase PTPN12 expressed in dendritic cells. *Mol Cell Biol.* 2014;34(5):888-899.
 37. Pike KA, Tremblay ML. TC-PTP and PTP1B: Regulating JAK-STAT signaling, controlling lymphoid malignancies. *Cytokine.* 2016;82:52-57.
 38. Tiganis T, Bennett AM, Ravichandran KS, Tonks NK. Epidermal growth factor receptor and the adaptor protein p52Shc are specific substrates of T-cell protein tyrosine phosphatase. *Mol Cell Biol.* 1998;18(3):1622-1634.
 39. Bourdeau A, Trop S, Doody KM, Dumont DJ, Tremblay ML. Inhibition of T cell protein tyrosine phosphatase enhances interleukin-18-dependent hematopoietic stem cell expansion. *Stem Cells.* 2013;31(2):293-304.
 40. Panayotou G, Bax B, Gout I, et al. Interaction of the p85 subunit of PI 3-kinase and its N-terminal SH2 domain with a PDGF receptor phosphorylation site: structural features and analysis of conformational changes. *EMBO J.* 1992;11(12):4261-4272.
 41. Kashishian A, Kazlauskas A, Cooper JA. Phosphorylation sites in the PDGF receptor with different specificities for binding GAP and PI3 kinase in vivo. *EMBO J.* 1992;11(4):1373-1382.
 42. Lee H, Morales LD, Slaga TJ, Kim DJ. Activation of T-cell protein-tyrosine phosphatase suppresses keratinocyte survival and proliferation following UVB irradiation. *J Biol Chem.* 2015;290(1):13-24.
 43. Lee H, Kim M, Baek M, et al. Targeted disruption of TC-PTP in the proliferative compartment augments STAT3 and AKT signaling and skin tumor development. *Sci Rep.* 2017;7:45077.
 44. Wiede F, La Gruta NL, Tiganis T. PTPN2 attenuates T-cell lymphopenia-induced proliferation. *Nat Commun.* 2014;5:3073.
 45. Patterson S, Gross J, Webster AD. DNA probes bind non-specifically to eosinophils during in situ hybridization: carbol chromotrope blocks binding to eosinophils but does not inhibit hybridization to specific nucleotide sequences. *J Virol Methods.* 1989;23(2):105-109.

A high-content cytokine screen identifies myostatin propeptide as a positive regulator of primitive chronic myeloid leukemia cells



Sofia von Palffy,¹ Niklas Landberg,¹ Carl Sandén,¹ Dimitra Zacharaki,² Mansi Shah,³ Naoto Nakamichi,⁴ Nils Hansen,¹ Maria Askmyr,¹ Henrik Lilljebjörn,¹ Marianne Rissler,¹ Christine Karlsson,¹ Stefan Scheduling,^{2,5} Johan Richter,⁵ Connie J. Eaves,⁴ Ravi Bhatia,³ Marcus Järås¹ and Thoas Fioretos¹

¹Division of Clinical Genetics, Department of Laboratory Medicine, Lund University, Lund, Sweden; ²Division of Molecular Hematology, Lund Stem Cell Center, Lund University, Lund, Sweden; ³Division of Hematology, Oncology and Bone Marrow Transplantation, University of Alabama at Birmingham, Birmingham, AL, USA; ⁴Terry Fox Laboratory, British Columbia Cancer Agency, Vancouver, British Columbia, Canada and ⁵Department of Hematology, Oncology and Radiation Physics, Skåne University Hospital, Lund, Sweden

Haematologica 2020
Volume 105(8):2095-2104

ABSTRACT

A aberrantly expressed cytokines in the bone marrow (BM) niche are increasingly recognized as critical mediators of survival and expansion of leukemic stem cells. To identify regulators of primitive chronic myeloid leukemia (CML) cells, we performed a high-content cytokine screen using primary CD34⁺ CD38^{low} chronic phase CML cells. Out of the 313 unique human cytokines evaluated, 11 were found to expand cell numbers ≥ 2 -fold in a 7-day culture. Focusing on novel positive regulators of primitive CML cells, the myostatin antagonist myostatin propeptide gave the largest increase in cell expansion and was chosen for further studies. Herein, we demonstrate that myostatin propeptide expands primitive CML and normal BM cells, as shown by increased colony-forming capacity. For primary CML samples, retention of CD34-expression was also seen after culture. Furthermore, we show expression of *MSTN* by CML mesenchymal stromal cells, and that myostatin propeptide has a direct and instant effect on CML cells, independent of myostatin, by demonstrating binding of myostatin propeptide to the cell surface and increased phosphorylation of STAT5 and SMAD2/3. In summary, we identify myostatin propeptide as a novel positive regulator of primitive CML cells and corresponding normal hematopoietic cells.

Introduction

Chronic myeloid leukemia (CML) is a myeloproliferative neoplasm caused by an acquired 9;22-chromosomal translocation in a hematopoietic stem cell (HSC) resulting in the expression of the BCR-ABL1 fusion protein.¹ The BCR-ABL1 fusion protein is a constitutively active tyrosine kinase and triggers a cascade of aberrant downstream signaling pathways leading to clonal outgrowth of CML cells and subsequent disease manifestation.^{1,2} There is growing evidence to suggest that primitive CML cells affect the bone marrow (BM) niche, contributing to deregulated cytokine levels.³ In CML, several pro-inflammatory cytokines, such as IL-6,^{4,5} IL-1 β ,⁶ and TNF- α ,⁴ have been shown to be up-regulated in patient serum. Cytokines are essential for the function and maintenance of cells, and altered cytokine levels influence not only leukemic cells, but also the normal HSC within the BM. A pro-inflammatory environment is thought to provide a selective advantage for the leukemic stem cells (LSC).⁷ In CML and acute myeloid leukemia (AML), we and others have shown that IL-1 is a positive regulator of LSC, and blocking IL-1 signaling inhibits the LSC.⁸⁻¹⁰ By contrast, chronic exposure to IL-1

Correspondence:

SOFIA VON PALFFY
sofia.von_palffy@med.lu.se

THOAS FIORETOS
thoas.fioretos@med.lu.se

Received: February 26, 2019.

Accepted: September 26, 2019.

Pre-published: October 3, 2019.

doi:10.3324/haematol.2019.220434

Check the online version for the most updated information on this article, online supplements, and information on authorship & disclosures: www.haematologica.org/content/105/8/2095

©2020 Ferrata Storti Foundation

Material published in *Haematologica* is covered by copyright. All rights are reserved to the Ferrata Storti Foundation. Use of published material is allowed under the following terms and conditions:

<https://creativecommons.org/licenses/by-nc/4.0/legalcode>.

Copies of published material are allowed for personal or internal use. Sharing published material for non-commercial purposes is subject to the following conditions:

<https://creativecommons.org/licenses/by-nc/4.0/legalcode>, sect. 3. Reproducing and sharing published material for commercial purposes is not allowed without permission in writing from the publisher.



leads to exhaustion of normal HSC.¹¹ Therefore, inhibition of the pro-inflammatory environment in the disease might have therapeutic potential.⁷ Hence, a better understanding of the autocrine and paracrine signaling important for LSC survival and maintenance will not only be of great importance for characterizing disease biology and progression, but might also translate into the development of novel therapies targeting the LSC.

To identify key positive regulators of CML stem cells, we conducted a high-content cytokine screen on stem cell enriched primary chronic phase CML cells using an arrayed library of 313 unique human cytokines. This screen confirmed the positive regulatory effect of IL-3,^{12,13} IL-1 α / β ,⁸ GM-CSF,¹⁴ IL-6,^{15,16} and IFN- γ ,¹⁷ cytokines previously reported to expand primitive CML cells, and also identified several novel positive regulators. Among the novel positive regulators, we identified myostatin propeptide (MSTNpp), a muscle secreted protein not previously implicated in the regulation of normal or malignant hematopoiesis, and demonstrate that MSTNpp promotes the growth and survival of both primitive CML and normal hematopoietic cells.

Methods

Patient samples and CD34 enrichment

Bone marrow and peripheral blood (PB) from untreated chronic phase CML patients, AML patients or blast crisis CML patients were obtained after written informed consent and in accordance with the Declaration of Helsinki. The Regional Ethics Committee (Dnr 2017/391) approved the study. All cellular chronic phase CML samples included in the study are summarized in the *Online Supplementary Table S1*. For information on cell preparation, see the *Online Supplementary Methods*.

Cytokine screening

Chronic myeloid leukemia PB samples with high IL1RAP expression within the CD34⁺CD38^{low} compartment, correlating with a high fraction of BCR-ABL1 positive cells,^{18,19} were selected for the screen (*Online Supplementary Figure S1*). IL1RAP expression in the CD34⁺CD38^{low} cells was assessed by flow cytometry as previously described.¹⁹ In brief, 500 CD34⁺CD38^{low} cells were sorted into pre-prepared cytokine plates containing 313 unique cytokines, and cell numbers were evaluated after seven days. For detailed information on cytokine library preparation, antibody staining, cell sorting, experimental read out and screen validation, see the *Online Supplementary Methods*.

Cell cultures

In all cell culture experiments, cells were cultured in serum free StemSpan™ SFEM media (Stem Cell Technologies, Canada). Cell numbers were evaluated using CountBright Absolute Counting Beads (Thermo Fisher Scientific, USA) and Draq7 (BioStatus, UK) on a LSR Fortessa (BD Biosciences, USA).

Cell cultures of transgenic BCR-ABL mouse cells

Transgenic *ScltA/BCR-ABL* mice²⁰ were taken off tetracycline pellets to induce CML-like disease. Leukemic mice and age-matched wild-type B6.SJL mice were sacrificed 8-10 weeks post induction. Five thousand Lin⁻Sca-1⁺c-Kit⁺ (LSK) BM cells were sorted into individual wells of a 96-well plate containing 500 ng/mL of MSTNpp (catalog# 12012, lot# 0603297, Peprotech) or no cytokine control, and cell numbers were analyzed after seven days. For detailed information on cell isolation, antibody stain-

ing, sorting, and cell culture see the *Online Supplementary Methods*.

Colony-forming assays

CD34⁺ chronic phase CML cells, CD34⁺CD38^{low} chronic phase CML cells, or equivalent normal BM cells, were cultured for a week with or without cytokine, prior to transfer to H4435 MethoCult (Stem Cell Technologies) according to the manufacturer's instructions. See the *Online Supplementary Methods* for details on readout and colony replating.

Co-culture experiments with primitive chronic myeloid leukemia cells and mesenchymal stromal cells

CD34⁺CD38^{low} CML cells were sorted as described above, and plated onto mesenchymal stromal cells (MSC) established from primary CML BM cells in a 1:5 ratio. Details on MSC cultures and culture conditions can be found in the *Online Supplementary Methods*.

MSTNpp binding experiment

KU812²¹ cells were resuspended in PBS with 2% FBS. Two ug/mL of MSTNpp (catalog# 12012, lot# 0603297, Peprotech) or no cytokine was added together with a polyclonal rabbit IgG anti-MSTNpp antibody (Antibodies-online, USA), and stained on ice in the dark for 30 minutes (min). Cells were washed twice in PBS with 2% FBS, resuspended in goat anti-rabbit BV421 (BD Biosciences) and stained on ice in the dark for another 30 min. After a final wash, cells were analyzed on a LSRFortessa (BD Biosciences). Draq7 (BioStatus) was used as a viability marker.

MSTNpp ELISA

MSTNpp concentrations in PB plasma samples from 12 CML patients and four healthy donors, and BM plasma from five healthy donors, were diluted 1:20 and analyzed using Human Myostatin ELISA (prodomain specific) (BioVendor, Czech Republic) according to the manufacturer's instructions.

MSTN reverse transcriptase-quantitative polymerase chain reaction

Relative *MSTN* expression in CD34⁺ cells, MNC and MSC from CML BM was assessed using reverse transcriptase quantitative polymerase chain reaction (RT-qPCR). For detailed methodology and assays used, see the *Online Supplementary Methods*.

RNA sequencing and gene set enrichment analysis

Regarding the gene set enrichment analysis (GSEA), CD34⁺CD38^{low} (lowest 5% of CD38-expressing cells) cells from PB of five chronic phase CML patients were sorted into flat bottom 96-well plates with or without 500 ng/mL of MSTNpp (Peprotech), with cell numbers ranging from 2,000-11,000 cells, and incubated for 3 h or 24 h. For detailed information on RNA-extraction, cDNA synthesis, library preparation, sequencing and analysis pipeline, see the *Online Supplementary Methods*.

Phospho-flow cytometry

Cells were resuspended in serum free StemSpan™ SFEM medium (Stem Cell Technologies) and incubated for 3 h at 37°C 5% CO₂, prior to 15 min stimulation with 500 ng/mL of MSTNpp (Peprotech) or 10 ng/mL of TGF- β 1 (Peprotech). Following fixation with 1.6% paraformaldehyde for 10 min at room temperature and permeabilization with 90% ethanol at -80°C, cells were stained with phospho-specific antibodies. Details on staining and the antibodies used are described in the *Online Supplementary Methods*.

Statistical analysis

All bar graphs show mean values and standard deviation. Differences between groups were assessed by unpaired Student's *t*-test using Prism 6 software (GraphPad Software, USA).

Results

Cytokine screening identifies MSTNpp as a positive regulator of CD34⁺CD38^{low} chronic myeloid leukemia cells

To identify positive regulators of primitive CML cells, we established a high-content cytokine screen using 313 unique human cytokines (Online Supplementary Table S2). CD34⁺CD38^{low} chronic phase CML PB samples with high

leukemic burden (Online Supplementary Figure S1) were sorted into 384-well plates with one cytokine condition per well. After a 7-day culture, the number of live cells was enumerated with automated fluorescence microscopy (Figure 1A).

In total, we identified 11 cytokines that increased cell numbers at least 2-fold compared to a no cytokine control (Figure 1B). Of these, the cytokines IL-3,^{12,13} IL-1 α /b,⁸ GM-CSF,¹⁴ IL-6,^{15,16} and IFN- γ ¹⁷ have previously been described as positive regulators of CML stem and progenitor cells, thus validating the robustness of the screen. Notably, five cytokines not previously described as positive regulators of CML stem and progenitor cells were identified: MSTNpp, soluble CD14 (sCD14), Interleukin 21 (IL-21), Interleukin 13 variant (IL-13v), and chemokine

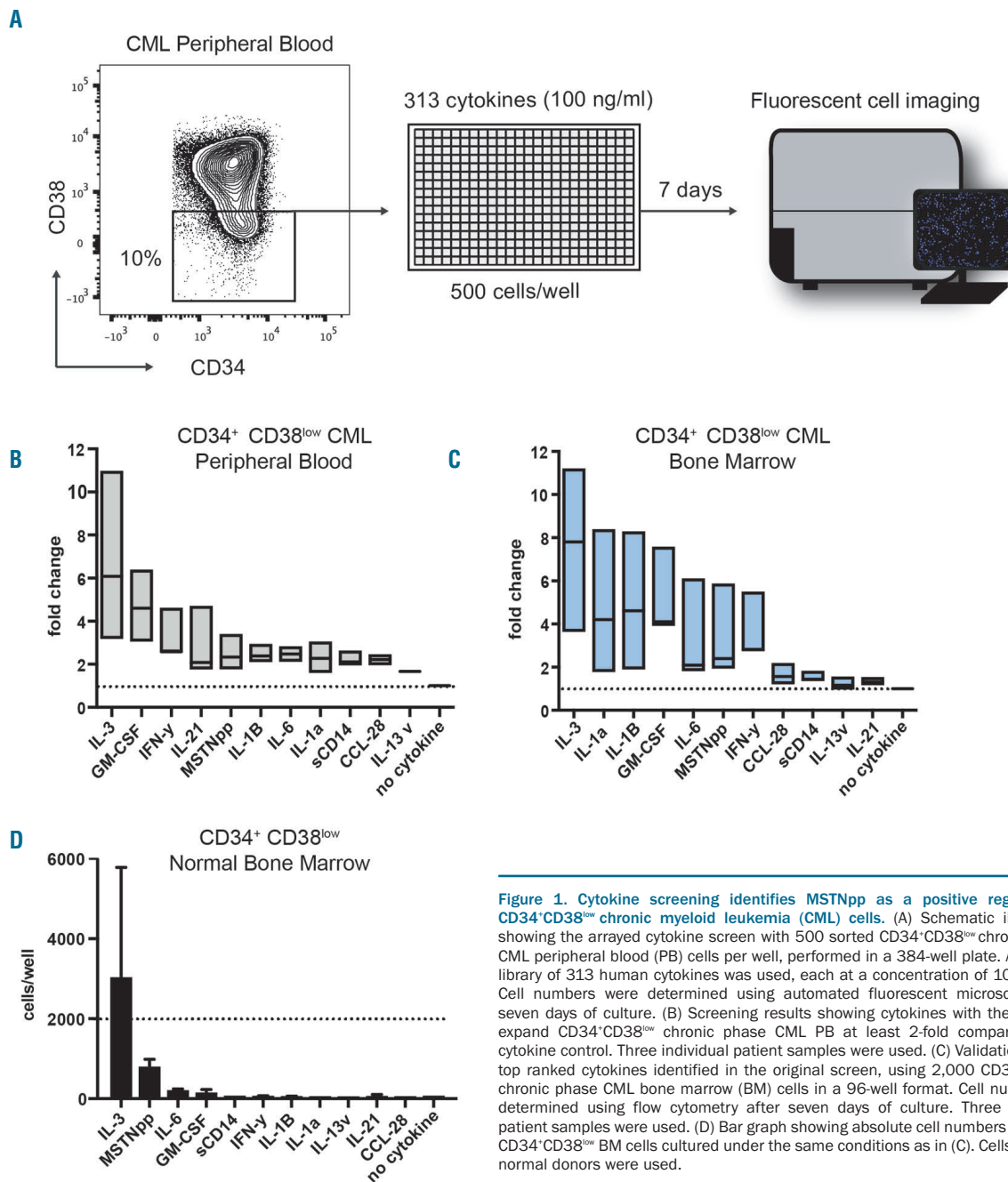


Figure 1. Cytokine screening identifies MSTNpp as a positive regulator of CD34⁺CD38^{low} chronic myeloid leukemia (CML) cells. (A) Schematic illustration showing the arrayed cytokine screen with 500 sorted CD34⁺CD38^{low} chronic phase CML peripheral blood (PB) cells per well, performed in a 384-well plate. A cytokine library of 313 human cytokines was used, each at a concentration of 100 ng/mL. Cell numbers were determined using automated fluorescent microscopy after seven days of culture. (B) Screening results showing cytokines with the ability to expand CD34⁺CD38^{low} chronic phase CML PB at least 2-fold compared to no cytokine control. (C) Validations of the top ranked cytokines identified in the original screen, using 2,000 CD34⁺CD38^{low} chronic phase CML bone marrow (BM) cells in a 96-well format. Cell number was determined using flow cytometry after seven days of culture. Three individual patient samples were used. (D) Bar graph showing absolute cell numbers of normal CD34⁺CD38^{low} BM cells cultured under the same conditions as in (C). Cells from two normal donors were used.

(C-C motif) ligand 28 (CCL28). To investigate whether the positive regulators identified also affected CD34⁺CD38^{low} CML cells from BM, we performed a more focused screen using only the top regulating cytokines in a 96-well format. All cytokines identified as positive regulators of primitive CML PB cells also increased the number of primitive CML BM cells (Figure 1C). However, only IL-3, IL-1 α /b, GM-CSF, IL-6, MSTNpp, and IFN- γ were able to expand cell numbers at least 2-fold, which was used as the cut-off in the original screen.

We next investigated whether the positive regulators identified also expanded normal CD34⁺CD38^{low} BM cells, enriched for HSC (Figure 1D). Whereas IL-3 expanded the normal BM cells during a 7-day culture, none of the other cytokines increased the total cell number. However, MSTNpp promoted their survival, as indicated by a higher cell number compared to the no cytokine control.

MSTNpp increases the progenitor potential of chronic myeloid leukemia and normal bone marrow cells

Of the top regulators identified, we selected MSTNpp for further studies given its strong effect on primary CML cells and its previously unexplored role in normal and malignant hematopoiesis. MSTNpp is produced by muscle cells and secreted into the bloodstream where its recognized function is to bind and regulate the muscle inhibiting myokine myostatin (also known as GDF-8).²² To study the growth dynamics of CML cells in response to different concentrations of MSTNpp, a dose titration experiment was performed on CD34⁺ CML cells. In a 7-day culture, MSTNpp increased the cell number in all treated wells in a dose-dependent manner (Figure 2A), with similar results observed during three days of culture (*Online Supplementary Figure S2A*). Adding a polyclonal anti-MSTNpp antibody to the culture reduced the growth promoting effect of MSTNpp on CML cells, confirming the specificity of the observed response (Figure 2B).

To investigate whether MSTNpp had a positive effect also on primitive murine CML cells, Lin⁻ Sca-1⁺ c-Kit⁺ (LSK) BM cells from transgenic *Scl-tTA/BCR-ABL* mice²⁰ were cultured *in vitro* with or without MSTNpp. In a 7-day culture, MSTNpp greatly increased the cell number compared to untreated cells (Figure 2C). For wild-type murine LSK BM cells from B6.SJL mice, MSTNpp nearly maintained the cell number, hence promoting cell survival compared to no cytokine control (Figure 2D). These results are in agreement with our findings using human CD34⁺CD38^{low} chronic phase CML PB and BM cells (Figure 1B and C), as well as for normal CD34⁺CD38^{low} BM cells (Figure 1D).

Given the robust response of MSTNpp in chronic phase CML, we hypothesized that MSTNpp could have a similar growth promoting effect on other myeloid malignancies. Therefore, we cultured primary blasts from five AML patients and three CD34⁺ blast crisis CML patients with and without MSTNpp, and evaluated the cell numbers at day 3 or 4 and day 7 (*Online Supplementary Figure S2B and C*). Out of the five AML patients tested, two responded to MSTNpp with a slight increase in survival at day 3. At day 7, however, this effect was no longer seen. Another AML patient showed a response to MSTNpp only at day 7, but not at day 3. For the CD34⁺ blast crisis CML cells, one out of the three samples responded to MSTNpp stimulation with increased sur-

vival; the other two, including a sample with a T315I-mutation, did not respond. These results suggest that, unlike chronic phase CML cells, blast crisis CML cells and AML blasts are not consistent in their response to MSTNpp.

Next, we investigated the possible effects of MSTNpp on cellular differentiation of primary human CD34⁺CD38^{low} CML cells. Since CD34 expression, in contrast to CD38 expression, correlates with stem cell activity of *in vitro* cultured cells,^{23,24} we used CD34 as a marker to assess whether the identified cytokines would maintain the CML cells in a primitive state. Notably, whereas cells cultured in IL-3 and GM-CSF displayed reduced CD34 expression, IL-1 α /b, IL-6, and MSTNpp stimulation resulted in retained CD34 expression, suggesting that these cytokines maintained the primitive state of the cells better (Figure 2E).

As CD34 expression of MSTNpp expanded cells was retained in liquid culture, we further investigated whether MSTNpp stimulation promotes the colony forming capacity of CML CD34⁺ cells. To this end, CD34⁺ or CD34⁺CD38^{low} cells were cultured with or without MSTNpp for seven days in serum free media, prior to plating in methylcellulose media. MSTNpp significantly increased the number of CML colonies compared to control cells without cytokine (Figure 2F). Moreover, pre-stimulation with MSTNpp increased the colony output upon replating (Figure 2F), suggesting that MSTNpp expands CML cells with self-renewal capacity.

We also investigated the effects of MSTNpp on the colony forming ability of normal CD34⁺CD38^{low} BM cells after one week in culture. Although MSTNpp did not expand normal CD34⁺CD38^{low} BM cells during a 7-day culture (Figure 1D), MSTNpp had a marked effect on the subsequent colony forming ability of the stimulated cells as compared to no cytokine control (Figure 2G and *Online Supplementary Figure S2D*). These findings show that MSTNpp promotes the colony forming capacity of both CML cells and normal hematopoietic stem and progenitor cells (HSPC).

Finally, to study the effect of MSTNpp on primitive CML cells in a setting that more closely resembles the BM microenvironment, we performed co-culture experiments where CD34⁺CD38^{low} CML cells were cultured on a monolayer of MSC established from primary CML BM (Figure 2H). When cultured on stroma, there were twice as many CML cells in the culture after three days, compared to the no stroma control. This suggests that the CML MSC produce growth factors important for the growth and survival of primitive CML cells. When adding MSTNpp to the co-culture, the cell numbers increased even further (approx. 2-fold), showing that primitive CML cells respond to MSTNpp also in a setting where other stimuli are present. These findings suggest that the effect of MSTNpp on CML cells is physiologically relevant.

MSTNpp affects chronic myeloid leukemia cells through mechanisms independent of myostatin

Myostatin is a transforming growth factor beta (TGF- β) superfamily member,²⁵ synthesized as part of the myostatin gene (*MSTN*) and produced primarily by muscle cells. The *MSTN* gene encodes a biologically-inactive precursor protein consisting of a signaling peptide, the MSTNpp-domain and the myostatin-domain. Proteolytic

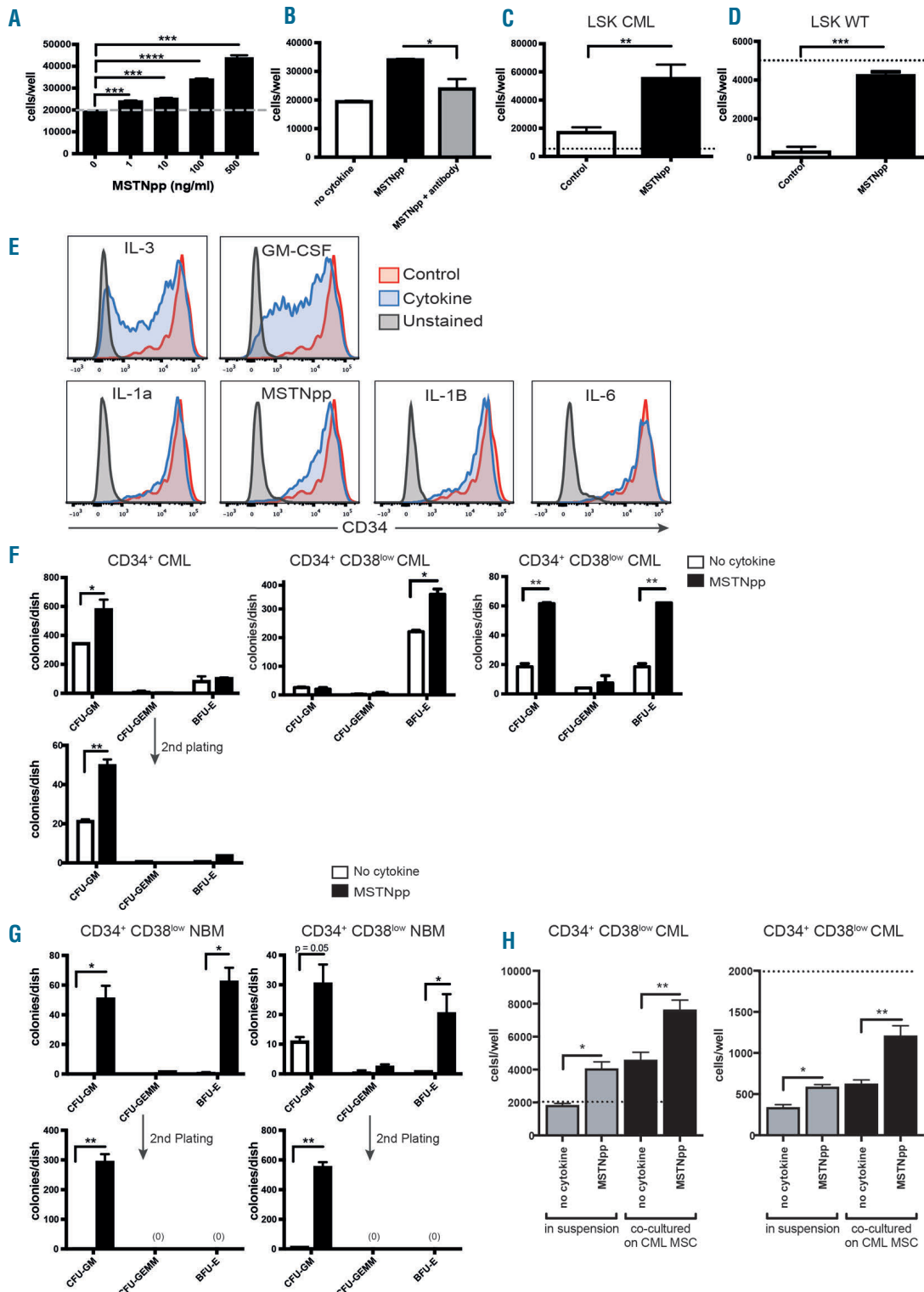


Figure 2. MSTNpp increases progenitor potential of chronic myeloid leukemia (CML) and normal bone marrow (BM) cells. (A) Bar graph showing total cell numbers of CD34⁺ chronic phase CML cells from a single patient after 7-day culture with increasing concentrations of MSTNpp. The dotted line indicates the number of seeded cells at day 0 (n=3). (B) Bar graph showing total cell numbers after culture of 100 ng/mL of MSTNpp with a polyclonal anti-MSTNpp antibody. The same cells and culturing conditions as in (A) were used (n=3). (C) Bar graph showing absolute cell numbers of Lin⁻Sca-1⁺c-Kit⁺ (LSK) BM cells from *ScfIT/BCR-ABL* mice after 7-day culture with or without 500 ng/mL of MSTNpp (n=3). (D) Bar graph showing total cell numbers of LSK BM cells from WT B6.SJL mice after 7-day culture with or without 500 ng/mL of MSTNpp (n=3). (E) Representative histograms showing CD34 expression of CD34⁺CD38^{low} chronic phase CML BM cells after a 7-day culture with indicated cytokines. (F) Colony type and number of chronic phase CD34⁺ and CD34⁺ CD38^{low} CML cells, pre-cultured for seven days with or without 500 ng/mL of MSTNpp prior to plating in methylcellulose. A cell equivalent of 500 starting cells was plated. Three individual patient samples were used in triplicates. Replating was performed after two weeks in colony culture for one of the samples. No colonies were seen after the 3rd replating. (G) Colony type and number of CD34⁺CD38^{low} normal BM cells using the same experimental setup as in (F). Cells from two normal donors were used in triplicates. (H) Bar graph showing total cell numbers of CD34⁺ CD38^{low} CML cells after 3-day culture with and without 100 ng/mL of MSTNpp. Gray bars: cells cultured in suspension; black bars: cells co-cultured with CML mesenchymal stromal cells (MSC). Two individual patient samples were used in triplicates. The dotted line indicates the number of seeded cells. *P<0.05, **P<0.01, ***P<0.001 and ****P<0.0001. WT: wild type.

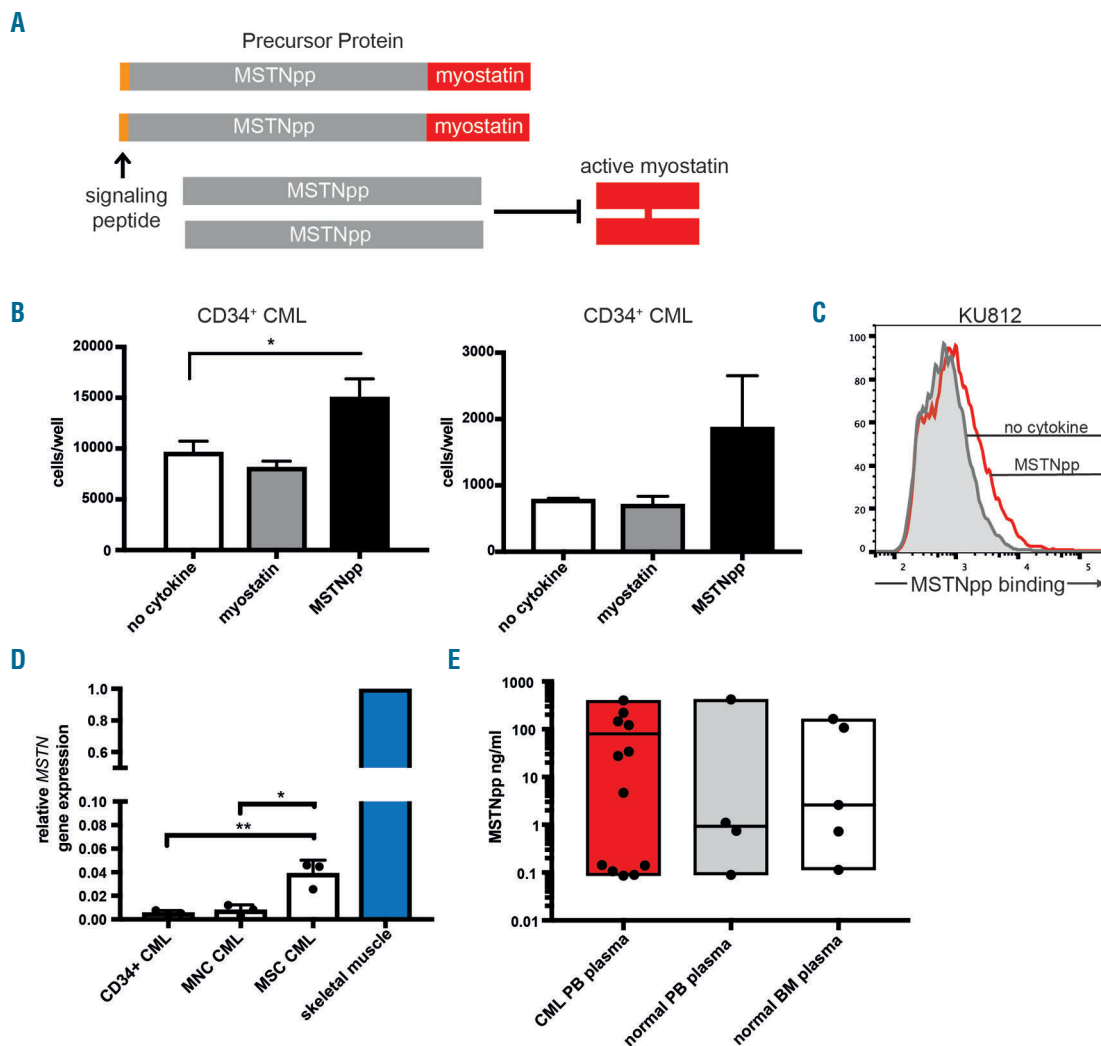


Figure 3. MSTNpp acts through mechanisms independent of myostatin in chronic myeloid leukemia (CML) and is produced by CML mesenchymal stromal cells (MSC). (A) Schematic illustration showing the MSTN precursor protein before and after enzymatic cleavage, generating MSTNpp and myostatin. (B) Bar graphs showing total cell numbers of CD34⁺ chronic phase CML cells after 7-day culture with 100 ng/mL of myostatin, 100 ng/mL of MSTNpp or no cytokine control. Two individual patient samples were used in triplicates. (C) Histogram showing binding of MSTNpp to the surface of KU812 cells, as compared to no cytokine control. (D) Bar graph showing relative *MSTN* gene expression of CD34⁺ cells, mononuclear cells (MNC) and cultured MSC from three chronic phase CML patients, in relation to expression in human skeletal muscle. (E) MSTNpp concentration in plasma of peripheral blood (PB) from 12 chronic phase CML patients, PB from four healthy donors and bone marrow (BM) from five healthy donors. The middle line in each bar indicates the mean plasma concentration. * $P \leq 0.05$; ** $P \leq 0.01$.

cleavage of the precursor protein generates active and circulating MSTNpp and myostatin. Active myostatin is antagonized by MSTNpp by forming a latent complex which prevents binding of myostatin to its receptor (Figure 3A).²² To explore the mechanism by which MSTNpp exerts its growth promoting effects on CML cells, we first investigated if MSTNpp acts by blocking the activity of myostatin. CML CD34⁺ cells were cultured for seven days with or without myostatin and MSTNpp (Figure 3B). No difference in cell number was seen between myostatin cultured cells as compared to a no cytokine control, whereas MSTNpp, serving as a positive control, increased the total cell number. This finding indicates that myostatin does not exert a negative effect on CML-progenitor cell growth, suggesting that MSTNpp does not promote CML cells by inhibiting myostatin, but through another mechanism.

To investigate the possibility that MSTNpp acts direct-

ly on CML cells by binding to a receptor on the cell surface, KU812 cells were incubated with an anti-MSTNpp antibody together with MSTNpp, or with anti-MSTNpp antibody only, and analyzed by flow cytometry. MSTNpp was found to bind to the cell surface, as a shift in fluorescence intensity was observed when both MSTNpp and the anti-MSTNpp antibody were added to the cells (Figure 3C).

MSTNpp is produced by chronic myeloid leukemia mesenchymal stromal cells and is present in the plasma of chronic myeloid leukemia patients

It is known that MSTNpp is produced by muscle cells²⁶ and is present in the blood of healthy individuals.^{27,28} To investigate whether the leukemic cells or the MSC within the marrow are another source of MSTNpp, we performed a *MSTN* RT-qPCR on CD34⁺ cells and MNC from primary CML patients, as well as on cultured MSC from

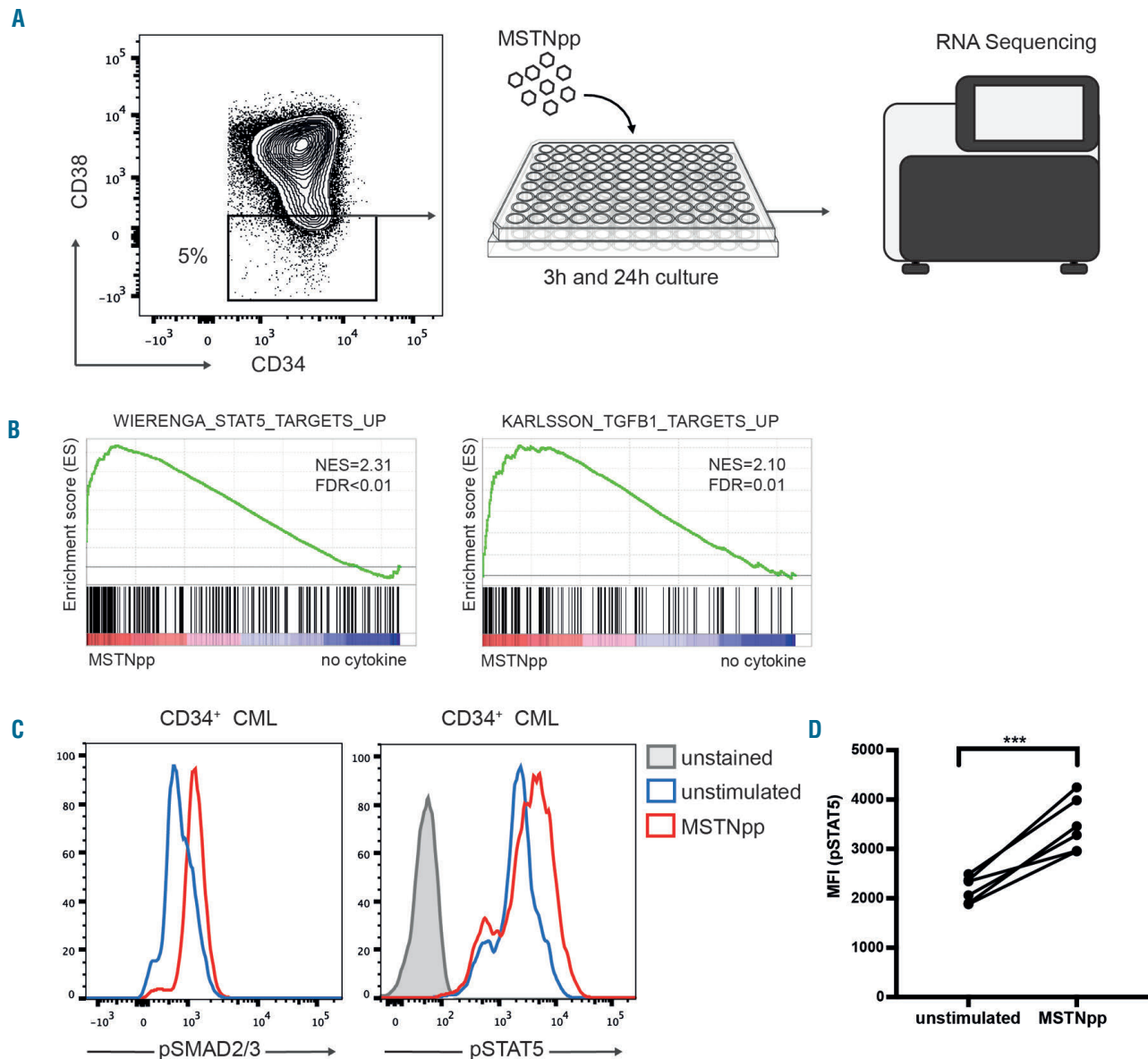


Figure 4. MSTNpp stimulation activates STAT5 and SMAD2/3 in chronic myeloid leukemia (CML) cells. (A) Schematic illustration of the RNA-sequencing experiment: CD34⁺ CD38^{low} chronic phase CML cells from five individual patient samples were sorted and cultured for 3 hours (h) and 24 h with or without MSTNpp prior to RNA-extraction and sequencing. (B) Gene set enrichment assay (GSEA) showing upregulation of STAT5 and TGF- β 1 target genes after 3 h MSTNpp stimulation. (C) Histograms showing activation of SMAD2/3 and STAT5 after 15 minutes stimulation with MSTNpp in CD34⁺ chronic phase CML cells, compared to unstimulated control. Unstained cells in gray, unstimulated cells in blue, and MSTNpp stimulated cells in red. (D) Median fluorescence intensity (MFI) of pSTAT5 with or without MSTNpp stimulation. Paired samples from six individual CD34⁺ chronic phase CML patient samples are shown. *** $P < 0.001$. NES: normalized enrichment score; FDR: false discovery rate.

the same patients (Figure 3D). All cell fractions tested expressed the *MSTN* gene, with the highest expression in MSC. Although the expression levels were approximately 20x lower in MSC than in skeletal muscle, these data suggest that the MSC in the BM are another source of MSTNpp, possibly contributing to the growth and survival of CML cells.

To evaluate whether the MSTNpp levels are different in leukemic and healthy individuals, we performed a MSTNpp specific ELISA on plasma from CML patients and healthy individuals (Figure 3E), as well as on plasma from healthy BM aspirates. All samples showed detectable levels of MSTNpp, but there was no significant

difference between MSTNpp levels in CML patients *versus* normal individuals. Moreover, the concentrations of MSTNpp varied greatly depending on the patient/donor, with levels ranging from ~0.1-400 ng/mL. As CML cells respond to MSTNpp even at 1 ng/mL (Figure 2A), the MSTNpp concentrations in the plasma from CML patients are within physiologically relevant levels for the leukemic cells

MSTNpp stimulation activates STAT5 and SMAD2/3 in chronic myeloid leukemia cells

To search for cellular programs and signaling pathways transcriptionally regulated by MSTNpp in primitive CML

cells, we performed RNA-sequencing following 3-h and 24-h culture of CD34⁺CD38^{low} cells with or without MSTNpp (Figure 4A). After 3 h, 147 genes were significantly up-regulated and 115 genes were significantly down-regulated in the MSTNpp stimulated cells compared to the non-stimulated control cells (FDR<0.01) (*Online Supplementary Table S3*). After 24 h, there were fewer differentially expressed genes, with 56 up-regulated genes and only 14 genes down-regulated (FDR<0.01) (*Online Supplementary Table S3*). To explore whether MSTNpp stimulation activates specific downstream pathways in CML cells, we performed GSEA. Following 3 h stimulation with MSTNpp, an enrichment of STAT5 target genes was observed (Figure 4B). In addition, MSTNpp, which is a TGF- β superfamily member, induced a significant enrichment of TGF- β 1 target genes both after 3 h and after 24 h (Figure 4B and *Online Supplementary Figure S3A*). After 24 h, genes associated with cell cycle and DNA-replication were also enriched (*Online Supplementary Figure S3A*), consistent with the increased proliferative response seen after stimulation by MSTNpp (Figures 1B and C and 2A and *Online Supplementary Figure S2A*).

Given that MSTNpp stimulation resulted in enrichment of STAT5 and the TGF- β 1 target genes, we performed phospho-flow cytometry of STAT5 and SMAD2/3 in CD34⁺ chronic phase CML cells. Already 15 min following MSTNpp stimulation, we observed an increase in the phosphorylation levels of STAT5 and SMAD2/3 (Figure 4C and D and *Online Supplementary Figures S3B and S4*). Interestingly, the MSTNpp-induced activation of SMAD2/3 was similar to that of TGF- β 1 (*Online Supplementary Figure S3C*), one of the well-known activators of SMAD2 and SMAD3.²⁹ However, culturing CD34⁺ CML cells with TGF- β 1 reduced cell numbers (*Online Supplementary Figure S3D*), whereas MSTNpp stimulation resulted in growth-promoting effects (Figure 2A and *Online Supplementary Figure S2A*). When an additional panel of phospho-antibodies was tested to evaluate changes in MAPK-pathways (pP38, pJNK and pERK1/2),³⁰ IL-1 signaling (NF- κ B and pAkt)^{31,32} and general phosphotyrosine activation (pTyr)³³ (*Online Supplementary Figure S4*), signaling pathways associated with cell proliferation and cancer,^{8,32,34} no changes were detected for any of these markers.

Discussion

Deregulation of cytokines in the BM niche is thought to play a major role in leukemic disease progression, with altered cytokine levels promoting the growth of LSC while suppressing normal HSC.^{7,35,36} In CML, a transgenic *BCR-ABL1* mouse model revealed extensive remodeling of the BM along with altered cytokine and chemokine levels, secreted both by proximal stroma cells and leukemic cells.³⁷ CML cells also produce and respond to autocrine stimulation by IL-3 and granulocyte-colony stimulating factor (G-CSF),¹⁵ and recent work by our group and others have highlighted IL-1 as a positive regulator of CML LSC.^{8,9} Hence, increased understanding of the cytokine-receptor interactions and signaling pathways activated in the immature cell population of both CML and normal BM cells might reveal disease dependencies that could translate into new treatment opportuni-

ties in CML and other malignancies.

We here conducted a high-content cytokine screen with the purpose of finding novel positive regulators of primitive CML cells. Previous studies have mainly investigated the effects on CML cells of single or a restricted set of cytokines.^{8,9,13,38,39} With a library of 313 cytokines screened, we identified 11 cytokines that at least doubled the cell number over seven days compared to no cytokine control. The screen confirmed the growth-promoting effect of IL-3,^{12,13} IL-1 α/β ,⁸ GM-CSF,¹⁴ IL-6,^{15,16} and IFN- γ ¹⁷ for CD34⁺CD38^{low} PB and BM chronic phase CML cells. The screen also identified five cytokines not previously reported to be important for CML; MSTNpp, sCD14, IL-21 and IL-13v, and CCL-28. Out of these novel cytokines, the TGF- β superfamily member MSTNpp was the most potent in promoting the growth of primitive CML cells.

Previously, most studies of MSTNpp had been carried out in the context of muscle physiology where it regulates the muscle inhibiting myokine myostatin.^{22,40} By binding free myostatin in the blood, MSTNpp hinders myostatin from binding to activin receptors and activating muscle wasting programs in the cell.^{22,41} Recently, it was also shown that MSTNpp can bind directly to activin receptors on muscle cells, blocking access by myostatin, and thus providing another mechanism of myostatin inhibition.⁴⁰ No studies describing MSTNpp effects independent of myostatin have been previously reported. However, our data strongly suggest that MSTNpp has a direct effect on hematopoietic cells, by binding to a receptor on the cell surface independently of myostatin. This conclusion is based on the following observations; the *in vitro* screen was performed in serum-free media with no myostatin present, and addition of myostatin had no adverse effects on the growth of CML cells. Therefore, the mechanism by which MSTNpp acts in normal and malignant hematopoiesis seems to differ from what has previously been described in muscle cells. Further, we confirmed that MSTNpp is present in the plasma of CML patients and normal individuals, and demonstrate for the first time that MSC, MNC and CD34⁺ cells from CML patients express *MSTN*. Out of these cell types, MSC expressed the highest levels of *MSTN*. Importantly, even though there was no difference in MSTNpp plasma concentration between the two groups, primitive CML cells are more responsive to MSTNpp stimulation than corresponding normal cells.

MSTNpp stimulation of chronic phase CML CD34⁺CD38^{low} cells greatly increased the number of cells in culture without loss of CD34-expression, suggesting that MSTNpp expands the primitive cells while keeping them in an immature state. This finding was further strengthened by colony-forming assays, where MSTNpp pre-stimulation increased the number of colonies of both CML and normal BM cells. This indicates that the growth promoting effect of MSTNpp is not restricted to CML cells, but also applies to normal hematopoietic stem and progenitor cells (HSPC). Whether MSTNpp would elicit a differential regulatory effect on primary CML LSC compared to normal HSC *in vivo* is difficult to assess, given that primary CML cells engraft poorly in immunodeficient mice.

The observation that MSTNpp stimulation expanded primitive CML cells and resulted in the activation of both STAT5 and SMAD2/3 is intriguing, as these signaling pathways are associated with different cellular effects. By

stimulation with TGF- β 1, we found SMAD2/3 phosphorylation as well as reduced growth and survival of primary CD34⁺ CML cells. This suggests that MSTNpp-induced SMAD2/3 activation is an unlikely cause of the growth-promoting effects. Instead, the increased STAT5 phosphorylation is a probable mechanism by which MSTNpp expands primitive CML cells. Although STAT5 phosphorylation was high in the unstimulated control cells (consistent with STAT5 being a well-known mediator and downstream target of the BCR-ABL1 fusion in CML)^{2,42} MSTNpp stimulation further activated STAT5. However, cross-talk between STAT5, TGF- β family signaling members and other signaling pathways might also contribute to the growth-promoting effects of MSTNpp in primitive CML cells.

In conclusion, we here identify several novel positive regulators of primitive CML cells using a high-content cytokine screen. We show that the myostatin antagonist MSTNpp binds to the surface of CML cells, induces activation of STAT5 and SMAD2/3, and has a previously unrecognized growth-promoting effect on primitive CML cells and corresponding normal cells. Further studies are needed to investigate whether interfering with MSTNpp

would translate into new therapeutic opportunities in CML.

Acknowledgments

We wish to thank Anna Hammarberg and the Multipark Cellomics Platform, Lund University, Lund, for help with the screening. We also thank Drs. Henrik Hjort-Hansen and Kourosh Lofti and the Nordic CML Study Group for providing clinical samples and patient characteristics.

Funding

This work was supported by the Swedish Cancer Society, the Swedish Children's Cancer Foundation, the Medical Faculty of Lund University, the Swedish Research Council, the ISREC Foundation by a joint grant to Swiss Cancer Center, Lusanne, CREATE Health Cancer Center, from the Biltrema foundation, the Medical Faculty of Lund University and the Knut and Alice Wallenberg Foundation. Grant support was also received from a Terry Fox Foundation New Frontiers Program Project (#1074), a Stem Cell Network of Centres of Excellence grant (#F17/DT2), and grants from the Canadian Cancer Society Research Institute (#704257 and #705047) and the Leukemia & Lymphoma Society of Canada (#417871).

References

- Ren R. Mechanisms of BCR-ABL in the pathogenesis of chronic myelogenous leukaemia. *Nat Rev Cancer*. 2005;5(3):172-183.
- Holyoake TL, Vetrie D. The chronic myeloid leukemia stem cell: stemming the tide of persistence. *Blood*. 2017;129(12):1595-1606.
- Schepers K, Campbell TB, Passegue E. Normal and leukemic stem cell niches: insights and therapeutic opportunities. *Cell Stem Cell*. 2015;16(3):254-267.
- Nievergall E, Reynolds J, Kok CH, et al. TGF- α and IL-6 plasma levels selectively identify CML patients who fail to achieve an early molecular response or progress in the first year of therapy. *Leukemia*. 2016;30(6):1263-1272.
- Anand M, Chodda SK, Parikh PM, Nadkarni JS. Abnormal levels of proinflammatory cytokines in serum and monocyte cultures from patients with chronic myeloid leukemia in different stages, and their role in prognosis. *Hematol Oncol*. 1998;16(4):143-154.
- Wetzler M, Kurzrock R, Estrov Z, et al. Altered levels of interleukin-1 beta and interleukin-1 receptor antagonist in chronic myelogenous leukemia: clinical and prognostic correlates. *Blood*. 1994;84(9):3142-3147.
- Pollyea DA, Jordan CT. Therapeutic targeting of acute myeloid leukemia stem cells. *Blood*. 2017;129(12):1627-1635.
- Agerstam H, Hansen N, von Palffy S, et al. IL1RAP antibodies block IL-1-induced expansion of candidate CML stem cells and mediate cell killing in xenograft models. *Blood*. 2016;128(23):2683-2693.
- Zhang B, Chu S, Agarwal P, et al. Inhibition of interleukin-1 signaling enhances elimination of tyrosine kinase inhibitor-treated CML stem cells. *Blood*. 2016;128(23):2671-2682.
- Agerstam H, Karlsson C, Hansen N, et al. Antibodies targeting human IL1RAP (IL1R3) show therapeutic effects in xenograft models of acute myeloid leukemia. *Proc Natl Acad Sci U S A*. 2015;112(34):10786-10791.
- Pietras EM, Mirantes-Barbeito C, Fong S, et al. Chronic interleukin-1 exposure drives haematopoietic stem cells towards precocious myeloid differentiation at the expense of self-renewal. *Nat Cell Biol*. 2016;18(6):607-618.
- Jiang X, Fujisaki T, Nicolini F, et al. Autonomous multi-lineage differentiation in vitro of primitive CD34⁺ cells from patients with chronic myeloid leukemia. *Leukemia*. 2000;14(6):1112-1121.
- Jiang X, Lopez A, Holyoake T, Eaves A, Eaves C. Autocrine production and action of IL-3 and granulocyte colony-stimulating factor in chronic myeloid leukemia. *Proc Natl Acad Sci U S A*. 1999;96(22):12804-12809.
- Emanuel PD, Bates LJ, Castleberry RP, Gualtieri RJ, Zuckerman KS. Selective hypersensitivity to granulocyte-macrophage colony-stimulating factor by juvenile chronic myeloid leukemia hematopoietic progenitors. *Blood*. 1991;77(5):925-929.
- Welner Robert S, Amabile G, Bararia D, et al. Treatment of Chronic Myelogenous Leukemia by Blocking Cytokine Alterations Found in Normal Stem and Progenitor Cells. *Cancer Cell*. 2015;27(5):671-681.
- Reynaud D, Pietras E, Barry-Holson K, et al. IL-6 controls leukemic multipotent progenitor cell fate and contributes to chronic myelogenous leukemia development. *Cancer Cell*. 2011;20(5):661-673.
- Schurch C, Riether C, Amrein MA, Ochsenschein AF. Cytotoxic T cells induce proliferation of chronic myeloid leukemia stem cells by secreting interferon-gamma. *J Exp Med*. 2013;210(3):605-621.
- Jaras M, Johnels P, Hansen N, et al. Isolation and killing of candidate chronic myeloid leukemia stem cells by antibody targeting of IL-1 receptor accessory protein. *Proc Natl Acad Sci U S A*. 2010;107(37):16280-16285.
- Landberg N, Hansen N, Askmyr M, et al. IL1RAP expression as a measure of leukemic stem cell burden at diagnosis of chronic myeloid leukemia predicts therapy outcome. *Leukemia*. 2016;30(1):253-257.
- Koschmieder S, Gottgens B, Zhang P, et al. Inducible chronic phase of myeloid leukemia with expansion of hematopoietic stem cells in a transgenic model of BCR-ABL leukemogenesis. *Blood*. 2005;105(1):324-334.
- Kishi K. A new leukemia cell line with Philadelphia chromosome characterized as basophil precursors. *Leuk Res*. 1985;9(3):381-390.
- Han HQ, Zhou X, Mitch WE, Goldberg AL. Myostatin/activin pathway antagonism: molecular basis and therapeutic potential. *Int J Biochem Cell Biol*. 2013;45(10):2333-2347.
- von Laer D, Corovic A, Vogt B, et al. Loss of CD38 antigen on CD34⁺CD38⁺ cells during short-term culture. *Leukemia*. 2000;14(5):947-948.
- Boitano AE, Wang J, Romeo R, et al. Aryl hydrocarbon receptor antagonists promote the expansion of human hematopoietic stem cells. *Science*. 2010;329(5997):1345-1348.
- McPherron AC, Lawler AM, Lee SJ. Regulation of skeletal muscle mass in mice by a new TGF- β superfamily member. *Nature*. 1997;387(6623):83-90.
- Schuelke M, Wagner KR, Stolz LE, et al. Myostatin mutation associated with gross muscle hypertrophy in a child. *N Engl J Med*. 2004;350(26):2682-2688.
- Furhata T, Kinugawa S, Fukushima A, et al. Serum myostatin levels are independently associated with skeletal muscle wasting in patients with heart failure. *Int J Cardiol*. 2016;220:483-487.
- Han DS, Huang CH, Chen SY, Yang WS. Serum reference value of two potential doping candidates-myostatin and insulin-like growth factor-I in the healthy young male. *J Int Soc Sports Nutr*. 2017;14:2.
- Blank U, Karlsson S. The role of Smad sig-

- naling in hematopoiesis and translational hematology. *Leukemia*. 2011;25(9):1379-1388.
30. Zhang W, Liu HT. MAPK signal pathways in the regulation of cell proliferation in mammalian cells. *Cell Res*. 2002;12(1):9-18.
 31. DiDonato JA, Mercurio F, Karin M. NF-kappaB and the link between inflammation and cancer. *Immunol Rev*. 2012;246(1):379-400.
 32. Multhoff G, Molls M, Radons J. Chronic inflammation in cancer development. *Front Immunol*. 2011;2:98.
 33. Blume-Jensen P, Hunter T. Oncogenic kinase signalling. *Nature*. 2001;411(6835):355-365.
 34. Hanahan D, Weinberg RA. Hallmarks of cancer: the next generation. *Cell*. 2011;144(5):646-674.
 35. Mirantes C, Passetgue E, Pietras EM. Pro-inflammatory cytokines: emerging players regulating HSC function in normal and diseased hematopoiesis. *Exp Cell Res*. 2014;329(2):248-254.
 36. Schepers K, Pietras EM, Reynaud D, et al. Myeloproliferative neoplasia remodels the endosteal bone marrow niche into a self-reinforcing leukemic niche. *Cell Stem Cell*. 2013;13(3):285-299.
 37. Zhang B, Ho YW, Huang Q, et al. Altered microenvironmental regulation of leukemic and normal stem cells in chronic myelogenous leukemia. *Cancer Cell*. 2012;21(4):577-592.
 38. Bhatia R, Munthe HA, Williams AD, Zhang F, Forman SJ, Slovak ML. Chronic myelogenous leukemia primitive hematopoietic progenitors demonstrate increased sensitivity to growth factor-induced proliferation and maturation. *Exp Hematol*. 2000;28(12):1401-1412.
 39. Bedi A, Griffin CA, Barber JP, et al. Growth factor-mediated terminal differentiation of chronic myeloid leukemia. *Cancer Res*. 1994;54(21):5535-5538.
 40. Ohsawa Y, Takayama K, Nishimatsu S, et al. The Inhibitory Core of the Myostatin Prodomain: Its Interaction with Both Type I and II Membrane Receptors, and Potential to Treat Muscle Atrophy. *PLoS One*. 2015;10(7):e0133713.
 41. Chen JL, Walton KL, Al-Musawi SL, et al. Development of novel activin-targeted therapeutics. *Mol Ther*. 2015;23(3):434-444.
 42. Hantschel O, Warsch W, Eckelhart E, et al. BCR-ABL uncouples canonical JAK2-STAT5 signaling in chronic myeloid leukemia. *Nat Chem Biol*. 2012;8(3):285-293.

Tuning mTORC1 activity dictates the response of acute myeloid leukemia to LSD1 inhibition

Amal Kamal Abdel-Aziz,^{1,2} Isabella Pallavicini,¹ Elena Ceccacci,¹ Giuseppe Meroni,³ Mona Kamal Saadeldin,^{1,4} Mario Varasi³ and Saverio Minucci^{1,5}

¹Department of Experimental Oncology, IEO, European Institute of Oncology IRCCS, Milan, Italy; ²Department of Pharmacology and Toxicology, Faculty of Pharmacy, Ain Shams University, Cairo, Egypt; ³Experimental Therapeutics IFOM-FIRC Institute of Molecular Oncology Foundation, Milan, Italy; ⁴Faculty of Biotechnology, October University for Modern Sciences and Arts, 6th October City, Cairo, Egypt and ⁵Department of Biosciences, University of Milan, Milan, Italy



Haematologica 2020
Volume 105(8):2105-2117

ABSTRACT

Lysine specific demethylase-1 (LSD1) has been shown to be critical in acute myeloid leukemia (AML) pathogenesis and this has led to the development of LSD1 inhibitors (LSD1i) which are currently tested in clinical trials. Nonetheless, preclinical studies reported that AML cells frequently exhibit intrinsic resistance to LSD1 inhibition, and the molecular basis for this phenomenon is largely unknown. We explored the potential involvement of mammalian target of rapamycin (mTOR) in mediating the resistance of leukemic cells to LSD1i. Strikingly, unlike sensitive leukemias, mTOR complex 1 (mTORC1) signaling was robustly triggered in resistant leukemias following LSD1 inhibition. Transcriptomic, chromatin immunoprecipitation and functional studies revealed that insulin receptor substrate 1 (IRS1)/extracellular-signal regulated kinases (ERK1/2) signaling critically controls LSD1i induced mTORC1 activation. Notably, inhibiting mTOR unlocked the resistance of AML cell lines and primary patient-derived blasts to LSD1i both *in vitro* and *in vivo*. In conclusion, mTOR activation might act as a novel pro-survival mechanism of intrinsic as well as acquired resistance to LSD1i, and combination regimens co-targeting LSD1/mTOR could represent a rational approach in AML therapy.

Introduction

Among the novel epigenetic druggable targets in acute myeloid leukemia (AML) therapy, lysine specific histone demethylase 1 (LSD1) has gained attention based on its preferential overexpression in primary AML compared to normal hematopoietic stem and progenitor cells.^{1,2} In cooperation with the oncogenic MLL-AF9 fusion protein, LSD1 actively sustains AML maintenance.³ Moreover, LSD1 inhibition reactivates an all-trans-retinoic acid (ATRA)-dependent differentiation pathway in AML.⁴ LSD1 overexpression has also been associated with poor prognosis in various types of tumors including colon and lung cancers.^{5,6} Mechanistically, LSD1 is a flavin adenine dinucleotide (FAD)-dependent amine oxidase that specifically removes mono- or dimethylated histone H3K4 and H3K9 resulting in context-specific transcriptional repression and activation respectively.⁷ Apart from chromatin, LSD1 demethylates and hence regulates a wide array of non-histone targets.^{8,9} All these activities account for the role of LSD1 in regulating tumor proliferation, metastasis and metabolism.^{2,10,11} We and others have developed LSD1 inhibitors (LSD1i) with potent and selective biochemical profiles and some of which are currently evaluated in clinical trials.¹²⁻¹⁵ Nonetheless, the preclinical antileukemic activity of LSD1i as a monotherapy is relatively modest.^{16,17} In solid tumors, specific DNA methylation signatures correlated with the sensitivity to LSD1i.¹⁶ However, the molecular mechanisms underlying the differential responsiveness of AML to LSD1i remain largely unknown.

Correspondence:

SAVERIO MINUCCI
saverio.minucci@ieo.it

Received: April 19, 2019.

Accepted: September 16, 2019.

Pre-published: September 19, 2019.

doi:10.3324/haematol.2019.224501

Check the online version for the most updated information on this article, online supplements, and information on authorship & disclosures: www.haematologica.org/content/105/8/2105

©2020 Ferrata Storti Foundation

Material published in *Haematologica* is covered by copyright. All rights are reserved to the Ferrata Storti Foundation. Use of published material is allowed under the following terms and conditions:

<https://creativecommons.org/licenses/by-nc/4.0/legalcode>.

Copies of published material are allowed for personal or internal use. Sharing published material for non-commercial purposes is subject to the following conditions:

<https://creativecommons.org/licenses/by-nc/4.0/legalcode>, sect. 3. Reproducing and sharing published material for commercial purposes is not allowed without permission in writing from the publisher.



Mammalian target of rapamycin (mTOR) signaling is frequently hyperactive in AML.¹⁸ mTOR exists in two distinct complexes; mTORC1 and mTORC2. mTORC1 primarily acts on substrates (as p70 S6 kinase) which controls glycolysis, protein synthesis and lipogenesis.¹⁹ mTORC2 regulates actin rearrangement, metabolism and survival (acting on substrates such as AKT).²⁰ Inactivating mTORC1 significantly prolongs the survival of mice transplanted with MLL-AF9 expressing AML cells.²¹ We and others have previously demonstrated that mTOR activation acts as a fundamental adaptive response exploited by cancer cells to evade the cytotoxic stimuli triggered by several anticancer drugs including epigenetic therapies.²²⁻²⁴ Therefore, in this study, we investigated the potential implication of mTOR in mediating the sensitivity/resistance of AML cells to LSD1i.

Methods

Cell lines and cell culture

AML cell lines were obtained from either DSMZ or ATCC. KASUMI-1, NB4 and THP-1 cells were cultured in RPMI-1640 media supplemented with 2 mM L-glutamine, 10% FBS and 1% penicillin-streptomycin. SKNO-1 cells were cultured in RPMI-1640 media supplemented with 10% FBS, 2 mM L-glutamine, 10 ng/mL GM-CSF and 1% penicillin-streptomycin. UF1 cells were cultured in RPMI-1640 media supplemented with 20% FBS and 2 mM L-glutamine. OCI-AML3 cells were cultured in α -MEM media supplemented with 20% FBS, 2 mM L-glutamine, and 1% penicillin-streptomycin. PhoenixTM-Ampho cells were cultured in DMEM media supplemented with 2 mM L-glutamine, 10% FBS and 1% penicillin-streptomycin. Cells were maintained in a humidified tissue culture incubator at 37°C with 5% CO₂.

Primary patient-derived AML blast and cord blood-derived CD34⁺ cells

A primary human AML sample (referred to as AML-IEO20; t(9;11);NPM WT;FLT3 WT) was obtained from the IEO Biobank according to the procedures approved by the Ethical Committee of the European Institute of Oncology. Mononuclear cells were isolated from the peripheral blood/bone marrow samples by Ficoll density centrifugation. For *ex vivo* studies, AML-IEO20 cells (passage no. 3, $\geq 90\%$ human leukemic blasts) were thawed and cultured in RPMI-1640 medium supplemented with 20% FBS, 1% S637 and 2mM L-glutamine. Primary human cord blood-derived CD34⁺ (non-transduced and hMLL-AF9 transduced) cells were cultured in HPGMTM Hematopoietic Growth Medium supplemented with 10% FBS, 2 mM L-glutamine, 100 ng/mL SCF, 100 ng/mL FLT3 and 100 ng/mL thrombopoietin. Before proceeding with *in vitro* experiments, cryopreserved cells were allowed to recover for at least three days.

In vivo studies

DDP38003 was dissolved in vehicle (40% PEG-400 in 5% glucose solution). A stock solution of rapamycin (10 mg/mL) was prepared in 100% ethanol and stored at -20°C until use. Immediately before administration, rapamycin was diluted in vehicle composed of 5% PEG-400 and 5% Tween-80. AML-IEO20 cells (0.25×10^6 cells/mouse) were transplanted *via* tail vein injection of 8-10 weeks old NOD-SCID-IL2R γ null (NSG) mice. One week post-transplantation, mice were randomly assigned into four different groups which were treated for five weeks. The first group served as vehicle treated group. The second group was administered DDP38003 (16.8 mg/kg, by oral gavage). The third group

received rapamycin (5 mg/kg, intraperitoneally). The fourth group received DDP38003 and rapamycin. The survival of the mice was analyzed and represented by a Kaplan-Meier survival plot. All animal studies were conducted in compliance with the Italian Legislative Decree No.116 dated January 1992 and European Communities Council Directive No.86/609/EEC concerning the protection of animals used for experimental purposes and other scientific purposes according to the institutional policy regarding the care and use of laboratory animals. Mice were housed according to the guidelines set out in Commission Recommendation 2007/526/EC – June 18, 2007, guidelines of the accommodation and care of animals used for experimental and other scientific purposes. The study was approved by both the Ethical Committee of the European Institute of Oncology and Italian Ministry of Health (Project license number 199/2017).

For additional methods, please refer to the *Online Supplementary Materials and Methods*.

Results

Heterogeneous AML responses to LSD1i do not correlate with basal LSD1 level

To explore the anti-leukemic activity of inhibiting LSD1, we initially used DDP38003 (previously referred to as Compound 15),¹⁵ a potent selective and irreversible LSD1i, against a panel of AML cell lines belonging to different subtypes. As previously reported,^{12,17} AML cells demonstrated heterogeneous responses to LSD1 inhibition. DDP38003 dramatically diminished the proliferation and viability (cellular ATP level) of KASUMI-1, SKNO-1 and UF1 cells (Figure 1A and *Online Supplementary Figure S1A*). Indeed, DDP38003 induced apoptotic cell death in sensitive AML cells (Figure 1B and *Online Supplementary Figure S1B*). Conversely, the viability and proliferation of NB4, OCI-AML3 and THP-1 cells were not significantly affected reflecting their resistance to DDP38003 (Figure 1A-B and *Online Supplementary Figure S1A-B*). Next, we investigated whether DDP38003 was efficiently inhibiting LSD1 in resistant AML. Indeed, genes reported to be directly repressed by LSD1^{12,25} were upregulated post-DDP38003 treatment in both resistant THP-1 and sensitive KASUMI-1 cells confirming efficient LSD1 inhibition (*Online Supplementary Figure S1C*). We then inquired whether such differential responsiveness of AML cells correlates with the basal level of LSD1. LSD1 levels in both sensitive and resistant AML were comparable ruling out this hypothesis (Figure 1C). Altogether, our findings indicate that assessing the changes in the transcript levels of direct target genes of LSD1 per se and/or basal LSD1 levels do not explain differential vulnerability/responsiveness of AML cells to LSD1i.

Activation of mTORC1 correlates with the resistance of AML cells to LSD1 inhibition

mTOR is constitutively activated in AML blasts²⁶ and mediates chemoresistance.²³ We therefore investigated the effect on mTOR signaling as a potential mechanism of resistance of AML cells to LSD1i. Indeed, DDP38003 triggered mTORC1 activation in resistant AML cells as shown by increased phosphorylation of its downstream targets: p70 S6 kinase (p70S6K), ribosomal S6 and 4 eukaryotic-binding protein 1 (4E-BP1) (Figure 1D). Conversely, treatment of sensitive AML with DDP38003 inactivated mTORC1 (Figure 1D). The activity of

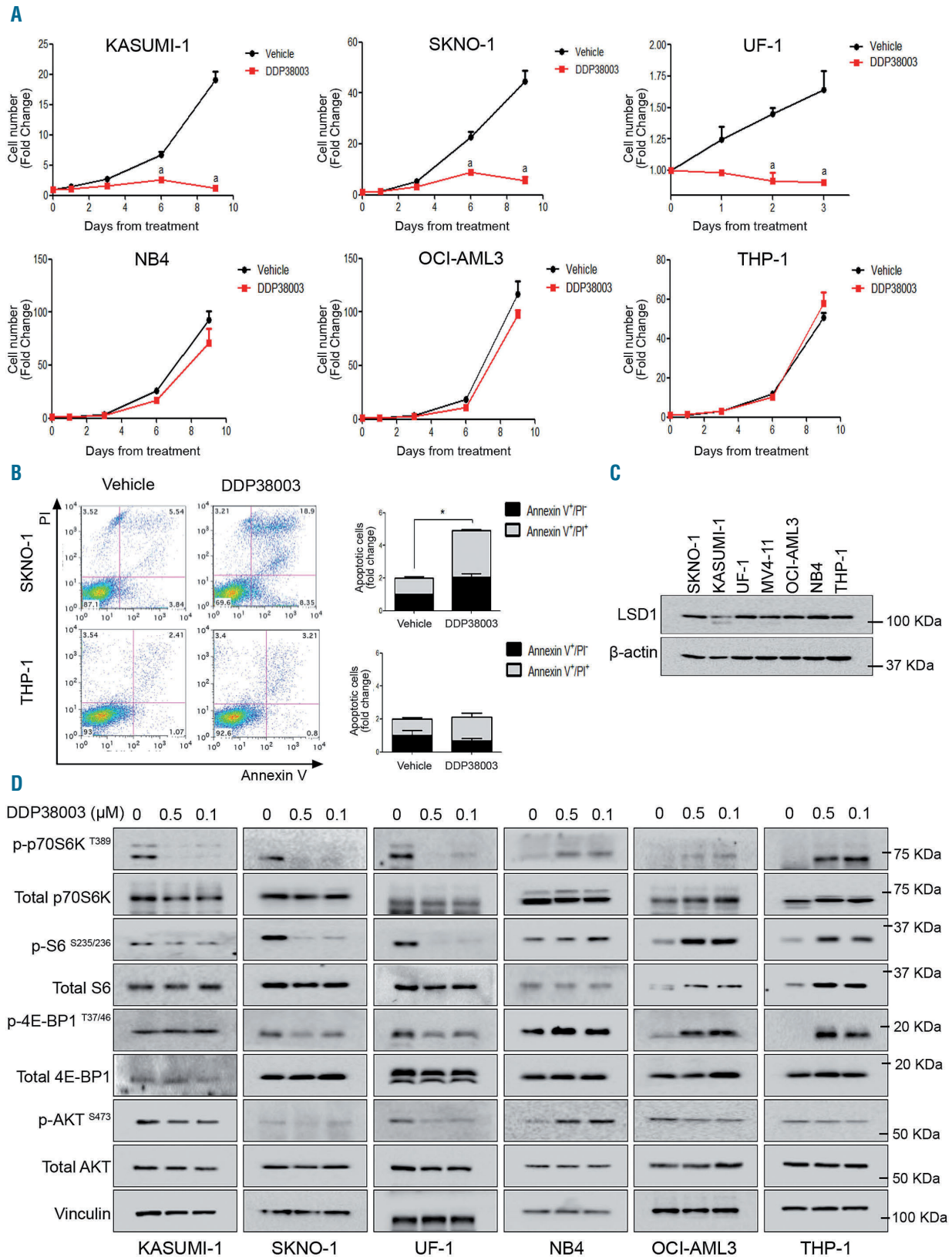


Figure 1. In contrast to acute myeloid leukemia cells sensitive to LSD1 inhibition, mTOR signaling is robustly activated in resistant AML cells in response to their treatment with DDP38003. (A) Growth curves of the indicated acute myeloid leukemia (AML) cell lines treated with either vehicle or DDP38003 (0.5 μM) for the indicated time points of treatment assessed using trypan blue cell counting. Data were statistically analyzed using two way ANOVA followed by Bonferroni post-hoc test. A: $P < 0.05$ compared to vehicle-treated cells ($n = 3$). (B) Representative flow cytometry dot plots depicting the effect of six days of vehicle or DDP38003 (0.5 μM) treatment on the viability/apoptosis of the indicated AML cells assessed by Annexin V/PI staining (left panel) and their quantitation (right panel). (C) Western blot analysis of LSD1 levels in the indicated AML cell lines. β-actin served as the loading control. (D) Immunoblotting analysis of mTOR signaling pathway in LSD1i-sensitive (KASUMI-1, SKNO-1 and UF1) and LSD1i-resistant (NB4, OCI-AML3 and THP-1) AML cells treated for six days with either vehicle or different concentrations of DDP38003 (0.1 and 0.5 μM). Vinculin served as the loading control. The presented blots are derived from replicate samples run on parallel gels and controlled for even loading. LSD1: lysine specific demethylase-1; LSD1i: LSD1 inhibitors.

mTORC2 (evaluated by assessing AKT phosphorylation at S473) was not consistently modulated in response to LSD1i in resistant and sensitive AML cells (Figure 1D). Collectively, these findings suggest that distinct fine-tuning of mTORC1 activity correlates with the differential responsiveness of AML cells to DDP38003.

Mirroring the response to DDP38003, mTORC1 was induced in resistant AML cells and inhibited in sensitive AML cells following their treatment with MC2580 (another selective LSD1i previously referred to as Compound 14e²⁷) (*Online Supplementary Figure S4D-G*). Finally, to confirm that LSD1 was the key molecular target for the phenotypic/molecular responses and exclude potential off-target effects associated with pharmacological inhibition, two different LSD1-targeting small hairpin RNA (shRNA) were used. Consistently, while *LSD1* knockdown sharply affected the proliferation of KASUMI-1 cells resulting in preferential counter-selection of one of the shRNA against wild-type cells, THP-1 and OCI-AML3 cells tolerated LSD1 knockdown (Figure 2A-C). shRNA against LSD1 efficiently reduced *LSD1* mRNA and protein levels, and subsequently upregulated the transcription of a direct target gene of LSD1 (CD11b) which was also modulated by DDP38003 (Figure 2D-L). Recapitulating the effect of pharmacological LSD1i, mTORC1 was inhibited in sensitive AML cells and induced in resistant AML cells following LSD1 knockdown (Figure 2J-L). Altogether, our data demonstrate that the sensitivity/resistance of AML cells to LSD1 inhibition is associated with distinctive modulation of mTORC1 activity.

Abrogating mTOR signaling counteracts the resistance of AML cells to LSD1 inhibition

Next, we explored the effect of inactivating mTOR on the response of AML cells resistant to LSD1 inhibition using different strategies. Inhibiting mTOR pharmacologically using either rapamycin (allosteric mTOR inhibitor) or AZD8055 (ATP competitive mTOR kinase inhibitor) sensitized resistant THP-1 cells to pharmacological LSD1i or genetic knockdown of LSD1 (Figure 3A-H). Mimicking nutritional stress using 2-deoxyglucose (2DG, a non-metabolizable glucose analogue)²⁸ also counteracted DDP38003-mediated mTOR activation and rendered THP-1 cells responsive to LSD1i (*Online Supplementary Figure S2A-C*).

A substantial proportion of initially responder cancer patients eventually relapses/progresses. Trying to simulate this scenario, parental KASUMI-1 cells (designated as KASUMI-1/P) were continuously exposed to increasing concentrations of DDP38003 for 12 months until they started to proliferate in the presence of DDP38003. Resistant descendent cells (named KASUMI-1/R) demonstrated a resistance index (RI) of 21 against DDP38003, and were also cross-resistant to MC2580 (RI of ~10) (*Online Supplementary Figure S4A-C*). As shown in the *Online Supplementary Figure S4D*, mTOR signaling was activated in KASUMI-1/R cells compared to their parental counter-part, and treatment with DDP38003, despite reducing the extent of mTOR activation, did not reach the low levels observed in parental cells. Besides boosting the responses of KASUMI-1/P cells to LSD1i, inhibiting mTOR dramatically reversed the acquired resistance of KASUMI-1/R cells to LSD1i *via* triggering apoptosis and this thereby indicates that compensatory mTOR activation protects AML cells against LSD1i-induced apoptotic

cell death (*Online Supplementary Figure S4E-G*). Collectively, our data suggest that targeting mTOR counteracts both intrinsic and acquired resistance of AML cells to LSD1i *in vitro*.

IRS1 and ERK1/2 signaling are involved in mTOR regulation by LSD1

We attempted to gain insights into the mechanism(s) through which LSD1 regulates mTOR. AMP activated protein kinase (AMPK) is a key negative regulator of mTOR.²⁹ Following LSD1i, AMPK activity was increased in both sensitive and resistant AML, as reflected by increased phosphorylation of AMPK and its downstream target, acetyl CoA carboxylase (ACC) (*Online Supplementary Figure S5A-D*). The levels of Raptor, a regulator and component of mTORC1, were not consistently modulated in response to LSD1 inhibition (*Online Supplementary Figure S5E-G*). Taken together, these results suggest that these mechanisms might not be critical for the observed modulatory effects on mTOR. We then monitored the activity of mTORC1 signaling in sensitive KASUMI-1 and resistant THP-1 cells at different time points following LSD1i. Even though six hours (h) of DDP38003 treatment were not enough to elicit any remarkable effects on the proliferation of sensitive KASUMI-1 cells, mTORC1 was dramatically inactivated (*Online Supplementary Figure S6A*). Conversely, 24 h post-LSD1i in resistant THP-1 cells, mTORC1 was robustly triggered (*Online Supplementary Figure S6B*). Such modulatory effects were maintained throughout the subsequent time points of treatment. Accordingly, we decided to perform transcriptomic analysis at the earliest detected and last tested time points in which mTORC1 activity was modulated secondary to LSD1i (*i.e.* 6 and 72 h in KASUMI-1 cells and 24 and 72 h in THP-1 cells). Consistent with the results of cell viability assays (Figure 1A-B and *Online Supplementary Figure S1A-B*), ingenuity pathway analysis (IPA) showed a significant modulation of gene sets involved in “cellular growth and proliferation” in sensitive KASUMI-1 but not resistant THP-1 cells post-LSD1i treatment (*Online Supplementary Figure S7A-B*). Notably, IPA predicted extracellular-signal regulated kinases 1 and 2 (ERK1/2) to be activated in resistant but not in sensitive AML following LSD1i (*Online Supplementary Table S1A-4*). ERK1/2 is reported to be an upstream activator of mTOR.²⁶ In parallel with mTOR modulation, DDP38003 inhibited ERK1/2 in sensitive AML cells (KASUMI-1) and activated ERK1/2 in resistant AML cells (THP-1 and NB4) cells (*Online Supplementary Figure S6A-C*). Inhibiting ERK1/2 using several unrelated selective MEK1/2 inhibitors as U0126, pimasertib and trametinib rendered resistant AML cells more vulnerable to LSD1 inhibition (*Online Supplementary Figure S6D-H*). These findings all suggest that ERK1/2 acts upstream of mTOR dysregulation by LSD1.

To further investigate how LSD1 regulates ERK1/2 and mTOR, we analyzed our RNA-Seq data which revealed that a subset of genes was differentially modulated in resistant *versus* sensitive AML following LSD1i (Figure 4A). Among those differentially expressed genes, insulin receptor substrate 1 (IRS1) was upregulated in resistant but not responsive AML cells after DDP38003 treatment (Figure 4A-B and *Online Supplementary Table S5*). IRS1 is an adaptor protein which regulates various pathways including ERK1/2 and mTOR.³⁰ Confirming RNA sequencing (RNA-Seq) data, treatment with pharmacological LSD1i or

LSD1 knockdown significantly increased IRS1 mRNA and protein levels in resistant AML cells, unlike sensitive AML cells (Figure 4C-K and *Online Supplementary Figure S8A*). Cistrome database analyses of previously deposited LSD1 ChIP-seq tracks¹² showed that LSD1 was associated to the IRS1 promoter in resistant NB4 cells, while it was not bound in sensitive KASUMI-1 and SKNO-1 cells (*Online Supplementary Figure S8B*). We confirmed LSD1 binding to the IRS1 promoter of LSD1i resistant AML cells by ChIP-

qPCR (Figure 4L-M and *Online Supplementary Figure S8C-D*). Following the induction of IRS1 by DDP38003 treatment, H3K4me3, H3K9Ac and H3K27Ac histone marks at IRS1 promoter were strongly increased compared to vehicle-treated cells (Figure 4N-P). Modest changes in H3K4me2 were found in THP-1 and KASUMI-1 cells following their treatment with LSD1 inhibitors (DDP38003, GSK690 and RN-1) (*Online Supplementary Figure S8E-F*).

To delineate the hierarchical relationship of IRS1 with

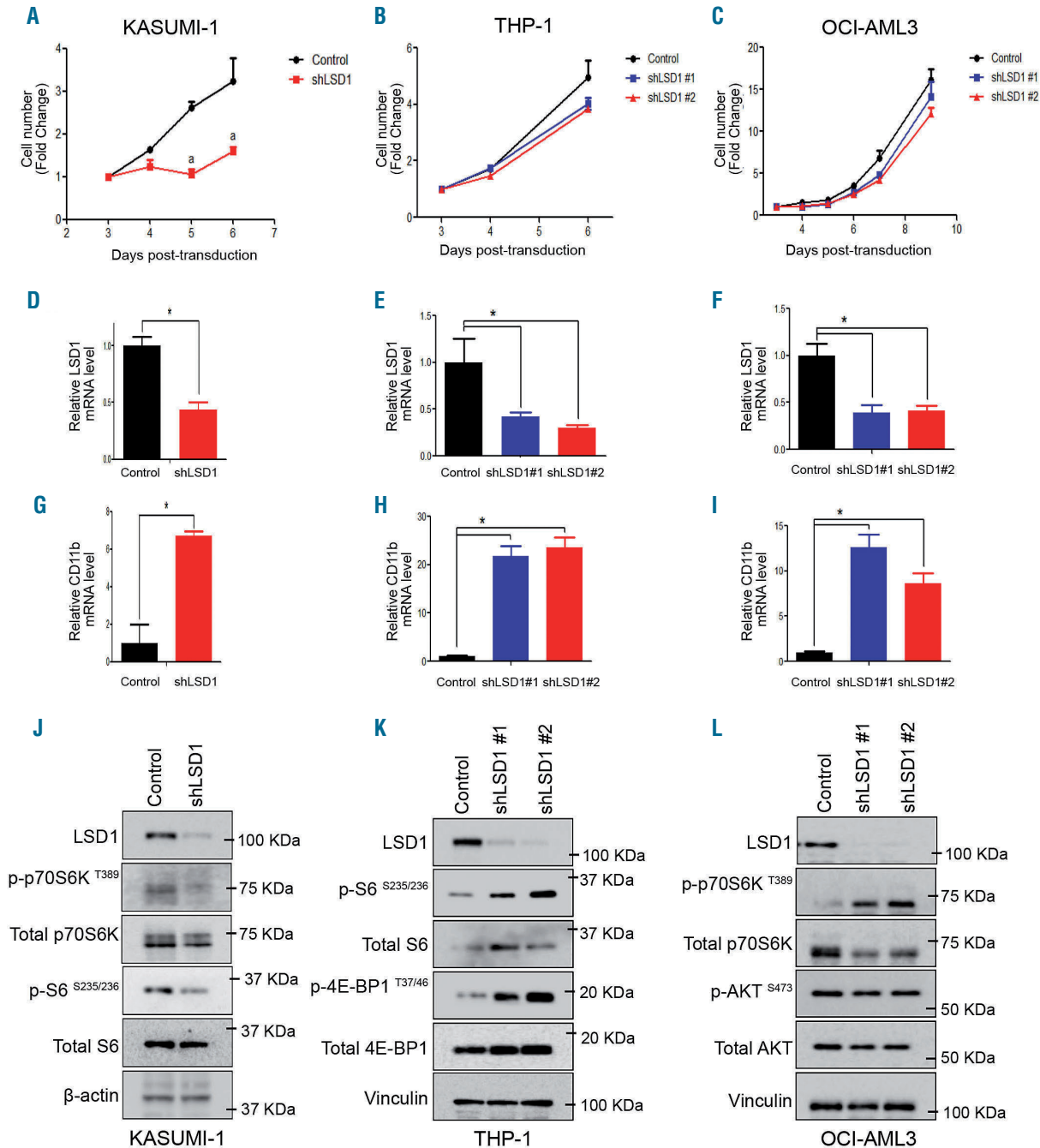


Figure 2. Genetic LSD1 knockdown recapitulates the effects of pharmacological LSD1 inhibition on mTOR signaling in sensitive and irresponsive acute myeloid leukemia cells. (A-C) Growth curves of KASUMI-1 (A), THP-1 (B) and OCI-AML3 (C) cells transduced with retroviral vectors expressing short hairpin RNA (shRNA) against control (scrambled) or LSD1 (*shLSD1* #1 and *shLSD1* #2) ($n=3$). (D-F) Normalized LSD1 and CD11b mRNA levels assessed in transduced KASUMI-1 (D), THP-1 (E), OCI-AML3 (F) cells expressing the indicated shRNA using real-time quantitative PCR (RT-qPCR). Data were statistically analyzed using either Student's *t*-test (A, D and G) or one way ANOVA followed by Bonferroni *post hoc* test (B, C, E, F, H and I). *: $P < 0.05$ compared to control (scrambled). (J-L) Western blot analysis of lysates obtained from transduced KASUMI-1 (J), THP-1 (K), OCI-AML3 (L) cells expressing the indicated shRNA. The presented blots are derived from replicate samples run on parallel gels and controlled for even loading.

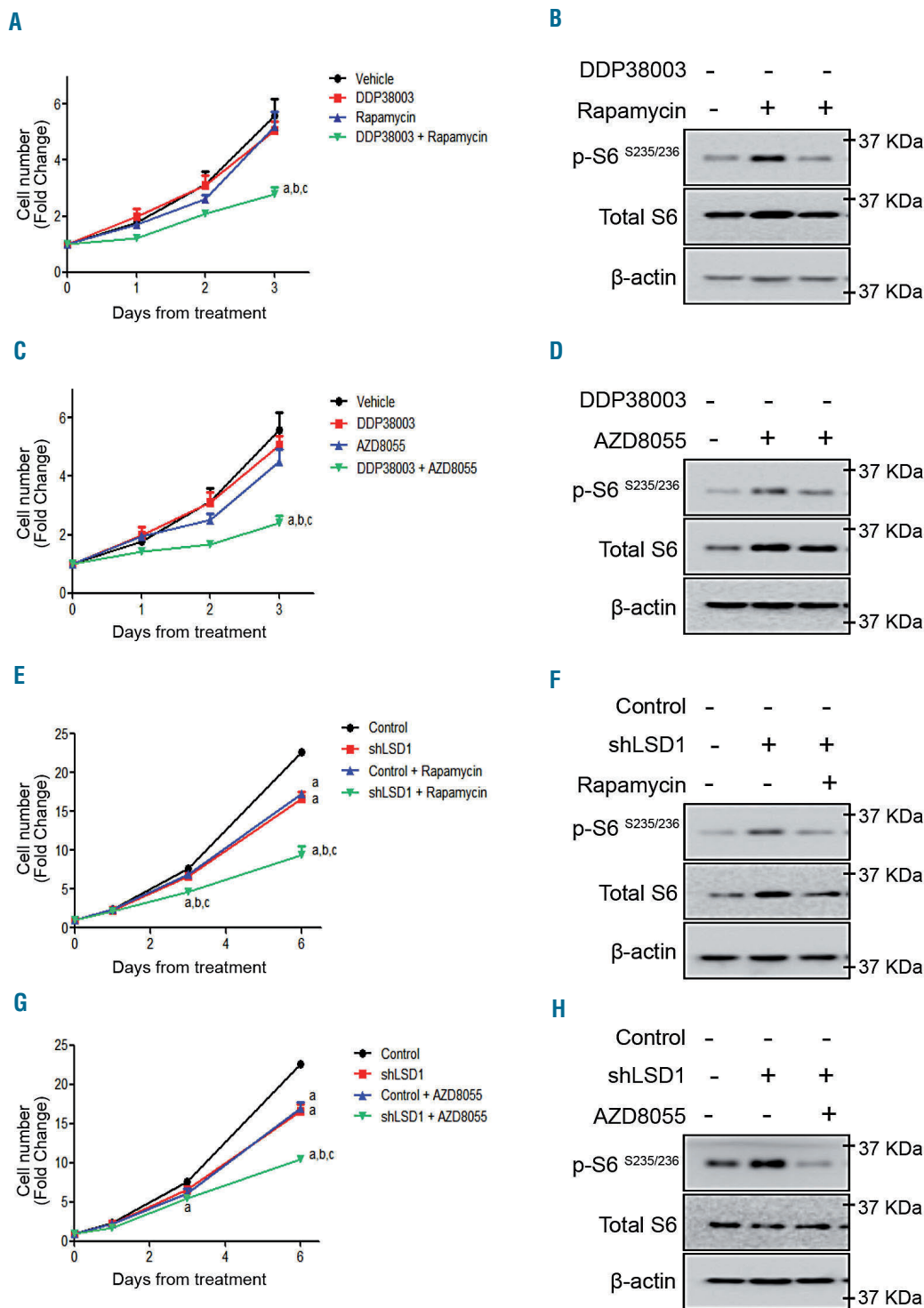


Figure 3. Inhibition of mTOR signaling reverses the resistance of acute myeloid leukemia cells to LSD1 inhibition. (A) Growth curves of THP-1 cells treated with vehicle, DDP38003 (0.5 μ M), rapamycin (10 nM) or DDP38003 and rapamycin for the indicated time points of treatment. Data were statistically analyzed using two way ANOVA followed by Bonferroni *post hoc* test, ^{a,b,c}: $P < 0.05$ compared to vehicle, DDP38003 or rapamycin alone treated groups respectively (n=3). Note that we have previously demonstrated that LSD1 inhibition affects THP-1 cells in clonogenic but not in liquid culture assays.³⁵ Indeed, co-inhibiting mTOR significantly augmented the anti-clonogenic activity of DDP38003 further promoting myeloid lineage differentiation of THP-1 cells (*Online Supplementary Figure S3A-B*). (B) Western blot analysis of lysates obtained from THP-1 cells (A) following 72 hours (h) of treatment. β -actin served as the loading control. (C) Proliferation curves of THP-1 cells treated with vehicle, DDP38003 (0.5 μ M), AZD8055 (20 nM) or DDP38003 and AZD8055 for the indicated time points of treatment. Data were statistically analyzed using two way ANOVA followed by Bonferroni *post hoc* test, ^{a,b,c}: $P < 0.05$ compared to vehicle, DDP38003 or AZD8055 alone treated groups respectively (n=3). (D) Western blot analysis of lysates obtained from THP-1 cells (C) following 72 h of treatment. β -actin served as the loading control. (E) Growth curves of transduced THP-1 cells expressing control shRNA or shRNA against LSD1 treated with vehicle or rapamycin for the indicated time points of treatment. Data were statistically analyzed using two way ANOVA followed by Bonferroni *post hoc* test, ^{a,b,c}: $P < 0.05$ compared to vehicle, shLSD1 or rapamycin alone treated groups respectively (n=3). (F) Western blot analysis of lysates obtained from THP-1 cells (E) following 144 h of treatment. β -actin served as the loading control. (G) Growth curves of transduced THP-1 cells expressing control shRNA or shRNA against LSD1 treated with vehicle or AZD8055 for the indicated time points of treatment. Data were statistically analyzed using two way ANOVA followed by Bonferroni *post hoc* test, ^{a,b,c}: $P < 0.05$ compared to vehicle, shLSD1 or AZD8055 alone treated groups respectively (n=3). (H) Western blot analysis of lysates obtained from THP-1 cells (G) following 144 h of treatment. β -actin served as the loading control.

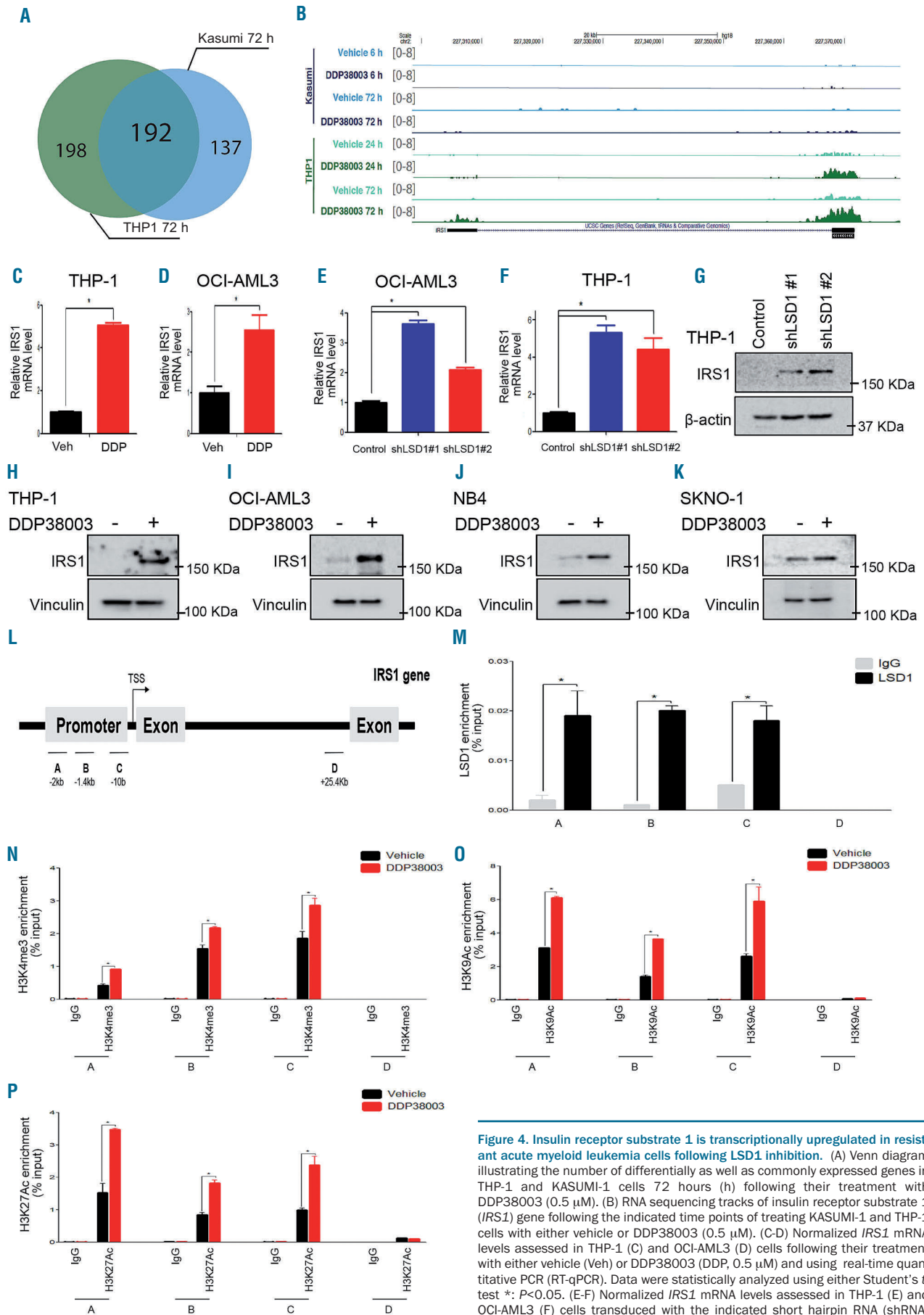


Figure 4. Insulin receptor substrate 1 is transcriptionally upregulated in resistant acute myeloid leukemia cells following LSD1 inhibition. (A) Venn diagram illustrating the number of differentially as well as commonly expressed genes in THP-1 and KASUMI-1 cells 72 hours (h) following their treatment with DDP38003 (0.5 μ M). (B) RNA sequencing tracks of insulin receptor substrate 1 (*IRS1*) gene following the indicated time points of treating KASUMI-1 and THP-1 cells with either vehicle or DDP38003 (0.5 μ M). (C-D) Normalized *IRS1* mRNA levels assessed in THP-1 (C) and OCI-AML3 (D) cells following their treatment with either vehicle (Veh) or DDP38003 (DDP, 0.5 μ M) and using real-time quantitative PCR (RT-qPCR). Data were statistically analyzed using either Student's *t*-test *: *P*<0.05. (E-F) Normalized *IRS1* mRNA levels assessed in THP-1 (E) and OCI-AML3 (F) cells transduced with the indicated short hairpin RNA (shRNA)

(control [scrambled] or LSD1 [*shLSD1* #1 and *shLSD1* #2]) using real-time quantitative PCR (RT-qPCR). Data were statistically analyzed using one way ANOVA followed by Bonferroni *post hoc* test. *: $P < 0.05$ compared to control (scrambled). (H-K) Western blot analysis of lysates obtained from THP-1 (H), OCI-AML3 (I), NB4 (J) and SKNO-1 (K) cells treated with either vehicle or DDP38003 (0.5 μM). Vinculin served as a loading control. (L) Schematic outline of the chromatin immunoprecipitation qPCR (ChIP-qPCR) primers designed to analyze the enrichment of LSD1 or histone marks on IRS1 promoter. (M) LSD1 ChIP-qPCR analyses were performed in THP-1 cells using antibody against LSD1 or IgG as a control. Enrichment values at the indicated sites (A–D) were normalized to input DNA. Values are means \pm standard deviation (SD). *: $P < 0.05$. (N–P) ChIP-qPCR analyses to assess H3K4me3 (N), H3K9Ac (O) and H3K27Ac (P) histone marks were performed in THP-1 cells 72 h following their treatment with either vehicle or DDP38003 (0.5 μM). Enrichment values at the indicated sites (A–D) were normalized to input DNA. Values are means \pm standard deviation (SD). *: $P < 0.05$.

ERK1/2 and mTOR, we investigated the effect of NT157, a selective IRS1/2 inhibitor.³¹ Co-treatment with NT157 reversed LSD1i-induced ERK/mTOR stimulation and sensitized tolerant AML cells to LSD1i, suggesting that IRS1 acts upstream of ERK/mTOR (Figure 5A–C).

All trans-retinoic acid (ATRA) has been reported to downregulate IRS1.^{32,33} Indeed, ATRA repressed IRS1 transcription and cooperated with LSD1i as previously reported (*Online Supplementary Figure S9A–E* and *Figure 5D–F*).⁴ Consistently, ATRA counteracted LSD1i-mediated induction of IRS1/ERK/mTOR in resistant AML cells and led to reduced H3K4me2 and, to a greater extent, H3K27Ac accumulation on IRS1 promoter (Figure 5F and *Online Supplementary Figure S9F–I*). Collectively, our data indicate that differential dysregulation of IRS1/ERK signaling might contribute at least partly to the modulation of mTOR following LSD1i.

Targeting mTOR sensitizes resistant primary human AML blasts to LSD1 inhibition *in vitro* and *in vivo*

We then checked the effect of LSD1i on primary human cells. mTOR signaling was not modulated in primary human hematopoietic CD34⁺ progenitor cells which tolerated DDP38003 (*Online Supplementary Figure S10A–C*). In contrast, mTOR was inhibited by LSD1i treatment in transduced human MLL-AF9 expressing CD34⁺ cells where LSD1i adversely affected their proliferation and clonogenicity while promoting myeloid differentiation (*Online Supplementary Figure S11A–G*).

Eventually, we explored the therapeutic value of co-inhibiting mTOR in primary patient derived AML blasts resistant to LSD1i (referred to as AML-IEO20, expressing the oncofusion protein MLL-AF9). Confirming the results seen in resistant AML cell lines, DDP38003 induced mTORC1 in resistant AML-IEO20 cells (Figure 6A–C). Inhibiting mTOR signaling sensitized AML-IEO20 cells to LSD1i (Figure 6D–F). This was associated with increased G₀/G₁ arrest and apoptotic cell death (*Online Supplementary Figure S12A–B*).

To validate our results *in vivo*, AML-IEO20 cells were transplanted into NSG mice. As shown in Figure 7A, one week post-transplantation, mice were randomly assigned into four cohorts and treated with: vehicle, DDP38003, rapamycin or their combination. After two weeks of treatment, DDP38003 as a monotherapy failed to lessen the percent of circulating human AML cells, while rapamycin caused a significant decrement (Figure 7C). DDP38003/rapamycin combinatorial regimen significantly reduced the percent of hCD45⁺ leukemic cells in the peripheral blood as compared to vehicle and DDP38003-treated groups (Figure 7C). Even though DDP38003/rapamycin co-treatment further lessened the percent of human AML cells by almost 60% compared to rapamycin alone, such a decrement was not statistically significant. At this stage of treatment, two mice from each

cohort were sacrificed, and spleen and bone marrow tissues were harvested. Rapamycin, but not DDP38003, reduced spleen and bone marrow infiltration by leukemic cells was comparable to the vehicle-treated group (Figure 7D–F). Notably, DDP38003/rapamycin combination elicited an even stronger reduction of leukemic infiltration (Figure 7E–F). May Grunwald/Giemsa-stained cytospin preparations of blood smear, spleen and bone marrow, histopathological and immunohistochemical examinations further confirmed the superior antileukemic activity of the LSD1i/mTORi combinatorial regimen (*Online Supplementary Figure S12C–F* and Table 1). After three weeks of treatment, circulating hCD45⁺ leukemic cells were present in the cohorts treated with vehicle, DDP38003 and rapamycin as monotherapies while they remained dramatically decreased by the combination treatment (Figure 7G). Indeed, the combination treatment significantly prolonged the survival of PDX mice as compared to vehicle ($P = 0.001$), DDP38003 ($P = 0.0004$) and rapamycin ($P = 0.0024$)-treated groups (Figure 7J). Altogether, our results provide the first proof of principle demonstrating preclinical evidence for a therapeutic strategy to restore the efficacy of LSD1i in irresponsive AML patients based on co-inhibiting LSD1/mTOR.

Discussion

AML cells have been reported to elicit heterogeneous responses to LSD1i.^{12,17} Here, we explored the mechanisms of sensitivity and resistance of AML cells to LSD1 inhibition. Initially, we ruled out the possibility that differential basal LSD1 levels might account for discrepant vulnerability of AML cells to LSD1i, consistent with what was described with T-cell lymphoblastic leukemias.³⁴ Moreover, global transcriptomic changes in the target genes of LSD1 (as CD11b) did not correlate with the discrepant responses of AML cells to LSD1i. Intriguingly, we found that distinctive modulation of mTORC1 activity acts as a key mediator of the susceptibility of AML cells to LSD1i therapy (Figure 7K). We and others have previously demonstrated that mTORC1 contributes to the resistance of diverse types of tumours to targeted anticancer therapies, such as histone deacetylase (HDAC) and tyrosine kinase inhibitors.^{25,35,36} Likewise, mTORC1 signaling was robustly triggered in AML cells that tolerated LSD1i. In contrast, mTORC1 was inhibited in LSD1i-sensitive AML, as recently described using S2101, another LSD1i, in responsive ovarian carcinoma cells.³⁷ Inhibiting mTOR *via* direct pharmacological inhibition, or mimicking energetic stress using the non-metabolizable glucose analogue, 2-deoxyglucose, reversed LSD1i-induced mTOR activation and counteracted the resistance of AML cells to LSD1i. Intriguingly, our findings with the glycolytic inhibitor, 2-deoxyglucose, could also be explained by Poulain *et al.*,

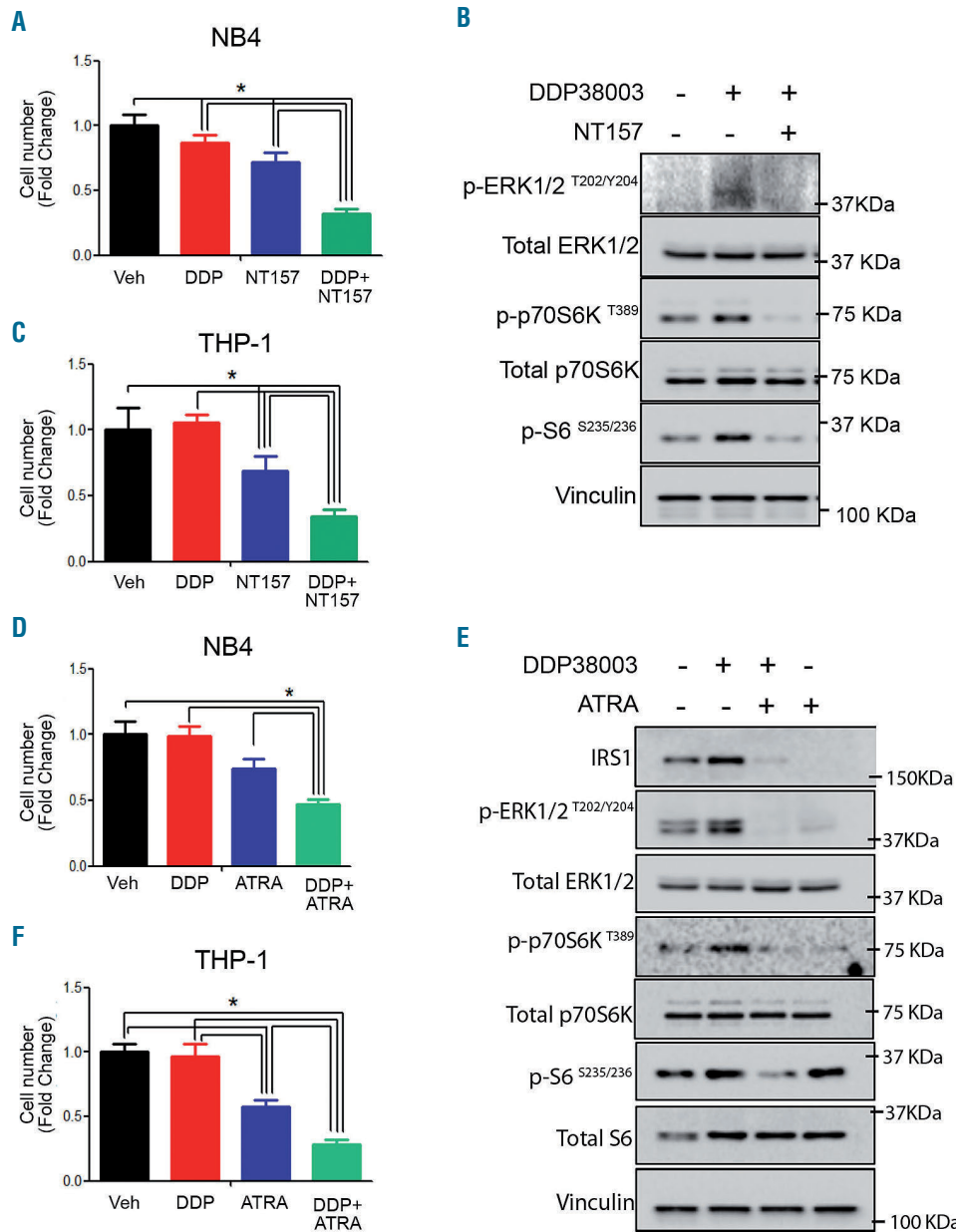


Figure 5. Inhibiting insulin receptor substrate 1 sensitizes resistant acute myeloid leukemia cells to LSD1 inhibition. (A) Relative cell number of NB4 cells treated with either vehicle (Veh), DDP38003 (DDP, 0.5 μM), NT-157 (1.25 μM) or their combination for 72 hours (h). Data were statistically analyzed using one way ANOVA followed by Bonferroni *post hoc* test (n=3). *: P<0.05. (C) Relative cell number of THP-1 cells treated with either vehicle (Veh), DDP38003 (DDP, 0.5 μM), NT-157 (1.25 μM) or their combination for 24 h. Data were statistically analyzed using one way ANOVA followed by Bonferroni *post hoc* test (n=3). *: P<0.05. (B) Western blot analysis of THP-1 cells treated as indicated. Vinculin served as a loading control. (D-E) Relative cell number of NB4 (D) and THP-1 (E) cells treated with either vehicle (Veh), DDP38003 (DDP, 0.5 μM), all-trans-retinoic acid (ATRA - 1 μM) or their combination. Data were statistically analyzed using one way ANOVA followed by Bonferroni *post hoc* test (n=3). *: P<0.05. (E) Western blot analysis. Vinculin served as a loading control.

who demonstrated that heightened mTORC1 activity promotes glycolysis and drives glucose addiction in AML cells.³⁸ Since mTOR acts as a fundamental metabolic checkpoint, LSD1-induced mTOR modulation might contribute to the epigenetic plasticity of cancer cell metabolism.¹¹ The ON/OFF regulatory effects of LSD1i on mTOR could also account for the previously reported regulatory effects of LSD1 on metabolic reprogramming.^{39,40}

Importantly, co-inhibiting LSD1 and mTOR significantly reduced the leukemic burden and prolonged the survival of mice xenotransplanted with primary patient-derived AML (with MLL-AF9 chromosomal translocations) compared to monotherapies. Consistent with the preclinically observed synergy between HDAC inhibitors and mTOR inhibitors, encouraging anticancer activities of vorinostat (HDAC inhibitor) when combined with sirolimus (mTOR inhibitor) have also been reported in patients with refractory Hodgkin lymphoma, perivascular

epithelioid tumor, and hepatocellular carcinoma.^{36,41} The observed synergy between LSD1i and mTOR inhibitors remains to be verified in patient-derived AML blasts exhibiting a diverse genetic background.

In addition, it is worth mentioning that while we have not noticed any potential impact of LSD1 inhibition on the proliferation as well as mTOR signaling of primary human CD34⁺ cord blood cells following three days of treatment, this does not exclude potential adverse effects on normal hematopoiesis following long-term LSD1 inhibition which was previously reported.⁴² Hence, this should carefully be considered while designing clinical trials evaluating the efficacy of LSD1i as a monotherapy or in combination regimens.

Acquired resistance is a frequently encountered hurdle in cancer therapy. Despite being formerly responsive, tumor cells have a formidable capability to develop resistance to indefinite spectra of anti-cancer agents when chal-

lenged for long periods.²³ After prolonged exposure of responsive AML (KASUMI-1/P) to DDP38003, secondarily resistant AML cells (KASUMI-1/R) started to grow in the presence of LSD1i. Such KASUMI-1/R cells were cross resistant to another LSD1i. Of note, mTOR activation was observed not only in AML cells intrinsically resistant to LSD1 inhibition, but also as a mechanism of acquired resistance to LSD1 inhibition in primarily sensitive AML cells. Analogously, imatinib triggered mTOR activation in a chronic phase chronic myelogenous leukemia (CML) patient which critically mediated CML survival during the early phase of acquired imatinib resistance before the acquisition of a kinase mutation.²² Although we have not analyzed the eventual genetic alterations in KASUMI-1/R cells, the observation that acquired resistance could be reverted by mTOR inhibition suggests that an adaptive rather than a genetic mechanism is involved in mediating mTOR activation and resistance to LSD1 inhibition. Nonetheless, this shall be systemically investigated in our

future studies on a larger subset of secondarily resistant AML.

Delving deeper, we have investigated how LSD1 differentially modulates mTOR in resistant *versus* sensitive AML cells. Intriguingly, we have observed mTORC1 activation in experimental conditions where AMPK - which in many cases acts as a mTOR inhibitor²⁹ - was activated and thereby excluding its involvement. In line with AMPK stimulation, we found that LSD1i increases the phosphorylation and hence inactivation of the down-stream target of AMPK, ACC which is the rate-limiting enzyme of fatty acid synthesis. In line with our data, LSD1 knockdown has been shown to reduce the triglyceride levels through modulating sterol regulatory element binding protein (SREBP1)-mediated activation of lipogenic gene transcription.⁴³ mTOR also promotes *de novo* lipogenesis *via* activating SREBP1 and phosphorylating serine/arginine protein kinases, thereby promoting the splicing of lipogenic pre-mRNA.⁴⁴ Our data highlighting the modulatory effects of

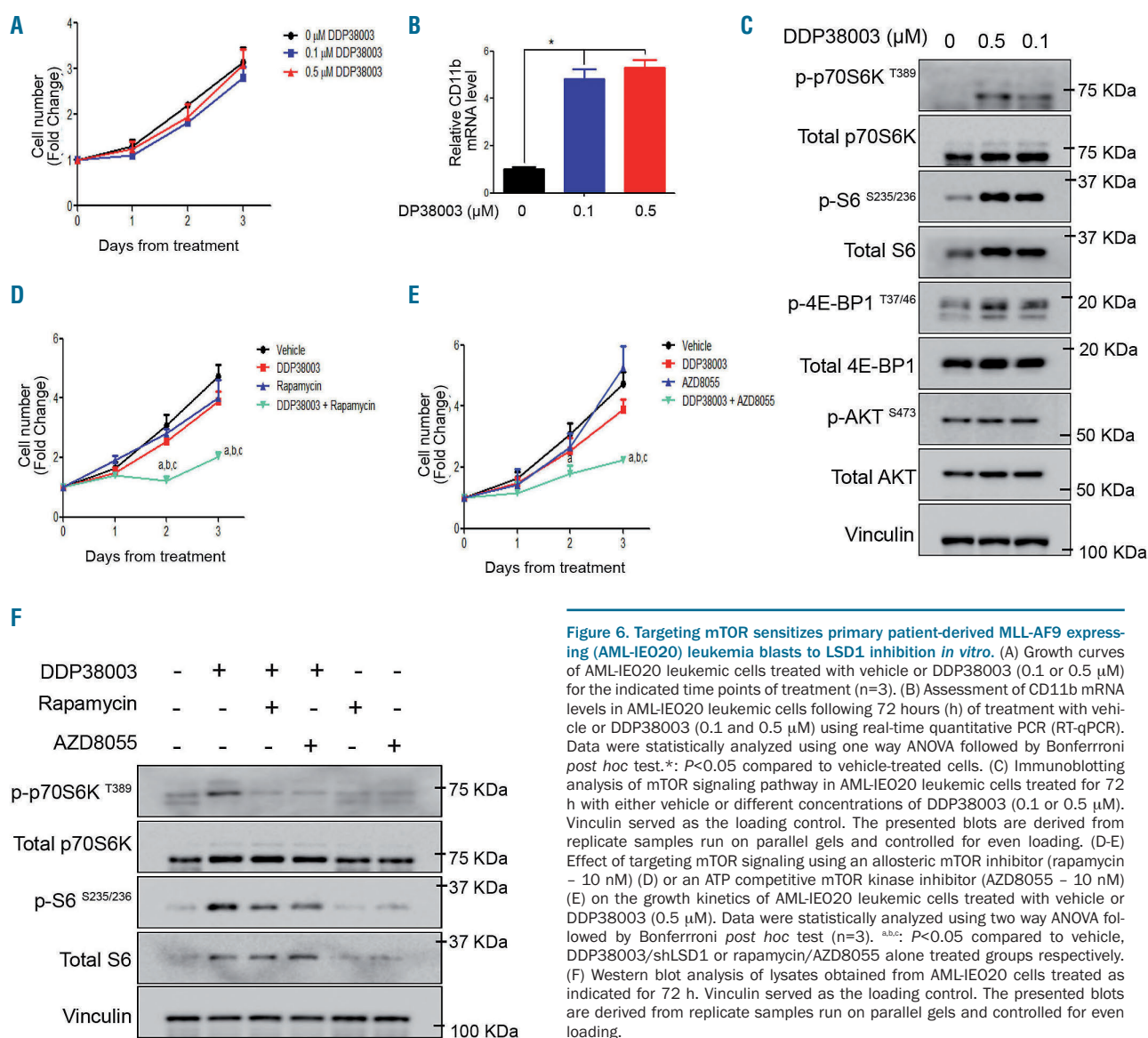


Figure 6. Targeting mTOR sensitizes primary patient-derived MLL-AF9 expressing (AML-IEO20) leukemia blasts to LSD1 inhibition *in vitro*. (A) Growth curves of AML-IEO20 leukemic cells treated with vehicle or DDP38003 (0.1 or 0.5 μM) for the indicated time points of treatment (n=3). (B) Assessment of CD11b mRNA levels in AML-IEO20 leukemic cells following 72 hours (h) of treatment with vehicle or DDP38003 (0.1 and 0.5 μM) using real-time quantitative PCR (RT-qPCR). Data were statistically analyzed using one way ANOVA followed by Bonferroni *post hoc* test.*: $P < 0.05$ compared to vehicle-treated cells. (C) Immunoblotting analysis of mTOR signaling pathway in AML-IEO20 leukemic cells treated for 72 h with either vehicle or different concentrations of DDP38003 (0.1 or 0.5 μM). Vinculin served as the loading control. The presented blots are derived from replicate samples run on parallel gels and controlled for even loading. (D-E) Effect of targeting mTOR signaling using an allosteric mTOR inhibitor (rapamycin - 10 nM) (D) or an ATP competitive mTOR kinase inhibitor (AZD8055 - 10 nM) (E) on the growth kinetics of AML-IEO20 leukemic cells treated with vehicle or DDP38003 (0.5 μM). Data were statistically analyzed using two way ANOVA followed by Bonferroni *post hoc* test (n=3). *abc*: $P < 0.05$ compared to vehicle, DDP38003/shLSD1 or rapamycin/AZD8055 alone treated groups respectively. (F) Western blot analysis of lysates obtained from AML-IEO20 cells treated as indicated for 72 h. Vinculin served as the loading control. The presented blots are derived from replicate samples run on parallel gels and controlled for even loading.

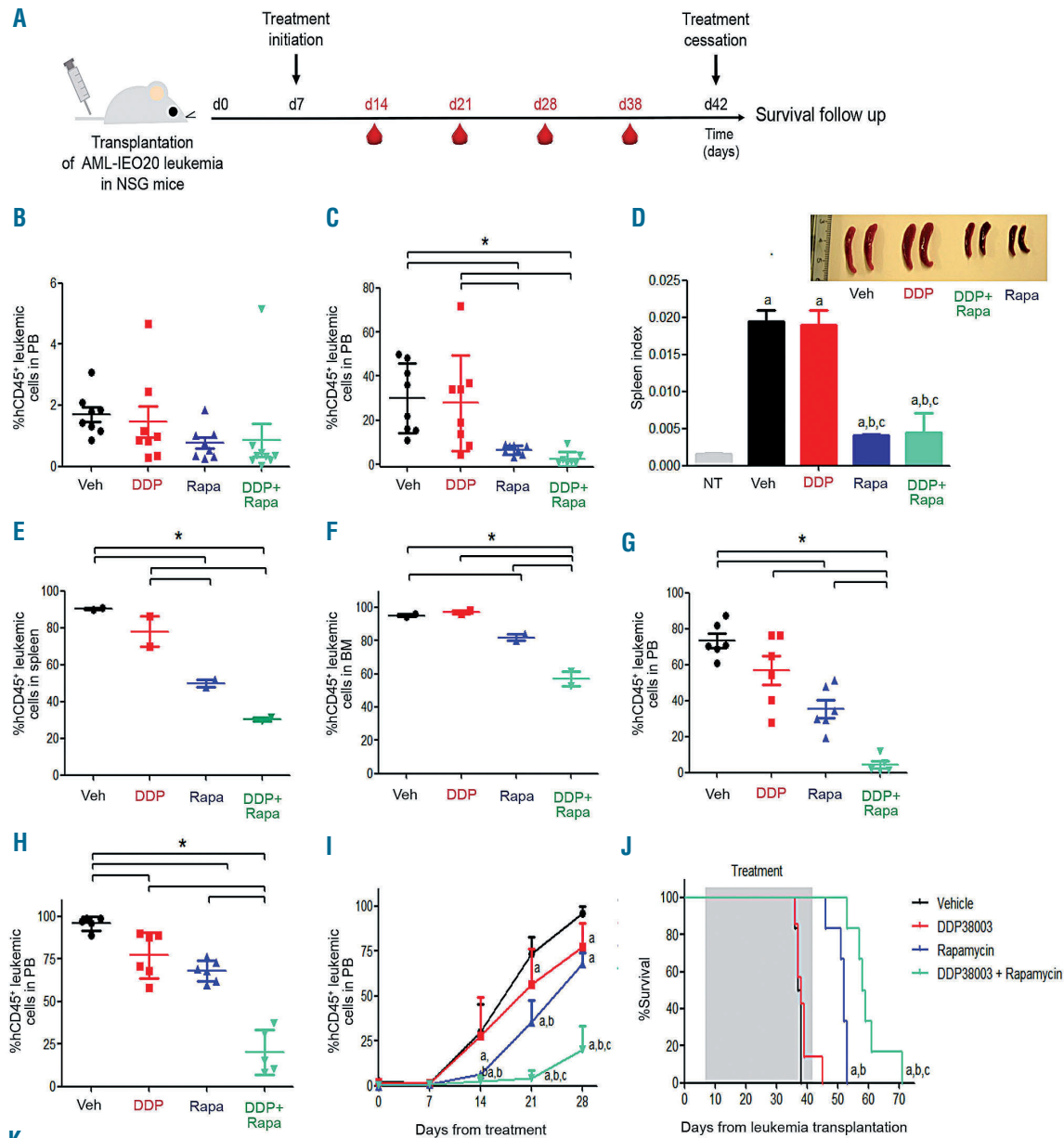
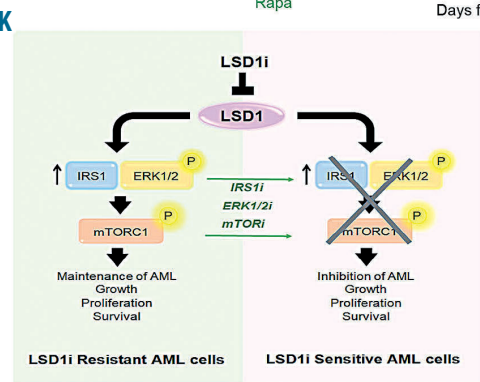


Figure 7. Targeting mTOR sensitizes primary patient-derived MLL-AF9 expressing (AML-IEO20) leukemia blasts to LSD1 inhibition *in vitro* and *in vivo*. (A) Schematic outline of the *in vivo* studies with the PDX model of AML-IEO20 leukemia. (B-I) Flow cytometric analyses of the percent of human CD45⁺ leukemic cells in the peripheral blood (PB) obtained from NSG mice transplanted with primary human AML-IEO20 cells and treated for 7 (B), 14 (C), 21 (G) and 28 (H) days with either: vehicle (Veh), DDP38003 (DDP, 16.8 mg/kg, PO), rapamycin (Rapa, 5 mg/kg, IP) or DDP38003 + rapamycin. (D) Effect of different treatments on the spleen index following 15 days of treatment. Data were statistically analyzed using one-way ANOVA followed by Tukey-Kramer *post hoc* test. ^{a,b,c}; *P*<0.05 compared to non-transplanted and vehicle-treated and DDP38003 alone xenotransplanted groups respectively. Upper right panel: image of spleens harvested from NSG mice 15 days following their treatment with either vehicle or DDP38003 or rapamycin or a combination of DDP38003 and rapamycin (n=2/group). (E-F) Flowcytometric analysis of AML-IEO20 leukemic engraftment depicted as percent of human CD45⁺ leukemic cells in the spleen (E) and bone marrow (F) after 15 days of treatment initiation (n=2/group). Data were statistically analyzed using one-way ANOVA followed by Tukey-Kramer *post hoc* test. *; *P*<0.05. Data represents mean ± standard deviation (SD). Data were statistically analyzed using one-way ANOVA followed by Tukey-Kramer *post hoc* test. *; *P*<0.05. (I) Flow cytometric analyses of the percent of human CD45⁺ leukemic cells in peripheral blood obtained from NSG mice transplanted with primary human AML-IEO20 cells and treated for the indicated time points with either: vehicle, DDP38003, rapamycin or their combination. (J) Kaplan Meier survival curve of mice engrafted with primary AML-IEO20 cells treated with vehicle, DDP38003, rapamycin or DDP38003 + rapamycin. Statistical significance was evaluated using log-rank (Mantel-Cox's) test. ^{a,b,c}; *P*<0.05 compared to vehicle, DDP38003 or rapamycin-only treated groups respectively. (K) Schematic representation of the proposed mechanism by which modulation of IRS1/ERK/mTOR signaling governs the sensitivity/resistance of acute myeloid leukemia (AML) cells to LSD1 inhibition (LSD1i).



LSD1 on ACC and mTOR enrich the evidences linking LSD1 to the regulation of lipid metabolism.

Upstream regulator IPA predicted ERK1/2 to be activated in resistant but not sensitive AML following LSD1i. Of note, ERK1/2 is known to positively regulate the activity of mTOR signaling *via* acting both upstream and downstream of mTOR.^{25,45} Inhibiting ERK1/2 inhibited mTOR and counteracted AML resistance to LSD1i. Moreover, transcriptomic studies showed that IRS1 was upregulated following LSD1i in resistant but not responsive AML cells. We found LSD1 to be associated with the IRS1 promoter only in AML cells resistant to LSD1i, suggesting that AML cells display different modes of regulation of this gene (negative regulation by LSD1 in resistant cells, other mechanisms in sensitive cells). Consistently, LSD1i led to remodeling of the IRS1 promoter in resistant AML cells, with a prominent accumulation of H3K4me3, H3K9Ac and H3K27Ac histone marks. Our findings are consistent with the previously reported studies which demonstrated that the transcriptional consequences of LSD1 inhibition are preceded by the preferential enrichment of H3K9Ac and H3K27Ac marks at LSD1-bound regulatory regions.^{14,46}

Notably, a selective IRS1/2 inhibitor, NT157,³¹ reversed LSD1i-induced ERK1/2 and mTOR activation and thereby sensitized resistant AML cells to LSD1i. Our data are in accordance with Machado-Neto and colleagues who reported that silencing IRS1 inactivates ERK1/2 and mTOR signaling in K562 CML cells.³⁰ In line with previous studies which reported that ATRA downregulates IRS1,^{32,33} we have further demonstrated that ATRA reduced H3K4me2 and H3K27Ac accumulation on IRS1 promoter. Indeed, ATRA dramatically abolished LSD1i-mediated IRS1 induction and rendered resistant AML vulnerable to LSD1i. Within this context, we speculate that LSD1i and ATRA cooperate by acting *via* distinct mechanisms. LSD1i unlocks ATRA-differentiation pathway⁴ whereas ATRA counteracts LSD1i-mediated upregulation of IRS1. These complementary activities might contribute to the synergistic antileukemic activity of their combination.⁴ Altogether, our findings imply that LSD1i-mediated modulation of IRS1 and ERK1/2 might contribute –at least

Table 1. Targeting mammalian target of rapamycin (mTOR) sensitizes primary patient-derived acute myeloid leukemia (AML) blasts (AML-IEO20) to LSD1 inhibition. Degree of leukemic cells infiltration of the spleen, bone marrow and surrounding muscular tissues harvested from NSG mice transplanted with human primary AML-IEO20 cells, sacrificed 15 days after initiation of treatment.

Treated Group (#designated labeled mouse number)	Extent of infiltration		
	Spleen	Bone marrow	Muscle
Non-transplanted	–	–	–
Vehicle-treated group (#A2)	+++	Necrotic	++
Vehicle-treated group (#A3)	+++	+++	++
DDP38003-treated group (#B11)	++	+++	+
DDP38003-treated group (#B12)	++	+++	+
Rapamycin-treated group (#D33)	++	+++	+
Rapamycin-treated group (#D36)	++	+++	+
DDP38003/Rapamycin co-treated group (#C21)	+	++	–
DDP38003/Rapamycin co-treated group (#C25)	+	++	–

Degree/extent of leukemia infiltration; null (–), mild (+), moderate (++), severe (+++).

partly–to mTOR regulation by LSD1 (Figure 7K).

In conclusion, our data underscore a pro-survival role of mTOR in mediating both intrinsic and acquired resistance of AML cells to LSD1i and provide an objective rationale for considering epigenetic (LSD1i)/metabolic (mTORi) combinatorial regimens for irresponsive AML patients.

Acknowledgments

We would like to thank Dr. Fabio Santoro, Dr. Roberto Ravasio and Prof. Pier Giuseppe Pelicci for their support and constructive discussions. We are also thankful to Dr. Federica Pisati who performed the histopathological and immunohistochemical analyses. AKA has been awarded a fellowship by AIRC (Italian Association for Cancer Research). Work in SM's lab is supported by AIRC, CNR (Epigen Flahsigij Project), Regione Lombardia (Progetto Neon) and Horizon 2020 (TRANSCAN DRAMA) grants. The funders had no role in study design, data collection and analysis, decision to publish, or preparation of the manuscript.

References

- Niebel D, Kirfel J, Janzen V, Holler T, Majores M, Gutgemann I. Lysine-specific demethylase 1 (LSD1) in hematopoietic and lymphoid neoplasms. *Blood*. 2014;124(1):151-152.
- Wada T, Koyama D, Kikuchi J, Honda H, Furukawa Y. Overexpression of the shortest isoform of histone demethylase LSD1 primes hematopoietic stem cells for malignant transformation. *Blood*. 2015;125(24):3731-3747.
- Harris WJ, Huang X, Lynch JT, et al. The histone demethylase KDM1A sustains the oncogenic potential of MLL-AF9 leukemia stem cells. *Cancer Cell*. 2012;21(4):473-487.
- Schenk T, Chen WC, Göllner S, et al. Inhibition of the LSD1 (KDM1A) demethylase reactivates the all-trans-retinoic acid differentiation pathway in acute myeloid leukemia. *Nat Med*. 2012;18(4):605-612.
- Lv T, Yuan D, Miao X, et al. Over-expression of LSD1 promotes proliferation, migration and invasion in non-small cell lung cancer. *PLoS One*. 2012;7(4):e35065.
- Jie D, Zhongmin Z, Guoqing L, et al. Positive expression of LSD1 and negative expression of E-cadherin correlate with metastasis and poor prognosis of colon cancer. *Dig Dis Sci*. 2013;58(6):1581-1589.
- Setzger E, Wissmann M, Yin N, et al. LSD1 demethylates repressive histone marks to promote androgen-receptor-dependent transcription. *Nature*. 2005;437(7057):436-439.
- Baek SH, Kim K Il. Regulation of HIF-1 alpha stability by lysine methylation. *BMB Rep*. 2016; 49(5):245-246.
- Feng J, Xu G, Liu J, et al. Phosphorylation of LSD1 at Ser112 is crucial for its function in induction of EMT and metastasis in breast cancer. *Breast Cancer Res Treat*. 2016;159(3):443-456.
- Hino S, Sakamoto A, Nagaoka K, et al. FAD-dependent lysine-specific demethylase-1 regulates cellular energy expenditure. *Nat Commun*. 2012;3:712-758.
- Sakamoto A, Hino S, Nagaoka K, et al. Lysine demethylase LSD1 coordinates glycolytic and mitochondrial metabolism in hepatocellular carcinoma cells. *Cancer Res*. 2015;75(7):1445-1456.
- McGrath JP, Williamson KE, Balasubramanian S, et al. Pharmacological inhibition of the histone lysine demethylase KDM1A suppresses the growth of multiple acute myeloid leukemia subtypes. *Cancer Res*. 2016;76(7):1975-1988.
- Vianello F, Botrugno OA, Cappa A, et al. Discovery of a novel inhibitor of histone lysine-specific demethylase 1A (KDM1A/LSD1) as orally active antitumor agent. *J Med Chem*. 2016;59(4):1501-1517.
- Maes T, Mascaro C, Tirapu I, et al. ORY-1001, a potent and selective covalent

- KDM1A inhibitor, for the treatment of acute leukemia. *Cancer Cell*. 2018;33(3): 495-511.
15. Abdel-Aziz AK, Minucci S. Comparing apples with oranges: Studying LSD1 inhibitors in cellular assays. *Pharmacol Res*. 2019;146:104345.
 16. Mohammad HP, Smitheman KN, Kamat CD, et al. A DNA Hypomethylation signature predicts antitumor activity of LSD1 inhibitors in SCLC. *Cancer Cell*. 2015; 28(1):57-69.
 17. Ishikawa Y, Gamou K, Yabuki M, et al. A novel LSD1 inhibitor T-3775440 disrupts GF11B-containing complex leading to trans-differentiation and impaired growth of AML cells. *Mol Cancer Ther*. 2017;16(2):273-284.
 18. Hoshii T, Tadokoro Y, Naka K, et al. mTORC1 is essential for leukemia propagation but not stem cell self-renewal. *J Clin Invest*. 2012;122(6):2114-2129.
 19. Martelli AM, Evangelisti C, Chiarini F, McCubrey JA. The phosphatidylinositol 3-kinase/Akt/mTOR signaling network as a therapeutic target in acute myelogenous leukemia patients. *Oncotarget*. 2010;1(2): 89-103.
 20. Zou Z, Chen J, Yang J, Bai X. Targeted inhibition of rictor/mTORC2 in cancer treatment: a new era after rapamycin. *Curr Cancer Drug Targets*. 2016;16(4):288-304.
 21. Gao Y, Gao J, Li M, et al. Rheb1 promotes tumor progression through mTORC1 in MLL-AF9-initiated murine acute myeloid leukemia. *J Hematol Oncol*. 2016;9:1-14.
 22. Burchert A, Wang Y, Cai D, et al. Compensatory PI3-kinase/Akt/mTOR activation regulates imatinib resistance development. *Leukemia*. 2005;19(10):1774-1782.
 23. Elgendy M, Abdel-Aziz AK, Renne SL, et al. Dual modulation of MCL-1 and mTOR determines the response to sunitinib. *J Clin Invest*. 2017;127(1):153-168.
 24. Malone CF, Emerson C, Ingraham R, et al. mTOR and HDAC inhibitors converge on the TXNIP/thioredoxin pathway to cause catastrophic oxidative stress and regression of RAS-driven tumors. *Cancer Discov*. 2017;7(12):1450-1463.
 25. Fang J, Ying H, Mao T, et al. Upregulation of CD11b and CD86 through LSD1 inhibition promotes myeloid differentiation and suppresses cell proliferation in human monocytic leukemia cells. *Oncotarget*. 2017;8(49): 85085-85101.
 26. Chow S, Minden MD, Hedley DW. Constitutive phosphorylation of the S6 ribosomal protein via mTOR and ERK signaling in the peripheral blasts of acute leukemia patients. *Exp Hematol*. 2006;34(9):1183-1191.
 27. Binda C, Valente S, Romanenghi M, et al. Biochemical, structural, and biological evaluation of tranlycypromine derivatives as inhibitors of histone demethylases LSD1 and LSD2. *J Am Chem Soc*. 2010;132(19): 6827-6833.
 28. Kovacs K, Decatur C, Toro M, et al. 2-Deoxy-glucose downregulates endothelial AKT and ERK via interference with N-linked glycosylation, induction of endoplasmic reticulum stress, and GSK3 β activation. *Mol Cancer Ther*. 2016;15(2): 264-275.
 29. Inoki K, Ouyang H, Zhu T, et al. TSC2 integrates Wnt and energy signals via a coordinated phosphorylation by AMPK and GSK3 to regulate cell growth. *Cell*. 2006; 126(5):955-968.
 30. Machado-Neto JA, Favaro P, Lazarini M, Costa FF, Olalla Saad ST, Traina F. Knockdown of insulin receptor substrate 1 reduces proliferation and downregulates Akt/mTOR and MAPK pathways in K562 cells. *Biochim Biophys Acta*. 2011;1813 (8):1404-1411.
 31. Fenerich BA, Machado-Neto JA, Alves AP, et al. The pharmacological IGF1R-IRS1/2 Inhibitor NT157 presents multiple antineoplastic effects in myeloproliferative neoplasms. *Blood*. 2017;130(Suppl 1):1253.
 32. Del Rincón S V, Guo Q, Morelli C, Shiu HY, Surmacz E, Miller WH. Retinoic acid mediates degradation of IRS-1 by the ubiquitin-proteasome pathway, via a PKC-dependant mechanism. *Oncogene*. 2004;23(57):9269-9279.
 33. Ravikumar S, Perez-Liz G, Del Vale L, Soprano DR, Soprano KJ. Insulin receptor substrate-1 is an important mediator of ovarian cancer cell growth suppression by all-trans retinoic acid. *Cancer Res*. 2007; 67(19):9266-9275.
 34. Goossens S, Peirs S, Loocke WV, et al. Oncogenic ZEB2 activation drives sensitivity towards KDM1A inhibition in T-cell acute lymphoblastic leukemia. *Blood*. 2017; 129(8):981-990.
 35. Abdel-Aziz AK, Abdel-Naim AB, Shouman S, Minucci S, Elgendy M. From resistance to sensitivity: insights and implications of biphasic modulation of autophagy by sunitinib. *Front Pharmacol*. 2017;8:1-10.
 36. Peng X, Zhang D, Li Z, Fu M, Liu H. mTOR inhibition sensitizes human hepatocellular carcinoma cells to resminostat. *Biochem Biophys Res Commun*. 2016;477(4):556-562.
 37. Feng S, Jin Y, Cui M ZJ. Lysine-specific demethylase 1 (LSD1) Inhibitor S2101 induces autophagy via the AKT/mTOR pathway in SKOV3 ovarian cancer cells. *Med Sci Monit*. 2016;22:4742-4748.
 38. Poulain L, Sujobert P, Zylbersztejn F, et al. High mTORC1 activity drives glycolysis addiction and sensitivity to G6PD inhibition in acute myeloid leukemia cells. *Leukemia*. 2017;31(11):2326-2335.
 39. Duteil D, Metzger E, Willmann D, et al. LSD1 promotes oxidative metabolism of white adipose tissue. *Nat Commun*. 2014;5:4093:1-31.
 40. Hino S, Kohrogi K, Nakao M. Histone demethylase LSD1 controls the phenotypic plasticity of cancer cells. *Cancer Sci*. 2016;107(9):1187-1192.
 41. Park H, Garrido-Laguna I, Naing A, et al. Phase I dose-escalation study of the mTOR inhibitor sirolimus and the HDAC inhibitor vorinostat in patients with advanced malignancy. *Oncotarget*. 2016;7 (41):67521-67531.
 42. Kerenyi MA, Shao Z, Hsu YJ, et al. Histone demethylase LSD1 represses hematopoietic stem and progenitor cell signatures during blood cell maturation. *Elife*. 2013;2:e00633.
 43. Abdulla A, Zhang Y, Hsu FN, et al. Regulation of lipogenic gene expression by lysine-specific histone demethylase-1 (LSD1). *J Biol Chem*. 2014;289(43):29937-29947.
 44. Lee G, Zheng Y, Cho S, et al. Post-transcriptional regulation of de novo post-transcriptional regulation of de novo lipogenesis by mTORC1-S6K1-SRPK2 signaling. *Cell*. 2017;171(7):1545-1549.
 45. Roux PP, Shahbazian D, Vu H, et al. RAS/ERK signaling promotes site-specific ribosomal protein S6 phosphorylation via RSK and stimulates Cap-dependent translation. *J Biol Chem*. 2007;282(19):14056-14064.
 46. Maiques-Diaz A, Spencer GJ, Lynch JT, et al. Enhancer activation by pharmacologic displacement of LSD1 from GF11 induces differentiation in acute myeloid leukemia. *Cell Rep*. 2018;22(13):3641-3659.



Ferrata Storti Foundation

EVI1 triggers metabolic reprogramming associated with leukemogenesis and increases sensitivity to L-asparaginase

Yusuke Saito,¹ Daisuke Sawa,¹ Mariko Kinoshita,¹ Ai Yamada,¹ Sachiyo Kamimura¹, Akira Suekane,² Honami Ogoh,² Hidemasa Matsuo,³ Souichi Adachi,³ Takashi Taga,⁴ Daisuke Tomizawa,⁵ Motomi Osato,^{6,7} Tomoyoshi Soga,⁸ Kazuhiro Morishita² and Hiroshi Moritake¹

Haematologica 2020
Volume 105(8):2118-2129

¹Division of Pediatrics, Faculty of Medicine, University of Miyazaki, Miyazaki; ²Division of Tumor and Cellular Biochemistry, University of Miyazaki, Miyazaki; ³Department of Human Health Science, Kyoto University, Kyoto; ⁴Department of Pediatrics, Shiga University of Medical Science, Shiga; ⁵Division of Leukemia and Lymphoma, Children's Cancer Center, National Center for Child Health and Development, Tokyo; ⁶Cancer Science Institute, National University of Singapore, Singapore; ⁷International Research Center for Medical Sciences, Kumamoto University, Kumamoto and ⁸Institute for Advanced Biosciences, Keio University, Yamagata, Japan

ABSTRACT

Metabolic reprogramming of leukemia cells is important for survival, proliferation, and drug resistance under conditions of metabolic stress in the bone marrow. Deregulation of cellular metabolism, leading to development of leukemia, occurs through abnormally high expression of transcription factors such as MYC and Ecotropic Virus Integration site 1 protein homolog (EVI1). Overexpression of EVI1 in adults and children with mixed lineage leukemia-rearrangement acute myeloid leukemia (MLL-r AML) has a very poor prognosis. To identify a metabolic inhibitor for EVI1-induced metabolic reprogramming in MLL-r AML, we used an XFp extracellular flux analyzer to examine metabolic changes during leukemia development in mouse models of AML expressing MLL-AF9 and Evi1 (Evi1/MF9). Oxidative phosphorylation (OXPHOS) in Evi1/MF9 AML cells accelerated prior to activation of glycolysis, with a higher dependency on glutamine as an energy source. Furthermore, EVI1 played a role in glycolysis as well as driving production of metabolites in the tricarboxylic acid cycle. L-asparaginase (L-asp) exacerbated growth inhibition induced by glutamine starvation and suppressed OXPHOS and proliferation of Evi1/MF9 both *in vitro* and *in vivo*; high sensitivity to L-asp was caused by low expression of asparagine synthetase (ASNS) and L-asp-induced suppression of glutamine metabolism. In addition, samples from patients with EVI1⁺MF9 showed low ASNS expression, suggesting that it is a sensitive marker of L-asp treatment. Clarification of metabolic reprogramming in EVI1⁺ leukemia cells may aid development of treatments for EVI1⁺MF9 refractory leukemia.

Correspondence:

HIROSHI MORITAKE
hiroshi_moritake@med.miyazaki-u.ac.jp

Received: May 2, 2019.

Accepted: October 24, 2019.

Pre-published: October 24, 2019.

doi:10.3324/haematol.2019.225953

Check the online version for the most updated information on this article, online supplements, and information on authorship & disclosures: www.haematologica.org/content/105/8/2118

©2020 Ferrata Storti Foundation

Material published in Haematologica is covered by copyright. All rights are reserved to the Ferrata Storti Foundation. Use of published material is allowed under the following terms and conditions:

<https://creativecommons.org/licenses/by-nc/4.0/legalcode>.

Copies of published material are allowed for personal or internal use. Sharing published material for non-commercial purposes is subject to the following conditions:

<https://creativecommons.org/licenses/by-nc/4.0/legalcode>,

sect. 3. Reproducing and sharing published material for commercial purposes is not allowed without permission in writing from the publisher.



Introduction

Acute myeloid leukemia (AML) is a cancer of myeloid lineage that results in genetically heterogeneous disease. Chromosomal translocations leading to fusion of the mixed lineage leukemia gene (MLL1) are common alterations associated with aggressive *de novo* and therapy-related acute leukemia in children and adults.^{1,2}

The ecotropic viral integration site-1 (EVI1) gene encodes a zinc finger protein that functions as a transcriptional regulator of hematopoietic stem cell self-renewal and long-term multilineage repopulating activity.^{3,4} Overexpression of EVI1 is an independent, adverse prognostic factor because of its association with reduced remission duration of AML with MLL rearrangement (MLL-r AML), particularly in patients harboring MLL-AF9 (MF9).⁵⁻⁷ EVI1 may play an important role in maintenance of cell quiescence and stem cell-like phenotypes in leukemia cells, thereby contributing to chemoresistance.^{8,9} Previously, we identified potential therapeutic

targets such as CD52 and GPR56 for the treatment of patients with EVI1^{high} leukemia; however, these potential targets did not prove effective in practice.^{10,11}

Dysregulation of metabolic pathways occurs through aberrant expression of transcription factors such as MYC.^{12,13} Transcriptional changes resulting from aberrantly activated MYC lead to increased glucose uptake and glycolytic activity; it also stimulates glutaminolysis and lipid biosynthesis during leukemogenesis. It is, however, still not known whether MLL positively regulates metabolic pathways. Therefore, we focused on metabolic reprogramming of MF9 AML with high EVI1 expression (EVI1⁺MF9 AML). A recent study shows that EVI1 alters cellular metabolism and increases activity of CKMT1, which affects mitochondrial respiration and ATP production.¹⁴ However, further studies are needed to resolve the metabolic relationship between MLL and EVI1.^{15,16}

Here, we developed transgenic (TG) mice with high expression of *Evi1* in hematopoietic progenitor cells and established a mouse model of EVI1⁺MF9 AML. We then examined metabolic changes in these cells during leukemia development using an XFp extracellular flux analyzer. We found that the leukemia cells showed accelerated oxidative phosphorylation (OXPHOS) prior to activation of glycolysis, along with greater dependency on glutamine as an energy source. In addition, treatment with L-asparaginase (L-asp) effectively inhibited proliferation of *Evi1*⁺MF9 AML cells by suppressing OXPHOS. Therefore, although patients with EVI1⁺MF9 AML usually have a poor prognosis, treatment with specific inhibitors of energy metabolic reprogramming induced by EVI1 (e.g. L-asp) may improve their outcomes.

Methods

TG mice

The +24 mCNE-mhsp68p vector was kindly provided by Dr. Motomi Osato (Kumamoto University, Kumamoto, Japan).¹⁷ +24mCNE is a stem cell-specific enhancer of *Runx1*, which is located +24 Kb downstream from the transcription start site in mice. Therefore, it is also called eR1(+24m) and is referred to hereafter as eR1. The mEvi1 transgenic construct was engineered by introducing mouse *Evi1* cDNA into the EcoR1 site of the eR1-mhsp68p vector. A 7.67 kb *Sap1/BsaA1* fragment of eR1-mhsp68p mEvi1 was then microinjected into fertilized mouse eggs (C57BL/6), and TG offspring were screened by polymerase chain reaction (PCR) using the following primers: 5'-ggc cac cat ggc gta tta gg-3' and 5'-tct tcc agc gga tag aat gg-3'. TG mice were backcrossed onto a C57BL/6 background and maintained as heterozygotes. All procedures were approved by the University of Miyazaki Animal Care and Use Committee.

Retroviral bone marrow transduction assays

The pMIG-FLAG-MLL-AF9 plasmid was a kind gift from Daisuke Nakada (Addgene plasmid # 71443).¹⁸ Plat-E cells were transiently transfected with MSCV vectors harboring the pCL-Eco plasmid using polyethylenimine (PEI). At four days post injection of wild-type (WT) and *Evi1*-TG mice with 5-fluorouracil (5-FU) (150 mg/kg; Kyowa Kirin), bone marrow (BM) cells were harvested and incubated for 24 hours (h) in X-Vivo 15 (Lonza, Allendale, NJ, USA) supplemented with 50 ng/mL SCF; 50 ng/mL TPO, 10 ng/mL IL-3, and 10 ng/mL IL-6 (all from Peprotech, Rocky Hill, NJ, USA). After incubation, cells in retronectin (Clontech, Mountain View, CA, USA)-coated plates were spin-infected

[490 g for 45 minutes (min) at 20°C] with retroviral supernatant supplemented with polybrene (8 µg/mL). BM cells (500,000) were then transplanted into lethally irradiated C57BL/6 mice. For secondary transplantations, GFP⁺ cells from primary recipient mice were transplanted into sublethally irradiated recipients.

Measurement of oxygen consumption rate

Oxygen consumption rate (OCR) was measured using an XFp extracellular flux analyzer (Agilent Technologies, Santa Clara, CA, USA). Leukemia cells were suspended in XF Assay Medium supplemented with 10 mM glucose, 1 mM pyruvate, and 2 mM glutamine. Cells (200,000 per well) were seeded in a culture plate pre-coated with Cell-Tak (Fisher Scientific). The plate was centrifuged and left to equilibrate for 60 min in a CO₂-free incubator before being transferred to the XFp extracellular flux analyzer. The Mito Stress Test was performed as follows: 1) basal respiration was measured in XF Base Medium (1 mM sodium pyruvate, 10 mM glucose, 2 mM glutamine); 2) oligomycin (1 µM) was injected to measure respiration linked to ATP production; 3) the uncoupler carbonyl cyanide 4-(trifluoromethoxy) phenylhydrazone (FCCP, 1 µM) was added to measure maximal respiration; and 4) rotenone and antimycin A (0.5 µM each) were applied together to measure non-mitochondrial respiration. Measurement of fuel dependency and fuel flexibility was performed according to the manufacturer's Mito fuel flex test kit protocol (Agilent Technologies).

Statistical analysis

Statistical analysis was performed using a paired Student's *t*-test, the Mann-Whitney U test, or the log-rank test as appropriate. Calculations were performed using Prism software (GraphPad). Group data are expressed as the mean±standard deviation. No mice were excluded from data analysis.

Results

EVI1 induces aggressive MLL-AF9 leukemia to activate mitochondrial respiration

Initially, we created a series of TG mice with high *Evi1* expression (*Evi1*-TG) in lineage^{low}Sca-1⁺c-kit⁺ (LSK) and granulocyte/macrophage progenitor (GMP) cells (Figure 1A) under the control of the eR1 enhancer, which shows hematopoietic-specific enhancer activity in both zebrafish and mouse models (*Online Supplementary Figure S1A*).¹⁷ There were no differences in blood cell counts or the percentage of normal hematopoietic progenitors including hematopoietic stem cells (HSC), multipotent progenitors (MPP), and GMP between WT and *Evi1*-TG mice (*Online Supplementary Figure S1B and C*). *Evi1*-TG mice do not develop leukemia and hematopoietic disorders until at least 16 weeks.

To examine whether EVI1 regulates energy metabolism in MLL-rearranged leukemia cells, we used a murine model in which AML is driven by the MF9 oncogene.^{19,20} Murine hematopoietic progenitor cells from WT and *Evi1*-TG were transduced with retrovirus encoding both MF9 and GFP, and serial colony forming assays were performed. BM cells showing MF9 expression were transplanted into irradiated syngeneic mice (Figure 1B). The colony assay revealed that the colony numbers and percentages of GFP⁺ AML cells from *Evi1*-TG were higher than those from WT *in vitro* (Figure 1C and D). After establishing primary MF9-induced AML in WT or *Evi1*-TG (WT/MF9 or *Evi1*/MF9) mice, we noted significantly higher expression of *Evi1* in GFP⁺ whole leukemia cells and in

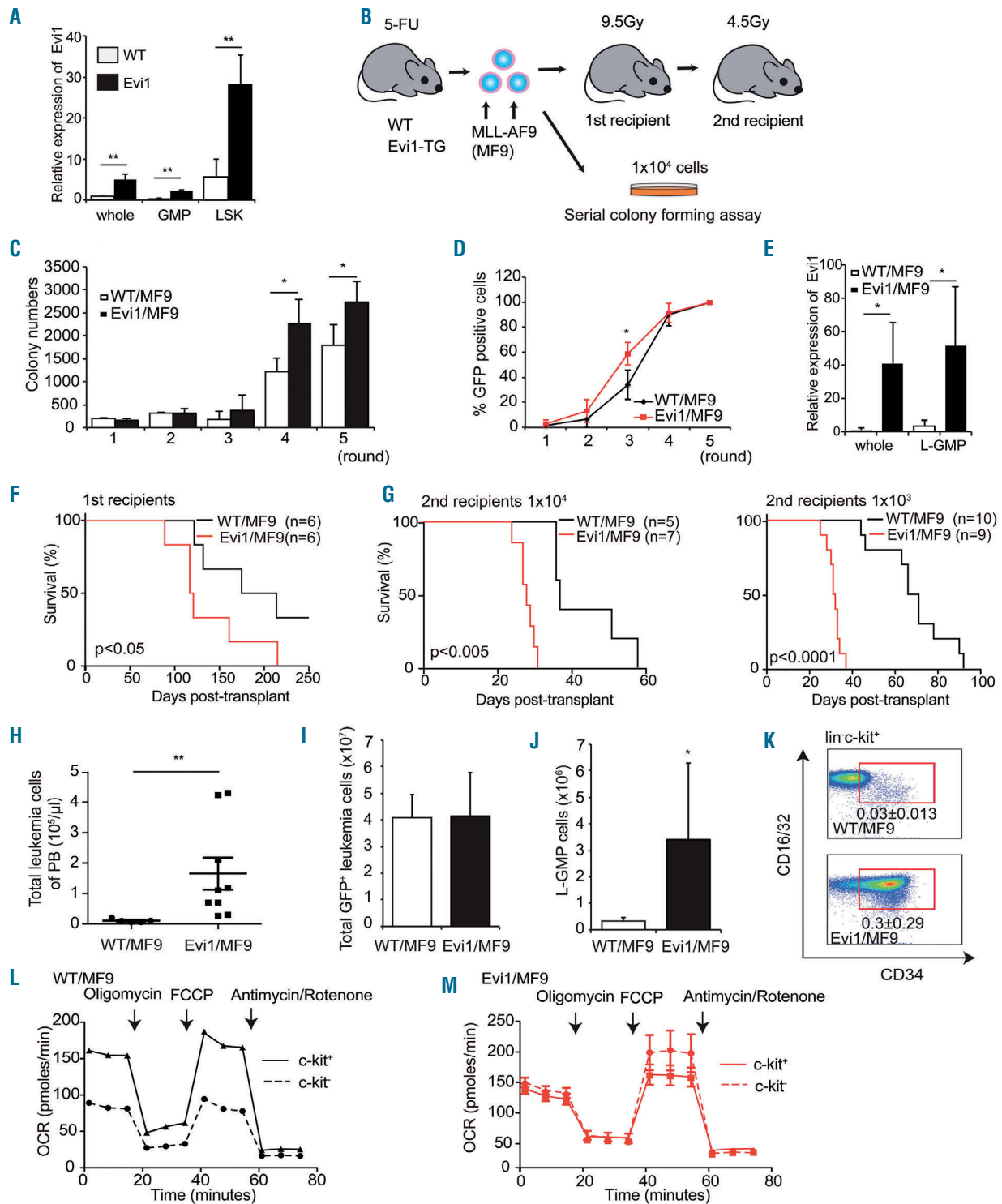


Figure 1. EVI1 induces aggressive MLL-AF9 leukemia cells to activate mitochondrial respiration. (A) Evi1 expression was detected in the LSK fraction, the GMP fraction, and whole bone marrow cells (BM) from wild-type (WT) (white bar) and Evi1-TG mice (black bar) by quantitative real-time polymerase chain reaction (qRT-PCR). Relative expression of Evi1 was normalized against that of β -actin on whole BM cells. (B) Schematic outline of the mouse model of WT/MF9 and Evi1/MF9. The experimental details are described in the Methods. (C and D) Hematopoietic progenitors from WT (white bar) and Evi1-TG (black bar) mice infected with an MF9 retrovirus were cultured in methylcellulose medium and replated every five days. The colony numbers for each round of replating are indicated in (C). The percentage of GFP-positive cells for each replating round is presented as a line graph (D). (E) Relative expression of Evi1 in the GFP⁺ and L-GMP fractions from WT/MF9 or Evi1/MF9 mice, as measured by qRT-PCR. Relative expression of Evi1 was normalized against that of β -actin on GFP⁺ cells from WT/MA9. (F) Kaplan-Meier survival curves of mice transplanted with MLL-AF9-transduced WT (n=6) or Evi1-TG cells (n=6 mice; three independent experiments). (G) Secondary transplantation of 10^4 or 10^3 GFP⁺ AML cells revealed increased leukemogenesis by Evi1-TG cells (n=5–10 mice; three independent experiments). (H) Total number of GFP⁺ leukemia cells in peripheral blood from secondary recipients. (I and J) Total number of acute myeloid leukemia (AML) cells and L-GMP cells in the BM of secondary recipients. Secondary recipients of Evi1/MF9 had significantly more L-GMP in the BM. (K) Representative FACS profiles (gated on lin-c-kit⁺ cells) show reduced numbers of CD34⁺CD16/32⁻ L-GMP (red box). (L and M) Oxygen consumption rate (OCR) of the c-kit⁺ or c-kit⁻ fractions from WT/MF9 (L) and Evi1/MF9 (M). Mitochondrial respiration in c-kit⁺ WT/MF9 cells was higher than that in c-kit⁻ cells. By contrast, there was no difference between c-kit⁺ and c-kit⁻ cells from Evi1/MF9 mice. All data are expressed as the mean \pm standard deviation. * $P < 0.05$; ** $P < 0.005$; *** $P < 0.0005$ (Student's t-test). Survival curves were compared using the log-rank test.

the leukemic granulocyte/macrophage progenitor (L-GMP) fraction from Evi1/MF9-recipients (Figure 1E). After the first round of transplantation of BM cells from WT/MF9 or Evi1/MF9, recipient mice receiving Evi1/MF9 cells survived for a significantly shorter time than mice transplanted with WT/MF9 cells (Figure 1F). After a second round of transplantation with 10^4 or 10^5 leukemia cells isolated from primary recipient mice, the survival of secondary recipient mice transplanted with Evi1/MF9 cells was significantly shorter than that of those transplanted with WT/MF9 (Figure 1G). Recipients of Evi1/MF9 cells harbored an increased total number of blast cells in peripheral blood and in the L-GMP fraction in the BM, although there was no difference between these mice and WT/MF9 mice with respect to the total number of GFP⁺ cells in the BM (Figure 1H-K). A recent report shows that mitochondrial respiration in leukemic stem and progenitor cells is higher than that in differentiated leukemia cells.^{21,22} Therefore, to examine the metabolic advantages conferred by Evi1/MF9 AML cells, we measured the mitochondrial OCR of the stem cell-enriched c-kit-positive (c-kit⁺) and differentiated c-kit-negative (c-kit⁻) fractions from WT/MF9 or Evi1/MF9 mice. The basal and maximum OCR of c-kit⁺ cells from WT/MF9 mice was higher than that of c-kit⁻ cells (Figure 1L). However, there was no difference in the OCR between c-kit⁺ and c-kit⁻ cells from Evi1/MF9 mice (Figure 1M). These data indicate that EVI1 activates mitochondrial respiration in differentiated leukemia cells as efficiently as in the stem cell-enriched fraction, thereby providing a metabolic advantage.

Oxidative phosphorylation is activated before enhanced glycolysis during development of EVI1⁺ MLL-AF9 leukemia

To examine the potential role of EVI1 during development of MF9 leukemia, we measured mitochondrial function (i.e. OCR) and glycolytic activity (i.e. ECAR) of serially replated colonies of WT/MF9 and Evi1/MF9 leukemia cells at different replating times using a XFp extracellular flux analyzer. Basal OCR and maximal respiratory capacity in normal c-kit⁺ hematopoietic progenitor cells from Evi1-TG mice were lower than in those from WT mice (Figure 2A). However, after the second round of plating, the OCR of Evi1/MF9 progenitor cells at each replating time was higher than that of WT/MF9 cells (Figure 2B-E). To clarify whether mitochondrial respiration is activated by the metabolic environment in BM, we measured OCR in *ex vivo* WT/MF9 and Evi1/MF9 leukemia cells isolated from the BM of leukemic mice. Evi1/MF9 mice showed a significantly higher basal and maximal respiratory capacity of OCR than WT/MF9 mice (Figure 2F). Of note, the glycolytic activity of Evi1/MF9 cells increased after the 3rd plating (Figure 2G); in addition, there was no difference between *ex vivo* ECAR of WT/MF9 leukemia cells and that of Evi1/MF9 cells (Figure 2H). These data suggest that EVI1 activates both OXPHOS and glycolysis; therefore, mitochondrial respiration may play an important role in development of MF9 leukemia and correlate with biological aggressiveness.

EVI1 expression is associated with metabolic reprogramming

To identify the metabolic pathways regulated by EVI1, we performed capillary electrophoresis time-of-flight mass spectrometry-based metabolome profiling of

WT/MF9 and Evi1/MF9 leukemia cells.²³ We found significant differences between the cells in terms of the amounts of metabolites derived from the glycolytic and TCA cycles. The amounts of F1,6P and lactate in Evi1/MF9 leukemia cells were higher, implying activation of glycolysis. Moreover, the amounts of fumarate and malate (metabolites of the TCA cycle) were significantly higher in Evi1/MF9 cells (Figure 3A). To identify genes co-expressed with EVI1, we performed DNA microarray analysis of GFP⁺ whole leukemia cells from WT/MF9 and Evi1/MF9 mice (Figure 3B and *Online Supplementary Figure S2*) (GSE118096), and compared the results with those for EVI1-over-expressing normal Lin^{low} BM cells (GSE34729).¹⁴

Expression profiling of Evi1-transduced normal BM cells¹⁴ and MF9 leukemia cells identified upregulation of *Idh2* and downregulation of *Idh1* in both (Figure 3B and *Online Supplementary Figure S2*); the expression of *Idh1* and *Idh2* was confirmed by quantitative real-time polymerase chain reaction (qRT-PCR) (Figure 3C). Upregulation of *Idh2* may induce increased production of metabolites such as fumarate and malate (metabolites of the TCA cycle). In addition, qRT-PCR revealed increased expression of genes involved in glycolysis including *Glut-1* in whole AML cells (Figure 3C and *Online Supplementary Figure S3*). Collectively, these data indicate that EVI1 induces changes in glucose metabolism and the TCA cycle.

EVI1 activates oxidative phosphorylation via glutaminolysis

To determine how EVI1 regulates mitochondrial metabolism, we measured mitochondrial mass by flow cytometry after staining with MitoTracker Deep Red FM. We also measured mitochondrial superoxide production by staining cells with CellROX or MitoSOX. The mitochondrial mass in Evi1/MF9 cells was equivalent to that in WT/MF9 cells (Figure 4A); however, reactive oxygen species (ROS) levels and mitochondrial superoxide production were significantly higher in Evi1/MF9 cells (Figure 4B and C), suggesting that EVI1 expression may facilitate accumulation of ROS. Next, to determine which glycolysis and OXPHOS pathways are important for energy production in Evi1/MF9 cells, we examined the OCR/ECAR ratio in two MF9 murine leukemia lines and various human AML cell lines under conditions of basal respiration. Overall, a higher OCR/ECAR ratio was observed in Evi1/MF9 and EVI1^{high} AML cell lines than in WT/MF9 and EVI1^{low} AML cell lines, suggesting that energy production in EVI1⁺ leukemia cells is mainly dependent on oxidative phosphorylation (Figure 4D and E). To measure the dependency, capacity, and flexibility of leukemia cells to oxidize three major mitochondrial fuels (glutamine, long-chain fatty acids and glucose), we used the XF Mito Fuel Flex Test to examine mitochondrial respiration in MF9 cells in the presence or absence of a specific inhibitor of each fuel pathway. Compared with those in WT/MF9 cells, mitochondria in Evi1/MF9 cells were more dependent on glutamine than on glucose and fatty acids (Figure 4F). Moreover, when Evi1/MF9 or WT/MF9 cells were cultured in the presence of different low concentrations of glucose or glutamine, Evi1/MF9 cells survived significantly longer in the presence of <0.1 g/L glucose (Figure 4G); however, survival decreased significantly when cultured in the presence of <0.2 mM glutamine (Figure 4H), suggesting that survival of Evi1/MF9 cells is very dependent on the glutamine concentration.

When Evi1/MF9 or WT/MF9 cells were treated with the glutaminase inhibitor BPTES, Evi1/MF9 cells (but not WT/MF9 cells) were sensitive to inhibition of OCR (Figure 4I). Collectively, these data indicate that EVI1 plays an essential role in mitochondrial energy reprogramming in MF9 AML cells by activating glutaminolysis (Figure 4J).

To identify the specific mutation that drives this metabolic phenotype (i.e. increased OXPHOS capacity in Evi1/MF9 cells), we measured OXPHOS levels and performed glucose/glutamine starvation experiments on cells infected with Evi1-targeting shRNA (shEvi1) or cells treated with a DOT1L inhibitor (EPZ004777). We found that

shEvi1 and EPZ004777 suppressed OXPHOS in Evi1/MF9 cells (*Online Supplementary Figure S4A*). When cells transfected with shEvi1 or treated with EPZ004777 were cultured in the presence of different low concentrations of glucose or glutamine, shEvi1 cells survived for a significantly longer time in lower concentrations of glutamine (*Online Supplementary Figure S4B*). This suggests that EVI1 is important for glutamine dependency. We performed quantitative PCR analysis of Glut-1, Idh1, and Idh2, and found that expression of Idh2 was lower in shEvi1 and in Evi1/MF9 cells treated with EPZ004777 (*Online Supplementary Figure S4C*). To investigate whether altered

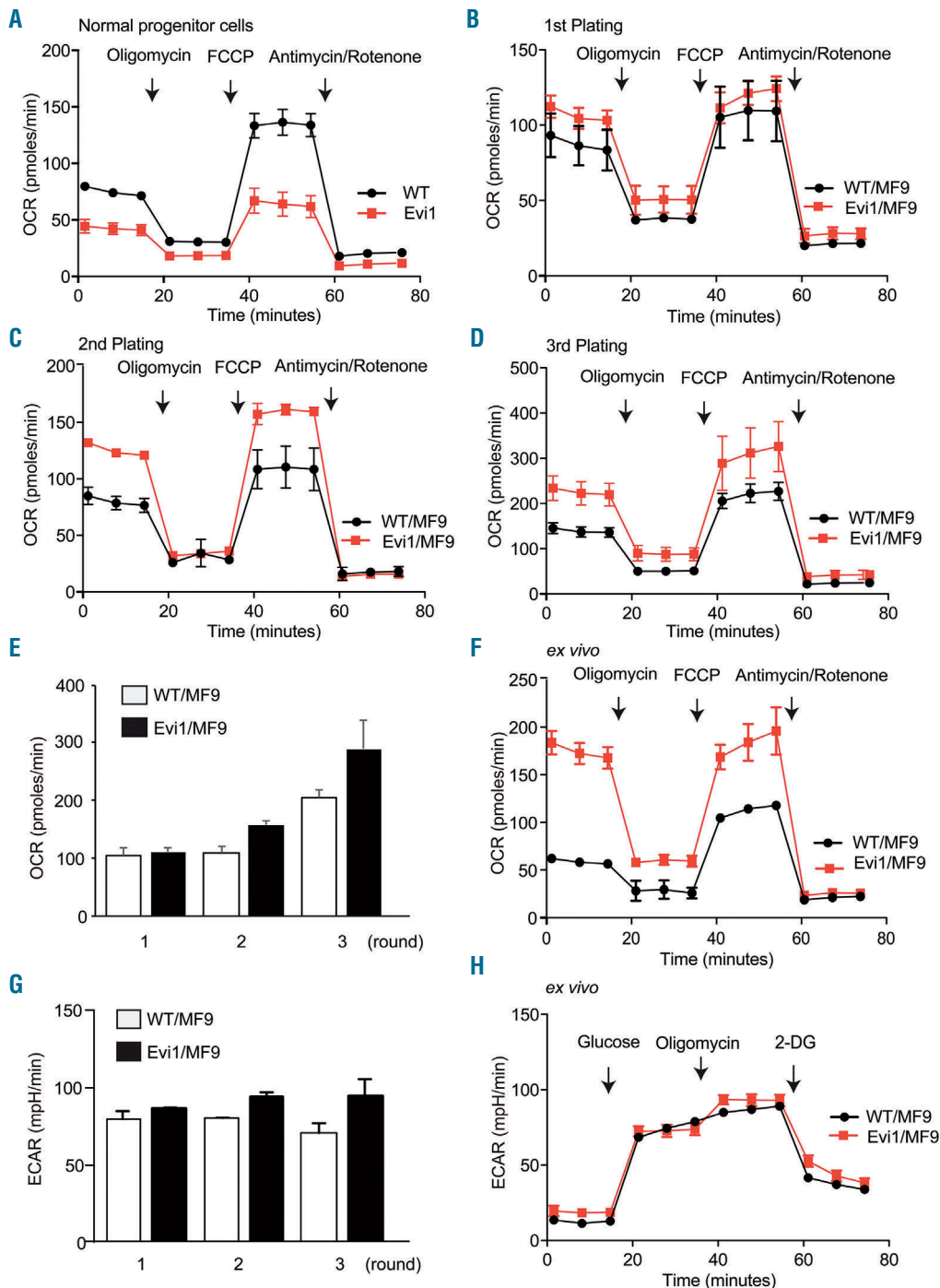
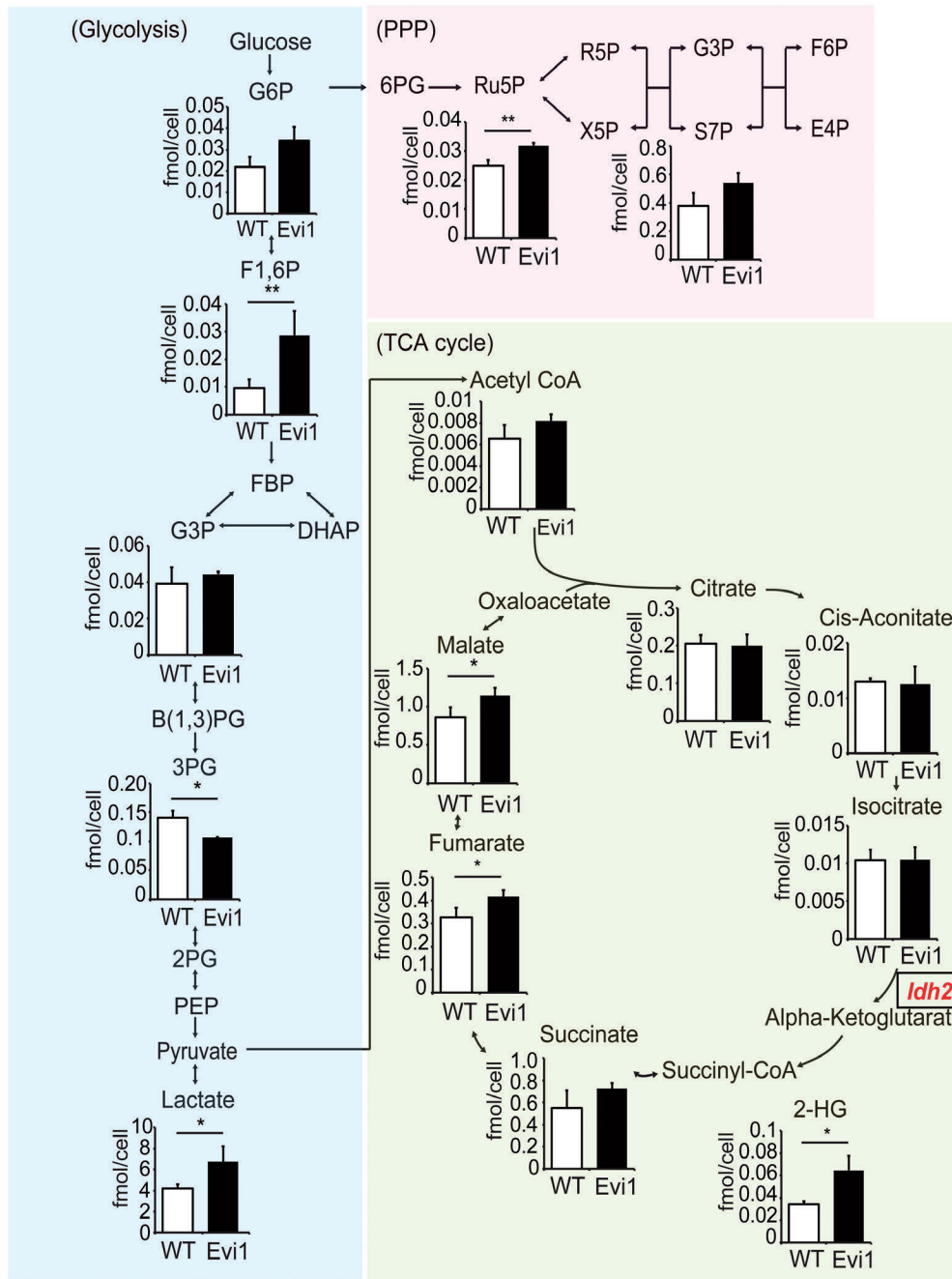
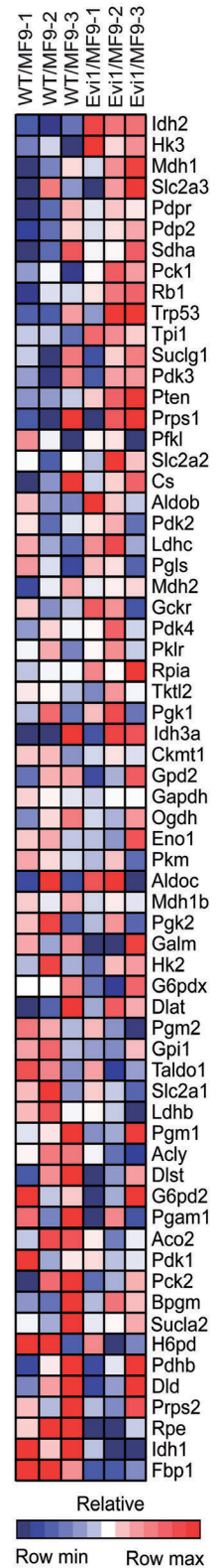


Figure 2. EVI1 increases oxidative phosphorylation (OXPHOS) and glycolysis during development of MLL-AF9 leukemia. (A) The basal oxygen consumption rate (OCR) and maximal respiratory capacity in Evi1-TG normal progenitor cells were significantly lower than those in wild-type (WT) progenitor cells. (B-D) After the 2nd plating, the OCR of Evi1-TG progenitor cells infected with MLL-AF9 increased gradually when compared with that of WT cells. (E) After the 2nd plating, the maximal respiratory capacity of Evi1/MF9 increased gradually when compared with that of WT cells. (F) The basal and capacity OCR of Evi1/MF9 bone marrow cells were significantly higher than those of WT/MF9 cells. (G) The basal ECAR of Evi1/MF9 cells increased slightly after the 3rd plating. (H) There was no significant difference between ECAR of ex vivo leukemia cells from WT/MF9 and from Evi1/MF9 mice. All samples were collected at least in duplicate.

A



B



C

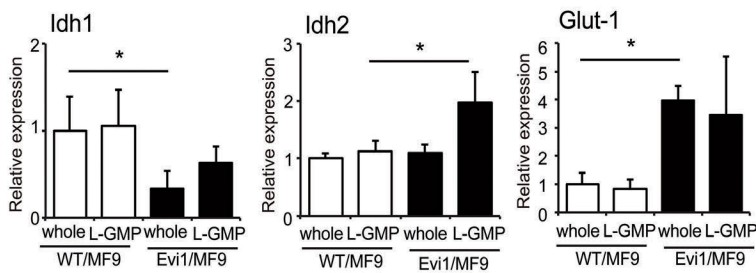


Figure 3. Expression of EVI1 is associated with metabolic reprogramming. (A) “Map” of the metabolic pathways and metabolite concentrations in the glycolysis, PPP, and TCA cycle pathways. The concentrations of F1,6P, lactate, fumarate, and malate were significantly higher in Evi1/MF9 cells (n=3). (B) Heat map of genes encoding metabolism-related factors differentially expressed upon genomic profiling of WT/MF9 or Evi1/MF9 leukemia cells (n=3). (C) Expression of Idh1, Idh2, and Glut-1 operating in the glycolytic pathways and TCA cycle, as measured by qRT-PCR. Expression was normalized to that of β -actin and to that of whole WT/MF9 cells (n=4).

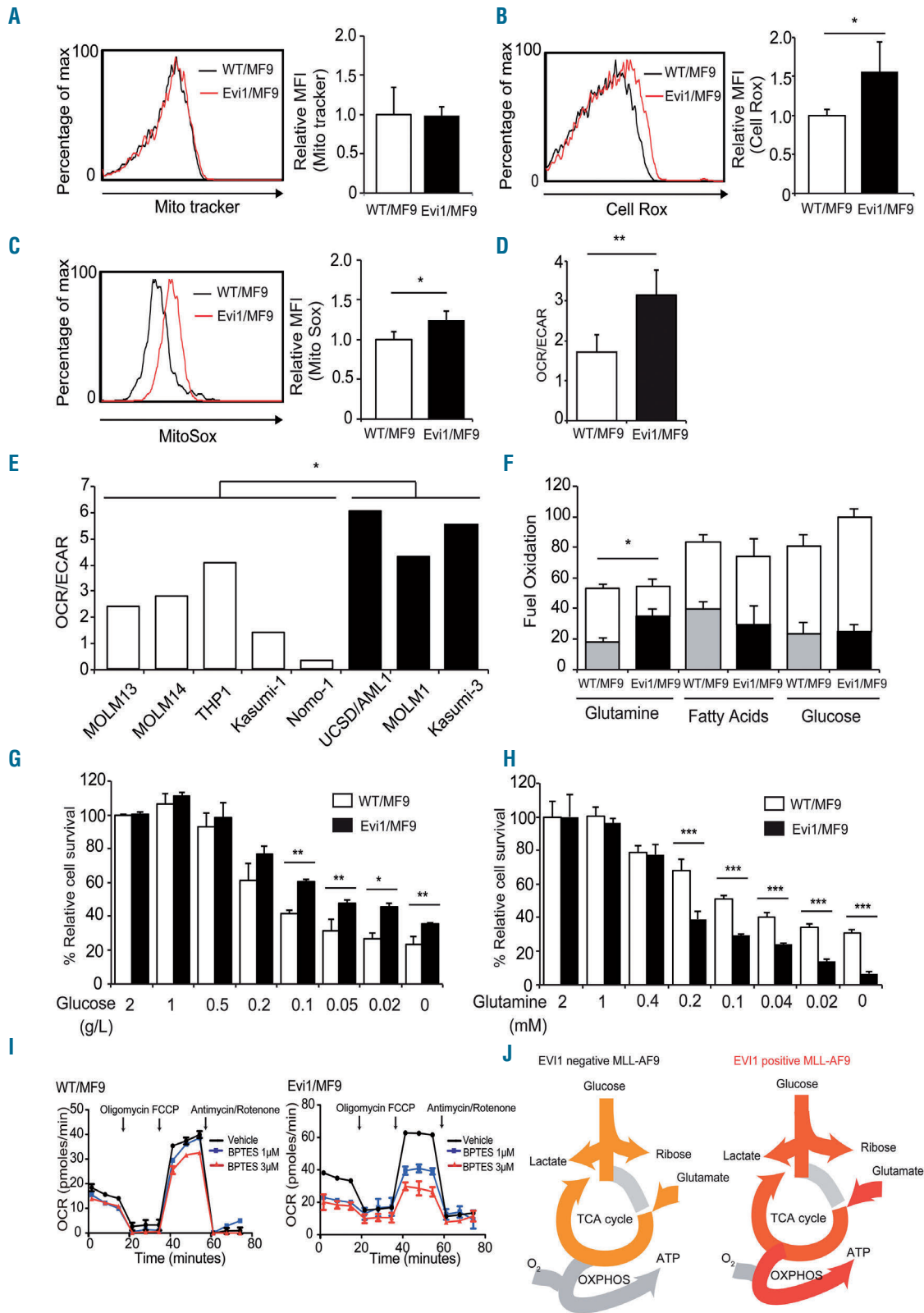


Figure 4. Evi1 activates oxidative phosphorylation (OXPHOS) via glutaminolysis. (A) Mitochondrial mass in Evi1/MF9 (red line) cells was equivalent to that in WT/MF9 (black line) (n=3). (B and C) Reactive oxygen species (ROS) levels and mitochondrial superoxide production were significantly higher in Evi1/MF9 (n=3). (D and E) The oxygen consumption rate (OCR)/extracellular acidification rate (ECAR) ratio under conditions of basal respiration in Evi1/MF9 (D) and Evi1^{high} acute myeloid leukemia (AML) cell lines (E) was significantly higher than that in WT/MF9 cells and Evi1^{low} AML cell lines. (F) The XF Mito Fuel Flex Test calculates the rate of oxidation of a given fuel as a percentage of oxidation of all three fuels being tested. Fuel dependency (black or gray) is a measurement of reliance on a particular fuel pathway to maintain baseline respiration. Fuel flexibility (white) is the ability of cells to increase oxidation of a particular fuel to compensate for inhibition of an alternative fuel pathway. Evi1/MF9 showed an increased dependency on glutamine, but not glycolysis and fatty acids. (G) Evi1/MF9 cells showed increased resistance to glucose starvation. (H) Evi1/MF9 cells were sensitized to glutamine starvation. **P*<0.05; ***P*<0.005; ****P*<0.0005 (Student's *t*-test). (I) The OCR of glutaminolysis inhibitor (BPTES)-treated WT/MF9 leukemia cells remained unchanged. The basal and maximum OCR of BPTES-treated Evi1/MF9 leukemia cells were lower than those of vehicle-treated cells. (J) Schematic representation of metabolic reprogramming upon Evi1 expression.

expression of *Idh1/Idh2* is functionally linked to the increased OXPHOS levels observed in *Evi1/MF9* cells, we measured OXPHOS in *Evi1/MF9* cells transfected with *shIdh1* or *shIdh2*. *Evi1/MF9-shIdh2* cells showed markedly lower levels of OXPHOS than *shScr-* and *shIdh1-*transfected cells (*Online Supplementary Figure S4D*). This suggests that upregulation of *Idh2* via EVI1 may increase OXPHOS activity, which is important for energy production in *Evi1/MF9* cells.

L-asp inhibits EVI1-mediated oxidative phosphorylation activity

To develop a novel strategy for treatment of *Evi1/MF9* cells, we tested the effect of specific inhibitors of glycolysis by 2-deoxyglucose (2-DG) and STF31 (a GLUT-1 inhibitor) and glutaminolysis by BPTES (a glutamine synthetase inhibitor); L-asparaginase (L-asp) is an enzyme that catalyzes hydrolysis of asparagine and glutamine.

Evi1/MF9 cells were more sensitive to glycolysis and glutaminolysis inhibitors than WT leukemia cells (Figure 5A). Moreover, treatment with L-asp led to marked suppression of *Evi1/MF9* cell growth (Figure 5B). Analysis of several human AML cells revealed that the IC_{50} of L-asp against three *EVI1^{high}* AML cell lines and two primary *EVI1⁺* AML cells was lower than that against *EVI1^{low}* AML cell lines and two primary *EVI1-* AML cells (Figure 5C and D). To confirm whether L-asp treatment affects mitochondrial respiration, we used the XFp extracellular flux analyzer to measure energy metabolism by murine *Evi1/MF9* and human *EVI1⁺* AML cells after L-asp treatment. The basal and maximum OCR values for mitochondria in L-asp-treated *Evi1/MF9* cells and human *EVI1⁺* AML cells were markedly lower than in non-treated cells, suggesting that *EVI1⁺* AML cells are more sensitive to L-asp (Figure 5E). WT/MF9 and *Evi1/MF9* do not express surface markers for B- and T-lymphoid cells (*Online Supplementary Figure S5A*). Addition of L-asp led to a marked reduction in the OCR of normal progenitor cells in *Evi1-TG* mice (*Online Supplementary Figure S5B*); however, there was no difference in the IC_{50} between WT and *Evi1-TG* mice (*Online Supplementary Figure S5C*). Some metabolic pathways may play a role in normal BM progenitor cells but not in leukemia cells. To examine whether suppression of OCR by L-asp depends on glutamine depletion, we studied the effects of high glutamine concentration on the OCR of cultured cells. In WT/MF9, L-asp treatment showed no OCR-suppressing effect, which was not affected by glutamine concentration. Meanwhile, in *Evi1/MF9*, high concentration of glutamine attenuated the OCR-suppressing effect (*Online Supplementary Figure S5D*). Taken together, these results indicate that L-asp treatment suppresses growth of *EVI1⁺* AML cells by blocking EVI1-mediated OXPHOS activity.

To examine the therapeutic potential of L-asp *in vivo*, recipient mice transplanted secondarily with *Evi1/MF9* AML cells were treated with L-asp *via* intraperitoneal injection beginning on day 5 post transplantation; L-asp (1,000 U/kg) was injected five times per week for four weeks (Figure 6A). L-asp treatment led to a significant reduction in the number of GFP⁺ AML cells in the peripheral blood (Figure 6B) and extended the survival time of recipient mice (Figure 6C). Although L-asp treatment reduced the total number of leukemia cells in the BM, there was no increase in the number of L-GMP cells in the BM (Figure 6D). Moreover, the basal and maximum OCR

in L-asp-treated BM cells were significantly lower than those in untreated cells (Figure 6E). By contrast, L-asp treatment did not reduce the number of leukemia cells in WT/MF9 mice and did not prolong their survival (*Online Supplementary Figure S6A-C*). Next, we examined the effect of L-asp treatment in a subcutaneous xenograft model of human AML. Immunodeficient NOG mice were injected with UCSD/AML1 cells and treated with L-asp (Figure 6F). L-asp treatment suppressed the growth of human *EVI1^{high}* AML tumors effectively (Figure 6G-I). Overall, these findings indicate that inhibition of OXPHOS by L-asp is a potential effective treatment for *EVI1^{high}* AML.

Low expression of ASNS by MLL-AF9 leukemia cells is associated with high sensitivity to L-asp

High sensitivity to L-asp is due to active glutaminolysis and low expression of asparagine synthetase (Asns). Therefore, we examined expression of the glutamine transporter (*Slc1a5*) and *Asns* in MF9 cells. Expression of *Asns* by *Evi1/MF9* cells was significantly lower than that by WT/MF9 cells (Figure 7A). By contrast, expression of *Slc1a5* by *Evi1/MF9* cells was significantly higher than that by WT/MF9 cells (Figure 7B). WT/MF9 cells transfected with *shAsns* showed a lower IC_{50} for L-asp (*Online Supplementary Figure S7*). These findings suggest that sensitivity to L-asp correlates with ASNS expression in MF9 leukemia.

Next, we examined expression of *IDH2*, *ASNS*, and *SLC1A5* in human leukemia cell lines. L-asp-sensitive *EVI1^{high}* AML cell lines and two primary *EVI1⁺* AML cells showed low expression of ASNS (*Online Supplementary Figure S8A and B*).

Finally, to determine whether these genes are clinically useful markers for predicting L-asp sensitivity, we examined their expression in leukemia samples from patients in JPLSG AML-05.⁷ In the MLL-r AML cohort (n=48), there was no significant difference in ASNS expression between *EVI1-* and *EVI1⁺* AML (Figure 7C). However, expression of ASNS in MF9 AML was significantly lower than that in non-MF9 AML (Figure 7D). Moreover, expression of ASNS in *EVI1⁺*MF9 AML (n=11) was significantly lower than that in those with *EVI1-MF9* (n=17); however, *EVI1* expression did not affect ASNS expression in non-MF9 AML (n=20) (Figure 7E and F). We found no significant difference between *EVI1⁺* and *EVI1-* MF9 AML patients with respect to expression of *IDH2* and *SLC1A5* (Figure 7G and H). These findings suggest that lower expression of ASNS in *EVI1⁺*MF9 AML is associated with higher sensitivity to L-asp.

Discussion

Previously, it was thought that activation of glycolysis was responsible primarily for metabolic reprogramming at onset of leukemia. In addition, clones that promote the survival of BM cells are produced when genes involved in onset of leukemia directly activate glycolytic metabolism.²⁴⁻²⁷ However, recent studies report a direct connection between mitochondrial metabolic activity and refractory AML; this is because: (i) production of adenosine triphosphate (ATP) by mitochondria is higher in leukemia stem cells than in differentiated blast cells or normal HSC; (ii) chemotherapy-resistance of AML correlates

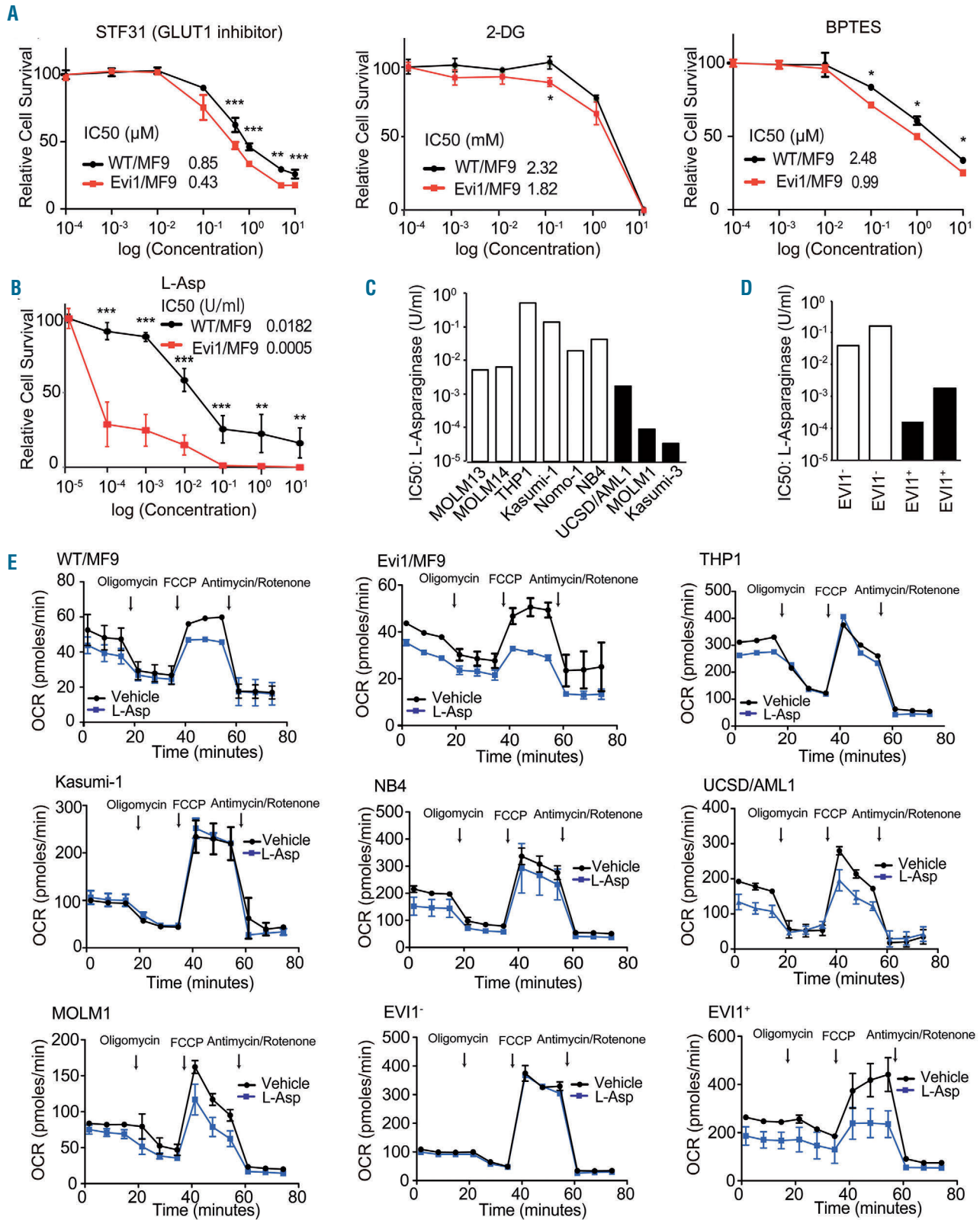


Figure 5. L-asparaginase (L-asp) inhibits EVI1-mediated activation of oxidative phosphorylation (OXPHOS). (A) Survival of MF9 acute myeloid leukemia (AML) cells after brief exposure to glycolysis inhibitors (STF31 and 2-DG) and a glutaminolysis inhibitor (BPTES). Evi1/MF9 cells were more sensitive to glycolysis and glutaminolysis inhibitors than wild-type (WT) leukemia cells. (B) Lasp suppressed proliferation of Evi1/MF9 cells. (C) EVI1^{high} AML cell lines were more sensitive to L-asp than EVI1^{low} AML cell lines. (D) AML cells from two EVI1⁺ AML patients were more sensitive to L-asp than those from EVI1⁻ AML patients. (E) Energy metabolism was analyzed by the XFp extracellular flux analyzer after L-asp treatment (1 U/mL) of AML cells. Basal and maximum OCR in mitochondria were much lower in L-asp-treated Evi1/MF9 than in L-asp-treated WT/MF9 cells. L-asp does not suppress mitochondrial oxidation in EVI1^{low} AML cell lines (THP1, Kasumi-1 and NB4) and primary EVI1⁻ AML cells. L-asp suppressed basal and maximum OCR in mitochondria of EVI1^{high} AML cell lines (UCSD/ANL1, MOLM1) and primary EVI1⁺ leukemia cells.

strongly with OXPHOS activation to a greater extent than with leukemic stemness; and (iii) high OXPHOS activity in cells showing stemness properties induces tyrosine kinase inhibitor-resistance in those with chronic myelocytic leukemia.^{21,22,28} Here, we found that OXPHOS is activated before glycolysis during onset of leukemia, thereby reconfirming the importance of mitochondrial metabo-

lism. A previous study reports that EVI1 plays an important role in metabolic regulation of leukemia, and that a metabolic pathway involving creatinine is the key.¹⁴ However, it is unclear how EVI1 controls metabolism and contributes to malignant alterations in MLL-r AML cells. The leukemia mouse model used in the present study did not show any alterations in creatine gene expression;

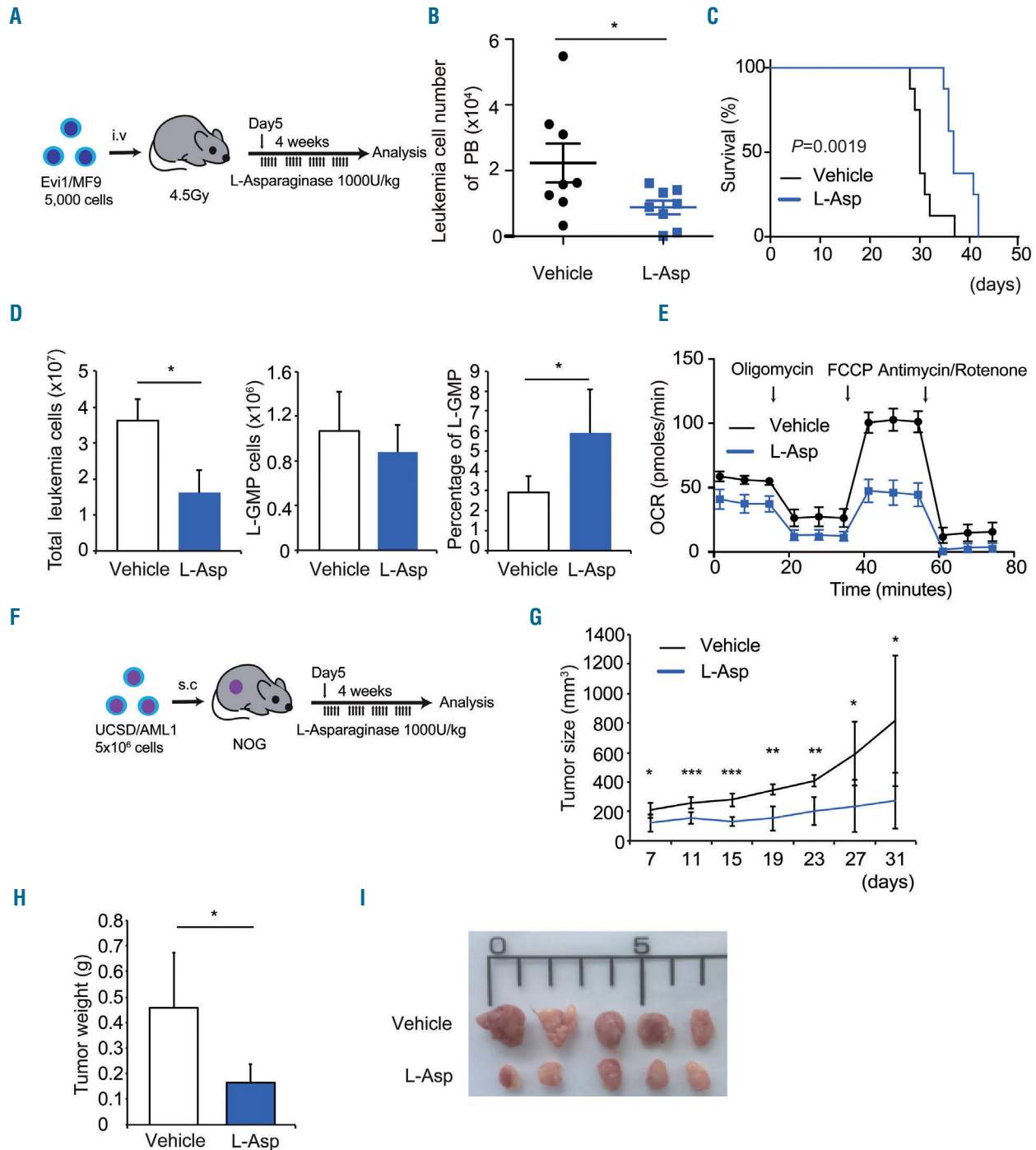


Figure 6. L-Asp inhibits growth of EVI1^{hsp} acute myeloid leukemia (AML) tumor cells *in vivo*. (A) Schematic outline of the Evi1/MF9 mouse model treated with L-asp. Treatment began five days post transplantation. (B) L-asp led to a significant reduction in the number of circulating GFP⁺ AML cells in peripheral blood (n=8). (C) L-asp treatment extended the survival of recipient mice significantly (n=8). (D) The total number of whole AML cells in the bone marrow fell significantly after exposure to L-asp, but the percentage of L-GMP increased significantly. (E) The oxygen consumption rate (OCR) of L-asp-treated leukemia cells in MF9 mice was lower than that of vehicle-treated cells. (F) Schematic outline of the UCSD/AML1 xenograft mouse model treated with L-asp. Treatment began five days post transplantation. (G-I) L-asp inhibited growth of AML tumors significantly (G). Tumor weight (H) and tumor size (I) (n=5).

however, it did show that an advantage in terms of mitochondrial metabolism-dependent energy production could be obtained by activating glutamine metabolism. Furthermore, we suggest that high EVI1 expression maintains OXPHOS activity, even in differentiated cells, and contributes to treatment resistance. Although we did not identify the genes controlled directly by EVI1, we believe that ASNS, IDH2, and SLC1A5 are candidates. IDH2 is mutated in 8-19% of AML cases; therefore, a mutant

IDH2 inhibitor is under development. Future studies should examine whether metabolic reprogramming or increased 2-HG production are induced upon high expression of IDH2.²⁹ In addition, we identified L-asp as a metabolic inhibitor for EVI1⁺ leukemia. L-asp exerts an anti-tumor effect by depleting both asparagine and glutamine.^{30,31} Sensitivity to L-asp correlates with ASNS expression, but the clinical marker is unknown.³²

Although some AML cases are highly sensitive to L-asp,

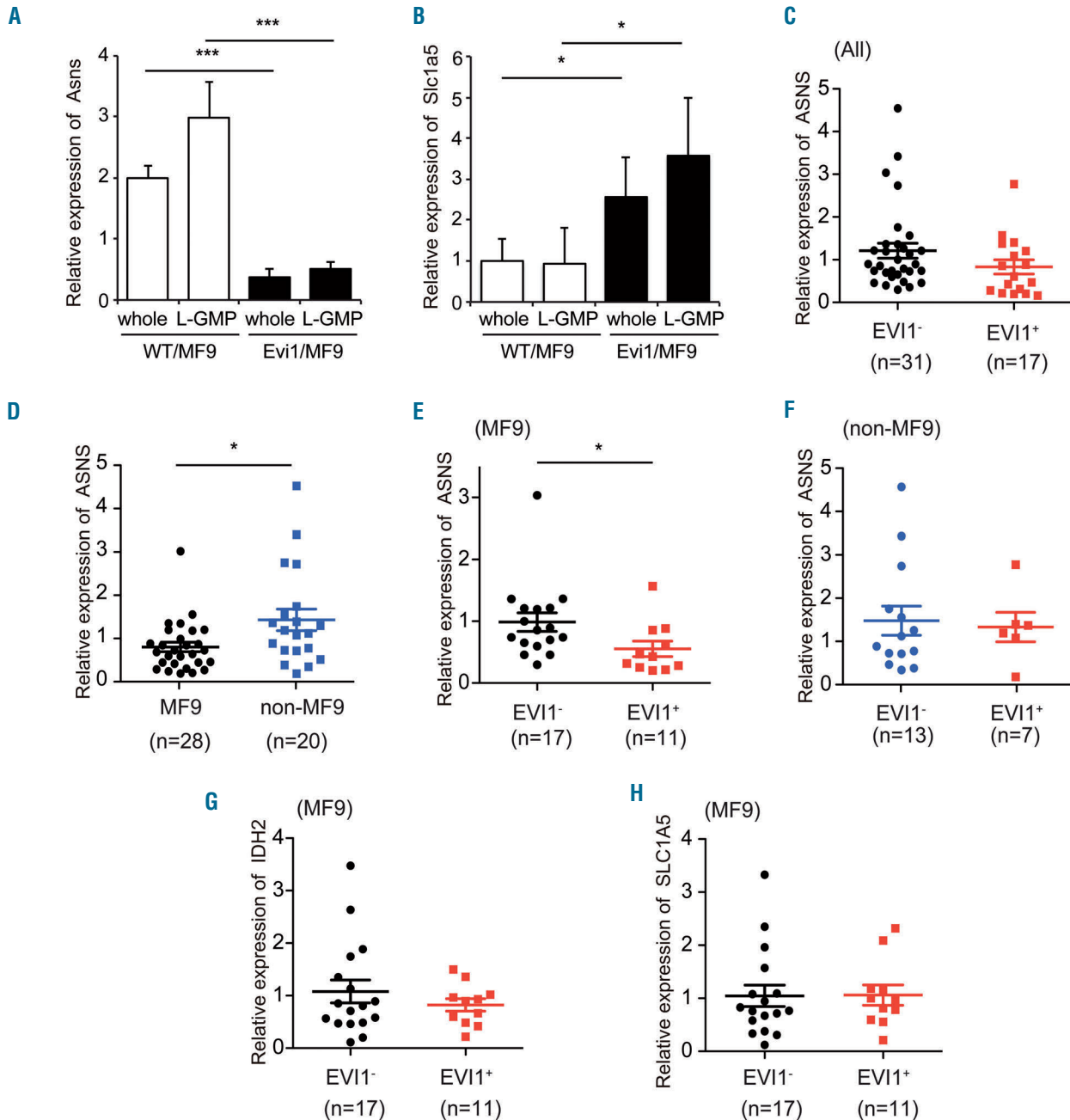


Figure 7. Low expression of ASNS in MF9 leukemia cells increases their sensitivity to L-asp. (A and B) Expression of the glutamine transporter (Slc1a5) and ASNS by MF9 leukemia cells. Expression of ASNS by Evi1/MF9 cells was significantly lower than that by wild-type (WT) cells. Expression of Slc1a5 by Evi1/MF9 cells was significantly higher than that by WT cells. (C-H) Gene expression in samples from JPLSG AML-05. In the acute myeloid leukemia (AML) with MLL rearrangement (MLL-r AML) cohort (n=48), there was no significant difference in ASNS expression between those with EVI1⁻ and those with EVI1⁺ AML (C). (D) MF9 AML showed significantly lower expression of ASNS than non-MF9 MLL-r AML. Expression of ASNS by EVI1⁻ MF9 cells was significantly lower than that of EVI1⁺ MF9 (n=28) (E) but not that of the non-MF9 cohort (n=20) (F). (G and H) Expression of IDH2 (G) and SLC1A5 (H) in the MF9 cohort.

the underlying mechanism is unclear.³³ AML showing high EVI1 expression is often accompanied by monosomy 7. Reduced expression of ASNS in AML with monosomy 7 is caused by haplodeletion of chromosome 7, making it highly sensitive to L-asp.³⁴ Here, since EVI1⁺ AML showed high sensitivity to L-asp despite its low glutamine dependence, it is likely that monosomy 7 is involved. Furthermore, we clarified that increased glutamine dependency by MF9 AML cells showing high EVI1 expression and low ASNS expression makes them sensitive to L-asp. Blockade of the creatine kinase pathway, which is essential for mitochondrial respiration, reduces glutamate levels in EVI1⁺ AML cells.¹⁴ Future studies should examine whether expression of ASNS by refractory MLL-r AML may increase the therapeutic potential of L-asp and improve treatment outcomes.

In conclusion, we found that the energy advantage of AML cells is acquired *via* transcription factor-mediated activation of mitochondrial metabolism, leading to a poor prognosis. Furthermore, we show that new therapeutic options can be identified by examining the energy-based metabolic characteristics of leukemia cells.

Funding

This research was supported by JSPS KAKENHI Grants (Number JP.16K19581 and AMED under Grant Number JP.17cm0106126h0002) and grants from the Takeda Science Foundation, the Friends of Leukemia Research Fund, The Shinnihon Foundation of Advanced Medical Treatment Research, and the Japanese Society of Hematology Research. Microarray data have been deposited in the Gene Expression Omnibus (GSE118096). The authors have no conflicts of interest to declare.

References

- Muntean AG, Hess JL. The pathogenesis of mixed-lineage leukemia. *Annu Rev Pathol.* 2012;7:283-301.
- Balgobind BV, Zwaan CM, Pieters R, Van den Heuvel-Eibrink MM. The heterogeneity of pediatric MLL-rearranged acute myeloid leukemia. *Leukemia.* 2011;25(8):1239-1248.
- Morishita K, Parker DS, Mucenski ML, et al. Retroviral activation of a novel gene encoding a zinc finger protein in IL-3-dependent myeloid leukemia cell lines. *Cell.* 1988;54(6):831-840.
- Morishita K, Parganas E, William CL, et al. Activation of EVI1 gene expression in human acute myelogenous leukemias by translocations spanning 300-400 kilobases on chromosome band 3q26. *Proc Natl Acad Sci U S A.* 1992;89(9):3937-3941.
- Lugthart S, Gröschel S, Beverloo HB, et al. Clinical, molecular, and prognostic significance of WHO type inv(3)(q21q26.2)/t(3;3)(q21;q26.2) and various other 3q abnormalities in acute myeloid leukemia. *J Clin Oncol.* 2010;28(24):3890-3898.
- Gröschel S, Schlenk RF, Engelmann J, et al. Deregulated expression of EVI1 defines a poor prognostic subset of MLL-rearranged acute myeloid leukemias: a study of the German-Austrian Acute Myeloid Leukemia Study Group and the Dutch-Belgian-Swiss HOVON/SAKK Cooperative Group. *J Clin Oncol.* 2013;31(1):95-103.
- Matsuo H, Kajihara M, Tomizawa D, et al. EVI1 overexpression is a poor prognostic factor in pediatric patients with mixed lineage leukemia-AF9 rearranged acute myeloid leukemia. *Haematologica.* 2014;99(11):e225-227.
- Valk PJ, Verhaak RG, Beijin MA, et al. Prognostically useful gene-expression profiles in acute myeloid leukemia. *N Engl J Med.* 2004;350(16):1617-1628.
- Verhaak RG, Wouters BJ, Erpelinck CA, et al. Prediction of molecular subtypes in acute myeloid leukemia based on gene expression profiling. *Haematologica.* 2009;94(1):131-134.
- Saito Y, Nakahata S, Yamakawa N, et al. CD52 as a molecular target for immunotherapy to treat acute myeloid leukemia with high EVI1 expression. *Leukemia.* 2011;25(6):921-931.
- Saito Y, Kaneda K, Suekane A, et al. Maintenance of the hematopoietic stem cell pool in bone marrow niches by EVI1-regulated GPR56. *Leukemia.* 2013;27(8):1637-1649.
- Wise DR, DeBerardinis RJ, Mancuso A, et al. Myc regulates a transcriptional program that stimulates mitochondrial glutaminolysis and leads to glutamine addiction. *Proc Natl Acad Sci U S A.* 2008;105(48):18782-18787.
- Cantor JR, Sabatini DM. Cancer cell metabolism: one hallmark, many faces. *Cancer Discov.* 2012;2(10):881-898.
- Fenouille N, Bassil CF, Ben-Sahra I, et al. The creatine kinase pathway is a metabolic vulnerability in EVI1-positive acute myeloid leukemia. *Nat Med.* 2017;23(3):301-313.
- Zhang Y, Owens K, Hatem L, et al. Essential role of PR-domain protein MDS1-EVI1 in MLL-AF9 leukemia. *Blood.* 2013;122(16):2888-2892.
- Stavropoulou V, Kaspar S, Brault L, et al. MLL-AF9 Expression in Hematopoietic Stem Cells Drives a Highly Invasive AML Expressing EMT-Related Genes Linked to Poor Outcome. *Cancer Cell.* 2016;30(1):43-58.
- Ng CE, Yokomizo T, Yamashita N, et al. A Runx1 intronic enhancer marks hemogenic endothelial cells and hematopoietic stem cells. *Stem Cells.* 2010;28(10):1869-1881.
- Saito Y, Chapple RH, Lin A, Kitano A, Nakada D. AMPK Protects Leukemia-Initiating Cells in Myeloid Leukemias from Metabolic Stress in the Bone Marrow. *Cell Stem Cell.* 2015;17(5):585-596.
- Krivtsov AV, Armstrong SA. MLL translocations, histone modifications and leukaemia stem-cell development. *Nat Rev Cancer.* 2007;7(11):823-833.
- Somervaille TC, Cleary ML. Identification and characterization of leukemia stem cells in murine MLL-AF9 acute myeloid leukemia. *Cancer Cell.* 2006;10(4):257-268.
- Farge T, Saland E, de Toni F, et al. Chemotherapy-resistant human acute myeloid Leukemia cells are not enriched for leukemic stem cells but require oxidative metabolism. *Cancer Discov.* 2017;7(7):716-735.
- Kuntz EM, Baquero P, Michie AM, et al. Targeting mitochondrial oxidative phosphorylation eradicates therapy-resistant chronic myeloid leukemia stem cells. *Nat Med.* 2017;23(10):1234-1240.
- Hirayama A, Kami K, Sugimoto M, et al. Quantitative metabolome profiling of colon and stomach cancer microenvironment by capillary electrophoresis time-of-flight mass spectrometry. *Cancer Res.* 2009;69(11):4918-4925.
- Vander Heiden MG, Cantley LC, Thompson CB. Understanding the Warburg effect: the metabolic requirements of cell proliferation. *Science.* 2009;324(5930):1029-1033.
- Ju HQ, Zhan G, Huang A, et al. ITD mutation in FLT3 tyrosine kinase promotes Warburg effect and renders therapeutic sensitivity to glycolytic inhibition. *Leukemia.* 2017;31(10):2143-2150.
- Poulain L, Sujobert P, Zylbersztejn F, et al. High mTORC1 activity drives glycolysis addiction and sensitivity to G6PD inhibition in acute myeloid leukemia cells. *Leukemia.* 2017;31(11):2326-2335.
- Wang YH, Israelsen WJ, Lee D, et al. Cell-state-specific metabolic dependency in hematopoiesis and leukemogenesis. *Cell.* 2014;158(6):1309-1323.
- Lagadinou ED, Sach A, Callahan K, et al. BCL-2 inhibition targets oxidative phosphorylation and selectively eradicates quiescent human leukemia stem cells. *Cell Stem Cell.* 2013;12(3):329-341.
- Medeiros BC, Fathi AT, DiNardo CD, et al. Isocitrate dehydrogenase mutations in myeloid malignancies. *Leukemia.* 2017;31(2):272-281.
- Chan WK, Lorenzi PL, Anishkin A, et al. The glutaminase activity of L-asparaginase is not required for anticancer activity against ASNS-negative cells. *Blood.* 2014;123(23):3596-3606.
- Offman MN, Krol M, Patel N, et al. Rational engineering of L-asparaginase reveals importance of dual activity for cancer cell toxicity. *Blood.* 2011;117(5):1614-1621.
- Ando M, Sugimoto K, Kitoh T, et al. Selective apoptosis of natural killer-cell tumours by L-asparaginase. *Br J Haematol.* 2005;130(6):860-868.
- Willems L, Jacque N, Jacquelin A, et al. Inhibiting glutamine uptake represents an attractive new strategy for treating acute myeloid leukemia. *Blood.* 2013; 122(20):3521-3532.
- Bertuccio SN, Serravalle S, Astolfi A, et al. Identification of a cytogenetic and molecular subgroup of acute myeloid leukemias showing sensitivity to L-Asparaginase. *Oncotarget.* 2017;8(66):109915-109923.



Ferrata Storti Foundation

Disrupting the leukemia niche in the central nervous system attenuates leukemia chemoresistance

Leslie M. Jonart,^{1,2} Maryam Ebadi,^{1,2} Patrick Basile,^{1,2} Kimberly Johnson,^{1,2} Jessica Makori^{1,2} and Peter M. Gordon^{1,2}

¹Division of Pediatric Hematology and Oncology, Department of Pediatrics, University of Minnesota and ²Masonic Cancer Center, University of Minnesota, Minneapolis, MN, USA.

Haematologica 2020
Volume 105(8):2130-2140

ABSTRACT

Protection from acute lymphoblastic leukemia relapse in the central nervous system (CNS) is crucial to survival and quality of life for leukemia patients. Current CNS-directed therapies cause significant toxicities and are only partially effective. Moreover, the impact of the CNS microenvironment on leukemia biology is poorly understood. In this study we showed that leukemia cells associated with the meninges of xenotransplanted mice, or co-cultured with meningeal cells, exhibit enhanced chemoresistance due to effects on both apoptosis balance and quiescence. From a mechanistic standpoint, we found that leukemia chemoresistance is primarily mediated by direct leukemia-meningeal cell interactions and overcome by detaching the leukemia cells from the meninges. Next, we used a co-culture adhesion assay to identify drugs that disrupted leukemia-meningeal adhesion. In addition to identifying several drugs that inhibit canonical cell adhesion targets we found that Me6TREN (Tris[2-(dimethylamino)ethyl]amine), a novel hematopoietic stem cell-mobilizing compound, also disrupted leukemia-meningeal adhesion and enhanced the efficacy of cytarabine in treating CNS leukemia in xenotransplanted mice. This work demonstrates that the meninges exert a critical influence on leukemia chemoresistance, elucidates mechanisms of relapse beyond the well-described role of the blood-brain barrier, and identifies novel therapeutic approaches for overcoming chemoresistance.

Correspondence:

PETER GORDON,
gord0047@umn.edu

Received: June 24, 2019.

Accepted: October 14, 2019.

Pre-published: October 17, 2019.

doi:10.3324/haematol.2019.230334

Check the online version for the most updated information on this article, online supplements, and information on authorship & disclosures: www.haematologica.org/content/105/8/2130

©2020 Ferrata Storti Foundation

Material published in Haematologica is covered by copyright. All rights are reserved to the Ferrata Storti Foundation. Use of published material is allowed under the following terms and conditions:

<https://creativecommons.org/licenses/by-nc/4.0/legalcode>.

Copies of published material are allowed for personal or internal use. Sharing published material for non-commercial purposes is subject to the following conditions:

<https://creativecommons.org/licenses/by-nc/4.0/legalcode>,

sect. 3. Reproducing and sharing published material for commercial purposes is not allowed without permission in writing from the publisher.



Introduction

Central nervous system (CNS) relapse is a common cause of treatment failure among patients with acute lymphoblastic leukemia (ALL).¹⁻³ Relapses occur despite CNS-directed therapies which include high-dose systemic chemotherapy, intrathecal chemotherapy, and cranial irradiation in some high-risk patients. These current CNS-directed therapies are also associated with significant acute and long-term toxicities.⁴⁻¹⁰ Accordingly, novel CNS-directed leukemia therapies are needed to improve long-term outcomes in ALL while decreasing treatment-related morbidity.

Historically, the ability of leukemia cells and chemotherapy to access the restricted CNS environment has been posited as a critical factor in the pathophysiology of CNS leukemia and relapse. However, several lines of evidence suggest that this is an overly simplistic model. First, high rates (>50%) of CNS leukemia occur in patients in the absence of adequate CNS-directed therapies as well as in mice transplanted with human, primary B-cell precursor leukemia cells.¹¹⁻¹⁴ Moreover, clonal analyses of paired leukemia cells isolated from both the bone marrow and CNS of patients and xenotransplanted mice demonstrated that all, or most, B-cell ALL clones are capable of disseminating to the CNS.^{14,15} Third, CNS leukemia relapses occur despite high-dose systemic and intrathecal chemotherapy. These therapies either overcome or bypass the blood-brain barrier. Fourth, it was shown that high Mer kinase-expressing, t(1;19) leukemia cells co-cultured with CNS-derived cells exhibit G0/G1 cell cycle arrest, suggestive of dormancy or quiescence, as well as

methotrexate resistance.¹⁶ Similarly, Akers *et al.* showed that co-culture of leukemia cells with astrocytes, choroid plexus epithelial cells, or meningeal cells enhanced leukemia chemoresistance.¹⁷ Together these observations suggest that the pathophysiology of CNS leukemia extends beyond the role of the blood-brain barrier. We hypothesize that the ability of leukemia cells to persist in the unique CNS niche and escape the effects of chemotherapy and immune surveillance likely also play critical roles in CNS leukemia and relapse.

However, while extensive research has demonstrated a critical role of the bone marrow niche in leukemia biology, the impact of the CNS niche on leukemia biology is less well understood.^{18,19} Herein, we demonstrate that the meninges exert a unique and critical influence on leukemia biology by enhancing leukemia resistance to the chemotherapy agents currently used in the therapy of CNS leukemia. We then leveraged this new understanding of the mechanisms of meningeal-mediated leukemia chemoresistance to identify a novel drug, Me6TREN (Tris[2-(dimethylamino)ethyl]amine), which overcomes leukemia chemoresistance by disrupting the interaction between leukemia and meningeal cells.

Methods

Cells and tissue culture

Leukemia cells were obtained from the American Type Culture Collection (ATCC) or *Deutsche Sammlung von Mikroorganismen und Zellkulturen* (DSMZ) and cultured in RPMI medium (Sigma-Aldrich) supplemented with fetal bovine serum 10% (Seradigm) and penicillin-streptomycin (Sigma-Aldrich). Leukemia cell lines included both B-cell (NALM-6, SEM) and T-cell (Jurkat, SEM, MOLT-13) immunophenotypes. The HCN-2 neuronal cell line was obtained from the ATCC. Leukemia cells expressing green fluorescent protein (GFP) were generated as described elsewhere.²⁰ Murine leukemia cells, generated by BCR/ABL p190 expression in hematopoietic cells from CD45.1 *Arf*^{-/-} mice,^{21,23} were provided by Dr. Michael Farrar (University of Minnesota, MN, USA). Primary B-ALL cells for co-culture experiments were obtained from the University of Minnesota Hematologic Malignancy Bank (IRB #: 0611M96846; pediatric patient at diagnosis). Primary B-ALL cells for *in vivo* experiments were obtained from the Public Repository of Xenografts [PRoXe;²⁴ sample CBAB-62871-V1; pediatric patient at diagnosis with a t(4;11) translocation]. Primary meningeal cells were obtained from ScienCell and cultured in meningeal medium supplemented with fetal bovine serum 2%, growth supplement, and penicillin-streptomycin. Meningeal cells were isolated from multiple different donor specimens and were typically used between passages 3-5.

Murine experiments

NSG (*NOD.Cg-Prkdcscid, Il2rgtm1Wjl/SzJ*; Jackson Laboratory) mice were housed under aseptic conditions. Mouse care and experiments were in accordance with a protocol approved by the Institutional Animal Care and Use Committee at the University of Minnesota (IRB#1704-34717A). Mice 6-8 weeks old were injected intravenously via the tail vein with $\sim 1-2 \times 10^6$ human leukemia cells. Experiments were then performed 3-5 weeks after injection. In general, after euthanasia of the mice, the heart was perfused with phosphate-buffered saline and the meninges or other tissues were removed using a dissecting microscope, and dissociated by gently washing through a 0.40

μm filter (Millipore). Cells were then stained with fluorescent antibodies against CD19 (NALM-6; eBioscience) or CD3 (Jurkat, eBioscience) and assessed for apoptosis or cell cycle as described. Alternatively, leukemia cells could be purified from meningeal cells using immunomagnetic separation and either CD19 or CD3 antibodies (Stem Cell Technologies or Miltenyi Biotec) and placed back into suspension. In drug treatment experiments, Me6TREN 10 mg/kg and cytarabine 50 mg/kg were given by subcutaneous and intraperitoneal injection, respectively. Cerebrospinal fluid was obtained from mice as described elsewhere.²⁵ Briefly, mice were euthanized and a scalp incision was made at the midline to expose the dura mater overlying the cisterna magna. Under a dissection microscope, a tapered, pulled glass capillary tube was then inserted through the dura and into the cisterna magna to obtain clear cerebrospinal fluid. Experiments with murine leukemia cells (BCR/ABL p190 expression in hematopoietic cells from *Arf*^{-/-} mice; CD45.1 background) used C57BL/6 mice. In these experiments, ~ 3000 leukemia cells/mouse were injected via the tail vein.

Statistical analysis

Results are shown as the mean \pm standard error of mean of the results of at least three experiments. The Student *t*-test or analysis of variance was used for statistical comparisons between groups. The log-rank (Mantel-Cox) test was used to calculate *P* values comparing the mouse survival curves. *P* values < 0.05 were considered statistically significant. Statistical analyses were conducted using GraphPad Prism 7 software (GraphPad Software, La Jolla, CA, USA).

Results

Leukemia cells reside in the meninges of the mouse central nervous system

In order to identify the anatomic site(s) in the CNS within which the leukemia cells reside, we transplanted multiple human ALL cell lines, including NALM-6, Jurkat, and SEM, into immune-compromised mice (NSG) via tail vein injection (*Online Supplementary Figure S1A*). Mice were not irradiated or conditioned with busulfan prior to transplantation to avoid perturbing leukemia niches. The mice were then euthanized and the CNS examined by histopathology and immunohistochemistry. We identified both the meninges and, to a lesser extent, the choroid plexus as the predominant CNS sites that harbor leukemia cells both before and after treatment with systemic cytarabine (*Online Supplementary Figure S1B*). In contrast, parenchymal involvement by leukemia was a rare, and often late, finding. It is possible that the altered immune system of NSG mice could influence CNS leukemia involvement or anatomic distribution. Accordingly, we also tested a pre-B-ALL mouse leukemia model that utilizes BCR/ABL p190 expression in hematopoietic cells from *Arf*^{-/-} mice transplanted into immunocompetent mice.^{21,22,26} Similar to the xenotransplantation results, leukemia extensively involved the meninges in these mice (*Online Supplementary Figure S1C*).

The meninges enhance leukemia chemoresistance

We then developed *ex vivo* co-culture approaches to focus more specifically on the effects of the meninges on leukemia chemosensitivity. We selected meningeal cells based on our immunohistochemical analyses of brains

from transplanted mice (*Online Supplementary Figure S1B, C*) as well as histopathological examinations of brains from patients with leukemia.¹¹⁻¹⁴ We found that leukemia cells adhered to primary human meningeal cells in a co-culture system (Figure 1A). Moreover, leukemia cells co-cultured with meningeal cells were significantly more resistant to cytarabine and methotrexate-induced apoptosis, as measured by annexin-V and viability staining, relative to the same cells grown in suspension or adherent to the HCN-2 neural precursor cell line (Figure 1B and *Online Supplementary Table S1*). In these experiments, chemotherapy had only very modest effects on meningeal cell viability

(*Online Supplementary Figure S2*). Additionally, primary pre-B leukemia cell survival both in the presence and absence of chemotherapy was also enhanced when the cells were co-cultured with primary meningeal cells (Figure 1C). These results show that meningeal cells protect leukemia cells from the effects of cytotoxic chemotherapy.

We then used conditioned media from primary human meningeal cells to test whether direct cell-cell contact is required for meningeal-mediated leukemia chemoresistance. As shown in Figure 1D, meningeal conditioned media conferred moderate chemoresistance on leukemia cells, but to a lesser extent than co-culture. Together these

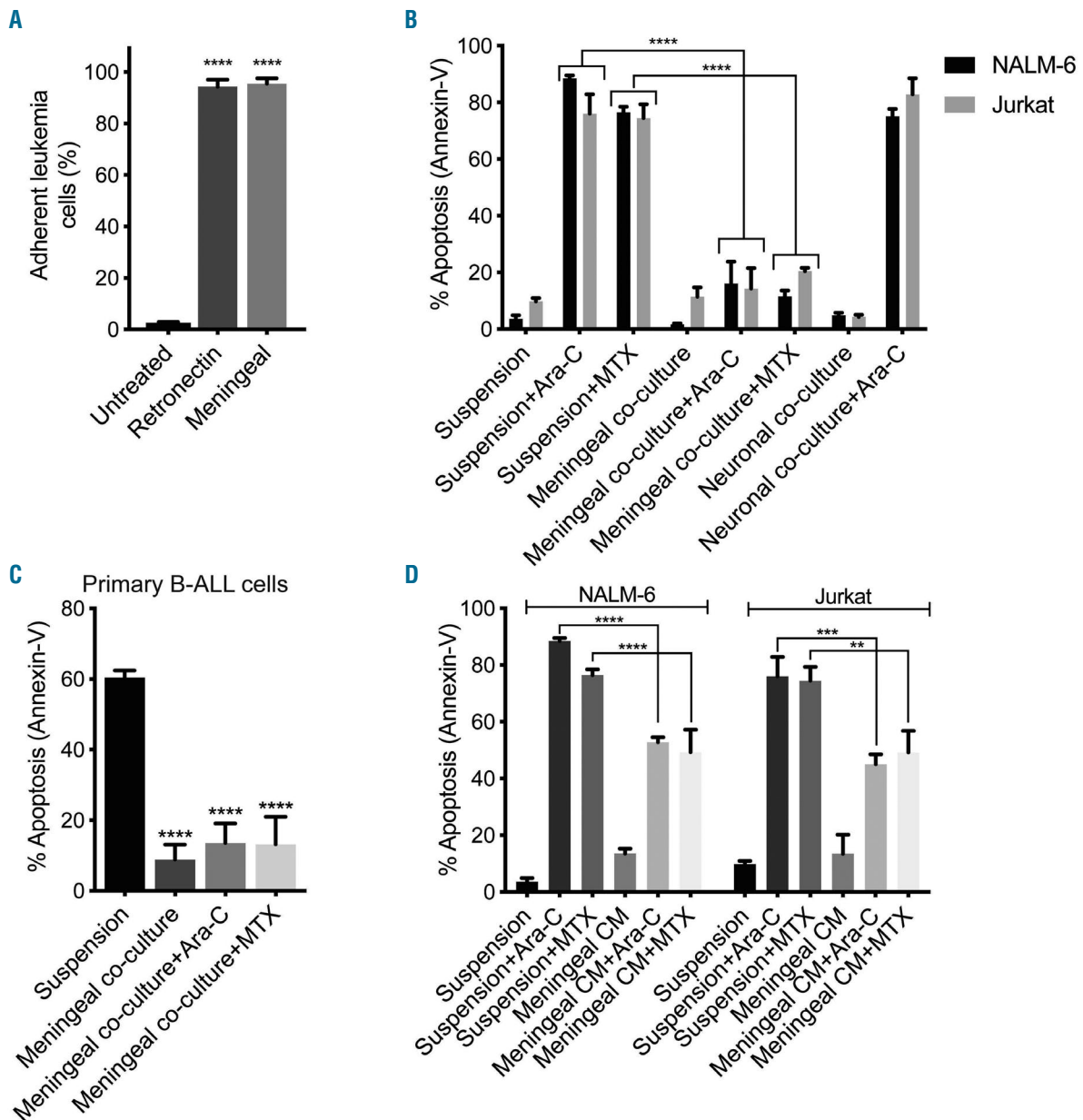


Figure 1. Leukemia cells exhibit increased chemoresistance when co-cultured with meningeal cells. (A) Percent of NALM-6 leukemia cells adherent to primary human meningeal cells, retronectin (recombinant fibronectin fragment) positive control, or non-tissue culture treated well after 2 h. (B, C) NALM-6 and Jurkat leukemia cells (B) or primary B-cell acute lymphocytic leukemia cells (C) cultured in suspension or adherent to central nervous system-derived cells (primary human meningeal cells or the HCN-2 neuronal cell line) were treated with cytarabine 500 nM or methotrexate 500 nM for 48 h and then apoptosis was measured using annexin-V and viability staining and flow cytometry. (D) NALM-6 and Jurkat cells were cultured in either regular media or meningeal conditioned media (CM; 100%) and treated with cytarabine 500 nM or methotrexate 500 nM for 48 h before apoptosis was measured using annexin-V staining and flow cytometry. For all graphs, data are the mean \pm standard error of mean from three independent experiments. ** $P < 0.01$, *** $P < 0.001$, **** $P < 0.0001$ by analysis of variance.

data suggest that meningeal-mediated leukemia chemoresistance is primarily dependent upon cell-cell contact with smaller contributions from a soluble factor(s) secreted by meningeal cells.

Meningeal cells shift the apoptotic balance toward survival in leukemia cells

In order to define the mechanism of meningeal-mediated leukemia chemoresistance we next examined the effects of co-culture on the apoptosis pathway in leukemia cells. In agreement with the annexin-V results (Figure 1B), co-culture of leukemia cells with primary meningeal cells attenuated apoptosis caused by cytarabine or methotrexate treatment as determined by both caspase 3/7 activity and measurement of leukemia cell mitochondrial potential with the dye TMRE (Figure 2A, B and *Online Supplementary Figure S3*). Next, we used an apoptosis antibody array to identify changes in the expression of multiple apoptosis family proteins in leukemia cells co-cultured with meningeal cells relative to suspension. In particular, the levels of several pro-apoptotic proteins (BID, caspase 3 & 8) decreased in leukemia cells co-cultured with meningeal cells (Figure 2C). However, assessing how the dynamic levels, activities, and complex interactions of these and other BCL-2 family of pro- and anti-apoptotic proteins (BH3 proteins) integrate to regulate the overall apoptotic balance is experimentally challenging. To try and capture the overall effect of the meninges on leukemia apoptotic balance, we then utilized BH3 profiling, a functional apoptosis assay that uses the response of mitochondria to perturbations by BH3 domain peptides, such as BIM, to predict the degree to which cells are primed to undergo apoptosis by the mitochondrial pathway.^{27,28} Importantly, decreased mitochondrial priming following drug treatment has been shown to be highly predictive of chemotherapy resistance *in vitro* and *in vivo*.^{27,28} Accordingly, we found that leukemia cells co-cultured with meningeal cells exhibited increased cytochrome C retention upon exposure to the BIM peptide compared to leukemia cells in suspension (Figure 2D). These data suggest that leukemia cells co-cultured with meningeal cells are significantly less primed to undergo apoptosis through the mitochondrial pathway than the same leukemia cells in suspension.

Meningeal cells increase leukemia quiescence

We also examined the effect of the meninges on leukemia cell cycle and quiescence. As shown in Figure 3A-C, leukemia cells co-cultured with primary meningeal cells are less proliferative, as determined by decreased Ki-67 staining, significantly decreased S phase, and increased G0/G1 phase. We next used Hoechst-pyronin Y staining to better distinguish between G0 and G1 phases.²⁹ As shown in Figure 3D-F, leukemia cells in co-culture with primary meningeal cells exhibited increased G0 phase, indicative of quiescence, relative to leukemia cells in suspension. Glucose uptake also diminished in leukemia cells co-cultured with meningeal cells, further supporting that these leukemia cells are quiescent (*Online Supplementary Figure S4*).

We then examined cell cycle and quiescence in leukemia cells isolated from the meninges of xenotransplanted mice. As shown in Figure 4A-C, leukemia cells isolated from the meninges of transplanted mice exhibited increased G0/G1 phase and decreased Ki-67 staining rela-

tive to leukemia cells isolated from peripheral blood or bone marrow. In order to assess whether the meninges harbor long-term quiescent leukemia cells, we labeled leukemia cells with a fluorescent membrane dye (DiR or DiD) that is retained in dormant, non-cycling cells but is diluted to undetectable levels within three to five generations in proliferating leukemia cells.³⁰⁻³⁴ Dye-labeled leukemia cells were then transplanted into immunodeficient mice. After having developed systemic leukemia in ~4 weeks, the mice were euthanized and their meninges harvested. Within the meninges we detected low levels of dye-retaining, quiescent leukemia cells by flow cytometry (<1% of total leukemia population) (Figure 4D, E). Further supporting that these dye-retaining leukemia cells are quiescent, the dye-retaining leukemia cells from the meninges exhibited low expression of the proliferation marker Ki-67 (Figure 4F). We also detected these quiescent leukemia cells within the meninges using confocal microscopy (Figure 4G-I).

We next treated these xenotransplanted mice with cytarabine and measured the percentage of dye-retaining leukemia cells in the meninges by flow cytometry. Cytarabine was given at a dose previously shown to result in plasma levels in the range produced by human high-dose cytarabine regimens that cross the blood-brain barrier.^{35,36} Cytarabine, compared to phosphate-buffered saline, also significantly reduced the CNS leukemia burden in xenotransplanted mice, providing functional data that cytarabine is crossing the blood-brain barrier in our murine experiments (*Online Supplementary Figure S5*). Moreover, the relative increase in dye-retaining leukemia cells after cytarabine treatment is consistent with these cells having increased chemoresistance compared to the dye-negative, proliferating leukemia cells (Figure 4J). Together these data suggest that the meninges harbor quiescent leukemia cells that are resistant to chemotherapy.

Meningeal-mediated leukemia chemoresistance is a reversible phenotype

We then tested whether removal of leukemia cells from co-culture with meningeal cells restored chemosensitivity. Leukemia cells were dissociated from meningeal cells, purified with CD19 (NALM-6) or CD3 (Jurkat) magnetic beads, and placed back in suspension. As shown in Figure 5A, leukemia cells removed from co-culture exhibited similar sensitivity to methotrexate and cytarabine as leukemia cells in suspension. Likewise, leukemia cells grown in suspension after isolation from the meninges of xenotransplanted mice also exhibited sensitivity to cytarabine (Figure 5B). Further supporting these results, the cell cycle and apoptosis characteristics of leukemia cells placed back into suspension after co-culture reverted back to baseline (Figure 5C-E). These results suggest that drugs that disrupt adhesion between leukemia and meningeal cells may restore leukemia chemosensitivity in the CNS niche.

Overcoming meningeal-mediated leukemia chemoresistance by disrupting adhesion

Given that meningeal-mediated leukemia chemoresistance is a reversible phenotype, we next identified several cell adhesion inhibitors that disrupted leukemia-meningeal adhesion in co-culture (*Online Supplementary Figure S6A*). We selected Me6TREN for further testing based upon its effectiveness in co-culture, small molecular

weight (increasing its likelihood of CNS penetration), tolerability in mice, lack of prior testing in leukemia, and likely multifactorial mechanism of action.^{37,38} Me6TREN significantly disrupted the adhesion of both NALM-6 and Jurkat leukemia cells to primary meningeal cells in a dose-dependent fashion (Figure 6A and *Online Supplementary Figure S6B, C*). This effect of Me6TREN on adhesion was not due to toxicity to leukemia or meningeal cells (*Online Supplementary Figure S6D*). We then quantified non-adherent leukemia cells in the cerebrospinal fluid of xenotransplanted mice after treatment with either Me6TREN or phosphate-buffered saline control in order to measure dis-

ruption of leukemia adhesion *in vivo*. As shown in Figure 6B, Me6TREN-treated mice showed a modest, but significant, increase in leukemia cells in the cerebrospinal fluid, consistent with the co-culture experiment. Moreover, by disrupting leukemia adhesion, Me6TREN significantly attenuated leukemia chemoresistance in co-culture with meningeal cells (Figure 6C). We next assessed the *in vivo* ability of Me6TREN to enhance the efficacy of cytarabine in treating leukemia in the meninges. We tested NALM-6, Jurkat, and primary B-ALL leukemia cells with dosing regimens shown in *Online Supplementary Figure S7*. In all cases, Me6TREN significantly enhanced the efficacy of

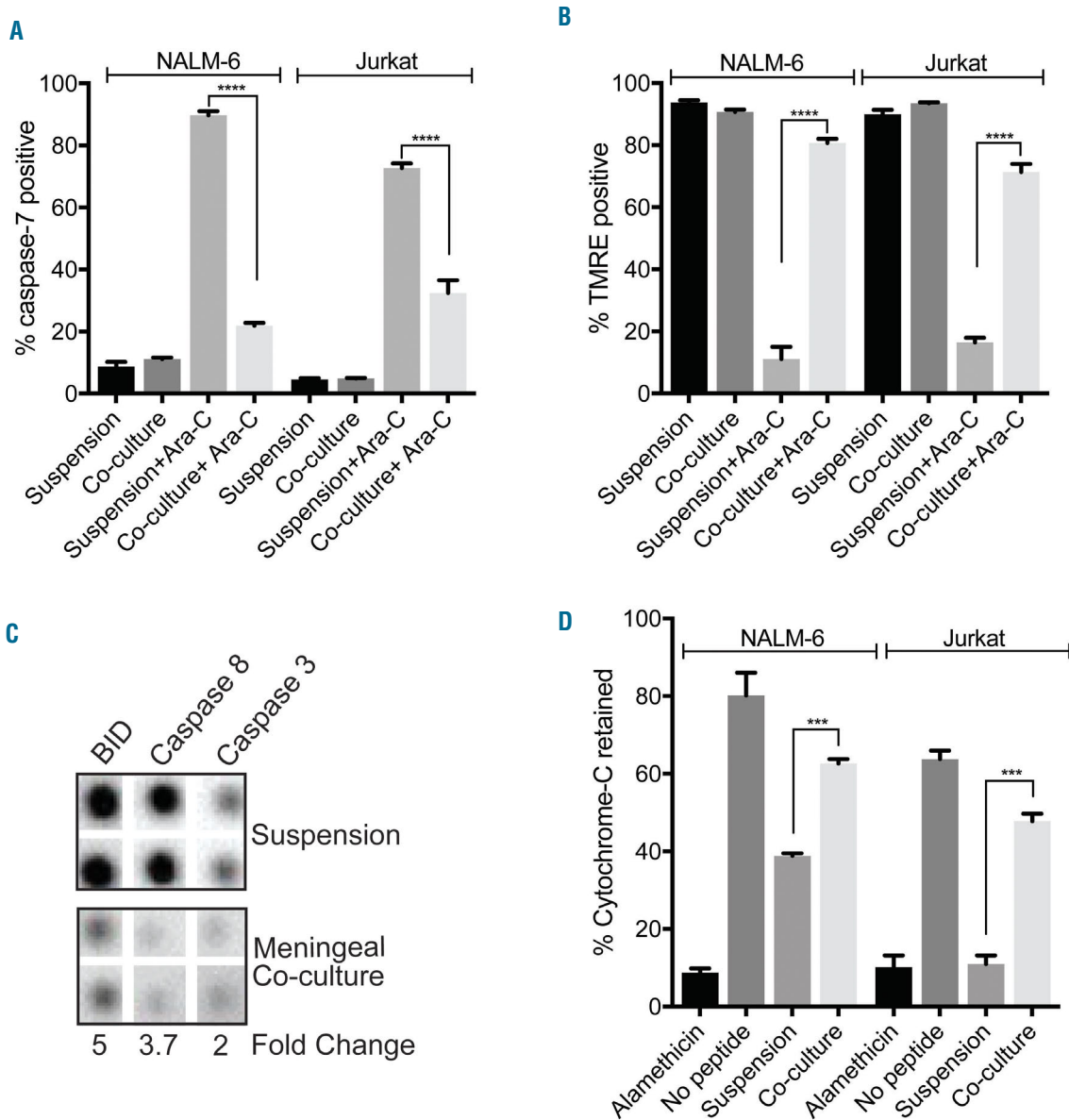


Figure 2. Meningeal cells tilt the apoptotic balance of leukemia cells toward survival. (A, B) NALM-6 and Jurkat leukemia cells cultured in suspension or adherent to meningeal cells were treated with cytarabine 500 nM for 48 h and caspase-7 activity (A) and TMRE staining (B) assessed by flow cytometry. (C) NALM-6 leukemia cells were grown in suspension or adherent to meningeal cells for 48 h. Acute lymphocytic leukemia cells were then isolated and lysed. Protein lysate was used to probe a Human Apoptosis Antibody Array (Abcam). Representative portions of the membrane are shown. Relative protein expression was calculated after normalization using the IgG positive control. (D) BH3 profiling was performed using the BIM peptide on NALM-6 and Jurkat leukemia cells grown in suspension or adherent to meningeal cells for 24 h (NALM-6) or 48 h (Jurkat). Cytochrome c retention was measured by flow cytometry. Alamethicin is a peptide antibiotic that permeabilizes the mitochondrial membrane and serves as a positive control. For all graphs, data are the mean \pm standard error of mean from three independent experiments. *** $P < 0.01$, **** $P < 0.001$, ***** $P < 0.0001$ by analysis of variance.

cytarabine in reducing the number of viable leukemia cells in the meninges (Figure 6D-G). Moreover, Me6TREN significantly extended the survival of mice treated with cytarabine in the patient-derived xenotransplantation model (Online Supplementary Figure S8). Despite Me6TREN disrupting the bone marrow hematopoietic niche,³⁸ mice receiving cytarabine/Me6TREN or cytarabine alone exhibited comparable hematologic toxicities (Online Supplementary Figure S9). Finally, disruption of the CNS leukemia niche with Me6TREN did not result in an increased leukemia burden in other organs or tissues (Online Supplementary Figure S10).

We then performed gene expression profiling on primary, human meningeal cells treated with Me6TREN in order to take an unbiased approach toward identifying the mechanisms by which Me6TREN disrupts leukemia-meningeal adhesion. As predicted, pathway analyses identified cell adhesion and migration as being among the most differentially regulated in meningeal cells treated with Me6TREN (Online Supplementary Figure S11A and Online Supplementary Table S2). The gene expression data also showed that Me6TREN significantly downregulated the cell-surface/adhesion proteins VCAM-1 and CD99 (Online Supplementary Figure S11B). Supporting a functional role for CD99 and VCAM-1 in leukemia-meningeal

adhesion we found that antibodies targeting either of these proteins attenuated the adhesion of leukemia and meningeal cells (Online Supplementary Figure S11C, D). We also examined matrix metalloproteases (MMP) because Me6TREN has been shown to upregulate MMP-9 in the context of hematopoietic stem cells and the bone marrow niche.³⁸ Supporting a similar role in the CNS niche, two different MMP inhibitors diminished the ability of Me6TREN to disrupt leukemia-meningeal adhesion (Online Supplementary Figure S11C, D). In contrast, Me6TREN did not significantly perturb the CXCR4 and CCR7 signaling pathways, which have been previously implicated in leukemia infiltration into the CNS (Online Supplementary Figure S12 and Online Supplementary Table S3).^{39,40}

Discussion

Protection from leukemia relapse in the CNS is crucial to long-term survival and quality of life of patients with leukemia.¹⁻³ One strategy for developing novel CNS-directed therapies has focused on identifying, and potentially targeting, the factors that facilitate leukemia cell trafficking to the CNS from the bone marrow.^{39,41-49} At the

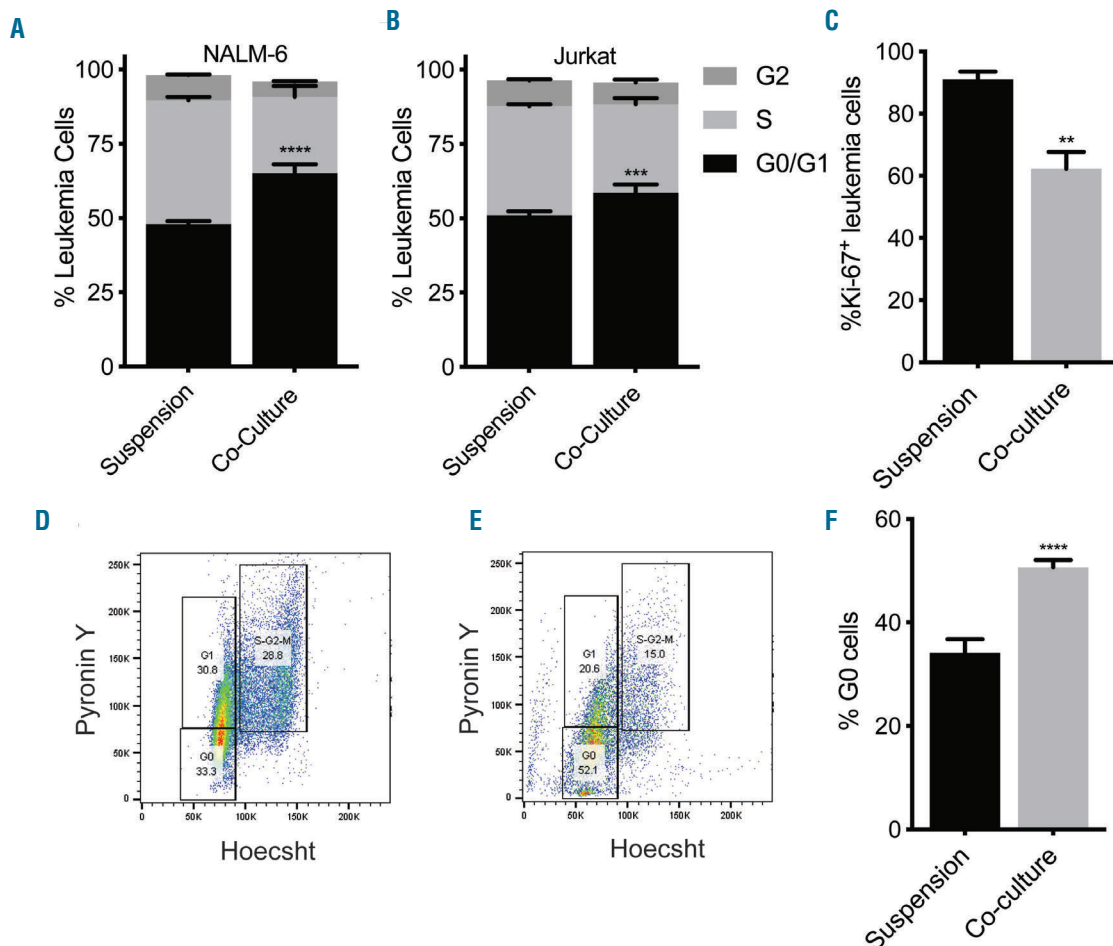


Figure 3. Meningeal cells increase leukemia quiescence *in vitro*. (A, B) NALM-6 and Jurkat leukemia cells cultured in suspension or adherent to primary meningeal cells for 48 h were assessed for cell cycle and proliferation using a Click-iT Plus EdU kit and flow cytometry. (C-F) NALM-6 leukemia cells cultured in suspension or adherent to primary meningeal cells for 48 h were stained for Ki-67 (C) or Hoechst-pyronin Y (D-F) and analyzed by flow cytometry. Representative flow plots for Hoechst-pyronin Y staining are shown (D-E). For all graphs, * $P < 0.05$, ** $P < 0.01$, *** $P < 0.001$, **** $P < 0.0001$ by analysis of variance.

same time, additional evidence suggests that the ability of leukemia cells to infiltrate the CNS is a general property of most leukemia cells and not restricted to rare clones that acquire a metastatic phenotype.^{14,15} Accordingly, we sought to address the question of how leukemia cells adapt to this unique niche and escape the effects of chemotherapy after infiltrating the CNS. We found that, within the CNS, leukemia cells primarily localize to the meninges and that parenchymal involvement by leukemia was a rare finding. This observation is in agreement with a larger body of literature demonstrating that leukemia

xenografts accurately model the anatomic distribution of leukemia observed within the CNS of humans.¹¹⁻¹⁴ As a result, we focused our work on the meninges. However, it is certainly possible, and perhaps even likely, that other cells or tissues within the CNS, such as the choroid plexus, may also affect leukemia biology.^{17,20} This may be analogous to the bone marrow microenvironment in which distinct niches (endosteal, vascular) exert unique effects on hematopoietic stem and leukemia cells.⁵⁰

We then used co-culture and *in vivo* xenotransplantation approaches to further characterize the effects of the

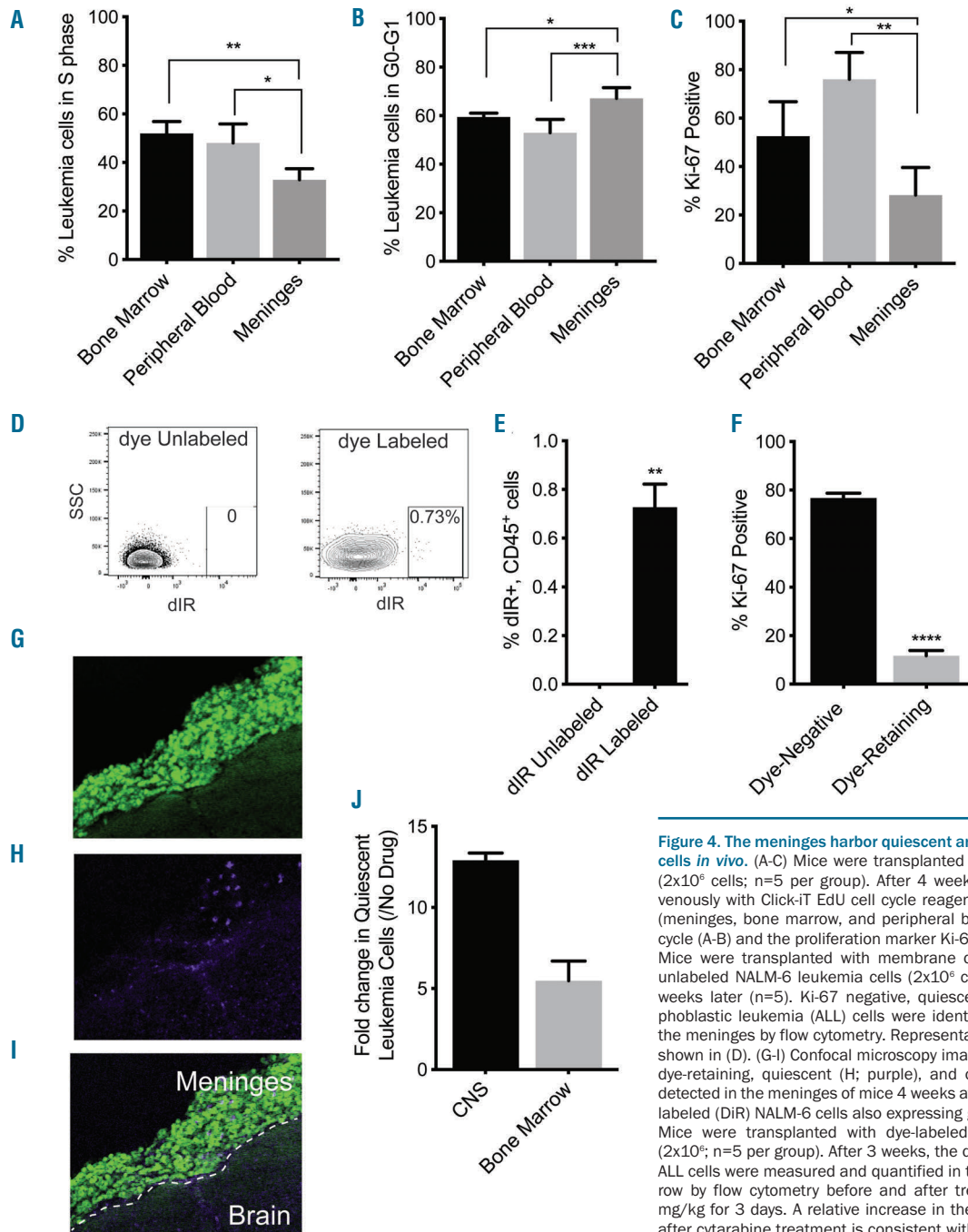


Figure 4. The meninges harbor quiescent and chemoresistant leukemia cells *in vivo*. (A-C) Mice were transplanted with NALM-6 leukemia cells (2×10^6 cells; $n=5$ per group). After 4 weeks, mice were injected intravenously with Click-IT EdU cell cycle reagent prior to harvesting tissues (meninges, bone marrow, and peripheral blood) and assessing for cell cycle (A-B) and the proliferation marker Ki-67 (C) by flow cytometry. (D-F) Mice were transplanted with membrane dye-labeled (DiD) or control, unlabeled NALM-6 leukemia cells (2×10^6 cells) and then euthanized 4 weeks later ($n=5$). Ki-67 negative, quiescent (dye-positive) acute lymphoblastic leukemia (ALL) cells were identified and quantified (D-F) in the meninges by flow cytometry. Representative flow cytometry plots are shown in (D). (G-I) Confocal microscopy images showing total (G; green), dye-retaining, quiescent (H; purple), and overlay (I) of leukemia cells detected in the meninges of mice 4 weeks after transplantation with dye-labeled (DiR) NALM-6 cells also expressing green fluorescent protein. (J) Mice were transplanted with dye-labeled human NALM-6 ALL cells (2×10^6 ; $n=5$ per group). After 3 weeks, the dye-positive and dye-negative ALL cells were measured and quantified in the meninges and bone marrow by flow cytometry before and after treatment with cytarabine 50 mg/kg for 3 days. A relative increase in the dye-positive leukemia cells after cytarabine treatment is consistent with dye-positive leukemia cells being chemoresistant relative to the dye-negative leukemia cells. For all graphs, * $P < 0.05$, ** $P < 0.01$, *** $P < 0.001$, **** $P < 0.0001$ by analysis of variance or a t-test.

meninges on leukemia biology. We found that the meninges enhance leukemia resistance to cytarabine and methotrexate, the primary drugs currently used in the treatment of CNS leukemia, by altering the apoptotic balance in leukemia cells to favor survival and increasing leukemia quiescence.^{1,2} Quiescence allows cancer cells to escape cytotoxic chemotherapy and has been shown to be critical for leukemia relapse and stem cell biology.^{32,51,52} In agreement, it was previously shown that high Mer kinase-expressing, t(1;19) leukemia cells co-cultured with CNS-derived cells exhibit G0/G1 cell cycle arrest, suggestive of dormancy or quiescence, as well as methotrexate resistance.¹⁶

To define the mechanism by which the meninges exert these effects on leukemia biology, we also tested the ability of meningeal conditioned media to enhance leukemia chemoresistance. While meningeal conditioned media partially attenuated the sensitivity of leukemia cells to chemotherapy, the effect was significantly less than when leukemia cells were in direct contact with meningeal cells. This result supports a model in which leukemia chemoresistance is primarily dependent upon direct interactions between the leukemia and meningeal cells with smaller contributions from a soluble factor(s) secreted by the meningeal cells. Together these results further support that the pathophysiology of CNS leukemia and relapse is more complex than simply the ability of leukemia cells or chemotherapy to access the restricted CNS microenvironment and complement other extensive laboratory and clinical data demonstrating that cell-autonomous factors play an essential role in leukemia biology.^{50,53,54}

Importantly, we also found that meningeal-mediated leukemia chemoresistance was a reversible phenotype. Leukemia cells removed from co-culture with meningeal cells or the meninges of xenotransplanted mice reverted back to baseline cell cycle, quiescence, apoptosis balance, and sensitivity to methotrexate and cytarabine. Ebinger *et al.* recently identified a similar population of relapse-inducing ALL cells within the bone marrow that exhibited dormancy, stemness, and treatment resistance.³¹ However, similar to our results, these therapeutically adverse properties were reversed when these leukemia cells were dissociated from the bone marrow microenvironment.

We then identified drugs capable of disrupting leukemia-meningeal adhesion. In addition to identifying several drugs that inhibit canonical cell adhesion targets, we also found that Me6TREN, a novel hematopoietic stem cell mobilizing compound, also disrupted leukemia-meningeal adhesion *in vitro* and *in vivo*. Moreover, Me6TREN enhanced the efficacy of cytarabine in treating CNS leukemia in xenotransplanted mice. *In vivo* efficacy against two leukemia cell lines with distinct immunophenotypes (T- and B-cell) and a primary B-ALL patient-derived xenotransplant support the possibility that drugs, or biologic agents, that target leukemia-niche interactions may exhibit broader specificity than mutation-specific therapeutics that are limited by the genetic heterogeneity of leukemia.

The mechanism by which Me6TREN disrupts the leukemia-meningeal niche is an active area of investigation in our laboratory. The ability of MMP inhibitors to diminish the efficacy of Me6TREN agrees with other work showing that Me6TREN upregulates MMP-9 in the bone marrow niche.³⁸ Our gene expression data also showed that Me6TREN significantly downregulated the

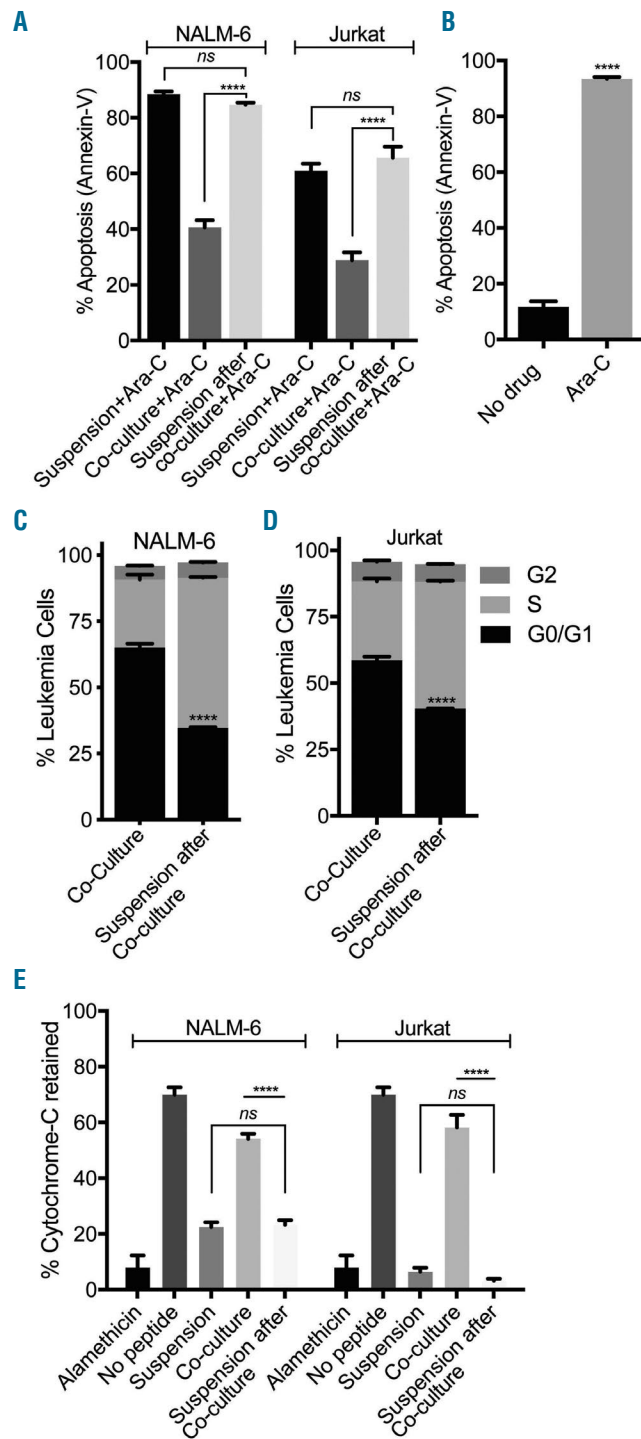


Figure 5. The effects of the meninges on leukemia cells are reversible. (A) NALM-6 and Jurkat cells grown in suspension, co-cultured with meningeal cells, or isolated from co-culture and placed back in suspension were treated with Ara-C (cytarabine) 500 nM and apoptosis was assessed by annexin-V staining and flow cytometry. (B) NALM-6 leukemia cells were isolated from the meninges of xenotransplanted mice and then grown in suspension for 48 h prior to treatment with cytarabine 500 nM and assessment of viability using annexin-V staining and flow cytometry. (C, D) NALM-6 (C) and Jurkat (D) leukemia cells were co-cultured with meningeal cells or isolated from co-culture and placed back in suspension and then cell cycle assessed using Click-IT Plus EdU cell cycle reagent and flow cytometry. (E) BH3 profiling was performed using the BIM peptide on NALM-6 and Jurkat leukemia cells co-cultured with meningeal cells or placed back into suspension after co-culture with meningeal cells. Cytochrome c retention was measured by flow cytometry. For all graphs, data are the mean \pm standard error of mean from three independent experiments. **** $P < 0.0001$ by analysis of variance. ns: not significant.

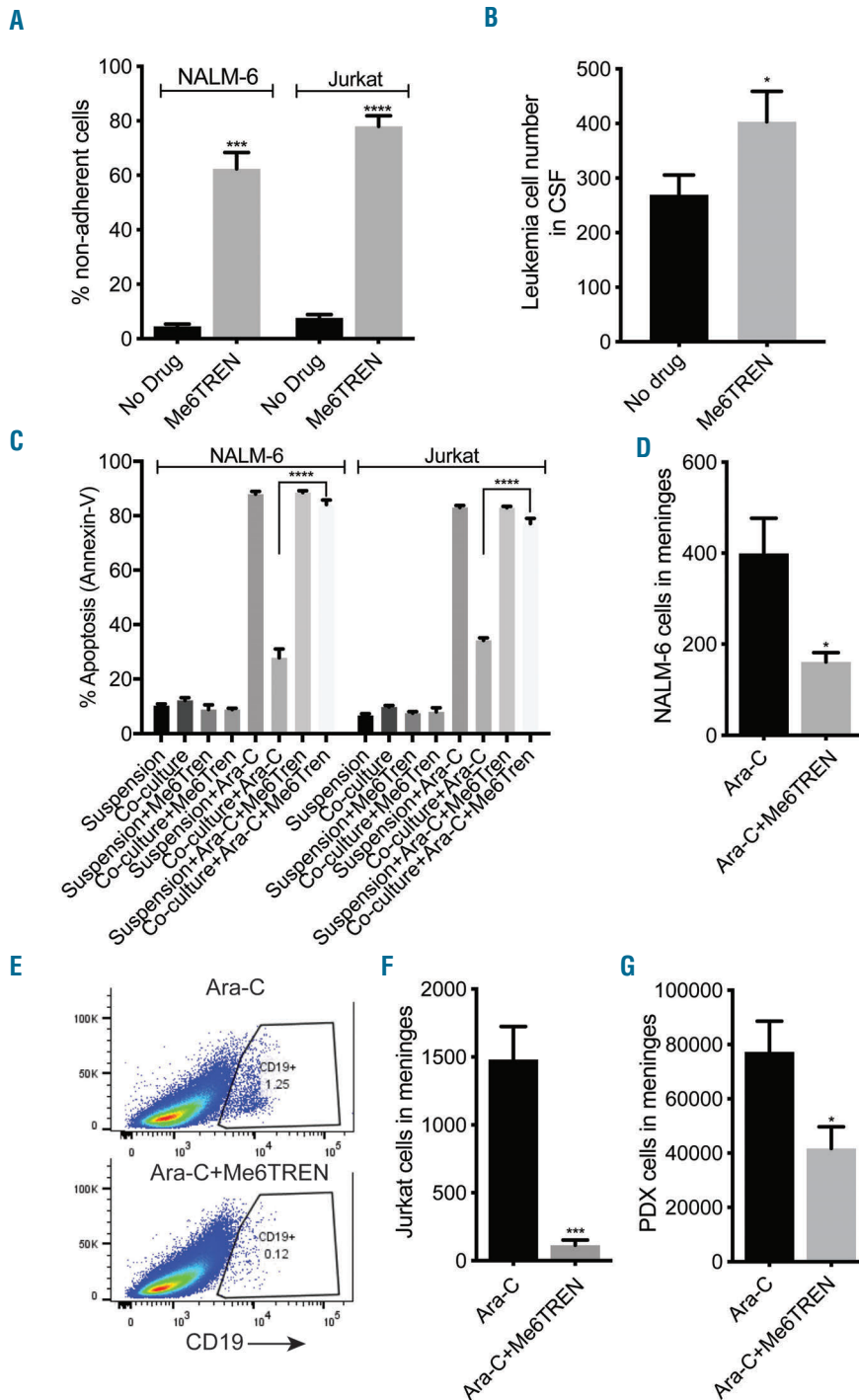


Figure 6. Me6TREN disrupts the meningeal-leukemia niche and attenuates leukemia chemoresistance *in vitro* and *in vivo*. (A) NALM-6 leukemia cells were co-cultured with meningeal cells in the presence or absence of Me6TREN 100 μ M. After 24 h, non-adherent leukemia cells were removed and quantified. (B) Mice were transplanted with NALM-6 leukemia cells (2×10^6 cells; $n=5$ per group). After 16 days, mice were treated with Me6TREN 10 mg/kg subcutaneous or phosphate-buffered saline control for 3 days. After an additional 24 h, 5–10 μ L of cerebrospinal fluid were removed from the cisterna magna and leukemia cells were quantified using flow cytometry and counting beads. (C) Leukemia cells in suspension or co-cultured with primary meningeal cells were treated with Me6TREN \pm cytarabine 500 nM and after 48 h viability was assessed with annexin-V staining and flow cytometry. (D–G) Mice transplanted with NALM-6 (2×10^6 cells; $n=5$ per group; D & E), Jurkat (2×10^6 cells; $n=5$ per group; F), or primary B-cell acute lymphocytic leukemia (PROx Sample CBAB-62871-V1; 1×10^6 cells; $n=5$ per group; G) cells were treated with cytarabine (50 mg/kg intraperitoneal) or cytarabine + Me6TREN (10 mg/kg subcutaneous). Forty-eight hours after completing therapy mice were euthanized, the heart was perfused, the meninges were isolated, dissociated and stained with human CD19 (NALM-6 & PDX) or CD3 (Jurkat) antibody, and leukemia cells were quantified by flow cytometry and counting beads (D, F, G). Representative flow plots for NALM-6 are shown in (E). For all graphs, * $P < 0.05$, ** $P < 0.01$, *** $P < 0.001$, **** $P < 0.0001$ by analysis of variance or a *t*-test.

cell-surface/adhesion proteins VCAM-1 and CD99. Supporting a functional role for CD99 and VCAM-1 in leukemia-meningeal adhesion, antibodies targeting either of these proteins attenuated the adhesion of leukemia and meningeal cells. CD99 has not been previously implicated in the mechanism of action of Me6TREN or the ALL niche. Importantly, in addition to directly participating in cell-cell adhesion through homo/heterotypic interactions, CD99 also regulates multiple other adhesion molecules/pathways including LFA-1, $\alpha 4\beta 1$, ELAM-1, VCAM-1, ICAM-1, MMP, and CXCR4/CXCL12.⁵⁵ As many of these adhesion pathways contribute to the bone marrow leukemia niche, Me6TREN may also diminish

leukemia chemoresistance in other leukemia niches.^{53,56} This possibility is potentially supported by our data demonstrating that Me6TREN extended the overall survival of mice treated with cytarabine. However, if upon further testing Me6TREN only disrupts leukemia-meningeal adhesion and the effect on survival is due only to decreased CNS leukemia progression, Me6TREN could still be effective in treating isolated CNS relapses, for use in upfront therapy to reduce the risk of CNS relapse, or potentially to reduce the dose or intensity of current CNS-directed therapies that carry significant risks of short- and long-term toxicity.

Given the complexity of cell-cell interactions, this mul-

tifaceted mechanism of action of Me6TREN may provide an advantage relative to other niche-disrupting agents being developed for leukemia therapy that target a single mechanism of retention or adhesion (i.e. inhibitors of SDF-1 or a single extracellular adhesion factor).⁵⁷ An alternative approach to overcome the complexity and redundancy of cellular adhesion would be to combine multiple inhibitors that target different adhesion molecules (*Online Supplementary Figure S6A*).

A potential risk of combining Me6TREN, or other niche-disrupting agents, and chemotherapy is that normal hematopoietic stem cells mobilized into the circulation by Me6TREN may be sensitized to chemotherapy with resulting marrow aplasia or delayed hematopoietic recovery. However, we found that mice receiving cytarabine/Me6TREN or cytarabine alone exhibited comparable hematologic toxicities. Moreover, preclinical and clinical studies combining other hematopoietic stem cell-mobilizing agents, such as AMD3100 or granulocyte colony-stimulating factor, with chemotherapy have also shown an acceptable toxicity profile.^{58,59} Another potential limitation to this approach of disrupting leukemia cell adhesion to the niche is that soluble factors secreted by the niche can also interact with non-adherent leukemia cells and affect leukemia biology, as we saw with meningeal conditioned media.^{46,60} Combination therapies that target both adhesion and secreted factors

may be the most efficacious in treatment of CNS leukemia.

In summary, this work demonstrates that the meninges enhance leukemia chemoresistance in the CNS, elucidates mechanisms of CNS relapse beyond the role of the blood-brain barrier, and identifies niche disruption as a novel therapeutic approach for enhancing the ability of chemotherapy to eradicate CNS leukemia.

Acknowledgments

This work was supported in part by the Children's Cancer Research Fund (PMG), the Timothy O'Connell Foundation (PMG), and an American Cancer Society Institutional Research Grant (PMG). PB was partially supported by NIH Training Grant T32 CA099936. We thank Dr. Michael Farrar for providing mouse BCR/ABL p190 leukemia cells, Dr. Juan Abrahante Lloréns (University of Minnesota Genomics Center) for assistance with RNA-sequencing data analyses, Dr. Mark Sanders (University of Minnesota Imaging Center) for providing expert assistance with confocal microscopy and sample preparation, and Mike Ehrhardt (University of Minnesota Cytokine Reference Laboratory) for assistance with measuring cytokine levels. This work utilized the University of Minnesota Masonic Cancer Center shared flow cytometry and comparative pathology resources and the Hematological Malignancy Tissue Bank, which are supported in part by NCI 5P30CA077598-18, Minnesota Masonic Charities, and the Killebrew-Thompson Memorial Fund.

References

- Pui C-H, Howard SC. Current management and challenges of malignant disease in the CNS in paediatric leukaemia. *Lancet Oncol.* 2008;9(3):257-268.
- Pui C-H, Thiel E. Central nervous system disease in hematologic malignancies: historical perspective and practical applications. *Semin Oncol.* 2009;36(4 Suppl 2):S2-16.
- Pui C-H. Central nervous system disease in acute lymphoblastic leukemia: prophylaxis and treatment. *Hematology Am Soc Hematol Educ Program.* 2006;142-146.
- Silverman LB. Balancing cure and long-term risks in acute lymphoblastic leukemia. *Hematology Am Soc Hematol Educ Program.* 2014;2014(1):190-197.
- Hijjiya N, Hudson MM, Lensing S, et al. Cumulative incidence of secondary neoplasms as a first event after childhood acute lymphoblastic leukemia. *JAMA.* 2007;297(11):1207-1215.
- Conklin HM, Krull KR, Reddick WE, Pei D, Cheng C, Pui CH. Cognitive outcomes following contemporary treatment without cranial irradiation for childhood acute lymphoblastic leukemia. *J Natl Cancer Inst.* 2012;104(18):1386-1395.
- Krull KR, Brinkman TM, Li C, et al. Neurocognitive outcomes decades after treatment for childhood acute lymphoblastic leukemia: a report from the St Jude lifetime cohort study. *J Clin Oncol.* 2013;31(35):4407-4415.
- Bhojwani D, Sabin ND, Pei D, et al. Methotrexate-induced neurotoxicity and leukoencephalopathy in childhood acute lymphoblastic leukemia. *J Clin Oncol.* 2014;32(9):949-959.
- Iyer NS, Balsamo LM, Bracken MB, Kadan-Lottick NS. Chemotherapy-only treatment effects on long-term neurocognitive functioning in childhood ALL survivors: a review and meta-analysis. *Blood.* 2015;126(3):346-353.
- Pui C-H, Cheng C, Leung W, et al. Extended follow-up of long-term survivors of childhood acute lymphoblastic leukemia. *N Engl J Med.* 2003;349(7):640-649.
- Price RA. Histopathology of CNS leukemia and complications of therapy. *Am J Pediatr Hematol Oncol.* 1979;1(1):21-30.
- Price RA, Johnson WW. The central nervous system in childhood leukemia. I. The arachnoid. *Cancer.* 1973;31(3):520-533.
- Evans AE, Gilbert ES, Zandstra R. The increasing incidence of central nervous system leukemia in children. (Children's Cancer Study Group A). *Cancer.* 1970;26(2):404-409.
- Williams MTS, Yousafzai YM, Elder A, et al. The ability to cross the blood-cerebrospinal fluid barrier is a generic property of acute lymphoblastic leukemia blasts. *Blood.* 2016;127(16):1998-2006.
- Bartram J, Goulden N, Wright G, et al. High throughput sequencing in acute lymphoblastic leukemia reveals clonal architecture of central nervous system and bone marrow compartments. *Haematologica.* 2018;103(3):e110-114.
- Krause S, Pfeiffer C, Strube S, et al. Mer tyrosine kinase promotes the survival of t(1;19)-positive acute lymphoblastic leukemia (ALL) in the central nervous system (CNS). *Blood.* 2015;125(5):820-830.
- Akers SM, Rellick SL, Fortney JE, Gibson LF. Cellular elements of the subarachnoid space promote ALL survival during chemotherapy. *Leuk Res.* 2011;35(6):705-711.
- Gossai NP, Gordon PM. The role of the central nervous system microenvironment in pediatric acute lymphoblastic leukemia. *Front Pediatr.* 2017;5:90.
- Frishman-Levy L, Izraeli S. Advances in understanding the pathogenesis of CNS acute lymphoblastic leukaemia and potential for therapy. *Br J Haematol.* 2017;176(2):157-167.
- Gaynes JS, Jonart LM, Zamora EA, Naumann JA, Gossai NP, Gordon PM. The central nervous system microenvironment influences the leukemia transcriptome and enhances leukemia chemo-resistance. *Haematologica.* 2017;102(4):e136-139.
- Williams RT, Sherr CJ. The ARF tumor suppressor in acute leukemias: insights from mouse models of Bcr-Abl-induced acute lymphoblastic leukemia. *Adv Exp Med Biol.* 2007;604:107-114.
- Mishra S, Zhang B, Cunnick JM, Heisterkamp N, Groffen J. Resistance to imatinib of bcr/abl p190 lymphoblastic leukemia cells. *Cancer Res.* 2006;66(10):5387-5393.
- Williams RT, Roussel ME, Sherr CJ. Arf gene loss enhances oncogenicity and limits imatinib response in mouse models of Bcr-Abl-induced acute lymphoblastic leukemia. *Proc Natl Acad Sci USA.* 2006;103(17):6688-6693.
- Townsend EC, Murakami MA, Christodoulou A, et al. The public repository of xenografts enables discovery and randomized phase II-like trials in mice. *Cancer Cell.* 2016;29(4):574-586.
- Liu L, Duff K. A technique for serial collection of cerebrospinal fluid from the cisterna magna in mouse. *J Vis Exp.* 2008;(21).
- Manlove LS, Schenkel JM, Manlove KR, et al. Heterologous vaccination and checkpoint blockade synergize to induce antileukemia

- immunity. *J Immunol.* 2016;196(11):4793-4804.
27. Montero J, Sarosiek KA, DeAngelo JD, et al. Drug-induced death signaling strategy rapidly predicts cancer response to chemotherapy. *Cell.* 2015;160(5):977-989.
 28. Bholra PD, Mar BG, Lindsley RC, et al. Functionally identifiable apoptosis-insensitive subpopulations determine chemoresistance in acute myeloid leukemia. *J Clin Invest.* 2016;126(10):3827-3836.
 29. Kim KH, Sederstrom JM. Assaying cell cycle status using flow cytometry. *Curr Protoc Mol Biol.* 2015;111:28.6.1-11.
 30. Tario JD, Muirhead KA, Pan D, Munson ME, Wallace PK. Tracking immune cell proliferation and cytotoxic potential using flow cytometry. *Methods Mol Biol.* 2011;699:119-164.
 31. Ebinger S, Özdemir EZ, Ziegenhain C, et al. Characterization of rare, dormant, and therapy-resistant cells in acute lymphoblastic leukemia. *Cancer Cell.* 2016;30(6):849-862.
 32. Boyerinas B, Zafrir M, Yesilkartal AE, Price TT, Hyjek EM, Sipkins DA. Adhesion to osteopontin in the bone marrow niche regulates lymphoblastic leukemia cell dormancy. *Blood.* 2013;121(24):4821-4831.
 33. Sipkins DA, Wei X, Wu JW, et al. In vivo imaging of specialized bone marrow endothelial microdomains for tumour engraftment. *Nature.* 2005;435(7044):969-973.
 34. Colmone A, Amorim M, Pontier AL, Wang S, Jablonski E, Sipkins DA. Leukemic cells create bone marrow niches that disrupt the behavior of normal hematopoietic progenitor cells. *Science.* 2008;322(5909):1861-1865.
 35. Zuber J, Radtke I, Pardee TS, et al. Mouse models of human AML accurately predict chemotherapy response. *Genes Dev.* 2009;23(7):877-889.
 36. Hiddemann W. Cytosine arabinoside in the treatment of acute myeloid leukemia: the role and place of high-dose regimens. *Ann Hematol.* 1991;62(4):119-128.
 37. Chen H, Wang S, Zhang J, et al. A novel molecule Me6TREN promotes angiogenesis via enhancing endothelial progenitor cell mobilization and recruitment. *Sci Rep.* 2014;4:6222.
 38. Zhang J, Ren X, Shi W, et al. Small molecule Me6TREN mobilizes hematopoietic stem/progenitor cells by activating MMP-9 expression and disrupting SDF-1/CXCR4 axis. *Blood.* 2014;123(3):428-441.
 39. Buonamici S, Trimarchi T, Ruocco MG, et al. CCR7 signalling as an essential regulator of CNS infiltration in T-cell leukaemia. *Nature.* 2009;459(7249):1000-1004.
 40. Alsadeq A, Fedders H, Vokuhl C, et al. The role of ZAP70 kinase in acute lymphoblastic leukemia infiltration into the central nervous system. *Haematologica.* 2017;102(2):346-355.
 41. Münch V, Trentin L, Herzig J, et al. Central nervous system involvement in acute lymphoblastic leukemia is mediated by vascular endothelial growth factor. *Blood.* 2017;130(5):643-654.
 42. Cario G, Izraeli S, Teichert A, et al. High interleukin-15 expression characterizes childhood acute lymphoblastic leukemia with involvement of the CNS. *J Clin Oncol.* 2007;25(30):4813-4820.
 43. Wigton EJ, Thompson SB, Long RA, Jacobelli J. Myosin-IIA regulates leukemia engraftment and brain infiltration in a mouse model of acute lymphoblastic leukemia. *J Leukoc Biol.* 2016;100(1):143-153.
 44. Holland M, Castro FV, Alexander S, et al. RAC2, AEP, and ICAM1 expression are associated with CNS disease in a mouse model of pre-B childhood acute lymphoblastic leukemia. *Blood.* 2011;118(3):638-649.
 45. Yao H, Price TT, Cantelli G, et al. Leukaemia hijacks a neural mechanism to invade the central nervous system. *Nature.* 2018;560(7716):55-60.
 46. Williams MTS, Yousafzai Y, Cox C, et al. Interleukin-15 enhances cellular proliferation and upregulates CNS homing molecules in pre-B acute lymphoblastic leukemia. *Blood.* 2014;123(20):3116-3127.
 47. Alsadeq A, Lenk L, Vadakumchery A, et al. IL7R is associated with CNS infiltration and relapse in pediatric B-cell precursor acute lymphoblastic leukemia. *Blood.* 2018;132(15):1614-1617.
 48. Naumann JA, Gordon PM. In vitro model of leukemia cell migration across the blood-cerebrospinal fluid barrier. *Leuk Lymphoma.* 2017;58(7):1747-1749.
 49. Akers SM, O'Leary HA, Minnear FL, et al. VE-cadherin and PECAM-1 enhance ALL migration across brain microvascular endothelial cell monolayers. *Exp Hematol.* 2010;38(9):733-743.
 50. Krause DS, Scadden DT. A hostel for the hostile: the bone marrow niche in hematologic neoplasms. *Haematologica.* 2015;100(11):1376-1387.
 51. Essers MAG, Trumpp A. Targeting leukemic stem cells by breaking their dormancy. *Mol Oncol.* 2010;4(5):443-450.
 52. Norkin M, Uberti JB, Schiffer CA. Very late recurrences of leukemia: why does leukemia awake after many years of dormancy? *Leuk Res.* 2011;35(2):139-144.
 53. Chiarini F, Lonetti A, Evangelisti C, et al. Advances in understanding the acute lymphoblastic leukemia bone marrow microenvironment: From biology to therapeutic targeting. *Biochim Biophys Acta.* 2016;1863(3):449-463.
 54. Moses BS, Slone WL, Thomas P, et al. Bone marrow microenvironment modulation of acute lymphoblastic leukemia phenotype. *Exp Hematol.* 2016;44(1):50-9.e1.
 55. Pasello M, Manara MC, Scotlandi K. CD99 at the crossroads of physiology and pathology. *J Cell Commun Signal.* 2018;12(1):55-68.
 56. Gaudichon J, Jakobczyk H, Debaize L, et al. Mechanisms of extramedullary relapse in acute lymphoblastic leukemia: reconciling biological concepts and clinical issues. *Blood Rev.* 2019;36:40-56.
 57. Sison EAR, Magoon D, Li L, et al. Plerixafor as a chemosensitizing agent in pediatric acute lymphoblastic leukemia: efficacy and potential mechanisms of resistance to CXCR4 inhibition. *Oncotarget.* 2014;5(19):8947-8958.
 58. Uy GL, Rettig MP, Stone RM, et al. A phase 1/2 study of chemosensitization with plerixafor plus G-CSF in relapsed or refractory acute myeloid leukemia. *Blood Cancer J.* 2017;7(3):e542-e542.
 59. Cooper TM, Sison EAR, Baker SD, et al. A phase 1 study of the CXCR4 antagonist plerixafor in combination with high-dose cytarabine and etoposide in children with relapsed or refractory acute leukemias or myelodysplastic syndrome: a Pediatric Oncology Experimental Therapeutics Investigators' Consortium study (POE 10-03). *Pediatr Blood Cancer.* 2017;64(8).
 60. Laurence ADJ. Location, movement and survival: the role of chemokines in haematopoiesis and malignancy. *Br J Haematol.* 2006;132(3):255-267.

Quantification of minimal disseminated disease by quantitative polymerase chain reaction and digital polymerase chain reaction for *NPM-ALK* as a prognostic factor in children with anaplastic large cell lymphoma

Christine Damm-Welk,¹ Nina Kutscher,¹ Martin Zimmermann,² Andishe Attarbaschi,³ Jutta Schieferstein,¹ Fabian Knörr,⁴ Ilske Oeschli,⁵ Wolfram Klapper⁵ and Wilhelm Woessmann^{1,4}

¹NHL-BFM Study Center, Department of Pediatric Hematology and Oncology, Giessen, Germany; ²Department of Pediatric Hematology and Oncology, Hannover Medical School, Hannover, Germany; ³Department of Pediatric Hematology and Oncology, St. Anna Children's Hospital, Medical University of Vienna, Vienna, Austria; ⁴Pediatric Hematology and Oncology, University Medical Center Hamburg-Eppendorf, Hamburg, Germany and ⁵Institute of Pathology, Hematopathology Section and Lymph Node Registry, Kiel, Germany.

[°]Present address: Pediatric Hematology and Oncology, University Medical Center Hamburg-Eppendorf, Hamburg, Germany



Haematologica 2020
Volume 105(8):2141-2149

ABSTRACT

Detection of minimal disseminated disease is a validated prognostic factor in ALK-positive anaplastic large cell lymphoma. We previously reported that quantification of minimal disease by quantitative real-time polymerase chain reaction (RQ-PCR) in bone marrow applying a cut-off of 10 copies *NPM-ALK*/10⁴ copies of *ABL1* identifies very high-risk patients. In the present study, we aimed to confirm the prognostic value of quantitative minimal disseminated disease evaluation and to validate digital polymerase chain reaction (dPCR) as an alternative method. Among 91 patients whose bone marrow was analyzed by RQ-PCR, more than 10 normalized copy-numbers correlated with stage III/IV disease, mediastinal and visceral organ involvement and low anti-ALK antibody titers. The cumulative incidence of relapses of 18 patients with more than 10 normalized copy-numbers of *NPM-ALK* was 61±12% compared to 21±5% for the remaining 73 patients ($P=0.0002$). Results in blood correlated with those in bone marrow ($r=0.74$) in 70 patients for whom both materials could be tested. Transcripts were quantified by RQ-PCR and dPCR in 75 bone marrow and 57 blood samples. Copy number estimates using dPCR and RQ-PCR correlated in 132 samples ($r=0.85$). Applying a cut-off of 30 copies *NPM-ALK*/10⁴ copies *ABL1* for quantification by dPCR, almost identical groups of patients were separated as those separated by RQ-PCR. In summary, the prognostic impact of quantification of minimal disseminated disease in bone marrow could be confirmed for patients with anaplastic large cell lymphoma. Blood can substitute for bone marrow. Quantification of minimal disease by dPCR provides a promising tool to facilitate harmonization of minimal disease measurement between laboratories and for clinical studies.

Introduction

ALK-positive anaplastic large cell lymphomas (ALCL) in children and adolescents are characterized by translocations involving the *ALK* gene on chromosome 2p23.¹ About 90% of ALK-positive ALCL carry the translocation t(2;5)(p23;q35) resulting in the fusion gene *NPM-ALK*.²⁻⁴ Between 25% and 35% of patients relapse with current treatment protocols.⁵⁻⁹

Correspondence:

CHRISTINE DAMM-WELK
c.damm-welk@uke.de

WILHELM WOESSMANN
w.woessmann@uke.de

Received: July 17, 2019.

Accepted: October 24, 2019.

Pre-published: October 24, 2019.

doi:10.3324/haematol.2019.232314

Check the online version for the most updated information on this article, online supplements, and information on authorship & disclosures: www.haematologica.org/content/105/8/2141

©2020 Ferrata Storti Foundation

Material published in *Haematologica* is covered by copyright. All rights are reserved to the Ferrata Storti Foundation. Use of published material is allowed under the following terms and conditions:

<https://creativecommons.org/licenses/by-nc/4.0/legalcode>.

Copies of published material are allowed for personal or internal use. Sharing published material for non-commercial purposes is subject to the following conditions:

<https://creativecommons.org/licenses/by-nc/4.0/legalcode>, sect. 3. Reproducing and sharing published material for commercial purposes is not allowed without permission in writing from the publisher.



Detection of blasts in bone marrow (BM) and blood by cytomorphological analysis is a rare event in ALCL.^{6,7} The chimeric fusion gene transcript *NPM-ALK* has been used to investigate the prognostic value of submicroscopic minimal disseminated disease (MDD) in BM and blood at diagnosis in independent cohorts of patients.¹⁰⁻¹³ Polymerase chain reaction (PCR) analysis allows the reliable detection of one circulating tumor cell among 100,000 normal cells.¹⁰ The detection of MDD by qualitative PCR in BM or blood (55% of patients) conferred a relapse risk of 50% in several studies.^{10-12,14} Measurement of minimal residual disease (MRD) using the qualitative PCR assay enabled identification of a very high-risk group of patients.¹⁴

We previously reported the possibility of identifying patients bearing a very high risk of relapse already at diagnosis by quantification of fusion gene transcripts using an *NPM-ALK*-specific quantitative real-time (RQ)-PCR assay. Applying a cut off of 10 copies *NPM-ALK* per 10⁴ copies of the reference transcript *ABL1* (normalized copy numbers, NCN), 16 patients (22%) with more than 10 NCN *NPM-ALK* in the BM at diagnosis had a 5-year probability of event-free survival of 23±11% compared to 78±6% for the 58 patients with NCN below the cut-off. MDD levels measured in blood provided comparable results.¹²

The Japanese NHL study group recently reported the outcomes of 60 ALCL-patients according to MDD in blood or BM using the same cut-off of 10 NCN *NPM-ALK*.¹³ The patients received comparable therapies. Compared to the Berlin-Frankfurt-Münster (BFM) group, however, more patients showed MDD levels above 10 NCN. The progression-free survival of 37 patients with >10 NCN *NPM-ALK* in blood or BM was 58±12% compared to 85±6% for the 22 patients with ≤10 NCN.¹³

The differences regarding the prognostic value of MDD assessment by RQ-PCR in these two studies illustrate the need for standardization before the implementation of quantification of *NPM-ALK* transcripts for initial risk assessment or MRD evaluation in clinical studies. Currently, quantitative values from different laboratories cannot be directly compared to each other, whereas MRD quantification within one laboratory has been reported to enable the course of the disease to be monitored.¹⁵⁻¹⁷

To achieve comparability of MRD quantification for *NPM-ALK* obtained by RQ-PCR in different reference laboratories, extensive protocol harmonization is necessary, as was done for the quantification of *BCR-ABL1* fusion gene transcripts in acute lymphoblastic leukemia and chronic myelogenous leukemia.^{18,19} Since quantification is performed at the lowest end of the necessary standard curve in *NPM-ALK*-specific RQ-PCR, a quantitative PCR approach with improved reproducibility without the need for a standard curve would be advantageous. Digital PCR (dPCR) may represent a quantitative PCR method that could be used as a replacement for RQ-PCR for *NPM-ALK* copy number estimation in ALK-positive ALCL. dPCR is a quantitative PCR method based on the distribution of the target RNA or DNA molecules in many partitions.²⁰ The amount of partitions with a positive PCR results allows the concentration of a given target to be determined without the need for standard curve calibration.²¹

The aim of this work was to validate the prognostic meaning of quantitative MDD measurements of *NPM-ALK* fusion gene transcripts by RQ-PCR in an independent cohort of uniformly treated ALK-positive ALCL patients of the BFM group. In addition, in an effort to facilitate quali-

ty-controlled quantification between different laboratories, a dPCR assay for quantification of *NPM-ALK* transcripts was developed and validated.

Methods

Patients

Patients with ALCL from Austria, Germany and Switzerland enrolled in the ALCL99 trial or the NHL-BFM registry 2012 between January 2006 and December 2016 were eligible after confirmation of *NPM-ALK* positivity of the ALCL. Both studies were approved by the institutional ethics committee of the primary investigators. Informed consent from the patients/caregivers to the studies included consent for future research on MDD.

Controls and cell lines

Blood from 20 healthy donors and eight ALK-negative ALCL patients included in ALCL99 or the NHL-BFM registry served as negative controls after written informed consent.

The cell lines HL-60 (acute myeloid leukemia), SU-DHL-1 and Karpas-299 (*NPM-ALK*-positive ALCL) were obtained from the *Deutsche Sammlung von Mikroorganismen und Zellkulturen* (DSMZ, Braunschweig, Germany).

Complementary DNA synthesis and quantitative real-time polymerase chain reaction

Complementary DNA (cDNA) synthesis and RQ-PCR were performed as described previously.¹² In total four replicates were analyzed (two with undiluted cDNA and two with 1+1 diluted cDNA, as an additional control for RQ-PCR inhibition). Samples which were positive for *NPM-ALK* in one to three of four replicates only or had NCN below one copy were considered as low positive not quantifiable. Negativity for *NPM-ALK* in all four replicates was considered as negative.

Digital polymerase chain reaction assay

Primer and probe sequences for the *NPM-ALK*- and *ABL1*-specific dPCR assay were identical to those used for the RQ-PCR assay.¹² Probes used for dPCR were ordered with 5'FAM™ as the reporter dye and the double quencher dyes ZEN™ and 3'Iowa-Black®FQ (IDT, Leuven, Belgium).

Ten microliters of dPCR™ supermix for probes (no dUTP; BIO-RAD, Munich, Germany), 0.6 µL forward primers, 0.6 µL reverse primers (10 µM, final concentration 300 pM) and 1 µL probe (final concentration 250 pM) were used in a reaction volume of 20 µL. Droplets were generated with the QX-200 droplet generator (BIO-RAD, Munich, Germany). The PCR was performed at 95°C for 10 min for enzyme activation, 44 cycles at 94°C for 30 s, followed by 1 min at 54.1°C for annealing and extension, and enzyme inactivation at 98°C for 10 min. Droplets were measured with the QX200 droplet reader and were analyzed with Quanta Soft pro analysis software (BIO-RAD, Munich, Germany). Four replicates per sample were measured. Only replicates with ≥10,000 accepted droplets were included in the analysis. The threshold for discrimination between positive and negative droplets was set manually with an adequate distance from the background. cDNA from the ALK-positive cell line SU-DHL-1 (positive control), HL-60 (negative control) and no template controls were included in each measurement. Copy numbers were normalized to 10,000 copies of the reference gene *ABL1* (NCN). Samples with <1,000 copies of *ABL1* were excluded. Samples with detectable fusion gene transcripts in one to three, but not in all four replicates were defined as low positive, not quantifiable. Samples were defined as negative if no positive droplets were observed.

Statistical analysis

Event-free survival and overall survival were analyzed using the Kaplan-Meier method with differences compared by the log-rank test. Cumulative incidence functions for relapse were constructed using the method of Kalbfleisch and Prentice. Functions were compared with the Gray test. Quantification by RQ-PCR and dPCR was compared using Spearman correlation. All analyses were performed using SAS (SAS-PC, version 9.4, SAS Institute Inc., Cary, NC, USA).

Results

Quantification of NPM-ALK fusion gene transcripts by quantitative real-time polymerase chain reaction (validation cohort)

Patients' characteristics

MDD was quantified by RQ-PCR in initial BM samples from 91 NPM-ALK-positive ALCL patients. Parallel blood samples for quantification were available from 70 of those patients. The clinical and biological characteristics of the 91 patients are shown in Table 1. Twenty-six of the 91 patients relapsed, one patient died from initial tumor complications. The cumulative incidence of relapse at 3 years of the 91 patients was 29±5%, the event-free survival at 3 years was 70±5% and the overall survival 92±3%. More than 10 NCN NPM-ALK were measured in the BM of 18 patients and ≤10 NCN NPM-ALK were detected in the remaining 73 patients.

The detection of >10 NCN NPM-ALK in BM correlated with stage III/IV disease, mediastinal and visceral organ involvement, as well as low anti-ALK antibody titers (Table 1). No association of NPM-ALK copy numbers above 10 NCN and histological subtype was observed (Table 1).

Prognostic impact of quantitative minimal disseminated disease in bone marrow

The cumulative incidence of relapse of 18 patients with more than 10 NCN NPM-ALK in BM was 61±12% compared to 21±5% for the remaining 73 patients (P=0.0002). The event-free survival rates at 3 years were 33±11% and 79±5%, respectively (P<0.0001), the overall survival rates were 83±9% and 94±3%, respectively (P=0.099) (Online Supplementary Figure S4). Application of the cut-off of 10 NCN NPM-ALK allowed the separation of a group of patients with a very high risk of relapse in the validation cohort.

Prognostic impact of quantitative minimal disseminated disease in blood

In 70 of the 91 patients for whom MDD was measured in the BM, NPM-ALK transcripts could be measured in blood, as well. The results for blood and BM in the same patients correlated (r=0.74). Notably, more patients were MDD-positive and showed higher copy numbers in blood compared to BM (Figure 1).

At 3 years the cumulative incidence of relapse of the 70 patients for whom MDD measurements were available in both BM and blood was 26±5%, the event-free survival was 74±5% and the overall survival 94±3%. To analyze a possible influence of the biological medium used for the quantitative MDD measurement on the detection of very high-risk patients, outcome was compared according to quantitative MDD in blood and BM using the same cut-

off among these 70 patients. The cumulative incidence of relapse of the 17 patients with >10 NCN NPM-ALK measured in blood was 59±13% compared to 15±5% in 53 patients with ≤10 NCN NPM-ALK (P=0.0004). In comparison, the cumulative incidence of relapse of the 13 patients with >10 NCN NPM-ALK measured in BM was 62±14% compared to 18±5% in the 57 patients with ≤10 NCN (P=0.0007) (Figure 2).

Establishment and validation of a digital droplet polymerase chain reaction assay

To overcome some limitations of RQ-PCR we tested an NPM-ALK-specific dPCR assay for fusion gene and reference gene quantification.

A gradient PCR was performed to optimize the performance of the dPCR assays for NPM-ALK and ABL1.¹² The amplification and elongation temperature was set to

Table 1. Association of the quantity of NPM-ALK transcripts in bone marrow with patients' characteristics, clinical and biological risk factors in the validation cohort.

	All patients	MDD		P
		≤10 NCN NPM-ALK	>10 NCN NPM-ALK	
	91	73	18	
Gender, n (%)				
Male	59	47 (64%)	12 (67%)	1.0
Female	32	26 (36%)	6 (33%)	
Stage*, n (%)				
I	5	5 (7%)	0 (0%)	0.002
II	20	20 (27%)	0 (0%)	
III	56	42 (58%)	14 (78%)	
IV	6	2 (3%)	4 (22%)	
n.a.	4	4 (5%)		
Age, n (%)				1.0
Age <10 years	24	19 (26%)	5 (28%)	
Age ≥10 years	67	54 (74%)	13 (72%)	
CNS, n (%)				
Negative	83	67 (100%)	16 (100%)	
Positive	-	-	-	
Bone marrow, n (%)				0.004
Negative	86	72 (99%)	14 (78%)	
Positive	5	1 (1%)	4 (22%)	
Bone, n (%)				0.14
No	77	64 (88%)	13 (72%)	
Yes	14	9 (12%)	5 (28%)	
Skin, n (%)				1.0
No	73	58 (80%)	15 (83%)	
Yes	18	15 (20%)	3 (17%)	
Mediastinum, n (%)				0.001
No	52	48 (66%)	4 (22%)	
Yes	39	25 (34%)	14 (78%)	
Visceral organs**, n (%)				0.01
No	68	59 (81%)	9 (50%)	
Yes	23	14 (19%)	9 (50%)	
Histology				0.59
Non-common	35	27 (39%)	8 (47%)	
Common	52	43 (61%)	9 (53%)	
Anti-ALK titer				0.03
≤750	24	15 (28%)	9 (60%)	
>750	44	38 (72%)	8 (40%)	

MDD: minimal disseminated disease; NCN: normalized copy number; n.a.: not available; CNS: central nervous system. * St. Jude staging system; ** liver, spleen, lung.

54.1°C after optimization. A serial limited 10-fold dilution of the ALK-positive cell line Karpas 299 in peripheral blood mononuclear cells from 10^{-1} to 10^{-5} was performed to evaluate the sensitivity and specificity of the dPCR assay (Table 2). Normalized copies of *NPM-ALK* were detected in cDNA prepared from dilutions of 10 ALK-positive cells in 1,000,000 normal cells in one out of four replicates. The peripheral blood mononuclear cells used for dilution had no detectable copies of *NPM-ALK*.

To estimate the rate of false positivity, blood from 20 healthy controls and BM or blood from eight ALK-negative ALCL patients was analyzed. No positive droplets were detected in BM or blood from ALK-negative ALCL patients or 20 healthy controls. All samples were negative by RQ-PCR. Since higher copy numbers of *NPM-ALK* were measured by dPCR compared to RQ-PCR, the cut-off for outcome analysis was set at 30 NCN for the dPCR.

Comparison of *NPM-ALK* quantification by digital and quantitative real-time polymerase chain reaction analyses in bone marrow and blood samples

Measurement of circulating tumor cells using RQ-PCR and dPCR was possible in 132 initial BM (n=75) or blood (n=57) samples from ALCL patients. Forty-five samples were negative by both RQ-PCR as well as dPCR (31/75

BM, 14/57 blood samples). Of the 75 BM samples, 19 and 15 were low positive, not quantifiable by dPCR and RQ-PCR, respectively. Of the 57 blood samples, 21 and 14 were low positive by dPCR and RQ-PCR, respectively. The results of dPCR and RQ-PCR correlated with a correlation coefficient of $r=0.85$ (Figure 3). Above the threshold of 10 NCN *NPM-ALK* measured by RQ-PCR the copy numbers obtained by both methods were highly correlated with a correlation coefficient of $r=0.96$, but generally higher with dPCR.

Comparison of patient stratification according to the results of quantitative real-time and droplet polymerase chain reaction analyses in bone marrow and blood

The cumulative incidence of relapse, event-free survival and overall survival of patients with dPCR quantification of MDD in BM (n=75) and blood (n=57) by dPCR using a threshold of 30 NCN are shown in Figure 4. The comparable data according to RQ-PCR, using the cut-off of 10 NCN, were almost identical. The patients' distribution according to MDD measured in BM was concordant with both quantification methods (Table 3). Among the 57 patients for whom MDD was quantified in blood, only one patient had a discordant result with ≤ 30 (dPCR) but >10 NCN (RQ-PCR) (Table 3b).

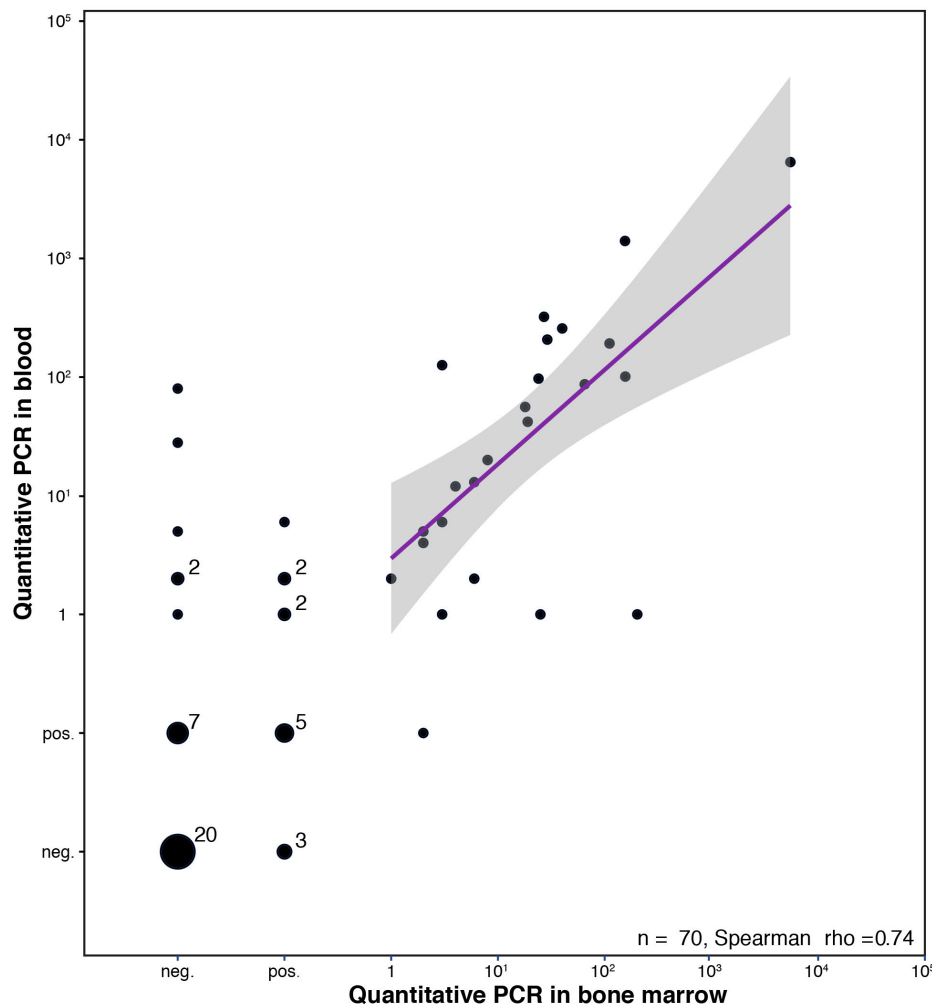


Figure 1. Normalized copy numbers of *NPM-ALK* in blood and bone marrow measured by quantitative real-time polymerase chain reaction. Copy numbers of *NPM/ALK*/ 10^4 copy numbers of *ABL1* were measured in 70 patients in initial blood and bone marrow samples. PCR: polymerase chain reaction.

Discussion

In our previous study, quantitative measurement of *NPM-ALK* fusion gene transcripts in blood or BM using a cut-off of 10 NCN in the RQ-PCR analysis allowed us to identify the group of patients with the highest risk of relapse. We were able to confirm these results in the validation cohort of uniformly treated *NPM-ALK*-positive ALCL patients. As in our previous analysis, only 20% of patients had more than 10 NCN *NPM-ALK* detectable in BM. Two-thirds of those patients relapsed in both series of altogether 175 ALCL patients.

When comparing the event-free survival of the very high-risk group determined by quantification of MDD in blood between the two cohorts, the EFS of high-risk patients was somewhat higher in the validation cohort than in the earlier cohort. This difference might be attributable to a selection bias with a higher event-free survival in the current cohort analyzed in blood compared to the previously reported cohort (previous cohort 61±6%, current cohort 74±5%). In the current validation cohort,

MDD results measured in blood and BM of the same patients were comparable and had the same prognostic impact. For future studies, investigation of peripheral blood could therefore be sufficient for quantitative MDD evaluation. This is especially helpful bearing in mind the application of MRD to follow the course of disease in very high-risk patients or after relapse.

Compared to the earlier cohort including patients diagnosed until 2005, the survival of the very high-risk patients, as defined by more than 10 NCN in BM, improved in the validation cohort (83% compared to 46%). New therapeutic options became available for patients with relapsed ALCL, ranging from vinblastine monotherapy, brentuximab vedotin, ALK kinase inhibitors to PD-L1 checkpoint inhibitors.^{15,17,22-28} In addition, allogeneic blood stem cell transplantation was increasingly used for consolidation in relapse.²⁹⁻³²

Our results show that separation of patients with a high risk of relapse can be achieved by quantification of MDD in patients with ALCL with the prerequisites that quantitative PCR evaluation is performed in the same laboratory

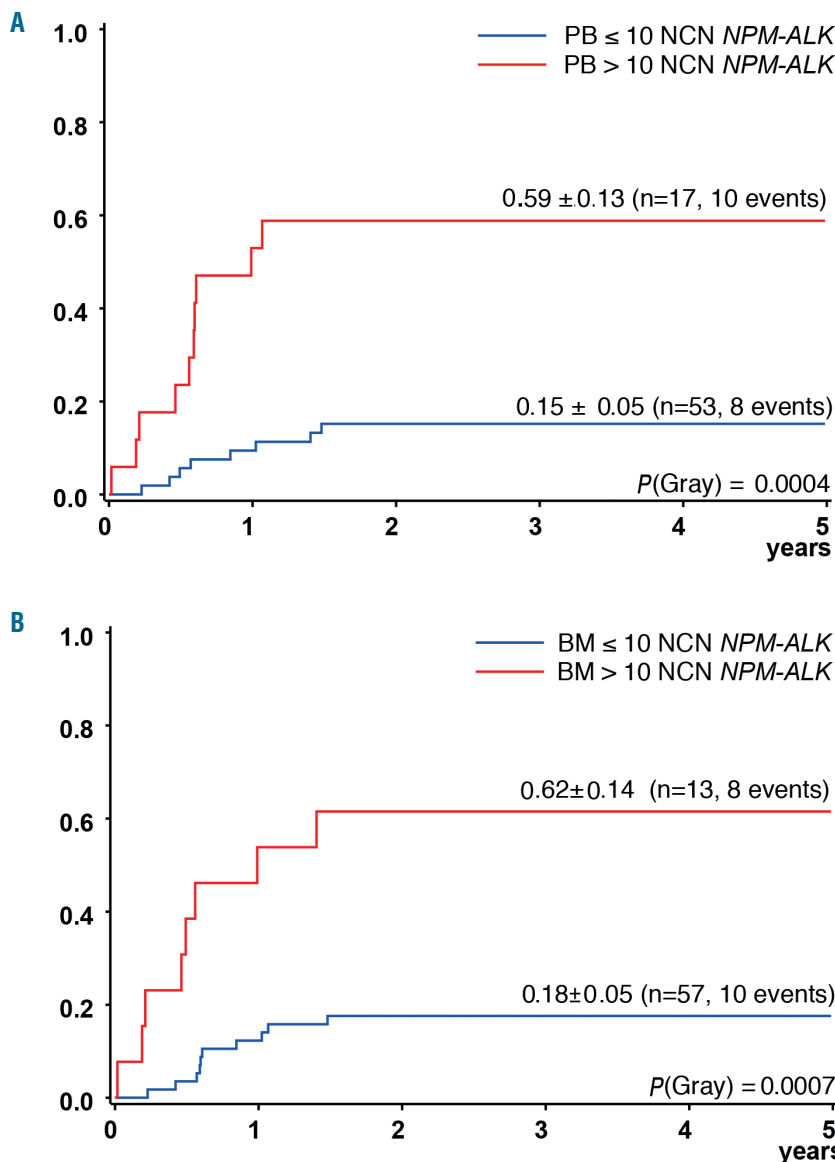


Figure 2. Outcome according to *NPM-ALK* copy numbers measured by quantitative real-time polymerase chain reaction in blood and bone marrow. Cumulative incidence of relapse (according to a cut-off of 10 normalized copy numbers of *NPM/ALK*/10⁴ copy numbers of *ABL1*) measured in initial (A) blood and (B) bone marrow samples in 70 patients. PB: blood; BM: bone marrow; NCN: normalized copy number.

by the same persons, according to standard operating procedures for RQ-based MDD measurement and analysis. However, there are still significant inter-laboratory differences and quantification of minimal disease in patients with ALCL can currently not be compared between laboratories.^{12,13,17,33} This is exemplified by the comparison of the Japanese study group's data with our data. Both groups used the same therapy and the same RQ-PCR assay for quantification. Twenty per cent of patients showed >10 NCN *NPM-ALK* in our cohorts and 37% of patients had high copy numbers in the Japanese cohort even though the relapse rate in the Japanese cohort was somewhat lower. Accordingly, the relapse risk of patients with >10 NCN *NPM-ALK* was higher in our cohorts (65%) than in the Japanese cohort (40%). In order to use quantification of copy numbers for patient stratification or to follow the course of individual patients in multinational studies, the RQ-PCR method needs very strict protocol harmonization and quality control. The experiences from quantification of *BCR-ABL1* transcripts can partly guide this development.³⁴ The introduction of calibrators, specific conversion factors to the calibrators for each laboratory and calibrated reference material led to a high standardization of *BCR-ABL1* measurements.^{19,35-37} In Philadelphia-positive acute leukemia the optimization and standardization process for RQ-PCR-based measurement of m-*BCR-*

ABL1 transcripts underscores the importance of standardization of all steps for quantitative PCR, including data interpretation and quality controls.³⁸ In the standardization process of MRD assessment of m-*BCR-ABL1* fusion gene transcripts organized by the Euro MRD consortium, the usage of a common primer and probe set as well as a centrally distributed plasmid standard curve had the greatest impact on overcoming inter-laboratory variability.³⁸

Since the same primer/probe sets and the same RQ-PCR protocol were applied by the Japanese and BFM study

Table 2. Normalized copy numbers of *NPM-ALK* measured by digital polymerase chain reaction analysis in a 10-fold serial dilution of a *NPM-ALK* anaplastic large cell lymphoma cell line in 10⁶ mononuclear cells.

Dilution	ALK ⁺ cells in 10 ⁶ MNC	Copies of <i>NPM-ALK</i> /10 ⁴ <i>ABL1</i>
10 ⁻¹	100,000	9222
10 ⁻²	10,000	974
10 ⁻³	1,000	93
10 ⁻⁴	100	8
10 ⁻⁵	10	0.4
0	0	0

MNC: mononuclear cells.

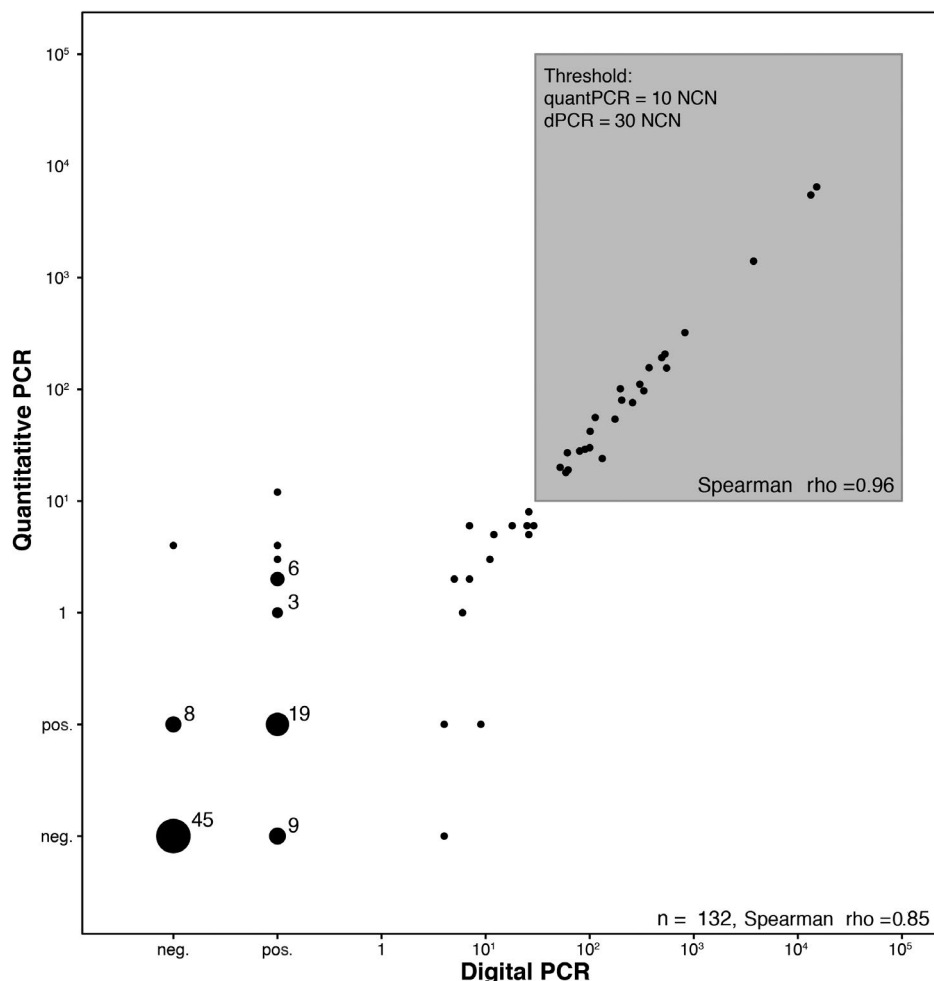


Figure 3. Comparison of *NPM-ALK* copy numbers measured by quantitative real-time polymerase chain reaction and digital polymerase chain reaction. Normalized copy numbers of *NPM/ALK*/10⁴ copy numbers of *ABL1* measured in 132 blood and bone marrow samples. quantPCR: quantitative real-time polymerase chain reaction; dPCR: digital polymerase chain reaction; NCN: normalized copy number.

groups, the differences in results might be related to the use of standard curves that were not centrally distributed and to the fact that the cut-off at 10 NCN *NPM-ALK* is close to the detection limit of the assay. The latter point is an unchangeable limitation to inter-laboratory comparability for quantification of *NPM-ALK* transcripts and a major difference from MRD quantification in leukemia.

In order to overcome some of the technical problems inherent to RQ-PCR we developed a dPCR method for the quantification of *NPM-ALK* transcripts and compared the

results obtained with this method to those obtained with RQ-PCR in a large cohort of patients. Using dPCR with a cut-off at 30 NCN *NPM-ALK* for quantitative measurements of MDD in blood and BM in the presented study allowed measurements near to the detection limit without needing standard curve calibration. The dPCR assay might be more suitable for quantitative measurements of *NPM-ALK* in a multinational setting, because it overcomes several limitations of the RQ-PCR assay. First, it is independent of a calibration curve, thereby excluding the impact of

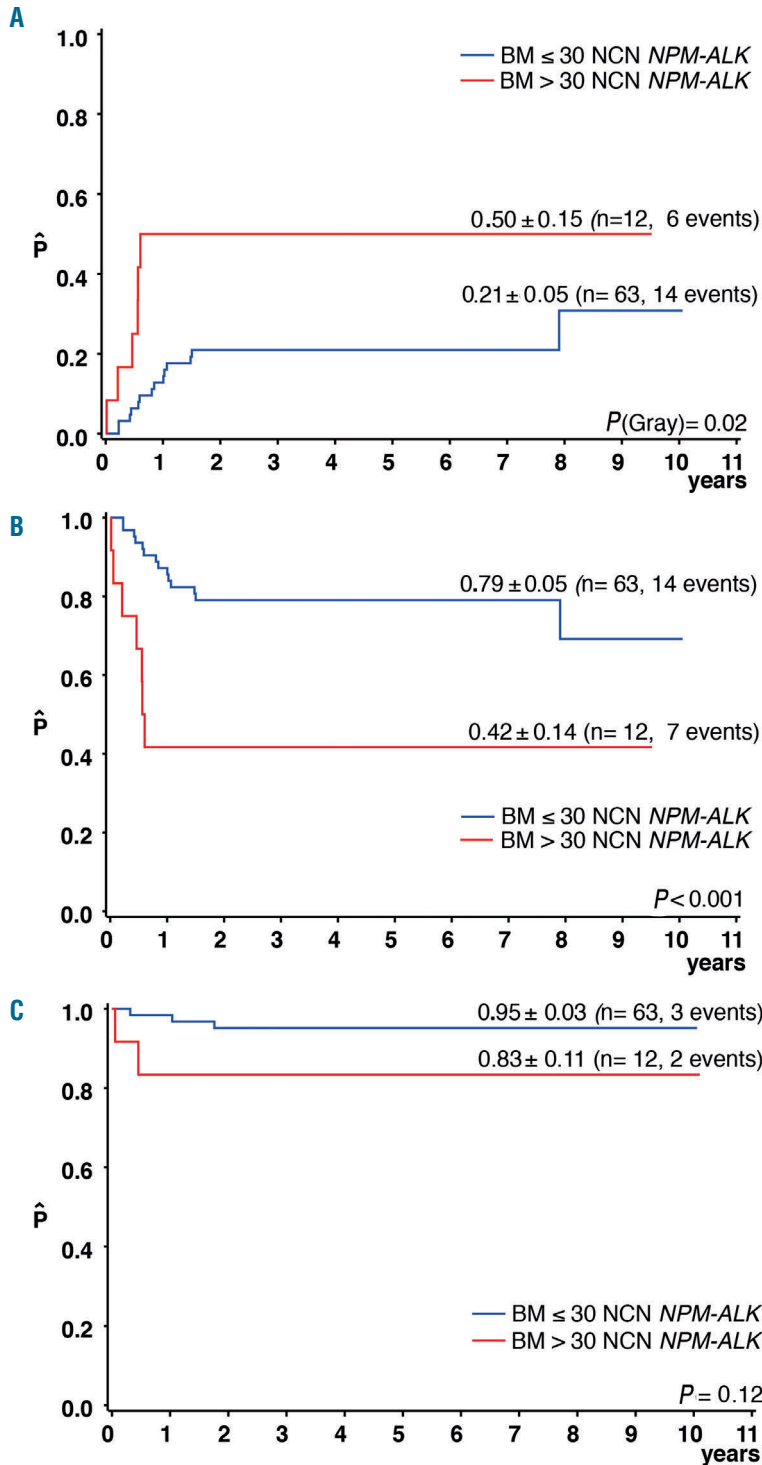


Figure 4. Outcome according to *NPM-ALK* copy numbers measured by digital polymerase chain reaction in bone marrow. (A) Cumulative incidence of relapse, (B) event-free survival and (C) overall survival at 3 years according to a cut-off of 30 normalized copy numbers of *NPM/ALK/10⁴* copy numbers of *ABL1*. BM: bone marrow, NCN: normalized copy numbers.

standard curve differences for inter-laboratory comparisons. Second, partitioning of target molecules leads to a more precise detection especially of rare events so that the assay is able to detect low copy numbers more accurately than RQ-PCR.^{39,40} To exclude that templates are not amplifiable during the dPCR reaction it is still unavoidable to verify the quality of a given cDNA by parallel estimation of a reference gene. Furthermore, for measurement of clinical samples, appropriate positive and negative controls must be included in order to control for the overall performance of a given dPCR experiment.

The applicability of dPCR for MRD measurement has already been shown for several hematologic malignancies. The accuracy of dPCR and high concordance with RQ-PCR was demonstrated for DNA-based MRD measurements of the *BCL2/IGH* rearrangement in blood and BM from patients with low stage follicular lymphoma⁴¹ and immunoglobulin/T-cell receptor rearrangements in patients with acute lymphoblastic leukemia.⁴² dPCR was shown to be reliable for quantifying *BCR-ABL1* transcripts for MRD monitoring in chronic myeloid leukemia and Philadelphia-positive acute lymphoblastic leukemia.⁴³⁻⁴⁶ Altogether, dPCR is a valuable tool for highly reproducible quantification of minimal disease at both DNA and RNA levels in patients' samples without requiring standard curves. In addition, for MDD and MRD in ALCL, it might have the advantage over RQ-PCR that the quantification is more accurate at lower copy numbers. Stringent protocol standardization and quality control are needed for this technique, as well.^{47,48}

In summary, our data validate that quantification of *NPM-ALK* transcripts by RQ-PCR using a cut-off of 10 NCN identifies very high-risk patients if performed in one laboratory. Quantification of MRD is indicated to follow the course of disease and response to treatment modules in MDD-positive or relapsed ALCL patients. In a rare disease such as ALCL, with planned and ongoing international trials, both methods for transcript quantification require

Table 3. Concordance of patients' stratification according to quantity of *NPM-ALK* transcripts determined using digital polymerase chain reaction and quantitative real-time polymerase chain reaction in (A) bone marrow and (B) blood.

(A)

		dPCR	
		≤30 NCN	>30 NCN
RQ-PCR	≤10 NCN	63	0
	>10 NCN	0	12

(B)

		dPCR	
		≤30 NCN	>30 NCN
RQ-PCR	≤10 NCN	44	0
	>10 NCN	1	12

The cut-off for the digital polymerase chain reaction was 30 normalized copy numbers (NCN), while that for quantitative real-time polymerase chain reaction was 10 NCN. dPCR: digital polymerase chain reaction; RQ-PCR: quantitative real time polymerase chain reaction.

inter-laboratory comparability of measurements. Since harmonization is difficult and expensive with RQ-PCR, we developed and validated a dPCR assay enabling reliable quantification of *NPM-ALK* transcripts at very low copy numbers without the need for standard calibration curves.

Acknowledgments

The authors would like to thank Claudia Keller for excellent technical assistance and Ulrike Meyer for excellent assistance with data management. The NHL-BFM Registry 2012 is supported by the Deutsche Kinderkrebsstiftung. CDW, NK, JS and WW were additionally supported by Forschungshilfe Peiper. The pediatric lymphoma research of IO and WK is supported by the KinderKrebsInitiative Buchholz, Holm-Seppensen.

References

- Morris SW, Kirstein MN, Valentine MB, et al. Fusion of a kinase gene, *ALK*, to a nucleolar protein gene, *NPM*, in non-Hodgkin's lymphoma. *Science*. 1994;263(5151):1281-1284.
- Perkins SL, Pickering D, Lowe EJ, et al. Childhood anaplastic large cell lymphoma has a high incidence of *ALK* gene rearrangement as determined by immunohistochemical staining and fluorescent in situ hybridisation: a genetic and pathological correlation. *Br J Haematol*. 2005;131(5):624-627.
- Damm-Welk C, Klapper W, Oschlies I, et al. Distribution of *NPM1-ALK* and *X-ALK* fusion transcripts in paediatric anaplastic large cell lymphoma: a molecular-histological correlation. *Br J Haematol*. 2009;146(3):306-309.
- Lamant L, McCarthy K, D'Amore E, et al. Prognostic impact of morphologic and phenotypic features of childhood *ALK*-positive anaplastic large-cell lymphoma: results of the ALCL99 study. *J Clin Oncol*. 2011;29(35):4669-4676.
- Brugieres L, Deley MC, Pacquement H, et al. CD30(+) anaplastic large-cell lymphoma in children: analysis of 82 patients enrolled in two consecutive studies of the French Society of Pediatric Oncology. *Blood*. 1998;92(10):3591-3598.
- Brugieres L, Le Deley MC, Rosolen A, et al. Impact of the methotrexate administration dose on the need for intrathecal treatment in children and adolescents with anaplastic large-cell lymphoma: results of a randomized trial of the EICNHL Group. *J Clin Oncol*. 2009;27(6):897-903.
- Seidemann K, Tiemann M, Schrappe M, et al. Short-pulse B-non-Hodgkin lymphoma-type chemotherapy is efficacious treatment for pediatric anaplastic large cell lymphoma: a report of the Berlin-Frankfurt-Munster Group Trial NHL-BFM 90. *Blood*. 2001;97(12):3699-3706.
- Williams DM, Hobson R, Imeson J, Gerrard M, McCarthy K, Pinkerton CR. Anaplastic large cell lymphoma in childhood: analysis of 72 patients treated on the United Kingdom Children's Cancer Study Group chemotherapy regimens. *Br J Haematol*. 2002;117(4):812-820.
- Rosolen A, Pillon M, Garaventa A, et al. Anaplastic large cell lymphoma treated with a leukemia-like therapy: report of the Italian Association of Pediatric Hematology and Oncology (AIEOP) LNH-92 protocol. *Cancer*. 2005;104(10):2133-2140.
- Mussolin L, Pillon M, d'Amore ES, et al. Prevalence and clinical implications of bone marrow involvement in pediatric anaplastic large cell lymphoma. *Leukemia*. 2005;19(9):1643-1647.
- Mussolin L, Damm-Welk C, Pillon M, et al. Use of minimal disseminated disease and immunity to *NPM-ALK* antigen to stratify *ALK*-positive ALCL patients with different prognosis. *Leukemia*. 2013;27(2):416-422.
- Damm-Welk C, Busch K, Burkhardt B, et al. Prognostic significance of circulating tumor cells in bone marrow or peripheral blood as detected by qualitative and quantitative PCR in pediatric *NPM-ALK*-positive anaplastic large-cell lymphoma. *Blood*. 2007;110(2):670-677.
- Iijima-Yamashita Y, Mori T, Nakazawa A, et al. Prognostic impact of minimal disseminated disease and immune response to *NPM-ALK* in Japanese children with *ALK*-positive anaplastic large cell lymphoma. *Int J Hematol*. 2018;107(2):244-250.
- Damm-Welk C, Mussolin L, Zimmermann M, et al. Early assessment of minimal resid-

- ual disease identifies patients at very high relapse risk in NPM-ALK-positive anaplastic large-cell lymphoma. *Blood*. 2014;123(3):334-337.
15. Hebart H, Lang P, Woessmann W. Nivolumab for refractory anaplastic large cell lymphoma: a case report. *Ann Intern Med*. 2016;165(8):607-608.
 16. Gambacorti-Passerini C, Mussolin L, Brugieres L. Abrupt relapse of ALK-positive lymphoma after discontinuation of crizotinib. *N Engl J Med*. 2016;374(1):95-96.
 17. Mosse YP, Voss SD, Lim MS, et al. Targeting ALK with crizotinib in pediatric anaplastic large cell lymphoma and inflammatory myofibroblastic tumor: a Children's Oncology Group study. *J Clin Oncol*. 2017;35(28):3215-3221.
 18. Branford S, Cross NC, Hochhaus A, et al. Rationale for the recommendations for harmonizing current methodology for detecting BCR-ABL transcripts in patients with chronic myeloid leukaemia. *Leukemia*. 2006;20(11):1925-1930.
 19. Hughes T, Deininger M, Hochhaus A, et al. Monitoring CML patients responding to treatment with tyrosine kinase inhibitors: review and recommendations for harmonizing current methodology for detecting BCR-ABL transcripts and kinase domain mutations and for expressing results. *Blood*. 2006;108(1):28-37.
 20. Vogelstein B, Kinzler KW. Digital PCR. *Proc Natl Acad Sci U S A*. 1999;96(16):9236-9241.
 21. Dube S, Qin J, Ramakrishnan R. Mathematical analysis of copy number variation in a DNA sample using digital PCR on a nanofluidic device. *PloS One*. 2008;3(8):e2876.
 22. Brugieres L, Pacquement H, Le Deley MC, et al. Single-drug vinblastine as salvage treatment for refractory or relapsed anaplastic large-cell lymphoma: a report from the French Society of Pediatric Oncology. *J Clin Oncol*. 2009;27(30):5056-5061.
 23. Mosse YP, Lim MS, Voss SD, et al. Safety and activity of crizotinib for paediatric patients with refractory solid tumours or anaplastic large-cell lymphoma: a Children's Oncology Group phase 1 consortium study. *Lancet Oncol*. 2013;14(6):472-480.
 24. Rigaud C, Abbou S, Minard-Colin V, et al. Efficacy of nivolumab in a patient with systemic refractory ALK+ anaplastic large cell lymphoma. *Pediatr Blood Cancer*. 2018;65(4):e26902.
 25. Pro B, Advani R, Brice P, et al. Brentuximab vedotin (SGN-35) in patients with relapsed or refractory systemic anaplastic large-cell lymphoma: results of a phase II study. *J Clin Oncol*. 2012;30(18):2190-2196.
 26. Gambacorti-Passerini C, Farina F, Stasia A, et al. Crizotinib in advanced, chemoresistant anaplastic lymphoma kinase-positive lymphoma patients. *J Natl Cancer Inst*. 2014;106(2):dj1378.
 27. Gambacorti-Passerini C, Messa C, Pogliani EM. Crizotinib in anaplastic large-cell lymphoma. *N Engl J Med*. 2011;364(8):775-776.
 28. Locatelli F, Mauz-Koerholz C, Neville K, et al. Brentuximab vedotin for paediatric relapsed or refractory Hodgkin's lymphoma and anaplastic large-cell lymphoma: a multicentre, open-label, phase 1/2 study. *Lancet Haematol*. 2018;5(10):e450-e461.
 29. Woessmann W, Peters C, Lenhard M, et al. Allogeneic haematopoietic stem cell transplantation in relapsed or refractory anaplastic large cell lymphoma of children and adolescents—a Berlin-Frankfurt-Munster group report. *Br J Haematol*. 2006;133(2):176-182.
 30. Gross TG, Hale GA, He W, et al. Hematopoietic stem cell transplantation for refractory or recurrent non-Hodgkin lymphoma in children and adolescents. *Biol Blood Marrow Transplant*. 2010;16(2):223-230.
 31. Fukano R, Mori T, Kobayashi R, et al. Hematopoietic stem cell transplantation for relapsed or refractory anaplastic large cell lymphoma: a study of children and adolescents in Japan. *Br J Haematol*. 2015;168(4):557-563.
 32. Strullu M, Thomas C, Le Deley MC, et al. Hematopoietic stem cell transplantation in relapsed ALK+ anaplastic large cell lymphoma in children and adolescents: a study on behalf of the SFCE and SFGM-TC. *Bone Marrow Transplant*. 2015;50(6):795-801.
 33. Mussolin L, Bonvini P, it-Tahar K, et al. Kinetics of humoral response to ALK and its relationship with minimal residual disease in pediatric ALCL. *Leukemia*. 2009;23(2):400-402.
 34. Hughes TP, Kaeda J, Branford S, et al. Frequency of major molecular responses to imatinib or interferon alfa plus cytarabine in newly diagnosed chronic myeloid leukemia. *N Engl J Med*. 2003;349(15):1423-1432.
 35. Cross NC, White HE, Muller MC, Saglio G, Hochhaus A. Standardized definitions of molecular response in chronic myeloid leukemia. *Leukemia*. 2012;26(10):2172-2175.
 36. Branford S, Fletcher L, Cross NC, et al. Desirable performance characteristics for BCR-ABL measurement on an international reporting scale to allow consistent interpretation of individual patient response and comparison of response rates between clinical trials. *Blood*. 2008;112(8):3330-3338.
 37. White H, Deprez L, Corbisier P, et al. A certified plasmid reference material for the standardisation of BCR-ABL1 mRNA quantification by real-time quantitative PCR. *Leukemia*. 2015;29(2):369-376.
 38. Pfeifer H, Cazzaniga G, van der Velden VHJ, et al. Standardisation and consensus guidelines for minimal residual disease assessment in Philadelphia-positive acute lymphoblastic leukemia (Ph+ ALL) by real-time quantitative reverse transcriptase PCR of e1a2 BCR-ABL1. *Leukemia*. 2019;33(8):1910-1922.
 39. Whale AS, Cowen S, Foy CA, Huggett JF. Methods for applying accurate digital PCR analysis on low copy DNA samples. *PloS One*. 2013;8(3):e58177.
 40. Sanders R, Mason DJ, Foy CA, Huggett JF. Evaluation of digital PCR for absolute RNA quantification. *PloS one*. 2013;8(9):e75296.
 41. Cavalli M, De Novi LA, Della Starza I, et al. Comparative analysis between RQ-PCR and digital droplet PCR of BCL2/IGH gene rearrangement in the peripheral blood and bone marrow of early stage follicular lymphoma. *Br J Haematol*. 2017;177(4):588-596.
 42. Della Starza I, Nunes V, Cavalli M, et al. Comparative analysis between RQ-PCR and digital-droplet-PCR of immunoglobulin/T-cell receptor gene rearrangements to monitor minimal residual disease in acute lymphoblastic leukaemia. *Br J Haematol*. 2016;174(4):541-549.
 43. Bonvini P, Zin A, Alaggio R, Pawel B, Bisogno G, Rosolen A. High ALK mRNA expression has a negative prognostic significance in rhabdomyosarcoma. *Br J Cancer*. 2013;109(12):3084-3091.
 44. Jennings LJ, George D, Czech J, Yu M, Joseph L. Detection and quantification of BCR-ABL1 fusion transcripts by droplet digital PCR. *J Mol Diagn*. 2014;16(2):174-179.
 45. Iacobucci I, Lonetti A, Venturi C, et al. Use of a high sensitive nanofluidic array for the detection of rare copies of BCR-ABL1 transcript in patients with Philadelphia-positive acute lymphoblastic leukemia in complete response. *Leuk Res*. 2014;38(5):581-585.
 46. Wang WJ, Zheng CF, Liu Z, et al. Droplet digital PCR for BCR/ABL(P210) detection of chronic myeloid leukemia: A high sensitive method of the minimal residual disease and disease progression. *Eur J Haematol*. 2018;101(3):291-296.
 47. Huggett JF, Foy CA, Benes V, et al. The digital MIQE guidelines: minimum information for publication of quantitative digital PCR experiments. *Clin Chem*. 2013;59(6):892-902.
 48. Huggett JF, Cowen S, Foy CA. Considerations for digital PCR as an accurate molecular diagnostic tool. *Clin Chem*. 2015;61(1):79-88.



Specific interactions of BCL-2 family proteins mediate sensitivity to BH3-mimetics in diffuse large B-cell lymphoma

Victoria M. Smith,^{1,2} Anna Dietz,³ Kristina Henz,³ Daniela Bruecher,³ Ross Jackson,^{1,2} Lisa Kowald,³ Sjoerd J.L. van Wijk,³ Sandrine Jayne,^{1,2} Salvador Macip,¹ Simone Fulda,^{3,4,5} Martin J.S. Dyer^{1,2} and Meike Vogler^{1,3}

¹Department of Molecular and Cell Biology, University of Leicester, Leicester, UK; ²Ernest and Helen Scott Haematological Research Institute, University of Leicester, Leicester, UK; ³Institute for Experimental Cancer Research in Pediatrics, Goethe-University, Frankfurt, Germany; ⁴German Cancer Research Centre (DKFZ), Heidelberg, Germany and ⁵German Cancer Consortium (DKTK), Partner Site Frankfurt, Germany

Haematologica 2020
Volume 105(8):2150-2163

ABSTRACT

The BCL-2-specific inhibitor, ABT-199 (venetoclax) has exhibited remarkable clinical activity in nearly all cases of chronic lymphocytic leukemia. In contrast, responses are usually much less in diffuse large B-cell lymphoma (DLBCL), despite high level expression of BCL-2 in over 40% of cases, indicating that co-expression of related anti-apoptotic BCL-2 family proteins may limit the activity of ABT-199. We have investigated the roles of BCL-2 proteins in DLBCL cells using a panel of specific BCL-2 homology 3 (BH3)-mimetics and identified subgroups of these cells that exhibited marked and specific dependency on either BCL-2, BCL-X_L or MCL-1 for survival. Dependency was associated with selective sequestration of the pro-apoptotic proteins BIM, BAX and BAK by the specific anti-apoptotic BCL-2 protein which was important for cellular survival. Sensitivity to BH3-mimetics was independent of genetic alterations involving the BCL-2 family and only partially correlated with protein expression levels. Treatment with ABT-199 displaced BAX and BIM from BCL-2, subsequently leading to BAK activation and apoptosis. In contrast, apoptosis induced by inhibiting BCL-X_L with A1331852 was associated with a displacement of both BAX and BAK from BCL-X_L and occurred independently of BIM. Finally, the MCL-1 inhibitor S63845 induced mainly BAX-dependent apoptosis mediated by a displacement of BAK, BIM and NOXA from MCL-1. In conclusion, our study indicates that in DLBCL, the heterogeneous response to BH3-mimetics is mediated by selective interactions between BAX, BAK and anti-apoptotic BCL-2 proteins.

Correspondence:

MEIKE VOGLER
m.vogler@kinderkrebsstiftung-frankfurt.de

Received: February 26, 2019.

Accepted: October 10, 2019.

Pre-published: October 10, 2019.

doi:10.3324/haematol.2019.220525

Check the online version for the most updated information on this article, online supplements, and information on authorship & disclosures: www.haematologica.org/content/105/8/2150

©2020 Ferrata Storti Foundation

Material published in Haematologica is covered by copyright. All rights are reserved to the Ferrata Storti Foundation. Use of published material is allowed under the following terms and conditions:

<https://creativecommons.org/licenses/by-nc/4.0/legalcode>.

Copies of published material are allowed for personal or internal use. Sharing published material for non-commercial purposes is subject to the following conditions:

<https://creativecommons.org/licenses/by-nc/4.0/legalcode>,

sect. 3. Reproducing and sharing published material for commercial purposes is not allowed without permission in writing from the publisher.



Introduction

Deregulated apoptosis is a key hallmark of cancer, and high expression of anti-apoptotic proteins is frequently observed in cancer cells. Apoptosis is initiated by ligation of death receptors on the cell surface or by the release of cytochrome c into the cytosol followed by formation of the apoptosome (intrinsic apoptosis). Among the most important regulators of apoptosis is the BCL-2 protein family, which consists of both pro- and anti-apoptotic proteins.¹ The pro-apoptotic BCL-2 proteins BAX and BAK are essential for the execution of intrinsic apoptosis, as they mediate the release of cytochrome c from the mitochondrial intermembrane space. The anti-apoptotic proteins (BCL-2, BCL-X_L, MCL-1, BCL-w, BCL2A1 and BCL-B) inhibit the activation of BAX and BAK, thus preventing the release of cytochrome c. BAX and BAK can be bound and inhibited directly by the anti-apoptotic BCL-2 proteins; alternatively, their activation can be inhibited by sequestration of BIM or related BCL-2 homology domain 3 (BH3)-only proteins. In this latter model, the release of BH3-only proteins from anti-apoptotic BCL-2 proteins is required in order to allow the BH3-only proteins to interact and directly activate BAX/BAK.

BCL-2 was identified as the target for the t(14;18)(q32.3;q21.3) chromosomal translocation involving the *BCL2* gene with the immunoglobulin heavy chain transcriptional enhancer in follicular lymphoma and related B-cell malignancies including diffuse large B-cell lymphoma (DLBCL).² This chromosomal translocation results in constitutive expression of BCL-2 and increased resistance to apoptosis. About 40% of DLBCL display high expression of BCL-2, not only due to t(14;18)(q32.3;q21.3) but also due to gene copy number alterations and amplifications.³ These genetic changes are associated with poor prognosis, particularly when combined with those affecting *MYC* in double-hit lymphomas.^{4,5} Apart from these genetic changes, *BCL2* is also among the most commonly mutated genes in DLBCL,⁶ with 91/393 cases reported as mutated in the COSMIC database (cancer.sanger.ac.uk/cosmic). In comparison, mutations involving MCL-1 (3/391) or BCL-X_L (0/391) are rare in DLBCL. A recent study analyzed the protein expression of BCL-2, BCL-X_L and MCL-1 in a large set of DLBCL cell lines and patients' tissues and confirmed high expression of these anti-apoptotic proteins.⁷ RNA sequencing data obtained from a large cohort of DLBCL patients (n=584) indicated high expression of all main anti-apoptotic BCL-2 proteins in DLBCL.⁸

Elevated expression of anti-apoptotic BCL-2 proteins in cancer makes these proteins promising targets for the development of novel therapeutics. The first inhibitor for clinical use, ABT-199 (venetoclax), selectively targets BCL-2 and has been approved for the treatment of chronic lymphocytic leukemia and acute myeloid leukemia.⁹⁻¹¹ Chronic lymphocytic leukemia cells display uniform sensitivity to ABT-199 and clinical responses are observed irrespective of genotype, demonstrating that the most important anti-apoptotic protein in chronic lymphocytic leukemia is BCL-2.¹²

In this study, we hypothesized that other BCL-2 family proteins, such as BCL-X_L and MCL-1, are important therapeutic targets in DLBCL. Here, for the first time directly comparing specific BH3-mimetics that target either BCL-2 (ABT-199),¹³ BCL-X_L (A1331852)¹⁴ or MCL-1 (S63845)¹⁵ in an extensive panel of DLBCL cell lines and primary cells, we identified subgroups of DLBCL that depended on individual BCL-2 family proteins for survival. Dependency was associated with the presence of pre-formed complexes of the respective anti-apoptotic BCL-2 protein with BIM, BAX and BAK, indicating that sensitive cells were highly primed and that sequestration of BAX/BAK by anti-apoptotic BCL-2 proteins was necessary for cellular survival.

Methods

Materials

All chemicals apart from ABT-199, A1331852, A1155463, A1210477 (Selleck Chemicals, Houston, TX, USA), and S63845 (ApexBio, Taiwan) were from Sigma (Deisenhofen, Germany). Most cell lines used in this study were obtained from *Deutsche Sammlung von Mikroorganismen und Zellkulturen* (DSMZ; Braunschweig, Germany) except Pfeiffer and SUDHL2 cells (American Type Culture Collection; Manassas, VA, USA), OCI-LY10 (Sandeep Dave, Duke University, Durham, NC, USA), MedB1¹⁶ (Peter Moeller, University of Ulm, Ulm, Germany) and Karpas-1106¹⁷ (Abraham Karpas, University of Cambridge,

Cambridge, UK). All cell lines were authenticated by short tandem repeat profiling and routinely tested for mycoplasma contamination. Primary patient-derived samples were obtained from patients attending the University Hospital of Leicester, UK. Local ethical approval (Leicestershire, Northamptonshire and Rutland REC06/Q2501/122) and patients' consent were obtained through the Haematological Tissue Bank of the Ernest and Helen Scott Haematological Research Institute, Leicester, UK. Peripheral blood mononuclear cells were isolated from the blood of patients presenting in leukemic phase and the CellTiterGlo assay (Promega, Mannheim, Germany) was used to assess these cells' viability.

Western blotting and immunoprecipitation

For western blotting, proteins were obtained using Tris-lysis buffer containing 1% TritonX. Western blotting was performed using the following antibodies: mouse anti-BCL-2 (M088701-2, Dako Agilent, Hamburg, Germany), rabbit anti-BCL-X_L (2762S, Cell Signaling, Beverly, MA, USA), rabbit anti-MCL-1 (ADI-AAP-240F, Enzo, Farmindale, NY, USA), rabbit anti-BIM (3183S, Cell Signaling), mouse anti-NOXA (ALX-804-408, Enzo), rabbit anti-BAK (06-536, Upstate/Merck), mouse anti-BAX (2772S, Cell Signaling) and mouse anti-GAPDH (5G4-6C5, BioTrend, Hy Test Ltd., Turku, Finland). Immunoprecipitation was performed using the following antibodies: hamster anti-BCL-2 (551051, BD Bioscience, Heidelberg, Germany), rabbit anti-BCL-X_L (ab32370, Abcam), rabbit anti-MCL-1 (ADI-AAP-240F, Enzo), mouse anti-BAX (610983, BD Bioscience), and rabbit anti-BAK (ab32371, Abcam). Antibodies were crosslinked to protein G dynabeads (Invitrogen, Karlsruhe, Germany). CHAPS containing lysates were incubated overnight at 4°C with the antibody-protein G complexes before the precipitates were washed in lysis buffer and analyzed by western blotting.

BH3-profiling

Cells were gently permeabilized with 0.0025% digitonin before exposure to 0.1, 1 or 10 μM of synthetic peptides (BIM, BAD, XXa1_Y4eK¹⁸). Loss of mitochondrial membrane potential was measured using 1 μM JC-1 via a Hidex Sense plate reader as described previously.¹⁹ Results were normalized to those of dimethylsulfoxide (DMSO) and carbonyl cyanide-4-(trifluoromethoxy)phenylhydrazone (FCCP) controls.

Genetic modifications

For silencing of individual genes, cells were electroporated with a neon transfection system (ThermoFisher) using two pulses of 20 ms at 1200 V. The following silencer select short interfering (si)RNA (ThermoFisher) were used at 100 nM: BAX (#1s1888, #3s1890), BAK (#1s1880, #2s1881), BIM (#1s195011, #2s195012, #3s223065), BCL-X_L (s1921), MCL-1 (s8583), and NOXA (s10709, s10710). CRISPR/Cas9 engineering was done as described previously.²⁰ Briefly, three guide (g)RNA against human BAK (GGTAGACGTGTAGGGCCAGA, TCACCTGC-TAGGTTGCAG, AAGACCCTTACCAGAAGCAG) or against green fluorescent protein as a non-human target (NHT) (GGAGCGCACCATCTTCTTCA, GCCACAAGTTCAGCGT-GTC, GGGCGAGGAGCTGTTACCG) were cloned in pLentiCRISPRv2 (Addgene # 52961). Lentiviral particles were generated by co-transfecting pLenti-CRISPRv2 NHT and BAK with pPAX2 (Addgene # 12260) and pMD2.G (Addgene # 12259) in HEK293T cells and used to transduce U2946 or SUDHL8 target cells using spin transduction followed by puromycin selection and isolation of BAK-deleted single clones using limited dilution. The BAK expression status was assessed using western blotting.

Results

BCL-2, BCL-X_L and MCL-1 are important therapeutic targets in diffuse large B-cell lymphoma

To investigate the roles of the main anti-apoptotic BCL-2 proteins in DLBCL, we assessed the effects of selective BH3-mimetics in DLBCL cells. We focused on commercially available inhibitors that target BCL-2 (ABT-199), BCL-X_L (A1331852, A1155463) or MCL-1 (A1210477,²¹ S63845). Primary cells isolated from patients' tissues were exposed to different concentrations of BH3-mimetics before analysis of cell viability using a CellTiterGlo Assay (Figure 1A). The direct comparison of ABT-199, A1331852 and S63845 revealed that the response to BH3-mimetics was highly heterogeneous, with three of seven samples (#1, #2, and #3) responding to low nanomolar concentrations of S63845, sample #4 responding best to

ABT-199, and samples #5, #6 and #7 being more resistant to all three BH3-mimetics. Notably, sample #3 displayed a better response to A1331852 than to ABT-199, indicating that although none of these primary samples displayed the highest sensitivity to A1331852, all three main anti-apoptotic BCL-2 proteins may be relevant therapeutic targets in DLBCL.

As primary patient-derived DLBCL cells are limited and freshly isolated malignant B cells rapidly lose viability *ex vivo*, we continued our investigations in a panel of 18 DLBCL cell lines comprising the main subtypes of DLBCL defined by gene expression profiling,²² namely activated B-cell, germinal center and primary mediastinal B-cell lymphoma-like cells (Table 1). In addition, based on their mutation/translocation signature derived from public databases, we characterized the cell lines according to their genetic drivers into MCD (*MYD88* and *CD79b*

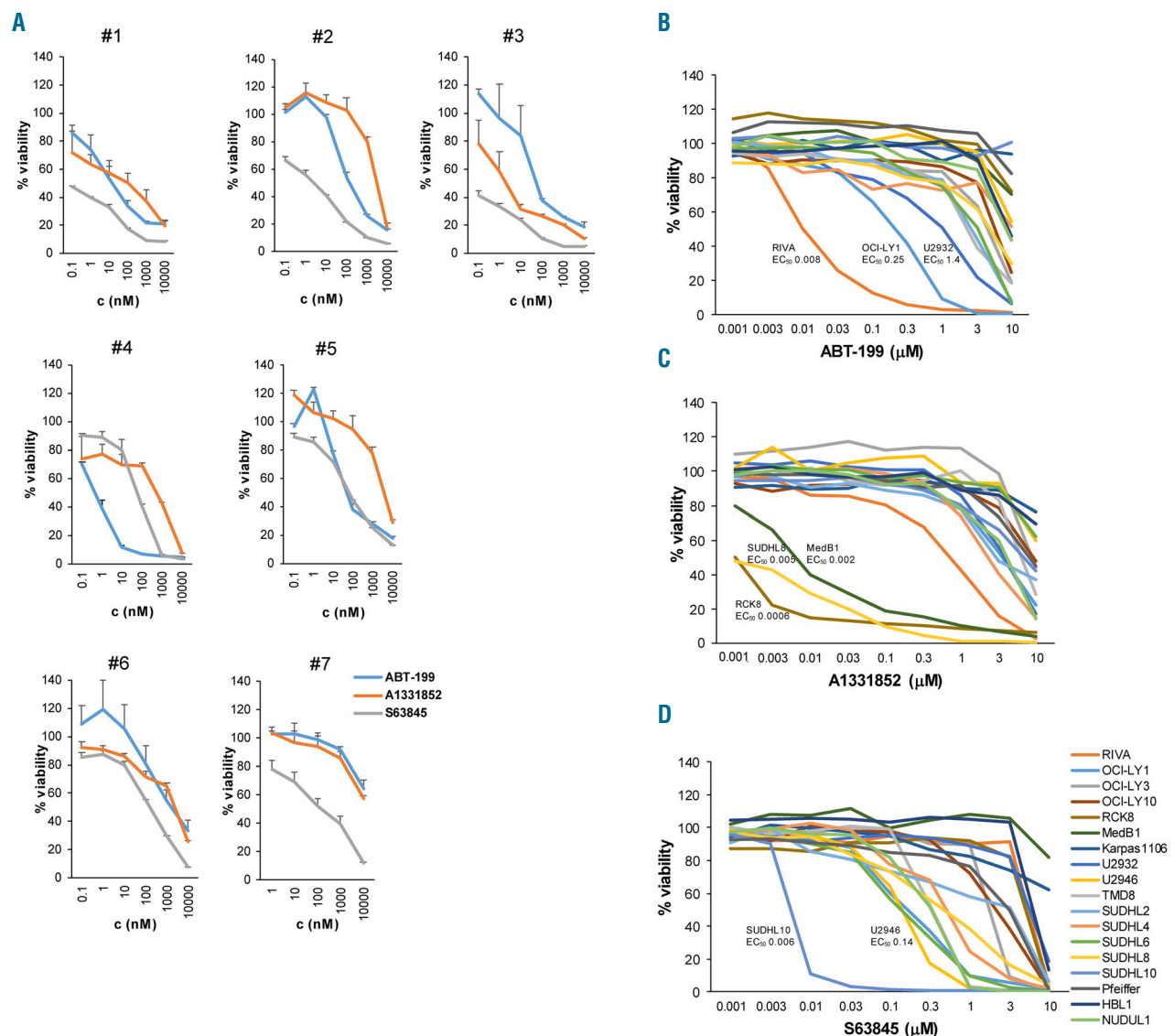


Figure 1. Diffuse large B-cell lymphoma cells display a heterogeneous sensitivity to selective BH3-mimetics. (A) Primary cells isolated from patients' tissues were incubated with different concentrations of ABT-199, A1331852 or S63845 for 24 h before analysis of cell viability using CellTiterGlo. Experiments were performed in triplicate and data shown are the mean and standard deviation (SD) for each individual sample (n=7). (B-D) Diffuse large B-cell lymphoma cell lines were exposed to different concentrations of ABT-199 (B), A1331852 (C) or S63845 (D) before analysis of cell viability using CellTiterGlo at 72 h. Data shown are the mean and SD (n=4-6). Half maximal effective concentration (EC₅₀) values, as displayed in Table 1, are indicated for highly sensitive cell lines.

Table 1. Characteristics of the cell lines.

Cell line	Gene expr. subtype	Genetic driver subtype	Driver mutations	Genetic modifications Alterations of BCL2 genes	BCL2 family mutations	Targeting BCL-2 ABT-199 EC ₅₀	Targeting BCL-XL A1331852 EC ₅₀ A1154463 EC ₅₀	Targeting MCL-1 S63845 EC ₅₀ A1210477 EC ₅₀	Original ref.	Mutation ref.
RIVA/Ri-1	ABC	Other ABC		BCL2 amp, PMAIP1 amp		0,008	1,127 7,500	5,500 >10	40	31
U2932	ABC	Other ABC		BCL2 amp, PMAIP1 amp		1,439	4,520 ND	5,260 5,466	41	31
OCL-LY1	GC	EZB	EZH2, CREBBP, KMT2D	t(14;18)	BCL2	0,245	6,0390 ND	0,170 >10	42	Cosmic
SUDHL4	GC	EZB	EZH2	t(14;18)	BCL2	5,000	2,224 ND	0,470 >10	43	Cosmic
OCL-LY10	ABC	MCD	CARD11, CD79a, MYD88		BCL2 (silent)	5,625	5,740 ND	2,320 >10	42	CCLL
RC-K8	GC	BN2	BCL6 translocation, RELN, TNFAIP3, SPEN			>10	0,0006 0,005	4,870 >10	44	Cosmic
SUDHL8	GC	Other GC	KMT2D, CREBBP, EP300, SOCS1			6,170	0,005 0,012	0,530 >10	43	Cosmic
MedB1	PMBL	Other GC	SOCS1			>10	0,002 0,067	>10 >10	16	Cosmic
SUDHL6	GC	EZB	EZH2, KMT2D, CREBBP, RELN	t(14;18)	BCL2	3,016	>10 >10	0,160 >10	43	Cosmic
TMD8	ABC	MCD	CD79b, MYD88, PIM1			1,635	3,598 >10	0,330 4,253	45	Unpublished
NU-DUL-1	GC	Other GC	KMT2D			9,846	3,603 ND	0,320 6,973	46	Cosmic
U2946	GC	Other GC		MCL1 amp		>10	>10 ND	0,140 >10	47	27
SUDHL10	GC	EZB	EZH2, PTEN, EP300	t(14;18)		>10	>10 >10	0,006 1,723	43	Cosmic
Karpas-1106	PMBL	EZB	EZH2, KMT2D, TNFAIP3, NFKB1E, RELT			>10	>10 ND	>10 >10	17	Cosmic
SUDHL2	ABC	BN2	TNFAIP3, MYD88, EP300			2,740	1,824 ND	not calc 3,666	48	Cosmic
HBL-1	ABC	MCD	CD79b, MYD88			8,742	>10 4,000	5,900 >10	49	Cosmic
OCL-LY3	ABC	MCD	CARD11, MYD88, HLA-A, IRF4, PIM1, PRDM1	BCL2 amp	BCL2 (silent)	4,127	6,653 ND	1,850 >10	42	CCLL
Pfeiffer	GC	EZB	EZH2, KMT2D	t(14;18)	BIM, BCL2 (silent)	>10	>10 ND	3,430 >10	50	Cosmic

Characteristics of diffuse large B-cell lymphoma cell (DLBCL) lines are displayed including the subtype of DLBCL and genetic modifications affecting the BCL2 proteins. The EC₅₀ values for the five BH3-mimetics used in this study are shown as calculated from the CellTiterGlo data displayed in Figure 1B-D and *Online Supplementary Figure S1A, B* (in μ M). ABC: activated B-cell; GC: germinal center B cell; PMBL: primary mediastinal B-cell-Hike; MCD: MYD88 and CD79b mutations; BN2: BCL6 fusion and NOTCH2 mutations; EZB: EZH2 mutations and BCL2 translocations; ref: reference; EC₅₀: half maximal effective concentration.

mutations), BN2 (*BCL6* fusion and *NOTCH2* mutations), N1 (*NOTCH1* mutations) and EZB (*EZH2* mutations and *BCL2* translocations) as recently described.⁸ An initial comparison of different selective BH3-mimetics indicated that A1331852 was more potent than A1155463, and S63845 displayed significantly higher potency than A1210477 (Figure 1B-D, *Online Supplementary Figure S1*, Table 1).

DLBCL cell lines displayed highly heterogeneous responses to BH3-mimetics (Figure 1B-D). RIVA, U2932 and OCI-LY1 cells responded primarily to ABT-199, indicating a dependency on BCL-2 for survival. In contrast, RCK8, SUDHL8 and MedB1 cells were highly sensitive to A1331852, demonstrating BCL- X_L dependency. Notably, these three cell lines displayed sensitivity to low nanomolar/picomolar concentrations of A1331852, with half maximal effective concentrations (EC_{50}) of 0.0006, 0.005 and 0.002 μ M, respectively, highlighting its potency in cellular systems. Susceptibility to S63845 was more homogeneous than that to ABT-199 or A1331852, with ten of the 18 cell lines responding to less than 3 μ M. The most sensitive cell line in our panel was SUDHL10 (EC_{50} 0.006 μ M), which was previously described to be resistant to BH3-mimetics.²³

Most cell lines were primarily sensitive to one specific BH3-mimetic, indicating firstly that in each cell line one particular BCL-2 family protein was functionally most dominant and, secondly and unexpectedly, that expression of the other anti-apoptotic BCL-2 proteins could not prevent induction of apoptosis. However, four cell lines (OCI-LY1, RIVA, SUDHL8 and TMD8) were sensitive to multiple inhibitors. Notably, five of the 18 cell lines did not respond to any inhibitor at submicromolar concentrations (OCI-LY10, Pfeiffer, OCI-LY3, Karpas-1106 and HBL1) (Table 1).

BH3-profiling using XXa1_Y4eK may predict sensitivity to A1331852

To confirm that BCL- X_L and MCL-1 are important therapeutic targets in DLBCL, we utilized a genetic approach to silence BCL- X_L or MCL-1. Knockdown of BCL- X_L by siRNA was sufficient to induce apoptosis in RCK8, SUDHL8 and MedB1 cells but not in the BCL-2-dependent RIVA or U2932 cells, whereas knockdown of MCL-1 was sufficient to induce apoptosis in SUDHL10, TMD8 and U2946 cells but not in BCL- X_L -dependent MedB1 cells, which correlated with susceptibility to A1331852 and S63845, respectively (Figure 2A-D). BH3-profiling may serve as a surrogate assay to investigate priming in tumor samples.²⁴ To examine whether BH3-profiling may predict the sensitivity to BH3-mimetics in DLBCL, permeabilized cells were exposed to BH3-peptides from BIM, which binds to all anti-apoptotic BCL-2 proteins, BAD, which binds to BCL-2 and BCL- X_L , and the engineered peptide XXa1_Y4eK, which binds with high affinity selectively to BCL- X_L .¹⁸ All tested cell lines displayed a dose-dependency towards BIM (Figure 2E). Both RIVA and RCK8 cells also responded to BAD and XXa1_Y4eK, congruent with a dependency on BCL-2 and/or BCL- X_L for survival. In contrast, the MCL-1-dependent cell line SUDHL10 did not respond to BAD or XXa1_Y4eK, as observed in previous studies.²⁵ Next, we asked whether the response to XXa1_Y4eK may correlate with the sensitivity to A1331852 in a larger panel of cell lines. The EC_{50} for A1331852 displayed a significant correlation with

the response to XXa1_Y4eK ($P < 0.001$), indicating that BH3-profiling could serve as a biomarker to predict responses to BH3-mimetics provided that specific and potent peptides, such as XXa1_Y4eK, are available (Figure 2F).

BCL-2 protein expression was highly variable but only partially associated with sensitivity to BH3-mimetics

Next, we aimed to understand the heterogeneity in the response to BH3-mimetics in the panel of DLBCL cell lines. Western blot analysis revealed that the expression of BCL-2 proteins was highly variable (Figure 2G, *Online Supplementary Figure S2A*). Several of the cell lines have genetic alterations involving *BCL2* e.g. t(14;18)(q32.3;q21.3) chromosomal translocation or gene amplifications (Table 1). Quantification of protein expression indicated that gene alterations of *BCL2* correlated partially with high protein expression (*Online Supplementary Figure S2B*). Although there was a tendency for cells with genetic alterations of *BCL2* to be more sensitive to ABT-199, as reported previously,²⁵ this difference was not statistically significant (*Online Supplementary Figure S2C*). Of note, although SUDHL4 and SUDHL6 cells are reported to contain missense mutations of *BCL2*, which may prevent antibody recognition,²⁶ BCL-2 protein expression was detectable with the antibody used in our study.

The highest expression of BCL- X_L was detected in RCK8, SUDHL8 and MedB1 cells, which were most sensitive to A1331852. Expression of MCL-1 was more homogeneous, with all cell lines expressing detectable MCL-1 protein and the highest expression being in the *MCL1* amplified U2946 cells.²⁷ The pore-forming BCL-2 proteins BAK and BAX were expressed in all cell lines while BH3-only protein expression was highly variable (Figure 2G).

To test whether susceptibility to BH3-mimetics was associated with the levels of expression of their targeted BCL-2 proteins, the EC_{50} values were correlated with BCL-2 protein expression. Linear regression analysis showed a significant correlation between the response to ABT-199 and expression of BCL-2, but this appeared to be driven by the very high or very low BCL-2-expressing cell lines. Sensitivity to ABT-199 also correlated significantly with the ratio of BCL-2 to MCL-1 expression (*Online Supplementary Figure S3A*). Although the cell lines with highest sensitivity to A1331852 expressed BCL- X_L strongly, the correlation of BCL- X_L expression and sensitivity to A1331852 was not statistically significant, which may be explained by several cell lines expressing BCL- X_L strongly but nevertheless being resistant to A1331852 (HBL1, Pfeiffer and Karpas-1106). Susceptibility to A1331852 was more strongly correlated with the ratio of BCL- X_L expression to a combined expression of the other anti-apoptotic proteins BCL-2 and MCL-1, although the resistant Pfeiffer and Karpas-1106 cells still displayed a high ratio and made this correlation weak ($R^2=0.23$) (*Online Supplementary Figure S3B*). Sensitivity to S63845 did not correlate with expression of its target MCL-1 (*Online Supplementary Figure S3C*) but, as described previously,¹⁵ did to some extent inversely correlate with expression of BCL- X_L . In addition, we found a significant correlation of S63845 sensitivity with the ratio of MCL-1 to BIM expression.

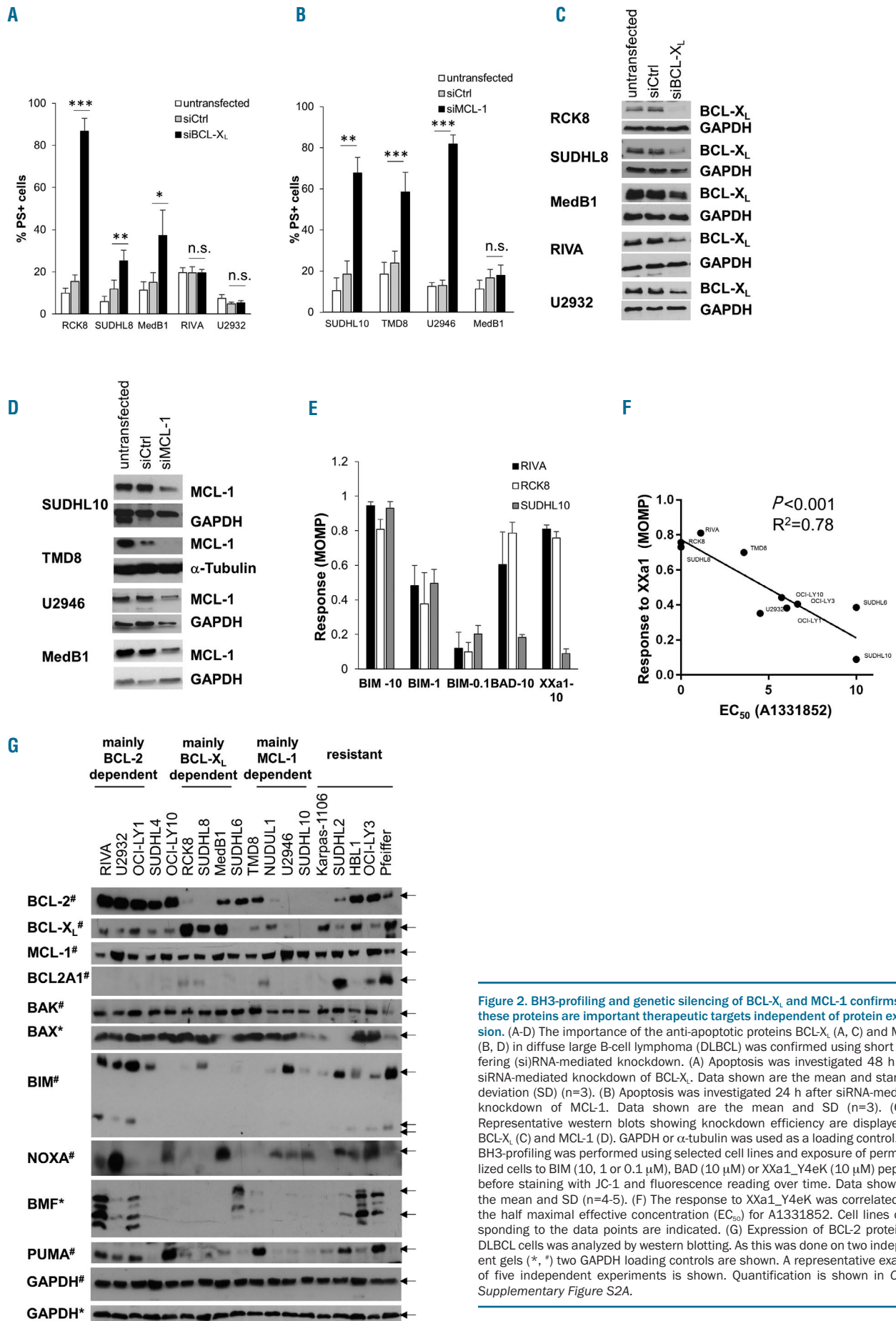


Figure 2. BH3-profiling and genetic silencing of BCL-X_L and MCL-1 confirms that these proteins are important therapeutic targets independent of protein expression. (A-D) The importance of the anti-apoptotic proteins BCL-X_L (A, C) and MCL-1 (B, D) in diffuse large B-cell lymphoma (DLBCL) was confirmed using short interfering (si)RNA-mediated knockdown. (A) Apoptosis was investigated 48 h after siRNA-mediated knockdown of BCL-X_L. Data shown are the mean and standard deviation (SD) (n=3). (B) Apoptosis was investigated 24 h after siRNA-mediated knockdown of MCL-1. Data shown are the mean and SD (n=3). (C, D) Representative western blots showing knockdown efficiency are displayed for BCL-X_L (C) and MCL-1 (D). GAPDH or α -tubulin was used as a loading control. (E, F) BH3-profiling was performed using selected cell lines and exposure of permeabilized cells to BIM (10, 1 or 0.1 μ M), BAD (10 μ M) or XXa1_Y4eK (10 μ M) peptides before staining with JC-1 and fluorescence reading over time. Data shown are the mean and SD (n=4-5). (F) The response to XXa1_Y4eK was correlated with the half maximal effective concentration (EC₅₀) for A1331852. Cell lines corresponding to the data points are indicated. (G) Expression of BCL-2 proteins in DLBCL cells was analyzed by western blotting. As this was done on two independent gels (*, *) two GAPDH loading controls are shown. A representative example of five independent experiments is shown. Quantification is shown in *Online Supplementary Figure S2A*.

Sensitivity to BH3-mimetics correlated with sequestration of pro-apoptotic BCL-2 proteins

To interrogate whether the interactions of anti- and pro-apoptotic BCL-2 proteins might influence susceptibility to BH3-mimetics, we selected ten representative cell lines and performed immunoprecipitation of the main anti-apoptotic proteins (Figure 3). In the BCL-2-dependent cell lines (RIVA, U2932 and OCI-LY1), BIM was highly bound to BCL-2, with no detectable binding of BIM to BCL-X_L or MCL-1, despite high protein expression of BCL-X_L and MCL-1. In contrast, BIM was highly bound by MCL-1 in the MCL-1-dependent cell lines SUDHL10 and U2946. These two cell lines expressed low levels of BCL-2 and BCL-X_L, which may explain why BIM was bound to MCL-1. In the BCL-X_L-dependent SUDHL8 and RCK8 cells, BIM expression was comparatively low, and some BIM appeared bound to BCL-X_L but not to BCL-2 or MCL-1. Collectively, these data suggest a relationship between the sequestration of BIM by the different anti-apoptotic BCL-2 proteins and a dependency on the respective anti-apoptotic BCL-2 protein for survival. However, the resistant cells OCI-LY3 and Pfeiffer, which did not respond to any BH3-mimetic, also displayed binding of BIM to BCL-2 and/or BCL-X_L and MCL-1. Pfeiffer cells have been reported to contain a missense mutation in BIM (S10C), but this mutation did not prevent binding of BIM to its anti-apoptotic binding partners. In line with its published binding profile,²⁸ the BH3-only protein NOXA was exclusively bound by MCL-1 but not by BCL-2 or BCL-X_L in all cell lines.

Besides binding BH3-only proteins, the anti-apoptotic BCL-2 proteins can also sequester BAX and BAK.²⁹ Intriguingly, we found that both BAX and BAK are bound by the anti-apoptotic BCL-2 proteins, highlighting that in DLBCL the anti-apoptotic BCL-2 proteins may act by

inhibiting already partially activated BAX and BAK, in which the BH3-domain is exposed and accessible for interaction with the anti-apoptotic BCL-2 proteins.³⁰ Thus, BAX was sequestered by BCL-2 predominantly in the BCL-2-dependent cell lines, and predominantly sequestered by BCL-X_L in the BCL-X_L-dependent cell lines, indicating that the binding of BAX by the respective anti-apoptotic BCL-2 protein was associated with sensitivity to specific inhibitors (Figure 3). Besides BAX, BAK was also bound by BCL-X_L in the BCL-X_L-dependent cell lines and by MCL-1 in the MCL-1-dependent cell lines. Taken together, our investigations show that sensitive DLBCL cell lines were highly primed and that direct sequestration of BAX and BAK by the anti-apoptotic BCL-2 proteins could be the last step preventing apoptosis in these cells.

BH3-mimetics induced cell death by displacing and activating BAX and BAK

Next, we asked how BH3-mimetics induced cell death in DLBCL cell lines. Exposure to BH3-mimetics induced caspase-3 cleavage, caspase-dependent phosphatidylserine externalization and loss of mitochondrial membrane potential (*Online Supplementary Figure S4*). The activation and oligomerization of BAX and/or BAK are key events in the intrinsic apoptotic pathway and require conformational changes. Treatment with BH3-mimetics induced conformational changes associated with activation and oligomerization of BAX and BAK in all sensitive cell lines (*Online Supplementary Figure S5A-C*). Of note, some active BAK was detectable in untreated cells, but the amount of constitutively active BAK did not correlate with sensitivity (*Online Supplementary Figure S5D*).

To investigate how BH3-mimetics induced the activation of BAX and BAK we interrogated how the interac-

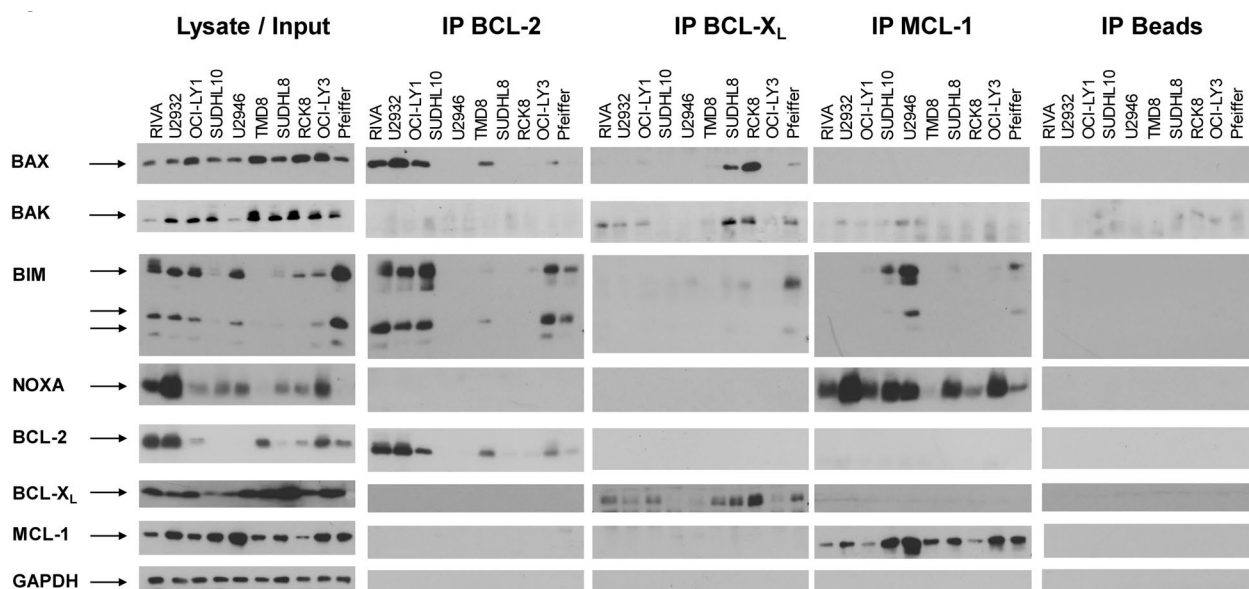


Figure 3. Priming correlates with sensitivity to BH3-mimetics. The interaction of anti- and pro-apoptotic BCL-2 proteins was investigated in a selection of ten cell lines with varying sensitivities to BH3-mimetics. Immunoprecipitation of BCL-2, BCL-X_L and MCL-1 was performed in untreated cell lysates followed by analysis of binding of pro-apoptotic BCL-2 proteins (BIM, NOXA, BAX and BAK) using Western blotting. Protein G beads without primary antibody were used to control for unspecific binding. Staining with BCL-2, BCL-X_L, MCL-1 and GAPDH was performed to demonstrate efficient immunoprecipitation and equal protein loading, respectively. Representative western blots of two independent experiments are shown.

tion of pro- and anti-apoptotic proteins changed upon exposure to BH3-mimetics (Figure 4). In the BCL-2-dependent cell lines RIVA and U2932, the recently described displacement of BIM from BCL-2³¹ was difficult to detect but some reduction in binding of BIM to BCL-2 was found in U2932 cells. In RIVA cells, a minor amount of BIM appeared bound to BCL-X_L following treatment with ABT-199, which may indicate a low level of BIM displacement from BCL-2. In both cell lines, less BAX was bound to BCL-2 following treatment with ABT-199, indicating a direct displacement of BAX from BCL-2 (Figure 4A). Similarly, in the BCL-X_L-dependent cell lines, BIM binding to BCL-X_L was reduced upon treatment with A1331852. Strikingly, both BAX and BAK were less bound by BCL-X_L upon A1331852 treatment, supporting the hypothesis that BH3-mimetics can directly displace BAX and BAK (Figure 4B). Treatment with S63845 in the

MCL-1-dependent cell lines resulted in less binding of BIM and BAK to MCL-1 (Figure 4C). In summary, these studies demonstrate that treatment with BH3-mimetics resulted in reduced binding of pro-apoptotic BCL-2 proteins.

The displacement of BIM could be functionally important for apoptosis induction, as released BIM could initiate apoptosis by binding directly to BAX and BAK and activating them. To investigate whether BIM is necessary, we performed siRNA-mediated knockdown of BIM followed by treatment with BH3-mimetics. Combined use of two distinct siRNA partially inhibited BH3-mimetic induced cell death in a treatment- and cell-line-dependent manner, as BIM knockdown reduced cell death in RIVA, SUDHL10 and to a lesser extent in U2946 cells (Figure 5A-C, *Online Supplementary Figure S6*), although efficient knockdown was achieved in all cell lines (Figure 5D). As

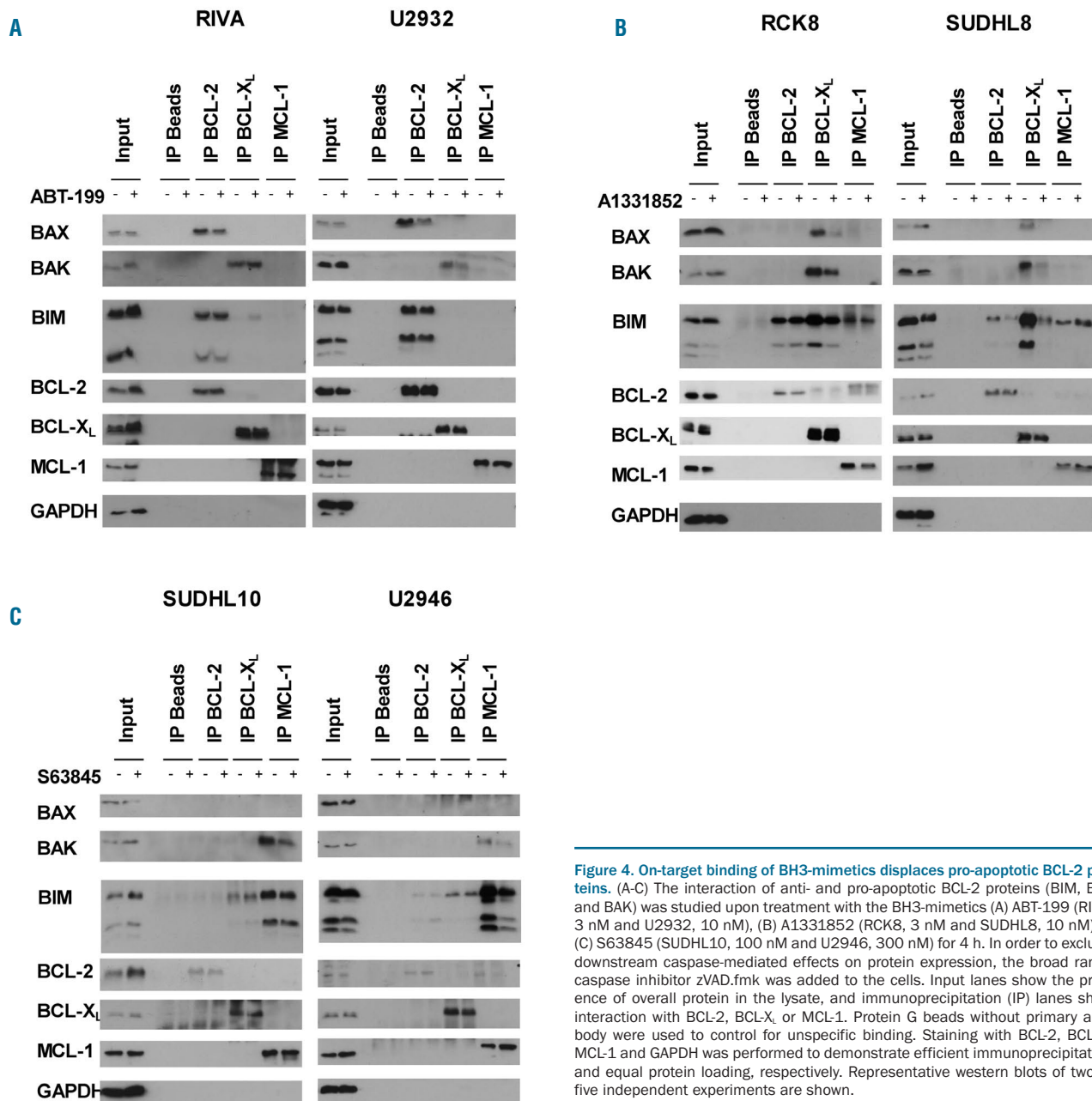


Figure 4. On-target binding of BH3-mimetics displaces pro-apoptotic BCL-2 proteins. (A-C) The interaction of anti- and pro-apoptotic BCL-2 proteins (BIM, BAX and BAK) was studied upon treatment with the BH3-mimetics (A) ABT-199 (RIVA, 3 nM and U2932, 10 nM), (B) A1331852 (RCK8, 3 nM and SUDHL8, 10 nM) or (C) S63845 (SUDHL10, 100 nM and U2946, 300 nM) for 4 h. In order to exclude downstream caspase-mediated effects on protein expression, the broad range caspase inhibitor zVAD.fmk was added to the cells. Input lanes show the presence of overall protein in the lysate, and immunoprecipitation (IP) lanes show interaction with BCL-2, BCL-X_L or MCL-1. Protein G beads without primary antibody were used to control for unspecific binding. Staining with BCL-2, BCL-X_L, MCL-1 and GAPDH was performed to demonstrate efficient immunoprecipitation and equal protein loading, respectively. Representative western blots of two to five independent experiments are shown.

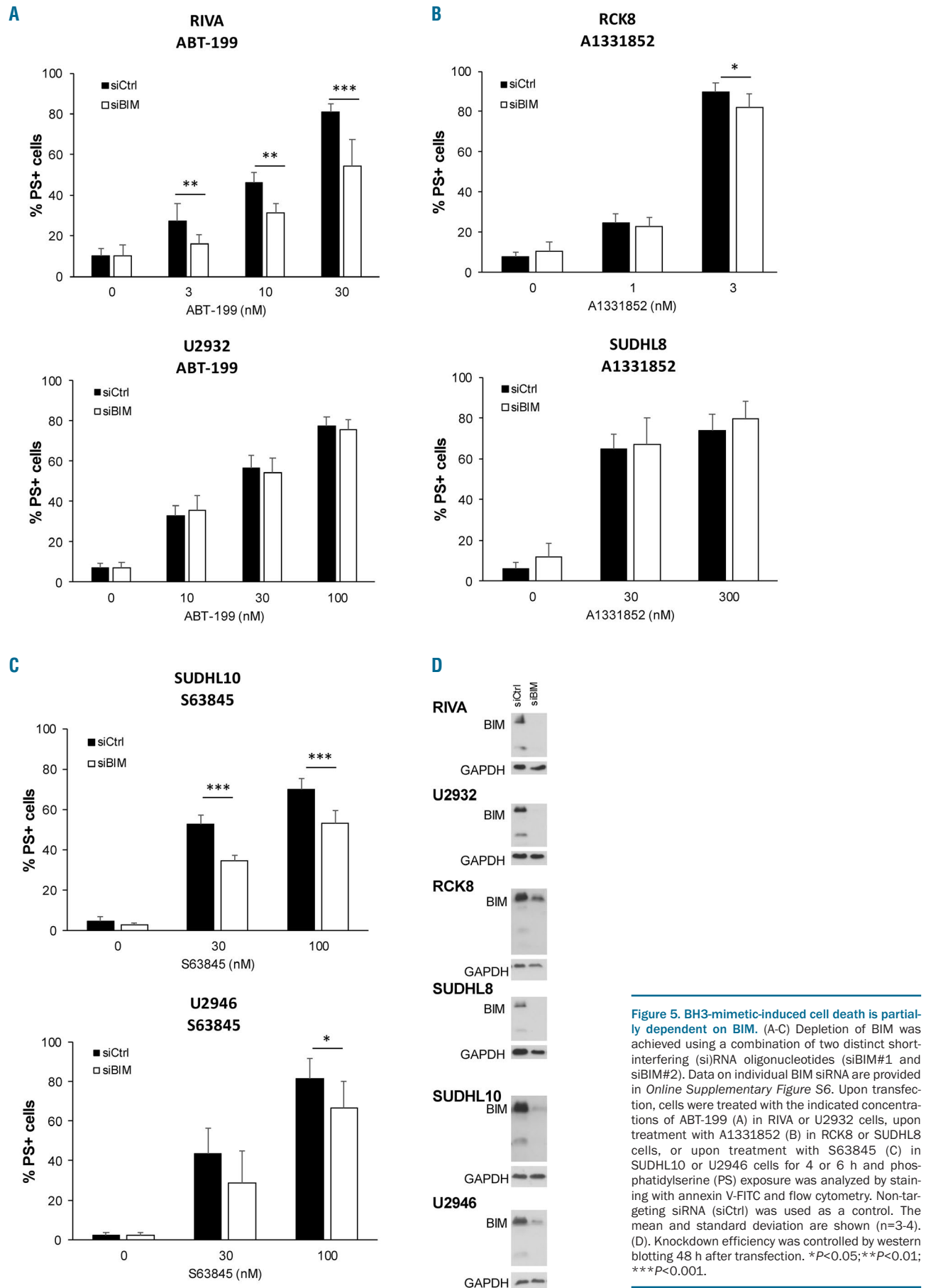


Figure 5. BH3-mimetic-induced cell death is partially dependent on BIM. (A-C) Depletion of BIM was achieved using a combination of two distinct short-interfering (si)RNA oligonucleotides (siBIM#1 and siBIM#2). Data on individual BIM siRNA are provided in *Online Supplementary Figure S6*. Upon transfection, cells were treated with the indicated concentrations of ABT-199 (A) in RIVA or U2932 cells, upon treatment with A1331852 (B) in RCK8 or SUDHL8 cells, or upon treatment with S63845 (C) in SUDHL10 or U2946 cells for 4 or 6 h and phosphatidylserine (PS) exposure was analyzed by staining with annexin V-FITC and flow cytometry. Non-targeting siRNA (siCtrl) was used as a control. The mean and standard deviation are shown (n=3-4). (D). Knockdown efficiency was controlled by western blotting 48 h after transfection. * $P < 0.05$; ** $P < 0.01$; *** $P < 0.001$.

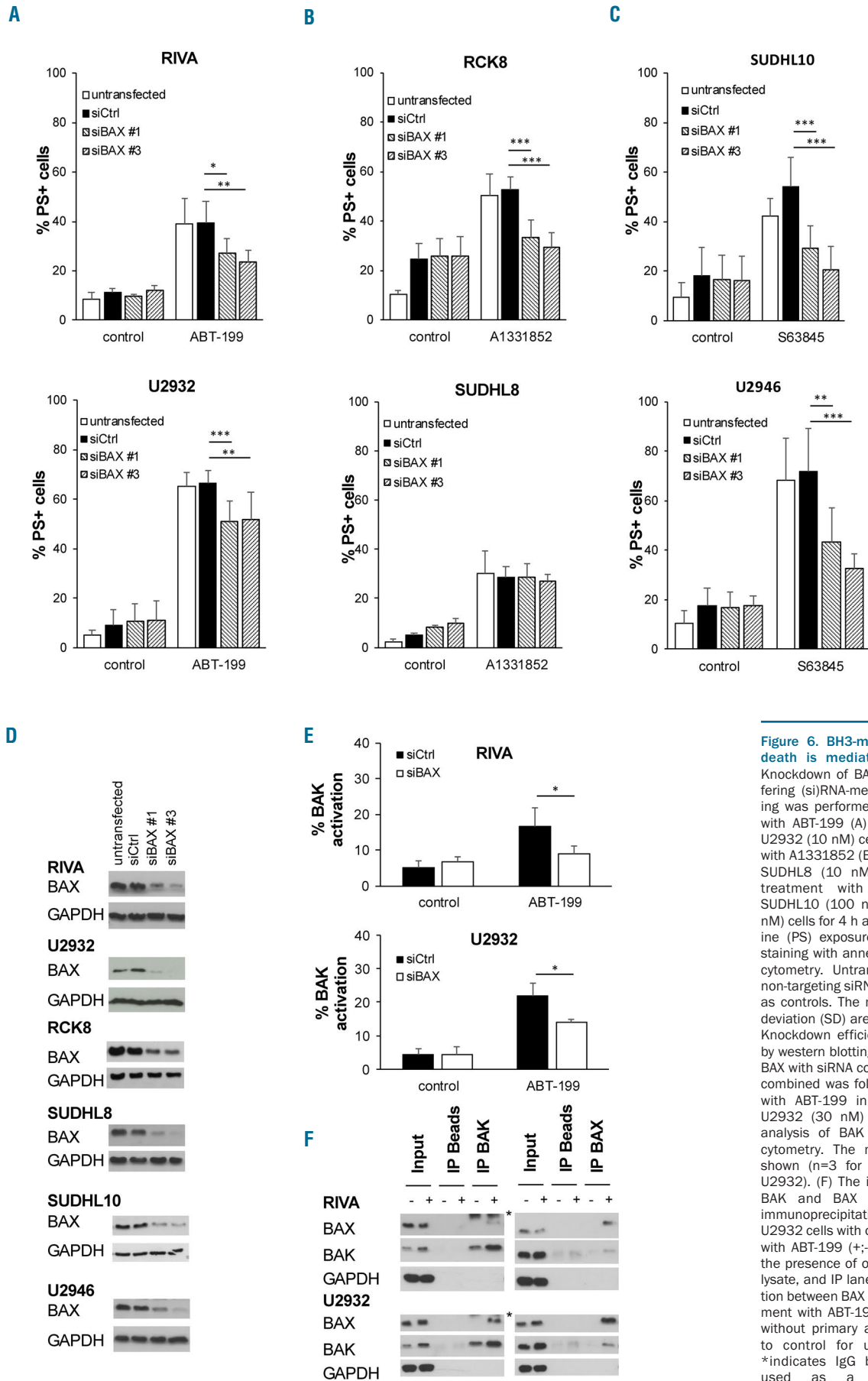


Figure 6. BH3-mimetic-induced cell death is mediated by BAX.

(A-D) Knockdown of BAX using short-interfering (si)RNA-mediated gene silencing was performed before treatment with ABT-199 (A) in RIVA (3 nM) or U2932 (10 nM) cells, upon treatment with A1331852 (B) in RCK8 (3 nM) or SUDHL8 (10 nM) cells, and upon treatment with S63845 (C) in SUDHL10 (100 nM) or U2946 (300 nM) cells for 4 h and phosphatidylserine (PS) exposure was analyzed by staining with annexin V-FITC and flow cytometry. Untransfected cells and non-targeting siRNA (siCtrl) were used as controls. The mean and standard deviation (SD) are shown (n=3-4). (D) Knockdown efficiency was assessed by western blotting. (E) Knockdown of BAX with siRNA constructs #1 and #3 combined was followed by treatment with ABT-199 in RIVA (10 nM) or U2932 (30 nM) cells for 4 h and analysis of BAK activation by flow cytometry. The mean and SD are shown (n=3 for RIVA and n=2 for U2932). (F) The interaction between BAK and BAX was assessed by immunoprecipitation (IP) in RIVA or U2932 cells with or without treatment with ABT-199 (+;-). Input lanes show the presence of overall protein in the lysate, and IP lanes show the interaction between BAX and BAK upon treatment with ABT-199. Protein G beads without primary antibody were used to control for unspecific binding. *indicates IgG band. GAPDH was used as a loading control. *P<0.05; **P<0.01; ***P<0.001.

RIVA cells also expressed high levels of the BH3-only protein BMF we asked whether BMF could be functionally important, but silencing of BMF did not affect ABT-199-induced apoptosis (*Online Supplementary Figure S7*).

BAX and BAK were required to mediate ABT-199-induced apoptosis

Next, we explored the role of BAX in BH3-mimetic-induced cell death. Silencing of BAX using siRNA indicated that BAX was essential for the cell death induced by BH3-mimetics, as cell death was significantly reduced in RIVA, U2932, RCK8, SUDHL10 and U2946 cells (Figure 6A-D). In contrast, knockdown of BAK only reduced apoptosis upon treatment with ABT-199 but not upon treatment with A1331852 or S63845, highlighting a prominent role for BAK only in ABT-199-induced apoptosis (*Online Supplementary Figure S8*).

We also investigated how BAK was involved in ABT-199-induced apoptosis. As no direct inhibition of BAK by BCL-2 was observed, we hypothesized that BAX inhibition by BCL-2 is the initial target of ABT-199, and that once BAX is released, BAK is also activated and accelerates cell death. To test this hypothesis, the activation of BAK was assessed upon silencing of BAX and treatment with ABT-199. In both RIVA and U2932 cells, silencing of BAX resulted in significantly less active BAK induced by ABT-199, suggesting that BAX contributed to activation of BAK (Figure 6E). To investigate whether BAX could directly activate BAK, the interaction between BAK and BAX was investigated. Treatment with ABT-199 induced complex formation between BAX and BAK in both RIVA and U2932 cells (Figure 6F).

BAX rather than BAK is functionally required for A1331852- or S63845-induced apoptosis

To exclude that the absence of an influence of BAK silencing on A1331852- or S63845-induced apoptosis may be caused by insufficient knockdown, we performed genetic deletion of BAK using CRISPR/Cas9. Deletion of BAK in SUDHL8 cells had only a minor effect on A1331852-induced cell death as compared to cells transfected with NHT control gRNA (*Online Supplementary Figure S9A, B*). To investigate whether BAX could be activated in the absence of BAK, BAX activation was quantified upon treatment with A1331852 using a conformation-specific antibody and flow cytometry. Although the deletion of BAK had a minor influence on the activation of BAX, BAX could clearly still be activated even though BAK was deleted (*Online Supplementary Figure S9C*).

To interrogate the role of BAK in S63845-induced apoptosis, BAK was deleted in U2946 cells. In contrast to the data obtained by siRNA-mediated knockdown, genetic deletion of BAK had a significant influence on S63845-induced apoptosis in all BAK-deleted clones investigated (Figure 7A). However, S63845-induced apoptosis was not completely inhibited, suggesting that BAX may play a prominent role also upon S63845 treatment. To confirm that S63845-mediated apoptosis involved BAX, knockdown of BAX was performed in BAK-deleted cells (Figure 7B). Knockdown of BAX by siRNA had a stronger influence than BAK deletion on S63845-induced apoptosis. Combined deletion of BAK and depletion of BAX resulted in complete inhibition of S63845-induced apoptosis (Figure 7C). To investigate how BAX may be activated upon inhibition of MCL-1, we first asked whether BAK

was essential in activating BAX. Analysis of BAX activation in BAK-deleted cells indicated that BAK may be involved in activating BAX, as BAX activation was significantly reduced in BAK-deleted cells. However, some active BAX was still present in BAK-deleted cells, indicating that other factors may be involved in activating BAX. To explore a role of the BH3-only proteins BIM and NOXA, siRNA-mediated knockdown of BIM and NOXA was performed in BAK-deleted cells. In line with the minor reduction of S63845-induced apoptosis by BIM knockdown (Figure 5C), BIM knockdown also reduced S63845-induced apoptosis in NHT- or BAK-deleted U2946 cells (Figure 7E, F). In addition to BIM, NOXA may also be involved in S63845-induced cell death, as knockdown of NOXA partially reduced S63845-induced apoptosis (Figure 7G,H). These data indicate that NOXA may participate in activating BAX upon S63845 treatment. To explore how NOXA may activate BAK we next investigated the binding of NOXA to MCL-1 and observed a prominent displacement of NOXA from MCL-1 by S63845 (Figure 7I). Taken together, these data indicate that BH3-only proteins displaced from MCL-1 by S63845 may contribute to an activation of BAX which primarily mediates S63845-induced apoptosis.

Discussion

By investigating the response to selective BH3-mimetics we have identified subgroups of DLBCL cells that depend on either BCL-2, BCL-X_i or MCL-1 for survival. Our side-by-side comparison of selective BH3-mimetics targeting the main anti-apoptotic proteins suggests that BCL-2, BCL-X_i and MCL-1 are all important therapeutic targets in DLBCL. However, we have not investigated the role of other BCL-2 family proteins, such as BCL2A1 or BCLw, due to the lack of specific inhibitors.

In line with previous studies, our data indicate a correlation of ABT-199 sensitivity with high BCL-2 protein expression.^{7,25} However, in our study sensitivity to ABT-199 was independent of genetic alterations of BCL-2 and not all cells expressing high BCL-2 levels were sensitive to ABT-199, highlighting the need to better understand the mechanisms of resistance in cells with high expression of BCL-2, such as HBL1 and OCI-LY3. Although RIVA and U2932 also expressed high levels of BCL-X_i and MCL-1, BAX and BIM were exclusively sequestered by BCL-2, indicating that in these cells BCL-2 is the preferred binding partner for the pro-apoptotic proteins. The molecular basis for this preferential binding is not known. Increased binding to BCL-2 instead of the related protein BCL-X_i cannot be explained by different binding affinities, as BIM BH3-peptides bind more strongly to BCL-X_i than to BCL-2,^{28,32} but may be explained by the amount of accessible protein at the mitochondria or by enhanced protein stability.³³ Our data indicate that ABT-199 released pro-apoptotic BAX and BIM and that the released BAX induced activation of BAK, as knockdown of BAX significantly reduced BAK activation (Figure 6E). The involvement of BIM in ABT-199-induced apoptosis appears to be cell-type-dependent, as BIM knockdown reduced apoptosis in RIVA but not in U2932 cells (Figure 5).

In contrast, in the BCL-X_i-dependent cell lines RCK8 and SUDHL8, BAX and BAK were exclusively bound to BCL-X_i. These cell lines expressed high levels of BCL-X_i

but low levels of BCL-2 and MCL-1, which may explain why BCL-X_i was the preferred binding partner. Treatment with A1331852 displaced both BAX, BAK and BIM from BCL-X_i. Knockdown experiments indicated that although BIM was displaced, it did not contribute to A1331852-induced apoptosis, whereas both BAX and

BAK were involved. Taken together, these experiments indicate that the marked sensitivity of RCK8 and SUDHL8 cells reflected the high levels of BAX and BAK bound by BCL-X_i and that the displacement of these proteins by A1331852 was sufficient to induce apoptosis. Another study has shown a requirement for BH3-only

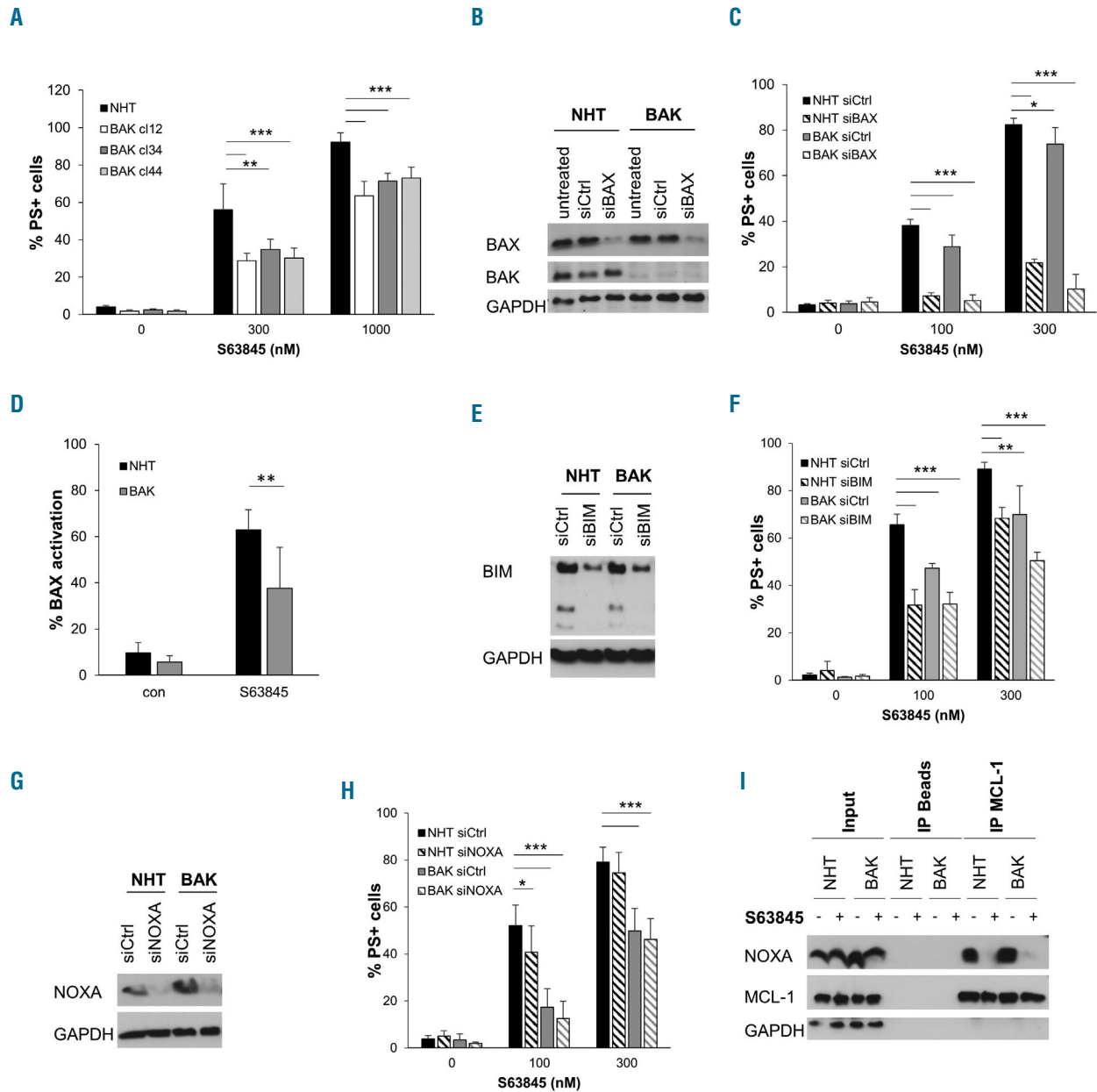


Figure 7. S63845 induced apoptosis is mainly independent of BAK. (A) BAK was deleted from U2946 cells using CRISPR/Cas9. Cells were transduced with pLentiCRISPRv2 either carrying non-human target (NHT) control guide (g)RNA or BAK gRNA (BAK) followed by selection of stable clones with BAK deletion. NHT or BAK-deleted clones were exposed to different concentrations of S63845 for 4 h before analysis of phosphatidylserine (PS) exposure by staining with annexin V-FITC and flow cytometry. The mean and standard deviation (SD) are shown (n=3). (B, C) To achieve efficient knockdown, BAX was silenced in U2946 NHT control or BAK-deleted cells (clone 12) using siRNA#1 and #3 combined. (B, C) Cells were exposed to different concentrations of S63845 for 4 h before analysis of PS exposure by staining with annexin V-FITC and flow cytometry. The mean and SD are shown (n=4). (D) NHT or BAK-deleted cells were treated with 100 nM S63845 for 4 h before analysis of BAX activation using intracellular staining with an active conformation-specific BAX antibody and flow cytometry. The mean and SD are shown (n=3). (E, F) BIM was silenced using short-interfering (si)RNA in U2946 NHT control or BAK-deleted cells (clone 12). (E, F) Knockdown of BIM was confirmed by Western blotting. (F) Cells were exposed to different concentrations of S63845 for 4 h before analysis of PS exposure by staining with annexin V-FITC and flow cytometry. The mean and SD are shown (n=4). (G, H) NOXA was silenced using siRNA in U2946 NHT control or BAK-deleted cells (clone 12). (G, H) Knockdown of NOXA was confirmed by Western blotting. (H) Cells were exposed to different concentrations of S63845 for 4 h before analysis of PS exposure by staining with annexin V-FITC and flow cytometry. The mean and SD are shown (n=4). (I) NHT or BAK-deleted clones were exposed to S63845 (100 nM) for 4 h before lysis in CHAPS-containing buffer and immunoprecipitation (IP) of MCL-1. The interaction with NOXA is demonstrated by Western blotting. Input lanes showing the presence of overall protein in the lysate, and IP lanes show the interaction with MCL-1. Protein G beads without primary antibody were used to control for unspecific binding. A representative blot of two independent experiments is shown. * $P < 0.05$; ** $P < 0.01$; *** $P < 0.001$.

proteins for A1331852-induced apoptosis in HCT-116 cells,³⁴ highlighting important differences from DLBCL.

In terms of S63845-induced apoptosis, the MCL-1-dependent cell lines SUDHL10 and U2946 did not express especially high levels of MCL-1, but both cell lines expressed only small amounts of BCL-2 and BCL-X_L. BIM and BAK were predominantly sequestered by MCL-1 in these cells. BAK has previously been identified as an essential mediator of S63845-induced cell death in breast cancer cells,³⁵ but our data demonstrate that BAX may be more important for MCL-1 inhibition in DLBCL. Thereby, BAK and/or BH3-only proteins displaced from MCL-1 contributed to the activation of BAX and apoptosis. Besides BIM, our data also indicate that NOXA is a potential mediator of S63845-induced apoptosis. NOXA is highly bound by MCL-1 and displaced by S63845, which may enable NOXA to act as a direct activator for BAX, as suggested previously.^{36,37}

Taken together, our study demonstrates that the sensitivity to BH3-mimetics is underlined by sequestration of BIM, BAX and/or BAK by the anti-apoptotic BCL-2 proteins, a phenomenon that is disrupted by BH3-mimetics, leading to predominantly BAX-mediated apoptosis. Therefore, our data support a model in which the major

function of the anti-apoptotic BCL-2 proteins in DLBCL cells is to directly sequester or inhibit BAX. Dependent on the abundance of the different anti-apoptotic BCL-2 proteins, the pro-apoptotic proteins preferentially bind to either BCL-2, BCL-X_L or MCL-1 which renders these cells highly sensitive to selective BH3-mimetics. However, our data also highlight that besides BCL-2, BCL-X_L or MCL-1 additional anti-apoptotic BCL-2 proteins such as BCL2A1³⁸ and BCL-w³⁹ may play important roles in DLBCL, as some cell lines, including Pfeiffer and OCI-LY3, display high priming but are nevertheless not responsive to inhibition of BCL-2, BCL-X_L or MCL-1. A more detailed understanding of the molecular mechanisms of resistance in these cell is required to enable the best use of potent BCL-2 family inhibitors in clinical practice.

Acknowledgments

The authors would like to thank C. Hugenberg for expert secretarial assistance and Sandeep Dave for providing us with OCI-LY10 cells. This work was partially supported by the Else Kröner-Fresenius-Stiftung (to MV), the Experimental Cancer Medicine Center Leicester and funding from the Scott Waudby Trust (to SJ and MJSD).

References

- Adams JM, Cory S. The Bcl-2 apoptotic switch in cancer development and therapy. *Oncogene*. 2007;26(9):1324-1337.
- Tsujiimoto Y, Ikegaki N, Croce CM. Characterization of the protein product of bcl-2, the gene involved in human follicular lymphoma. *Oncogene*. 1987;2(1):3-7.
- Aukema SM, Siebert R, Schuurin E, et al. Double-hit B-cell lymphomas. *Blood*. 2011;117(8):2319-2331.
- Sarkozy C, Traverse-Glehen A, Coiffier B. Double-hit and double-protein-expression lymphomas: aggressive and refractory lymphomas. *Lancet Oncol*. 2015;16(15):e555-e567.
- Hom H, Ziepert M, Becher C, et al. MYC status in concert with BCL2 and BCL6 expression predicts outcome in diffuse large B-cell lymphoma. *Blood*. 2013;121(12):2253-2263.
- Schuetz JM, Johnson NA, Morin RD, et al. BCL2 mutations in diffuse large B-cell lymphoma. *Leukemia*. 2012;26(6):1383-1390.
- Klanova M, Andera L, Brazina J, et al. Targeting of BCL2 family proteins with ABT-199 and homoharringtonine reveals BCL2- and MCL1-dependent subgroups of diffuse large B-cell lymphoma. *Clin Cancer Res*. 2016;22(5):1138-1149.
- Schmitz R, Wright GW, Huang DW, et al. Genetics and pathogenesis of diffuse large B-cell lymphoma. *N Engl J Med*. 2018;378(15):1396-1407.
- Vogler M, Walter HS, Dyer MJS. Targeting anti-apoptotic BCL2 family proteins in haematological malignancies - from pathogenesis to treatment. *Br J Haematol*. 2017;178(3):364-379.
- Davids MS, Roberts AW, Seymour JF, et al. Phase I first-in-human study of venetoclax in patients with relapsed or refractory non-Hodgkin Lymphoma. *J Clin Oncol*. 2017;35(8):826-833.
- DiNardo CD, Pratz K, Pullarkat V, et al. Venetoclax combined with decitabine or azacitidine in treatment-naive, elderly patients with acute myeloid leukemia. *Blood*. 2019;133(1):7-17.
- Anderson MA, Tam C, Lew TE, et al. Clinicopathological features and outcomes of progression of CLL on the BCL2 inhibitor venetoclax. *Blood*. 2017;129(25):3362-3370.
- Souers AJ, Levenson JD, Boghaert ER, et al. ABT-199, a potent and selective BCL-2 inhibitor, achieves antitumor activity while sparing platelets. *Nat Med* 2013;19(2):202-208.
- Levenson JD, Phillips DC, Mitten MJ, et al. Exploiting selective BCL-2 family inhibitors to dissect cell survival dependencies and define improved strategies for cancer therapy. *Sci Transl Med*. 2015;7(279):279ra240.
- Kotschy A, Szlavik Z, Murray J, et al. The MCL1 inhibitor S63845 is tolerable and effective in diverse cancer models. *Nature*. 2016;538(7626):477-482.
- Moller P, Bruderlein S, Strater J, et al. MedB-1, a human tumor cell line derived from a primary mediastinal large B-cell lymphoma. *Int J Cancer*. 2001;92(3):348-353.
- Nacheva E, Dyer MJ, Metivier C, et al. B-cell non-Hodgkin's lymphoma cell line (Karpas 1106) with complex translocation involving 18q21.3 but lacking BCL2 rearrangement and expression. *Blood*. 1994;84(10):3422-3428.
- Dutta S, Ryan J, Chen TS, Kougentakis C, Letai A, Keating AE. Potent and specific peptide inhibitors of human pro-survival protein Bcl-xL. *J Mol Biol*. 2015;427(6 Pt B):1241-1253.
- Ryan J, Letai A. BH3 profiling in whole cells by fluorimeter or FACS. *Methods*. 2013;61(2):156-164.
- van Wijk SJL, Fricke F, Herhaus L, et al. Linear ubiquitination of cytosolic Salmonella typhimurium activates NF-kappaB and restricts bacterial proliferation. *Nat Microbiol*. 2017;2:17066.
- Levenson JD, Zhang H, Chen J, et al. Potent and selective small-molecule MCL-1 inhibitors demonstrate on-target cancer cell killing activity as single agents and in combination with ABT-263 (navitoclax). *Cell Death Dis*. 2015;6:e1590.
- Alizadeh AA, Eisen MB, Davis RE, et al. Distinct types of diffuse large B-cell lymphoma identified by gene expression profiling. *Nature*. 2000;403(6769):503-511.
- Deng J, Carlson N, Takeyama K, Dal Cin P, Shipp M, Letai A. BH3 profiling identifies three distinct classes of apoptotic blocks to predict response to ABT-737 and conventional chemotherapeutic agents. *Cancer Cell*. 2007;12(2):171-185.
- Del Gaizo Moore V, Letai A. BH3 profiling-measuring integrated function of the mitochondrial apoptotic pathway to predict cell fate decisions. *Cancer Lett*. 2013;332(2):202-205.
- Pham LV, Huang S, Zhang H, et al. Strategic therapeutic targeting to overcome venetoclax resistance in aggressive B-cell lymphomas. *Clin Cancer Res*. 2018;24(16):3967-3980.
- Masir N, Campbell LJ, Jones M, Mason DY. Pseudonegative BCL2 protein expression in a t(14;18) translocation positive lymphoma cell line: a need for an alternative BCL2 antibody. *Pathology*. 2010;42(3):212-216.
- Quentmeier H, Drexler HG, Hauer V, et al. Diffuse large B cell lymphoma cell line U-2946: model for MCL1 inhibitor testing. *PLoS One*. 2016;11(12):e0167599.
- Chen L, Willis SN, Wei A, et al. Differential targeting of pro-survival Bcl-2 proteins by their BH3-only ligands allows complementary apoptotic function. *Mol Cell*. 2005;17(3):393-403.
- Willis SN, Chen L, Dewson G, et al. Proapoptotic Bak is sequestered by Mcl-1 and Bcl-xL, but not Bcl-2, until displaced by BH3-only proteins. *Genes Develop*. 2005;19(11):1294-1305.
- Westphal D, Kluck RM, Dewson G.

- Building blocks of the apoptotic pore: how Bax and Bak are activated and oligomerize during apoptosis. *Cell Death Diff.* 2014;21(2):196-205.
31. Liu Y, Mondello F, Erazo T, et al. NOXA genetic amplification or pharmacologic induction primes lymphoma cells to BCL2 inhibitor-induced cell death. *Proc Natl Acad Sci U S A.* 2018;115(47):12034-12039.
 32. Kong W, Zhou M, Li Q, Fan W, Lin H, Wang R. Experimental characterization of the binding affinities between proapoptotic BH3 peptides and antiapoptotic Bcl-2 proteins. *ChemMedChem.* 2018;13(17):1763-1770.
 33. Rooswinkel RW, van de Kooij B, de Vries E, et al. Antiapoptotic potency of Bcl-2 proteins primarily relies on their stability, not binding selectivity. *Blood.* 2014;123(18):2806-2815.
 34. Greaves G, Milani M, Butterworth M, et al. BH3-only proteins are dispensable for apoptosis induced by pharmacological inhibition of both MCL-1 and BCL-XL. *Cell Death Diff.* 2019;26(6):1037-1047.
 35. Merino D, Whittle JR, Vaillant F, et al. Synergistic action of the MCL-1 inhibitor S63845 with current therapies in preclinical models of triple-negative and HER2-amplified breast cancer. *Sci Transl Med.* 2017;9(401):eaam7049.
 36. Chen HC, Kanai M, Inoue-Yamauchi A, et al. An interconnected hierarchical model of cell death regulation by the BCL-2 family. *Nat Cell Biol.* 2015;17(10):1270-1281.
 37. Du H, Wolf J, Schafer B, Moldoveanu T, Chipuk JE, Kuwana T. BH3 domains other than Bim and Bid can directly activate Bax/Bak. *J Biol Chem.* 2011;286(1):491-501.
 38. Vogler M. BCL2A1: the underdog in the BCL2 family. *Cell Death Diff.* 2012;19(1):67-74.
 39. Adams CM, Mitra R, Gong JZ, Eischen CM. Non-Hodgkin and Hodgkin lymphomas select for overexpression of BCLW. *Clin Cancer Res.* 2017;23(22):7119-7129.
 40. Th'ng KH, Garewal G, Kearney L, et al. Establishment and characterization of three new malignant lymphoid cell lines. *Int J Cancer.* 1987;39(1):89-93.
 41. Amini RM, Berglund M, Rosenquist R, et al. A novel B-cell line (U-2932) established from a patient with diffuse large B-cell lymphoma following Hodgkin lymphoma. *Leuk Lymphoma.* 2002;43(11):2179-2189.
 42. Tweeddale ME, Lim B, Jamal N, et al. The presence of clonogenic cells in high-grade malignant lymphoma: a prognostic factor. *Blood.* 1987;69(5):1307-1314.
 43. Epstein AL, Levy R, Kim H, Henle W, Henle G, Kaplan HS. Biology of the human malignant lymphomas. IV. Functional characterization of ten diffuse histiocytic lymphoma cell lines. *Cancer.* 1978;42(5):2379-2391.
 44. Kubonishi I, Niiya K, Miyoshi I. Establishment of a new human lymphoma line that secretes plasminogen activator. *Jpn J Cancer Res.* 1985;76(1):12-15.
 45. Tohda S, Sato T, Kogoshi H, Fu L, Sakano S, Nara N. Establishment of a novel B-cell lymphoma cell line with suppressed growth by gamma-secretase inhibitors. *Leuk Res.* 2006;30(11):1385-1390.
 46. Epstein AL, Variakojis D, Berger C, Hecht BK. Use of novel chemical supplements in the establishment of three human malignant lymphoma cell lines (NU-DHL-1, NU-DUL-1, and NU-AMB-1) with chromosome 14 translocations. *Int J Cancer.* 1985;35(5):619-627.
 47. Fridberg M, Servin A, Anagnostaki L, et al. Protein expression and cellular localization in two prognostic subgroups of diffuse large B-cell lymphoma: higher expression of ZAP70 and PKC-beta II in the non-germinal center group and poor survival in patients deficient in nuclear PTEN. *Leuk Lymphoma.* 2007;48(11):2221-2232.
 48. Epstein AL, Kaplan HS. Biology of the human malignant lymphomas. I. Establishment in continuous cell culture and heterotransplantation of diffuse histiocytic lymphomas. *Cancer.* 1974;34(6):1851-1872.
 49. Abe M, Nozawa Y, Wakasa H, Ohno H, Fukuhara S. Characterization and comparison of two newly established Epstein-Barr virus-negative lymphoma B-cell lines. Surface markers, growth characteristics, cytogenetics, and transplantability. *Cancer.* 1988;61(3):483-490.
 50. Gabay C, Ben-Bassat H, Schlesinger M, Laskov R. Somatic mutations and intraclonal variations in the rearranged V κ genes of B-non-Hodgkin's lymphoma cell lines. *Eur J Haematol.* 1999;63(3):180-191.



Ferrata Storti Foundation

Vitamin K-dependent carboxylation of coagulation factors: insights from a cell-based functional study

Zhenyu Hao, Da-Yun Jin, Darrel W. Stafford, and Jian-Ke Tie

Department of Biology, the University of North Carolina at Chapel Hill, Chapel Hill, NC, USA

Haematologica 2020
Volume 105(8):2164-2173

ABSTRACT

Vitamin K-dependent carboxylation is a post-translational modification essential for the biological function of coagulation factors. Defects in carboxylation are mainly associated with bleeding disorders. With the discovery of new vitamin K-dependent proteins, the importance of carboxylation now encompasses vascular calcification, bone metabolism, and other important physiological processes. Our current knowledge of carboxylation, however, comes mainly from *in vitro* studies carried out under artificial conditions, which have a limited usefulness in understanding the carboxylation of vitamin K-dependent proteins in native conditions. Using a recently established mammalian cell-based assay, we studied the carboxylation of coagulation factors in a cellular environment. Our results show that the coagulation factor's propeptide controls substrate binding and product releasing during carboxylation, and the propeptide of factor IX appears to have the optimal affinity for efficient carboxylation. Additionally, non-conserved residues in the propeptide play an important role in carboxylation. A cell-based functional study of naturally occurring mutations in the propeptide successfully interpreted the clinical phenotype of warfarin's hypersensitivity during anticoagulation therapy in patients with these mutations. Unlike results obtained from *in vitro* studies, results from our cell-based study indicate that although the propeptide of osteocalcin cannot direct the carboxylation of the coagulation factor, it is required for the efficient carboxylation of osteocalcin. This suggests that the coagulation factors may have a different mechanism of carboxylation from osteocalcin. Together, results from this study provide insight into efficiently controlling one physiological process, such as coagulation without affecting the other, like bone metabolism.

Correspondence:

JIAN-KE TIE
jktie@email.unc.edu

Received: June 13, 2019.

Accepted: October 11, 2019.

Pre-published: October 17, 2019.

doi:10.3324/haematol.2019.229047

Check the online version for the most updated information on this article, online supplements, and information on authorship & disclosures: www.haematologica.org/content/105/8/2164

©2020 Ferrata Storti Foundation

Material published in *Haematologica* is covered by copyright. All rights are reserved to the Ferrata Storti Foundation. Use of published material is allowed under the following terms and conditions:

<https://creativecommons.org/licenses/by-nc/4.0/legalcode>.

Copies of published material are allowed for personal or internal use. Sharing published material for non-commercial purposes is subject to the following conditions:

<https://creativecommons.org/licenses/by-nc/4.0/legalcode>, sect. 3. Reproducing and sharing published material for commercial purposes is not allowed without permission in writing from the publisher.



Introduction

Vitamin K-dependent (VKD) carboxylation is a post-translational modification that converts specific glutamate residues (Glu) to gamma-carboxyglutamate residues (Gla) in VKD proteins. It is essential for the biological function of proteins that control blood coagulation, vascular calcification, bone metabolism, and other important physiological processes.¹ Carboxylation has mostly been associated with coagulation, since it was originally observed in the clotting factor, prothrombin (PT).² Defects of VKD carboxylation have long been known to cause bleeding disorders.³ There are two types of coagulation factors, one is procoagulant proteins which include PT, FVII, FIX, and FX. The other is anticoagulant proteins which include PC, PS, and PZ. The biological functions of these clotting factors require 9-13 Glu residues at the N-terminus of the mature protein (referred to as the Gla domain) to be properly modified by VKD carboxylation.

Carboxylation is catalyzed by an integral membrane protein gamma-glutamyl carboxylase (GGCX), which utilizes the reduced form of vitamin K, carbon dioxide, and oxygen as co-factors. This modification involves the subtraction of the gamma-hydrogen from the Glu residue followed by the addition of a carbon dioxide (carboxyl group). Simultaneously, reduced vitamin K is oxidized to vitamin K epoxide to provide the energy required for the carboxylation reaction. The enzy-

matic activity of GGCX was first discovered in the 1970s, showing that radioactive $^{14}\text{CO}_2$ was incorporated into PT in rats, and that the amount incorporated was dependent upon the administration of vitamin K.⁴ Two decades later, the GGCX gene was cloned⁵ and the enzyme was purified⁶ by our laboratory, making it possible to study GGCX function at the molecular level.

Gamma-glutamyl carboxylase recognizes its protein substrate by binding tightly to the propeptide of the substrate, which tethers the substrate to the enzyme.⁷ The Glu residues within the Gla domain of the substrate propeptide are progressively modified so that multiple carboxylation reactions occur during a single enzyme and substrate binding event.⁸ In addition, binding of the propeptide to GGCX has been shown to significantly stimulate the activity of the enzyme toward non-covalently linked Glu-containing substrates.^{9,10} The propeptide of most VKD proteins is located at the N-terminus of the precursor protein that is proteolytically removed after carboxylation to form the mature protein. Notably, a propeptide can also be found at the C-terminus of the precursor protein¹¹ or even within the mature VKD protein.¹² Removal of the propeptide from the precursor of coagulation factors abolishes their carboxylation,^{7,13} suggesting the pivotal role of the propeptide for carboxylation. Nevertheless, the propeptide of osteocalcin (or referred to as bone Gla protein, BGP) appears to be unnecessary for its carboxylation.¹⁴ Moreover, high-affinity binding sites within the mature BGP were identified, which appeared to bind to GGCX through a different binding site to the propeptide binding site.¹⁵

Propeptides of coagulation factors are essential for the carboxylation of precursor proteins. These propeptide sequences are highly conserved, especially at residues -16, -10, -6, -4, and -1. It has been proposed that the N-terminal sequence of the propeptide is necessary for GGCX recognition, while the C-terminal sequence is required for propeptidase recognition.¹⁵ Despite the high sequence conservation, in an *in vitro* study, the apparent affinities of the coagulation factors' propeptide for GGCX varied over 100-fold.¹⁶ Nevertheless, these coagulation factors appear to be fully carboxylated in physiological conditions. It has been shown that replacing FX propeptide with a reduced affinity propeptide (PT's propeptide) enhanced the carboxylation of FX, which presumably increased substrate turnover.¹⁷ However, a similar strategy of replacing FIX propeptide failed to increase the carboxylation efficiency of FIX,¹⁸ although the reason for this discrepancy remains unclear.

It is worth noting that most of our knowledge of GGCX function and its interaction with natural protein substrates was obtained from *in vitro* studies carried out under artificial conditions using the pentapeptide FLEEL as the substrate.¹⁹ Consequently, we do not know how GGCX carboxylates natural VKD proteins in their native milieu.

Here, we studied the carboxylation of coagulation factors in a cellular environment with different chimeric reporter-proteins using our recently established cell-based assay.²⁰ We compared the contribution of the propeptide, the Gla domain, and the C-terminal functional domain of the coagulation factor to its carboxylation. In addition, we examined the effect of naturally occurring mutations in the propeptide on the coagulation factor's carboxylation to gain an insight into the corresponding phenotype of warfarin hypersensitivity. Our results confirmed the piv-

otal role of the propeptide in coagulation factor carboxylation and interpreted the clinical phenotype of the hypersensitivity of warfarin during anticoagulation therapy.

Methods

Materials and cell lines

The mammalian expression vector pcDNA3.1Hygro(+), mouse anti-carboxylated BGP monoclonal antibody, Alexa Fluor-488 conjugated donkey anti-mouse IgG, Alexa Fluor-568 conjugated donkey anti-sheep IgG, and Hoechst 33342 were from ThermoFisher Scientific (Waltham, MA, USA). The fluorescent protein-tagged marker proteins of the endoplasmic reticulum (ER) (mCherry-Sec61-N-18) and Golgi apparatus (pmScarlet_Giantin_C1) were gifts from Dr. Michael Davidson (Addgene plasmid # 55130) and Dr. Dorus Gadella (Addgene plasmid # 85048), respectively. The Ca^{2+} -dependent monoclonal antibody to carboxylated Gla domain of PC (PCgla) was a gift from Dr. Paul Bajaj (University of California, Los Angeles, CA, USA).²¹ The horseradish peroxidase-conjugated goat anti-mouse IgG was from Jackson ImmunoResearch Laboratories Inc. (West Grove, PA, USA). The monoclonal antibody against Gla residues was from Sekisui Diagnostics LLC (Stamford, CT, USA). The HEK293 and COS-7 cell lines were from ATCC (Manassas, VA, USA).

DNA manipulations and plasmid constructions

The pcDNA3.1Hygro(+) vector, with the cDNA of FIXgla-PC (PC with its Gla domain exchanged with that of FIX) cloned onto the XbaI site, was used as the cloning and expression vector, as previously described.²⁰ All other chimeric reporter-proteins, with the different propeptides and/or Gla domains used in this study, were obtained by overlap polymerase chain reaction (PCR). Replacement of FIX epidermal growth factor (EGF) domain and the following domains with cell organelle marker proteins was performed by PCR. The nucleotide sequences of all constructs were verified by DNA sequencing at Eton Bioscience Inc. (RTP, NC, USA).

Reporter-protein carboxylation in HEK293 cells

The efficiency of reporter-protein (FIXgla-PC) carboxylation was determined in HEK293 cells, as previously described.²⁰ For the warfarin resistance study, HEK293 cells stably expressing the corresponding mutant reporter-protein were cultured in complete medium containing 20 nM vitamin K with increasing concentrations of warfarin. The cell culture medium was collected 48 hours (h) later and used for the sandwich-based ELISA to determine the level of carboxylated reporter-proteins.²⁰ For the BGP-PC reporter-protein (PC with its Gla domain replaced by BGP) detection, sheep anti-human PC IgG was used as the capture antibody, and mouse anti-carboxylated BGP antibody was used as the detection antibody. Experimental data were analyzed using GraphPad Prism.

To purify carboxylated chimeric reporter-proteins for use as a standard for ELISA, different chimeric proteins were stably expressed in HEK293/VKOR cells (HEK293 cells over-expressing VKOR). Carboxylated reporter-proteins were purified from the collected medium using 2-step chromatography, as previously described.¹⁷ Protein concentrations were quantified using the BCA protein assay kit.

Immunofluorescence confocal imaging

The subcellular localization of reporter-proteins were examined by immunofluorescence confocal imaging, as previously described.²² To examine the effect of the propeptide on reporter-protein carboxylation, different propeptide attached reporter-pro-

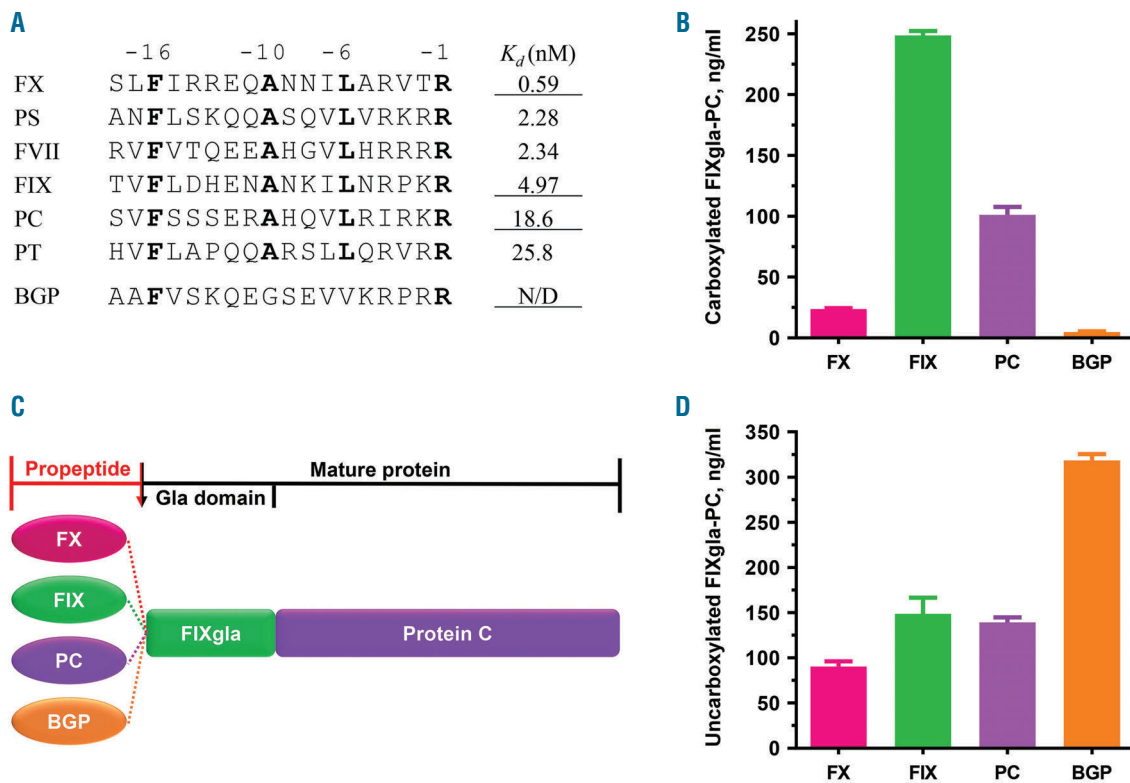


Figure 1. Effect of propeptides on coagulation factor carboxylation. (A) Sequence alignment of propeptides of vitamin K-dependent (VKD) coagulation factors and bone Gla protein (BGP), and their relative K_d values for gamma-glutamyl carboxylase (GGCX). Highly conserved residues are indicated by bold letters. The K_d values of different propeptides (adapted from Higgins-Gruber *et al.*²³) are a relative measure of propeptides' affinity for GGCX. The underlined K_d values correspond to the propeptides used in this study. (B) Carboxylation efficiency of the reporter-protein in HEK293 cells as directed by different propeptides. Reporter-proteins with different propeptides were transiently expressed in HEK293 cells, and the transfected cells were cultured in complete medium containing 11 μ M vitamin K. The carboxylated reporter-protein in the cell culture medium was determined by ELISA. (C) Domain structure of the reporter-protein, factor IX gla-protein C (FIXgla-PC), with different propeptides. The propeptide is proteolytically removed after carboxylation to form the mature protein. (D) Expression of uncarboxylated reporter-proteins with different propeptides as in (B). Reporter-proteins were transiently expressed in HEK293 cells and the transfected cells were incubated in complete medium containing 5 μ M warfarin. The total amount of uncarboxylated reporter-protein in the cell culture medium was determined by ELISA.

tein fusions were transiently expressed in COS-7 cells on coverslips. For the localization of carboxylated reporter-proteins at different cell organelles, fluorescent protein-tagged cell organelle marker protein fusions, and the corresponding marker protein fused with FIXgla, were transiently co-expressed in COS-7 cells. Transfected cells were cultured with 11 μ M vitamin K for 48 h, fixed with 4% paraformaldehyde, permeabilized with 0.20% Triton X-100, and immuno-stained with corresponding antibodies. The cell nuclei were stained with 2 μ M Hoechst 33342.

Results

Contribution of the propeptide to coagulation factor carboxylation

To explore the role of the propeptide on coagulation factor carboxylation in a cellular milieu, we used our recently established mammalian cell-based assay.²⁰ Propeptides with different affinities for GGCX (Figure 1A) were fused to the N-terminus of the chimeric reporter-protein FIXgla-PC (Figure 1C). These chimeric fusion proteins were transiently expressed in HEK293 cells, and the efficiency of their carboxylation was determined by ELISA.²⁰ We selected propeptides of FX, FIX, PC, and BGP for this study. Results from our cell-based study show that BGP propeptide cannot direct reporter-protein carboxylation (Figure 1B), which agrees with results from *in vitro* studies.¹⁴⁻¹⁶ In

addition, FIX propeptide is the most efficient propeptide for reporter-protein carboxylation, which is approximately 10-fold higher than that of FX propeptide and 2.5-fold higher than PC propeptide. However, this cell-based result of carboxylation of propeptide attached protein substrate is different from the previous *in vitro* study showing that all of the propeptides stimulated carboxylation of the non-covalently linked substrate to a similar extent.²³

To confirm that the significantly decreased production of carboxylated reporter-proteins, directed by the propeptides of FX and BGP, was not due to the effect of the propeptide on reporter-protein expression, we determined the expression levels of the reporter-proteins in cell culture medium without carboxylation by feeding the cells with warfarin. The reporter-protein has similar expression levels when fused to different coagulation factor propeptides (FX, FIX, and PC) (Figure 1D). However, a significant amount of uncarboxylated reporter-protein was produced when BGP propeptide was used. Nevertheless, these results suggest that the significant difference in reporter-protein carboxylation, when fused to different propeptides (Figure 1B), is not due to the effect of the propeptide on reporter-protein expression, but rather to its carboxylation.

The unaffected expression and non-carboxylation characteristics of the reporter-protein, when fused to BGP propeptide, were confirmed further by immunofluores-

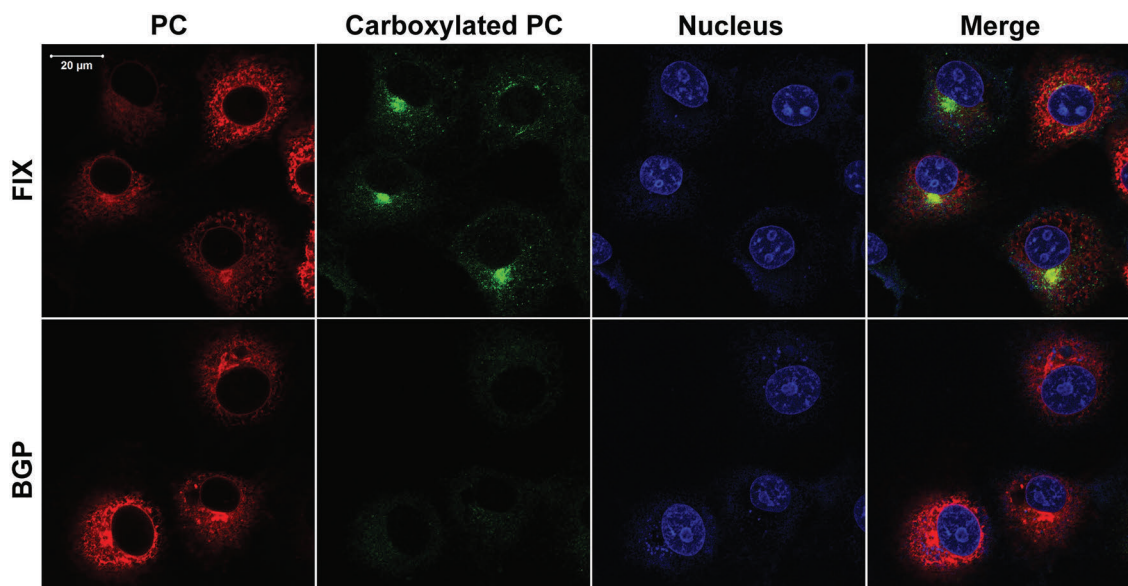


Figure 2. Localization of reporter-proteins by immunofluorescence confocal imaging. The reporter-protein factor IX gla-protein C (FIXgla-PC) with the propeptide of FIX or bone Gla protein (BGP) was transiently expressed in COS-7 cells. The transfected cells were cultured with complete medium containing 11 μ M vitamin K. The carboxylated reporter-protein (carboxylated PC) was immuno-stained by the mouse anti-carboxylated FIXgla monoclonal antibody as the primary antibody, and Alexa Fluor-488 conjugated donkey anti-mouse IgG as the secondary antibody (green image). The total reporter-protein (PC) was probed by the sheep anti-PC polyclonal antibody as the primary antibody and the Alexa Fluor-568 conjugated donkey anti-sheep IgG as the secondary antibody (red image). The cell nucleus was stained by Hoechst 33342 (blue image).

cence confocal imaging (Figure 2). The reporter-protein (fused with either a FIX or BGP propeptide) was properly synthesized and directed to the ER (Figure 2, red images, total reporter-protein), but only the fusion with FIX propeptide was properly carboxylated (Figure 2, green image, carboxylated reporter-protein). The location of the carboxylated reporter-protein appears to be in both the ER and Golgi apparatus, which is consistent with previous observations.²⁴ Together, these results suggest that the propeptide plays an essential role in coagulation factor carboxylation.

The entire N-terminal sequence of the propeptide determines the efficiency of coagulation factor's carboxylation

The alanine residue at -10 and leucine residue at -6 of the coagulation factor propeptide are highly conserved (Figure 1A). However, BGP propeptide has a glycine at -10 and valine at -6. The *in vitro* study shows that substituting alanine for glycine at -10 (G-10A) in BGP propeptide increased its affinity for GGCX 45-fold, and substituting leucine for valine at -6 (V-6L) increased its affinity approximately 100-fold.²⁵ When both G-10A and V-6L are mutated in BGP propeptide, its apparent affinity for GGCX is similar to that of FIX propeptide. To examine how these mutations affect carboxylation efficiency *in vivo*, we made the same BGP propeptide substitutions in the chimeric reporter-protein of FIXgla-PC (Figure 1C) and examined their effect on reporter-protein carboxylation in HEK293 cells. The V-6L mutant increased reporter-protein carboxylation approximately 20-fold and the G-10A mutant increased reporter-protein carboxylation approximately 7-fold (Figure 3A). Mutating both residues increased reporter-protein carboxylation approximately 23-fold, a carboxylation efficiency close to that of FIX propeptide. These results, consistent with our previous *in vitro* study,²⁵

suggest that the conserved residues at positions -6 and -10 in the propeptide are essential for its binding to GGCX and for substrate carboxylation.

Factor X propeptide is the tightest binding propeptide of the coagulation factors, and carboxylation of FX has a slow turnover rate. Based on these observations and the above result (Figure 3A), we replaced the conserved residues of FX propeptide at -10 or -6 to that of the BGP in the chimeric reporter-protein of FIXgla-PC. We assumed these replacements would decrease the affinity of FX propeptide for GGCX and therefore increase the turnover rate of reporter-protein carboxylation. Unexpectedly, our results show that neither the single mutation (L-6V or A-10G) nor the double mutation (L-6V/A-10G) increased reporter-protein carboxylation (Figure 3C), suggesting that the non-conserved residues of the coagulation factor's propeptide play a role in GGCX's binding and substrate carboxylation.

To explore the contribution of the propeptide's non-conserved residues to carboxylation, we replaced FX propeptide sequence between -11 and -18 with that of PC (FX/PC1) (Figure 3B), a propeptide that has approximately 90-fold lower affinity for GGCX.¹⁶ Results from our cell-based study show that this replacement does not show an obvious effect on reporter-protein carboxylation (Figure 3D). However, when we exchanged the propeptide sequence between -5 and -9 (FX/PC2) (Figure 3), reporter-protein carboxylation was increased approximately 3-fold. Further replacement of FX propeptide between -5 and -18 with that of PC (FX/PC3) (Figure 3), increased reporter-protein carboxylation approximately 6-fold, a level similar to the full-length propeptide of PC (Figure 3D). These results suggest that the entire N-terminal sequence of the propeptide (-5 to -18) determines the carboxylation efficiency of coagulation factors, which is consistent with previous observations.¹³

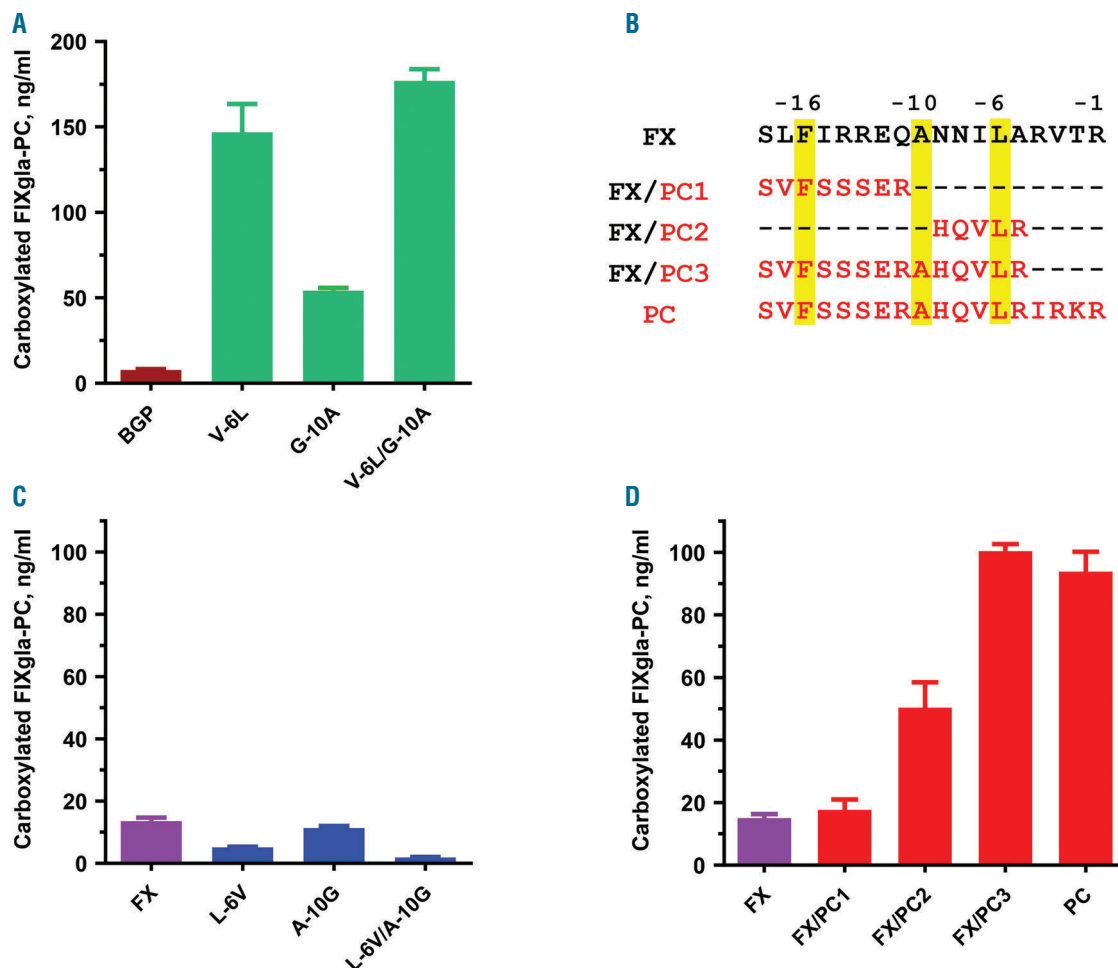


Figure 3. Contribution of propeptide's conserved and non-conserved residues to reporter-protein carboxylation. Effect of conserved residues at -6 and -10 of the propeptide of bone Gla protein (BGP) (A) and factor X (FX) (C) on the carboxylation of reporter-proteins as evaluated by cell-based assay. Chimeric reporter-proteins with wild-type or mutant propeptides were transiently expressed in HEK293 cells and the carboxylated reporter-protein was determined by ELISA, as described in B. (B) Propeptide sequence of FX and the replacement of part of its sequence with that of protein C (PC) (highlighted in red). Highly conserved residues are highlighted in yellow. (D) Carboxylation of the reporter-protein directed by chimeric propeptide sequences of FX and PC as indicated in (B).

Effect of naturally occurring propeptide mutations on coagulation factor carboxylation

Naturally occurring mutations have been identified at positions -1, -4, -9 and -10²⁵⁻³⁰ in the propeptide of coagulation factors. Patients bearing mutations at positions -9 and -10 of FIX propeptide possess near-normal levels of active FIX; but, these levels are reduced to <1% of normal during anticoagulation therapy (referred to as warfarin hypersensitivity).^{27,28,31-33} Meanwhile, other VKD clotting factor levels only decreased to 30-40%. To examine the effect of these mutations on coagulation factor carboxylation in a cellular milieu, we introduced these mutations to FIX propeptide in our reporter-protein for cell-based functional study. Our results show that, despite significant differences in GGCX affinity *in vitro*,²⁵ these mutations have only a moderate effect on reporter-protein carboxylation in a cellular environment (Figure 4A), which is consistent with clinical observations of patients bearing these mutations that have near-normal levels of active FIX.

To clarify the warfarin hypersensitivity phenotype during anticoagulation therapy of patients carrying these mutations, we examined the response of the mutant

reporter-proteins' carboxylation to increasing concentrations of warfarin. We stably expressed the individual mutant or wild-type reporter-protein in HEK293 cells and examined their carboxylation efficiency under different warfarin or vitamin K concentrations. Results showed that, compared with the wild-type reporter-protein, the N-9K mutant has a moderate effect on warfarin inhibition, while the warfarin response curve of the A-10T and A-10V mutants significantly shifts to lower concentrations of warfarin (Figure 4B), suggesting that they are more sensitive to warfarin inhibition. The half-maximal inhibition concentration (IC₅₀) of warfarin for the A-10T and A-10V mutants decreased 11.6-fold and 4.5-fold, respectively (Figure 4C), which is consistent with a recent similar cell-based study.²⁶ As warfarin blocks the vitamin K recycling, we also examined the effect of vitamin K on the carboxylation of these mutant reporter-proteins. We determined the half-maximal effective concentration (EC₅₀) of vitamin K for the carboxylation of these mutant reporter-proteins. Compared to the wild-type reporter-protein, the A-10T and A-10V mutants required a significantly higher concentration of vitamin K (5.8-fold and 2.9-fold, respectively) to

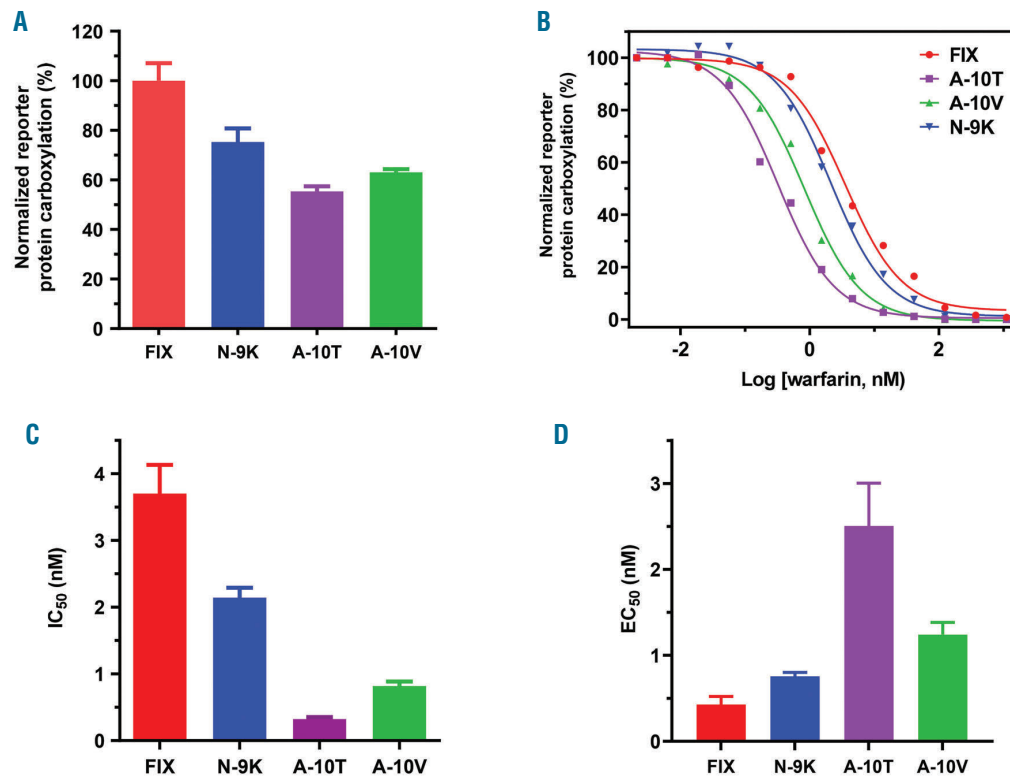


Figure 4. Effect of naturally occurring propeptide mutations on reporter-protein carboxylation. (A) Carboxylation efficiency of the chimeric reporter-protein with wild-type factor IX (FIX) propeptide or with its naturally occurring mutations N-9K, A-10T, and A-10V. The wild-type and corresponding mutant reporter-proteins were transiently expressed in HEK293 cells and the carboxylated reporter-protein was determined by ELISA, as described in the legend to Figure 1C. (B) Warfarin titration of reporter-protein carboxylation as directed by FIX propeptide with naturally occurring mutations at positions -9 and -10. The wild-type and corresponding mutant reporter-proteins were stably expressed in HEK293 cells. The corresponding reporter cells were cultured in complete medium containing 20 nM vitamin K with increasing concentrations of warfarin. (C) Inhibition efficiency of warfarin on the carboxylation of mutant reporter-proteins. The half-maximal inhibition concentration (IC₅₀) of warfarin was determined from (B) using GraphPad software. (D) Effect of vitamin K concentration on reporter-protein carboxylation. HEK 293 cells stably expressing wild-type and corresponding mutant reporter-proteins were cultured with complete medium containing increasing concentrations of vitamin K. The efficiency of reporter-protein carboxylation was determined by ELISA and the half-maximal effective concentration (EC₅₀) of vitamin K was determined using GraphPad software.

achieve half-maximal carboxylation (Figure 4D). Together, these results suggest that mutations at -9 and -10 of the propeptide are more sensitive to warfarin inhibition.

Naturally occurring mutations at position -4 and -1 of the propeptide preclude post-translational cleavage of the propeptide, resulting in secretion of the pro-coagulation factor with its propeptide still attached.^{29,30,34,35} To examine the effect of these mutations on carboxylation, we mutated R-1 (R-1S) or R-4 (R-4Q) of the propeptide in our reporter-protein and transiently expressed them in HEK293 cells. Transfected cells were cultured with vitamin K. However, we were unable to detect reporter-protein carboxylation using ELISA (*data not shown*). This could be due to the un-cleaved propeptide which prevents the recognition of the carboxylated Gla domain by the conformational specific antibody, as observed previously.²⁹ To test this hypothesis, we examined reporter-protein carboxylation from cell culture medium using western blot analysis with an antibody that recognizes Gla residues. Our result shows that, compared to the wild-type reporter-protein, the R-1S and R-4Q mutants appear to be properly carboxylated, but migrate slower (Figure 5). This suggests that mutations at -1 and -4 do not affect reporter-protein carboxylation but prevent the cleavage of the propeptide, in agreement with previous observations.^{29,30,34}

Contribution of other sequences of coagulation factor to vitamin K-dependent carboxylation

To test whether the Gla domain of the coagulation factor contributes to VKD carboxylation, we compared the carboxylation efficiency of the Gla domains of FIX (containing 12 Gla residues) and PC (containing 9 Gla residues) in our chimeric reporter-protein (Figure 6A). These reporter-proteins were transiently expressed in HEK293 cells, and their carboxylation efficiency was examined by ELISA using antibodies that specifically recognize the corresponding carboxylated Gla domains. Both reporter-proteins can be efficiently carboxylated to a similar level (Figure 6C). Together with previous observations,^{7,13} this suggests that the Gla domain of the coagulation factor contributes very little to GGCX binding and substrate carboxylation, and that the propeptide is sufficient to direct the following Gla domain of coagulation factors to GGCX for carboxylation.³⁶

It should be noted that BGP propeptide has an undetectable affinity to GGCX *in vitro*,¹⁶ which has been suggested to be unnecessary for BGP carboxylation.^{14,15} To test this hypothesis, we removed BGP propeptide in the chimeric reporter-protein BGP-PC (Figure 6B), as previously described in the coagulation factor study.⁷ Our result from the cell-based study showed that the removal of BGP

propeptide significantly decreased (10-fold) reporter-protein carboxylation (Figure 6D), suggesting that BGP propeptide plays an essential role in BGP carboxylation, which differs from *in vitro* studies.^{14,15}

To examine the effect of coagulation factor's remaining domains on its carboxylation, we used chimeric reporter-proteins of FIX with its EGF and following domains replaced by different cell organelle marker proteins, including Sec61B for ER, Giantin for Golgi, and tissue factor for the plasma membrane. As controls, cell organelle marker proteins were fused to the N-terminal of the mCherry fluorescent protein. The cell organelle specific FIXgla chimeric reporter-proteins and the corresponding controls were transiently co-expressed in COS-7 cells. The transfected cells were cultured with vitamin K, and the carboxylated reporter-protein was immuno-stained with an antibody that specifically recognizes the carboxylated Gla domain of FIX. These reporter-proteins were properly carboxylated (Figure 7, green image) and transported to the destined locations (Figure 7, red image), supporting the view that the remaining domains of FIX do not affect its carboxylation.

Discussion

The aim of this study was to explore carboxylation of coagulation factors in a cellular environment in order to explain the clinical phenotypes of naturally occurring mutations in coagulation factors, as related to their carboxylation modifications. Previous studies have shown that the propeptide is essential for directing coagulation factor carboxylation.^{7,13} Despite a significant variation in affinity, once the propeptide binds to GGCX, it has been proposed that it induces a conformational change in the GGCX active site that stimulates carboxylation of its substrate to a similar extent.²⁵ The *in vitro* study shows that the carboxylation rate is much faster than the rate of product release,³⁷ and the release of the carboxylated product from GGCX can be detected in coagulation factors with a lower affinity propeptide but not with a higher affinity propeptide.³⁸ Therefore, it was hypothesized that exchanging the higher affinity propeptide with a reduced affinity propeptide would enhance coagulation factor carboxylation by allowing for a higher substrate turnover. For example, it has been shown that substituting FX propeptide with a lower affinity propeptide (PT propeptide) significantly increased FX carboxylation.¹⁷ However, it is not clear why this hypothesis applies to carboxylation of FX¹⁷ but not to that of FIX.¹⁸

Results from this study show that FIX propeptide is the most efficient propeptide for directing coagulation factor carboxylation and that the propeptide with either a higher (FX propeptide) or lower (PC propeptide) affinity has a reduced carboxylation efficiency (Figure 1). The affinity of FIX propeptide is approximately 8-fold lower than that of FX and is approximately 4-fold higher than that of PC.^{16,23} The efficiency of FX propeptide to direct reporter protein carboxylation is only approximately 10% of that of FIX. This result suggests that the affinity of FIX propeptide for GGCX is optimal, as it balances the rate of carboxylation and product releasing. This explains why the propeptide exchanging strategy increased carboxylation of FX but not that of FIX.^{17,18}

It has been proposed that the propeptide contains two

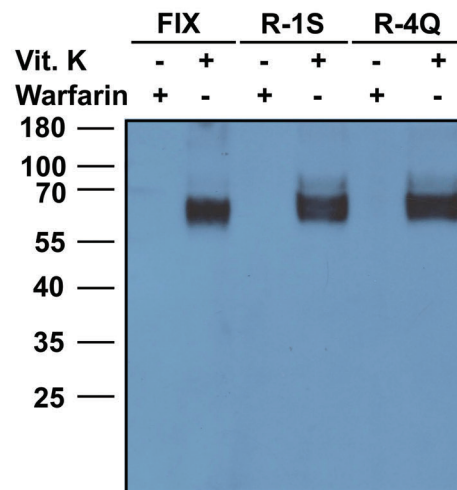


Figure 5. Effect of naturally occurring propeptide mutations at positions -1 and -4 on reporter-protein carboxylation. Wild-type and -1 and -4 mutant reporter-proteins were transiently expressed in HEK293 cells; the transfected cells were cultured with a serum-free medium containing 11 μ M vitamin K (Vit. K) or 5 μ M warfarin (Warfarin). The cell culture medium was collected 48 hours post-transfection and loaded to SDS-PAGE for Western blot analysis. Carboxylated protein bands were probed by a mouse monoclonal antibody that recognizes Gla residues.

recognition elements: one for GGCX recognition (located towards the N-terminus) and one for propeptidase recognition (located near the C-terminus). For GGCX recognition, it appears that only a few conserved residues are essential for GGCX binding.^{25,39} Several naturally occurring mutations have been identified in the GGCX recognition region of FIX propeptide. These mutations are clinically silent in normal conditions, but selectively decrease FIX activity dramatically during warfarin therapy, which could cause life-threatening bleeding complications.²⁷ To explore the role of the propeptide on coagulation factor carboxylation and the clinical consequence of mutations in the propeptide, we examined these questions using our recently established cell-based assays.⁴⁰ Unlike previous *in vitro* studies, our results show that the entire N-terminal sequence of the propeptide, rather than a few conserved residues, determines the carboxylation efficiency of coagulation factors (Figure 3). This explains why the essential residues for GGCX binding in the propeptide of all coagulation factors are highly conserved, while the affinity of the propeptides for GGCX varies over 100-fold.¹⁶

Our results also show that mutations in FIX propeptide have a moderate effect on reporter-protein carboxylation at a higher vitamin K concentration (Figure 4A), but a significant effect on warfarin sensitivity (Figure 4B and C), which is consistent with the clinical phenotype of warfarin hypersensitivity in patients bearing these mutations during anticoagulation therapy.

The C-terminus of the propeptide is thought to be the propeptidase recognition site, essential for the propeptide cleavage to form mature coagulation factors.¹⁵ Naturally occurring mutations were found in this region at positions -4 and -1. Patients carrying these mutations in FIX have a bleeding diathesis and have a propeptide attached FIX (proFIX) detected in their plasma.³⁰ This proFIX loses lipid binding ability and has no coagulation activity.⁴¹ Our results show that mutations at -4 and -1 do not affect reporter-protein carboxylation, although the propeptide is

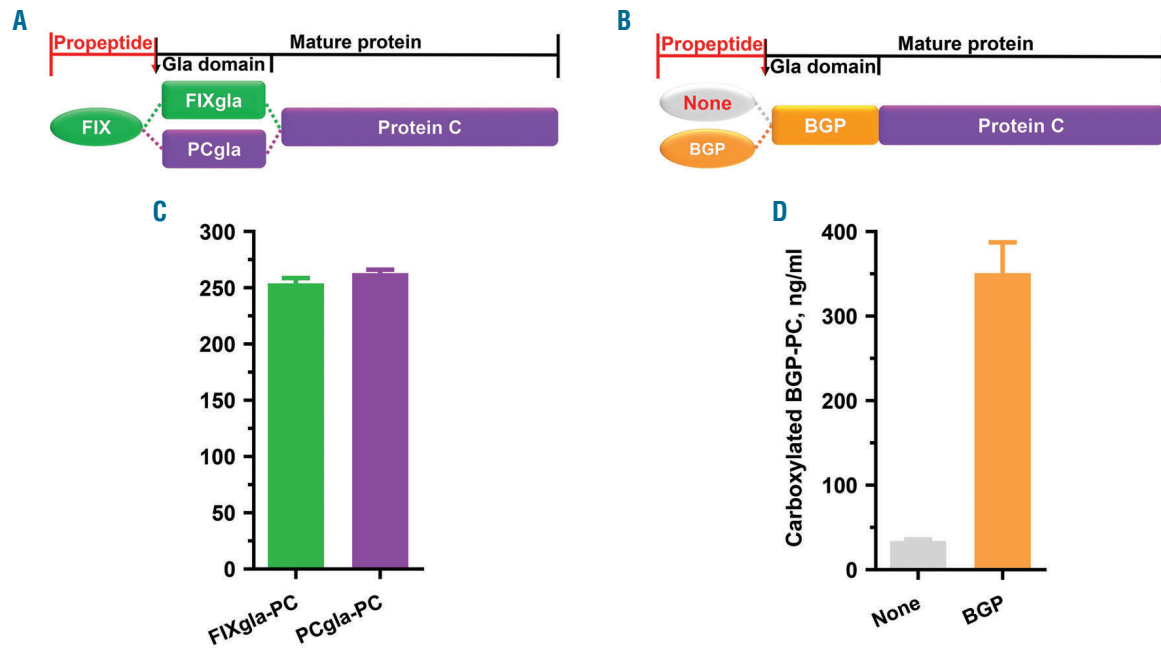


Figure 6. Effect of coagulation factor's Gla domain and bone Gla protein (BGP) propeptide on reporter-protein carboxylation. (A) Domain structure of the chimeric reporter-protein of protein C (PC) with different Gla domains. (B) Domain structure of BGP-PC chimeric reporter-protein with and without the BGP propeptide. (C) Carboxylation efficiency of the chimeric reporter-proteins factor IX gla-protein C (FIXgla-PC) and PCgla-PC. The corresponding reporter-protein was transiently expressed in HEK293 cells and the carboxylation efficiency of the reporter-protein was determined, as in B. (D) Carboxylation efficiency of the chimeric reporter-proteins in (B).

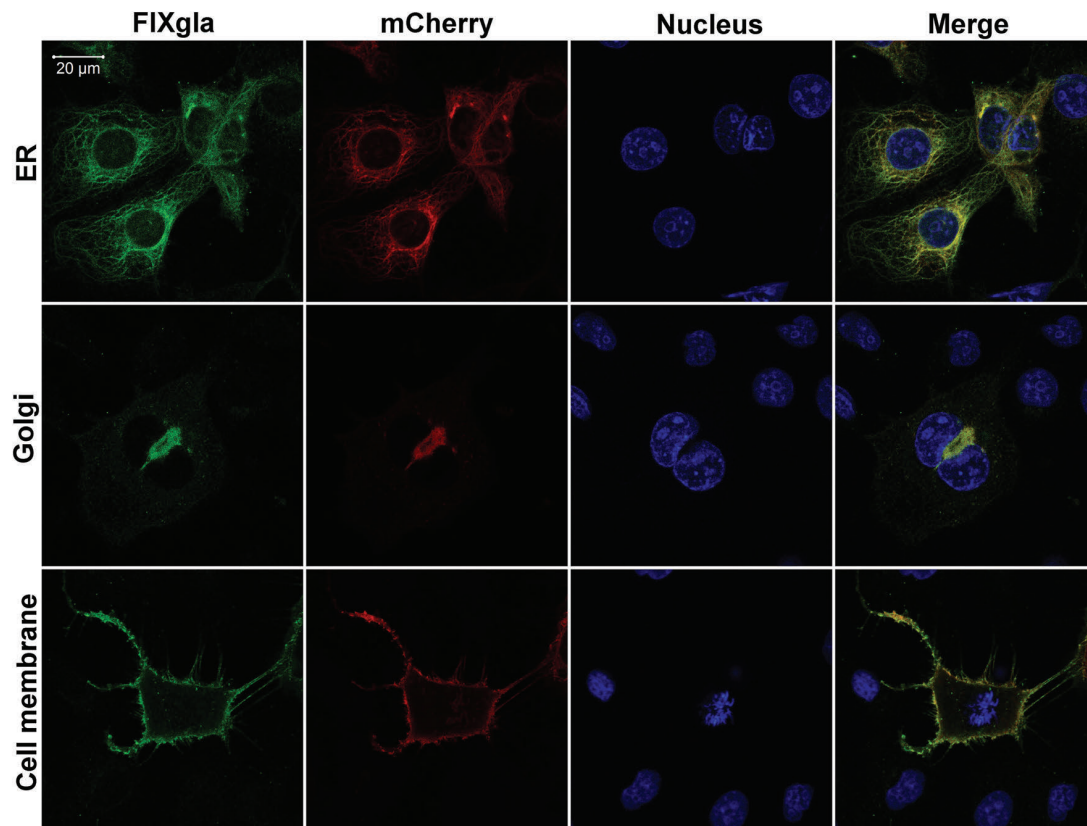


Figure 7. Localization of carboxylated factor IX (FIX)gla fused chimeric cell organelle marker proteins. FIXgla and mCherry (control) fused cell organelle marker proteins (Sec61B for ER, Giantin for Golgi, and tissue factor for Cell membrane) were transiently co-expressed in COS-7 cells. The transfected cells were cultured with 11 µM vitamin K. Forty-eight hours post transfection, cells were fixed with 4% paraformaldehyde and permeabilized with 0.20% Triton X-100. Carboxylated reporter-proteins (FIXgla) were immuno-stained with a mouse anti-carboxylated FIXgla monoclonal antibody as the primary antibody, and Alexa Fluor-488 conjugated donkey anti-mouse IgG as the secondary antibody (green image). mCherry fusion proteins (mCherry) were directly visualized as a fluorescent protein (red image), and the cell nucleus was stained by Hoechst 33342 (blue image).

still attached to the carboxylated protein (Figure 5). These mutant proteins cannot be recognized by a calcium-dependent conformational specific antibody, suggesting a loss of function.⁴¹ However, contradictory results exist on whether these mutations affect FIX carboxylation. It has been shown that proFIX purified from hemophilia patients, carrying mutations at -4, is properly carboxylated,^{30,34} others have shown that proFIX with a mutation at -4 in a hemophilia patient is only partially carboxylated.³⁵ This discrepancy may result from the different approaches used in determining the extent of carboxylation. Nevertheless, it has been confirmed that these mutations interfere with propeptide cleavage, and therefore affect the function of FIX (mainly by destabilizing the calcium-binding conformation),³⁴ impair FIX binding to the lipid membrane, and affect FIX activity for coagulation.^{29,41}

In contrast to numerous studies which indicate that the propeptide of BGP is not required for GGCX binding and its carboxylation,¹⁴⁻¹⁶ results from this study show that the removal of BGP propeptide dramatically decreased BGP carboxylation (Figure 6D). This result is consistent with previous studies showing that a non-covalently attached propeptide stimulates BGP carboxylation and a covalently

attached propeptide directs complete carboxylation of BGP.^{42,43} In addition, consistent with previous studies, our results show that BGP propeptide cannot direct coagulation factor carboxylation (Figures 1B and 2). Together, these results suggest that BGP may have a different mechanism for carboxylation than coagulation factors. This supports observations that vitamin K intake affects the carboxylation of coagulation factors and of BGP in different ways.⁴⁴⁻⁴⁷ Further studies are ongoing to clarify the mechanistic differences in the carboxylation of a variety of VKD proteins. Results from these studies will continue to provide insights into efficiently controlling one physiological process without affecting the other.

Acknowledgments

The authors would like to thank Dr. Paul Bajaj from the University of California, Los Angeles for helpful discussions and for providing the Ca²⁺-dependent monoclonal antibody against carboxylated Gla domain of protein C.

Funding

This work is supported by grant HL131690 from the National Institutes of Health (to JKT and DWS).

References

- Shearer MJ, Okano T. Key Pathways and Regulators of Vitamin K Function and Intermediary Metabolism. *Annu Rev Nutr.* 2018;38:127-151.
- Stenflo J, Fernlund P, Egan W, Roepstorff P. Vitamin K dependent modifications of glutamic acid residues in prothrombin. *Proc Natl Acad Sci U S A.* 1974;71(7):2730-2733.
- Napolitano M, Mariani G, Lapecorella M. Hereditary combined deficiency of the vitamin K-dependent clotting factors. *Orphanet J Rare Dis.* 2010;5:21.
- Girardot JM, Delaney R, Johnson BC. Carboxylation, the completion step in prothrombin biosynthesis. *Biochem Biophys Res Commun.* 1974;59(4):1197-1203.
- Wu SM, Cheung WF, Frazier D, Stafford DW. Cloning and expression of the cDNA for human gamma-glutamyl carboxylase. *Science.* 1991;254(5038):1634-1636.
- Wu SM, Morris DP, Stafford DW. Identification and purification to near homogeneity of the vitamin K-dependent carboxylase. *Proc Natl Acad Sci U S A.* 1991;88(6):2236-2240.
- Jorgensen MJ, Cantor AB, Furie BC, Brown CL, Shoemaker CB, Furie B. Recognition site directing vitamin K-dependent gamma-carboxylation resides on the propeptide of factor IX. *Cell.* 1987;48(2):185-191.
- Morris DP, Stevens RD, Wright DJ, Stafford DW. Processive post-translational modification. Vitamin K-dependent carboxylation of a peptide substrate. *J Biol Chem.* 1995;270(51):30491-30498.
- Cheung A, Engelke JA, Sanders C, Suttie JW. Vitamin K-dependent carboxylase: influence of the "propeptide" region on enzyme activity. *Arch Biochem Biophys.* 1989;274(2):574-581.
- Knobloch JE, Suttie JW. Vitamin K-dependent carboxylase. Control of enzyme activity by the "propeptide" region of factor X. *J Biol Chem.* 1987;262(32):15334-15337.
- Brown MA, Begley GS, Czerwicz E, et al. Precursors of novel Gla-containing conotoxins contain a carboxy-terminal recognition site that directs gamma-carboxylation. *Biochemistry.* 2005;44(25):9150-9159.
- Price PA, Fraser JD, Metz-Virca G. Molecular cloning of matrix Gla protein: implications for substrate recognition by the vitamin K-dependent gamma-carboxylase. *Proc Natl Acad Sci U S A.* 1987;84(23):8835-8839.
- Foster DC, Rudinski MS, Schach BG, et al. Propeptide of human protein C is necessary for gamma-carboxylation. *Biochemistry.* 1987;26(22):7003-7011.
- Vermeer C, Soute BA, Hendrix H, de Boer-van den Berg MA. Decarboxylated bone Gla-protein as a substrate for hepatic vitamin K-dependent carboxylase. *FEBS Lett.* 1984;165(1):16-20.
- Houben RJ, Rijkers DT, Stanley TB, et al. Characteristics and composition of the vitamin K-dependent gamma-glutamyl carboxylase-binding domain on osteocalcin. *Biochem J.* 2002;364(Pt 1):323-328.
- Stanley TB, Jin DY, Lin PJ, Stafford DW. The propeptides of the vitamin K-dependent proteins possess different affinities for the vitamin K-dependent carboxylase. *J Biol Chem.* 1999;274(24):16940-16944.
- Camire RM, Larson PJ, Stafford DW, High KA. Enhanced gamma-carboxylation of recombinant factor X using a chimeric construct containing the prothrombin propeptide. *Biochemistry.* 2000;39(46):14322-14329.
- Blosteim M, Cuerquis J, Landry S, Galipeau J. The carboxylation efficiency of the vitamin K-dependent clotting factors: studies with factor IX. *Haemophilia.* 2008;14(5):1063-1068.
- Rishavy MA, Berkner KL. Vitamin K oxygenation, glutamate carboxylation, and processivity: defining the three critical facets of catalysis by the vitamin K-dependent carboxylase. *Adv Nutr.* 2012;3(2):135-148.
- Tie JK, Jin DY, Straight DL, Stafford DW. Functional study of the vitamin K cycle in mammalian cells. *Blood.* 2011;117(10):2967-2974.
- Ndonwi M, Broze GJ Jr, Agah S, Schmidt AE, Bajaj SP. Substitution of the Gla domain in factor X with that of protein C impairs its interaction with factor VIIa/tissue factor: lack of comparable effect by similar substitution in factor IX. *J Biol Chem.* 2007;282(21):15632-15644.
- Wu S, Chen X, Jin DY, Stafford DW, Pedersen LG, Tie JK. Warfarin and vitamin K epoxide reductase: a molecular accounting for observed inhibition. *Blood.* 2018;132(6):647-657.
- Higgins-Gruber SL, Mutucumarana VP, Lin PJ, Jorgenson JW, Stafford DW, Straight DL. Effect of vitamin K-dependent protein precursor propeptide, vitamin K hydroquinone, and glutamate substrate binding on the structure and function of 42-glutamyl carboxylase. *J Biol Chem.* 2010;285(41):31502-31508.
- Bristol JA, Ratcliffe JV, Roth DA, Jacobs MA, Furie BC, Furie B. Biosynthesis of prothrombin: intracellular localization of the vitamin K-dependent carboxylase and the sites of gamma-carboxylation. *Blood.* 1996;88(7):2585-2593.
- Stanley TB, Humphries J, High KA, Stafford DW. Amino acids responsible for reduced affinities of vitamin K-dependent propeptides for the carboxylase. *Biochemistry.* 1999;38(47):15681-15687.
- Pezeshkpoor B, Czogalla KJ, Caspers M, et al. Variants in FIX propeptide associated with vitamin K antagonist hypersensitivity: functional analysis and additional data confirming the common founder mutations. *Ann Hematol.* 2018;97(6):1061-1069.
- Sekhri A, Lisinschi A, Furqan M, et al. The

- Conundrum of "Warfarin Hypersensitivity": Prolonged Partial Thromboplastin Time From Factor IX Propeptide Mutation. *Am J Ther*. 2016; 23(3):e911-915.
28. Chu K, Wu SM, Stanley T, Stafford DW, High KA. A mutation in the propeptide of Factor IX leads to warfarin sensitivity by a novel mechanism. *J Clin Invest*. 1996; 98(7):1619-1625.
 29. Ware J, Diuguid DL, Liebman HA, et al. Factor IX San Dimas. Substitution of glutamine for Arg-4 in the propeptide leads to incomplete gamma-carboxylation and altered phospholipid binding properties. *J Biol Chem*. 1989;264(19):11401-11406.
 30. Bentley AK, Rees DJ, Rizza C, Brownlee GG. Defective propeptide processing of blood clotting factor IX caused by mutation of arginine to glutamine at position -4. *Cell*. 1986;45(3):343-348.
 31. Ulrich S, Brand B, Speich R, Oldenburg J, Asmis L. Congenital hypersensitivity to vitamin K antagonists due to FIX propeptide mutation at locus -10: a (not so) rare cause of bleeding under oral anticoagulant therapy in Switzerland. *Swiss Med Wkly*. 2008;138(7-8):100-107.
 32. Aegerter C, Fontana S, Fux C, Demarmels Biasiutti F. Life threatening bleeding under adequate oral anticoagulation. Cases 4a, b. *Hamostaseologie*. 2003;23(3):113-116.
 33. Baker P, Clarke K, Giangrande P, Keeling D. Ala-10 mutations in the factor IX propeptide and haemorrhage in a patient treated with warfarin. *Br J Haematol*. 2000;108(3):663.
 34. Wojcik EG, Van Den Berg M, Poort SR, Bertina RM. Modification of the N-terminus of human factor IX by defective propeptide cleavage or acetylation results in a destabilized calcium-induced conformation: effects on phospholipid binding and activation by factor XIa. *Biochem J*. 1997;323 (Pt 3):629-636.
 35. de la Salle C, Charmantier JL, Ravanat C, et al. The Arg-4 mutant factor IX Strasbourg 2 shows a delayed activation by factor XIa. *Nouv Rev Fr Hematol*. 1993;35(5):473-480.
 36. Furie BC, Ratcliffe JV, Tward J, et al. The gamma-carboxylation recognition site is sufficient to direct vitamin K-dependent carboxylation on an adjacent glutamate-rich region of thrombin in a propeptide-thrombin chimera. *J Biol Chem*. 1997;272 (45):28258-28262.
 37. Hallgren KW, Hommema EL, McNally BA, Berkner KL. Carboxylase overexpression effects full carboxylation but poor release and secretion of factor IX: implications for the release of vitamin K-dependent proteins. *Biochemistry*. 2002;41(50):15045-15055.
 38. Wallin R, Martin LF. Early processing of prothrombin and factor X by the vitamin K-dependent carboxylase. *J Biol Chem*. 1988;263(20):9994-10001.
 39. Sanford DG, Kanagy C, Sudmeier JL, Furie BC, Furie B, Bachovchin WW. Structure of the propeptide of prothrombin containing the gamma-carboxylation recognition site determined by two-dimensional NMR spectroscopy. *Biochemistry*. 1991;30(41):9835-9841.
 40. Tie JK, Stafford DW. Functional Study of the Vitamin K Cycle Enzymes in Live Cells. *Methods Enzymol*. 2017;584:349-394.
 41. Bristol JA, Freedman SJ, Furie BC, Furie B. Profactor IX: the propeptide inhibits binding to membrane surfaces and activation by factor XIa. *Biochemistry*. 1994;33(47):14136-14143.
 42. Benton ME, Price PA, Suttie JW. Multi-site-specificity of the vitamin K-dependent carboxylase: in vitro carboxylation of des-gamma-carboxylated bone Gla protein and Des-gamma-carboxylated pro bone Gla protein. *Biochemistry*. 1995;34(29):9541-9551.
 43. Engelke JA, Hale JE, Suttie JW, Price PA. Vitamin K-dependent carboxylase: utilization of decarboxylated bone Gla protein and matrix Gla protein as substrates. *Biochim Biophys Acta*. 1991;1078(1):31-34.
 44. Theuwissen E, Cranenburg EC, Knapen MH, et al. Low-dose menaquinone-7 supplementation improved extra-hepatic vitamin K status, but had no effect on thrombin generation in healthy subjects. *Br J Nutr*. 2012;108(9):1652-1657.
 45. Kuwabara A, Fujii M, Kawai N, Tozawa K, Kido S, Tanaka K. Bone is more susceptible to vitamin K deficiency than liver in the institutionalized elderly. *Asia Pac J Clin Nutr*. 2011;20(1):50-55.
 46. Rejnmark L, Vestergaard P, Charles P, et al. No effect of vitamin K1 intake on bone mineral density and fracture risk in perimenopausal women. *Osteoporos Int*. 2006;17(8):1122-1132.
 47. Price PA, Kaneda Y. Vitamin K counteracts the effect of warfarin in liver but not in bone. *Thromb Res*. 1987;46(1):121-131.



Red blood cell metabolism in Rhesus macaques and humans: comparative biology of blood storage

Davide Stefanoni,¹ Hye Kyung H. Shin,² Jin Hyen Baek,² Devin P. Champagne,¹ Travis Nemkov,¹ Tiffany Thomas,³ Richard O. Francis,³ James C. Zimring,⁴ Tatsuro Yoshida,⁵ Julie A. Reisz,¹ Steven L. Spitalnik,³ Paul W. Buehler² and Angelo D'Alessandro^{1,6}

¹Department of Biochemistry and Molecular Genetics, University of Colorado Denver – Anschutz Medical Campus, Aurora, CO; ²Center for Biologics Evaluation and Research, Food and Drug Administration, Silver Spring, MD; ³Department of Pathology & Cell Biology, Columbia University, New York, NY; ⁴BloodWorks Northwest, Seattle, WA; ⁵Hemanext Inc, Lexington, MA and ⁶Department of Medicine, Division of Hematology, University of Colorado Denver – Anschutz Medical Campus, Aurora, CO, USA

Haematologica 2020
Volume 105(8):2174-2186

ABSTRACT

Macaques are emerging as a critical animal model in transfusion medicine, because of their evolutionary similarity to humans and perceived utility in discovery and translational science. However, little is known about the metabolism of Rhesus macaque red blood cells (RBC) and how this compares to human RBC metabolism under standard blood banking conditions. Metabolomic and lipidomic analyses, and tracing experiments with [1,2,3-¹³C₃]glucose, were performed using fresh and stored RBC (sampled weekly until storage day 42) obtained from Rhesus macaques (n=20) and healthy human volunteers (n=21). These results were further validated with targeted quantification against stable isotope-labeled internal standards. Metabolomic analyses demonstrated inter-species differences in RBC metabolism independent of refrigerated storage. Although similar trends were observed throughout storage for several metabolic pathways, species- and sex-specific differences were also observed. The most notable differences were in glutathione and sulfur metabolites, purine and lipid oxidation metabolites, acylcarnitines, fatty acyl composition of several classes of lipids (including phosphatidylserines), glyoxylate pathway intermediates, and arginine and carboxylic acid metabolites. Species-specific dietary and environmental compounds were also detected. Overall, the results suggest an increased basal and refrigerator-storage-induced propensity for oxidant stress and lipid remodeling in Rhesus macaque RBC cells, as compared to human red cells. The overlap between Rhesus macaque and human RBC metabolic phenotypes suggests the potential utility of a translational model for simple RBC transfusions, although inter-species storage-dependent differences need to be considered when modeling complex disease states, such as transfusion in trauma/hemorrhagic shock models.

Correspondence:

ANGELO D'ALESSANDRO
angelo.dalessandro@ucdenver.edu

PAUL W. BUEHLER,
Paul.Buehler@fda.hhs.gov

Received: June 19, 2019.

Accepted: October 10, 2019.

Pre-published: November 7, 2019.

doi:10.3324/haematol.2019.229930

Check the online version for the most updated information on this article, online supplements, and information on authorship & disclosures: www.haematologica.org/content/105/8/2174

©2020 Ferrata Storti Foundation

Material published in Haematologica is covered by copyright. All rights are reserved to the Ferrata Storti Foundation. Use of published material is allowed under the following terms and conditions:

<https://creativecommons.org/licenses/by-nc/4.0/legalcode>.

Copies of published material are allowed for personal or internal use. Sharing published material for non-commercial purposes is subject to the following conditions:

<https://creativecommons.org/licenses/by-nc/4.0/legalcode>,

sect. 3. Reproducing and sharing published material for commercial purposes is not allowed without permission in writing from the publisher.



Introduction

Rhesus macaques (*Macaca mulatta*, hereafter RM) are one of the most thoroughly studied non-human primates, in part because of their broad geographic distribution, reaching from Afghanistan and India, and across to China. In addition, RM evolutionarily diverged from human ancestors ~25 million years ago (by comparison, rodents and human ancestors diverged ~70 million years ago). Indeed, macaques share an average sequence identity of ~93% with *Homo sapiens*¹ and preclinical models often rely on macaques to investigate mechanisms and test interventions in the context of leading causes of human disease, including trauma/hemorrhagic shock,² human immunodeficiency virus,³ cancer, and cardiovascular disease.⁴ For example,

by metabolomic phenotyping plasma from rodents, swine, macaques, and humans,² hemorrhage in macaques was found to recapitulate human metabolic dysfunction in trauma⁵ more closely than other animal species. In transfusion medicine, the study of non-human primates facilitated a landmark discovery by Landsteiner and Wiener in the late 1930s, i.e., identification of the Rhesus blood group – after a factor found in Rhesus monkey blood.⁶

Red blood cell (RBC) transfusions can be modeled in animal species prior to pursuing costly and complex human clinical trials, or when human studies are deemed unethical (e.g., in acute radiation sickness). Nonetheless, animal modeling requires a rational approach toward species selection; in particular, blood group system diversity and variations in RBC physiology and biophysical properties across species/strains provide unique challenges when interpreting animal data in transfusion medicine. Additional complexity is introduced when refrigerated storage and blood component preservation are part of the experimental design.⁷ Refrigerated storage of RBC induces a series of biochemical and morphological modifications, collectively denoted “the storage lesion.”⁸ For example, stored RBC progressively lose their capacity to cope with oxidant stress,⁹ which is paralleled by their decreased ability to sustain energy metabolism.

Metabolic investigations of human RBC units stored using all currently licensed storage additives¹⁰⁻¹² helped to identify the impact of processing strategies (including leukoreduction¹³ and storage solutions¹⁴) on the molecular heterogeneity of stored units. Several factors complicate the study of the potential impact of “age of blood” on clinical outcomes.³ For example, units from some donors may store better than others for genetic, dietary, and/or environmental reasons, and the metabolic age of a RBC unit may differ from its chronological age.¹⁵ Findings from the Recipient Epidemiology and Donor evaluation Study (REDS-III) demonstrate donor-dependent heterogeneity in the propensity of RBC to hemolyze *in vitro* in response to storage duration, oxidative stress, and mechanical/osmotic insults.¹⁶ Therefore, improving RBC storage quality through increased understanding of RBC metabolism could enhance RBC quality for all donated units, independently of donor-specific factors, and improve transfusion outcomes overall.

Differences in storage quality become even more complex when comparing various animal species and strains; therefore, approximating human RBC function and storage outcomes is critical to pre-clinical, proof-of-concept studies. As such, it is important to use pre-clinical models of novel blood transfusion strategies that reliably approximate clinically relevant scenarios in humans. Although murine and canine models of blood storage and transfusion are available,¹⁷⁻²¹ macaques are generally perceived as a more relevant pre-clinical model,⁴ because of their evolutionary similarity to humans. For example, hematologic parameters in humans and RM are comparable. The RM hematocrit is $43 \pm 2\%$ in males and $41 \pm 2\%$ in females with corresponding hemoglobin levels of 13.1 ± 0.9 and 12.5 ± 0.2 g/dL, respectively.²² RM RBC distribution width and disc diameter are $13.0 \pm 0.7\%$ and $8 \mu\text{m}$, respectively, values similar to those of human RBC.²² Furthermore, the average life span of RM RBC is 98 ± 21 days,^{23,24} which is similar to that of human RBC (100-120 days), and significantly longer than that of murine RBC (55-60 days²⁵).

However, little is known about refrigerated storage of RM RBC under standard blood banking conditions. Although prior preliminary studies explored similarities and differences in the proteomes of fresh RBC from mice, humans, and macaques,²⁶ to the best of our knowledge, no previous study compared the metabolome and lipidome of human and RM RBC throughout 42 days of refrigerated storage. Thus, the current data provide a comparative analysis of RBC metabolic pathways and lipidomic changes occurring over time and identify dietary and environmental compounds unique to each species.

Methods

Extensive methodological details are provided in the *Online Supplementary Methods*.

Blood collection, processing and storage

Blood from 5-year old RM (n=20; 10 male/10 female) was collected into a syringe, using a 20 G needle, from the femoral vein under ketamine/dexmedetomidine (7 mg/kg/0.2 mg/kg) anesthesia according to the Food and Drug Administration (FDA) White Oak Animal Care and Use protocol 2018-31. All blood donor animals originated from the same colony located on Morgan Island, South Carolina and were naïve to experimentation at the time of blood collection.

The blood from 30- to 75-year old human volunteers (n=21; 11 male/10 female) was collected into a syringe, using a 16 G needle, from the median cubital vein under informed consent according to National Institutes of Health (NIH) study Institutional Research Board #99-CC-0168 “Collection and Distribution of Blood Components from Healthy Donors for In Vitro Research Use” under an NIH-FDA material transfer agreement. Blood was collected into acid citrate dextrose, leukofiltered, and stored in AS-3 in pediatric-sized bags, designed to hold 20 mL volumes, which mimicked the composition of standard full-sized units (i.e., incorporating polyvinylchloride and phthalate plasticizers).

The RBC were stored at 4-6°C for 42 days. The RBC and supernatants were separated via centrifugation upon sterile sampling of each unit on days 0, 7, 14, 21, 28, 35, and 42.

Ultra-high pressure liquid chromatography - mass spectrometry metabolomics and lipidomics

Frozen RBC aliquots of 50 μL volume were extracted 1:10 in ice-cold extraction solution (methanol:acetonitrile:water 5:3:2).²⁷ Samples were vortexed and insoluble material pelleted, as described elsewhere.²⁸ Analyses were performed using a Vanquish UHPLC coupled online to a Q Exactive mass spectrometer (Thermo Fisher, Bremen, Germany). Samples were analyzed using a 3 min isocratic condition²⁹ or a 5, 9, and 17 min gradient, as described previously.^{30,31} Additional analyses, including untargeted analyses and fragment ion search (FISH) score calculation via mass spectrometry,² were performed with Compound Discoverer 2.0 and LipidSearch (Thermo Fisher, Bremen, Germany). For targeted quantitative experiments, extraction solutions were supplemented with stable isotope-labeled standards, and endogenous metabolite concentrations were quantified against the areas calculated for heavy isotopologues for each internal standard.^{30,31} Graphs and statistical analyses (either a *t*-test or repeated measures analysis of variance) were prepared with GraphPad Prism 5.0 (GraphPad Software, Inc, La Jolla, CA, USA), GENE E (Broad Institute, Cambridge, MA, USA), and MetaboAnalyst 4.0.³²

Results

Fresh red blood cells from macaques and humans differ metabolically

Metabolomic analyses were performed on leukocyte-filtered, fresh (day 0) RBC from healthy human volunteers (n=21) and RM (n=20) (Figure 1A; *Online Supplementary Table S1*). Significant differences between species were determined by partial least squares-discriminant analysis, *t*-test-informed hierarchical clustering, and volcano plots (Figure 1B-D, respectively). Significant changes were noted in the levels of purines (e.g., hypoxanthine, urate), arginine and sulfur metabolites (e.g., glutathionylcysteine, glutathione, phytochelatins), carnitines, and xenometabolites (e.g., caffeine) in fresh RBC from the two species (Figure 1D). In the light of these changes, correlation analyses (Spearman) were performed across all metabolites to define the level of metabolic linkage in RBC from either species (Figure 1E). Identifying correlates in one species (e.g., macaques), disruptions of such correlations, and generation of novel correlations indicate metabolic rewiring (Figure 1F, from left to right). These measurements can then be used to subtract the correlations observed for every pair of metabolites in each species, resulting in a differential heat map (Figure 1F, rightmost panel). This map highlights pathways that are preserved (Figure 1G, leftmost panel), and those that undergo metabolic rewiring in RBC from these species (>30% Δr between species, $P < 0.05$), such as those involving glutathione homeostasis, sulfur, purine, carboxylic acid, and arginine metabolism (Figure 1G).

Metabolic tracing experiments with [1,2,3-¹³C₃]glucose in fresh human or macaque red blood cells

In light of metabolic differences in glutathione homeostasis observed at steady state, we hypothesized that species-specific alterations of glucose fluxes affect the NADPH-generating pentose phosphate pathway (PPP). NADPH is required to preserve RBC redox homeostasis by favoring reduction of glutathione and other reversibly oxidized thiols. To test this hypothesis, leukoreduced RBC lysates from RM (n=20) and humans (n=21) were incubated with [1,2,3-¹³C₃]glucose for 1 h at 37°C (Figure 2). This allows comparisons of ¹³C incorporation through glycolysis (+3 isotopologues) and the PPP (+2) in RM and human RBC at steady state (Figure 2; *Online Supplementary Figure S1*), as described previously.^{9,33} Importantly, RM and human RBC showed similar rates of glucose consumption, along with comparable levels of the glycolytic products pyruvate and lactate, in the absence of any apparent preference in glycolysis/PPP fluxes (*Online Supplementary Figure S1*). However, early steps of glycolysis showed significantly different rates between these species, with higher levels of ¹³C₃-glucose 6-phosphate (and hexose phosphate isobars) in human RBC and higher levels of ¹³C₃-fructose biphosphate in RM (Figure 2). RM RBC showed significantly higher levels of ¹³C accumulation in intermediates of the glyoxylate pathway (e.g., ¹³C₃-methylglyoxal and ¹³C₃- and ¹³C₅-lactoyl-glutathione) and late PPP products (e.g., ¹³C₂-ribose), but lower levels of labeled glutathione and purines (e.g., ¹³C₂-AMP) (Figure 2). Further focusing on reducing equivalents,³⁴ there were species-specific preferences in substrates used to generate carboxylic acids, with ¹³C₃-malate preferred in RM and ¹³C₂-malate in humans (Figure 2).

Interspecies comparison of the red blood cell metabolome during refrigerated storage

Metabolomic analyses were performed on 574 samples of stored RBC and supernatants from RM and humans (Figure 3A; *Online Supplementary Table S1*). Partial least squares-discriminant analysis of RBC data showed significant species- and time-dependent clustering of these samples across principal component 1 (28.8% of total variance) and principal component 2 (18.6%), respectively (Figure 3B). The Venn diagram in Figure 3C, D shows the number of significant metabolites by repeated measures two-way analysis of variance and related pathway analyses. Hierarchical clustering analyses further highlighted significant storage- and species-dependent differences (Figure 3E; a vectorial version of this figure, including metabolite names, is provided in *Online Supplementary Figure S2*).

Targeted metabolomic analyses were accompanied by untargeted metabolomic analyses (*Online Supplementary Figure S3A-D*). Interestingly, these analyses expanded on the targeted metabolomic data by highlighting species-specific changes in levels of xenometabolites stored RBC (*Online Supplementary Figure S3E*) derived from personal habits (e.g., cotinine from smoking in 2 of 21 donors), chemical exposure (e.g., aniline, nitrosopiperidine), therapeutic drugs (e.g., acetaminophen, in 2 subjects), and diet (e.g., caffeine and theophylline in humans; methyl-histidine, phloionic acid, lupinine, gallic acid, azelaic acid, and asarone in RM).

Although limited by the relatively small numbers of male and female human and RM donors evaluated, a preliminary breakdown by sex identified a significant impact in RM, especially regarding carboxylic acid, arginine, fatty acid, and purine metabolism (*Online Supplementary Figure S4A-D*).

Species-specific differences in metabolic phenotypes of stored red blood cells

Significant differences were observed in RBC levels of sulfur-containing metabolites involved in one-carbon and glutathione metabolism (Figure 4), including taurine, S-adenosylmethionine (SAM), cysteine, cystathionine, and glutathione [both reduced (GSH) and oxidized (GSSG)]; all were higher in RM than human RBC throughout storage, except GSH. Increased glutathione pools and activation of the gamma-glutamyl cycle, ascorbate metabolism, and glutaminolysis were observed in RM, as compared to human, RBC (Figure 4). These observations were not accompanied by significantly different levels of PPP intermediates (except for higher levels of the non-oxidative phase PPP metabolite sedoheptulose phosphate in humans). However, in contrast to what was observed in fresh RBC, stored RM RBC showed higher levels of intracellular glucose in supernatants and cells (Figure 4), despite comparable levels of intracellular and supernatant levels of lactate (i.e., ~10% increase in RM, $P < 0.05$) (*Online Supplementary Table S1*). Of note, human RBC showed lower levels of 2,3-diphosphoglycerate, but higher levels of ATP, during the first 2 weeks of storage (Figure 4).

Expanding on these observations, a deeper focus on purine metabolism revealed significantly higher levels of all purines and purine-containing metabolites in RM RBC. However, dramatic species-specific changes in purine oxidation metabolites were observed (Figure 5A), with RM RBC showing significantly higher levels of hypoxanthine (accumulating during storage in both species) and human

RBC showing significantly higher levels of urate and hydroxyisourate (decreasing during storage).

Purine oxidation and salvage of deaminated purines involve using the amine group from aspartate through a reaction that generates fumarate, a minimally active pathway in mature RBC.³⁵ Consistent with dysregulation of purine oxidation and salvage, species-specific changes in the levels of aspartate (higher in RM) and fumarate (higher in humans) were noted, suggesting a decreased rate of salvage reactions in RM RBC (Figure 5B). Similarly, RBC lev-

els of some carboxylic acids (e.g., malate, 2-hydroxyglutarate) were higher in humans, whereas others (e.g., citrate, α -ketoglutarate, succinate, oxaloacetate, itaconate) were higher in RM (Figure 5B), suggesting species-specific differences in transamination reactions (e.g., those dependent on the activity of alanine and aspartate aminotransferases) or carboxylic acid metabolism via cytosolic isoforms of Krebs cycle enzymes, all of which are active in mature RBC.^{34,36-38}

In cells with mitochondria, carboxylate metabolism is

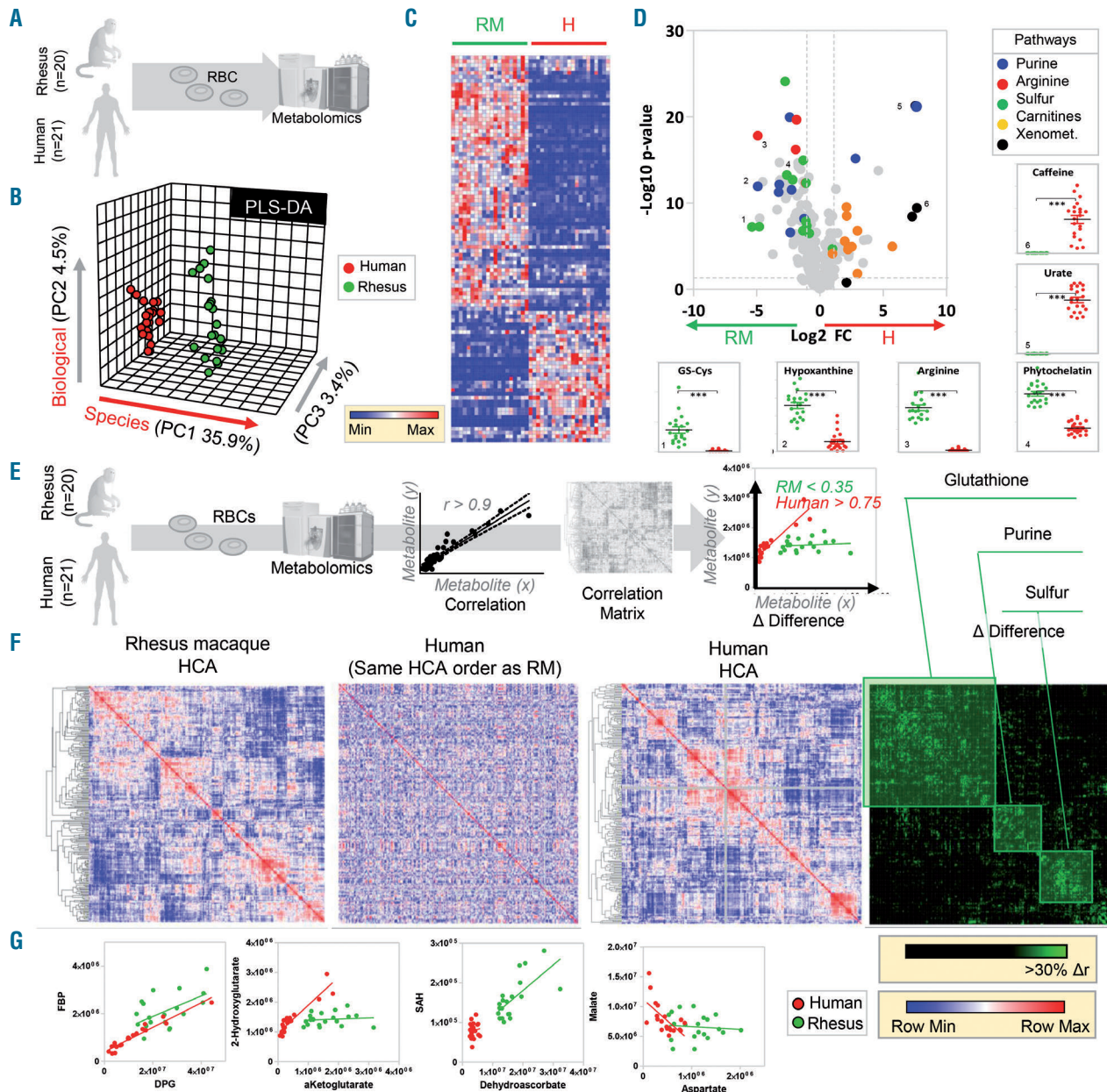


Figure 1. Metabolomics of fresh red blood cells from healthy human volunteers and Rhesus macaques. (A) An overview of the experimental design. (B) Partial least square-discriminant analysis (PLS-DA) of red blood cells from 21 humans (red) or 20 Rhesus macaques (RM) (green). (C) An overview of the metabolites that were significantly different between the two groups (a vectorial version of the heat map is provided in *Online Supplementary Figure S2*). (D) A volcano plot highlighting the major pathways differing between humans (red) and RM (green). (E) Metabolite levels were correlated among each other (Spearman) in humans (red) and RM (green). (F) These correlations were used to map hierarchical clustering profiles in RM and humans. RM and human RBC showed significantly different metabolic correlation maps. Metabolites whose linear correlations differed significantly between species ($>30\% \Delta r$ between species, $P < 0.05$) are highlighted in the rightmost panel in (F). (G) Some representative examples of correlations that are preserved (left) or lost (other panels) between species. PC: principal component; RBC: red blood cells; DPG: 2,3-diphosphoglycerate; HCA: hierarchical clustering analysis.

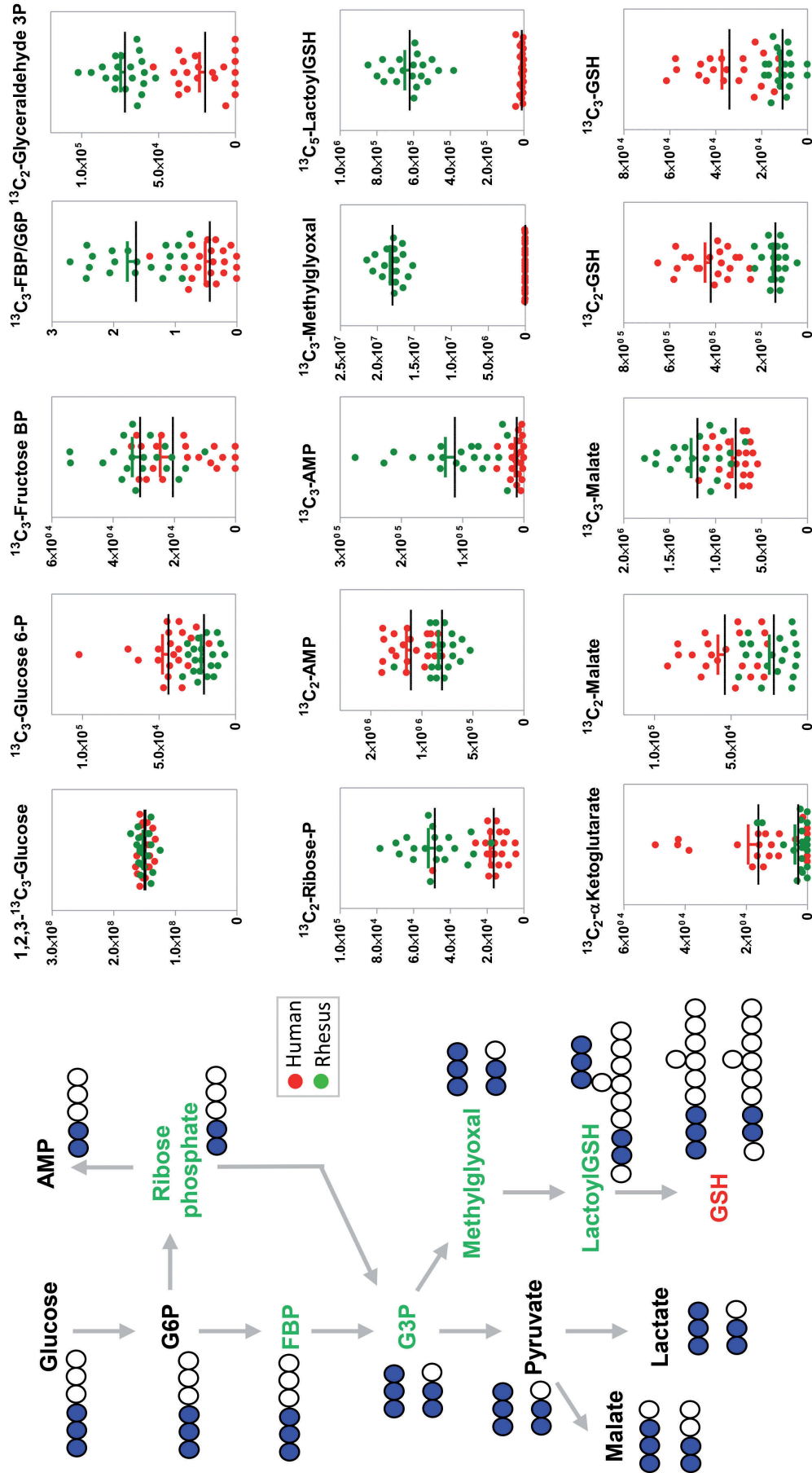


Figure 2. Metabolic tracing experiments with [1,2,3- ^{13}C]-glucose in human or Rhesus macaque red blood cells. Incubation with the tracer for 1 h at 37°C allowed comparisons of the rate of ^{13}C incorporation through glycolysis (+3 isotopologues) and the pentose phosphate pathway (PPP) (+2) in red blood cells from Rhesus macaques (green) and humans (red) at steady state. Rhesus macaque red blood cells showed significantly higher levels of ^{13}C accumulation in intermediates of the glyoxylate pathway and late PPP products, but lower levels of labeled glutathione and purines. GSH: glutathione

intertwined with the urea cycle, which is incomplete in mitochondria-devoid mature RBC. Arginine metabolism differed significantly between human and RM RBC, the latter having significantly higher RBC (and supernatant) levels of arginine, but with significantly lower levels of citrulline, ornithine, and creatine (Figure 5B). Although RM RBC had higher levels of polyamines (including sper-

midine), these increases (10-20% by storage day 42; $P < 0.0025$) were not sufficient to explain the >100-fold increase in arginine levels in RM RBC. However, comparable fold-change increases in asymmetric dimethylarginine (and isobaric isomers) were noted in RM RBC, as seen by untargeted metabolomics (Online Supplementary Figure S3C).

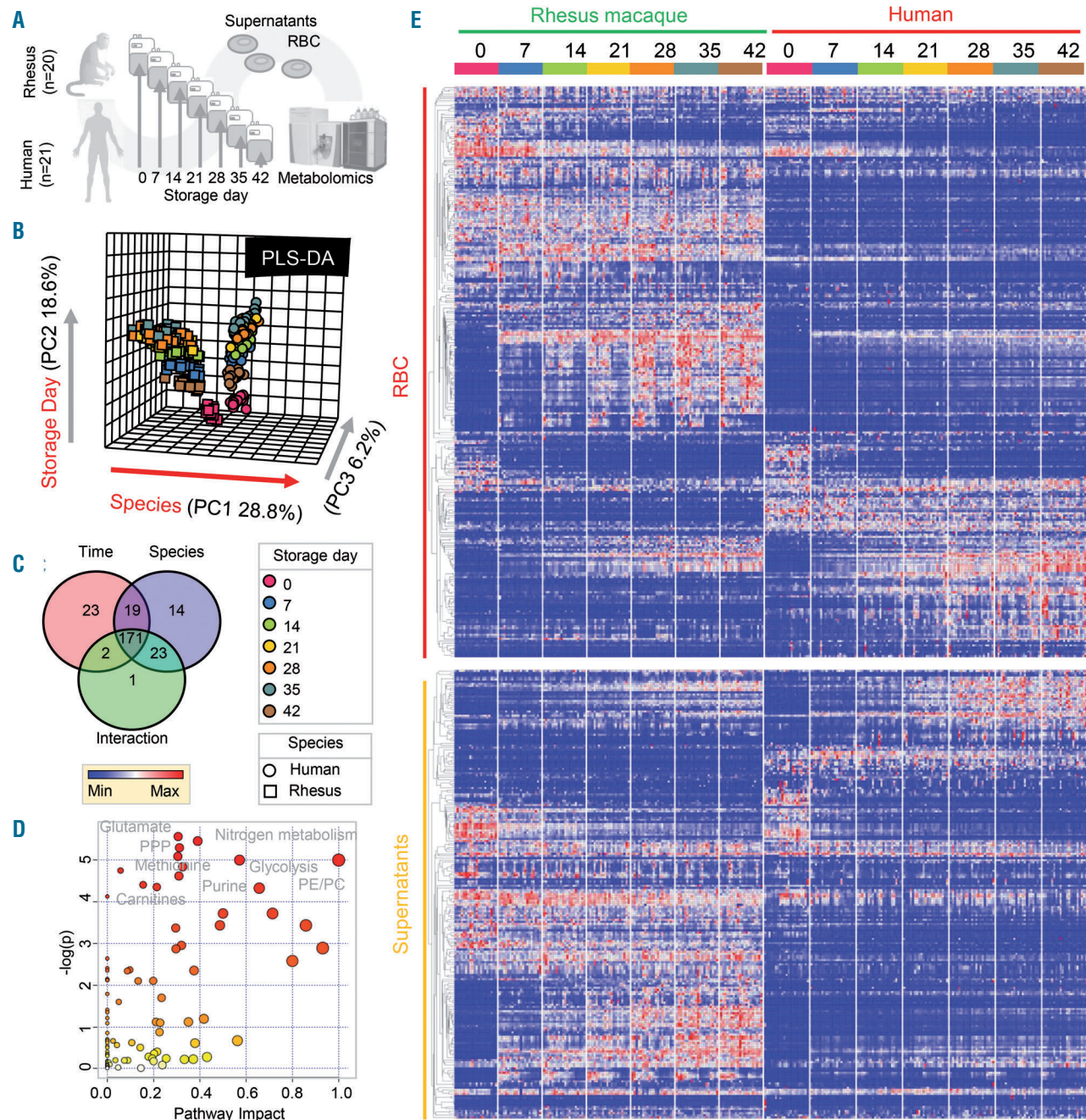


Figure 3. Interspecies comparison of the red blood cell metabolome during refrigerated storage. (A) Comparison of the metabolome of red blood cells (RBC) from humans and Rhesus macaques (RM). (B) Partial least squares-discriminant analysis (PLS-DA) shows significant species- and time-dependent clustering of samples across principal components (PC1 and PC2, respectively). (C, D) Venn diagram (C) showing the number of significant metabolites by repeated measures two-way analysis of variance and related pathway analyses (D). (E) A heat map showing significant metabolic changes in stored RBC and supernatants as a function of storage duration in humans and RM. A vectorial version of this figure is provided in Online Supplementary Figure S2.

Storage-induced lipid remodeling and oxidant damage of membrane lipids is higher in Rhesus macaque, as compared to human, red blood cells

Interestingly, untargeted analyses revealed significantly higher levels of diethylhexyl-, monoethylhexyl- and free phthalate plasticizers in RM RBC as a function of storage (*Online Supplementary Figure S3*). Since both human and RM RBC samples were stored in the same polyvinylchloride units under identical conditions, we hypothesize that these results could, at least in part, be explained by differential species-specific storage-dependent membrane dynamics. Further analyses of targeted metabolomic data indicated that RBC acylcarnitines increased with storage duration. RM RBC were characterized by higher levels of short and medium chain acylcarnitines (C2-12), and lower levels of long and very-long acylcarnitines (C16-22

or longer), as compared to human RBC (Figure 6). Similarly, free fatty acids (medium and long-chain, but not very long-chain fatty acids) were higher in RM RBC (Figure 6), along with higher levels of sphingosine 1-phosphate and lipid peroxidation products, including 4-hydroxynonenal (4-HNE) and its glutathionylated form (GS-HNE). Consistent with increased oxidant stress in stored RM RBC, along with tracing experiments in fresh RBC (Figure 2), RM RBC showed significantly higher storage-dependent increases in lactoyl-glutathione levels (Figure 6).

To expand on these observations, untargeted lipidomic analyses were performed on fresh (day 0) and end of storage (day 42) RM and human RBC (summarized by lipid classes in *Online Supplementary Figure S5* and volcano plots in *Online Supplementary Figure S6A, B*). Notably,

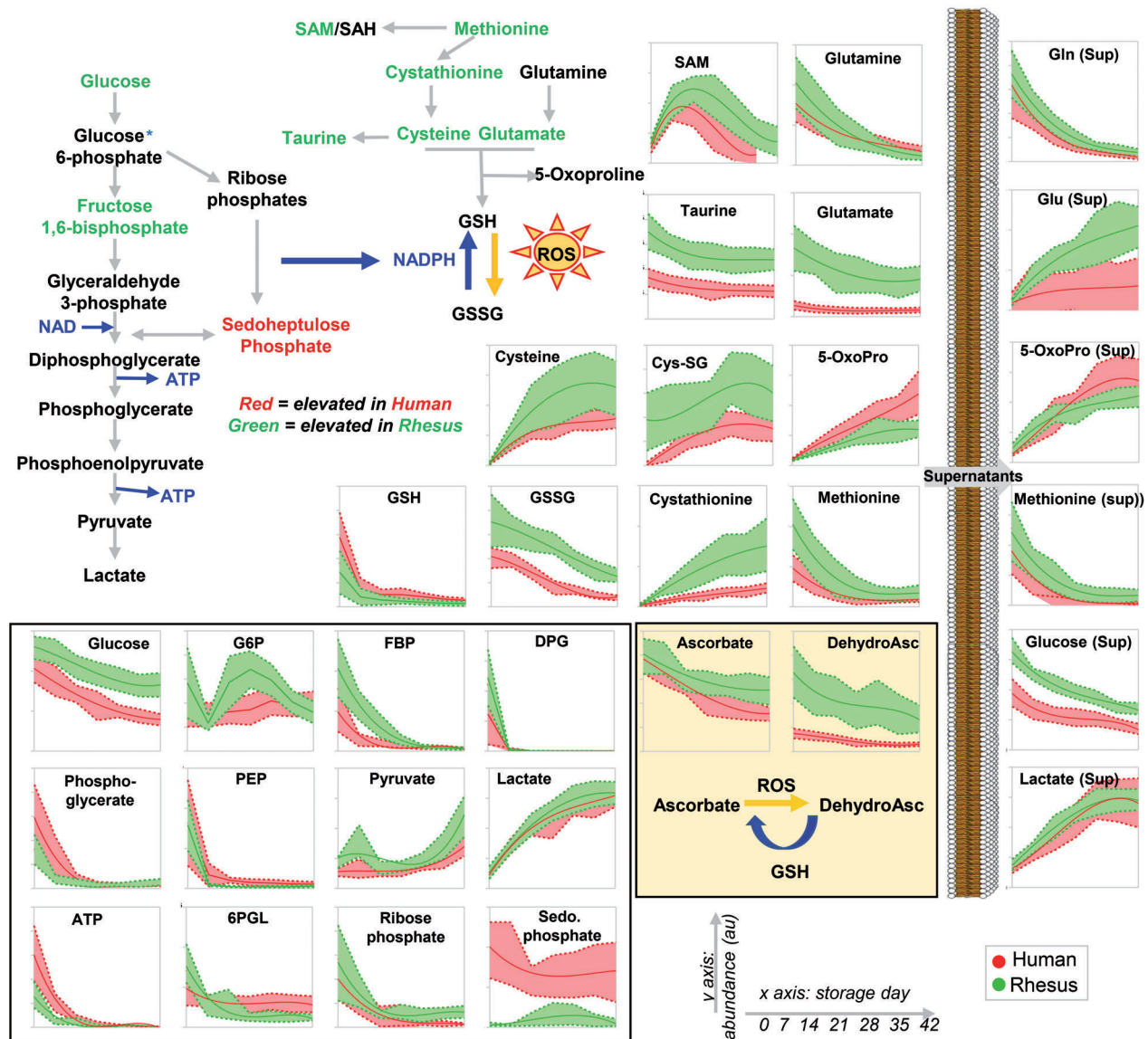


Figure 4. Species- and storage time-specific metabolic changes in Rhesus macaque and human red blood cells: focus on glycolysis, the pentose-phosphate pathway, glutathione, and one-carbon homeostasis. Data for Rhesus macaques are shown in green, those for humans are represented in red. Supernatant metabolites are shown in the right-hand side of the figure, outside the representative lipid bilayer of the cellular membrane.

fresh and stored RM RBC had significantly higher levels of most phosphatidylserines (*Online Supplementary Figure S6C-E*) and short/medium-chain, but not long and very-long chain, fatty acyl-phosphatidylethanolamines (*Online Supplementary Figure S6F, G*).

Validation using targeted quantitative metabolomics and lipidomics

The initial, global approach generated extensive, but relative, quantification data for several pathways. To confirm critical observations, we performed validation exper-

iments on all RBC and supernatant samples using targeted quantitative methods with stable isotope-labeled internal standards (Figure 7A). Results are reported in tabular and vectorial formats (*Online Supplementary Table S2* and *Online Supplementary Figure S7*). There was a substantial overlap ($r^2 > 0.75$) between relative and absolute values for critical metabolites in amino acid, redox (glutathione and purine oxidation), and fatty acid metabolic pathways, which demonstrated significant differences between the two species as a function of storage duration (Figure 7B-F) and sex (*Online Supplementary Figure S4E-G*).

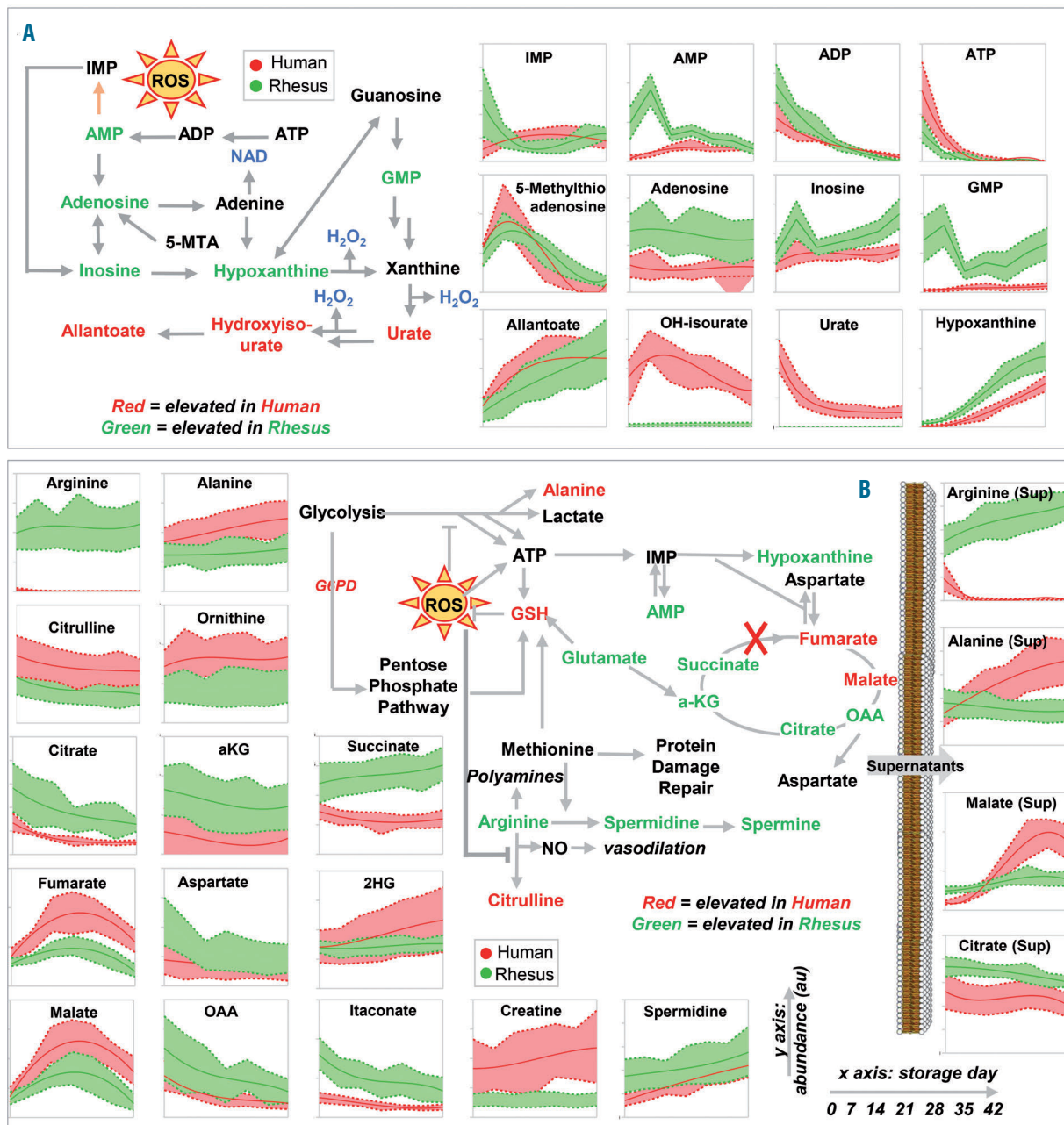


Figure 5. Species- and storage time-specific metabolic changes in Rhesus macaque and human red blood cells and supernatants: focus on purine metabolism, urea cycle, and carboxylate metabolism. (A, B) Data for Rhesus macaques are shown in green, those for humans are represented in red. Supernatant metabolites are shown in the right-hand side of panel (B), outside the representative lipid bilayer of the cellular membrane.

Discussion

Over the past two decades, animal models have helped to identify potential mechanisms critical to RBC storage biology and transfusion outcomes. Murine and canine models of RBC storage and transfusion were critical in identifying (i) etiological contributions to transfusion-related acute lung injury, including the two-hit model;³⁹ (ii) the impact of storage duration on mortality,²¹ and (iii)

the role that iron overload plays in increasing the risk of septic complications.¹⁹ These models have limited genetic variability and a more homogeneous exposome than humans. This controlled strain-specific heterogeneity of genetic background in rodent models enables mechanistic studies to identify genetic and metabolic contributors to RBC storage quality and the post-transfusion performance of the RBC.^{17,18} In addition, animal models can be modified in a controlled fashion to allow for selective

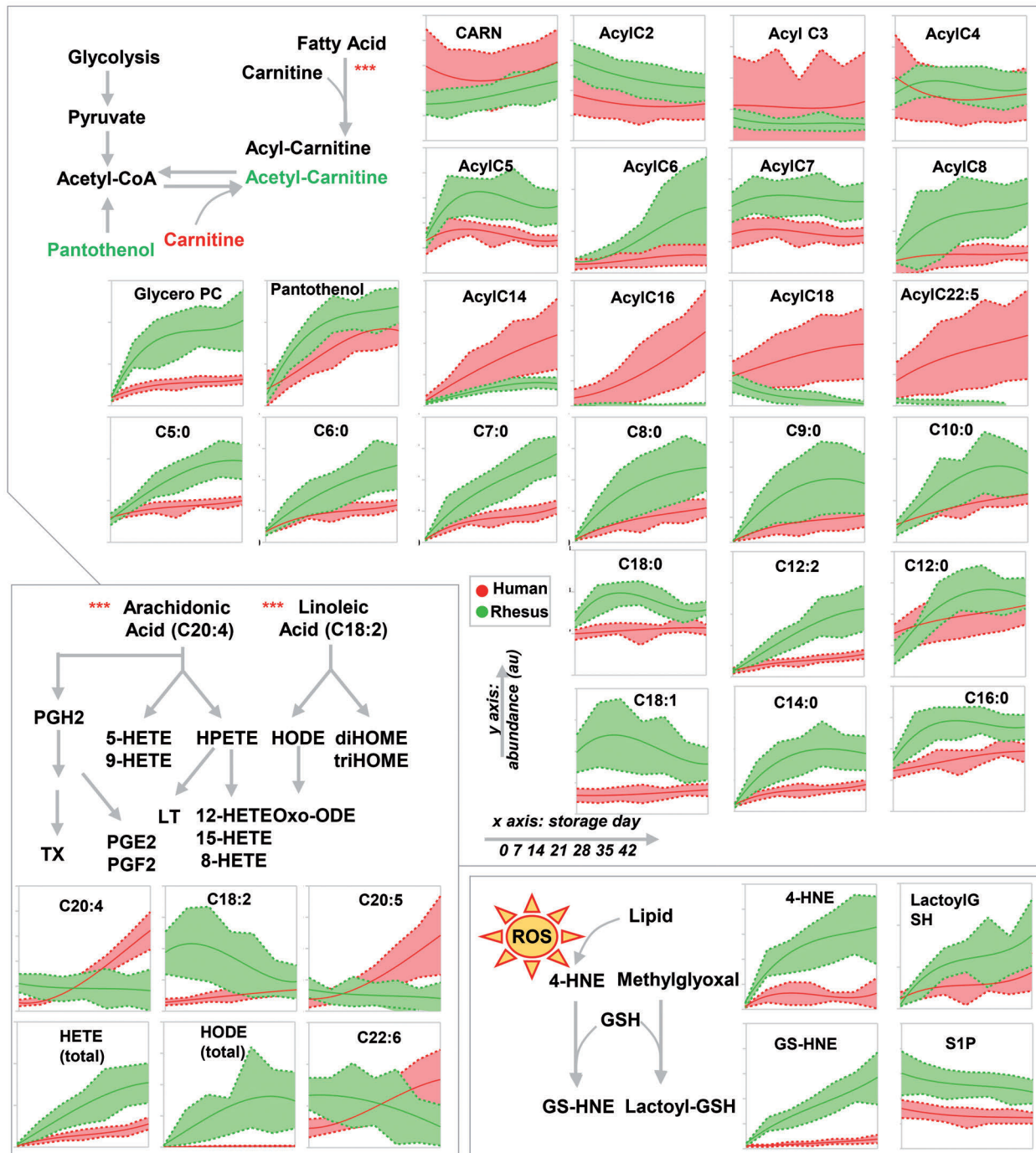


Figure 6. Species- and storage time-specific metabolic changes in Rhesus macaques and human red blood cells: focus on acyl-carnitines, free fatty acid metabolism, and lipid peroxidation products. Data for Rhesus macaques are shown in green, those for humans are represented in red.

genetic, pharmacological, dietary, or surgical interventions, which are difficult, and sometimes impossible, to achieve with humans. Given their phylogenetic similarity to humans, RM may provide a particularly relevant RBC storage and transfusion model. For example, RM demon-

strate similar pathobiology and metabolic derangements common to human trauma patients.²

By combining state-of-the-art targeted and untargeted metabolomics and lipidomics, as well as tracing experiments with [1,2,3-¹⁵C₃]glucose, the present study shows

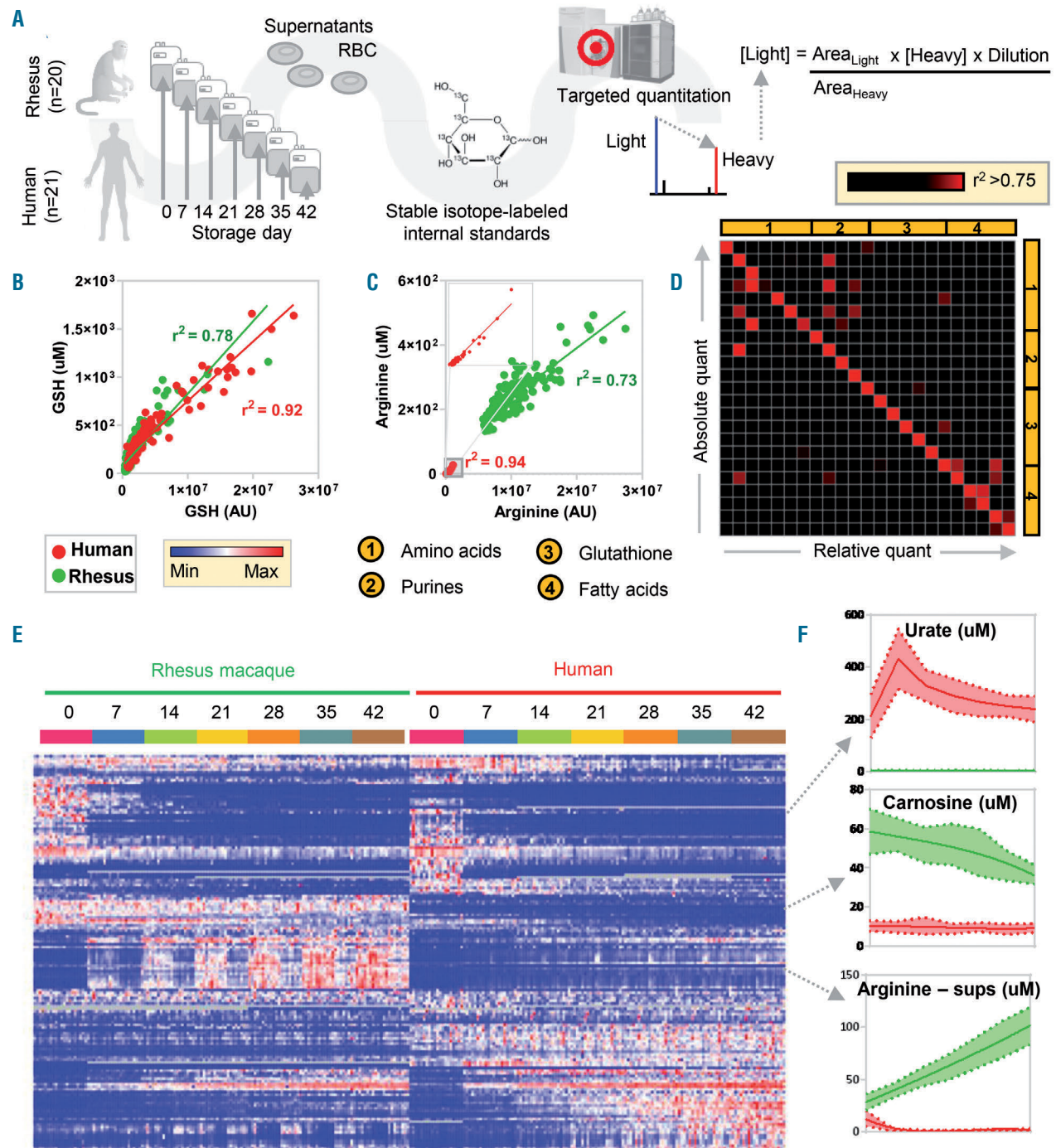


Figure 7. Validation experiments on red blood cells and supernatants. (A) Validation via targeted quantitative mass spectrometry-based measurements against stable isotope-labeled internal standards. (B, C) There was a substantial overlap of relative and absolute quantitative measurements for both metabolites showing similar interspecies concentrations (e.g., glutathione – GSH (B) and significantly different interspecies levels (e.g., arginine) (C). This is further exemplified in (D), in which red dots in the heat map show metabolites from different pathways (including amino acids, glutathione homeostasis, purines, and fatty acids), whose measurements by either method correlated significantly ($r^2 > 0.75$). (E) Notably, significant metabolic changes during storage, illustrated in the heat map, recapitulate the relative quantification measurements in Figure 1 and related supplements. For example, quantitative measurements of urate, carnosine, and arginine are consistent with respective measurements from the exploratory analysis. All measurements are provided in tabular form in *Online Supplementary Table S2* and in vectorial form in *Online Supplementary Figure S7*.

that fresh and stored human and RM RBC have comparable glycolytic and PPP fluxes. However, RM RBC have higher baseline levels of glutathione oxidation and turnover (i.e., the gamma-glutamyl cycle), along with increased transamination reactions (e.g., higher levels of glutamine, aspartate, alanine, and glutamate) and sulfur metabolism (e.g., cysteine, taurine, and SAM). Glutathionylated lipid and sugar oxidation products (e.g., GS-HNE and lactoyl-glutathione) suggest that increased sulfur metabolism in this species could result from enhanced basal oxidant stress and/or decreased activity of the deglutathionylation protein machinery. These results were confirmed by tracing experiments, highlighting significant activation of the glyoxylate pathway in RM, as compared to human, RBC; this pathway is usually associated with oxidant stressors (e.g., diabetes⁴⁰). Alternatively, this observation suggests that evolution has driven species-specific changes in sulfur metabolism resulting from sulfur-rich diets in the wild, as suggested by increased plant-derived⁴¹ phytochelatin in RM RBC. Combining targeted and untargeted metabolomics identified additional dietary metabolites of plant origin in RM, supporting a significant impact of diet on the molecular composition of their RBC. Based on this observation, one could test whether differences in free fatty acids, fatty acyl composition of carnitines and phosphatidylethanolamines (but not phosphatidylserines) in RM RBC result from differing fatty acyl contents of their dietary lipids, as compared to humans. Since fatty acyl-conjugation to carnitines depends on high-energy ATP and co-enzyme A availability, and is involved in lipid damage repair, one could speculate that differential levels of acyl-carnitines in humans and RM could be explained by a differential species-specific capacity to preserve ATP stores or prevent/repair lipid damage during storage. In this view, species-specific differences in carnitine metabolism suggest a differential impact of storage on membrane phospholipid homeostasis.⁴² Such phenomena may be explained, in part, by simply considering that the RBC storage additive used here was designed to optimize human RBC storage. Higher phosphatidylserine levels in RM RBC suggest the potential for increased erythrophagocytosis by mononuclear phagocytes; this could be tested by post-transfusion RBC recovery studies. Nonetheless, the present study assessed the total RBC phosphatidylserine content, rather than its cellular compartmentalization (i.e., exposure on the RBC membrane outer leaflet⁴³). On the other hand, phthalate plasticizers, which accumulate up to millimolar levels in human RBC by the end of storage, appeared to be present at even higher levels in RM RBC, despite virtually identical storage conditions; one possible explanation, consistent with the current data, is an increase in lipid oxidation and remodeling in RM RBC.

Xenometabolites, including environmental and dietary metabolites, can affect RBC integrity. Interestingly, all human blood donors in this study consumed caffeine (a purine metabolite that could modulate stored RBC metabolism via signaling through adenosine receptors⁴⁴), based on detecting the parent compound and its metabolites. Additionally, cotinine (a nicotine metabolite and marker of smoking⁴⁵) was detected in two of 21 donors, similar to the overall smoking incidence in USA donors (14% in 2017). Similarly, metabolites of chemical exposure, such as aniline, were only detected in human donor RBC, with broad inter-donor variability.

Sex-specific signatures were detected, especially in RM,

consistent with recent observations about the potential impact of sex on RBC storability and capacity to cope with oxidant and osmotic stressors; these parameters appear to be improved in female donor RBC.^{16,46} Metabolic pathways affected by sex include arginine, carboxylic acid metabolism, and purine oxidation, which were validated using targeted quantitative measurements.

Perhaps the study's most interesting finding is that purine oxidation products were all higher in RM, as compared to human, RBC, except for the antioxidant urate.⁴⁷ This is particularly relevant in light of the recently described role of ATP breakdown and oxidation products upstream of urate (e.g., hypoxanthine as a critical marker of post-transfusion recovery in humans³⁵). Similarly, arginine and asymmetric dimethylarginine (isobaric isomers could not be resolved in this study) were >100-fold higher in RM RBC throughout storage. This suggests that RM RBC have an altered capacity for metabolizing arginine to ornithine or citrulline via arginase and nitric oxide synthase, a phenomenon previously connected to a potential impact of blood storage and transfusion on nitric oxide metabolism and transfusion-related vasodilatory capacity.⁴⁸

There are limitations to the study despite our attempt to keep blood experimental conditions constant between RM and humans. For example, blood collection from RM required mild anesthesia/sedation with ketamine-dexmedetomidine. In one study, anesthetics and sedatives alone or in combination transiently increased circulating glucose levels and promoted insulin resistance (within the hour after dosing).⁴⁹ Although we are unaware of any association between donor age and RBC storage quality, the RM RBC evaluated in this study were donated by adolescent or young adult animals, whereas the human donors represented the general age range of individuals volunteering for blood donation. The RM RBC were collected from animals originating on Morgan Island, South Carolina, whose ancestors were transferred from the Caribbean Primate Research Center in Puerto Rico in 1979-1980. The Morgan Island RM form a large, free-ranging colony, with more than 4,000 animals and ~75% female predominance.⁵⁰ The colony comprises animals that descended from India with little or no known Chinese RM introgression. Although most large national primate research centers in the USA conduct extensive genetic testing of animals in their care to promote gene flow, diverse genetic composition remains a challenge. Conversely, little genetic testing was performed on the Morgan Island colony. Nonetheless, although it is not expected that mixed Chinese-India hybrid animals occur there, it is likely that this colony experiences some genetic drift and genetic homozygosity due to the potential for inbreeding.

Conclusion

By describing the metabolic landscape of human and RM RBC throughout 42 days of refrigerated storage, we identified storage-, diet-, and sex-specific metabolites that may affect human biology and the potential translatability of future pre-clinical studies using RM as a model for RBC storage and transfusion. Although species-specific differences were certainly anticipated, identifying molec-

ular similarities and differences in metabolic phenotypes of fresh and stored RBC when comparing these two species will inform the appropriateness of RM as a model in transfusion medicine and, specifically, of RBC storage in the context of specific interventions (e.g., testing novel storage additives). As such, our results suggest that several metabolic pathways in RM RBC overlap those in human RBC at baseline and during storage. This assessment of comparative RBC biology will likely be relevant in pre-clinical and clinical transfusion medicine and hematology. Nonetheless, clear differences emerged in this initial comparison, which provide opportunities for

further investigation of uniquely different biochemical pathways that affect RBC under baseline conditions and during refrigerated storage.

Acknowledgments

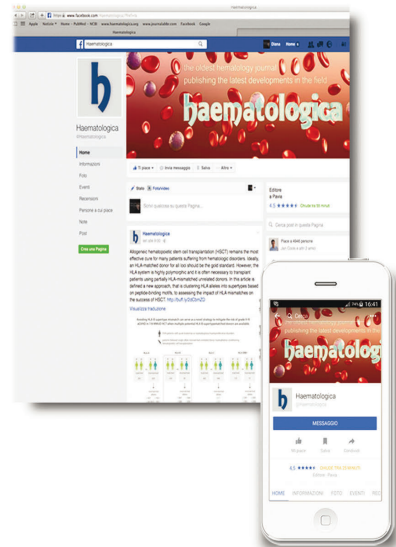
Research reported in this publication was supported by funds from the Boettcher Webb-Waring Investigator Award (to ADA), RM1GM131968 from the National Institute of General and Medical Sciences (to ADA), R01HL146442 (to ADA) and R01HL148151 (to SLS, ADA, and JCZ) from the National Heart, Lung and Blood Institutes (to ADA) and a Shared Instrument grant from the National Institute of Health (S10OD021641).

References

- Rhesus Macaque Genome Sequencing and Analysis Consortium, Gibbs RA, Rogers J, et al. Evolutionary and biomedical insights from the rhesus macaque genome. *Science*. 2007;316(5822):222-234.
- Reisz JA, Wither MJ, Moore EE, et al. All animals are equal but some animals are more equal than others: plasma lactate and succinate in hemorrhagic shock - a comparison in rodents, swine, nonhuman primates, and injured patients. *J Trauma Acute Care Surg*. 2018;84(3):537-541.
- Hatzioannou T, Ambrose Z, Chung NPY, et al. A macaque model of HIV-1 infection. *Proc Natl Acad Sci U S A*. 2009;106(11):4425-4429.
- Lankau EW, Turner PV, Mullan RJ, Galland GG. Use of nonhuman primates in research in North America. *J Am Assoc Lab Anim Sci*. 2014;53(3):278-282.
- D'Alessandro A, Moore HB, Moore EE, et al. Early hemorrhage triggers metabolic responses that build up during prolonged shock. *Am J Physiol Regul Integr Comp Physiol*. 2015;308(12):R1034-1044.
- Schwarz H, Dörner F, Karl Landsteiner and his major contributions to haematology. *Br J Haematol*. 2003;121(4):556-565.
- Waterman HR, Kapp LM, Howie HL, et al. Analysis of 24-h recovery of transfused stored RBCs in recipient mice of distinct genetic backgrounds. *Vox Sang*. 2015;109(2):148-154.
- Yoshida T, Prudent M, D'Alessandro A. Red blood cell storage lesion: causes and potential clinical consequences. *Blood Transfus*. 2019;17(1):27-52.
- Reisz JA, Wither MJ, Dzieciatkowska M, et al. Oxidative modifications of glyceraldehyde 3-phosphate dehydrogenase regulate metabolic reprogramming of stored red blood cells. *Blood*. 2016;128(12):e32-42.
- D'Alessandro A, Reisz JA, Culp-Hill R, et al. Metabolic effect of alkaline additives and guanosine/gluconate in storage solutions for red blood cells. *Transfusion*. 2018;58(8):1992-2002.
- Rolfsson Ó, Sigurjonsson ÓE, Magnusdottir M, et al. Metabolomics comparison of red cells stored in four additive solutions reveals differences in citrate anticoagulant permeability and metabolism. *Vox Sang*. 2017;112(4):326-335.
- Cancelas JA, Dumont LJ, Maes LA, et al. Additive solution-7 reduces the red blood cell cold storage lesion. *Transfusion*. 2015;55(3):491-498.
- Pertinhez TA, Casali E, Baroni F, et al. A comparative study of the effect of leukoreduction and pre-storage leukodepletion on red blood cells during storage. *Front Mol Biosci*. 2016;3:13.
- D'Alessandro A, Culp-Hill R, Reisz JA, et al. Heterogeneity of blood processing and storage additives in different centers impacts stored red blood cell metabolism as much as storage time: lessons from REDS III - Omics. *Transfusion*. 2019;59(1):89-100.
- D'Alessandro A, Zimring JC, Busch M. Chronological storage age and metabolic age of stored red blood cells: are they the same? *Transfusion*. 2019;59(5):1620-1623.
- Kanias T, Lanteri MC, Page GP, et al. Ethnicity, sex, and age are determinants of red blood cell storage and stress hemolysis: results of the REDS-III RBC-Omics study. *Blood Adv*. 2017;1(15):1132-1141.
- Zimring JC, Smith N, Stowell SR, et al. Strain-specific red blood cell storage, metabolism, and eicosanoid generation in a mouse model. *Transfusion*. 2014;54(1):137-148.
- de Wolski K, Fu X, Dumont LJ, et al. Metabolic pathways that correlate with post-transfusion circulation of stored murine red blood cells. *Haematologica*. 2016;101(5):578-586.
- Hod EA, Zhang N, Sokol SA, et al. Transfusion of red blood cells after prolonged storage produces harmful effects that are mediated by iron and inflammation. *Blood*. 2010;115(21):4284-4292.
- Klein HG. The red cell storage lesion(s): of dogs and men. *Blood Transfus*. 2017;15(2):107-111.
- Solomon SB, Wang D, Sun J, et al. Mortality increases after massive exchange transfusion with older stored blood in canines with experimental pneumonia. *Blood*. 2013;121(9):1663-1672.
- Chen Y, Qin S, Ding Y, et al. Reference values of clinical chemistry and hematology parameters in rhesus monkeys (*Macaca mulatta*). *Xenotransplantation*. 2009;16(6):496-501.
- Fonseca LL, Alezi HS, Moreno A, et al. Quantifying the removal of red blood cells in *Macaca mulatta* during a *Plasmodium coatneyi* infection. *Malar J*. 2016;15(1):410.
- Fonseca LL, Joyner CJ, Saney CL, et al. Analysis of erythrocyte dynamics in Rhesus macaque monkeys during infection with *Plasmodium cynomolgi*. *Malar J*. 2018;17(1):410.
- Kaestner L, Minetti G. The potential of erythrocytes as cellular aging models. *Cell Death Differ*. 2017;24(9):1475-1477.
- Pasini EM, Kirkegaard M, Mortensen P, Mann M, Thomas AW. Deep-coverage rhe-
- sus red blood cell proteome: a first comparison with the human and mouse red blood cell. *Blood Transfus*. 2010;8(Suppl 3):s126-139.
- Reisz JA, Nemkov T, Dzieciatkowska M, et al. Methylation of protein aspartates and deamidated asparagines as a function of blood bank storage and oxidative stress in human red blood cells. *Transfusion*. 2018;58(12):2978-2991.
- Nemkov T, Hansen KC, Dumont LJ, D'Alessandro A. Metabolomics in transfusion medicine. *Transfusion*. 2016;56(4):980-993.
- Nemkov T, Hansen KC, D'Alessandro A. A three-minute method for high-throughput quantitative metabolomics and quantitative tracing experiments of central carbon and nitrogen pathways. *Rapid Commun Mass Spectrom Rapid Commun Mass Spectrom*. 2017;31(8):663-673.
- Fu X, Felcyn JR, Odem-Davis K, Zimring JC. Bioactive lipids accumulate in stored red blood cells despite leukoreduction: a targeted metabolomics study. *Transfusion*. 2016;56(10):2560-2570.
- D'Alessandro A, Nemkov T, Yoshida T, et al. Citrate metabolism in red blood cells stored in additive solution-3. *Transfusion*. 2017;57(2):325-336.
- Chong J, Soufan O, Li C, et al. MetaboAnalyst 4.0: towards more transparent and integrative metabolomics analysis. *Nucleic Acids Res*. 2018;46(W1):W486-W494.
- D'Alessandro A, Nemkov T, Yoshida T, et al. Citrate metabolism in red blood cells stored in additive solution-3. *Transfusion*. 2017;57(2):325-336.
- Nemkov T, Sun K, Reisz JA, et al. Metabolism of citrate and other carboxylic acids in erythrocytes as a function of oxygen saturation and refrigerated storage. *Front Med*. 2017;4:175.
- Nemkov T, Sun K, Reisz JA, et al. Hypoxia modulates the purine salvage pathway and decreases red blood cell and supernatant levels of hypoxanthine during refrigerated storage. *Haematologica*. 2018;103(2):361-372.
- Nemkov T, Hansen KC, D'Alessandro A. A three-minute method for high-throughput quantitative metabolomics and quantitative tracing experiments of central carbon and nitrogen pathways. *Rapid Commun Mass Spectrom Rapid Commun Mass Spectrom*. 2017;31(8):663-673.
- D'Alessandro A, Dzieciatkowska M, Nemkov T, Hansen KC. Red blood cell proteomics update: is there more to discover? *Blood Transfus*. 2017;15(2):182-187.

38. Reisz JA, Slaughter AL, Culp-Hill R, et al. Red blood cells in hemorrhagic shock: a critical role for glutaminolysis in fueling alanine transamination in rats. *Blood Adv.* 2017;1(17):1296-1305.
39. Silliman CC, Paterson AJ, Dickey WO, et al. The association of biologically active lipids with the development of transfusion-related acute lung injury: a retrospective study. *Transfusion.* 1997;37(7):719-726.
40. Knight J, Wood KD, Lange JN, Assimios DG, Holmes RP. Oxalate formation from glyoxal in erythrocytes. *Urology.* 2016;88:226.
41. D'Alessandro A, Taamalli M, Gevi F, et al. Cadmium stress responses in *Brassica juncea*: hints from proteomics and metabolomics. *J Proteome Res.* 2013;12(11):4979-4997.
42. Tokarska-Schlattner M, Epand RF, Meiler F, et al. Phosphocreatine interacts with phospholipids, affects membrane properties and exerts membrane-protective effects. *PLoS One.* 2012;7(8):e43178.
43. Nguyen DB, Wagner-Britz L, Maia S, et al. Regulation of phosphatidylserine exposure in red blood cells. *Cell Physiol Biochem.* 2011;28(5):847-856.
44. Sun K, D'Alessandro A, Xia Y. Purinergic control of red blood cell metabolism: novel strategies to improve red cell storage quality. *Blood Transfus.* 2017;15(6):535-542.
45. Vuk T, O i T, Juki I. Influence of cigarette smoking on haemoglobin concentration - do we need a different approach to blood donor selection? *Transfus Med.* 2019;29(Suppl 1):70-71.
46. Kanas T, Sinchar D, Osei-Hwedie D, et al. Testosterone-dependent sex differences in red blood cell hemolysis in storage, stress, and disease. *Transfusion.* 2016;56(10):2571-2583.
47. Tzounakas VL, Karadimas DG, Anastasiadi AT, et al. Donor-specific individuality of red blood cell performance during storage is partly a function of serum uric acid levels. *Transfusion.* 2018;58(1):34-40.
48. D'Alessandro A, Reisz JA, Zhang Y, et al. Effects of aged stored autologous red blood cells on human plasma metabolome. *Blood Adv.* 2019;3(6):884-896.
49. Monestier M, Bona CA. Antibodies possessing multiple antigen specificities and exhibiting extensive idiotypic cross-reactivity. *Int Rev Immunol.* 1988;3(1-2):59-70.
50. Taub DM, Mehlman PT. Development of the Morgan Island rhesus monkey colony. *Pr R Health Sci J.* 1989;8(1):159-169.

RESEARCH, READ & CONNECT



We reach more than
6 hundred thousand readers each year

The first Hematology Journal in Europe

Impressions YTD

9,621,645

Digital Readers

4,431

Total Audience

554,484

Worldwide rank

7th

Impact factor

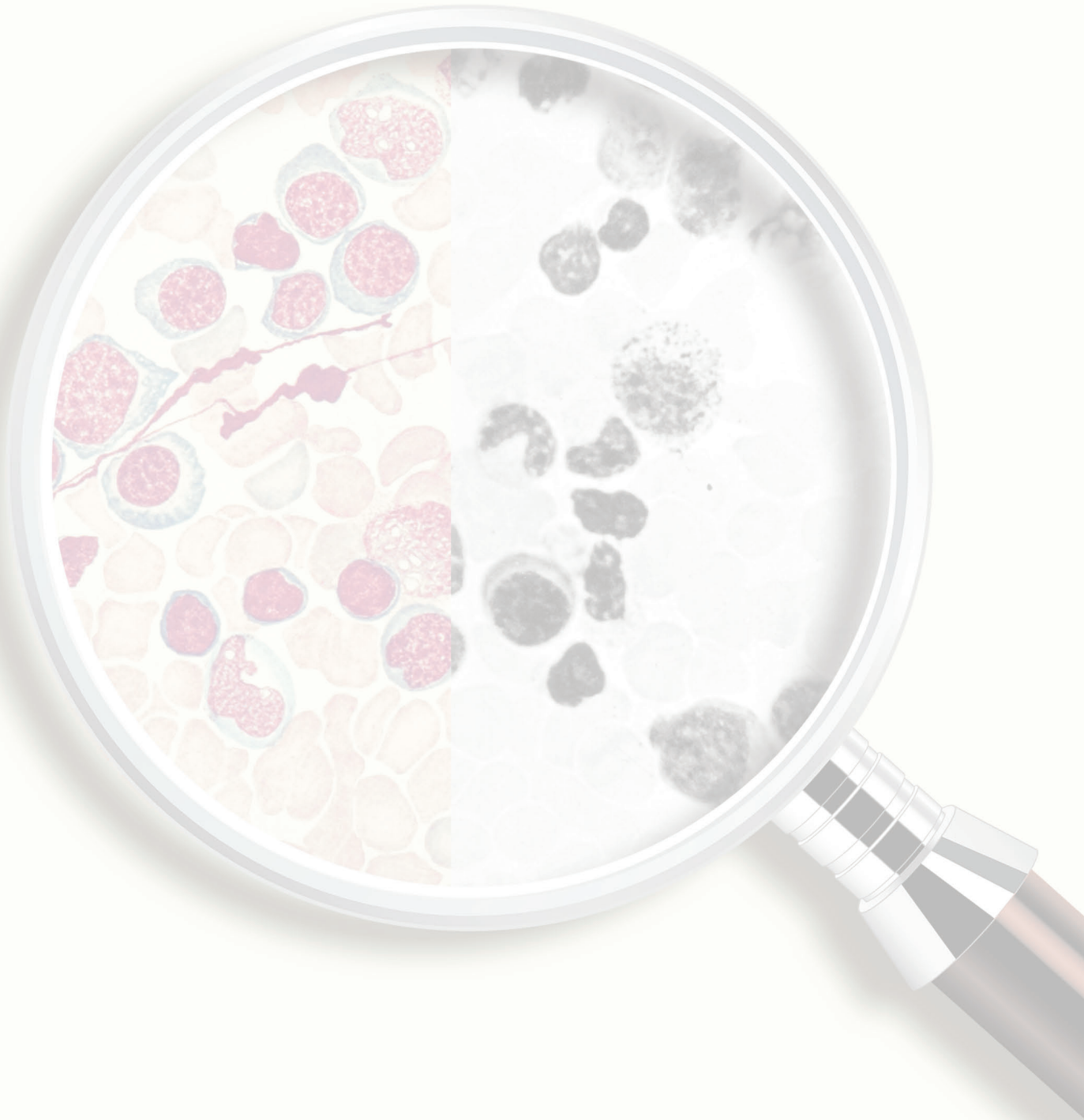
7.570

Total citations

16,255

 **haematologica**

Journal of the Ferrata Storti Foundation



haematologica — Vol. 105 n. 8 — August 2020 — 1985-2186